ELSEVIER

THE TEXTILE INSTITUTE BOOK SERIES

Advanced Characterization and Testing of Textiles

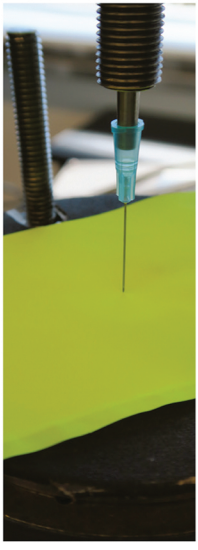

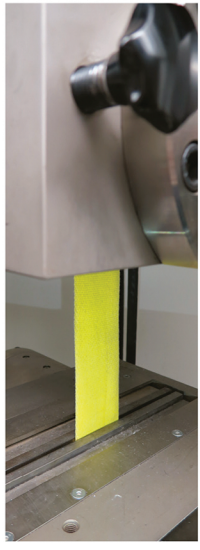


Edited by Patricia Dolez, Olivier Vermeersch, and Valerio Izquierdo

Advanced Characterization and Testing of Textiles

The Textile Institute Book Series

Incorporated by Royal Charter in 1925, The Textile Institute was established as the professional body for the textile industry to provide support to businesses, practitioners and academics involved with textiles and to provide routes to professional qualifications through which Institute Members can demonstrate their professional competence. The Institute's aim is to encourage learning, recognise achievement, reward excellence and disseminate information about the textiles, clothing and footwear industries and the associated science, design and technology; it has a global reach with individual and corporate members in over 80 countries.

The Textile Institute Book Series supersedes the former 'Woodhead Publishing Series in Textiles', and represents a collaboration between The Textile Institute and Elsevier aimed at ensuring that Institute Members and the textile industry continue to have access to high calibre titles on textile science and technology.

Books published in The Textile Institute Book Series are offered on the Elsevier web site at: store.elsevier.com and are available to Textile Institute Members at a substantial discount. Textile Institute books still in print are also available directly from the Institute's web site at: www.textileinstitute.org

To place an order, or if you are interested in writing a book for this series, please contact Matthew Deans, Senior Publisher: m.deans@elsevier.com

Recently Published and Upcoming Titles in The Textile Institute Book Series:

Handbook of Technical Textiles, Volume 1, 2nd Edition, A. Richard Horrocks and Subhash C. Anand, 9781782424581
Handbook of Technical Textiles, Volume 2, 2nd Edition, A. Richard Horrocks and Subhash C. Anand, 9781782424659
Geotextiles, Robert Koerner, 9780081002216
Advances in Braiding Technology, Yordan Kyosev, 9780081009260
Antimicrobial Textiles, Gang Sun, 9780081005767
Active Coatings for Smart Textiles, Jinlian Hu, 9780081002636
Advances in Women's Intimate Apparel Technology, Winnie Yu, 9781782423690
Smart Textiles and Their Applications, Vladan Koncar, 9780081005743
Advances in Technical Nonwovens, George Kellie, 9780081005750
Activated Carbon Fiber and Textiles, Jonathan Chen, 9780081006603
Performance Testing of Textiles, Lijing Wang, 9780081005705
Colour Design, Janet Best, 9780081012703
Forensic Textile Science, Debra Carr, 9780081018729
Principles of Textile Finishing, Asim Kumar Roy Choudhury, 9780081006467
High-Performance Apparel, John McLoughlin and Tasneem Sabir, 9780081009048

The Textile Institute Book Series

Advanced Characterization and Testing of Textiles

Patricia Dolez

Olivier Vermeersch

Valério Izquierdo

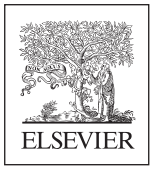

WP
WOODHEAD
PUBLISHING
An imprint of Elsevier

Woodhead Publishing is an imprint of Elsevier
The Officers' Mess Business Centre, Royston Road, Duxford, CB22 4QH, United Kingdom
50 Hampshire Street, 5th Floor, Cambridge, MA 02139, United States
The Boulevard, Langford Lane, Kidlington, OX5 1GB, United Kingdom

Notices
Knowledge and best practice in this field are constantly changing. As new research and experience broaden our understanding, changes in research methods, professional practices, or medical treatment may become necessary.

Practitioners and researchers must always rely on their own experience and knowledge in evaluating and using any information, methods, compounds, or experiments described herein. In using such information or methods they should be mindful of their own safety and the safety of others, including parties for whom they have a professional responsibility.

To the fullest extent of the law, neither the Publisher nor the authors, contributors, or editors, assume any liability for any injury and/or damage to persons or property as a matter of products liability, negligence or otherwise, or from any use or operation of any methods, products, instructions, or ideas contained in the material herein.

Library of Congress Cataloging-in-Publication Data
A catalog record for this book is available from the Library of Congress

British Library Cataloguing-in-Publication Data
A catalogue record for this book is available from the British Library

ISBN: 978-0-08-100453-1 (print)
ISBN: 978-0-08-100454-8 (online)

Publisher: Matthew Deans
Acquisition Editor: David Jackson
Editorial Project Manager: Sabrina Webber
Production Project Manager: Omer Mukthar
Cover Designer: Victoria Pearson

Typeset by SPi Global, India

Contents

Contributors xi
About the editors xiii

Part One Principles of textile characterization and testing 1

1 Introduction to advanced characterization and testing of textiles 3
P.I. Dolez, O. Vermeersch
1.1 Introduction 3
1.2 Importance of textile testing 4
1.3 Variety of textile applications 6
1.4 Objectives of characterization and testing 7
1.5 Introduction to test methods 9
1.6 Testing management and infrastructure 12
1.7 Defective products 15
1.8 Future trends 16
1.9 Sources of further information and advice 18
References 19

Part Two Testing by properties 23

2 Advanced strength testing of textiles 25
D.C. Adolphe, P.I. Dolez
2.1 Introduction 25
2.2 Mechanical behavior of textiles 25
2.3 Textile elasticity 26
2.4 Tensile and multiaxial tensile strength 28
2.5 Compression 34
2.6 Burst strength 36
2.7 Shear properties 38
2.8 Flexion properties 39
2.9 Puncture resistance 40
2.10 Tear resistance measurement 44
2.11 Cut resistance 49
2.12 Impact resistance 52
2.13 Abrasion resistance 53

2.14 Future trends **55**
2.15 Conclusion **55**
2.16 Sources of further information and advice **56**
References **56**

3 Comfort testing of textiles **59**
E. Classen
3.1 Introduction **59**
3.2 Fabric comfort properties **60**
3.3 Thermophysiological comfort testing **61**
3.4 Skin sensorial wear comfort testing **62**
3.5 Ergonomic comfort testing **66**
3.6 Psychological comfort testing **67**
3.7 Future trends **67**
3.8 Conclusion **68**
References **68**

4 Testing thermal properties of textiles **71**
D. Tessier
4.1 Introduction **71**
4.2 Thermal properties of textiles **74**
4.3 Testing thermal properties **75**
4.4 Applications **83**
4.5 Future trends **86**
4.6 Conclusion **88**
4.7 Sources of further information and advice **88**
References **89**
Further reading **92**

5 Tests for evaluating textile aging **93**
M. Fulton, M. Rezazadeh, D. Torvi
5.1 Introduction **93**
5.2 Textile aging **93**
5.3 Tests for textile aging **95**
5.4 Nondestructive tests **106**
5.5 Methods to predict useful life of textiles **114**
5.6 Conclusions and future work **116**
5.7 Sources of further information **117**
References **118**
Further reading **124**

6 Advanced chemical testing of textiles **127**
Y. Shao, V. Izquierdo, P.I. Dolez
6.1 Introduction **127**
6.2 Measurement of extractable content **128**
6.3 Analysis of fiber content **129**

6.4 Chemical testing of functional finishes **134**
6.5 Measurement of the resistance to chemicals **140**
6.6 Measurement of the permeability to air, water vapor, solvents, particles, and toxic chemicals **142**
6.7 Biodegradability testing **144**
6.8 Future trends **145**
6.9 Conclusions **146**
References **146**
Further reading **149**

7 Toxicity testing of textiles **151**
P.I. Dolez, H. Benaddi
7.1 Introduction **151**
7.2 Testing for heavy metals **153**
7.3 Testing for VOCs **159**
7.4 Testing for toxic dyes **165**
7.5 Testing for pesticide residues **168**
7.6 Testing for flame retardants **173**
7.7 Testing for phthalates **175**
7.8 Testing for other toxic chemicals **176**
7.9 Eco-textile certifications **177**
7.10 Conclusion and future trends **179**
7.11 Sources of further information and advice **179**
References **180**

8 Testing fabrics for flammability and fire safety **189**
V. Izquierdo
8.1 Introduction **189**
8.2 Flammability properties of fabrics **189**
8.3 Testing the flammability of fabrics **192**
8.4 Test methods for fire-resistant fabrics **196**
8.5 Future trends **205**
8.6 Conclusion **205**
8.7 Sources of further information and advice **205**
References **206**
Further reading **209**

9 Testing of hot-water and steam protective performance properties of fabrics **211**
S. Mandal, M. Camenzind, S. Annaheim, R.M. Rossi
9.1 Introduction **211**
9.2 Tests for evaluating the hot water and steam protective performance of the clothing used by high-risk sector workers **212**
9.3 Characterization of the hot water and steam protective performances of clothing used by the high-risk sector workers **225**

9.4 Key issues related to the hot water and steam protective performance of clothing **230**
9.5 Summary and conclusion **231**
9.6 Sources for further information **232**
References **232**

Part Three Testing by applications **237**

10 Specific testing of geotextiles and geosynthetics **239**
P.I. Dolez
10.1 Introduction **239**
10.2 Geotextiles **240**
10.3 Geogrids **264**
10.4 Geosynthetic clay liners **270**
10.5 Drainage geocomposites **277**
10.6 Future trends **285**
10.7 Conclusion **287**
10.8 Sources of further information and advice **287**
Acknowledgments **287**
References **287**

11 Specific testing of protective clothing **301**
P.I. Dolez, V. Izquierdo
11.1 Introduction **301**
11.2 Testing of industrial/domestic protective clothing **303**
11.3 Testing of law enforcement protective clothing **312**
11.4 Testing of first responder protective clothing **316**
11.5 Testing of military protective clothing **320**
11.6 Testing of medical protective clothing **324**
11.7 Testing of electrical protective clothing **326**
11.8 Testing of construction protective clothing **329**
11.9 Testing of marine protective clothing **330**
11.10 Testing of sports protective clothing **333**
11.11 Future trends **335**
11.12 Conclusions **337**
11.13 Sources for further information and advice **337**
Acknowledgments **338**
References **338**

12 Specific testing for smart textiles **351**
J. Decaens, O. Vermeersch
12.1 Introduction **351**
12.2 Testing conductive textile materials **353**
12.3 Testing smart thermoregulating textiles **358**
12.4 Testing ECG, EMG, EEG, and other embedded textile sensors **363**

12.5 Testing cosmetotextiles and smart dermotextiles **367**
12.6 Conclusion **371**
References **371**

13 Specific testing for filtration **375**
N. Petillon
13.1 Structural properties **375**
13.2 Hydraulic properties **379**
13.3 Separative properties **381**
13.4 Physical and physicochemical properties **386**
13.5 Existing standards to qualify filter media **389**
13.6 Source of further information **394**
References **395**

14 Specific testing of textiles for transportation **399**
M. Richaud, O. Vermeersch, P.I. Dolez
14.1 Introduction **399**
14.2 Performance testing related to safety **404**
14.3 Testing related to flammability, smoke generation, and toxicity **410**
14.4 Testing related to hygiene **414**
14.5 Testing of textile-reinforced composites **415**
14.6 Durability testing **419**
14.7 Future trends **423**
14.8 Conclusion **425**
14.9 Sources of further information and advice **425**
Acknowledgments **426**
References **426**

15 Specific testing for performance sportswear **433**
R.M. Rossi
15.1 Introduction **433**
15.2 Heat and moisture transfer through sportswear **433**
15.3 Pressure and friction **438**
15.4 Aero- and hydrodynamics **440**
15.5 Conclusions and future trends **441**
15.6 Sources of further information **442**
References **443**

Index **449**

This page intentionally left blank

Contributors

D.C. Adolphe University of Haute-Alsace, ENSISA, Mulhouse, France

S. Annaheim Empa, Swiss Federal Laboratories for Materials Science and Technology, St. Gallen, Switzerland

H. Benaddi CTT Group, Saint-Hyacinthe, QC, Canada

M. Camenzind Empa, Swiss Federal Laboratories for Materials Science and Technology, St. Gallen, Switzerland

E. Classen Hohenstein Institute, Bönnigheim, Germany

J. Decaens CTT Group, Saint-Hyacinthe, QC, Canada

P.I. Dolez CTT Group, Saint-Hyacinthe, QC, Canada

M. Fulton University of Saskatchewan, Saskatoon, SK, Canada

V. Izquierdo CTT Group, Saint-Hyacinthe, QC, Canada

S. Mandal Empa, Swiss Federal Laboratories for Materials Science and Technology, St. Gallen, Switzerland

N. Petillon IFTS, Foulayronnes, France

M. Rezazadeh University of Saskatchewan, Saskatoon, SK, Canada

M. Richaud CTT Group, Saint-Hyacinthe, QC, Canada

R.M. Rossi Empa, Swiss Federal Laboratories for Materials Science and Technology, St. Gallen, Switzerland

Y. Shao CTT Group, Saint-Hyacinthe, QC, Canada

D. Tessier CTT Group, Saint-Hyacinthe, QC, Canada

D. Torvi University of Saskatchewan, Saskatoon, SK, Canada

O. Vermeersch CTT Group, Saint-Hyacinthe, QC, Canada

This page intentionally left blank

About the editors

Patricia Dolez has recently joined the Department of Human Ecology at the University of Alberta, Canada, to work as an assistant professor in textile science. Before that, she had been a researcher at CTT Group in Saint-Hyacinthe, Quebec, Canada, since 2012. She holds an engineering degree in materials science and a PhD in physics. Her expertise includes textiles, polymers, and composites. She is especially interested in the application of nanotechnologies, smart textiles, natural fibers, and recycled materials in personal protective equipment and other textile-based products, as well as in the aging behavior of protective materials. Dr. Dolez has authored more than 100 articles in books, scientific and technical journals, and conference proceedings. She is also the editor of a book entitled, "Nanoengineering: Global Approaches to Health & Safety Issues," published in 2015 by Elsevier.

Olivier Vermeersch is a graduate of ENSISA (engineering school in Mulhouse, France) and the University of Haute Alsace in France in textile materials and processes engineering. Dr. Vermeersch has been involved in the technical textile industry since 1990 within the CTT Group, the largest R&D laboratory in Canada in the areas of technical textiles, geosynthetics, and flexible materials. He is vice-president of R&D as well as chairholder of the NEXTEX Industrial Chair of Saint-Hyacinthe College, a Canadian NSERC Level 2 Chair that focuses on 3D textiles and preforms for composites and smart textiles. He is the author of several patents, which are commercially exploited by some of his industrial partners. He was also involved in organizing EXPO HIGHTEX editions for a decade, was co-editor-in-chief of "The Textile Journal" until 2016, and is the author of numerous technical and scientific publications. In 2014, he was awarded the prestigious Excellence Award from the Fonds de recherche Nature et Technologies du Québec.

Valerio Izquierdo graduated in textile engineering from the Institut Textile et Chimique de Lyon (ITECH—France) in 1998. After 3 years at the Institut Textile de France, he joined the CTT Group (Saint-Hyacinthe, Canada) as a project leader to pilot innovative research and development projects and laboratory testing. Valerio became lab manager for the textile laboratories of the CTT Group in 2006 and extended his expertise in the various testing methods routinely used to assess textile performance and quality. He is now vice-president of the Textile Laboratories and Expertise branch of the CTT Group, involved in the characterization of textile and polymeric materials for the benefit of manufacturers, distributors, and end-users. The CTT Group Textile Laboratories perform testing of various chemical and

physical textile properties, as well as flame resistance, accelerated ageing, comfort parameters, toxicity, high visibility, moisture management, and applicability for personal protective equipment. Valerio also sits as a leading expert on various boards emitting regulatory and specification guidelines for the industry and governing agencies.

Part One

Principles of textile characterization and testing

This page intentionally left blank

Introduction to advanced characterization and testing of textiles

1

P.I. Dolez, O. Vermeersch
CTT Group, Saint-Hyacinthe, QC, Canada

1.1 Introduction

The earliest evidence of textile processes may be dated to 35,000–15,000 BC with dyed flax fibers discovered in a cave in the Caucasus and sewing needles found in France (Hearle, 2002; Jenkins, 2003). The first manufactured textiles were most probably felt, produced with wool. Some articles demonstrating a high level of development of the felt-making technology have been found in Siberia in a tomb dated from the 5th century BC. Weaving may have been known since the Paleolithic era as indicated by cloth burnt remnants and imprints in clay found in the Czech Republic and dated around 25,000 BC. Around 5000–3500 BC, textile manufacturing was well implanted in many parts of the world with hemp in the Middle East, cotton and wool in South America, linen in Egypt, cotton in India, and silk in China, for example. Production techniques further improved over the centuries. Then, in the period of 1750–1850, textile manufacturing transitioned from crafting to industrialization with the mechanization of the equipment. More recently, new high performance fibers/materials were developed, leading to the emergence of a high value-added technical textiles market. This market is projected to reach 42.2 million metric tons by 2020, at a compound annual growth rate (CAGR) of 4.68% between 2015 and 2020 (M&M, 2015a). As a whole, the global textile sector is currently valued at USD 439.1 billion (EHER, 2017).

Textile manufacturing involves the transformation of fibers into fabrics. The four main textile structures are wovens, knits, braids, and nonwovens. In the case of weaving, knitting, and braiding, fibers are first made into yarns, which are then used to produce the textile structure. Nonwovens are manufactured directly from fibers. Woven textiles are produced by interlacing warp and weft yarns according to a regular pattern. They are generally stronger but less stretchable than the other textile structures. Knitted textiles are manufactured by interlacing symmetrically disposed loops together. They offer a very large extensibility and display directional mechanical performance. Braids are formed by interlacing three or more yarns to yield a long and narrow product. Finally, nonwovens are produced by disposing fibers in a more or less random manner to form a three-dimensional structure. The web is further consolidated using mechanical, thermal, and/or chemical means. The advantages of the nonwoven process include a high manufacturing rate, low cost, capacity to handle a wide variety

Advanced Characterization and Testing of Textiles. https://doi.org/10.1016/B978-0-08-100453-1.00001-5

of fibers, lower level of requirements in terms of fiber properties, and a wide range of functions. Textile structures may then receive a finishing treatment, for instance, to provide them with flame-resistance properties; they may be dyed; and/or they may be coated with a polymer, for example, to make them water-tight. More information about textile manufacturing techniques is available in Horrocks and Anand (2000). The wide variety of technologies available for each type of textile structure, with the additional possibility of combining them into hybrid structures, gives rise to a myriad of products with different characteristics. These engineered materials have found countless applications in a whole range of different markets.

Textiles are produced using natural and/or man-made fibers. Natural fibers include plant-based fibers such as cotton, hemp, flax, and jute; protein-based fibers such as silk and wool; and mineral fibers. Man-made fibers include cellulose-based or regenerated fibers, e.g., rayon, acetate, and triacetate fibers; organic fibers, e.g., polyethylene, polypropylene, acrylic, nylon, polyester, spandex, modacrylic, para-aramid (e.g. Kevlar® and Twaron®), and meta-aramid (e.g., Nomex®); and inorganic fibers, e.g., glass, carbon, and basalt. Depending on the fibers, a wide range of properties may be observed: for instance, low density and biodegradability for plant-based fibers; very high strength for para-aramid, ultra-high molecular weight polyethylene (Dyneema® and Spectra®), and carbon fibers; and flame resistance for para- and meta-aramids. More information about the characteristics and properties of natural and man-made fibers may be found in Kozłowski (2012), Eichhorn, Hearle, Jaffe, and Kikutani (2009), McIntyre (2004), and Hearle (2001).

Raw materials available for textile manufacturing evolved from natural fibers with very high inherent variability to synthetic fibers produced with commodity polymers to high performance fibers. Simultaneously, production techniques and equipment gained in precision. The resulting ability to better control the quality and performance of what was produced gave rise to large efforts to develop test methods that could characterize textile properties and performance at the different stages of production, i.e., from the raw material to the finished product. These properties include physical, mechanical, chemical, barrier, and thermal properties as well as comfort, flammability, and durability.

1.2 Importance of textile testing

The primary objective of textile testing is to assess the product properties and predict its performance during use. The information obtained may be used for the following (Anonymous, 2014):

- Research and development
- Selection of raw materials/inputs
- Process development
- Process control
- Quality control
- Product testing
- Product failure analysis
- Comparative testing and benchmarking
- Conformity with government regulations and specifications

1.2.1 Manufacturers' perspective

For a manufacturer, the two main purposes of testing are to check the quality of his inputs and his outputs. Depending on his position in the value chain, his input materials might be fibers, yarns, or fabrics. The properties of his inputs will affect both his ability to process them smoothly and in an efficient manner, and the quality and properties of the product obtained. For instance, a yarn with a low strength will have a larger probability of failure during weaving, increasing the machine down time; the woven fabric produced will also display a lower strength and eventually not meet the requirements.

The control of the manufacturer's outputs is also critical to ensure the viability of his processes: manufacturing parameters are optimized to allow a high production rate while limiting machine down time and achieving the level of quality and performance expected. Process control strategies include the use of statistical process control (SPC) methods, multistage process surveillance, and fault diagnosis (Majumdar, Das, Alagirusamy, & Kothari, 2012). Statistical quality control makes use of variability measurement, differences between means, significance of variables, control charts, and hypothesis testing, for instance.

Originally, the requirements products had to meet mostly dealt with the material properties, for instance, the yarn or the fabric tensile strength. Increasingly, more complex aspects related to the performance in service have been included; flammability and breathability are examples. Some of these properties may also be exclusive features that are part of the manufacturer's strategy to protect his share of the market with a monopoly based on particular functions only offered by his product.

Testing of outputs is also a key element for the manufacturer to ensure that he is in the desired bracket of performance/cost ratio. Indeed, it is critical for him to maximize his margin of profits by avoiding exceeding the required quality levels. Quality control over outputs is also part of the toolbox in case of disputes with clients.

1.2.2 Specifiers' perspective

The specifier is generally the one setting up the requirements. It may be the buyer, who is generally not the end-user in the case of finished products, or organisms representing consumers and end-users. Examples of these organisms include the International Organization for Standardization (ISO), ASTM International, the National Fire Protection Association (NFPA), and SAE International. If specifications were originally drafted by manufacturers independently of the product application, considerations related to end-users gradually gained importance: nowadays, requirements in terms of performance take into account criteria associated with the area of application of the product and its conditions of use.

For specifiers, testing allows parametrizing the exchange of money for goods using precise sets of requirements. The product selected has to meet the prescribed requirements while generally being the least expensive. With standard test methods, it is possible to compare different products and identify those meeting the requirements. For specifiers, testing is also a powerful driver of technical innovation because it sets new targets for performance. In addition, it can promote sociopolitical changes; examples include “green” products, local content, and fair trade.

1.2.3 End-users' perspective

For the end-user, testing ensures that his expectations in terms of quality, properties, and performance are met by the product. The characteristics he will be looking for may be related to safety, aesthetics, function, comfort, and durability, for instance, depending on the application and his use of the product. If end-users' criteria were initially mostly aimed at performance without any consideration to the production process, the increase awareness of the general public about the socio-politico-economic aspects of goods manufacturing leads to a new purchase paradigm where, for some, local content and fair trade may prevail over price.

Testing also allows end-users to make an informed selection among the products available. For instance, the standardization of test methods has made comparing different materials/products characteristics possible, while third-party certification guarantees that the product they choose meets the level of performance set by the specification. Some companies have also developed a branding strategy where some unique characteristics or performance are associated with a specific brand.

1.2.4 Market development issues

The development of high performance materials has enabled the manufacture of highly specialized products with application-specific and even task-specific functions. For example, if fire resistance is needed, para-aramid might be preferred over ultra-high molecular weight polyethylene for cut-resistant protective clothing.

This large segmentation of specifications and markets has led to a corresponding breakdown in test methods. One typical example is flammability testing: depending if the textile is used for upholstered seating structures, mattresses, tents, bedcovers and pillows, floor covering, protective clothing or children's sleepwear, the flammability test may involve different ignition sources, intensities, and durations of exposure, specimen sizes, angles between the specimen and the flame, parameters measured, etc. (see Chapter 8 on flammability testing). The same is true if the textile is used in the aircraft, automotive, railway, or marine industry (see Chapter 14 on testing of transportation textiles). One of the reasons for these differences in the testing methods is the attempt to reproduce as much as possible the conditions experienced by the material or the product during service.

1.3 Variety of textile applications

Textiles have found applications in a wide range of sectors. The following provides some examples:

- Clothing and linen: street wear, business suits, felt hats, swimsuits, towels, sleepwear, bedsheets, blankets, dishtowels, microfiber dust rags, etc.
- Home furnishing, appliances and household items: upholstered furniture, cushions, curtains, blinds, carpets, rugs, umbrellas, dusting clothes, mops, absorbent paper, air and liquid filters, composite reinforcement for panels, etc.

- Transportation (aircrafts, road vehicles, railway, marine vessels, recreational vehicles, aerospace, etc.): seat upholstery, seat belts, airbags, reinforcements for tires, air and liquid filters, carpets, wall coverings, composite reinforcements for nonstructural and structural parts, etc.
- Medical: scaffolds, stents, cardiovascular implants, soft-tissue implants, suture threads, sterile pads, wound dressings, bandages, compression stockings, splints, casts, cervical collars, braces, orthopedic implants, extracorporeal devices, operating fields, surgical gowns, bed linens, incontinence pads, etc.
- Hygiene and cosmetics: tissues, diapers, panty liners, wipes, makeup removal pads, cosmetotextiles, etc.
- Protection: lab coats, clean laboratory coveralls, cut-resistant gloves, boot liners, fire bunker suits, bulletproof vests, harnesses, lanyards, dust masks, mask filters, etc.
- Sports: motorcycle jackets, ski suits, ballerina pointe shoes, ice hockey neck protectors, composite reinforcements for hockey sticks and bicycle frames, etc.
- Military: underwear, combat uniforms, ballistic vests, tents, packsacks, sleeping bags, composite reinforcements for armor vehicles, etc.
- Industrial: dust collection filters, solid-liquid separation filters, straps, ropes, hoses, transmission and conveyor belts, etc.
- Construction: acoustic panels, insulating batts, reinforcements for fiber reinforced plastics used as patio grating, reinforcement for bituminous membranes, etc.
- Civil engineering: geotextiles, erosion control products, geogrids, geocomposite clay liners, drainage composites, reinforcements for geomembranes, etc.
- Energy: composite reinforcements for wind turbine rotor blades, battery separators, wearable energy harvesting systems, etc.

When testing is considered, this large variety of applications leads to a multiplication of tests with different experimental conditions in order to simulate as closely as possible the material/product behavior in service. For instance, textiles for application in the automotive and geosynthetics industry are generally conditioned and tested at 23°C and 50% relative humidity. On the other hand, a temperature of 20°C or 21°C and a relative humidity of 65% are typically required for firefighter protective clothing and general-use garment testing. For a company willing to explore different markets, this may involve testing each property and performance according to the different standard test methods relevant to each market. Because there may not be any correlation between the tests performed using these different test methods, this situation may also apply during the product development phase as well as for quality control in production.

1.4 Objectives of characterization and testing

The two main purposes of textile testing are quality control during manufacturing and certification involving third-party testing.

1.4.1 Manufacturing quality control

Quality control is a major component of the manufacturing process. The objective is to ensure that the characteristics of the part produced are within the level of tolerance expected by the customer: quality is defined by the average value of the property as well

as its standard deviation. Quality control may be conducted on-line, i.e., without stopping the production process—for example, with an automatic system for the detection of broken needles in nonwovens. Tests may also be conducted off-line, by collecting samples and measuring them aside. More details about textile quality control may be found in Grover and Hamby (1960) and Majumdar et al. (2012).

Quality control starts at the raw material level. The objectives at that stage are to make sure that the properties of the raw materials are compatible with the manufacturing process as well as with the requirements of the finished product. For spinners, for instance, raw materials may be staple fibers of natural or synthetic origin for the manufacture of yarns and threads as well as polymers for the production of mono- or multifilaments by extrusion. Some nonwoven processes like flash spinning may also directly use polymers as raw materials. Nature/composition, diameter, length, mass per unit length, strength, elongation at break, stiffness, breaking twist angle, crimp, fiber aggregation, and presence of contaminants are some of the critical parameters for fibers while composition, melting and degradation temperatures, and viscosity may be measured for polymers. In addition, in the case of polymers, molded plate specimens may be prepared and tested to verify other characteristics such as tensile strength and durability.

Further down the value chain, nonwoven manufacturers will receive fibers or chopped filaments while weavers, knitters, and braiders will use staple fiber or filament yarns. Fibers used for nonwoven manufacturing will be checked for length distribution, diameter, stiffness, and strength among others. Characteristics assessed on yarns include count, titer, twist, strength, hairiness, evenness, and neps. At the next step, finishes, coatings, and color may be added to textile structures. In addition to the characteristics of the fabric itself, converters have to check its ability to take the treatment and retain it. At the last step, garment or textile product manufacturers receive finished, dyed, and/or coated fabrics as well as all the necessary add-on components such as zippers, buttons, and fasteners, and assemble them into a finished product. They will assess the physical characteristics as well as the short- and long-term performance of the fabric they receive. They may also verify that the fabric will resist the assembly process, for instance, by stitching.

Quality control is also performed at the different stages of each textile process. The objective is to fine tune the process parameters so that the production quality and efficiency are optimized. For instance, quality control in yarn spinning involves the blowroom, carding, drawing, combing, speed frame, and spinning operations. This assessment may also reveal some maintenance issues or equipment malfunction. Production quality monitoring is conducted by collecting samples in the production line according to a well-defined protocol and measuring a series of characteristics selected to be indicative of the level of quality of the material. Statistical methods have been developed to provide a meaningful assessment of the production quality.

Finally, quality control testing is also made by manufacturers on final products. This allows them to verify that they meet the targeted requirements both in terms of mean value and standard deviation. Properties measured generally include physical characteristics, e.g., garment/product dimensions, tensile strength, and the presence of defects; short-term performance, e.g., tear strength, resistance to puncture, and water vapor permeability; and long-term performance, e.g., resistance to abrasion, UV resistance, and creep. Some of these characteristics are specific to the application targeted by the product.

1.4.2 Certification and third-party testing

Aside from the tests performed by the manufacturer, a third-party certification may be sought for the finished product. This assessment is conducted for a fee by an independent laboratory. It warrantees that the product complies with a certain set of requirements referring to safety, quality, and/or performance. Tests are performed using specific standard test methods.

For manufacturers, the advantages of third-party certification include demonstrating the compliance with standards and regulations, providing an independent validation and verification of their commitment to safety and quality, and increasing their credibility and acceptance with their clients as well as regulators. For buyers and end-users, this avoids the need to test the product before purchasing/using it.

Certifications may be issued by a country. The accreditation body may then give notified bodies the authority to provide verification services to ensure compliance with standards and regulations in order to deliver declarations of conformity. For instance, there are about 1400 notified bodies for CE marking worldwide (EU, 2017). In Canada, the list of product, process, and service certification bodies accredited by the Standards Council of Canada and relevant to textiles includes the Bureau de normalisation du Québec, the Canadian General Standards Board, CSA Group, Intertek Testing Services Inc., and the Underwriters Laboratories of Canada (SCC, 2017).

Systems of certification have also been set by private organizations on a business or sector-basis. For instance, the OEKO-TEX association, which stands for the International Association for Research and Testing in the Field of Textile and Leather Ecology, is formed of 18 independent textile research and test institutes in Europe and Japan (OEKO-TEX, 2017). They develop test methods, establish limit values, and perform laboratory tests and site audits in relation with the awarding of the different OEKO-TEX product labels and production site certifications. These include the OEKO-TEX Standard 100 relative to banned and harmful substances. It applies to raw, semifinished, and finished textile products at all stages of processing as well as to accessory materials. The companion OEKO-TEX Standard 1000 refers to environmentally friendly production sites in the textile and clothing industry.

1.5 Introduction to test methods

Test methods may be divided into two categories depending on the type of feature they measure: a property or a performance. This section also discusses standardization bodies, which are in charge of developing standard test methods.

1.5.1 Property-based test methods

A property-based test method measures a product/material physical or chemical characteristic. It may be, for example, a fiber chemical nature and length distribution, a yarn count and twist, the type of fabric weave or knit pattern and its weight, the spectral characteristics of a dye, or the mass per unit area of a certain substance used as a finish or a coating.

Prescriptive regulations are solely based on property tests: they correspond to a partial description of the product. However, they do not set any requirements about the performance of the product and how it would behave in service conditions. In addition, prescriptive regulations may limit innovation by excluding new products on the basis of their chemical and physical characteristics even if they perform better than the current technology.

1.5.2 Performance-based test methods

In contrast, performance-based test methods are designed to simulate the conditions of the product/material use. As such, they inform about the product/material short- and long-term behavior in service. Short-term performance assessment may include flammability and toxic fume testing, tear and puncture strength measurement, and air flow and water vapor permeability. Long-term performances comprise resistance to UV, abrasion, chemicals, biodegradation, creep, etc.

Even if they are considered a critical complement to property-based test methods, performance-based test methods may also lead to the unfortunate exclusion of some products, for example, if the size of the specimens specified in the test method is inappropriate for the product. In addition, simulating service conditions might be a challenge because of the infinite number of specific cases encountered as well as the difficulty in replicating the complexity of the real situation experienced in service (Ohlemiller et al., 1993).

1.5.3 Standardization

The objective of standardization is ensuring the consistency of essential features of goods and services (e.g., quality, ecology, safety, economy, reliability, compatibility, interoperability, efficiency, and effectiveness) so that the product, process, or service is fit for its purpose (ISO, 2017). It can also allow a widespread adoption of formerly custom processes. The primary activity of standardization bodies is producing technical standards to address the needs of a relatively wide range of users: tasks consist in developing, coordinating, promulgating, revising, amending, reissuing, and interpreting documents that provide requirements, specifications, test methods, guidelines, and characteristics.

Five principles are at the basis of the standardization process: consensus, democratic legitimacy, transparency, willingness, and coherence (ISO, 2017). The development of an ISO standard usually takes about three years. First, experts within a work group discuss a new work item that is proposed. When they reach a consensus, the draft moves to the relevant technical committee or subcommittee where it is improved to reach a consensus. The document then becomes a draft international standard (DIS). An inquiry on the proposed DIS is first conducted, after which the document turns into a final draft international standard (FDIS), which is subjected to a formal vote. Upon approval, it is published as an international standard. These standards may then be referred to in regulations.

Standardization bodies exist at the international, regional, and national level. For instance, the International Organization for Standardization (ISO) is an international standard-setting body composed of representatives of national standards organizations from 164 countries, one per country (ISO, 2017). A technical committee on textiles, ISO/TC 38, was formed from the beginning to coin test methods, terminology, and definitions of fibers, yarns, threads, cords, rope, cloth, and other fabricated textile materials, and elaborate specifications for textile products (ISO/TC 38, 2017). ISO/TC 38 also covers textile industry raw materials, auxiliaries, and chemical products required for textile processing and testing. A total of 382 standards are under its direct responsibility or that of its subcommittees. Other technical committees dealing with textile or textile-based products include the following:

- ISO/TC 20 on aircraft and space vehicles
- ISO/TC 22 on road vehicles
- ISO/TC 31 on tires, rims, and valves
- ISO/TC 41 on pulleys and belts (including veebelts)
- ISO/TC 72 on textile machinery and accessories
- ISO/TC 94 on personal safety—protective clothing and equipment
- ISO/TC 136 on furniture
- ISO/TC 194 on biological and clinical evaluation of medical devices
- ISO/TC 216 on footwear
- ISO/TC 219 on floor coverings
- ISO/TC 221 on geosynthetics

At the regional level, the CEN/TC 248 technical committee of the European Committee for Standardization oversees the test methods, terms and definitions, specifications, and classification aspects of textiles, textile products, and textile components of products (CEN/TC 248, 2017). It also covers equipment relevant for the testing and use of textiles. It has 350 standards under its responsibility. Other regional standardization bodies may also be found in other parts of the world.

Standardization agencies also exist at the national level. For instance, in the United States, there are about 600 private and public standardization agencies, including ASTM International, the American Association of Textile Chemists and Colorists (AATCC), the National Institute of Standards and Technology (NIST), the American National Standards Institute (ANSI), the National Fire Protection Association (NFPA), the National Institute of Justice (NIJ), and the Geosynthetic Research Institute (GRI). In Europe, each member country has one standardization agency, for example, AFNOR in France, BSI in the United Kingdom, and DIN in Germany. In Canada, four standards development organizations are certified by the Standards Council of Canada (SCC): CSA Group, BNQ (Bureau de normalisation du Québec), CGSB (Canadian General Standards Board), and ULC (Underwriters Laboratories of Canada). Some of these national agencies have technical committees dedicated to textiles: for example, the ASTM Committee D13 on Textiles, the BSI Committees TCI/66 on Apparel and interior textiles, TCI/24 on Physical testing of textiles, and TCI/80 on Chemical testing of textiles, and the joint Australian/New Zealand Committees CS/4 on Care labeling of textiles and CS/86 on Burning behavior of textile products, floor coverings and furniture.

1.6 Testing management and infrastructure

Testing laboratories use test methods to characterize the properties and performance of materials and products. These laboratories may be separate entities or a part of manufacturing companies. In Canada only, when all types of products are considered, laboratory testing services generate $2 billion in annual revenue (IBISWorld, 2016a). This value increases to $18 billion for the US market (IBISWorld, 2016b). The global textile testing, inspection, and certification market is expected to reach $7.2 billion by 2020, with a CAGR of 4.6% between 2015 and 2020 (M&M, 2015b). It is pulled by the introduction of new regulations, standards, and technological innovations in the textile sector, and the increase in the worldwide trading of textiles. Top players in textile testing, inspection, and certification cited in the MarketsandMarkets report include SGS Group (Switzerland), Bureau Veritas SA (France), Intertek Group plc (United Kingdom), TUV SUD Group (Germany), TÜV Rheinland Group (Germany), Asia Inspection Ltd (Hong Kong), British Standards Institution (BSI) Group (United Kingdom), Centre Testing International (CTI) (China), Hohenstein Institute (Germany), SAI Global Ltd (Australia), TESTEX AG (Switzerland), and Eurofins Scientific (Luxembourg).

1.6.1 Conditioning and standard atmospheric conditions

The main peculiarity of textile testing is related to the hygroscopic behavior of most textile fibers. Their tendency to absorb moisture from the atmosphere if the relative humidity in the air is high or inversely give up moisture in a dry air environment affects the measure of their physical properties. For instance, cotton typically absorbs 8%–14% of moisture vapor, which produces an increase in weight and strength, and a change in a number of other properties (Iqbal et al., 2012). Conversely, silk can take up to 35% in moisture and sees a strong decrease in strength when its moisture content increases. Even polyester, which is hydrophobic, can gain up to 1% in weight due to moisture absorption.

As a result, standardized relative humidity and temperature conditions are used to ensure that meaningful and comparable results are obtained when testing textiles. These conditions are specified in the test method; they typically are $20 \pm 2°C$ and $65\% \pm 2\%$ RH for general-use textiles (CAN/CGSB 4.2 No. 2–M88, 2013) and $23 \pm 2°C$ and $50\% \pm 5\%$ RH for nonwovens (ASTM D1776, 2016). Specimens are conditioned prior to testing until they reach a constant weight. Testing is also conducted in the same controlled atmospheric conditions.

Some exceptions exist when the textile has to be tested in the conditions in which it was manufactured or retrieved. This is the case, for example, for geosynthetic clay liners (GCL). Samples collected in the manufacturing plant or at the installation site or exhumed from a project site after installation shall be immediately wrapped into at least two layers of plastic sheeting to limit changes in the GCL moisture content (ASTM D6072, 2009). The samples should then be transmitted to the testing laboratory using expedited delivery and tested rapidly. They should be unpacked immediately prior to testing and tested as received, i.e., without conditioning (ASTM D6768, 2004).

1.6.2 Laboratory equipment

A large variety of laboratory equipment exists for testing textiles. They may be grouped based on the type of properties and performance they give access to:

- Physical: Presser-foot apparatus equipped with a thickness gauge, analytical balance, etc.
- Morphology: Optical microscope, scanning electron microscope, porometer, dry sieving, wet sieving, bubble point tester, etc.
- Composition/chemical: Wet chemistry lab with fume hood, potentiometric titration device, Fourier transformed infrared spectroscope (FTIR), inductively coupled plasma atomic emission spectrometer (ICP-AES), gas chromatography-mass spectrometry (GC-MS), atomic absorption analysis (AAA), etc.
- Physicochemical: Contact angle analyzer, tensiometer, moisture management tester, tribometer, etc.
- Thermochemical: Differential scanning calorimeter (DSC), thermogravimetric analyzer (TGA), dynamic mechanical analyzer (DMA), thermomechanical analyzer (TMA), etc.
- Mechanical: Universal testing machine equipped with a controlled environment chamber, drop tower, Elmendorf tearing tester, bursting strength tester, etc.
- Biological: Incubator, water bath, spectrophotometer, luminescence photometer, etc.
- Thermal: Hot plate, gas burner, calorimeter, thermal manikin, etc.
- Flammability: Gas burner, fume hood, thermal protective performance (TPP) tester, instrumented flash fire manikin, etc.
- Barrier: Air permeameter, permeation cell, GC-MS, film permeability tester, water vapor transmission rate tester, oxygen gas transmission apparatus, man-in-simulant test chamber, hydrostatic pressure tester, Suter tester, UV spectrometer, etc.
- Hydraulic: Water flow apparatus, air flow apparatus, soil-geotextile permeameter, flexible wall permeameter, transmissivity test rig, etc.
- Comfort: Sweating guarded hotplate system, Kawabata testing suit, dexterity pegboard tester, etc.
- Visibility: Spectrophotometer, gray scales, light source, photoreceptor, etc.
- Durability: Oven, DSC, UV-accelerated weathering tester (xenon and fluorescent), abrasion tester (e.g., rotary, Taber, Martindale, Wyzenbeek), crock meter, pilling tester, washing/drying machine, spectrophotometer, immersion tank with temperature control, incubator, universal testing machine equipped with a controlled environment chamber, cyclic loading testing machine, etc.

The global textile testing equipment market is projected to grow to USD 102.17 million by 2021, at a CAGR of close to 2% between 2017 and 2021 (Technavio, 2017). This growth is fueled by the rise in the demand for technical textiles. The equipment may be designed for specific standard test methods as well as include specific accessories allowing performing tests according to specific standards. For instance, grips of different widths are used for tensile tests performed according to different test methods.

1.6.3 Laboratory information management systems

A laboratory information management system (LIMS) is a software that manages multiple aspects of laboratory informatics (LII, 2016): sample management; instrument and application integration; manual data entry; electronic laboratory notebook;

environment monitoring; data mining; data and trend analysis; automatic report creation; document management; electronic data exchange; audit management; QC/QA; customer relationship management; instrument calibration and maintenance; supplies inventory and equipment management; personal and workload management; time tracking; etc.

First developed in 1982, LIMS evolved from a single centralized minicomputer to become a dynamic enterprise resource planning tool (LII, 2016). It follows a sample along its five phases of processing by the laboratory:

- Receive sample and log information about sample and customer
- Assign and schedule tests on sample
- Perform tests with associated use of equipment and supplies
- Store data and analysis
- Inspect, approve, and compile sample data for reporting and/or further analysis

1.6.4 Laboratory accreditation

Laboratory accreditations recognize the technical competence of laboratories to perform specific tests, measurements, and calibrations (ILCA, 2001). It also allows customers to identify reliable testing, measurement, and calibration services that meet their needs. The accreditation process usually takes several days. It involves a thorough assessment of all the elements that contribute to the production of accurate and reliable test results. Laboratories may have all of their testing and calibration activities accredited or submit only specific ones for accreditation. Accredited laboratories are re-evaluated periodically by the accreditation body to ensure their continued compliance with requirements and verify that their standard of operation is maintained. Third-party testing is generally performed by an accredited laboratory.

Most testing laboratories seek accreditation under the international standard ISO/IEC 17025 (2005). It shares many aspects with the ISO 9000 standard. However, it applies directly to organizations that conduct testing and calibration operations. In addition, it is more specific in terms of requirements for competence to carry out tests and/or calibrations performed either using standard methods, nonstandard methods, or laboratory-developed methods. ISO/IEC 17025 includes two main sections: management requirements and technical requirements. The first section deals with the operation and effectiveness of the quality management system within the laboratory. The second section covers factors that determine the correctness and reliability of the tests and calibrations performed in the laboratory. Laboratories generally utilize ISO/IEC 17025 to implement a quality system in addition to using it as the basis for accreditation from an accreditation body. The International Laboratory Accreditation Cooperation (ILAC) includes over 90 accreditation bodies from more than 80 countries that deliver laboratory accreditations according to ISO/IEC 17025 (ILAC, 2017). This represents 52,000 accredited laboratories.

Other laboratory accreditation programs are encountered in the textile industry for product certification purposes. Some are regional; examples are the BNQ (Bureau de normalisation du Québec) in Quebec, Canada, and the European Union's CE mark-

ing. Other ones target specific application sectors, such as GAI-LAP (Geosynthetic Accreditation Institute-Laboratory Accreditation Program) for geosynthetics and BIFMA (Business and Institutional Furniture Manufacturers Association) for commercial furniture. There are also accreditation programs aimed at a specific purpose. One example is the OEKO-TEX Association, which targets environmentally friendly products and production sites in the textile and clothing industry.

1.7 Defective products

A defective product may be discovered by the manufacturer through quality control during production or at final inspection. It may also be identified as a result of a customer complaint. Defects may be visually apparent: for instance, a missed pick in a woven fabric, a ladder in a knit, or a barre (Ahmed, 2008). The product may also fail to meet the prescribed requirements in terms of properties and performance.

1.7.1 Detection

When a test performed on a raw, semifinished, or finished textile product does not yield the expected result, verification is first made that the problem is not due to the testing process itself: the specimen preparation, conditioning protocol, test conditions, data acquisition, data analysis, etc. For instance, specimens may slide in the grips during a tensile test, yielding a higher elongation at break. For verification purposes, the test may be performed a second time by the same laboratory or the sample sent to another laboratory.

If the problem with the textile product is detected by the product manufacturer, he may return the raw material to his supplier or ask the supplier for a rebate if the problem can be attributed to a defective input. However, market globalization makes product traceability along the value chain more difficult. If the problem is related to the manufacturer's process, he can try downgrading the defective product and sell it at a lower price. He may also have to discard the defective product, which could then be reintroduced upstream in the process, recycled, or landfilled depending on the situation.

If the problem is detected by the client, he may send the product back to the manufacturer if it has not been used yet and/or ask for a refund. Defective products may also be the source of disputes between the two (or more) parties involved, especially when the defective product has caused damage or harm. In these cases, which may end up in court, testing laboratories may be asked to provide an independent opinion. Once again, gaps in product traceability may add to the difficulties in establishing the responsibilities in the case settlement.

In all instances, it is critical that the defective product is identified as early as possible in the value chain because the associated financial impact increases at each step of the transformation process. For example, it has been estimated that defective fabrics lose 55%–65% of their value (Srinivasan, Dastor, Radhakrishnaihan, & Jayaraman, 1992).

1.7.2 Strategies for product improvements

When defects and problems in product properties and performance are detected, whether as a result of the manufacturer's own quality control program or following a complaint by a customer, it is essential that he takes the necessary actions to identify the exact cause(s) of the problem and set up solutions to avoid it reoccurring. This attitude is key to re-establishing and/or preserving the confidence of clients.

In addition, an in-depth defect analysis gives manufacturers the opportunity to improve their processes and increase the quality and performance of their products as well as their manufacturing efficiency. For that purpose, they may take advantage of the various tools available: for instance, process mapping, analysis, and control systems, and statistical quality control principles (Majumdar et al., 2012).

1.8 Future trends

The textile industry has already experienced two major phases of transformation that have had a large impact on testing: the Industrial Revolution in the period 1750–1850 and the development of synthetic/high performance fibers in the 20th century. New changes can be expected in the near future with the introduction of the next generation materials such as smart textiles and nanomaterials, a shift towards more environmentally friendly production processes, and changes in the procurement paradigm.

1.8.1 Next generation materials

New materials are entering the textile industry, bringing new functionalities and further increasing the level of performance. For instance, smart materials and wearable electronics allow textiles to become active and reactive. The previously lifeless textile product can provide active cooling and/or heating, adapt its breathability to environmental conditions, guide visually impaired people, allow integrated position location and communication, offer physiological monitoring, release active compounds and drugs at a controlled rate, monitor the structural health of composite structures, and harvest and transfer energy for example (Koncar, 2016). New test methods are required to characterize the specific characteristics of smart textiles—for instance, trigger threshold value, response delay, signal strength, and consumed power (Decaens, Vermeersch, Dolez, & Lachapelle, 2016). Durability, especially for connects, also needs to be assessed in an appropriate manner. In addition, testing should probe the eventual occurrence of unwanted side effects of these smart textiles—for example, the interference of conductive elements with dielectric performance.

Nanotechnology is another science that is finding its way into the textile industry, either through the use of nanofibers, the surface modification or coating of fibers and textile structures using nanomaterials, or the addition of nanofillers for the production of nanocomposite fibers and filaments (Brown & Stevens, 2007). Nanotechnology

offers great opportunities to improve the properties and performance of existing textile products and develop completely new functionalities. For instance, the tensile strength, thermal stability, thermal conductivity, and chemical resistance of polymer fibers can be improved with the dispersion of a small amount of carbon nanotubes in the matrix (Liu & Kumar, 2014); this can also make them become electrically conductive. As another example, growing zinc oxide nanorods on jute fibers followed by a fatty acid treatment provided the originally hydrophilic natural fibers with stable hydrophobic properties (Arfaoui, Dolez, Dubé, & David, 2017). If test methods may have to be adjusted to take into account the input of nanomaterials, the largest modification in product assessment will be related to the current level of uncertainty about the potential toxic effects of some nanomaterials on human health and the environment in the short and long term (Dolez, 2015).

1.8.2 Environmentally friendly production processes

A second driver of change in the textile industry and textile product testing is the shift towards more environmentally friendly manufacturing. This trend is fueled by new regulations aimed at better controlling the amount of chemicals used in textile processes and limiting those that are the most toxic. For instance, nonylphenol ethoxylates (NPEs), which are used as a cleaning, dyeing, and rinsing agent for textiles and a stabilizer for polymers, have been banned from use within its borders by the European Union for 20 years; they have now been voted by all EU member states to be excluded also from textile imports (Flynn, 2015). These changes are largely the result of the action of various lobby groups, for instance, the Ethical Fashion Forum (2015) and GreenPeace (2016); using mass-media campaigns, they raised the attention of the general public on the potential dangers on health and the environment of the use of certain chemicals and processes in the textile industry.

This trend has led to the creation of voluntary eco-textile certifications and labels: for instance OEKO-TEX (OEKO-TEX, 2017), GREENGUARD (Greenguard, 2016), and Bluesign (Bluesign, 2016); they aim at eliminating from textile products substances posing risks to people and the environment. In the case of natural fibers, the Global Organic Textile Standards sets up requirements for both ecology and labor conditions throughout the supply chain for textiles and apparel manufactured using organically produced raw materials (GOTS, 2016).

This new paradigm in textile manufacturing, which runs from fiber cultivation/production to product assembly, generates new needs in terms of testing. Among the 1900–2400 chemicals used in the textile industry, 165 have already been identified as carcinogenic, mutagenic, toxic to reproduction, allergenic, and/or with environmentally hazardous, long-term effects (KEMI, 2013). This includes heavy metals, volatile organic compounds, toxic dyes, pesticides, flame retardants, phthalates, nonylphenol ethoxylates, dioxins, and furans. As knowledge progresses, new chemicals will be added to the watch or exclusion list, while some others may find their way out of that list. In addition, as new processes and alternative chemical solutions are proposed for more eco-friendly textile products and processes, test methods will have to be adapted and/or developed to ensure that these improvements do not hide loopholes.

1.8.3 Trends in procurement

Goods and services purchases, including of textile products, have traditionally been based on the principle of the lowest conform bidder. This is even a rule for public procurement in a number of countries including Canada (PWGSC, 2013). However, deviations to this rule are increasingly observed, with other nontechnical aspects being taken into account.

For instance, the "green" trend already mentioned in Section 1.8.2 is also observed in procurement. Examples include the European Union green public procurement criteria for textile products and services, which defines ecological criteria for the award of the Community Ecolabel for textile products (EU GPP, 2011). Maximum concentration or emission values for a series of toxic substances are set for each type of fiber covered by the Ecolabel; criteria also deal with the type of process used and the biodegradability of released chemicals for instance. In Canada, a policy on green procurement was also established in 2006 (PSPC, 2016). By increasing the promotion of environmental sustainability and integrating environmental performance considerations in its procurement process, the Canadian federal government seeks to reduce the environmental impacts of its operations and foster environmental stewardship.

With a wider scope, sustainable procurement targets environmental, social, and ethical aspects in purchasing. Considerations in socially responsible procurement relevant to the textile industry include health and safety at work, the respect of international labor standards and quality of employment, the fight against illegal and child labor, and the ethical procurement of raw materials (Moschitz, Crippa, Defranceschi, & Ochoa Vidal, 2007). For instance, the Global Lead City Network for Sustainable Procurement brings together 14 cities worldwide committed to driving a transition to sustainable consumption and production through appropriate procurement strategies (GLCN, 2017). In Canada, the Municipal Collaboration for Sustainable Procurement network groups 20 Canadian municipalities, colleges, and universities wishing to share information, resources, and technical expertise in sustainable procurement (MCSP, 2017). However, if the cause is noble, its implementation is challenging due to the very long length of the value chain, which often extends across a number of countries, and the lack of product traceability.

1.9 Sources of further information and advice

Relevant standardization committees may be consulted for further information:

- ISO/TC 38: textiles (www.iso.org/committee/48148.html)
- ISO/TC 20: Aircraft and space vehicles (www.iso.org/committee/46484.html)
- ISO/TC 22: Road vehicles (www.iso.org/committee/46706.html)
- ISO/TC 31: Tires, rims, and valves (www.iso.org/committee/47670.html)
- ISO/TC 41: Pulleys and belts, including veebelts (www.iso.org/committee/48410.html)
- ISO/TC 72: Textile machinery and accessories (www.iso.org/committee/49924.html)
- ISO/TC 94: Personal safety - Protective clothing and equipment (www.iso.org/committee/50580.html)

- ISO/TC 136: Furniture (www.iso.org/committee/52448.html)
- ISO/TC 194: Biological and clinical evaluation of medical devices (www.iso.org/committee/54508.html)
- ISO/TC 216: Footwear (www.iso.org/committee/54972.html)
- ISO/TC 219: Floor coverings (www.iso.org/committee/54988.html)
- ISO/TC 221: Geosynthetics (www.iso.org/committee/270590.html)

References

Ahmed, A. (2008). *A catalogue of visual textile defects*. Word Press.

Anonymous. (2014). Practices and importance of testing and analysis of textiles. *Textile Today*, April 1, 2014. http://www.textiletoday.com.bd (Accessed 12 April 2017).

Arfaoui, M. A., Dolez, P. I., Dubé, M., & David, É. (2017). Development and characterization of a hydrophobic treatment for jute fibres based on zinc oxide nanoparticles and a fatty acid. *Applied Surface Science*, *397*, 19–29.

ASTM D1776. (2016). *Standard practice for conditioning and testing textiles*. West Conshohocken, PA: ASTM International.

ASTM D6072/D6072M. (2009). *Standard practice for obtaining samples of geosynthetic clay liners*. West Conshohocken, PA: ASTM International.

ASTM D6768/D6768M. (2004). *Standard test method for tensile strength of geosynthetic clay liners*. West Conshohocken, PA: ASTM International.

Bluesign. (2016). Bluesign® technologies. www.bluesign.com (Accessed 22 October 2016).

Brown, P. & Stevens, K. (Eds.), (2007). *Nanofibers and nanotechnology in textiles*. Cambridge, UK: Woodhead Publishing.

CAN/CGSB 4.2 No. 2–M88. (2013). *Textile test methods conditioning textile materials for testing*. Ottawa, Canada: Canadian General Standards Board.

CEN/TC 248. (2017). CEN/TC 248—Textiles and textile products. European Committee for Standardization. https://standards.cen.eu (Accessed 16 April 2017).

Decaens, J., Vermeersch, O., Dolez, P. I., & Lachapelle, D. (2016). *Development of test methods for smart textiles*. In: *Workshop on smart textiles*. Chicago, IL: ASTM International. June 26.

Dolez, P. (Ed.), (2015). *Nano engineering: Global approaches to health & safety issues*. Amsterdam, Netherlands: Elsevier.

EHER, (2017). Global sector report—Textile. Euler Hermes Economic Research. http://www.eulerhermes.com (Accessed 20 April 2017).

Eichhorn, S. J., Hearle, J. W. S., Jaffe, M., & Kikutani, T. (2009). *Handbook of textile fibre structure Natural, regenerated, inorganic and specialist fibres* (Vol. 2). Cambridge, UK: Woodhead Publishing.

Ethical Fashion Forum. (2015). *10 toxic chemicals to avoid in youber products*. The Ethical Fashion Forum. http://source.ethicalfashionforum.com/article/10-toxic-chemicals-to-avoid-in-your-products (Accessed 20 April 2017).

EU. (2017). *Nando (New approach notified and designated organisations) information system*. European Commission. ec.europa.eu/growth/tools-databases/nando/.

EU GPP. (2011). Green public procurement—textiles: Technical background report. European Commission, DG Environment.

Flynn, V. (2015). EU countries agree textile chemical ban. *The Guardian*, Tuesday 21 July 2015.

GLCN. (2017). The Global Lead City Network on Sustainable Procurement. http://www.glcn-on-sp.org/home/ (Accessed 20 April 2017).

GOTS. (2016). Global organic textile standard—Ecology & social responsibility. http://www.global-standard.org/about-us.html (Accessed 20 April 2017).

Greenguard. (2016). *GREENGUARD certification from UL environment*. GREENGUARD. greenguard.org (Accessed 22 October 2016).

GreenPeace. (2016). *You did it! Toxic chemical banned in EU textile imports*. GreenPeace International. http://www.greenpeace.org/international/en/news/Blogs/makingwaves/NPEtoxicchemicalbannedEUtextile/blog/53582/ (Accessed 14 August 2016).

Grover, E. B., & Hamby, D. S. (1960). *Handbook of textile testing and quality control*. New York, NY: Textile Book Publishers. [Interscience].

Hearle, J. (2002). *Creativity in the textile industries: A Story from pre-history to the 21st Century*. Manchester, UK: The Textile Institute.

Hearle, J. W. S. (Ed.), (2001). *High-Performance Fibres*. Cambridge, UK: Woodhead Publishing.

Horrocks, A. R., & Anand, S. C. (Eds.), (2000). *Handbook of technical textiles*. Cambridge, UK: Woodhead Publishing.

IBISWorld. (2016a). Laboratory testing services in Canada. Market research report. IBISWorld.

IBISWorld. (2016b). Laboratory testing services in the US. Market research report. IBISWorld.

ILAC. (2017). *About ILAC*. http://ilac.org/about-ilac/ [Accessed 19 April 2017].

ILCA. (2001). *Why become an accredited laboratory?* International Laboratory Accreditation Cooperation. http://www.cala.ca/ilac_why_become_accred_lab.pdf (Accessed 17 April 2017).

Iqbal, M., Sohail, M., Ahmed, A., Ahmed, K., Moiz, A., & Ahmed, K. (2012). Textile environmental conditioning: Effect of relative humidity variation on the tensile properties of different fabrics. *Journal of Analytical Sciences, Methods and Instrumentation*, *2*, 92–97.

ISO. (2017). *Consumers and standards: Partnership for a better world*. International Organization for Standardization. www.iso.org/sites/ConsumersStandards/index.html (Accessed 16 April 2017).

ISO/IEC 17025. (2005). *General requirements for the competence of testing and calibration laboratories*. Geneva, Switzerland: International Organization for Standardization.

ISO/TC 38. (2017). *ISO/TC 38: Textiles*. International Organization for Standardization. https://www.iso.org/committee/48148.html (Accessed 16 April 2017).

Jenkins, D. (Ed.), (2003). *The Cambridge history of western textiles*. Cambridge, UK: Cambridge University Press.

KEMI. (2013). Hazardous chemicals in textiles—Report of a government assignment. Swedish Chemicals Agency, 114 p.

Koncar, V. (Ed.), (2016). *Smart textiles and their applications* (1st ed.). Duxford, UK: Woodhead Publishing.

Kozłowski, R. (Ed.), (2012). *Types, properties and factors affecting breeding and cultivation*: Vol. 1. Handbook of natural fibres. Cambridge, UK: Woodhead Publishing.

LII. (2016). *The complete guide to LIMS & laboratory informatics*. Atlanta, GA: Laboratory Informatics Institute, Inc.

Liu, Y., & Kumar, S. (2014). Polymer/carbon nanotube nano composite fibers—A review. *ACS Applied Materials & Interfaces*, *6*(9), 6069–6087.

M&M. (2015a). *Technical textile market by product (fabric, unspun fiber, yarn-type products), technology (nonwoven, fabric, weaving, knitting, spinning), fiber (synthetic, natural, specialty), application (mobiltech, indutech, sportech, others), colorant (dye, pigment), fabric—Global forecast to 2020*. Maharashtra, India: MarketsandMarkets Research Private Ltd.

M&M. (2015b). *Textile testing, inspection and certification (TIC) market by application (textile testing, textile inspection, textile certification, & toys), and geography—Global forecast to 2020*. Maharashtra, India: MarketsandMarkets Research Private Ltd.

Majumdar, A., Das, A., Alagirusamy, R., & Kothari, V. K. (Eds.), (2012). *Process control in textile manufacturing*. Cambridge, UK: Woodhead Publishing.

McIntyre, J. E. (Ed.), (2004). *Synthetic fibres: Nylon, polyester, acrylic, polyolefin*. Cambridge, UK: Woodhead Publishing.

MCSP. (2017). *Municipal collaboration for sustainable procurement*. http://mcspgroup.com/portal/ (Accessed 20 April 2017).

Moschitz, S., Crippa, F., Defranceschi, P., & Ochoa Vidal, A. (2007). *RESPIRO guide on socially responsible procurement of textiles and clothing*. Brussels, Belgium: EUROCITIES.

OEKO-TEX. (2017). *OEKO-TEX® association*. www.oeko-tex.com (Accessed 16 April 2017).

Ohlemiller, T. J., Villa, K. M., Braun, E., Eberhardt, K. R., Harris, R. H., Jr., Lawson, J. R., & Gann, R. G. (1993). Test methods for quantifying the propensity of cigarettes to ignite soft furnishings. *NIST special publication 851-2*. Gaithersburg, MD: National Institute of Standards and Technology.

PSPC. (2016). *Policy on green procurement. Public services and procurement Canada*. http://www.tpsgc-pwgsc.gc.ca/ecologisation-greening/achats-procurement/politique-policy-eng.html (Accessed 20 April 2017).

PWGSC. (2013). *National goods and services procurement strategy—Clothing and textiles*. Public Works and Government Services Canada.

SCC. (2017). *Directory of accredited product, process and service certification bodies*. Standards Council of Canada. www.scc.ca/en/accreditation/product-process-and-service-certification/directory-of-accredited-clients.

Srinivasan, K., Dastor, P. H., Radhakrishnaihan, P., & Jayaraman, S. (1992). FDAS: A knowledge-based frame detection work for analysis of defects in woven textile structures. *Journal of the Textile Institute*, *83*, 431–447.

Technavio. (2017). *Global textile testing equipment market driven by rising demand for technical textiles*. London, UK: Infiniti Research Limited.

This page intentionally left blank

Part Two

Testing by properties

This page intentionally left blank

Advanced strength testing of textiles

2

D.C. Adolphe, P.I. Dolez*†

*University of Haute-Alsace, ENSISA, Mulhouse, France †CTT Group, Saint-Hyacinthe, QC, Canada

2.1 Introduction

Since the very beginning of the textile industry, textile products have been tested to evaluate their mechanical properties. Because of the specificity of textile materials (including possible variations depending on whether natural or synthetic fibers are used as raw material), standards have rapidly been developed to guide manufacturers in characterizing materials in a consistent manner.

In this chapter, international standard test methods will be presented whenever they exist; however, in some cases, no international standard is available. In those cases, methods generally used in the industry will be introduced instead.

In complement to the standardized or typically used methods, some prerequirements are assumed:

- All the tests are done in standardized conditions regulated by the ISO standard 139/A1 (2011): 20°C—65% RH.
- Sampling must follow the requirements of either the ad hoc standards or recommended methods, depending on the raw material.
- The data can be reported individually, but the more common usage is to present the data with the mean value[1] associated with the standard deviation (or CV%)[2].

In this chapter, different test methods are presented, some of which have been specifically developed for textile materials. These are associated with specific mechanical properties of textile products. In other instances, standards relative to textile products (garments) or nonwovens (geotextiles) are described.

2.2 Mechanical behavior of textiles

In terms of mechanical properties, textile products can generally be considered viscoplastic and ductile materials. However, different behaviors can be observed at the fiber, yarn, and fabric scale, and will also depend upon whether the fabric is woven, knitted, or nonwoven.

[1] The formula of the mean value is the following: $\bar{M} = \frac{\sum_{i=1}^{N} x_i}{N}$.

[2] The formula of the standard deviation is: $\sigma = \frac{\sum_{i=1}^{N} \sqrt{\left(\bar{M} - x_i\right)^2}}{N}$.

Advanced Characterization and Testing of Textiles. https://doi.org/10.1016/B978-0-08-100453-1.00003-9

Classical shapes of the stress-strain curve of different types of fibers are displayed in Fig. 2.1 (NPTEL, 2012a). It can be observed that that shape is strongly material-dependent.

At the yarn level, the stress-strain curve usually displays a S Shape as shown in Fig. 2.2 (NPTEL, 2012b); the slope OA corresponds to the Young modulus, and C is the yield point.

In the case of fabrics, different behaviors can be observed. Woven and knitted fabrics are generally orthotropic, that is to say, they present two orthogonal preferential directions (warp/weft or row/column). Therefore, their mechanical behavior can be very different depending on the direction of loading as shown in Fig. 2.3.

In the case of knitted fabrics, the same difference between row and column loading can be observed. However, the strain values usually are much higher; they can reach more than 400%, depending on the tested knitted fabric.

For nonwoven materials, two different behaviors can be observed (Adolphe, 2001): if the structure is blocked (e.g., with thermally bonded nonwovens), the stress strain curve presents the shape displayed in Fig. 2.4A; if the structure is loose (e.g., with needle-punched nonwovens), the curve shape is displayed in Fig. 2.4B. The difference in the shape is linked to structural reorganization, which occurs upon loading with loose structure; the fibers/filaments are reorganized during the tensile test, and a negative contraction phenomenon appears.

2.3 Textile elasticity

The determination of the elasticity of textiles is covered by the standard NF EN 14704-1 (2005). The test can be performed on a strip or a loop. For a strip, the specimen dimensions are the following: $(50 \pm 1.0) \times (250–300)\,\text{mm}^2$. For a loop, the specimen

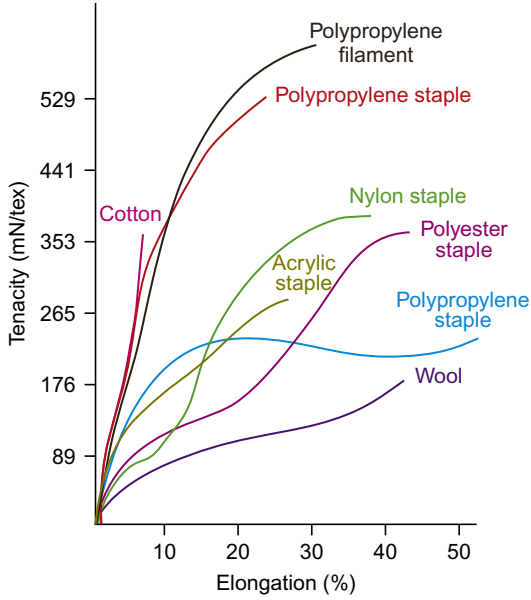

Fig. 2.1 Typical stress-strain curves for different types of fibers.
Reproduced from NPTEL. (2012a). Textile fibers. http://nptel.ac.in/courses/116102026/20.

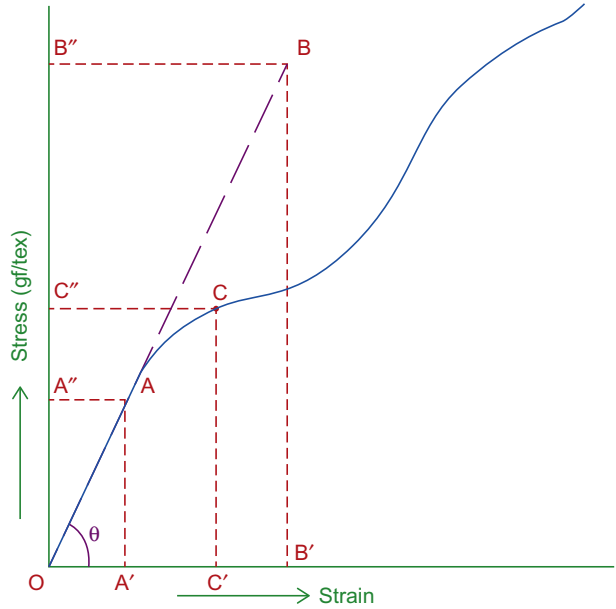

Fig. 2.2 Typical stress-strain curve of yarns.
Reproduced from NPTEL. (2012b). Textile testing. http://nptel.ac.in/courses/116102029/40.

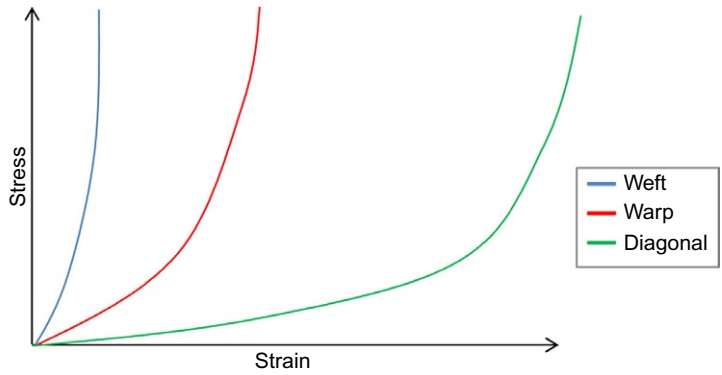

Fig. 2.3 Example of stress-strain curves for a woven fabric loaded in the weft, warp, and diagonal direction.
Based on Hedley, G.A., The Effect of Beeswax/Resin Impregnation on the Tensile Properties of Canvas, ICOM Committee for Conservation, 4th Triennial Meeting, Venice, Italia, 1975.

dimensions are $(75 \pm 1.0) \times (250 \pm 1)\,\text{mm}^2$. To form the loop, a 301-type stitch line is performed at 25 mm of each strip end with a density of 3.5 (±0.5) stitches/cm. Five specimens per direction are measured. The strip dimensions do not depend on the type of material (woven, nonwoven, or knitted fabrics) tested. For the strip test, the distance between the clamps is 200 mm for wovens and nonwovens, and 100 mm for knitted fabrics. This distance is adjusted to have a 200-mm loop in total for the loop test.

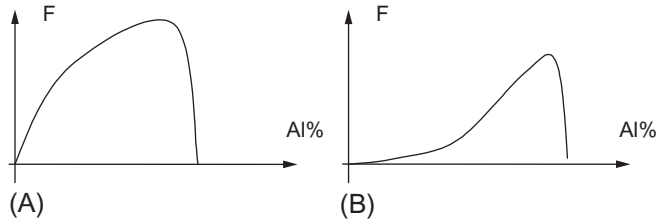

Fig. 2.4 (A) Stress-strain curve for a blocked structure. (B) Stress-strain curve for loose structure.
Courtesy Adolphe, D. C. (September 2001) Nonwoven lecture—ENSISA.

The measurement principle is that a fabric specimen of the required dimensions is extended at a constant rate to either a specified force or elongation for an agreed number of cycles. Specimen elasticity is calculated by measuring certain parameters.

The rate of extension and retraction of the specimen is fixed. It is equal to 100 mm/min for woven and nonwoven fabrics and 500 mm/min for knitted fabrics. The cycling limits are set at the gauge length and at a load of 6 N/cm of width for the woven and nonwoven fabrics. For knitted fabrics, the cycle can use a maximum load based on Table 2.1 or a fixed elongation (50%, 70%, 80%, or 100%).

Fig. 2.5 shows a typical cycling curve. Based on these curves, the following parameters can be extracted: maximum elongation, force decay due to time, force decay due to exercise (fatigue), unrecovered elongation, recovered elongation, and elastic recovery.

2.4 Tensile and multiaxial tensile strength

Because ISO standards are available for tensile tests on fabrics, they are presented here. In these standards, tests are carried out until the specimen ruptures. In addition, other mechanical characterization methods exist, such as the one developed by Kawabata & Niwa (1989) where the tests are carried out under low stress. For these tests the maximum load does not lead to the rupture of the specimen, but corresponds to a value which is representative of typical use conditions. In this case, both the loading and release behaviors are examined and considered in the analysis.

Table 2.1 Cycling loads according to NF EN 14704-1 (2005)

		Loading/cm of specimen width	
Weft knit	**Warp knit**	**Strip**	**Loop**
≤5% elastane	≤5% elastane	3 N	6 N
>5% but <12% elastane	>5% but < 12% elastane	4 N	8 N
	12% to 20% elastane	5 N	10 N
	>20% elastane	7 N	14 N

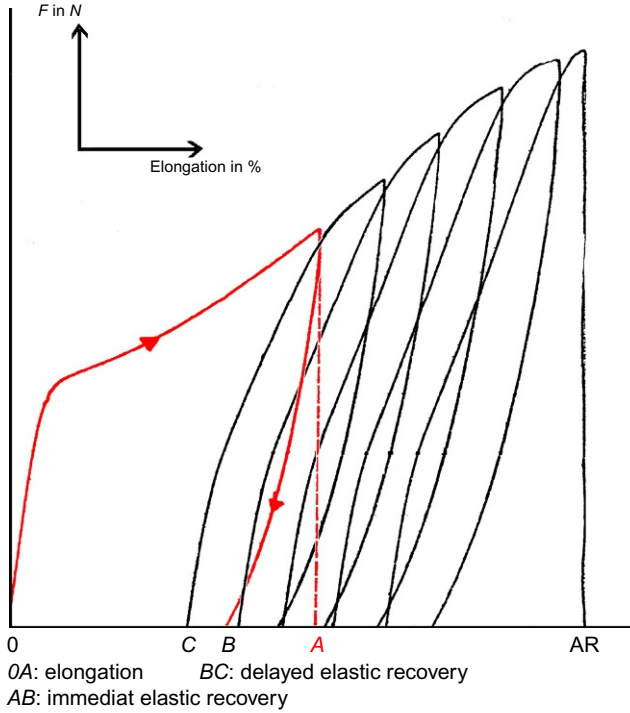

Fig. 2.5 Typical cycling curve.

2.4.1 Standard tensile test methods for fibres

ISO 5079 (1995) describes testing conditions in tension for individual fibers. The tensile test may also be conducted on fiber bundles. Two methods are available: the Pressley tensile tester (Fig. 2.6) that provides the breakage force of the bundle, and the Stelometer (Fig. 2.7) that provides the breakage force and the breakage elongation of the fiber bundle.

In the case of the Pressley tensile test, two options are offered: joined clamps or separated clamps (1/8 in.). The bundle is loaded at the constant rate. The force is increased up to bundle breakage. The result is called the "Pressley Index," expressed as (PI) in (lbs/mg). Usually, measurements conducted with separated clamps provide lower values than those done with joined clamps.

With the Stelometer (Fig. 2.7), two types of clamps are also proposed (ISO 3060, 1974). With the joined clamps, it is possible to have access to the tensile failure value while with the 1/8 in. separated clamps, the test provides the force and the elongation at failure. The Stelometer applies a constant stress rate (1 kgf/s) all along the test.

In the case of technical fibers, the standard ISO 11566 (1996) on the tensile properties of carbon fibers has been developed to characterize carbon filaments. This test method provides the sample size and speed/time to rupture. It also suggests a special handling protocol in order to avoid a filament breakage problem.

Fig. 2.6 Pressley fiber tensile tester.
Photo from TTF University of Zagreb.

Fig. 2.7 Stelometer.
Courtesy MB Trade Corporation.

2.4.2 Standard tensile test methods for yarns

ISO 2062 (2009) may be used to characterize the tensile properties of yarns. The standard provides the test conditions: the specimen length is 500 mm, the pretension is 0.5 cN + 0.1 cN per tex, and the time to rupture is 20 ± 3 s.

To carry out this test, preliminary measurements have to be performed in order to characterize the yarn count used for the pretension determination and some preliminary tests are carried out in order to adjust the rupture time to 20 ± 3 s.

2.4.3 Standard tensile test methods for fabrics

Tensile tests for fabrics are governed by two international standards: NF EN ISO 13934-1 (2013) and NF EN ISO 13934-2 (2014). The first one is performed on a fabric strip, while the second one corresponds to the grab test.

For the strip test, the specimen dimensions are the following: $(50 \pm 1.0) \times (250–300)\ mm^2$. The gauge length should be 200 mm. In the case of stretchable fabrics (with an elongation larger than 75%), this gauge length may be reduced to 100 mm; the specimen size is thus reduced to $(50 \pm 1.0) \times (150–200)\ mm^2$. The rate of elongation depends on the elongation at maximum force of the fabric as mentioned in Table 2.2.

The specimen can be installed with or without pretension; in the former case, the following rules apply:

- For stretchable fabrics, the pretension is equal to 0.5 N.
- For nonstretchable fabrics, the pretension is computed based on the mass per unit area as shown in Table 2.3.

Fig. 2.8 presents the typical force-elongation curve. The results can be considered valid if the rupture does not occur within 5 mm of the clamping line of the jaws. Otherwise, the result is recorded as a jaw break.

Based on the data obtained, the following parameters can be extracted: maximum force, force at rupture, elongation at maximum force, and elongation at rupture. The slope at the very beginning of the force-elongation curve gives the value of the Young modulus of the material.

Table 2.2 Rate of extension or elongation (NF EN ISO 13934-1, 2013)

Gauge length (mm)	Elongation at maximum force of the fabric (%)	Rate of elongation (%/min)	Rate of extension (mm/min)
200	<8	10	20
200	8–75	50	100
100	>75	100	100

Table 2.3 Pretension as a function of the mass per unit area of the fabric

Mass per unit area	≤200 g/m²	>200–500 g/m²	>500 g/m²
Pretension	2 N	5 N	10 N

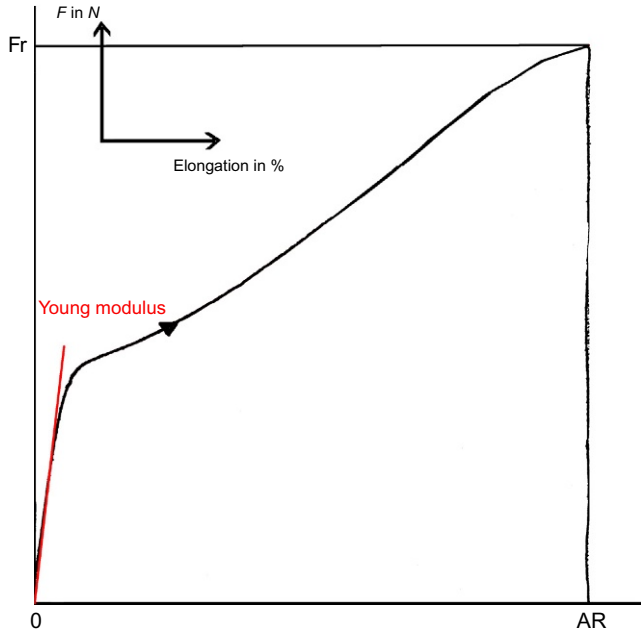

Fig. 2.8 Typical force-elongation curve.

The standard EN ISO 13934-2 (2014) deals with another tensile test, the grab test. This test is mainly dedicated to woven fabrics; it must be performed on a constant-rate-of-extension machine.

Contrary to the strip test, the clamping area ($(25 \pm 1) \times (25 \pm 1)\,mm^2$) is smaller than the specimen width, which is 100 ± 2 mm. The specimen length must be sufficient to allow a gauge length of 100 mm. A minimum of 5 specimens per direction are tested. No pretension is applied when the sample is secured in the clamps. The rate of extension is fixed at 50 mm/min. This test method provides the maximum force.

2.4.4 Low stress tensile characterization

As mentioned in the introduction, the Kawabata method allows a low-stress characterization of textiles. The specimen size is $200 \times 200\,mm^2$. It is subjected to a maximum load of 500 cN/cm of specimen width. The load is then released. The velocity of the mobile clamp is 12 mm/min. The loading and unloading behaviors are analyzed. The device developed for this measurement is the Kawabata Evaluation System—for Fabric 1 (KES-FB1 module, Fig. 2.9).

A typical curve is displayed on Fig. 2.10. The following parameters can be extracted from the data: linearity of the load-extension curve, tensile energy, tensile resilience, extensibility, and strain at 500 cN/cm.

Fig. 2.9 KES-FB1-tension tester.
Courtesy Dominique C. Adolphe.

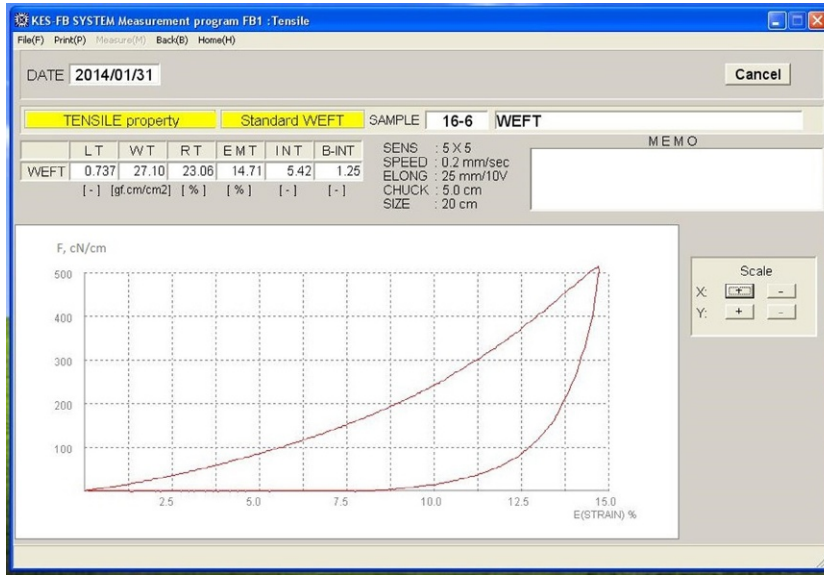

Fig. 2.10 Typical KES tensile curve.
Courtesy V. Kuzmichev.

2.5 Compression

2.5.1 Thickness measurement

This first apparatus is not intended to measure the compressibility of fabrics but their thickness under pressure. Fig. 2.11 presents an example of such a device. The measurement can be carried out following the NF EN ISO 5084 (1996) standard.

The size of the specimen surface used for the test is (2000 ± 20) mm^2, which corresponds to a pressure foot diameter of 50.5 ± 20 mm. The pressure applied for performing the measurement is 1 kPa. The measure is taken 1 min after the pressure has been applied. The parameter extracted from the measurement is T, the thickness of the fabric under 1 kPa pressure.

It is also possible to access the compression behavior of a fabric using this apparatus. In that case, measurement is carried out using different values of the applied pressure ranging between 0 and 1 kPa. The recorded thickness vs applied pressure curve is computed and analyzed.

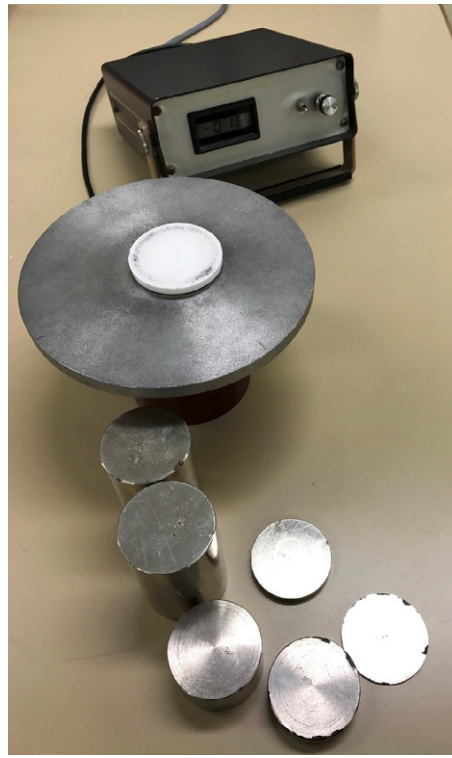

Fig. 2.11 Sodemat thickness measurement apparatus.
Courtesy Dominique C. Adolphe.

2.5.2 Kawabata compression measurement device

The compression behavior of fabrics may also be characterized using the Kawabata Evaluation System-FB3 (Fig. 2.12). This device measures the thickness of the fabric, but it also gives some information about the compression behavior of the specimen. The principle of the measurement is simple: a finger pushes on the fabric until a reaching a specific pressure value, then releases.

The surface of the pressure finger is 2 cm^2. The maximum applied pressure is 5 kPa. The displacement rate of the pressure finger is 1.2 mm/min.

Fig. 2.13 provides an example of the typical compression curve obtained with the KES-FB3 Compression tester. Five parameters are generally computed: T_0, the thickness at 0.5 cN/cm^2, T_m, the thickness at 5 kPa, the fabric compressibility, the energy of compression, the linearity of the compression, and the compression resilience of the fabric.

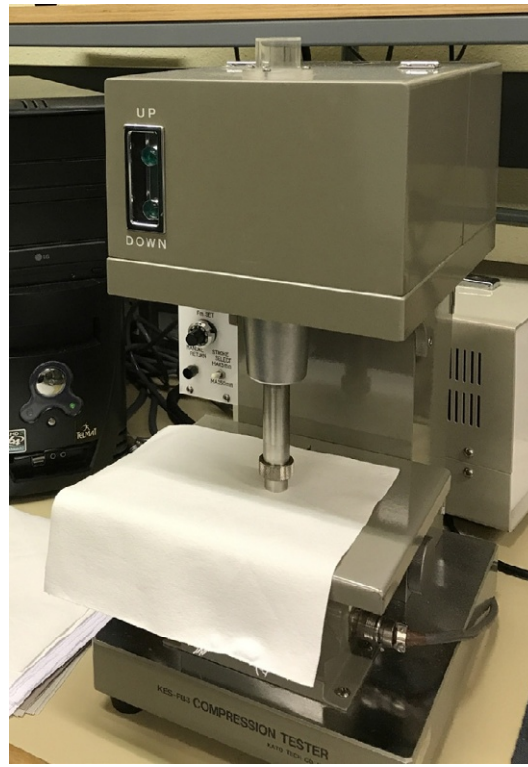

Fig. 2.12 KES-FB3 compression tester.
Courtesy Dominique C. Adolphe.

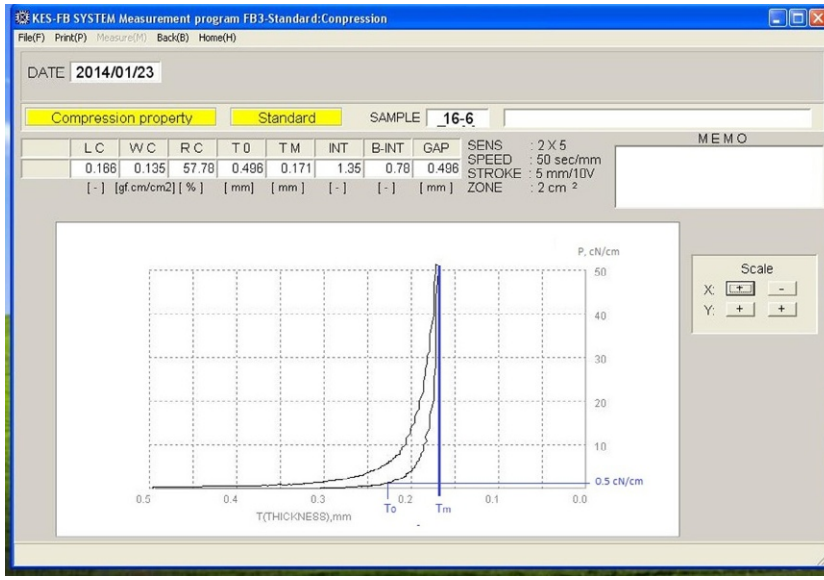

Fig. 2.13 Typical compression curve.
Courtesy V. Kuzmichev.

2.6 Burst strength

A textile could be submitted to multidirectional stresses during its use. Therefore, some special test methods have been developed to simulate these conditions.

Two different techniques may be used to characterize the burst strength of textiles: hydraulic and pneumatic. They can be applied to knitted, woven, nonwoven, and laminated fabrics. They may also be suitable for fabrics produced by other techniques. These tests may be performed on specimens either conditioned or in the wet state.

2.6.1 Hydraulic method

The principle of this test is defined in the standard NF EN ISO 13938-1 (1999). A test specimen is clamped over an expandable diaphragm by means of a circular clamping ring (Fig. 2.14). An increasing fluid pressure is applied to the underside of the diaphragm, causing the distension of both the diaphragm and the fabric. The volume of fluid is increased at a constant rate until the test specimen bursts. The bursting strength and bursting distension are determined.

The dimension of the testing area is generally 50 mm^2, but other sizes can be contemplated depending on the measurement device used (100, 10, or 7.3 cm^2). A constant rate of increase in liquid volume is selected between 100 and 500 cm^3/min depending on the test area and fabric requirements. If it is not possible to apply a constant volume increase rate, test conditions should be adjusted so that the time to burst is (20 ± 5) s.

Fig. 2.14 MTS burst tester.
Courtesy Dominique C. Adolphe.

The parameters extracted from this test are the following: the bursting pressure (kPa), height at burst (mm), and/or bursting volume (cm^3). The specimen bursting pressure is obtained by applying a correction for the diaphragm burst pressure, which is the pressure needed to deform the diaphragm up to burst without any fabric.

2.6.2 Pneumatic method

The second burst test method based on a pneumatic technique is described in the standard NF EN ISO 13938-2 (1999). In that case, compressed air is used to apply pressure on the membrane instead of oil. The standard NF EN ISO 13938-2 mentions that, based on the data available, there appears to be no significant difference in the bursting strength results for pressures up to 800 kPa when hydraulic or pneumatic burst testers are used.

With the pneumatic method, the dimension of the testing area is also equal to 50 mm^2, but other sizes can be envisioned depending on the measurement device used (100, 10, or 7.3 cm^2).

The parameters extracted from this test are the following: the bursting pressure (kPa), height at burst (mm), and/or bursting volume (cm^3). As with the hydraulic test method, the diaphragm burst pressure must be determined in order to correct the result of the measurement performed with the specimen.

2.7 Shear properties

No standard test method is available for textile shear. However, a well-known technique uses the Kawabata evaluation system KES-FB1 (Fig. 2.15).

In this technique, the fabric is submitted to an in-plane shear stress as shown in Fig. 2.16. The specimen size is $200 \times 200\,mm^2$. The gauge area is $200 \times 50\,mm^2$. The speed of the mobile clamp is 12 mm/min. The shear amplitude goes from −8 to +8 degrees.

Fig. 2.17 displays a typical curve provided by a shear test performed with the KES device. Based on the data, the following parameters can be obtained: the shear rigidity (G) and the value of the hysteresis at 0.5 degrees (2HG) and 5 degrees (2HG5).

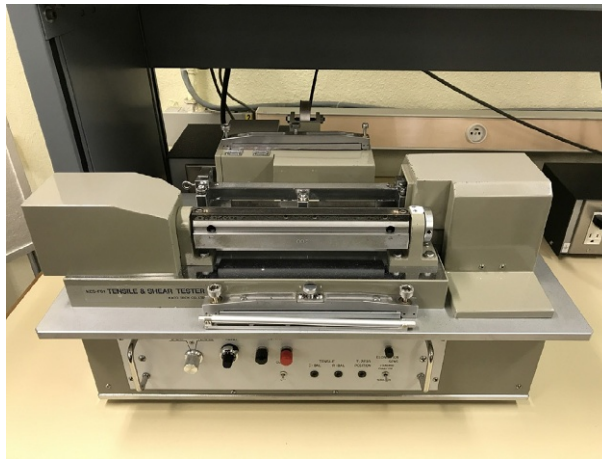

Fig. 2.15 KES-FB1-shear tester.
Courtesy Dominique C. Adolphe.

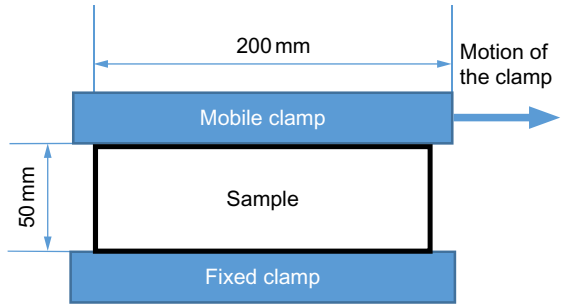

Fig. 2.16 Shear test principle.
Courtesy Dominique C. Adolphe.

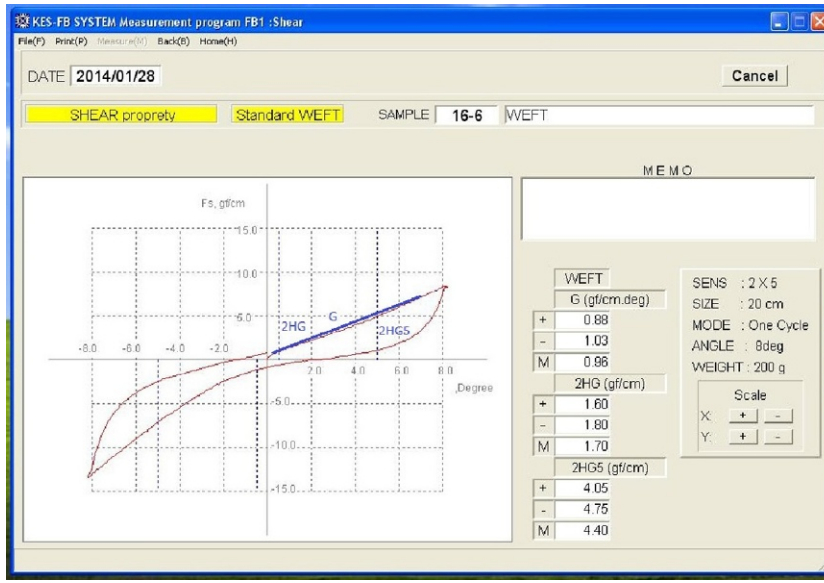

Fig. 2.17 Typical shear curve.
Courtesy V. Kuzmichev.

2.8 Flexion properties

Depending on the type of textile, different methods can be used to characterize textile bending properties. For instance, the test method described in the standard NF EN ISO 9073-7 (1998) is dedicated to nonwovens. However, it can be used for other types of textiles.

2.8.1 Bending length measurement

The device described in the standard NF EN ISO 9073-7 (1998) allows the measurement of the bending length. The standard also provides an equation to calculate the bending rigidity.

The principle of the measurement is the following: a rectangular strip of fabric is supported on a horizontal platform with the long axis of the strip parallel to the long axis of the platform (Fig. 2.18). The strip is moved in the direction of its length so that an increasing part of the specimen overhangs the platform and bends down under its own weight. The overhang is free at one end. It is maintained on the other end by a ruler applying a pressure on the part of the test piece still on the platform.

The overhanging length is determined when the leading edge of the test piece reaches a plane passing through the edge of the platform and inclined at an angle of 41.5 degrees below the horizontal. The bending length C is equal to half the overhanging length. The specimen size is $(25 \pm 1) \times (250 \pm 1)\,\text{mm}^2$. The recommended number of specimens tested is 6.

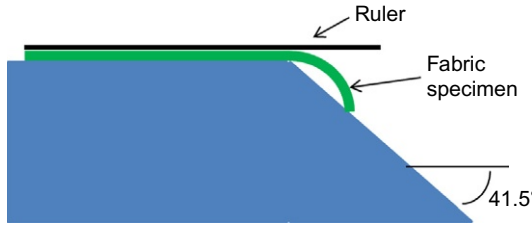

Fig. 2.18 Bending length measurement set-up.
Based on NF EN ISO 9073-7. (1998). Textiles. Test methods for nonwovens. Part 7: Determination of bending length.

In addition, the bending rigidity G can be computed using the following equation:

$$G = m \times C^3 \times 10^{-3}$$

with m being the mass of the test piece per unit area (g/m^2). This equation has been obtained by approximating the acceleration due to gravity g by 10 m/s^2 instead of 9.81 m/s^2.

2.8.2 Bending rigidity measurement

Kawabata has also developed a pure bending measurement device. Thanks to this device, it is possible to measure the bending rigidity of the textile material. The principle of this measurement is the following: the sample is folded at a constant rate of curvature, and the angular bending moment is recorded as a function of the specimen curvature angle.

Fig. 2.19 presents the KES-FB2 device. For this device, the sample size is 200×200 mm^2 and the gauge area is 200×10 mm^2.

Fig. 2.20 shows a typical curve provided by this test. Two parameters are computed from the data: the bending rigidity (B) and the hysteresis (2HB).

2.9 Puncture resistance

Several methods are proposed to characterize the puncture resistance of fabrics. For instance, standard test methods have been developed for geosynthetics but could be applied to other types of textiles. In addition to the different test methods described below, the ISO 13996 (1999) standard test method can be used for the evaluation of the puncture resistance of protective garments. Even if the relevance of the probe dimension to real puncture hazards may be questionable, this standard is used and recognized in the protective clothing industry.

2.9.1 Cone drop test

The standard NF EN ISO 13433 (2007) proposes the following test method: "The specimen is clamped horizontally between two steel rings. A stainless-steel cone is

Fig. 2.19 KES-FB2-bending measurement.
Courtesy Dominique C. Adolphe.

dropped, point first, from a distance of 500 mm onto the center of the specimen. The degree of penetration is measured by inserting a narrow-angle, graduated cone into the hole." A schematic representation of the proposed device is shown in Fig. 2.21.

The cone is made of stainless steel with a tip angle of 45 degrees and a mass of (1000 ± 5) g. The penetration depth is assessed using a measuring cone. This cone is graduated and has a mass of (600 ± 5) g.

The standard recommends using five samples per measurement. The sample size must be suitable with the dimension of the clamping device. The resistance to cone puncture is reported in terms of hole diameter.

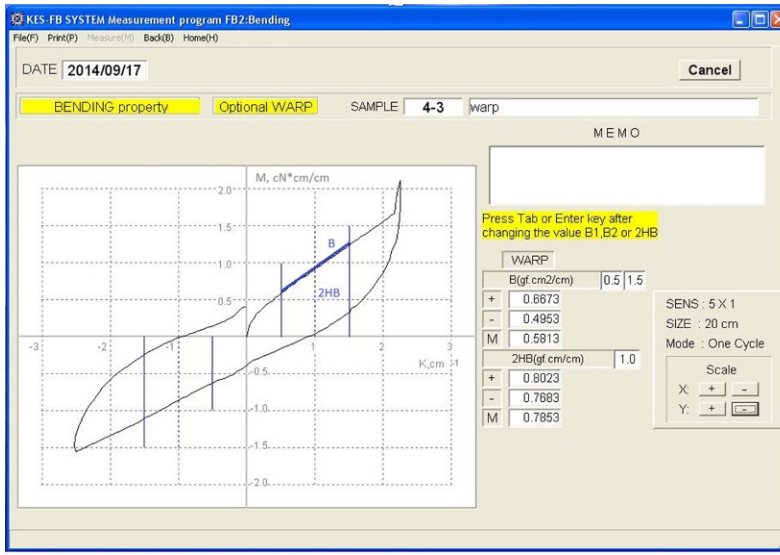

Fig. 2.20 Typical bending curve using the KES-FB2 device.
Courtesy V. Kuzmichev.

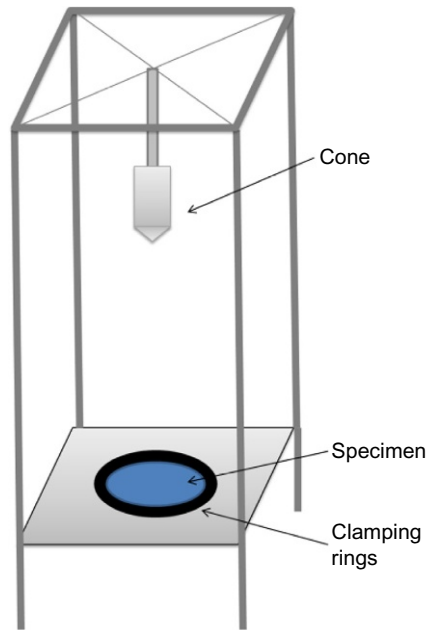

Fig. 2.21 Dynamic cone drop test.
Based on NF EN ISO 13433: 2007. Geosynthetics—Dynamic perforation test (cone drop test).

2.9.2 Pyramid puncture resistance

The standard NF EN 14574 (2015) proposes another test for the measurement of the puncture resistance of materials. It is also dedicated to geosynthetics. The principle of this measurement is illustrated in Fig. 2.22. A test specimen lies flat on an aluminum plate supported by a steel base. The whole assembly is secured in a testing machine set in compression mode. A force is exerted on the center of the test specimen by an inverted steel pyramid attached to the moving beam of the test frame. The perforation of the specimen is recorded when an electrical contact occurs between the pyramid indenter and the aluminum plate below the specimen.

The recorded push-through load is representative of the protection efficiency of the materials against puncture. The standard recommends testing at least 10 specimens of $100 \times 100\,\text{mm}^2$ dimension. The tensile machine speed must be constant at (1.0 ± 0.1) mm/min. The parameter provided by this method is the "push-through load" in N.

2.9.3 CBR test

The standard NF EN ISO 12236 (2006) proposes the following test method: "The specimen is clamped between two steel rings. A plunger is advanced at a constant rate on the center of the specimen and perpendicularly to it. The push-through force, push-through displacement, and force-displacement curve are recorded."

For this method, different accessories are required: a plunger which is a stainless-steel cylinder with a diameter of (50 ± 5) mm and a (2.5 ± 0.2) mm radius on the leading edge. The clamping system has an internal diameter of (150 ± 0.5) mm. A schematic representation of the set-up is displayed in Fig. 2.23.

The method recommends testing 5 specimens. The specimen dimension must be suitable with the dimension of the clamping device. The displacement rate of the plunger is fixed at (50 ± 5) mm/min. A preload of 20 N is used.

Fig. 2.24 shows a typical force-displacement curve. The following parameters can be extracted from the data: F_p, the push-through force and $h_{p,}$ the push-through displacement.

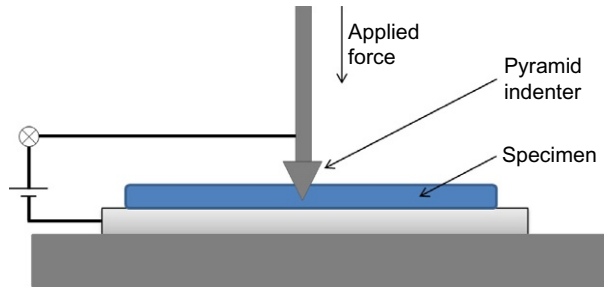

Fig. 2.22 Pyramid puncture set-up.
Based on NF EN 14574: 2015. Geosynthetics—Determination of the pyramid puncture resistance of supported geosynthetics.

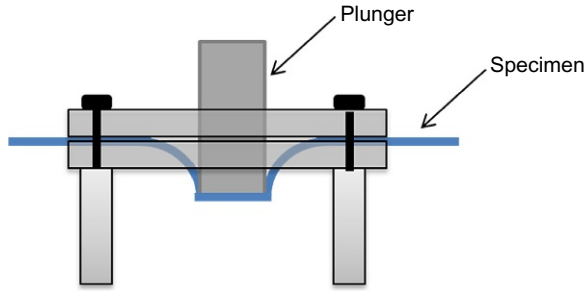

Fig. 2.23 Test set-up for the CBR test.
Based on NF EN ISO 12236: 2006. Geosynthetics—Static puncture test (CBR test).

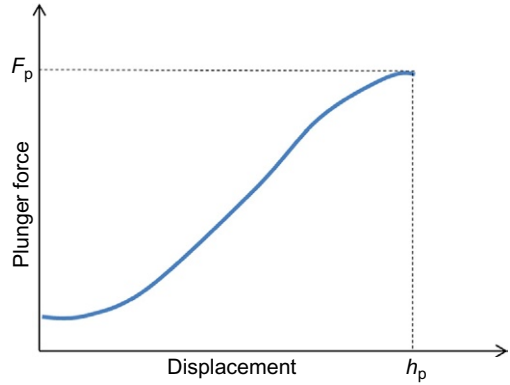

Fig. 2.24 Typical curve of plunger force versus displacement.
Based on NF EN ISO 12236: 2006. Geosynthetics—Static puncture test (CBR test).

2.10 Tear resistance measurement

ISO proposes four different characterization methods for the tear resistance of textiles.

2.10.1 Ballistic pendulum method (Elmendorf)

The tear properties of fabrics may be measured using the ballistic pendulum method (Elmendorf) according to NF EN ISO 13937-1 (2000). The principle of this method is explained in the standard: "The force required to continue a slit previously cut in a fabric is determined by measuring the work done in tearing the fabric through a fixed distance. The apparatus consists of a pendulum carrying a clamp, which is in alignment with a fixed clamp when the pendulum is in the raised, starting position with maximum potential energy. The specimen is fastened in the clamps, and the tear is started by cutting a slit in the specimen between the clamps. The pendulum is then released, and the specimen is torn completely as the moving jaw moves away from the fixed one. The tear force is measured."

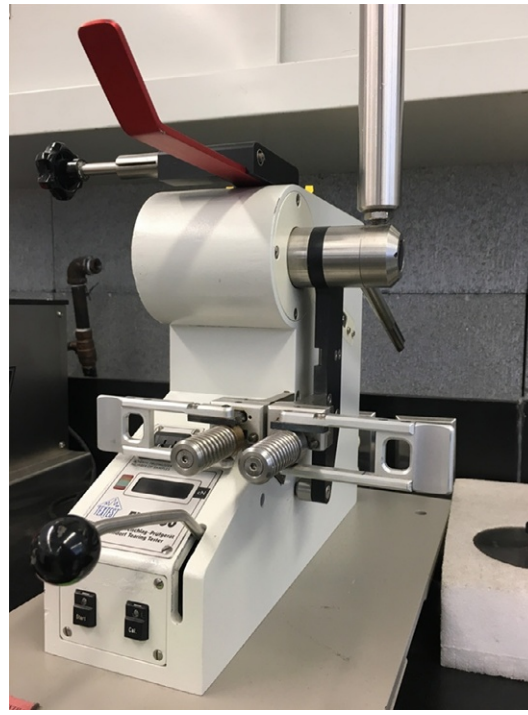

Fig. 2.25 Elmendorf pendulum testing machine.
Courtesy CTT Group, QC, Canada.

For this method, a pendulum testing machine (Fig. 2.25) is required. This machine is equipped with two jaws: one is fixed and the other is swinging. A sharp knife is situated between the two jaws to begin the tear of the test specimen by cutting a slit of 20 ± 0.5 mm.

The standard recommends testing at least five specimens per direction. The specimen size and shape are displayed in Fig. 2.26. The parameter provided by this measurement is the tear force, in newtons.

2.10.2 Single tear method with trouser-shaped test specimens

The determination of the tear properties of fabrics may also be conducted using trouser-shaped test specimens (NF EN ISO 13937-2, 2000). According to this test method, a slit is initially precut in the middle of a specimen strip along its length as shown in Fig. 2.27. The specimen is placed in a tensile machine that pulls on its two legs (Fig. 2.28). The test continues until the tearing reaches a location set as the end of the test as shown in Figs. 2.27 and 2.28.

The specimen dimensions are usually $(200 \pm 2) \times (50 \pm 1)\,\text{mm}^2$. But the test can also be performed on wide width trouser specimens; in that case, the specimen dimensions are $(200 \pm 2) \times (200 \pm 2)\,\text{mm}^2$. The other specimen dimensions are left unchanged. The gauge length is adjusted to 100 mm, and the rate of elongation is fixed at 100 mm/min.

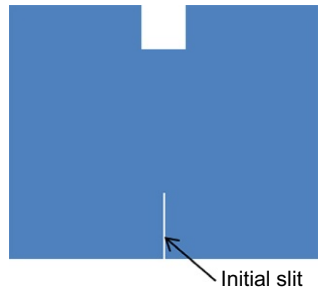

Fig. 2.26 Pendulum testing specimen.
Based on NF EN ISO 13937-1: 2000. Textiles—Tear properties of fabrics—Part 1: Determination of tear force using ballistic pendulum method (Elmendorf).

Fig. 2.27 Trouser-shaped test specimen.
Based on NF EN ISO 13937-2: 2000. Textiles—Tear properties of fabrics—Part 2: Determination of tear force of trouser-shaped test specimens (Single tear method).

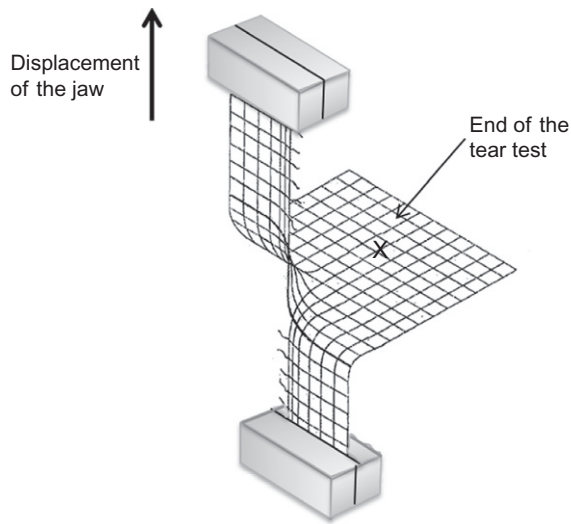

Fig. 2.28 Single tear test with a trouser-shaped test specimen.
Based on NF EN ISO 13937-2: 2000. Textiles—Tear properties of fabrics—Part 2: Determination of tear force of trouser-shaped test specimens (Single tear method).

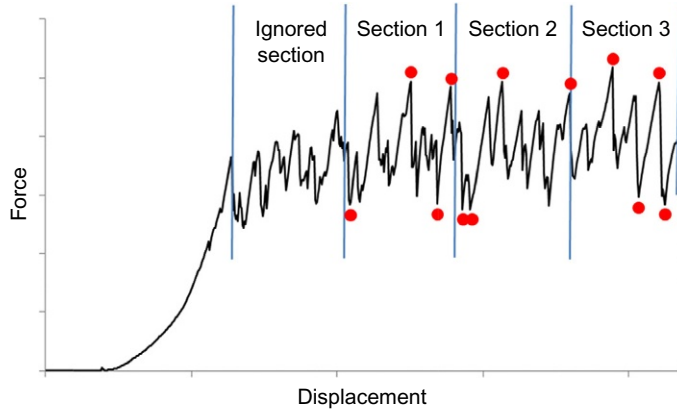

Fig. 2.29 Tear test force-displacement trace for a trouser-shaped elastomer-coated cotton knit specimen.

For tear force calculation, the peak trace is divided into four equal parts, beginning with the first peak and ending with the last peak (see Fig. 2.29). The first part shall not be used for the calculation of the mean value. From each of the three remaining subsections, the two highest and the two lowest peaks are located and recorded. A peak suitable for calculation is characterized by a 10% minimum rise and drop of the force.

2.10.3 Single tear method with wing-shaped test specimens

According to NF EN ISO 13937-3 (2000), "a specifically shaped test specimen cut to form two wings on one side is mechanically stressed so that the stress is concentrated at a cut to cause tearing in the desired direction. The wings of the specimen are clamped inclined to the direction of the threads to be torn. The force necessary to continue the tear over a specified length of tear is recorded. The tear force is calculated from force peaks of the autographic trace, or on-line by electronic means." As in the previous test method, a tensile machine is required to perform this test. Fig. 2.30 shows the shape and dimensions of the test specimen. The sample is installed in the tensile machine without any pretension as displayed in Fig. 2.31. The dimension

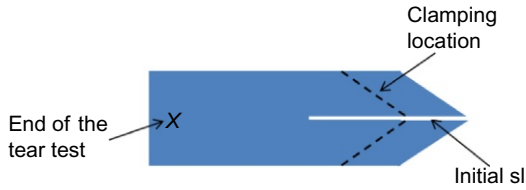

Fig. 2.30 Wing-shaped test specimen.
Based on NF EN ISO 13937-3: 2000. Textiles—Tear properties of fabrics—Part 3: Determination of tear force of wing-shaped test specimens (Single tear method).

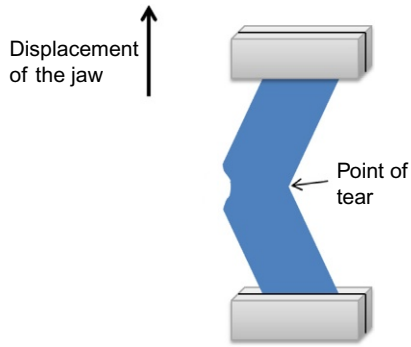

Fig. 2.31 Tear test using a wing-shaped specimen.
Based on NF EN ISO 13937-3. (2000). Textiles—Tear properties of fabrics—Part 3: Determination of tear force of wing-shaped test specimens (Single tear method).

of the test specimen is $(200 \pm 2) \times (100 \pm 1)\,mm^2$. The gauge length is set to 100 mm. The rate of extension is adjusted to 100 mm/min.

The shape of the "tear peak trace" for this test is similar to that for the previous test, and the calculation of the mean tear force value is done in the same manner.

In the case of a manual calculation, the mean tear force value is determined using the 12 peaks identified on the last three sections of the tear peak trace. The value of the force is expressed in newtons. In the case of an electronic evaluation, the mean value is calculated using all the peaks in the last three sections of the tear peak trace.

2.10.4 Double tear test

According to the standard NF EN ISO 13937-4 (2000), "Two parallel slits, connected by a slit at right angles to form a tongue are cut in a rectangular test specimen. The tongue is inserted in one jaw of a recording tensile-testing machine and the remaining part of the test specimen is clamped symmetrically in the other jaw to ensure both cuts each form straight parallel lines. A pulling force is applied in the direction of the cuts to simulate two parallel tears. The force to continue both tears over a specified length of tear is recorded. The tear force is calculated from the force peaks of the autographic trace, or on-line by electronics means." Fig. 2.32 shows the shape of the corresponding specimen.

The specimen is secured in a tensile machine without any pretension as displayed in Fig. 2.33. The dimensions of the test specimen are $(200 \pm 2) \times (200 \pm 2)\,mm^2$. The gauge length is set to 100 mm. The rate of extension is adjusted to 100 mm/min.

The shape of the "tear peak trace" for this test is similar to that for the test of the standard NF EN ISO 13937-2 (2000), and the calculation of the value is done in the same manner.

In the case of a manual calculation, the mean tear force value is calculated using the 12 peaks identified on the last three sections of the tear peak trace. The value of the force is expressed in newtons. In the case of an electronic evaluation, the mean value is calculated using all the peaks of the last three sections of the tear peak trace.

Fig. 2.32 Shape of the double tear tongue-shaped test specimen.
Based on NF EN ISO 13937-4: 2000. Textiles—Tear properties of fabrics—Part 4: Determination of tear force of tongue-shaped test specimens (Double tear test).

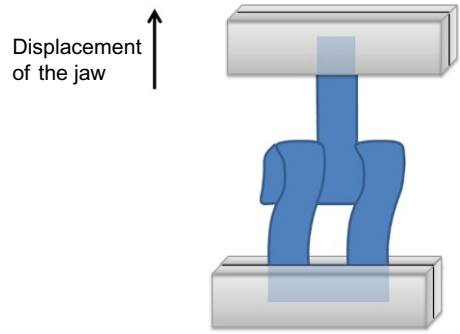

Fig. 2.33 Double tear test.
Based on NF EN ISO 13937-4: 2000. Textiles—Tear properties of fabrics—Part 4: Determination of tear force of tongue-shaped test specimens (Double tear test).

2.11 Cut resistance

Different tests, including EN and ISO standards, have been developed to assess the resistance to cutting of different types of materials. Here, only the tests dedicated to fabrics are presented.

2.11.1 Slicing-type cut by sharp objects

The standard NF EN ISO 13997 (1999) has been developed to characterize the resistance of protective clothing to slicing by sharp objects. The standard defines the test as follows: "The cut resistance of a material is its ability to resist being cut through by a blade. This is measured in a machine in which a sharp blade is drawn across a specimen. The cuts are achieved in blade movements of 3–50 mm length when a range of forces are applied to the blade normal to the specimen surface. The cut resistance of a sample material is expressed as the cutting force that is required to be applied to

a blade of standard sharpness to just cut through the material in a 20-mm blade stroke. The value of the cutting force may be used to classify materials."

Any apparatus that can maintain a constant force between the cutting edge and the specimen, and can accurately measure the distance the blade travels to cut through the specimen can be used to conduct the test. As an example, the standard proposes the device presented in Fig. 2.34.

For this measurement, the blades are crucial; the standard provides indications on how to assess the quality of these blades. The device will provide the cutting stoke length for an applied normal force value between 1 and 200 N. The sample dimensions are at least $(110 \times 32)\,mm^2$. The rate of displacement between the blade and the specimen holder is (2.5 ± 5) mm/min.

The test is repeated with different forces until at least 15 readings have been obtained with cutting stroke lengths distributed between 5 and 50 mm. Five readings should be obtained in each of the following cutting stroke length ranges: 5–15, 15–30, and 30–50 mm. The force corresponding to a 20-mm blade stroke is determined with a curve fit of the data points.

The NF EN ISO 13997 (1999) standard provides some cutting force values for typical protective clothing materials (Table 2.4).

2.11.2 Impact cut by hand knives

The NF EN 1082-3 (2000) standard describes an impact cut test for fabric, leather, and other materials used in gloves and arm guards simulating cuts and stabs by hand knives. The principle of the measurement is described in the standard as follows: "The leather

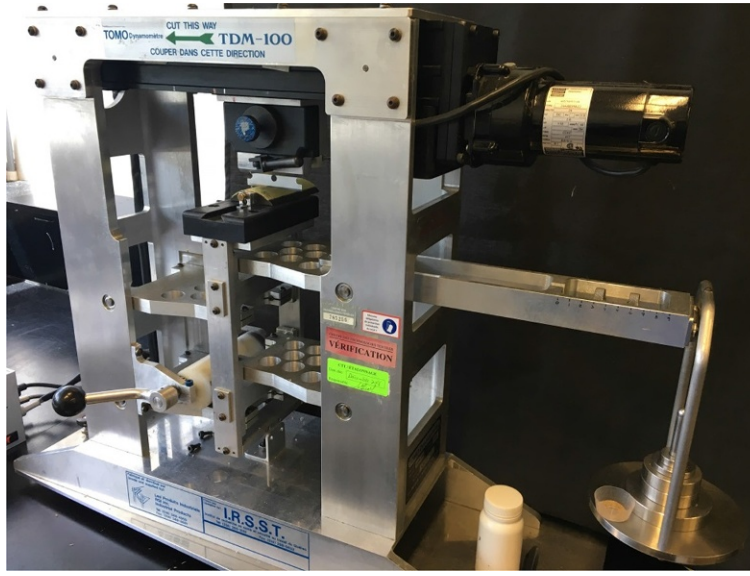

Fig. 2.34 TDM proposed for cutting resistance measurement.
Courtesy CTT Group, QC, Canada.

Table 2.4 Typical cutting force for protective clothing materials (NF EN ISO 13997, 1999)

Material	Mass per unit area (g/m^2)	Cutting force (N)	Application
Cotton	545	5.9	Work gloves
Latex	469	1.0	Surgical gloves
p-Aramid	688	11	Industrial gloves
Leather	754	2.3	Work gloves
Reinforced HMWPE[a]	581	20.8	Food-handling gloves
Reinforced HMWPE[a]	853	31.9	Food-handling gloves
Vinyl	590	3.5	Protective clothing liquid
p-Aramid	1900	38.7	Multilayer protective apron

[a] *HMWPE*, high molecular weight polyethylene.

or fabric gloves or materials are tested by impacts of standard knife blades held in a guided falling block."

The components of a possible test apparatus design are shown in Fig. 2.35. The device must allow measuring the velocity of the blade to an accuracy of ±0.05 m/s.

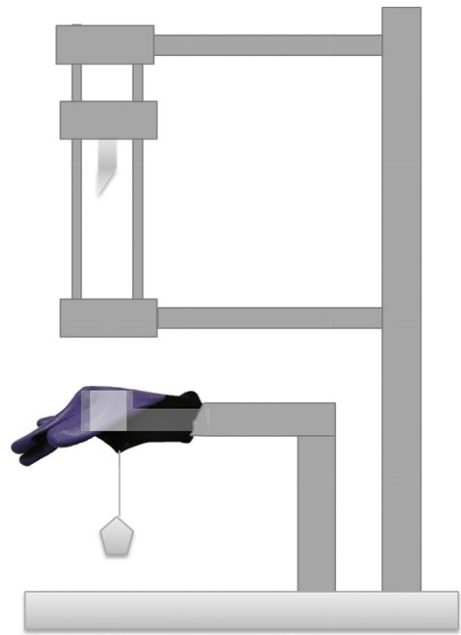

Fig. 2.35 Schematic representation of a testing device for impact cutting resistance. Based on NF EN 1082-3: 2000. Protective clothing—Gloves and arm guards protecting against cuts and stabs by hand knives—Part 3: Impact cut test for fabric, leather and other materials.

The size of the specimen must be adapted to the testing device. Flat materials are sewn or weld into a tube shape. This tube shall have a circular diameter of (100 ± 20) mm. A tension of 10 N has to be applied on the specimen.

The mass of the knife-holding block and knife shall be measured to an accuracy of ±0.5 g. The impact energy the knife tip would make on the specimen is calculated. Then, the height of the electromagnet is adjusted so that the mean impact energy of ten test drops is within 5% of the specified energy. The standard mentions that the impact energy generally used is 0.65 J and is provided by a drop from a height of 600 mm.

The parameter generated by this measurement is the relative cut penetration. It is calculated on the basis of penetration in a reference fabric. For the NF EN 1082-3 (2000) standard, the reference fabric is a cotton canvas defined in the standard EN 388 (2004).

The NF EN 1082-3 (2000) standard provides some typical penetration values for conventional glove and arm guard materials when tested with a 11-g block and 0.65 J as the impact energy (Table 2.5).

2.12 Impact resistance

No ISO standard is available to characterize the impact resistance of textile materials by themselves. However, some methods have been developed for garments aimed at specific applications such as horse riding and motorcycling and are described here.

2.12.1 Protective jackets, body and shoulder protectors for equestrian use

In the paragraph 5.8 of the standard NF EN 13158 (2009) on protective clothing for horse riders, horse drivers, and those working with horses, a test method is proposed to characterize the protection to impact offered by the garments. The testing device is made of hammers that are adjusted in order to fall down at ±2 mm of the center of the anvil (Fig. 2.36). The impact energy is controlled by additional weights affixed to the hammer.

Table 2.5 Values of impact cutting penetration for glove and arm guard materials when tested with a 11-g block and 0.65 J as the impact energy (NF EN 1082-3, 2000)

Materials	Penetration (mm)
Ceramic and polyethylene plain knit	24.3
Steel, aramid, and polyethylene plain knit	16.0
Terry loop knot aramid	23.8
Ceramic and polyethylene plain knit in a work glove	6.9
Glove with thin metal plates	3.6
Chain mail	4.8

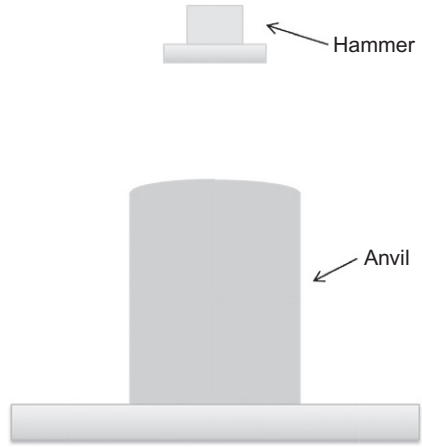

Fig. 2.36 Impact test device for equestrian protective clothing.
Based on NF EN 13158: 2009. Protective clothing—Protective jackets, body and shoulder protectors for equestrian use: For horse riders and those working with horses, and for horse drivers—Requirements and test methods.

The anvil is directly mounted on a force sensor. The whole system is secured to a concrete block with a minimum weight of 1000 kg. A continuous recording system is used in order to easily determine the force peak.

Different sizes and shapes of flat hammer and curved anvil are proposed in the standard to fit with the part of the garment to be tested. The proposed hammers have the following shapes and dimensions: circular shape (80 ± 2 mm diameter), and rectangular shape ($(80 \pm 2) \times (20 \pm 1)$ mm^2). All the anvils proposed have a (100 ± 2)-mm diameter. But they display different levels of curvature on the upper face (contact face). This curvature could go from 150 ± 5 mm to 50 ± 1 mm. Six specimens are tested. The parameter provided by this test is the peak force value. This standard is currently under revision.

2.12.2 Motorcyclists' back protectors

In the NF EN 1621-2 (2014) standard, the resistance of motorcyclists' back protectors to mechanical impact is tested using a bar impactor and an anvil (Fig. 2.37). The measurement is performed with a high-speed transducer. The sensor sensitivity should range from 1 to 70 kN.

2.13 Abrasion resistance

The standard NF EN ISO 12947-1 (1999) may be used to measure the abrasion resistance of textiles using a Martindale abrasion testing apparatus. The principle of this measurement is the following: “The Martindale abrasion tester subjects a circular specimen to a defined load and rubs it against an abrasive medium (i.e., standard

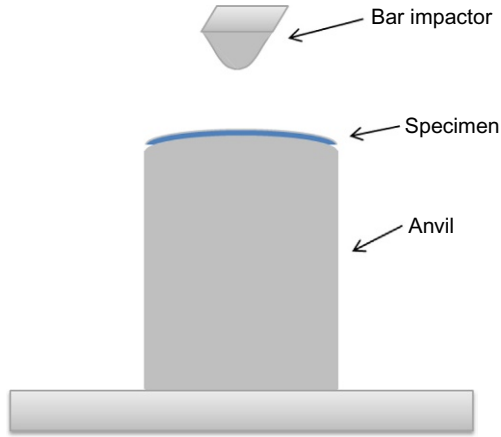

Fig. 2.37 Impact characterization device for motorcyclists' back protectors.
Based on NF EN 1621-2. (2014). Motorcyclists' protective clothing against mechanical impact—Part 2: Motorcyclists' back protectors—Requirements and test methods.

fabric) in a translational movement trancing a Lissajous figure. The specimen holder, containing either specimen or abrasive medium depending on which method is being used, is additionally freely rotatable around its own axis perpendicular to the horizontal plane. The specimen is subjected to abrasive wear for a predetermined number of rubs. The number of abrasion rubs making up the inspection interval depends upon the product type and method of assessment." (NF EN ISO 12947-1, 1999).

Fig. 2.38 shows different types of Martindale abrasion testers. The specimen surface area in contact with the abrader has a diameter of (38.1 ± 0.05) mm. Two loading pieces are available to perform the test: a large piece allows applying a nominal pressure of 12 kPa, and a small loading piece provides a nominal pressure of 9 kPa. The diameter of the abrading platform is (136 ± 0.5) mm. The rotational frequency of the outer drive unit is $(44.5 \pm 2.5)\,\text{mm}^{-1}$.

The main parameter that is generated by the test is the number of rotations the fabric can bear before it breaks down (NF EN ISO 12947-2, 2017). The end-point criteria for the test depend on the type of fabric tested (Table 2.6). Additional parameters may

Fig. 2.38 Martindale abrasion testers.
Courtesy VVC.

Table 2.6 Specimen breakdown criteria (NF EN ISO 12947-2, 2017)

Type of fabric	Breakdown point (end-point)	
	"Thread breakage" criterion	"Worn off area" criterion
Woven fabric (without pile)	Two threads completely broken	NA
Knitted fabric (without pile)	One thread completely broken	NA
Pile fabric		
Cut pile woven fabric Cut pile knitted fabric	One thread completely broken (knitted fabric)	
Fabric made with chenille yarns Uncut pile fabric	Two threads completely broken (woven fabric)	or fully worn-off area
Raised fabric	One thread completely broken (knitted fabric) Two threads completely broken (woven fabric)	NA
Flocked fabric	NA	Fully worn-off area
Nonwoven fabric	Hole in the fabric	

be obtained with this test, such as the loss of mass (NF EN ISO 12947-3, 1999) and the change in the aspect (NF EN ISO 12947-4, 1999).

2.14 Future trends

The different test methods presented in this chapter are a nonexhaustive list of what have been developed to assess the mechanical behavior of textiles. Several other methods, not standardized, can be used to characterize the textile complex elements as well as for comparison purposes.

In addition, some of the standards presented in this chapter are currently under revision; they might be changed in the near future.

Finally, large efforts must be put forward for developing new test methods (for instance, for electronic textiles). The availability of test methods and their standardizations is crucial for the development of new, innovative textiles (for example smart textiles, or fabrics with special properties).

2.15 Conclusion

All the tests and standards presented in this chapter have been mainly developed to respond to characterization needs and allow the comparison of performance results among the worldwide textile community. These standards are especially critical in the textile sector because of the large diversity of textile characteristics.

Some new standards might appear in a near future as a result of the improvement and innovation in textile functionalization.

2.16 Sources of further information and advice

More information about existing standards and standards under revision may be obtained from standardization committees dedicated to textiles, such as ISO/TC 38/SC 23 on fibers and yarns, and CEN/TC 248 on textiles and textile products.

References

Adolphe, D. C. (September 2001). *Nonwoven lecture—ENSISA*.
EN 388. (2004). *Protective gloves against mechanical risks*.
ISO 2062. (2009). *Textiles—Yarns from packages—Determination of single-end breaking force and elongation at break using constant rate of extension (CRE)*.
ISO 3060. (1974). *Textiles—Cotton fibers—Determination of breaking tenacity of flat bundles*.
ISO 5079. (1995). *Textile fibers—Determination of breaking force and elongation at break of individual fibers*.
ISO 11566. (1996). *Tensile properties of carbon fibre*.
ISO 13996. (1999). *Protective clothing—Mechanical properties—Determination of resistance to puncture*.
Kawabata, S., & Niwa, M. (1989). Fabric performance in clothing and clothing manufacture. *The Journal of Textile Institute*, *80*(1), 19–50.
NF EN 1082-3. (2000). *Protective clothing—Gloves and arm guards protecting against cuts and stabs by hand knives—Part 3: Impact cut test for fabric, leather and other materials*.
NF EN 1621-2. (2014). *Motorcyclists' protective clothing against mechanical impact—Part 2: Motorcyclists' back protectors—Requirements and test methods.*
NF EN 13158. (2009). *Protective clothing—Protective jackets, body and shoulder protectors for equestrian use: For horse riders and those working with horses, and for horse drivers—Requirements and test methods*.
NF EN 14574. (2015). *Geosynthetics—Determination of the pyramid puncture resistance of supported geosynthetics*.
NF EN 14704-1. (2005). *Determination of the elasticity of fabrics—Part 1: Strip tests—AFNOR*.
NF EN ISO 139/A1. (2011). *Textiles. Standard atmospheres for conditioning and testing*.
NF EN ISO 5084. (1996). *Textiles. Determination of thickness of textiles and textile products*.
NF EN ISO 9073-7. (1998). *Textiles. Test methods for nonwovens. Part 7: Determination of bending length*.
NF EN ISO 12236. (2006). *Geosynthetics—Static puncture test (CBR test)*.
NF EN ISO 12947-1. (1999). *Textiles—Determination of the abrasion resistance of fabrics by the Martindale method—Part 1: Martindale abrasion testing apparatus*.
NF EN ISO 12947-2. (2017). *Textiles—Determination of the abrasion resistance of fabrics by the Martindale method—Part 2: Determination of specimen breakdown*.
NF EN ISO 12947-3. (1999). *Textiles—Determination of the abrasion resistance of fabrics by the Martindale method—Part 3: Determination of mass loss*.

NF EN ISO 12947-4. (1999). *Textiles—Determination of the abrasion resistance of fabrics by the Martindale method—Part 4: Assessment of appearance change*.
NF EN ISO 13433. (2007). *Geosynthetics—Dynamic perforation test (cone drop test)*.
NF EN ISO 13934-1. (2013). *Textiles—Tensile properties of fabrics—Part 1: Determination of maximum force and elongation at maximum force using the strip method*.
NF EN ISO 13934-2. (2014). *Textiles—Tensile properties of fabrics—Part 2: Determination of maximum force using the grab method*.
NF EN ISO 13937-1. (2000). *Textiles—Tear properties of fabrics—Part 1: Determination of tear force using ballistic pendulum method (Elmendorf)*.
NF EN ISO 13937-2. (2000). *Textiles—Tear properties of fabrics—Part 2: Determination of tear force of trouser-shaped test specimens (Single tear method)*.
NF EN ISO 13937-3. (2000). *Textiles—Tear properties of fabrics—Part 3: Determination of tear force of wing-shaped test specimens (Single tear method)*.
NF EN ISO 13937-4. (2000). *Textiles—Tear properties of fabrics—Part 4: Determination of tear force of tongue-shaped test specimens (Double tear test)*.
NF EN ISO 13938-1. (1999). *Textiles—Bursting properties of fabrics—Part 1: Hydraulic method for determination of bursting strength and bursting distension*.
NF EN ISO 13938-2. (1999). *Textiles—Bursting properties of fabrics—Part 2: Pneumatic method for determination of bursting strength and bursting distension*.
NF EN ISO 13997. (1999). *Protective clothing—Mechanical properties—Determination of resistance to cutting by sharp objects*.
NPTEL. (2012a). *Textile fibers*. http://nptel.ac.in/courses/116102026/20.
NPTEL. (2012b). *Textile testing*. http://nptel.ac.in/courses/116102029/40.

This page intentionally left blank

Comfort testing of textiles

3

E. Classen
Hohenstein Institute, Bönnigheim, Germany

3.1 Introduction

The demands clothing has to meet in order to be competitive have steadily multiplied in recent years. With the current market situation, it is insufficient for garments to be fashionably designed and have good mechanical or technological properties. They must also function well physiologically. The wearing comfort of clothing is a main quality criterion. Comfort not only affects the well-being of the wearer, but also his performance and efficiency. Comfort is a complex, highly subjective quality, often defined as the absence of discomfort. Clothing should support the wearer during his activities. Physiological demands can also vary depending on the type of clothing, that is, sport, personal protection, work, casual, etc. The four important aspects of comfort in clothing are thermophysiological comfort, skin sensorial comfort, ergonomic comfort, and psychological comfort (Mecheels, 1998).

Thermophysiological comfort deals with the interaction between the body and the clothing and involves the transport of heat and moisture from the body through the clothing into the environment. Thermophysiological sensations include coolness, warmth, chilling, and sweating. Skin sensorial comfort, or skin sensory comfort, describes the contact and interaction between the textile and the skin. Skin sensory comfort is determined by the mechanical sensation a textile causes through direct contact with the skin. It includes pleasant perceptions like smoothness or softness as well as unpleasant perceptions such as scratchiness, stiffness, or clinginess (such as when a fabric clings to sweat-dampened skin). Textiles with poor skin sensorial wear comfort may even lead to mechanically induced skin irritations. Ergonomic comfort deals with the fit of clothing and the freedom of movement it allows. Essential properties for ergonomic comfort are the garment's pattern and the elasticity of its materials. Psychological comfort is affected by fashion, personal preferences, ideology, etc. The psychological aspect should not be undervalued: who would feel comfortable in clothing of a color he or she dislikes?

The wear comfort of fabrics is one of clothing's most important properties. Only comfortable textiles can have high market potential for clothing application. Different kinds of clothing are expected to have different fashion, technical, and physiological properties depending upon their intended use, for example, daily wear, sportswear, outdoor wear, work wear, personal protective clothing, and so on. Clothing must fulfil the needs created by its intended use.

Wear comfort is a complex phenomenon which cannot be properly judged by the customer through simply trying the garment on in the store, nor can it be defined by the sales representative. However, wear comfort can be measured because it is not

Advanced Characterization and Testing of Textiles. https://doi.org/10.1016/B978-0-08-100453-1.00004-0

entirely an undefined, purely subjective individual sensation. Wear comfort is a quantifiable consequence of the body-climate-clothing interaction.

3.2 Fabric comfort properties

Fabrics are engineered for a wide variety of uses, and demonstrate a wide range of properties. In garment applications, fabrics may be used for a variety of clothing types, for example, casual and urban wear, sportswear, summer and winter wear, work wear, and personal protective wear. Regardless of the clothing usage, fabrics are expected to provide comfort, functionality, and protection to the wearer from normal to extreme conditions.

Fabric properties are often divided into two main groups: aesthetics and functionality. Aesthetics involves all aspects of a fabric appearance. Functionality involves the fabric performance during usage. Typical fabric properties include stretch, handling, stiffness, smoothness, thermal and moisture transfer, electrical surface resistivity, and draping, for instance.

The properties of fabrics depend on their physical, chemical, and structural characteristics. Fiber type, yarn type, yarn smoothness, fabric structure, fabric thickness, and presence of additional materials like membranes influence the comfort of clothing. In addition, the dyeing, finishing, and coating processes can also influence a material's properties.

The fiber structure and constructional factors affect heat and moisture transport in textile materials. Natural fibers like wool and cotton have a higher ability to absorb large amounts of moisture due to their hygroscopic properties. The greater the fiber's ability to absorb sweat or moisture from the wearer's skin, the drier it keeps the skin. In addition, still air in a textile structure and between the fabric layers can improve the textile insulation value. A fabric porosity and the total volume of void space within the fabric affect its air permeability. Hairy fibers and fabrics provide a greater volume of still air than smooth ones; this increases their efficiency as an insulation barrier to heat and moisture. The wearer's motion causes air penetration through the clothing. The heat and moisture transfer resistance of the clothing system decreases depending on the fabric pore size.

Highly functionalized fabrics can perform differently from their original state. Raw cotton fiber usually absorbs or releases moisture into and out of the fiber interior. However, with a special finishing, cotton fabrics can gain the ability to repel water. In addition, the surface of wool fibers, which can mechanically irritate the skin, can be modified with physical and chemical treatments so that its scale structure is reduced, resulting in less irritation. Today's fabrics must demonstrate multiple functionalities at the same time, for example, moisture wicking, temperature control, pilling resistance, stain resistance, antimicrobial and antiodor properties, and the ability to block UV radiation. Therefore, it is increasingly difficult to judge the comfort of a fabric based solely upon the fiber material.

Skin sensorial wear comfort describes the mechanical contact sensations caused by the textile on the skin (Bartels & Umbach, 2001). The surface structure of the fiber, the fabric construction, and the absorption of sweat from the skin are important parameters for a pleasant sensation.

3.3 Thermophysiological comfort testing

In the early days of comfort testing, fabrics were field tested during wearer trials because no objective test method was available. These human subject trials evaluated the physiological impact of the clothing on human bodies. Today, the physiological function of textiles and whole garment systems can be measured by a set of laboratory test methods. Laboratory test methods are fast and cost less than wearer trials. They can easily determine different aspects of comfort with high reproducibility. Results obtained with testing devices have less variability than those measured on human beings. However, the results of laboratory test methods are the results of physical measurements and must be correlated with human perception in wearer trials. Laboratory tests do not directly measure comfort. They probe certain parameters which must be proven significant for comfort. This physiological validation is crucial because only then will test results of wear comfort be meaningful. As a result, mathematical correlations between the wearer's perception of comfort and results provided by laboratory devices have to be established (Bartels, 2011).

Wearer trials with human test subjects are performed in field tests or under controlled conditions. In field tests, environmental conditions may vary between individual tests; as a result, a huge number of test subjects are necessary to obtain a statistically significant result. In controlled-condition wearer trials, environmental conditions are controlled in a climatic chamber. This offers an advantage by allowing environmental conditions and test subjects' activity to be reproducibly repeated and controlled. Objective data can be recorded via sensors attached to the subject's body, for example heart rate, skin temperature, humidity in the microclimate, and body core temperature. However, wearer trials are time consuming and expensive, while laboratory tests can provide results at the material and clothing level for product development.

Thermophysiological wear comfort of textile materials can be determined with the sweating guarded hotplate (the Skin model), a thermoregulatory model of the human skin which has been internationally standardized (ISO 11092, 2014). The Skin model simulates heat and moisture transport from the skin. It consists of an electrically heated porous metal plate with a water supply. The metal plate is placed in a climatic cabinet with adjustable temperature, air humidity, and air movement, and it is highly reproducible. Normal wear situations with only moderate sweating can be simulated, as well as situations with increased or heavy sweating. A series of parameters characterizing the thermophysiological quality of a textile material can be determined: thermal insulation (R_{ct}, thermal resistance), breathability (R_{et}, water vapor resistance), sweat transport, sweat buffering, and drying time.

Thermal manikins can also be used to assess the thermophysiological properties of ready-made garments. Manikins have been used since 1945. Measurements are carried out according the ISO 15831 standard (ISO 15831, 2004; Wang, 2008). Thermal manikins have the size and shape of a so-called standard man. Different thermal manikin models differ in the number of segments corresponding to different parts of the body. The segments are separately controlled by computer and allow the simulation of characteristic temperature gradients at the body surface. The advantage of manikin testing is that it provides a realistic simulation of heat transfer from the body through

the clothing into the environment. Manikins can simulate different body postures relevant to the clothing's actual use, that is, standing, walking, sitting, and lying down. This allows evaluation of the influence of convection and ventilation in the garment's microclimate caused by the wearer's body movement on their physiological function. Today, sweating thermal manikins are also available to determine heat and moisture transfer through garments.

3.4 Skin sensorial wear comfort testing

Sensorial evaluation of textiles is important for the consumer. In his first contact with the fabric, the consumer examines the fabric properties by touching it with his hand to select a good clothing material according to his feeling and experience (Kawabata, 1980).

Touch is one of the sensations processed by the somatosensory system (Bishop, 1996; Dhinakaran, Sundaresan, & Dasaradan, 2007). The human tactile sensation with the hand is produced by somatic receptors in the hand. The three somatic senses in the hand are mechanoreceptors (which are stimulated by the mechanical displacement of various body tissues), thermoreceptors (which are stimulated by temperature changes), and nociceptors (which sense pain). When the hand touches materials, the skin's sense of touch is used, and sensory signals are sent to the brain. Subjective perceptions are formulated and clustered in terms of tactile, moisture, pressure, and thermal sensations. Tactile sensations can be described as prickly, tickly, rough, smooth, craggy, scratchy, itchy, or sticky. Moisture sensations can be described as clammy, damp, wet, sticky, sultry, nonabsorbent, or clingy. Pressure sensations can be described as snug, loose, lightweight, heavy, soft, or stiff. Thermal sensations can be described as cold, chill, cool, warm, or hot.

In 1930, Peirce started the first investigation of fabric bending rigidity, one of the factors which affect the handling and comfort of apparel (Peirce, 1930). Fifty years later, Kawabata's Hand Evaluation System of Fabric, the KES-F system, was developed in Japan (Kawabata, 1980).

The KES-F system consists of four specialized instruments to measure the following parameters (Kawabata, 1980): tensile and shearing with KES-F1; bending with KES-FB2; compression with KES-FB3; and surface friction and roughness with KES-FB4. These measurements simulate fabric deformations observed while in use. Sixteen different parameters are measured. Using extensive human subjective evaluation, Kawabata developed a ranking system of the characteristics of fabrics. However, the system requires experts to interpret the resulting data. The KES-F system is often used in scientific research projects to judge the sensory quality of fabrics.

Because of the high cost of the Kawabata instruments and the need for experts to interpret the data, the Australian CSIRO developed the FAST system (Fabric Assurance by Simple Testing) in the late 1980s. The FAST instruments are a simpler alternative to the KES-F system and give information about the characteristics of a fabric similar to the KES-F system. The FAST system consists of four instruments: FAST-1 for thickness; FAST-2 for bending; FAST-3 for extensibility; and FAST-4 for dimensional stability (Shishoo, 1995).

Other devices measure only individual parameters, for example, the Shirley stiffness tester, the Cusick drape meter, the universal tensile tester, thickness gauges, the universal surface tester or the cantilever stiffness tester (Kayseri et al., 2012). There are a lot of instruments on the market that determine various individual aspects of the feel of a textile's surface (e.g., touch, softness, fabric hand).

To evaluate the handle of a fabric, fingers slide on its surface, which is compressed between the thumb and the index finger. Fingers contain more than 250 sensors per cm^2 (Bensaid, Osselin, Schacher, & Adolphe, 2006); they are the most crucial organs for the determination of fabric quality. The whole hand may also be used, to judge seat covers or furniture upholstery, for instance. In this case, the whole hand is slightly moved over a covering material; this sensation differs from that provided by the finger. Touching with the hand does not provide the same perception as when a fabric is worn in direct contact with the body.

Skin sensorial comfort describes these perceptions while wearing clothing. Clothes worn next to the skin have to offer particularly good sensorial wear comfort to be accepted by the wearer (Bartels & Umbach, 2001). For that purpose, the Hohenstein Institutes in Germany have developed and improved a complex system of skin sensory test devices and assessment formulae over several decades (Bartels & Umbach, 2002; Mecheels, 1982). The research results show that the following parameters are important: the surface index, number of contact points, wet cling index, sorption index with the skin, and fabric stiffness. In particular, the skin sensitivity to mechanical irritation becomes stronger as moisture increases. Therefore, the textile must promote sweat transport from the skin into the environment.

For good skin sensorial comfort, the hairiness of the fabric is important (Bartels & Umbach, 2002; Mecheels, 1982). Hairiness depends on the number and length of fibers and yarns protruding from the fiber bulk. It varies widely from one material to another, for example, from filaments with no hair at all to fabrics with long and stiff fiber ends. It is influenced by the material used as well as the yarn structure. For instance, most of the fiber ends are at the surface in spun yarns, while filament yarns show no fiber ends. If a textile surface contains fiber ends, direct contact between the textile and the skin prevents the formation of a sweat film on the skin. On the other hand, if the number of fiber ends is too high and/or the fibers are too stiff, the textile becomes scratchy. For instance, coarse wool has long and stiff fiber ends while filament yarns have no fiber on their surface. However, extremely smooth or flat surfaces are disadvantageous because a sweat film easily builds up between the textile and the skin, leading to a strong clinging sensation.

A textile surface profile can be assessed by measuring the surface index (i_o) using optical methods like a microscope (Fig. 3.1). This index quantifies a textile hairiness, that is, the number and length of fiber ends protruding from the bulk. The value of i_o is determined from enlarged cross-cuttings of the fabric via an image-analyzing system. A fabric obtains a good sensorial comfort rating if the surface index (i_o) lies between 3 and 15.

The number of contact points between the skin and the textile, n_K, is also an important parameter (Bartels & Umbach, 2002; Mecheels, 1982). This number is determined optically with a topograph, which gives a 3-dimensional picture of the textile surface

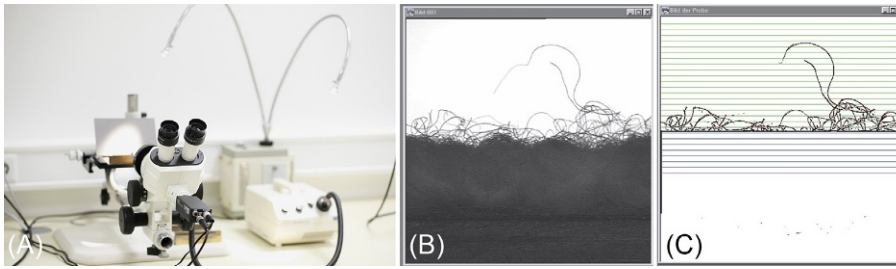

Fig. 3.1 Surface index measuring equipment (A), picture of the textile bulk (B), and digitized picture of the textile bulk (C).

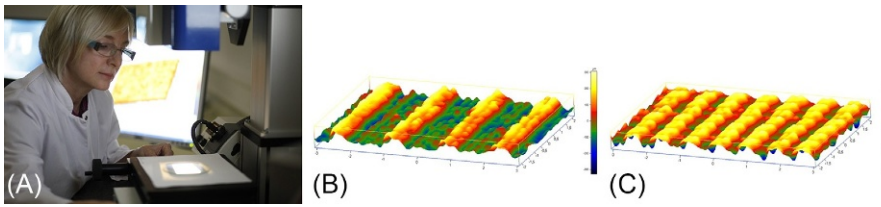

Fig. 3.2 Contact point index measuring device (A), and examples of topography of textiles: (B) fine rib ($n_K = 1722$) and (C) double rib ($n_K = 921$).

(Fig. 3.2). Metrics specific to the textile surface are quantified using this picture via an image-analyzing system, for example, the number of high and low points, the incline grade of the high points, etc. The number of contact points is computed using these data. The hairiness of textiles can vary in a wide range from a material which has no hair at all (e.g., filaments) to fabrics with long and stiff fiber ends. Spun yarns show the most fiber ends on the surface, and filament yarns show no fiber ends.

If a fabric clings to moist skin, it is extremely unpleasant to the wearer. The intensity of "wet cling" on the skin can be expressed by a wet cling index, i_K. A smaller i_K corresponds to a lower uncomfortable wet cling sensation. The index i_K is measured with a special apparatus equipped with a sintered glass plate which simulates the roughness of the human skin (Fig. 3.3). The textile sample is drawn horizontally across a moistened sintered glass plate. The force needed to draw the sample horizontally across the glass plate is measured with a sensor. The mean value of this force over the lengthwise and crosswise direction of the sample yields the wet cling index, i_K. The lower the i_K, the lower the fabric wet cling on the skin, and the better its sensorial comfort.

The importance of this clinging sensation is physiological: human beings have no humidity receptors on their skin and feel moisture only indirectly. There may be a temperature perception if wind enhances the cooling of wet skin. There could be a mechanical sensation if sweat drops run down. Clinging is a strong mechanical perception and signals the wearer that he is sweating, that is, feeling uncomfortable.

For skin sensorial comfort, it is thus important to keep the body's surface as dry as possible, even under high activity (Bartels & Umbach, 2002; Mecheels, 1982). Skin wetness leads to a faster abrasion of the upper part of the skin, a dilution of skin fats

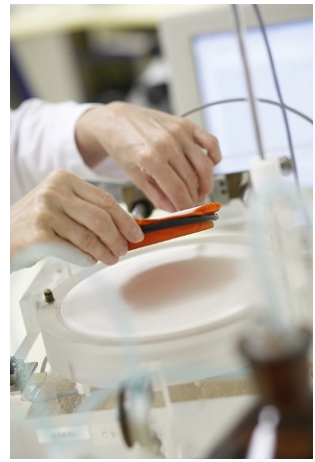

Fig. 3.3 Wet cling index measuring equipment.

and decrease of their protective function, a change in the skin pH-value, and a higher penetration of chemicals or allergenic substances through the skin. Wet skin is much more sensitive and can be irritated more easily than dry skin. Therefore, rapid sweat transport through the textile leads to better thermophysiological comfort and higher skin sensorial comfort.

For skin sensorial comfort, the "wettability" of a textile is significant (Bartels & Umbach, 2002; Mecheels, 1982). This is determined by the time needed for the textile to absorb a drop of water. To achieve reproducible results, a defined test geometry and drop volume are required. A water drop of a defined volume is deposited on the textile surface (Fig. 3.4). The variation of the water drop contact angle is recorded over time. The time lapse after which the water drop has been completely absorbed by the sample can be extrapolated from these data. This time lapse yields the sorption index, i_B.

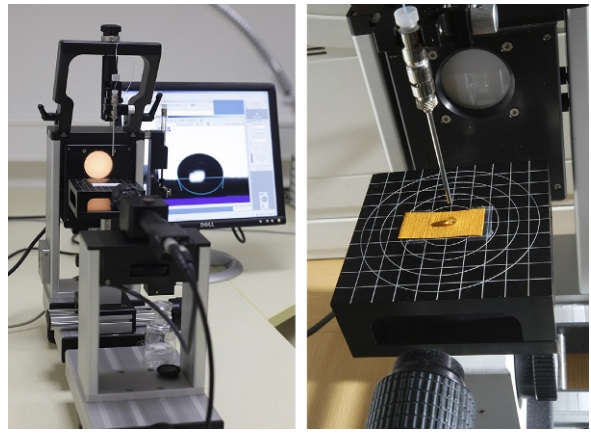

Fig. 3.4 Sorption index measuring equipment.

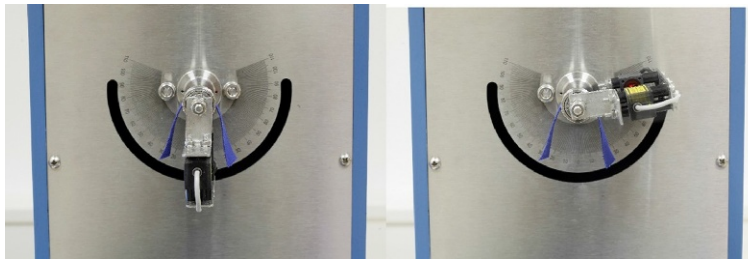

Fig. 3.5 Stiffness measurement device.

To prevent skin from getting wet, the textile should also offer a good water vapor transport, that is, breathability. The breathability of the textile may be determined via the water vapor permeability index i_{mt} defined in ISO 11092 (2014). This index expresses the relative breathability of the textile under consideration of its thermal insulation.

The fifth important parameter is stiffness, *s* (Bartels & Umbach, 2002; Mecheels, 1982). A textile can feel comfortably smooth or soft, or it may be unpleasantly stiff, or too limp or flabby. The stiffness (*s*) is expressed as the bending angle against the perpendicular direction of a fabric specimen with a 2×10 cm dimension (Fig. 3.5). By definition, *s* can assume values between 0 (completely flabby) and 90 (completely rigid).

Comprehensive skin sensorial wear comfort, WC_S, can be predicted using the different skin sensorial wear comfort parameters (Bartels & Umbach, 2002; Mecheels, 1982). The determination of WC_S differs for knitwear and woven fabrics because the wearer expects knitwear to be softer or smoother than a woven fabric. WC_S is given as a six-point scale ranging from 1 ("very good") to 6 ("unsatisfactory"). With the knowledge of WC_S, the skin sensorial wear comfort of different fabrics can be easily compared.

Different test methods for sensorial skin comfort were developed in a number of research projects (Bartels & Umbach, 2002; Mecheels, 1982). The same fabrics/garments were also examined in wearer trials to compare the objective data with the subjective perceptions of the test subjects. These perceptions depended upon different parameters and were influenced by the experiences of the test subjects and their description of the sensations. In addition, description of these perceptions required a set of linguistic terms which were dependent upon the cultural background of the subject.

3.5 Ergonomic comfort testing

Ergonomic comfort of clothing is especially important for work wear and personal protective clothing. Ergonomics is a scientific discipline concerned with understanding the interactions between humans and other elements of a system. Ergonomics applies theory, principles, data, and methods to design in a way that optimizes human well-being and overall system performance (IEA, 2017). Proper ergonomic design is necessary to prevent repetitive strain injuries and other musculoskeletal disorders,

which may develop over time and can lead to long-term disabilities. Ergonomics is concerned with the "fit" between the user, his/her equipment, and their environment.

If a garment fits the human body well, the wearer can easily move in the garment. Ergonomic comfort, sometimes also called aesthetic comfort, can be tested with different objective methods (Sinclair, 2014). One traditional method measures the space between the body and the clothing and calculates the fitting index. The ease of motion can be assessed through wearer trials. In these wearer trials, wearers are required to perform a series of activities, which normally occur in practice. The wearer rates the ease of body movement on a scale, for example, the Likert scale. To judge the ergonomic comfort of a whole garment, different assessments are made for different parts of the body and different activities. Photographs can be taken for additional subsequent visual assessment.

Another method is the symmetrized dot pattern technology (Sinclair, 2014). This new method is based on changes in dot patterns and imaging technologies which allow the capture and analysis of garment images. However, the garment surface may be folded or wrinkled. In this case, the space between body and garment cannot easily be measured with high precision and efficiency.

Additionally, 3D-scanning technology makes it possible to identify spaces between the body and the garment. Three-dimensional body data for both nude and dressed human subjects are necessary to build up the spaces between the body and the garment.

3.6 Psychological comfort testing

Psychological comfort represents how the individual feels in the clothing. It is influenced by different factors such as styling, color, fashion, and aesthetics. Psychological comfort is highly subjective because of the personal nature of positive association, and because the personal experiences of each subject are different. Therefore, expectations differ, resulting in a significant effect on their response. Subjective perceptions involve psychological processes in which all relevant sensory perceptions are formulated, weighed, combined, and evaluated against past experiences and present desires. This type of comfort is qualitative and cannot be measured.

3.7 Future trends

Today fabrics are often highly multifunctional and display new properties, for example, compression, shaping, heating, and cooling.

Compression textiles have been used for medical applications for a long time. For example, compression stockings reduce the expansion of veins; the compressive gradient enhances venous blood flow to the heart. Today, compression textiles are popular in sports, especially endurance sports like triathlon and marathon running. During sports activities, compressive textiles reduce wobbling masses, muscle vibration, and swelling. In addition, the pressure of the compression textile influences the skin. Until now this was not taken into account in the characterization of skin sensorial comfort.

Indeed, if new tools have been developed in the last years to measure the pressure applied on materials, most of the systems measure the influence of pressure on a flat area, not a three-dimensional body. Therefore, the development of the new measuring system is necessary.

Cooling influences the skin and body temperature and provides thermoregulation to the body. The use of cooling fabrics helps protect the human body from overheating. Yet, the influence of the cooling effect on skin sensorial comfort has not been investigated yet.

New properties require new laboratory test methods to determine the function and the effect of this function. However, sensorial comfort is difficult to predict as it involves a large number of different factors. Modeling and simulation of textile fabrics represent an important field of scientific research. Interdisciplinary cooperation of scientists in the fields of physics, mechanics, mathematics, and informatics is necessary for the simulation and prediction of textile properties and behavior. Modeling tools are useful for estimation of skin sensorial comfort, and further research activities are required.

3.8 Conclusion

Because of the direct physiological interaction between the body and the clothing (which has an essential influence on our well-being as well as our physical and mental performance), the measurement and evaluation of the physiological function of textiles and garments are at least as important as the testing of mechanical/technological properties which has been done for years. Wear comfort of clothing is not obtained automatically; it is only the result of a well-designed product development process, and is never determined by examining only a single constructional parameter. Today a powerful toolbox of laboratory test methods which have been correlated with the real perception of human subjects in wear trials is available for the determination of sensorial skin comfort.

References

Bartels, V. T. (2011). Improving comfort in sport and leisure wear. In G. Song (Ed.), Improving comfort in clothing. *Woodhead Publishing Series in textiles: Number 106*. Cambridge: Woodhead Publishing.

Bartels, V. T., & Umbach, K. H. (2001). *Skin sensorial wear comfort of sportswear*. In *40th international man made fibre congress, Dornbirn, Austria, September 19–21*.

Bartels, V. T., & Umbach, K. H. (2002). *Test and evaluation methods for the sensorial comfort of textiles*. In: *Euroforum "Toucher du textile", Paris, France*.

Bensaid, S., Osselin, J.-F., Schacher, L., & Adolphe, D. (2006). The effect of pattern construction on the textile feeling evaluated through sensory analysis. *The Textile Institute*, *97*(2), 137–145.

Bishop, D. P. (1996). Fabric: Sensory and mechanical properties. *The Textile Institute, Textile Progress*, *26*(3), 1–62.

Dhinakaran, M., Sundaresan, S., & Dasaradan, B. S. (2007). Comfort properties of apparels. *The Indian Textile Journal*, *32*, 2–10.

IEA. (2017). *What is ergonomics*. International Ergonomics Association. http://www.iea.cc/whats/.

ISO 11092. (2014). *Measurement of thermal and water-vapour resistance under steady-state condition*.

ISO 15831. (2004). *Clothing—Physical effects-Measurements of thermal insulation by means of a thermal manikin*.

Kawabata, S. (1980). *The standardisation and analysis of hand evaluation* (2nd ed.). Be Osaka: Textile Machinery Society of Japan.

Kayseri, G. Ö., Özdil, N., Mengüc, G. S. (06.05.2012). *Sensorial comfort of textile materials*. OpenTech. www.intechopen.com.

Mecheels, J. (1982). *Zur Komfortwirkung von Textilien auf der Haut*. Hohensteiner Forschungsberichte.

Mecheels, J. (1998). *Körper-Klima-Kleidung: Wie funktioniert unsere Kleidung?* Berlin: Schiele & Schiele.

Peirce, F. T. (1930). The "handle" of cloth as a measurable quality. *J Text Inst.*, *21*, T377–T416.

Shishoo, R. L. (1995). Importance of mechanical and physical properties of fabric, in the clothing manufactiring process. *International Journal of Clothing Science and Technology*, *7*(2/3), 35–42.

Sinclair, R. (2014). Textiles and fashion: Materials, design and technology. *Woodhead Publishing Series in textiles: Number 126*. Cambridge, UK: Elsevier Ltd.

Wang, F. (2008). *A comparative introduction on sweating thermal manikin Newton and Walter*. In: *7th International Thermal Manikin and Modelling Meeting, September*. University of Coimbra.

This page intentionally left blank

Testing thermal properties of textiles

4

D. Tessier
CTT Group, Saint-Hyacinthe, QC, Canada

4.1 Introduction

4.1.1 Thermal comfort

Thermal properties of textile materials have been investigated for several decades (Sale & Hedrick, 1924; National Bureau of Standards, 1938, 1944; Morris, 1953). One of the pioneer organizations involved was the National Bureau of Standards, known today as the National Institute of Standards and Technology (NIST). Thermal comfort is now an important concept for consumers. This is true not only for high-tech clothing and protective uniforms, but also for ready-to-wear garments. Thermal comfort is a complex concept that refers more specifically to the thermophysiological comfort where the "thermal balance" is achieved when heat loss equals heat production; therefore, the body keeps a constant temperature.

The following properties are part of the thermal comfort attributes of textiles:

- Water vapor resistance or breathability
- Thermal resistance, dry
- Air permeability
- Liquid wicking rate
- Water resistance (under hydrostatic pressure)
- Water repellency

Thermal comfort is also very dependent on the environment because particular environmental conditions will require specific textiles and material compositions. For example, very cold and dry environments will require high thermal insulation or thermal resistance textile materials while cold, humid/rainy, and windy conditions will be better managed using an insulated textile material in combination with a water vapor permeable membrane. To achieve appropriate thermal comfort, additional requirements are needed relative to the air permeability and the water vapor resistance (breathability). On the other hand, sportswear has to properly manage the perspiration or liquid wicking rate and body heat in order to provide a good level of thermal comfort. Finally, liquid water resistance is more relevant for high-tech clothing and protective uniforms at pressure points where liquid may enter and affect the ability of the clothing to provide thermal insulation. In fact, water is a very good thermal conductor so it strongly affects the thermal resistance of textiles and other insulation materials.

One key component in most multilayered clothing is the moisture barrier (Holmes, 2000): the moisture barrier is constructed of a moisture-resistant yet breathable film

Advanced Characterization and Testing of Textiles. https://doi.org/10.1016/B978-0-08-100453-1.00005-2

that is laminated to a substrate for support. It protects the wearer from water, steam, moisture penetration, chemicals, and blood-borne pathogens when required. Moisture barriers also allow the outward passage of moisture vapor so that some of the body heat can escape.

The thermal sensation on the skin is also an important attribute for textiles having direct contact with the skin. It is possible to assess the thermal sensation via thermal effusivity. A material's thermal effusivity is a measure of its ability to exchange thermal energy with its surroundings.

4.1.2 Cold protection

Nowadays, many different cold protection technologies and textile materials are available (Abdel-Rehim, Saad, El-Shakankery, & Hanafy, 2006; Vogt, 1998; Ukponmwan, 1993). A common denominator to cold protection is the air entrapped into the thermal insulation material. The air might be found between the fibers, inside the fibers (hollow fibers), inside cells, microcapsules, etc.

A well known natural material is duck down, which is very lightweight. There are now numerous types of high-performance synthetic insulations available, and several come close to down in terms of its warmth-to-weight ratio. Often, synthetic insulation is brought by a combination of two elements: polyester threading molded into long single yarns or short staples that mimic lofty down clusters and provide the resiliency in compression, and thinner and lighter yarns that fill voids and trap warm air.

Apart from fibers, fiber assemblies such as nonwovens or embossed nonwovens (Thinsulate from Dupont, Primaloft, Thermolite from Invista), fleece, and other knitted constructions (Polartec insulating fabrics) do provide high-performance thermal insulation. Thermolite offers hollow core polyester fibers. There are other hollow fibers made of polypropylene such as Dryarn or polyamide Meryl Nexten from Nylstar (Fig. 4.1). According to the technical information made available by Nylstar (Nylstar, 2014), Meryl Nexten fabrics are ultralight, i.e., 30% less heavy than fabrics with the same thickness and structure. They are made of standard polyamide.

There are also emerging, natural hollow fibers such as kapok and milkweed; the latter is also known as asclepias. The milkweed fibers are obtained from the floss. The milkweed floss is a hollow fiber (Fig. 4.2) with excellent thermal insulation qualities (McCullough, 1991). It has a tubular morphology, a length which may be typically about 3 cm, a mean diameter of 22 microns, and a wall thickness about 10% of the diameter (Tessier & Simard, 2014).

Given the wide variety of insulating fiber, microfiber, hollow fiber, nonwoven, and knitted constructions available, different test methods exist to assess the cold insulation properties for protection against cold. Conversely, fibrous materials may also be designed to protect against heat and reduce heat stress, for instance.

4.1.3 Heat stress protection

Firemen are exposed to flames, high temperatures, and extreme heat. Many industrial workers are also exposed to high temperatures in metallurgy and petrochemical

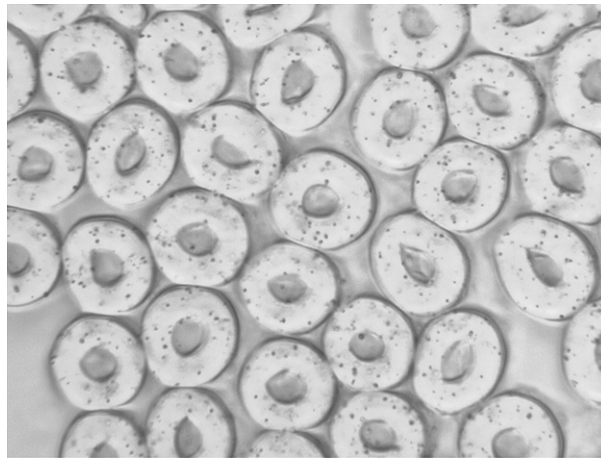

Fig. 4.1 Cross-section view of Meryl Nexten fabric made with hollow fibers.
Reproduced from Nylstar. (2014). Textile web article. http://www.textileweb.com/doc/meryl-nexten-0001. Corporate brochure, Nylstar_Meryl_Nexten_2014.pdf.

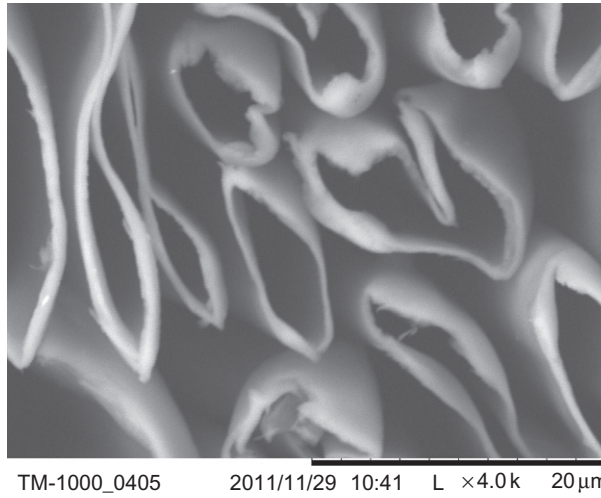

Fig. 4.2 SEM picture of milkweed floss, cross-section view.
Reproduced from Tessier, D., Simard, F. (2014). Oil absorption performance of milkweed hollow-fiber in sorbent pads & round booms. In: *The Institute of Textile Science, 112th Scientific Session, Banff, May* 6.

industries for instance. For example, state-of-the-art protective uniforms for firemen often called "turnout gear" have to meet minimal requirements of NFPA (NFPA, 1971). They are composed of three layers, with the inner layer called the thermal barrier. The main function of this thermal barrier is to protect from radiant heat. While it is effective at protecting from the heat moving toward the fireman, it is much less effective at allowing the metabolic heat to get out of the garment. So, gradually, the

heat can build up into the garment (in a space known as the microclimate).That microclimate temperature may increase and induce heat stress to the fireman. This risk increases with the activity level because the body heat cannot escape efficiently.

The thermal property of interest here is the thermal heat loss, known as the THL value. The THL indicates how much a material or combination of materials lets heat escape. It is important to consider it when heat stress is a concern.

4.2 Thermal properties of textiles

The thermal energy can be transferred through textile fabrics by direct conduction, heat convection, and radiation (Holman, 1986). The thermal resistance of textiles comprises one or more conductive, convective, and radiant components. The thermal conductivity corresponds to the conductive component.

4.2.1 Thermal resistance

The thermal resistance (ISO 11092, 2014) R_{ct} is the temperature difference between two faces of a material (T_m and T_a) divided by the resultant heat flux (H) per unit area (A) in the direction of the gradient. The dry heat flux may consist of one or more of the conductive, convective, and radiant components. Thermal resistance R_{ct}, expressed in square meters kelvin per watt (m^2K/W) as an SI unit, is a quantity specific to textile materials or composites that determines the dry heat flux across a given area in response to a steady temperature gradient. Applied R_{ct} can be calculated using Eq. (4.1):

$$R_{ct} = \frac{\left(T_m - T_a\right) * A}{\left(H - \Delta H_c\right)} - R_{ct0} \tag{4.1}$$

where T_a is the air temperature in the test enclosure, in degrees Celsius, T_m is the temperature of the measuring unit, H is the heating power supplied to the measuring unit, in watts, ΔH_c is a correction term for heating power for the measurement of thermal resistance R_{ct}, A is the area of the measuring unit, in square meters, and R_{ct0} is the apparatus constant.

The thermal resistance or clothing insulation I_{cl} can be expressed as the unit "clo." It is not a standard unit, but it is commonly used in America. One clo equals $0.155\,m^2K/W$. The use of the unit clo implicitly means that it relates to the whole body and thus includes heat transfer by exposed body parts (Vogt, 1998). The Shirley Institute in Manchester, England, developed another alternative unit called the tog as an easy-to-follow alternative to the SI unit that is still used to represent the thermal insulation of duvets. The equivalence for 1 tog is $0.1\,m^2K/W$ (BS 4745, 2005).

4.2.2 Thermal conductivity and effusivity

Heat transfer by conduction depends on the material heat conductivity, the thermal conductivity. Thermal effusivity is also gaining importance; the recent ASTM D 7984

standard test method has been developed for the measurement of thermal effusivity of fabrics using a modified transient plane source (MTPS) instrument.

The thermal conductivity k—sometimes called λ—is expressed in watts per meter Kelvin (W/m·K) and describes the transport of energy—in the form of heat—through a body of mass as the result of a temperature gradient, as described in Eq. (4.2):

$$k = \frac{\left(H - \Delta H_c\right) * L}{\left(T_t - T_0\right) * A} - k_0 \tag{4.2}$$

$(H-\Delta H_c)$ represents the net heat flux going through a material of thickness L and surface area A and k_0 is the apparatus constant. The temperature increase from initial time (T_0) to test time (T_t) is measured as the response to a steady applied power (heat flux).

As a result, the relation between the thermal conductivity and the thermal resistance of textile fabrics is influenced by the actual thickness of the material, as per Eq. (4.3):

$$k = L / R_{ct} \tag{4.3}$$

Effusivity e can be calculated as the square root of the product of the thermal conductivity, density, and heat capacity, as shown in Eq. (4.4):

$$e = \left(k \rho C_p\right) \frac{1}{2} \tag{4.4}$$

where ρ is the density (kg/m^3) and C_p is the heat capacity (J/kg·K).

4.3 Testing thermal properties

The thermal energy can be transferred through textile fabrics by direct conduction, heat convection, and radiation. So various test methods have been developed to take into account these heat transfer mechanisms.

4.3.1 Standard test methods

This section presents different test methods related to the evaluation of thermal resistance for textile fabrics. The tog test, clo test, sweating guarded hotplate and THL are closely related to the evaluation of thermophysiological comfort and thermal resistance.

Other standard test methods like thermal protective performance (TPP) and radiant heat resistance (RHR) refer to thermal protection performance of materials used in firefighter clothing where high heat fluxes are used (Mandal, Song, Ackerman, Paskaluk, & Gholamreza, 2013; Mandal & Song, 2014). Those methods could employ radiant heat, convective heat, contact heat, or a combination of different heat sources. In a review, Havenith (2009) provided an overview of laboratory tests for cold weather clothing that included physical measurements of fabrics (including THL) and physical

measurements for entire garments using thermal manikins. The search was extended to human wear trials and climatic chamber experimentation. Tests methods for innovative fabrics such as heated, variable insulation, and phase-change materials were discussed. Regarding the heat and flame protection perspective, Haase (2013) discussed flame-resistant clothing standards and regulations aspects including test methods such as TPP (and other test methods from ISO, EN, and ASTM), certification procedures for flame retardant (FR) products, and their applications for protective clothing in industrial, firefighting, and military use. Zhai and Li (2015) studied prediction methods of skin burns for performance evaluation of thermal protective clothing. They mentioned that new technologies may be used in the future to explore precise or suitable prediction methods for both flash fire tests and increasingly lower-intensity tests.

4.3.1.1 Tog test, BS 4745

Launched in the 1940s by The Shirley Institute, the Shirley Togmeter is the standard apparatus for rating thermal resistance of textiles, commonly known as the tog test (BS 4745, 2005). This apparatus, described in British Standard BS 4745, measures a textile sample, either between two metal plates (for underclothing) or between a metal plate and free air (for outer layers).

4.3.1.2 Clo test, ASTM D-1518

The measurement of the clo, a standard test method mainly used in the United States, is described in ASTM D-1518 (ASTM D1518, 2014). The thermal resistance of a batting or batting/fabric system is of considerable importance in determining its suitability for use in cold weather protective clothing, sleeping bags, and bedding systems.

This test method measures the heat transfer from a warm, dry, constant-temperature, horizontal flat plate up through a layer of the test material to a cool atmosphere and calculates the resistance of the material. The measurements are made under still air conditions (Option #1) or with a horizontal air flow over the specimen (Option #2).

For practical purposes, this test method is limited to specimens of batting and layered batting/fabric assembly having an intrinsic thermal resistance from 0.1 to 1.5 m^2K/W and thicknesses not in excess of 50 mm. The test method also provides a method for determining the bulk density of the material, the insulation per unit thickness, and the insulation per unit weight.

4.3.1.3 Sweating guarded hotplate, ISO 11092

ISO 11092 is often referred to as the "skin model." It simulates the heat transfer through the skin. The standard test method is used for two different tests (ISO 11092, 2014): the water vapor resistance and the thermal resistance. The thermal resistance, R_{ct} value, is provided in m^2K/W and the test is performed as follows: a fabric is placed on a copper plate that is regulated at 35°C. The surrounding conditions are 20°C and 65% RH. The air flow velocity on top of the fabric is maintained at 1 m/s. The heat flux (power) necessary to maintain the plate at 35°C is recorded. Alternatively, the thermal resistance can be reported in clo units. Thermal resistivity, r, expressed in mK/W, can also be obtained with this test.

4.3.1.4 THL, ASTM F1868

ASTM F1868 is a standard test method that is used for the evaluation of the thermal and evaporative resistance of clothing materials (ASTM F1868, 2014). The range of this measurement technique is from 0.002 to 0.5 m^2K/W for intrinsic thermal resistance and from 0.0 to 1.0 $kPa\,m^2/W$ for intrinsic evaporative resistance. ASTM F1868 is required by the standard NFPA 1971 with a minimum of 205 W/m^2. The total heat loss is a combination of dry heat loss and wet heat loss.

This method consists of placing textile fabrics and multilayer assemblies on a sweating hot plate for testing. The temperature of the test plate, guard section, and bottom plate is maintained at $35 \pm 0.5°C$ throughout the test. Other test conditions such as air temperature and relative humidity may vary depending on the procedure utilized. Generally, the air flow velocity on top of the fabric or fabric assembly is maintained at 1 m/s. The test evaluates two forms of heat transfer—wet and dry. Dry heat transfer is the THL, representing the conductive heat loss resulting from the external environment due to temperature gradient. Wet heat transfer refers to the evaporative heat loss to the external environment due to a vapor pressure gradient. The thermal resistance, R_{cf} value, is provided in m^2K/W and the evaporative resistance, R_{ef}^A value, is expressed in $Pa.m^2/W$. The THL, given by Q_t in Eq. (4.5) below, is expressed in W/m^2.

$$Q_t = \frac{10^{\circ}C}{R_{cf} + 0.04} + \frac{3.57\ kPa}{R_{ef}^A + 0.0035} \tag{4.5}$$

4.3.1.5 TPP, ISO 17492

This standard test method measures the heat transfer of horizontally mounted flame-resistant textile materials when exposed to a combination of convective and radiant energy (ISO 17492, 2003). Using this test method, the TPP test value is obtained and expressed in cal/cm^2.

The method can be applied to any type of textile material used either as a single layer or in a multilayer construction when all structures or subassemblies are made of flame-resistant materials. Layer compositions might be made of woven fabrics, nonwovens, and water vapor permeable membranes (WVPM) for example. It is not intended to be used on materials that are not flame resistant. This test method is required by the NFPA 1971 in the evaluation/certification of protective ensembles for firefighters. NFPA 1971 (2013) requires an average TPP test result of no less than 35.0.

This test method also refers to other test methods such as radiant heat only (ISO 6942, 2002) or flame contact only (ISO 9151, 1995). A review of thermal sensors for the performance evaluation of protective clothing against heat and fire is also available (Mandal & Song, 2015).

4.3.1.6 TPP of materials for hot surface contact, ASTM F1060

This test method (ASTM F1060, 2008), also known as the contact heat test, is used to measure the thermal insulation of materials used in protective clothing when exposed for a short period of time to a hot surface with a temperature of up to 600°F (316°C).

It is applicable to materials used in the construction of protective clothing that is intended to protect against exposure to hot surfaces. This includes woven fabrics, knit fabrics, battings, sheet structures, and composite materials/structures. The material to be tested is placed in contact with a standard hot surface. The amount of heat transmitted by the material is compared with the tolerance to heat of human tissue and the obvious effects of the heat on the material are noted. The temperature of the hot surface is measured/controlled with a thermocouple, and the heat transmitted by the test specimen is measured with a copper calorimeter. The calorimeter temperature increase is a direct measure of the heat energy received. A contact pressure of 3 kPa (0.5 psi) is used to compare material performance under controlled conditions. If a different pressure is chosen to represent a specific use condition, it should be noted under the test conditions. Time to pain and time to burn (second-degree burn) are reported respectively (in seconds). It is also possible to obtain a "no pain" and/or "no burn" test result depending on the test materials and test conditions. A post-test visual evaluation code (1–9) is also provided (1: Break open; 2: Charring; 3: Dripping; 4: Embrittlement; 5: Ignition; 6: Melting; 7: Shrinkage; 8: Sticking; 9: No noticeable change to specimen).

The thermal protection time as determined by this test method relates to the actual end-use performance only to the degree that the end-use exposure is identical to the exposure used in this test method; that is, the hot surface test temperature is the same as the actual end-use temperature and the test pressure is the same as the end-use pressure. This test method is limited to short exposure because the model used to predict burn injury is limited to predictions of time to burn of a maximum of 30 s and predictions of time to pain of up to 50 s. The use of this test method for longer exposure to hot surface requires a different model for determining burn injury or a different basis for reporting test results.

4.3.1.7 RHR, ASTM F1939

This test method, entitled "Radiant Heat Resistance of Flame Resistant Clothing Materials with Continuous Heating," rates the nonsteady state thermal resistance or insulating characteristics of flame-resistant clothing materials subjected to a continuous, standardized radiant heat exposure (ASTM F1939, 2008). This test method is intended for the determination of the RHR value of a material or a combination of materials, or for a comparison of different materials used in flame resistant clothing for workers exposed to radiant thermal hazards. However, it does not predict skin burn injury from the standardized radiant heat exposure. A standard radiant heat flux level must be selected for testing: 21 kW/m^2 (0.5 cal/cm^{2}s) or 84 kW/m^2 (2.0 cal/cm^{2}s). Other values of radiant heat flux can be selected to represent the conditions of an expected hazard. For example, protective apparel/clothing requiring flame resistance such as firefighter garments could be evaluated using this standard. The RHR test result is expressed/reported in J/cm^2 (cal/cm^2). The intersect time, t (which corresponds to where the sensor response intersects with the Stoll curve or exposure termination curve) may also be reported; if so, the test result is expressed in seconds (s).

ASTM F1939 is used in the NFPA 1971 (2013) specification for firefighters, "Standard on Protective Ensembles for Structural Fire Fighting and Proximity Fire

Fighting." Per the NFPA 1971 (2013) (Par. 7.3.2) requirement, the tested material shall have an intersect time of not less than 20 seconds. Other related test methods are provided in Chapter 8, "Testing Fabrics for Flammability and Fire Safety."

4.3.1.8 Differential scanning calorimetry, ASTM D7138, ISO 11357

Differential scanning calorimetry (DSC) measures changes in heat capacity and will detect the glass transition temperature, melting point, crystallization temperature, and thermal degradation (Lizak, Murarova, & Mojumdar, 2012; Lizak & Mojumdar, 2013). ASTM D7138 is a standard test method used to determine the melting temperature of synthetic fibers, i.e., to determine the temperature at which a synthetic fiber specimen changes from a solid to a liquid-like state (ASTM D7138, 2008). The glass transition is also measured for amorphous or semicrystalline polymers. It is worth mentioning that synthetic fibers may either be amorphous or semicrystalline thermoplastics or thermosets. Thermoplastic fibers made of semicrystalline polymers comprise crystalline and amorphous regions and may be manufactured with a range of molecular weights. As described in ASTM D7138, the amorphous and crystalline fiber structure and large polydispersity may lead to a melting temperature range instead of a discreet melting point.

The test method can be used to determine the melting temperature of thermoplastic fibers, yarns, or threads. The test method is considered satisfactory for acceptance testing of commercial shipments. If the test method is used to identify a fiber material type, it is important to test a known reference material at the same laboratory with the same test method to confirm the fiber identification. In addition, since some types of fibers have similar melting temperatures or overlapping melting temperature ranges, secondary methods such as those described in test methods ASTM D276 or CAN/CGSB 4.2 No 14 will be required for fiber identification.

ISO 11357 specifies several DSC methods for the thermal analysis of polymers and polymer blends, such as thermoplastics, thermosets and elastomers. ISO 11357 is intended for the observation and measurement of various properties of the above-mentioned materials, such as physical transitions (glass transition, phase transitions such as melting and crystallization, polymorphic transitions, etc.), chemical reactions (polymerization, crosslinking and curing of elastomers and thermosets, etc.), stability to oxidation, and heat capacity.

For example, Iqbal and Sun (2016) reported the heat transfer property of multifilament yarn incorporated with microencapsulated phase change materials (MPCM) using a finite element method. The results of simulation after post-processing have been validated against experimental values which were obtained by DSC. The DSC method therefore shows its relevancy when studying thermoregulating effects.

4.3.1.9 Thermogravimetric analysis, ASTM E1131, ISO 11358

Thermogravimetric analysis, TGA, mainly allows the determination of basic constituents by weight loss upon heating. The ASTM E1131 standard (alternatively ISO 11358) is a standard test method for compositional analysis of solids and liquids by thermogravimetry. Materials analyzed by TGA include polymers, composites, laminates, and coatings.

TGA uses heat to induce reactions and physical changes in materials. TGA provides a quantitative measurement of the mass change in materials associated with transitions and thermal degradation. TGA records changes in mass due to dehydration, decomposition, and oxidation of a sample with time and temperature. The TGA curve represents the percent mass (weight) loss or its derivative versus temperature when the sample is heated at a uniform rate (heating rate) in a specific environment. The change in mass over specific temperature ranges provides an indication of the composition of the sample, including volatiles such as water and solvents, and inert additives or fillers, as well as indications of thermal stability.

Here are the main capabilities of TGA that can be applied to textile materials:

- Thermal stability of a material.
- Determination of temperature and weight change of decomposition reactions.
- Quantitative (or qualitative) composition analysis of a material.
- Measurement of the weight fraction of inorganic materials used as additives or fillers, such as carbon black, TiO_2, $CaCO_3$, $MgCO_3$, Al_2O_3, $Al(OH)_3$, $Mg(OH)_2$, talc, kaolin clay, and silica in a material.

4.3.1.10 Textile testing with thermal or sweating thermal manikins, ASTM F1291, ASTM F2732, and ISO 15831

There are several standards related to thermal testing of clothing fabrics on thermal or sweating thermal manikins: ASTM F1291, 2010; ASTM F2732, 2011; ISO 15831, 2004. ASTM F1291 (2010) is a "Standard Test Method for Measuring the Thermal Insulation of Clothing Using a Heated Manikin." The test method covers the determination of the insulation value of clothing ensembles. It describes the measurement of the resistance to dry heat transfer from a heated manikin to a relatively calm, cool environment. The evaporative resistance of a clothing ensemble can be measured in accordance with Test Method ASTM F2370 (2010).

ASTM F2732 (2011) is a "Standard Practice for Determining the Temperature Ratings for Cold Weather Protective Clothing." This standard practice covers the determination of the temperature rating of cold weather protective clothing ensembles. It involves measuring the insulation value of a clothing ensemble with a heated manikin in accordance with Test Method ASTM F1291 (2010) and using a heat loss model to predict the lowest environmental temperature for comfort.

ISO 15831 (2004) is entitled "Measurement of Thermal Insulation by Means of a Thermal Manikin." This international standard describes the requirements of the thermal manikin and the test procedure used to measure the thermal insulation of a clothing ensemble. It was developed to better simulate the situation of a wearer either standing or moving in a relatively calm environment. The test method also refers to ISO 9920 "Ergonomics of the Thermal Environment—Estimation of the Thermal Insulation and Evaporative Resistance of a Clothing Ensemble". The result in terms of thermal insulation provided by ISO 15831 may be compared with the value of required clothing insulation (IREQ) evaluated based on the environmental thermal conditions and the level of activity using ISO 11079 (2007).

In addition, tests may be conducted on gloves using a hand model (EN 511, 2006) and on footwear using a foot model (GCTT 4006-13). The thermal resistance is also

computed from the energy consumed to maintain the hand or the foot at a certain temperature (30–35°C for the hand and 27°C for the foot) while they are exposed to cold temperature in an environmental chamber.

4.3.1.11 Thermal effusivity with the modified transient plane source technique, ASTM D7984

ASTM D7984 (2016) is a test method for the measurement of the thermal effusivity of fabrics using an MTPS (modified transient plane source) instrument. Studies have shown that the perceived "warmth" of a material in contact with the skin is directly correlated with the initial rate of skin cooling (Pavlović, Stanković, Popović, & Poparić, 2014; Tessier & Noujaim, 2012; Wongsriruksa, Howes, Conreen, & Miodownik, 2012; Tiest, 2010; Hes, Araujo, & Djulay, 1996). This cooling rate is determined by the thermal effusivity of the material, making it the most reliable physical metric for evaluating the tactile acceptability of performance textiles. These studies also provide a relationship between the measured thermal effusivity and the perception of warmth to the touch.

The modified transient plane source is inspired from the transient plane source method (Yoneda & Kawabata, 1985) and has the specific advantages of fast test preparation (no sample preparation) and no need for calibration. This test method is also rapid at delivering test results: it can be performed in <5 s. In addition, the test method is well suited for textile testing and is nondestructive. Various materials pertaining to clothing and thermal insulation materials, such as woven fabrics, knitted fabrics, membrane-laminated fabrics, coated fabrics, foams, nonwovens and polymers, can be evaluated using this technique. Dry- and wet-state sample testing can also be performed at different temperatures (with a thermal chamber).

The thermal conductivity and effusivity analyzer, TCi from C-Therm Technologies Ltd, is based on the modified transient plane source technique. It is a characterization equipment that allows very precise and fast measurement of thermal properties, both thermal conductivity and effusivity, without sample preparation. Fig. 4.3 presents the TCi. The left side of Fig. 4.3 shows the compression test accessory (CTA) specifically designed for textiles. The CTA enables users to precisely control the level of compression or compaction applied on the specimen while characterizing the material's thermal conductivity. It is thus suitable, among other things, for textile fabrics, fleece materials, interlinings, and nonwovens.

With the C-Them TCi analyzer, the textile sample is in close contact with the thermal conductivity sensor (shown on both left and right sides of the figure) in order to achieve consistent results. A fixed amount of thermal energy, a known current, is applied through the sensor's heating element, providing a small amount of heat to the sample. That heat causes a rise of 1 to 1.5 K in the temperature at the surface of the sample. The temperature rise at the interface induces a change in the voltage of the sensor element.

In addition, the C-Them TCi has the flexibility to measure the thermal effusivity, which is related to the "temperature feel" of an object. The formulation for the determination of effusivity is provided by Eq. (4.4) (Section 4.2.2). The sensor can detect the heat flow from the textile material sample so the effusivity value can be

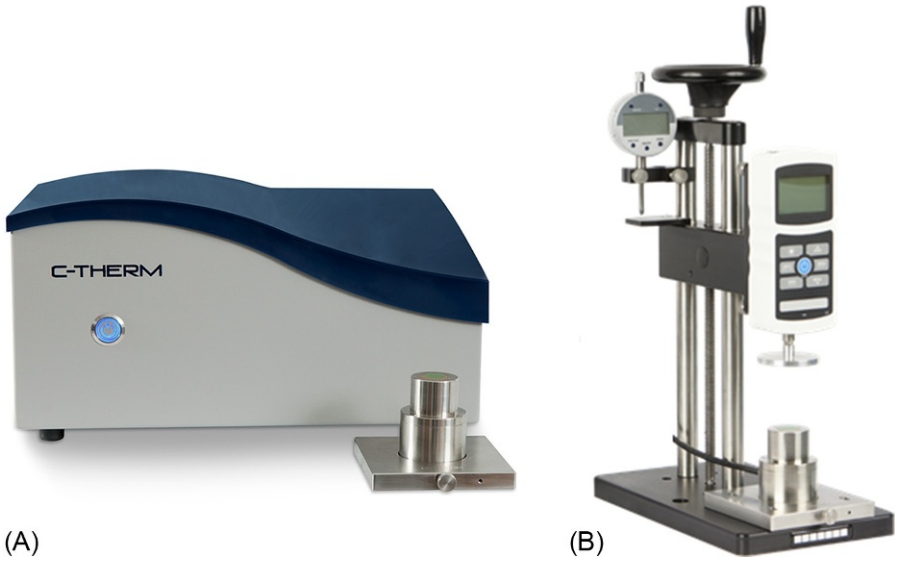

Fig. 4.3 Thermal conductivity and effusivity analyzer. (A) presents the TCi instrument and measuring device and (B) correspond to the compression test accessory (CTA) for textile testing that can be used with the TCi instrument and measuring device.
Courtesy of C-Therm Technologies Ltd.

obtained. Among other fabrics, layered sports textiles and nonwovens comprising aerogel particles have been characterized with the ASTM D7984 test method.

4.3.2 Other characterization techniques

4.3.2.1 Alambeta testing instrument

Özdil et al. (2007) evaluated the effect of yarn properties on the thermal comfort of knitted fabrics using the Alambeta testing instrument. The Alambeta testing instrument characterizes the thermal diffusion (heat transfer), thermal conductivity, and thermal resistance (insulation) of textile fabrics. A fabric specimen is placed between two plates, the bottom plate being heated, for example, at 40°C and the upper plate being maintained at a constant temperature. The upper plate comprises a measuring head containing a heat flow sensor. The upper plate moves downwards until it touches the sample placed on the bottom plate; at this moment, the surface temperature of the sample suddenly changes and the instrument computer registers the heat flow course. This allows the thermal energy to freely rise to the upper measuring plate through the specimen, without compressing the fabric specimen.

In addition, Hes and coworkers (Hes, 2008; Hes & Loghin, 2009; Bogusławska-Baczek & Hes, 2014; Mangat & Hes, 2015) showed that the Alambeta instrument is suitable for the investigation of the thermal properties of fabrics in the wet state. They were involved in the nondestructive determination of comfort parameters for functional garments and clothing and evaluated the heat, moisture, and air transfer properties of selected woven fabrics in wet state. Lately, they also determined the heat transfer by

radiation in textile fabrics by means of a method with known emissivity of plates using the Alambeta testing instrument (Bogusławska-Baczek & Hes, 2014). They also used this technique to assess the comfort aspects of denim garments (Mangat & Hes, 2015).

4.4 Applications

There are many types of products for which the evaluation of thermal properties is of importance such as for fibers, yarns, textile fabrics, multilayer fabrics, composite textiles, etc. Testing of thermal properties may be required, for example, in quality control, prototyping (R&D), and performance validation in order to meet specific thermal performance requirements. Not many thermal test methods apply to fibers; however, the thermal conductivity can be evaluated with the modified transient plane source technique. Otherwise, many test methods apply to textile fabrics and nonwovens.

4.4.1 Specialty fibers/yarns

Thermally insulating fibers and yarns are of high importance in the design of cold or hot protection clothing, boots, gloves, etc. Hollow fibers and microfibers are also gaining importance.

George and coworkers (George, Joseph, Nagarajan, Jose, & Skrifvars, 2013) investigated the thermal, calorimetric, and crystallization behavior of a polypropylene/jute yarn developed by the commingling technique. A commingled yarn is a yarn consisting of two or more individual yarns that have been combined, usually by means of air jets. In this particular development, the polypropylene continuous yarn filament formed the matrix around the jute yarn; heating lead to the consolidation of the resulting yarn. Within this study, TGA and DSC curves were obtained to study the effect of fiber content and also to follow the thermal decomposition (stability) and calorimetric (melting) behavior of untreated and various treated composite yarns.

4.4.2 Textile fabrics

Nonwoven, woven, or knitted fabrics play an important role in thermoregulation and hot/cold protection. Therefore, a lot of test methods apply such as those related to the thermal resistance: the tog test (Section 4.3.1.1), the clo test (Section 4.3.1.2), the sweating guarded hotplate (Section 4.3.1.3), and the TPP (Section 4.3.1.4). In addition, thermal conductivity can be assessed with the modified transient plane source technique (Section 4.3.1.11).

Weder, Rossi, and Crespy (2010) and Hes and Williams (2011) presented a review of test methods available for testing heat and mass transfer through textiles, membranes, and coatings for textiles; among those test methods are the sweating guarded hotplate (Section 4.3.1.3) and standard test methods with thermal manikins (Section 4.3.1.10).

4.4.3 Multilayer fabrics

There are many different possibilities related to multilayer fabrics and fabric assemblies. For example, these include membrane-laminated fabrics, coated fabrics, foam-coated fabrics, as well as assembly of different types of fabrics. For example,

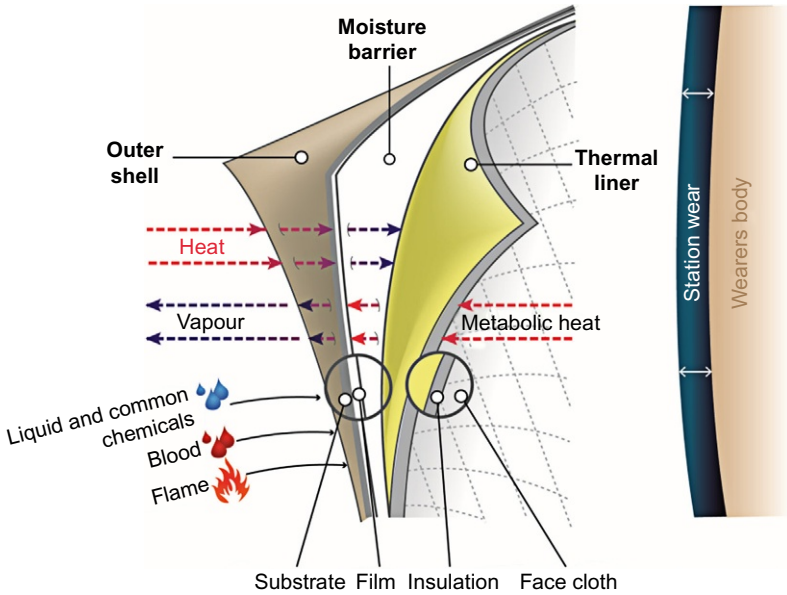

Fig. 4.4 Firefighter material assembly comprising three layers (Davis et al., 2010).

the THL test would be performed on a standard three-layer assembly used in firefighter protective clothing, which comprises a thermal barrier (representing the inner layer). Typically, the thermal barrier (thermal liner) may be comprised of a nonwoven fibrous material quilted with a face-cloth woven fabric that can be in a direct contact with the skin. A schematic representation of the firefighter material assembly (Davis, Chin, Lin, & Petit, 2010) is presented at Fig. 4.4. Also relevant to the firefighter, Barker (2011) published a chapter related to the evaluation of the heat stress and comfort of firefighter and emergency responder protective clothing. In his paper, thermal manikin and hot plate test methods (ISO 11092) are also discussed.

From another perspective, Paul and coworkers (Paul & Diller, 2003) compared the thermal insulation performance of different fibrous materials for an advanced space suit. They numerically analyzed the thermal conductivity performance for three candidate insulating fiber materials in terms of various denier (size), interstitial void fractions, interstitial void media, and orientations to the applied temperature gradient.

Recently, Rossi (2015) presented the basic construction of cold weather sportswear (base layer, middle layers, outer shell) and discussed the main properties of these layers. The author tried to show how the different layers interact with each other and how the layering concept can influence the performance of the clothing. Others, such as Mäkinen and Jussila (2014), presented a review about cold-protective clothing and related standard test methods used for their evaluations. Material properties were discussed and the role and function of different clothing layers for regulating thermal comfort and avoiding thermal stress were examined.

4.4.4 Phase change materials in textiles and clothing assemblies

A phase change material (PCM) is a thermoregulation material that can be used for its cooling, refreshing effect. The effect involves heat absorption during a reversible thermal transition from a solid to a liquid state. Most often, PCMs are microencapsulated, i.e., enclosed into microcapsules. These microcapsules can be incorporated into fibers, for example, in a melt extrusion process or applied as a coating using a liquid finishing process for instance. In the latter case, the liquid finishing formulation requires a polymeric binder in order to secure the microcapsules at the surface of the fibers and ensure durability to repeated washings.

The thermal analysis of fibers with PCM can be performed using DSC. From DSC test results, important information like the melting/fusion temperature transition range (the evolution toward the liquid state), the heat absorption (thermal storage capacity), and the stability upon thermal cycling (reusability) can be obtained. The energy absorption capacity is usually given in J/g. In addition, the freezing/crystallization temperature transition range (the evolution toward the solid state) and the heat exhaustion can be determined.

Tessier and Noujaim (2012) developed a novel flame-resistant PCM formulation and designed some leak-proof packets to contain it. Fig. 4.5 shows a DSC curve obtained with a PCM formulation made of a salt hydrate and other additives. On this

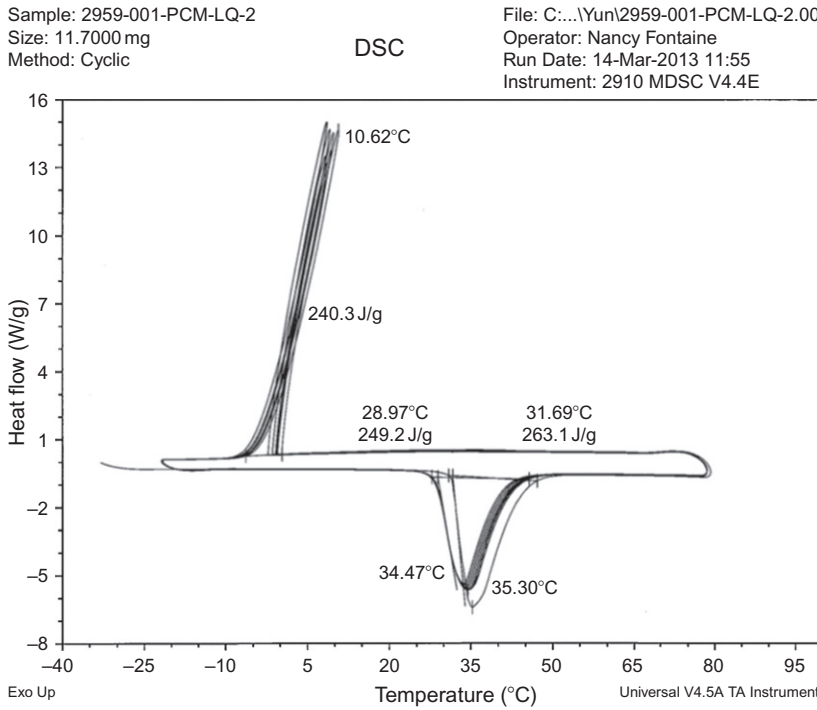

Fig. 4.5 DSC curve obtained from a PCM composition designed for a cooling (thermoregulating) vest.

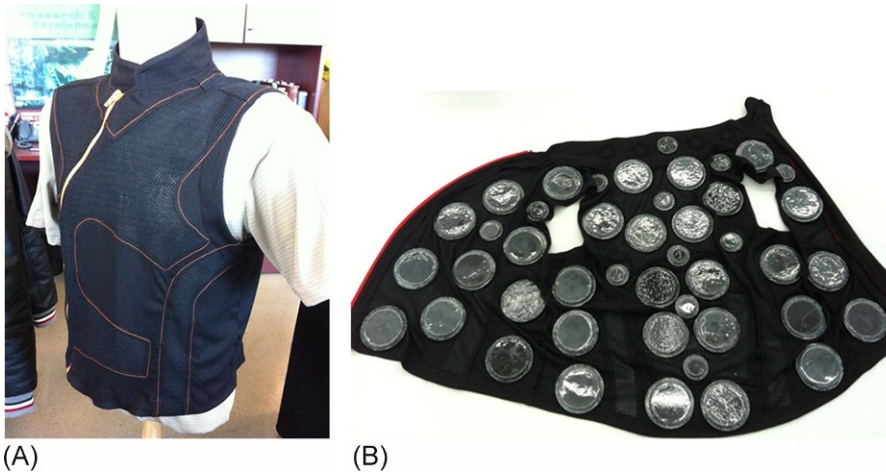

Fig. 4.6 Round PCM packets implemented into a thermoregulating vest.

figure, nine thermal cycles applied to the same PCM formulation are shown. The composition has a melting range spanning from about 28–29°C to 40–45°C and the crystallization is initiated around the water freezing point, for instance 0°C. In addition, the PCM formulation shows a very good freeze/melting stability after repeated thermal cycles. The heat absorption capacity of this PCM formulation is about 250 J/g.

PCM formulations shall be contained in leak-proof packets because the heating or temperature increase makes the PCM go from the solid to the liquid (molten) state. Then, the PCM packets can be inserted into or affixed to an underlayer (base layer) in order to obtain a cooling (thermoregulating) vest, as shown in Fig. 4.6. The PCM-cooling vest was developed in collaboration with Logistik Unicorp Inc., Quebec, Canada.

A thermophysiological study with human subjects wearing this PCM cooling vest was undertaken by Marchand et al. (2015). The PCM cooling vest was worn under a state-of-the-art firefighter uniform as well as a novel concept of uniform. The study, based on use of the ASTM F2300 (2010) standard, showed that the PCM cooling vest allowed a significant reduction of the thermophysiological stress when the cooling vest was worn next (close) to the skin. They observed that the PCM cooling vest allowed maintaining the microclimate temperature below 35°C, i.e., about five degrees lower than the control condition (without cooling vest), while performing the test. In addition, the relative humidity inside the garment (in the microclimate) was also reduced by ~17%, thereby improving comfort (Fig. 4.6).

4.5 Future trends

Thermal testing equipment and test methods such as ISO 11092 and ASTM F1868 were designed to assess performance of textile fabrics, nonwoven materials, and textile assemblies (multi-layer fabrics). On the other hand, the test method ASTM F2300

allows, among other things, the systematic evaluation of cooling garments worn by human subjects. This test method covers the physiological measurement of internal body core temperature, skin temperature, thermal exposure time, heart rate response, oxygen consumption, and whole body sweat rate. However, it requires a large number of human subjects and considerable budget and time to validate test results, i.e., to obtain statistically meaningful data.

Recently, advanced thermal testing equipment and manikins became available to evaluate thermal properties of socks, gloves, vests, jackets, boots and protective uniforms. For instance, a sweating thermal hand test set-up is presented in Fig. 4.7.

For testing that is specific to the thermal hand, only the EN511 standard applies. But because the system works on the principle of a sweating thermal manikin, typical thermal manikin standards could also theoretically be applied: ISO/DIS 15831, EN13537, ASTM F1291. Thermal manikins and sweating thermal manikins are becoming increasingly popular for thermal testing purposes. In addition, special designs could allow different motions like walking while testing.

In 2009, McCullough (2009) presented a paper related to the evaluation of cold weather clothing using manikins. Watson and co-workers (Watson, Nawaz, & Troynikov, 2013) also used a thermal manikin in order to design and evaluate sports garments for cold conditions. Testing was made with multilayered garment ensembles suitable for stop-go sport in subzero conditions. Wardiningsih, Troynikov, Nawaz, and Watson (2014) studied the influence of wearing impact protective garment on the thermophysiological comfort of the wearer. In their study, one commercially available hip impact protective garment was evaluated in terms of thermophysiological wear comfort by measuring, among other things, the dry thermal resistance and evaporative resistance using a thermal manikin. Another study from Troynikov and Ashyeri (2011) was focused on the thermoregulatory evaluation of triathlon suits, namely dry thermal resistance and evaporative resistance, carried out by means of a thermal manikin where the data were acquired in static, nonperspiring, and perspiring conditions.

Fig. 4.7 Thermal sweating hand test setup at the CTT Group.

Specific skin surface temperatures and sweating rates were allocated to different body zones relative to the triathlon activity.

Advanced thermal testing equipment often requires temperature and humidity chambers in order to have the flexibility to simulate different environmental conditions. Such set-ups allow performing testing, for example, in cold/dry or cold/humid conditions or, otherwise, in hot/dry or hot/humid conditions. Some chambers also offer air flow, i.e., wind-speed control, programmable thermal cycles, etc.

As the implementation of electrical devices for heating is progressing into fabrics and consumer goods, new test methods for the evaluation of thermal properties are being developed. Because controls allow increasing or reducing the heat rate, it is becoming more complex to evaluate. The market now offers battery-heated socks, gloves, vests, and jackets so the thermal properties may be adjusted in order to provide improved thermal comfort and cold protection.

4.6 Conclusion

As an introduction to this chapter focused on the testing of thermal properties of textiles, the important needs related to thermal comfort, cold protection, and protection against heat stress were discussed. Some of the state-of-the-art technologies and commercial products related to thermal comfort and protection have then been described.

The most relevant thermal properties related to textiles are thermal resistance, thermal conductivity, and effusivity. Test methods for thermal properties include tog and clo tests, sweated guarded hotplate, THL, TPP, contact heat test, radiant heat test, calorimetry and thermogravimetry analysis, thermal effusivity by modified transient plane source technique, and textile testing with thermal and sweating thermal manikins.

Applications related to thermal comfort, cold protection, and heat stress protection have been described with the use of specialty fibers/yarns, textile fabrics, multilayer fabrics and fibers, and textiles with PCMs. In terms of future trends, testing of thermal properties are progressively using advanced thermal testing equipment that is becoming available to evaluate thermal properties of socks, gloves, vests, jackets, boots, and protective uniforms. Several test methods exist to assess the performance of textile fabrics and textile assemblies (multilayer fabrics) in a coupon configuration. The arrival of thermal manikins, hands, and feet shows a need to include design, assembly, and textile making (garment making) considerations when designing thermally protective clothing. It is now necessary to consider both types of products—textile materials and ready-to-wear articles—in order to obtain a more complete picture for developers and end-users.

4.7 Sources of further information and advice

Novel thermal test methods for textiles are still being developed. Here are some references describing work in progress:

- Romeli D, Barigozzi G, Esposito S, Rosace G, Salesi G, High sensitivity measurements of thermal properties of textile fabrics, Polymer Testing, Volume 32 (6) 2013, pp 1029-1036.
- Hadded A, Benltoufa S, Fayala F, Jemni A, Thermo physical characterisation of recycled textile materials used for building insulating, Journal of Building Engineering, Vol 5, 2016, pp 34-40.
- Li W, Xu W, Wang H, Wang X, A dynamic tester to evaluate the thermal and moisture behaviour of the surface of textiles, Journal of Thermal Biology, Vol 55, 2016, pp 14-19.
- Zhu GC, Kremenakova D, Wang Y, Militky J, Mishra R, Study on air permeability and thermal resistance of textiles under heat convection, Textile Research Journal, vol 85 (16), 2015, pp 1681-1690.
- Neves SF, Campos JBLM, Mayor TS, On the determination of parameters required for numerical studies of heat and mass transfer through textiles – Methodologies and experimental procedures, International Journal of Heat and Mass Transfer, Vol 81, 2015, pp 272-282.

There are some interesting reviews on the subject of thermal test methods and thermal stress of protective clothing:

- Udayraj, Talukdar P, Das A, Alagirusamy R, Heat and mass transfer through thermal protective clothing – A review, International Journal of Thermal Sciences, Vol 106, 2016, pp 32-56.
- Crown EM, Batcheller JC, Technical textiles for personal thermal protection, Chap 9, Handbook of Technical Textiles (Second Edition), Woodhead Publishing (Ed), 2016, pp 271-285.
- Wang F, Chuansi Gao, Protective Clothing, Managing Thermal Stress, Woodhead Publishing (Ed), 1st Edition, 2014, pp 500.
- Tang Y, He Y, Shao H, Ji C, Assessment of comfortable clothing thermal resistance using a multi-scale human thermoregulatory model, International Journal of Heat and Mass Transfer, Vol 98, 2016, pp 568-583.

References

Abdel-Rehim, Z. S., Saad, M. M., El-Shakankery, M., & Hanafy, I. (2006). Textile fabrics as thermal insulators. *AUTEX Research Journal*, *6*(3), 148–161.

ASTM D1518. (2014). *Standard test method for thermal resistance of batting systems using a hot plate. Standard test method*.

ASTM D7138. (2008). *Standard test method to determine melting temperature of synthetic fibers. Standard test method*.

ASTM D7984. (2016). *Standard test method for measurement of thermal effusivity of fabrics using a modified transient plane source (MTPS) instrument*.

ASTM E1131. (2014). *Standard test method for compositional analysis by thermogravimetry*.

ASTM F1060. (2008). *Thermal protective performance of materials for protective clothing for hot surface contact*.

ASTM F1291. (2010). *Standard test method for measuring the thermal insulation of clothing using a heated manikin*.

ASTM F1868. (2014). *Standard test method for thermal and evaporative resistance of clothing materials using a sweating hot plate. Standard test method*.

ASTM F1939. (2008). *Radiant heat resistance of flame resistant clothing materials with continuous heating*.

ASTM F2300. (2010). *Standard test method for measuring the performance of personal cooling systems using physiological testing*.

ASTM F2370. (2010). *Standard test method for measuring the evaporative resistance of clothing using sweating manikin*.

Barker, R. (2011). Evaluating the heat stress and comfort of firefighter and emergency responder protective clothing. *Improving comfort in clothing*. Philadelphia, PA, USA: Woodhead Publishing. (chapter 12), pp. 305–319.

Bogusławska-Baczek, M., & Hes, L. (2014). Determination of heat transfer by radiation in textile fabrics by means of method with known emissivity of plates. *Journal of Industrial Textiles*, *44*(1), 115–129.

BS 4745. (2005). *Determination of the thermal resistance of textiles. Two-plate method: fixed pressure procedure, two-plate method: Fixed opening procedure, and single-plate method. Standard test method*.

Davis, R., Chin, J., Lin, C. C., & Petit, S. (2010). Accelerated weathering of polyaramid and polybenzimidazole firefighter protective clothing fabrics. *Polymer Degradation and Stability*, *95*(9), 1642–1654.

EN 511 Standard. (2006). *Protective gloves against cold*. European Committee for Standardization (32 p.).

GCTTG 4006-13 test method. (n.d.). Cote de confort thermique au niveau de pied à sec et humide (Thermal comfort index for the dry and wet foot). CTT Group.

George, G., Joseph, K., Nagarajan, E. R., Jose, E. T., & Skrifvars, M. (2013). Thermal, calorimetric and crystallisation behaviour of polypropylene/jute yarn bio-composites fabricated by commingling technique. *Composites Part A: Applied Science and Manufacturing*, *48*, 110–120.

Haase, J. (2013). Flame resistant clothing standards and regulations. *Handbook of fire resistant textiles*. Woodhead Publishing. (chapter 14), pp. 364–414.

Havenith, G. (2009). Laboratory assessment of cold weather clothing. *Textiles for cold weather apparel*. Boca Raton, FL, USA: Woodhead Publishing. (chapter 10), pp. 217–243.

Hes, L. (2008). Non-destructive determination of comfort parameters during marketing of functional garments and clothing. *Indian Journal of Fibre and Textile Research*, *33*, 239–245.

Hes, L., Araujo, M., & Djulay, V. (1996). Effect of mutual bonding of textile layers on thermal insulation and thermal contact properties of fabric assemblies. *Textile Research Journal*, *66*(4), 245–250.

Hes, L., & Loghin, C. (2009). Heat, moisture and air transfer properties of selected woven fabrics in wet state. *Journal of Fiber Bioengineering and Informatics*, *2*(3), 141–149.

Hes, L., & Williams, J. (2011). Laboratory measurement of thermo-physiological comfort. *Improving comfort in clothing*. Woodhead Publishing. (chapter 5), pp. 114–137.

Holman, J. P. (1986). *Heat transfer* (6th ed.). New York, NY: McGraw-Hill Book Company. pp. 373–472.

Holmes, D. A. (2000). Waterproof breathable fabrics. In A. R. Horrocks & S. Anand (Eds.), *Handbook of technical textiles* (pp. 282–315). CRC Press/Woodhead Publishing.

Iqbal, K., & Sun, D. (2016). Finite element analysis of functional yarn with thermal management characteristics. *Thermochimica Acta*, *636*, 33–41.

ISO 6942. (2002). *Protective clothing—Protection against heat and fire—Method of test: Evaluation of materials and material assemblies when exposed to a source of radiant heat. Standard test method*.

ISO 9151. (1995). *Protective clothing against heat and flame–Determination of heat transmission on exposure to flame, Standard test method*.

ISO 11079. (2007). *Ergonomics of the thermal environment—Determination and interpretation of cold stress when using required clothing insulation (IREQ) and local cooling effects. Standard test method*.

ISO 11092. (2014). *Textiles—Physiological effects—Measurement of thermal and water-vapour resistance under steady-state conditions (sweating guarded-hotplate test). Standard test method*.

ISO 11357. (2009). *Plastics—Differential scanning calorimetry (DSC), Standard test method*.

ISO 11358. (2014). *Plastics—Thermogravimetry (TG) of polymers*.

ISO 17492. (2003). *Clothing for protection against heat and flame—Determination of heat transmission on exposure to both flame and radiant heat. Standard test method*.

Lizak, P., & Mojumdar, S. C. (2013). Thermal properties of textile fabrics. *Journal of Thermal Analysis and Calorimetry*, *112*(2), 1095–1100.

Lizak, P., Murarova, A., & Mojumdar, S. C. (2012). Heat transfer through a textile layer composed of hollow fibres. *Journal of Thermal Analysis and Calorimetry*, *108*, 851–857.

Mäkinen, H., & Jussila, K. (2014). Cold-protective clothing: Types, design and standards. *Protective clothing*. Waltham, MA, USA: Woodhead Publishing. (chapter 1), pp. 3–38.

Mandal, S., & Song, G. (2014). An empirical analysis of thermal protective performance of fabrics used in protective clothing. *Annals of Occupational Hygiene*, *58*(8), 1065–1077.

Mandal, S., & Song, G. (2015). Thermal sensors for performance evaluation of protective clothing against heat and fire: A review. *Textile Research Journal*, *85*(1), 101.

Mandal, S., Song, G., Ackerman, M., Paskaluk, S., & Gholamreza, F. (2013). Characterization of textile fabrics under various thermal exposures. *Textile Research Journal*, *83*(10), 1005–1019.

Mangat, M. M., & Hes, L. (2015). Comfort aspects of denim garments. *Denim manufacture, finishing and applications*. Waltham, MA, USA: Woodhead Publishing. (chapter 15), pp. 461–479.

Marchand, D., Gauvin, C., Brien-Breton, A., Aubertin-Leheudre, M., Tessier, D., & Sadier, Y. (2015). Évaluation de nouvelles technologies visant à réduire le stress thermophysiologique associé au port de vêtements individuels de protection pour les pompiers. Rapport scientifique. Publications de l'IRSST, Rapport no R-891, 28 octobre 2015.

McCullough, E. A. (1991). Evaluation of milkweed floss as an insulative fill material. *Textile Research Journal*, *61*(4), 203–210.

McCullough, E. A. (2009). Evaluation of cold weather clothing using manikins. *Textiles for cold weather apparel*. Boca Raton, FL, USA: Woodhead Publishing. (chapter 11), pp. 244–255.

Morris, G. J. (1953). Thermal properties of textile materials. *Journal of the Textile Institute*, *44*, 449.

National Bureau of Standards. (1938). Improved apparatus for measuring the thermal transmission of textiles. *Journal of the Franklin Institute*, *225*(1), 97–98.

National Bureau of Standards. (1944). Thermal properties of moist fabrics. *Journal of the Franklin Institute*, *237*(6), 469–470.

NFPA 1971. (2013). *Standard on protective ensembles for structural fire fighting and proximity fire fighting, 2013*.

Nylstar. (2014). Textile web article. http://www.textileweb.com/doc/meryl-nexten-0001. Corporate brochure, Nylstar_Meryl_Nexten_2014.pdf.

Özdil, N., Marmaralı, A., & Kretzschmar, S. D. (2007). Effect of yarn properties on thermal comfort of knitted fabrics. *International Journal of Thermal Sciences*, *46*(12), 1318–1322.

Paul, H. L., & Diller, K. R. (2003). Comparison of thermal insulation performance of fibrous materials for the advanced space suit. *Journal of Biomechanical Engineering*, *125*(5), 639–647.

Pavlović, S. S., Stanković, S. B., Popović, D. M., & Poparić, G. B. (2014). Transient thermal response of textile fabrics made of natural and regenerated cellulose fibers. *Polymer Testing*, *34*, 97–102.

Rossi, R. M. (2015). Cold weather sports clothing. *Textiles for sportswear*. Waltham, MA, USA: Woodhead Publishing. (chapter 9), pp. 197–212.

Sale, P. D., & Hedrick, A. F. (1924). Measurement of heat insulation and related properties of blankets. *Journal of the Franklin Institute*, *198*(6), 827–829.
Tessier, D., & Noujaim, N. (2012). *Caracterisation of PCM pastes, powders and packets (macroencapsulation) using C-Therm Tci thermal conductivity and effusivity analyzer*. In *2012 North American Thermal Analysis Society Conference, Orlando, 12–15 August*.
Tessier, D., & Simard, F. (2014). *Oil absorption performance of milkweed hollow-fiber in sorbent pads & round booms*. In *The Institute of Textile Science, 112th Scientific Session, Banff, May 6*.
Tiest, W. M. B. (2010). Tactual perception of material properties. *Vision Research*, *50*(24), 2775–2782.
Troynikov, O., & Ashyeri, E. (2011). Thermoregulatory evaluation of triathlon suits in regards to their physiological comfort properties. *Procedia Engineering*, *13*, 357–362.
Ukponmwan, J. O. (1993). The thermal-insulation properties of fabrics. *Textile Progress*, *24*(4), 1–54.
Vogt, J. J. (1998). Heat and cold. In J. M. Stellman (Ed.), *Encyclopaedia of occupational health and safety* (pp. 42.1–42-55). USA: International Labour Organization [chapter 42].
Wardiningsih, W., Troynikov, O., Nawaz, N., & Watson, C. (2014). Influence of wearing impact protective garment on thermophysiological comfort of the wearer. *Procedia Engineering*, *72*, 551–556. The Engineering of Sport 10.
Watson, C., Nawaz, N., & Troynikov, O. (2013). Design and evaluation of sport garments for cold conditions using human thermoregulation modeling paradigm. *Procedia Engineering*, *60*, 151–156.
Weder, M., Rossi, R., & Crespy, D. (2010). Testing heat and mass transfer through membranes and coatings for textiles. *Smart textile coatings and laminates*. Boca Raton, FL, USA: Woodhead Publishing. (chapter 4), pp. 95–122.
Wongsriruksa, S., Howes, P., Conreen, M., & Miodownik, M. (2012). The use of physical property data to predict the touch perception of materials. *Materials and Design*, *42*, 238–244.
Yoneda, M., & Kawabata, S. (1985). Analysis of transient heat conduction and its application. *Journal of Textile Machinery Society of Japan*, *31*(4), 79.
Zhai, L. N., & Li, J. (2015). Prediction methods of skin burn for performance evaluation of thermal protective clothing. *Burns*, *41*(7), 1385–1396.

Further reading

ASTM F1930. (2015). *Standard test method for evaluation of flame resistant clothing for protection against fire simulations using an instrumented manikin*.
Kilinc-Balci, F. S. (2011). Testing, analyzing and predicting the comfort properties of textiles. *Improving comfort in clothing*. Philadelphia, PA, USA: Woodhead Publishing. (chapter 6), pp. 138–162.
Rossi, R. M. (2005). Interactions between protection and thermal comfort. *Textiles for protection*. Boca Raton, FL, USA: Woodhead Publishing. (chapter 10), pp. 233–260.
Venkataraman, M., Mishra, R., Jasikova, D., Kotresh, T. M., & Militky, J. (2014). Thermodynamics of aerogel-treated nonwoven fabrics at subzero temperatures. *Journal of Industrial Textiles*, *45*(3), 387–404. https://doi.org/10.1177/1528083714534711.
Zhu, G. C., Kremenakova, D., Wang, Y., Militky, J., & Mishra, R. (2015). Study on air permeability and thermal resistance of textiles under heat convection. *Textile Research Journal*, *85*(16), 1681–1690.

Tests for evaluating textile aging

5

M. Fulton, M. Rezazadeh, D. Torvi
University of Saskatchewan, Saskatoon, SK, Canada

5.1 Introduction

There are a large number of standard tests for evaluating the performance of textiles when they are new, many of which are described in the other chapters in this book. However, end users are not only interested in the performance of textiles when they are new, but the continuing performance of textiles, and the products that contain these materials, over their entire useful life. In many cases, end users also need methods to determine when to replace textile products. In some applications, such as protective clothing, the continuing performance of this clothing and the ability to determine when to replace it will have a significant impact of the safety of end users.

This chapter will briefly review textile aging processes, as well as how these processes affect important aspects of textile performance. Recent research to quantify the effects of aging on textile performance will be discussed, along with standard and nonstandard tests that can be used to evaluate the continuing performance of textiles. In many cases, the same tests that are used to evaluate the textiles when new are used to determine the change in one or more specific aspects of performance of used textiles.

One particular important issue with evaluating performance of in-use textiles is that most standard tests are destructive. Therefore, in many applications these tests cannot be practically used to evaluate the performance of in-use clothing, especially when this clothing is expensive, such as firefighters' protective clothing. To address this issue, nondestructive tests are being developed to provide information to aid in evaluating in-use textiles and determining whether or not to replace individual products, as is already being done in engineering applications, such as the evaluation of urban infrastructure. Therefore, this chapter will focus on recent developments in the use of nondestructive tests for fabrics. Statistical and other methods to use data from tests of in-use textiles to predict their remaining lifetime will also be discussed.

5.2 Textile aging

One general definition of aging, which can be applied to textiles, is the accumulation of all changes in a system with the passage of time (Timiras, Quay, & Vernadakis, 1995). Changes are irreversible and usually cause decline or loss of functionality, although some features may improve because of aging (Johnson, 2005). The major destructive consequence of textile aging is degradation.

Degradation is defined as weakening and loss of properties that are necessary for satisfactory performance due to changes that occur because of the aging process

Advanced Characterization and Testing of Textiles. https://doi.org/10.1016/B978-0-08-100453-1.00006-4

(Slater, 1991). It is possible for textile degradation to occur prior to use. However, this chapter will primarily focus on aging that occurs after textiles have begun to be used. This chapter will also mainly focus on methods used to evaluate thermal protective clothing for firefighters and other workers, but similar testing methods for aging exist for other textiles.

Slater (1991) discusses the main causes of degradation of textiles and the mechanisms by which this degradation can occur. Some degradation may occur before a product reaches the end user because of the processing of textiles, either in the various stages of production of a fabric (Zhang et al., 2014; Zhao, Zhang, Zhang, & Lu, 2012), or during dyeing or finishing. Once a product reaches the end user, some degradation may occur during storage. Often degradation that occurs during either normal or severe use is of primary concern to the end user and may have a large impact on performance (Cloud & Lowe, 1995). For example, for firefighters' protective clothing this degradation may be caused by a number of factors including:

- mechanical action (e.g., abrasion),
- environmental conditions (e.g., exposure to ultra-violet (UV) radiation, weathering, moisture),
- cleaning and maintenance procedures, and
- exposure to high temperatures and/or heat fluxes.

In some cases, end users are concerned with aging of textiles simply for aesthetic purposes (Slater, 1991). However, in other cases the aging of textiles may lead to a decrease in user safety. For example, thermal protective fabrics commonly used for outer shells in firefighters' protective clothing have been shown to degrade with wear associated with normal use as well as exposures to high temperatures and other conditions (Davis, Chin, Lin, & Petit, 2010; Rezazadeh, 2014; Thorpe, 2004). Therefore, it is very important for firefighters to understand how their protective clothing may degrade with use. While methods for evaluation and testing of new firefighters' protective clothing ensembles are well defined (e.g., NFPA 1971, 2013) many retirement criteria for high-performance protective clothing are mainly based on visual indicators (e.g., NFPA 1851, 2014). An ensemble may be retired after significant visual signs of aging (rips, tears, severe discoloration) appear or after a useful-lifespan criterion specified by the manufacturer or a relevant standard is reached.

One particular concern is that some types of damage to firefighters' protective clothing and other textiles, such as tears, fading, and brittleness are quite apparent during visual inspection. But the level of damage to the textiles may not be completely reflected by visible degradation. Slater (1986) noted performance may degrade below minimum accepted levels before emergence of any visual cues. He also defined two levels in degradation of fabrics: a functional level and a visual level. The functional level is the limit below which the fabric becomes functionally unacceptable. The visual level is the point at which visual indicators of deterioration like color fade or tears become visible to the naked eye, which usually does not coincide with the functional level threshold (Slater, 1986). This issue could bring about severe consequences in specialized clothing such as firefighters' protective clothing if degradation past the functional level occurred before the visible level was reached. For example,

Davis et al. (2010) could not determine if there was significant deterioration in mechanical strength of exposed specimens by means of visual inspection or pulling on the fabrics by hand. However, measured values of tensile and tear strength of these aged fabrics were lower than the values for new fabrics. Hence, there is a possibility that discoloration and manual inspection of a garment for physical damage (rips, tears, cuts, seam integrity, broken stitches) and thermal damage (charring, burn holes) will not identify an unacceptable level of deterioration (Thorpe, 2004).

Detailed discussions on the individual aging degradation mechanisms (e.g., UV radiation, thermal exposures) can be found in previous work by Slater (1991), Rezazadeh and Torvi (2011), and Rezazadeh (2014). In order to understand the overall effects of aging on individual textile products the effects of a number of factors will need to be understood (Rezazadeh, 2014) including:

- the type of material used to manufacture the textile;
- the nature of conditions under which textiles are used, including resulting exposures to high temperatures and heat fluxes, chemicals, and ultraviolet radiation;
- wear and abrasion patterns; and
- the specific maintenance procedures used for the textiles.

These factors may vary considerably even for textiles that are used for similar applications. The remainder of this chapter discusses methods that can be used to evaluate the effects of textile aging on performance in the laboratory and under field conditions.

5.3 Tests for textile aging

A study of the effects of aging on textile performance generally involves two phases. The first phase is either sampling in-use textiles or using laboratory tests to simulate the expected aging processes in the field. The second phase is to evaluate the performance of the textile, and to compare this performance to the same textile when it is new, or to some performance standard. This section will first describe some of the ways that are used to simulate aging of textiles in the laboratory. Methods of evaluating performance, most of which are destructive tests included in standards for new textiles, are briefly described. Examples of research in which these and other methods have been used to evaluate the effects of aging on performance of textiles are then provided.

5.3.1 Methods to simulate aging

It is very important to understand the similarities and differences between exposures in the laboratory and field when interpreting the results of performance testing. Field conditions will often expose a fabric to repeated and combined degradation factors. On the other hand, many laboratory testing procedures and testing devices are based on only one specific type of exposure. Bridging the gap between controlled laboratory conditions and real-world situations is an ongoing area of active research. Some examples of textile aging research are summarized in Tables 5.1 and 5.2.

Table 5.1 Summary of textile aging research

Investigator(s)	Textiles tested	Aging method(s)	Parameters studied
Abrasion			
Chen and Cloud (2000)	Nonwoven fabrics used in chemical protective clothing	Brush pilling tester (ASTM D3511) and random tumble pilling test (ASTM D3512) in wet and dry conditions	– Surface wetting – Liquid retention – Liquid penetration
Jasinska and Stempien (2014)	Lyocell, tencel, and cotton	Random tumble pilling test (ASTM D3512), brush pilling tester (ASTM D3511), and a modified Martindale method (ASTM D4966, EN ISO 12945-1/2:200)	– Gradation and degree of pilling on fabric surfaces (using digital image analysis)
In-use wear, field studies			
Makinen (1992)	Firefighters' protective clothing	Specimens taken from new and in-use clothing (4–10+ years of service) Laundering in the laboratory	– Flame resistance – Mechanical properties (tensile/tear strength) – Abrasion resistance
Vogelpohl (1996)	20 used firefighters' protective clothing specimens	Specimens donated from active service and training programs (1–5+ years of service)	– NFPA 1971 requirements – Mechanical properties (tensile/tear strength, seam strength) – Flame resistance – Water resistance – Abrasion resistance, zipper operation resistance
Vogelpohl and Easter (1997)	Used firefighters' protective clothing	1–5+ years in service	– Flame resistance (char length/after-flame time) – TPP – Water absorption and penetration resistance – Mechanical properties (tensile/tear strength)
House and Squire (2004)	Firefighters' protective hood	15–20 days of use (including daily laundering) at firefighter school	– Estimated burn injury after 1–10 s thermal mannequin exposures

Cinnamon (2013)	108 used firefighters' protective clothing specimens	Field studies, specimens in active service for 10–20 years	– Age (vs 10-year retirement guidelines) – TPP – Mechanical properties (tensile/tear strength, seam strength) – Water penetration – Visual inspection results (NFPA 1971; NFPA 1851)
McQuerry, Klausing, Cotterill, and Easter (2015)	108 used firefighters' protective clothing specimens	Field studies, specimens in active service for 2–10 years	– Age (vs. 10-year retirement guidelines) – TPP – Mechanical properties (tensile/tear strength, seam strength) – Water penetration – Visual inspection results (NFPA 1971; NFPA 1851)
Maintenance/cleaning procedures			
McSherry, Reeves, Markezich, and Cooper (1975)	Flame-resistant treated cotton fabrics	Laundering based on AATCC test method (varied detergent and number of cycles)	– Flame resistance (char length)
Hsu and Cheek (1989)	Ramie, cotton, and rayon knits	Laundering procedures (hand washing and machine washing) followed by tumble drying or flat drying	– Dimensional stability
Loftin (1992)	Treated and inherently flame resistant fabrics used in thermal protective clothing	Industrial laundering for up to 100 washing cycles	– Flame resistance (after-flame/afterglow time, char length) – Thermal protection – Mechanical properties (tensile/tear strength)
Stull, Dodgen, Connor, and McCarthy (1996)	Firefighters' protective clothing	Six different types of cleaning procedures	– Flame resistance (char length/after- flame) – Tear and seam strength – Water penetration resistance

(Continued)

Table 5.1 Continued

Investigator(s)	Textiles tested	Aging method(s)	Parameters studied
Mettananda (2009)	Treated and inherently flame resistant fabrics used in thermal protective clothing	Contaminated specimens with motor oil and then laundered using domestic washing machine and six laundering procedures	– Flame resistance (damaged length, after-flame time) – Limiting oxygen index – Remaining oil
Pinto, Carr, Helliker, Girvan, and Gridley (2012)	Military body armor	Residential dryer for up to 10 h	– Ballistic performance
Atalay, Bahadir, and Kalaoglu (2015)	Outer shell, moisture barrier, and thermal liner for firefighter protective clothing	EN469 washing standard, five cycles according to ISO 6330:2012 standard	– TPP (40 and 80 kW/m^2 heat fluxes) – Water vapor permeability
Chemical degradation			
Park, Seo, Ma, and Lee (2002)	Kevlar in a composite matrix	Chemical surface treatments (0–35 wt% phosphoric acid)	– pH, X-ray photoelectron spectroscopy, FTIR analysis – Interlaminar shear strength and fracture energy
Szostak-Kotowa (2004)	Natural (cotton, wool, silk) and synthetic fibers (polyester, polyurethane, polyaramid)	Biodeterioration, microbacterial and fungal growth	– Mechanical properties (tensile strength and elongation) – Color and appearance changes, aesthetics – Chemical structure changes
Ultraviolet radiation and weathering			
Barnett and Slater (1991)	Cotton/nylon blends	Xenon-arc exposure at specific temperature and relative humidity (RH) with and without water spray	– Mechanical properties (tensile and tear strength) – Abrasion resistance
	Dyed and undyed Inherently flame resistant fabrics	Xenon-arc lamp	– Color fastness – Mechanical properties (tensile strength) – Limiting oxygen index

Poli, Toniolo, and Sansonetti (2006)	Polymer coatings for protecting low porosity stones	Xenon-arc lamp	– Water-repellencey
Zhang et al. (2006)	Outer shell for firefighters' protective clothing	Carbon-arc lamp, 40°C and 45% RH	– Mechanical properties (tensile/tear strength) – XRD and SEM – Calorimetry – ATR-FTIR chemical changes
Davis et al. (2010)	Inherently flame resistant fabrics	Mercury-arc lamp, 50°C and 50% RH	– Mechanical properties (tensile/tear strength) – UV transmission and protection – Microscopy
Day, Cooney, and Suprunchuk (1988)	Outer shell and moisture barrier fabrics for firefighters' protective clothing	Xenon-arc lamp, 60°C and 30% RH	– Color fastness – Mechanical properties (tensile/tear strength) – Flame resistance (char length/after-flame time) – Thermal protection
Arrieta, David, Dolez, and Vu-Khanh (2011b)	Outer shell for firefighters' protective clothing	UV (50–80°C) and hydrolytic aging environmental chamber (50–80°C, 60%–80% RH)	– Mechanical properties (breaking force) – ATR-FTIR chemical changes
Nazare, Davis, Peng, and Chin (2012)	Outer shell for firefighters' protective clothing	Moisture influence (dried versus 50% RH) and SPHERE mercury-arc lamp UV aging at 50°C and 50% RH	– ATR-FTIR chemical changes – UV protection factor – Performance properties (stretching, tear resistance, elasticity)
Aidani, Nguyen-Tri, Malajati, Lara, and Vu-Khanh (2013)	Moisture barrier with Nomex backing	UV (50–80°C) exposure with weather tester	– Mechanical properties (tensile/tear strength) – Chemical changes (FTIR) – X-ray diffraction, SEM – Calorimetry – Atomic force microscopy – Vapor permeability
Houshyar, Padhye, Nayak, and Shanks (2015)	Outer shell for firefighters' protective clothing	Weather-O-meter xenon lamp UV exposure, 40°C and 50% RH (ASTM G155)	– Mechanical properties (tensile/tear strength) – Abrasion resistance (Martindale method) – FTIR, SEM, TGA results – Photo/UV degradation aging process

Table 5.2 Examples of research on effects of thermal aging

Investigator(s)	Thermal aging method	Duration of thermal aging	Parameters studied
Day et al. (1988)	Exposure to 150–250°C in an oven	5 min–7 days	– Thermal shrinkage and weight loss – Flame resistance (char length/after-flame time) – TPP – Tear strength
An, Barker, and Stull (1989)	Convective exposure at 94°C in an oven Conductive exposure at 94°C on a metal plate	4 h 5 min	– Mass per unit area – Mechanical properties (tensile/tear strength, bending flexibility) – Chemical permeation resistance
Iyer and Vijayan (1999) and Iyer et al. (2006)	Exposure to 150–550°C in a furnace	0.5–7000 h (1–12 stages)	– X-ray diffraction pattern – Weight loss – Mechanical properties (tensile strength) – Microstructural features
Jain and Vijayan (2002)	Exposure to 200–400°C in a furnace	0.5–2000 h (1 stage)	– X-ray diffraction pattern – Weight loss – Mechanical properties (tensile strength) – Microstructural features
Thorpe (2004)	Exposure to 5–30 kW/m^2 using radiant panel	30–3600 s	– Conductive and compressed heat resistance (CCHR) rating – Mechanical properties (tensile/tear strength) – Water penetration resistance
Rossi, Bolli, and Stampfli (2008)	Two exposures to 40 (quartz tubes) or 80 kW/m^2 (Meker burner)	17–33 s	– Required time for 12°C or 24°C temperature rise of a test sensor (t_{12} or t_{24}) – Mechanical properties (tensile/tear strength)

Arrieta, David, Dolez, and Vu-Khanh (2010)	Extended exposure, temperatures from 190°C to 320°C	From hours for high temperatures and weeks for low temperatures	– Mechanical properties (breaking strength, thermal life) – FTIR
Aidani, Dolez, and Vu-Khanh (2011)	Oven from 190°C to 320°C	1–1056 h	– Mechanical properties (tensile/tear strength, ASTM D5587) – Vapor permeability
Rezazadeh (2014)	Exposures to cone calorimeter (10–40 kW/m^2) Multiple exposures at 20 kW/m^2 (15–150 s)	10–2600 s	– Mechanical properties (tensile/tear strength) – SEM evaluation – Water vapor permeability/penetration – TPP – Colorimetry – NIR reflectance
Ozgen and Pamuk (2014)	Oven from 220°C to 300°C	1–30 days	– Mass loss – Mechanical properties (tensile strength)
Wang and Li (2015)	Repeated high heat flux exposure 84 kW/m^2 using a traversing thermal mannequin or a bench scale apparatus	Repeated 3 s exposures for both bench and mannequin test	– TPP – Mechanical properties (tensile/tear strength, shrinkage, fabric thickness) – SEM evaluation
Cui, Ma, and Lv (2015)	Exposure from a quartz tube (6.5 and 9.7 kW/m^2)	5–30 min	– Mechanical properties (tensile/tear strength and elongation at break) – TPP – SEM evaluation – FTIR-Raman spectroscopy

Selecting appropriate aging protocols is key to obtaining laboratory results that can be related to expected performance in the field. For example, variations between individual fire departments and individual firefighter roles make for a wide range of expected exposure conditions, in terms of both exposure intensity and frequency. One method that has been used in the past is to classify the heat flux and temperature exposures that firefighters are subjected to as routine, ordinary, and emergency conditions (Abbott & Schulman, 1979; Donnelly, Davis, Lawson, & Selepak, 2006). For each of these classifications, a temperature and heat flux range is given, which can then be used to set heat flux and temperature exposure levels for thermal aging in a laboratory environment. A more detailed breakdown of this process is outlined by Rezazadeh (2014) who used information from the literature and measurements made in field fire tests to develop laboratory exposures to simulate the range of conditions that firefighters face during their duties.

5.3.1.1 Mechanical action

Textiles and products containing textiles are used in physical activities which may result in abrasion. For example, textiles used in clothing can be subjected to large mechanical forces when they are in contact with other surfaces, and individual layers of fabric within the clothing system can also be in contact with each other (Rezazadeh & Torvi, 2011). Mechanical wear can also occur from laundering of fabrics (Vanderschaaf, Batcheller, & Torvi, 2015).

One concern is that research has shown that the actual abrasion of textiles cannot be completely simulated in the laboratory. Slater (1987) clarified how different tests used to simulate abrasion produce different modes of degradation in the fabrics. Two common testing procedures commonly used for experimental studies are outlined in ASTM D3512/D3512M (2014) and ASTM D3511/D3511M (2015) for random tumble pilling testing and brush pilling testing, respectively. ASTM D3512 is intended for use with knits or woven textiles and makes use of a machine containing a cylindrical test chamber lined with an abrasive material while ASTM D3511 requires a random brush pilling apparatus. Both posttest evaluation methods involve examination of the textile surface in a well-lit chamber accompanied with comparative notes to other tested samples. Alternatives to laboratory abrasion testing include real-world sampling of functional garments obtained from longer-term wear tests, but these field tests may take a longer period of time to complete and potentially destroy entire functional garments (Vanderschaaf et al., 2015).

Bresee, Annis, and Warnock (1994) explained that abrasion of fabrics through simulated methods in the laboratory could not bring about the same fuzzing and pilling on the fabrics as in actual use. Abrasion in the field is caused by a variety of frictional forces in different directions over a relatively long period, while the mechanism of simulated abrasion is based on exerting intensive force in specific directions. Bresee et al. (1994) examined specimens that had been abraded during simulated physical activity by volunteers and three different apparatus: the Fiber Transfer Abrasion Tester (Annis & Bresee, 1990), the Random Tumble Pilling Tester (ASTM D3512), and the Brush Pilling Tester (ASTM D3511). A qualitative comparison to other tested specimens is often used

to rank pilling and abrasion resistance, but more recent developments in digital image analysis has led to increased research in quantitative evaluation methods (Jasinska & Stempien, 2014).

5.3.1.2 Weathering, environmental, and UV aging

Laboratory simulated UV exposures require the use of specialized weathering equipment such as a Simulated Photodegradation via High Energy Radiant Exposure (SPHERE) device or a xenon-arc lamp (Davis et al., 2010). Conversions between sun irradiance to actual outdoor exposure will vary from machine to machine, but one example related to firefighting protective clothing aging in days can be found in Davis et al. (2010). Further information on outdoor weathering conditions and photodegradation predictions can be found in Pickett and Sargent (2009).

5.3.1.3 Maintenance/cleaning procedures

The repeated washing and drying of textile garments has been known to have a detrimental impact on both aesthetics and textile performance (Slater, 1991). Even a single incorrect washing procedure may have an immediate destructive impact on some types of clothing. Therefore, manufacturers will provide instructions on cleaning, and standards organizations have published detailed guidelines for cleaning and maintenance, including NFPA 2113 (2015) and NFPA 1851 (2014). Both of these NFPA standards make reference to either ASTM F2757-09 (2016) or ASTM F1449 (2015). Many standard tests (e.g., ASTM F2700; ASTM D3511) recommend laundering of fabric specimens prior to testing in order to remove both surface contamination and factory surface finishes, and then also refer to specific standards for instructions on this laundering (ASTM F2757-09; ASTM F1449-08; ASTM D3938). Collier, Bide, and Tortora (2009) also provides details on laundering procedures. Assuming that end users follow these instructions or guidelines, these same documents can be used in the laboratory to simulate aging of textile due to cleaning and maintenance. As fabrics can also become soiled and contaminated with use, determining the effectiveness of cleaning and maintenance procedures is also an important aspect of aging. One example of an evaluation of laundering considerations based on soiling release properties can be found in a study by Mettananda and Crown (2010).

5.3.1.4 Thermal aging

Firefighters and other workers can be exposed to both high temperatures and heat fluxes. Therefore, many research studies on aging of these types of fabrics focus on thermal exposures (Day et al., 1988). Intensity, temperature, duration of exposure, and frequency of exposure will all influence aging of fabrics (Rezazadeh, 2014). One other piece of information that is valuable when evaluating thermal aging is information on expected temperatures that a textile may reach during exposure, and temperatures which are necessary for changes to occur to the textile (e.g., dye loss and onset of

thermal-chemical changes). This information can be used to understand the possible material or chemical structure changes as will be discussed in Section 5.3.2.

Laboratory procedures used for thermal aging can be largely grouped into two main categories; full scale or bench scale tests. Full scale tests have the advantage of being able to test entire protective clothing ensembles, but have a relatively large cost and significant testing facility requirements. Bench scale tests are less expensive and facilities are more widely available. However, only a small fabric sample is tested.

Examples of tests that can be used to thermally age fabrics include thermal protection performance (TPP) (ASTM F2700-08, 2013) or radiative protective performance (RPP) (ASTM F1939-15, 2015) procedures included in NFPA 1971 (2013) and other standards used to evaluate new fabrics. Depending on the standard, specimens are exposed to a heat flux provided from a primarily convective (e.g., laboratory burner), primarily radiative (e.g., quartz tubes), or combined convective/radiative exposure. The differences in convective and radiative components and wavelengths of thermal radiation should be considered when comparing laboratory and field exposures (Torvi, Rezazadeh, & Bespflug, 2016). Others have used other radiative heat sources to produce heat fluxes, such as the heater from the cone calorimeter, a piece of fire testing equipment typically used to test building materials (ASTM E1354-16a, 2016; Torvi et al., 2016). Thermal aging can also be performed using ovens or furnaces.

Bench scale tests do not account for clothing features (zippers, ties, loops, stitching, etc.,) that would be found in a full scale garment. Full scale testing facilities may include life-sized thermal mannequins that can be used to gain significant insight into thermal protective clothing performance (ASTM F1930-15, 2015). Examples include DuPont's Thermo-Man, Pyro Man at the Textile Protection and Comfort Centre, and the Instrumented Mannequin at the University of Alberta (Sipe, 2004). Many of these high-tech thermal mannequins are stationary, but recent research has been conducted into the influence of movement or occupant sweat generation on protective performance during emergency fire scenarios (Sipe, 2004; Udayraj, Talukdar, Das, & Alagirusamy, 2016).

5.3.1.5 Field studies

Some studies will involve testing of textiles that have been used in the field. These textiles will experience combined exposures to a number of factors, which may include UV degradation, high intensity thermal exposures, mechanical wear and other factors over a period of time. Examples of this research can be found in Table 5.1. These field studies offer a wealth of information, but major disadvantages include the time required to obtain the specimens necessary to perform the research and the absence of detailed information on the exposure conditions over the lifetime of the garments.

In some industries, organizations will take a sample of garments from their inventory and use these to assess the condition of other garments that are still in use. For firefighters' protective clothing this approach would be prohibitively expensive. There have been some research studies that have examined used firefighting equipment

(Vogelpohl & Easter, 1997). These studies may take a relatively long period of time and require the cooperation of active firefighting departments with a variety of used garments. This research is particularly important as some firefighters have a preference towards wearing aged and worn gear even though it may not be clear whether these ensembles continue to provide required protection levels (McQuerry et al., 2015). A summary of select field study results can be found in Table 5.1.

5.3.2 Methods to evaluate performance

Destructive testing methods for evaluating performance criteria of new textiles can be adapted to evaluate aged textiles. Studies are often based on standards used to specify performance for new textiles (e.g., CAN/CGSB-155.1, 2001; EN 367, 1992; EN 469, 2005; ISO 13506, 2008; ISO 6942, 2002; NFPA 1971, 2013). For example, NFPA 1971 (2013) outlines over 50 destructive test methods, which are used to evaluate protective ensembles for structural and proximity firefighting. Tests include the constant-rate-of-extension (CRE) tensile tests (ASTM D2261, 2013; ASTM D5034, 2013), and flammability testing methods (ASTM D1230-10e1, 2016; ASTM D6413/D6413M-15, 2015), which expose a textile specimen to a standardized flame using a specialized mounting apparatus. In a similar manner, aged firefighters' protective fabrics can be tested for a number of aspects of performance including:

- thermal protection,
- flammability,
- thermal shrinkage resistance,
- heat resistance,
- water resistance,
- dimensional stability, and/or
- tear strength.

Supplemental information provided by thermogravimetric analysis (TGA), microscopy and other methods can help to interpret test results and explain the effects of aging on performance. TGA is a thermal compositional analysis method often utilized in conjunction with spectroscopy in order to gain information on decomposition chemical reactions taking place (ASTM E1131-08, 2014). In this method a known mass of a substance, either solid or liquid, is heated at a controlled rate in a controlled atmospheric environment. Changes in mass can be used to determine temperatures at which physical and chemical changes of the textile structure occur. An example of a TGA curve for a protective fabric from Rezazadeh (2014) is shown in Fig. 5.1. Further microscopic evaluations (e.g., SEM) can also give valuable information on the microstructural changes taking place during aging processes (Rezazadeh, 2014).

5.3.3 Research examples

Examples of research into effects of aging on textile performance are shown in Tables 5.1 and 5.2. Examples of abrasion, weathering, maintenance/cleaning,

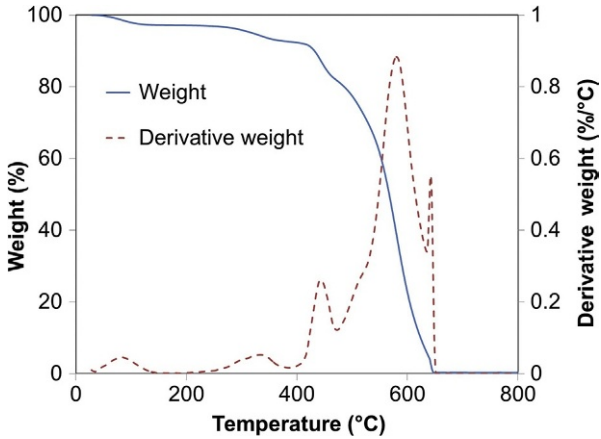

Fig. 5.1 Example of a mass-loss relation over a temperature range from TGA testing of a royal blue Nomex IIIA specimen (Rezazadeh, 2014).

environmental, UV, and chemical aging studies can be found in Table 5.1. A more detailed review of research in these areas can be found in (Rezazadeh & Torvi, 2011).

Table 5.2 provides a summary of examples of work on effects of thermal aging and continues a previous review (Rezazadeh & Torvi, 2011). Research has shown that flame resistance and mechanical properties of fabrics deteriorate more severely through thermal exposure than other aspects of performance (e.g., Rezazadeh & Torvi, 2011). Such a loss in mechanical strength is more noticeable during the early stages of exposure, while a loss in flame resistance properties may take longer to occur (Wang & Li, 2015). Wang and Li (2015) and others have noted that in some cases there can be an increase in TPP values after thermal exposures.

5.4 Nondestructive tests

As noted earlier, most standard tests used to evaluate textiles are destructive, and therefore are not suitable for evaluation of in-use textile products. A nondestructive test (NDT) technique is an evaluation method that gauges the current state of a material without influencing future performance (Rezazadeh, 2014). NDT methods may impact the material structure in some form, but these changes are often small enough to have a negligible influence on future performance. For example, acoustic impact testing can be used to find microdefects in a material structure while the material vibrations have no influence on future performance.

5.4.1 Purpose of NDT methods

In NDT methods some properties of the material serve as indicators of performance deterioration. Measurements of these properties are then used to determine

deterioration of the material, and possibly to estimate the remaining life of the material. Shull (2002) states that these selected physical properties must deteriorate with use and the physical degradation process must be known. NDT techniques are being used extensively in many areas of engineering to evaluate in-use conditions of materials and to estimate remaining service life (Shull, 2002). Although the interest level in the nondestructive evaluation of textile structures has been high for quite some time (e.g., Onions & Slater, 1967) work continues to develop new NDT methods for textile applications, or to apply NDT methods used in other branches of engineering and science.

Several NDT methods that have been studied for use in evaluating protective and other textiles are described in the following sections. Emphasis is placed on techniques that are based on color measurements and near infrared spectroscopy. Examples of how the results of these tests can be correlated with those from destructive tests are also given.

5.4.1.1 Visual inspections

One NDT method used in textile applications is visual inspections. For example, NFPA 1851 (2014) provides information on various levels of visual inspection of in-use firefighter's protective clothing. After each use, individual end users can look for visual indications of possible damage including soiling, contamination, and physical damage, such as tears and rips. Specially trained individuals can conduct more advanced inspections on a regular basis or as a result of an initial visual inspection.

While NFPA 1851 mainly includes visual inspections, a few other NDT procedures are also provided for evaluating the clothing. The inner layer of this clothing, which includes both the moisture barrier and thermal liner, is evaluated by using a light source and subjectively determining the amount of light that passes through the liner. Brighter areas may indicate a deficiency in the insulating layers. In another test method, which is also applicable to the inner layer, a cup of a water-alcohol mixture is poured on the moisture barrier side of the inner layer and the other side is visually inspected for leakage. In the third test method, the substrate of the moisture barrier is exposed to water pressure of 6.9 kPa (1 psi) and water leakage on the other side is determined visually.

5.4.1.2 Liquid penetrants

One example of the use of liquid penetrants is the work of Bray and Stull (1996), who investigated the feasibility of using liquid penetrants to detect defects in chemical/biological protective clothing, such as cracks, holes or other loss of integrity. Several liquid penetrants with different characteristics were used to evaluate eight fabrics after they had been abraded, and to determine how well the penetrants were able to indicate failure in chemical permeation and viral penetration tests. While this method showed promise for evaluation of protective clothing, it was thought that a penetrant should be specifically developed for firefighters' protective fabrics, which could penetrate through multiple layers of fabric in a reasonable length of time, and

be correlated with results of chemical permeation and viral penetration test standards (ASTM E165/E165M-12, 2012).

5.4.1.3 Active thermography

Thermography is an NDT method where specimens are excited with incident energy and an infrared camera is used to measure temperature distributions. Differences in thermal properties caused by changes to fabrics will result in differences in temperatures. One example of this technique is the work of Gralewicz and Wiecek (2009) who evaluated the use of active thermography as a nondestructive technique to detect defects in thermal protective fabrics. They cut out circles of diameters between 2 and 22 mm in different layers of multilayer systems to represent defects, and measured temperatures using an infrared camera when the specimens were exposed to a lamp. While the method was able to detect some larger defects, smaller defects caused by early stage degradation could be difficult to detect using this technique. For example, Gralewicz and Wiecek were unable to detect defects of diameter <8 mm in size.

5.4.1.4 Color measurements

Many visual inspections are based on color changes, such as those that occur when firefighter's protective clothing is exposed to high heat fluxes and temperatures (Fig. 5.2). However, color changes assessed using visual inspections are subjective (Randall, 1998). Therefore, NDT methods for textiles based on color measurements have been considered.

The discoloration of the fabric because of a thermal or other exposure, such as shown in Fig. 5.2, can be expressed as a color difference and related to mechanical or other properties. Thorpe (2004) used both a colorimeter and images from a computer scanner to measure color differences after exposures in the laboratory. Emphasis was placed on the computer scanner, as it was felt that this equipment would be easily available to firefighters. Discoloration, or color difference, was defined as the color difference between a new and exposed specimen, measured using two distinct color measurement systems, RGB and CIE L*a*b color space. He found that tensile strength of the outer shell fabrics could be correlated with color measurements.

Rezazadeh (2014) continued this work on color measurement by assessing the technique using fabrics with a range of initial color. Two trends in correlations between color change and tensile strength were observed. The first trend was observed for yellow, red, and undyed (light brown) fabrics, for which the color difference continually increased as dye was removed and char appeared (Fig. 5.3). The second trend was observed for blue and black fabrics (e.g., Fig. 5.2), for which the color difference increased as dye was removed, but then decreased when char appeared (Fig. 5.4). While this method shows promise, Thorpe (2004) identified a number of issues that would need to be addressed. A collection of baseline color changes for a variety of protective fabrics would need to be developed, and the sensitivity of the results to deposition of contaminants in the fabric and the required level of resolution of specimen image would need to be determined.

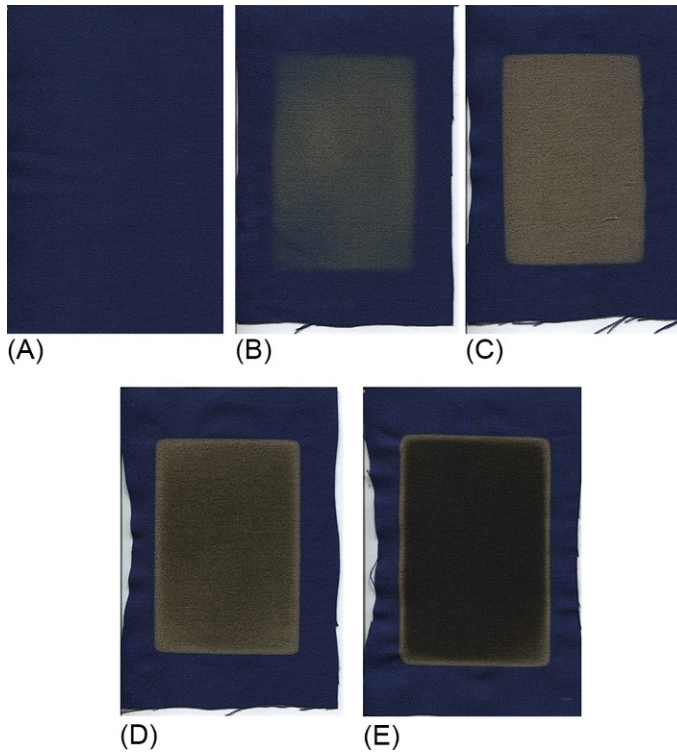

Fig. 5.2 Examples of color fade of royal blue Nomex IIIA specimens after different thermal exposures. (A) New, (B) 10 kW/m^2 for 2400 s, (C) 20 kW/m^2 for 30 s, (D) 30 kW/m^2 for 30 s, and (E) 40 kW/m^2 for 30 s (Rezazadeh, 2014).

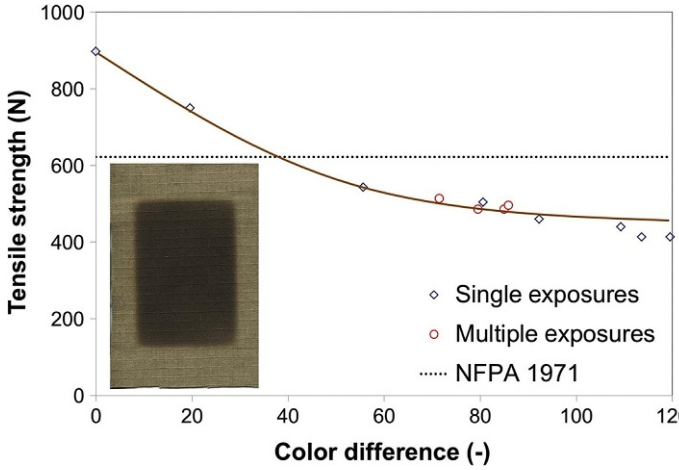

Fig. 5.3 Correlation between color difference and tensile strength of Kevlar/PBI outer shell measured after single and multiple exposures of firefighters' ensemble to 20 kW/m^2 (Rezazadeh, 2014).

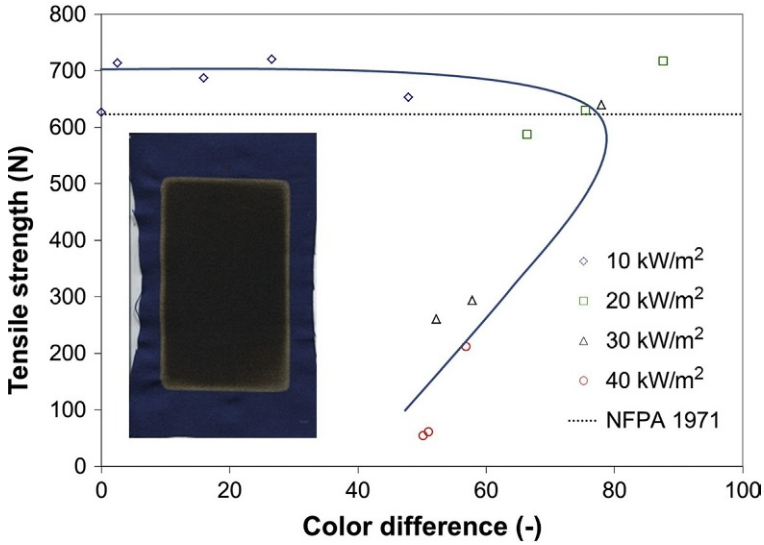

Fig. 5.4 Correlation between color difference and tensile strength of royal blue Nomex fabric measured after exposures to 10–40 kW/m^2 (Rezazadeh, 2014).

Digital image analysis can also be based on other visual parameters besides color changes. For example, Hadjianfar, Semnani, and Sheikhzadeh (2010) used digital image analysis to measure textile luster properties. The appearance of textile materials can often be classified by luster (gloss, glitter, sheen, shine, etc.), but in practice it is difficult to obtain theoretical and experimental luster values. Commercial devices, such as glarimeters and glossimeters, are available. However, Hadjianfar et al. created a new method that takes diffuse and scattered light from fabrics into account. This method can produce consistent results based on derived luminance values of textile images taken by a high-quality camera and a diffused nonpolarized lighting system.

5.4.1.5 Raman spectroscopy

Raman spectroscopy has been investigated as a tool for studying textile degradation, and a potential NDT method. Raman peaks and relative position may be an indication of performance or chemical changes in high performance fiber microstructures. Moreover, mechanical or thermal degradation could cause band shifts that will appear in the Raman spectra of the fibers. Galiotis (1992) was one of the first to look at the use of Raman spectroscopy for the evaluation of protective fibers such as Kevlar and Nomex. Ward and Young (2001) evaluated near-infrared (NIR) Raman spectroscopy changes following the deformation of thermotropic aromatic copolyesters. Washer, Brooks, and Saulsberry (2009) examined Raman spectra response to incident UV and thermal exposures. The vibrational modes of the Raman peaks were thought to change

in direct relation to the deterioration of the fiber. They showed that the average peak intensity of aged specimens decreased in comparison with that of unaged specimens while the average bandwidth of peaks in the Raman spectrum of aged specimens increased. Thorpe (2004) also examined NDT methods based on Raman spectroscopy. However, this method did not work particularly well for the specific outer shell fabric specimens he studied as there was a high fluorescence level and poor signal-to-noise ratios. Washer et al. (2009) noted that the use of an incident light of longer wavelength might enhance the resolution when using this technique. One other concern is that laser power levels should be kept low enough to prevent structural damage to textiles (Penn & Milanovich, 1979; Prasad & Grubb, 1990), and to give good spectral response (Washer et al., 2009).

5.4.1.6 X-ray diffraction

X-ray diffraction (XRD) has been used in a number of investigations of the effects of thermal aging on the structure and mechanical properties of fabrics. Iyer and Vijayan (1998, 1999) and Iyer, Sudhakar, and Vijayan (2006) used XRD to study the effects of multistage isothermal exposures on thermal degradation of Kevlar fibers, while Jain and Vijayan (2002) examined the thermal degradation of Nomex fibers after exposures to temperatures from 200°C to 400°C. Iyer and Vijayan (1999) and Iyer et al. (2006) used XRD to study the effects of thermal degradation of Kevlar fibers after exposures to temperatures from 150°C to 550°C. They correlated some features of the XRD pattern, such as position and half width of reflection peaks and integrated intensity of the diffraction profile, with temperature and duration of exposure.

Arrieta, David, Dolez, and Vu-Khanh (2011a) studied the effect of thermal aging on the crystallinity of outer shell specimens made of a 60% Kevlar/40% PBI blend. Specimens were thermally aged at temperatures from 190°C to 320°C inside an electric oven. Crystallinity was determined using X-ray diffraction and Raman spectroscopy. Zhu et al. (2013) used the Shanghai Synchrotron Radiation Facility to investigate small-angle X-ray scattering (SAXS) combined with a modified Pauw's scattering model in order to characterize voids in the fiber microstructure of aramid fiber bundles. These nonheat treated fiber bundles were not strength tested directly, but their given material strength predictions were compared to the SAXS obtained results. The group was able to show that larger voids directly lead to a weaker fiber.

5.4.1.7 Near infrared spectroscopy

Infrared spectroscopy has been used for identification of compounds and investigation of material composition in agricultural and other applications since the initial development of the technology (McClure, 2004). Peak intensity changes in the transmission spectrum can also be used to study degradation in materials or to analyze decomposition products. Examples of specific wavelengths or wavelength ranges that can be related to particular structural features, or changes that occur as a result of aging, can be found in Goddu and Delker (1960), Mosquera, Jamond, Martinez-Alonzo,

and Tascon (1994), Chalmers and Griffiths (2001), McClure (2004), and Arrieta et al. (2010, 2011a, 2011b).

Infrared spectroscopy has been used in various areas of engineering and science. Researchers in the field of heritage conservation (Garside, Wyeth, & Zhang, 2011; Richardson, Martin, Wyeth, & Zhang, 2008) compared the absorption spectra of new and aged silk specimens after exposure to heat, light, and humidity. They correlated tensile strength of specimens to changes in the intensity of peaks in the water absorption bands in the spectra of new and used specimens. Dispersive infrared spectroscopy was employed by Gu et al. (2008) to compare degradation of an epoxy coating system when exposed to ultraviolet radiation in the laboratory and the field. Many researchers have investigated methods of using infrared spectroscopy to evaluate or predict properties of wood, including density (Mora, 2009), moduli of rupture and elasticity (Kludt, 2003), compressive strength (Kelley, 2003) and stiffness and tensile strength (Hedrick, Bennett, Rials, & Kelley, 2007).

One application of IR spectroscopy to textiles is the work of Ghosh, Cannon, and Roy (1990) who implemented dispersive IR spectroscopy within the wavelength region of 1100–2500 nm to determine the amount of durable press resin in cotton fabrics. Based on the change in absorbance spectra, they picked three wavelengths and developed a model to predict the amount of fixed resin on cotton fabrics. Fortier et al. (2014) used attenuated total reflectance FTIR (ATR-FTIR) to evaluate the percentage change in moisture content of oven dried cotton in order to determine if oxidation of the cotton structure was occurring.

A number of investigators have used IR spectroscopy in applications related to protective fabrics and clothing. Davis et al. (2010) used FTIR within the wavelength region of 5500–12,500 nm to explain the degradation of fabrics containing PBI, Nomex, and Kevlar after exposure to ultraviolet radiation. Nazare et al. (2012) used FTIR spectroscopy within wavelength regions of 2800–3400 and 5500–6200 nm for interpretation of changes in mechanical properties of PBI, Nomex, and Kevlar after specimens had been exposed to ultraviolet radiation and a hot and humid environment, which were used to simulate routine firefighting operations and storage rooms. Infrared spectra of new and aged specimens were analyzed, and changes were related to alterations in chemical composition of specimens, and deterioration in tear and tensile strength.

Arrieta et al. (2011b) demonstrated that thermal degradation of a blend of 60% Kevlar/40% PBI after exposure to temperatures from 190°C to 320°C could not be detected in the absorption peaks of the infrared spectra within the wavelength region of 2500–20,000 nm using FTIR. Even though the tensile strength of the specimens decreased noticeably after a certain level of aging, the variation of the absorption peaks was subtle. Arrieta et al. (2011b) showed that ATR-FTIR results could be correlated with the photochemical (UV) aging of Kevlar/PBI blended fabrics. Decreases in the fabric breaking force after exposure to both UV radiation and humidity were correlated with ATR-FTIR measurements of the aged specimens. Cai and Yu (2011) used FTIR spectroscopy in the wavelength region of 2500–25,000 nm to analyze the volatiles produced during the thermal degradation of Kevlar and Nomex specimens.

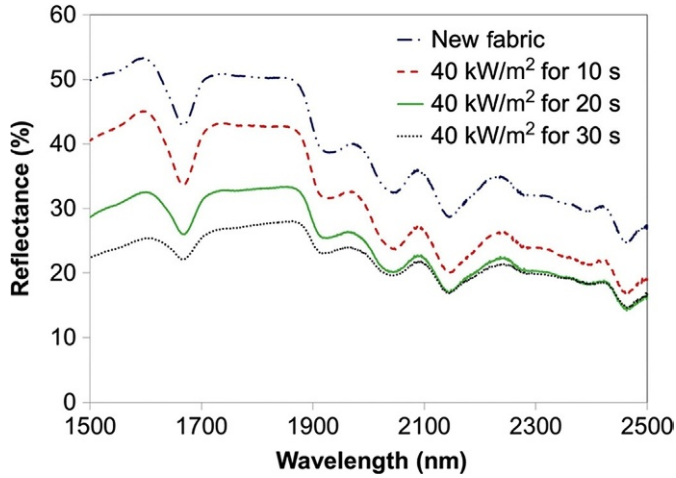

Fig. 5.5 Infrared reflectance spectrum of a royal blue Nomex fabric specimen after various lengths of exposed to 40 kW/m^2 (Rezazadeh, 2014).

Rezazadeh (2014) demonstrated that near infrared spectroscopy had the potential to be used to predict tensile strength of fabrics used in the outer shell of firefighters' protective clothing. Fig. 5.5 shows the shifts in reflectance spectra that were observed for the same royal blue Nomex fabric shown in Fig. 5.4 after exposures to 40 kW/m^2. Correlations were developed using multivariable linear regression models, and it was found that a model based on reflectance values at three wavelengths could be used to predict tensile strength. For example, Fig. 5.6 compares predicted and measured tensile strength values. The regression model was developed using reflectance at 1600, 1750 and 2425 nm and tensile strength values measured after exposures to 10–40 kW/m^2 (these points are shown using open squares). The model was then used to predict tensile strength for a second set of fabrics exposed to 5, 15 and 25 kW/m^2 based on reflectance at the same three wavelengths (shown using solid squares). The model did a very good job of predicting tensile strengths around 600 N, but was much less successful at predicting lower tensile strengths. One reason for the lower success in this range of tensile strength is that a much larger fraction of the data used to develop the regression model was for higher tensile strength values rather than for values of 400 N or less. Nevertheless, this research demonstrated that a practical device, which would measure reflectance at even a small number of wavelengths, could be a viable way to predict tensile strength of in-use protective clothing.

Understanding which particular wavelengths can be correlated with changes in fabric properties with aging, such as the work of Rezazadeh described previously, is important for the development of practical tools that can be used to evaluate in-use fabrics and other products in the field. For example, Hedrick et al. (2007) worked on predictions of stiffness and tensile strength of woods using dispersive IR spectroscopy

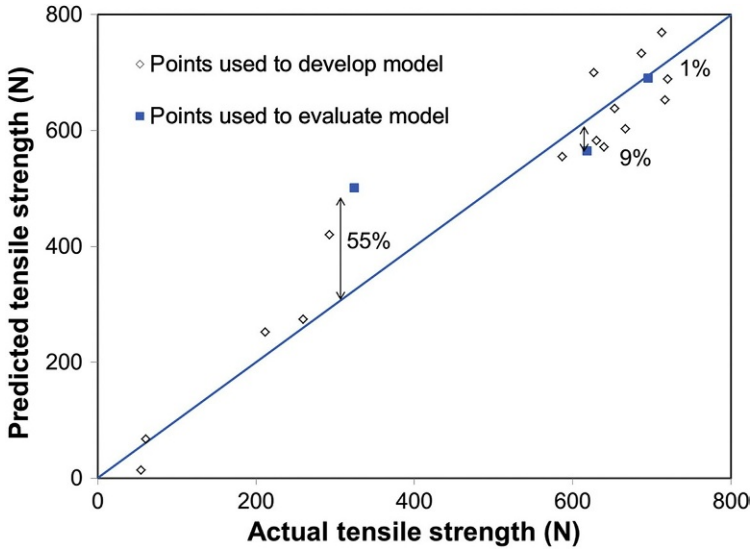

Fig. 5.6 Comparison of tensile strength measurements for thermally aged royal blue Nomex fabrics with values predicted using three-wavelength regression model (Rezazadeh, 2014).

over the wavelength range 350–2500 nm. They found that the prediction of desired parameters using a shorter spectra range of 950–1850 nm was almost as accurate as the prediction over the full range of 350–2500 nm, which can be used in developing small and inexpensive instruments.

Portable NIR evaluation tools have been in development for a number of decades in a number of areas, including the agricultural and medical fields (McClure, 2004). Portable textile evaluation methods based on NIR measurements have been developed successfully by Rodgers et al. (2010) for the evaluation of cotton fiber micronaire, a key property of cotton. Rodgers et al. (2010) found that results from handheld devices matched well with benchtop NIR devices; certain spectral shifts were noted, but could be minimized with baseline correction methods.

5.5 Methods to predict useful life of textiles

There are several reasons why useful life cannot be completely described using a deterministic parameter. These include complicated and relatively unknown mechanisms of degradation, a diverse range of exposure conditions, and different maintenance procedures (Kim, Jorgensen, King, & Czandema, 1996). Therefore, the development of a probabilistic model would be useful. Such a model would be based on results of deterministic tests in which physical properties of the fabric

are measured to demonstrate the condition of the clothing. These deterministic tests could include the nondestructive tests described in this chapter, the results of which would be used to predict the in-use performance of the textile. Statistical and predictive methods are already used successfully in many applications (You & Tonon, 2012).

Rezazadeh and Torvi (2011) provide a review of some statistical and predictive models that could be used for evaluating firefighters' protective clothing. Another approach could be to use information on the in-use properties of the fabric and/or garment in heat and mass transfer models that can predict the protection (or other aspect of performance) of the fabric or system. These models could range from models to predict the performance of fabrics in standard bench top tests (Torvi & Threlfall, 2006) to computational fluid dynamics (CFD) models of complete garments (e.g., Jiang et al., 2010; Tian, Wang, & Li, 2016). Wang and Li (2015), Wang et al. (2014), and Wang, Li, and Tian (2015) created a method to evaluate the thermal protective performance of thermal protective garments when the airgaps between the individual material construction layers are eliminated. Models such as this one could allow information on physical changes to garments, such as shrinkage, to be used to predict the resulting change in the performance of the garment.

Another potential part of predictive methods for determining the effects of aging would be a management system to keep a written record of use, care, and maintenance of a particular textile item. Torvi and Hadjisophocleous (2000) discuss the development of a system that could be used to assist in making a decision as to the proper time to retire an article of firefighters' protective clothing. In collaboration with a research committee, they proposed some guidelines which could be used in conjunction with visual inspections and records of service provided by the management system to assist the fire departments with determination of retirement age of firefighters' protective clothing.

Expected useful lifetime will depend greatly on the individual firefighters' role within the fire department (Rezazadeh, 2014). Some roles will face less severe exposure conditions than others. For example, turnout gear that has been used by an individual responsible for maintaining water pumping operations during a fire event will face much lower levels of thermal degradation than an individual entering the burning building. Different departments (e.g., rural versus urban settings) may also experience different levels of firefighting activity and therefore choose different retirement criteria for their protective clothing. On the other hand, standards organizations state that after any contact with CBRN terrorism agents (chemicals, biological agents, and radiological particulates) firefighters' protective clothing must be retired immediately regardless of physical appearance or repair cost (NFPA 1851). Economic considerations may also be used to retire a piece of clothing if the replacement cost is deemed to be lower than any required repair costs. Details on this calculation can be found in NFPA 1851 (2014). Recent work has been conducted into the service life of personal protective clothing (Dolez & Vu-Khanh, 2009) and the limitations of the current NFPA 1851 (2014) standard destructive testing methods (Nazare et al., 2012).

5.6 Conclusions and future work

The general process of textile aging has been discussed, along with some of the main factors that cause degradation, including mechanical action, environmental conditions, cleaning and maintenance procedures, and exposures to high temperatures and heat fluxes. One particular concern with aging of textiles is that it is possible for degradation in the performance of a textile to occur prior to changes in its visual appearance. In some applications, this may affect the safety of the end user. Therefore, understanding the effects of single and multiple types of aging on the performance of textiles is critical.

Several tests used to simulate aging and evaluate performance have been discussed in this chapter. Examples of research that uses these tests to better understand the effects of aging on fabric performance have also been provided. The development of standard tests to evaluate textile performance continues to be an active area of research. New tests are expected to simulate conditions textiles are exposed to in the field, produce repeatable and reproducible results, and assist end users, regulators, researchers, and industry in making informed decisions about textiles and products containing these textiles. Improvements in standard textile test methods will also assist in evaluating the effects of textile aging, as many of the methods used to evaluate performance of in-use textiles are the same tests used to evaluate new textiles. This chapter also provides examples of how standard tests are used to simulate conditions in the field in order to age textiles in the laboratory. Research is needed in many applications to better understand these field conditions, and to better relate laboratory and field exposures, in order to determine the limitations of laboratory testing.

While many laboratory studies are aimed at evaluating the performance of textiles after being subjected to one form of aging, in field conditions, these materials are subjected to several exposures simultaneously. Research is needed to study the combined effects of different types of exposure on the continuing performance of textiles. For example, during its useful life firefighters' protective clothing will be exposed to many types of aging, including high temperatures and heat fluxes, chemicals, ultraviolet radiation, abrasion, and cleaning and maintenance procedures. There are limited studies in which multiple aging factors are considered for this protective clothing. Another alternative is studies of used textiles. However, in order to make these studies as useful as possible, detailed records of the use, care and maintenance of the items considered in the study are needed.

To address the concern that most textile tests are destructive, and therefore not suitable for evaluating in-use textiles, research has been conducted into a number of nondestructive test methods for textiles. Some of these techniques are based on visual inspections, while more sophisticated methods use active thermography, liquid penetrants, X-ray diffraction, and Raman spectroscopy. Two methods that have shown promise in the evaluation of firefighters' protective clothing, color measurements and infrared spectroscopy, were discussed in this chapter. While results from these latter two methods have been correlated with changes in tensile strength for a limited number of fabrics that were aged in the laboratory, additional work is needed to

develop more general correlations between parameters in nondestructive tests and textile performance. Some changes to textiles, such as dirt, are not expected to seriously impact textile performance, but one concern with some nondestructive tests, such as color measurement, is differentiating these changes from charring and other changes which may also produce similar changes to the appearance of a textile. Therefore, for any nondestructive method to be practical, it must be able to differentiate between various phenomena. Developing practical devices based on the nondestructive methods used in laboratories will also be important for these methods to gain widespread use. For example, while entire NIR spectra can be used to evaluate fabrics, determining the most important wavelengths for this analysis will be critical if small, handheld devices are to be developed for use in the field.

5.7 Sources of further information

Readers looking for additional information on textile aging tests may wish to consult publications from the following standards, research and other organizations.

5.7.1 Standards organizations

The following organizations publish relevant textile standards:

- American Society for Testing and Materials (ASTM) www.astm.org;
- Canadian General Standards Board (CGSB) http://www.tpsgc-pwgsc.gc.ca/ongc-cgsb/index-eng.html;
- European Commission for Standardization (CEN) www.cen.eu;
- International Organization for Standardization (ISO) www.iso.org; and
- National Fire Protection Association (NFPA) www.nfpa.org (performance of new and in-use protective clothing and equipment for firefighters).

ASTM has also sponsored a series of Performance of Protective Clothing symposia (http://www.astm.org/DIGITAL_LIBRARY/SYMPOSIA/PAGES/F23.htm), which have included papers that describe textile aging research and tests. NFPA publishes fire statistics reports, including numbers and causes of fires, firefighter and civilian injuries and deaths, and fire department activities (www.nfpa.org/news-and-research). NFPA's Fire Protection Research Foundation has sponsored research of relevance to the study of the continuing performance of firefighters' protective clothing and equipment.

5.7.2 Research organizations

The following academic, government and other organizations have conducted research related to textile aging, and methods to evaluate in-use performance of textiles:

- CTT Group www.gcttg.com;
- Donghua University http://english.dhu.edu.cn/;
- Finnish Institute of Occupational Health www.ttl.fi/en;

- National Institute of Standards and Technology (NIST) www.nist.gov/el/fire_research/firesafety/fireontheweb.cfm;
- National Research Council of Canada www.nrc-cnrc.gc.ca;
- North Carolina State University, College of Textiles https://textiles.ncsu.edu/;
- Swiss Federal Laboratories for Materials Science and Technology (EMPA) www.empa.ch;
- University of Alberta, Departments of Human Ecology and Mechanical Engineering www.ualberta.ca;
- University of Kentucky, School of Human Environmental Sciences https://hes.ca.uky.edu;
- University of Maryland, Department of Fire Protection Engineering www.fpe.umd.edu/;
- University of Saskatchewan, Department of Mechanical Engineering http://engineering.usask.ca/mech/; and
- Worcester Polytechnic Institute, Department of Fire Protection Engineering www.wpi.edu/academics/fpe.

5.7.3 Other organizations

Many manufacturers of protective clothing include information on the care, maintenance, and use of their products in user manuals and/or on their websites. Two examples are:

- Globe's website (http://globefiresuits.com), which includes training material and videos on protective clothing standards, care, maintenance, inspection, and retirement; and
- Lion Group's Fire Academy website (http://lionfireacademy.com/), which includes training materials and videos on care, maintenance, and inspection of firefighters' protective clothing.

References

Abbott, N., & Schulman, S. (1979). Protection from fire: Non-flammable fabrics and coatings. *Journal of Industrial Textiles*, *6*, 48–64.

Aidani, R., Dolez, P., & Vu-Khanh, T. (2011). Effect of thermal aging on the mechanical and barrier properties of an e-PTFE/Nomex moisture membrane used in firefighters' protective suits. *Journal of Applied Polymer Science*, *121*(5), 3101–3110.

Aidani, R., Nguyen-Tri, P., Malajati, Y., Lara, J., & Vu-Khanh, T. (2013). Photochemical aging of an e-PTFE/NOMEX membrane used in firefighter protective clothing. *Polymer Degradation and Stability*, *98*(7), 1300–1310.

An, S., Barker, R., & Stull, J. (1989). Measurement of the flammability and thermal aging of chemical protective suit materials. *Chemical protective clothing performance in chemical emergency response*. ASTM. STP 1037 (pp. 86–101).

Annis, P., & Bresee, R. (1990). An abrasion machine for evaluating single fiber transfer. *Textile Research Journal*, *60*(9), 541–548.

Arrieta, C., David, E., Dolez, P., & Vu-Khanh, T. (2010). Thermal aging of a blend of high-performance fibers. *Journal of Applied Polymer Science*, *93*(5), 3031–3039.

Arrieta, C., David, E., Dolez, P., & Vu-Khanh, T. (2011a). X-ray diffraction, Raman, and differential thermal analyses of the thermal aging of a Kevlar-PBI blend fabric. *Polymer Composites*, *32*(3), 362–367.

Arrieta, C., David, E., Dolez, P., & Vu-Khanh, T. (2011b). Hydrolytic and photochemical aging studies of a Kevlar-PBI blend. *Polymer Degradation and Stability*, *96*(8), 1411–1419.

ASTM D1230-10e1. (2016). *Standard test method for flammability of apparel textiles*. West Conshohocken, PA: ASTM International.

ASTM D2261-13. (2013). *Standard test method for tearing strength of fabrics by the tongue (Single rip) procedure (Constant-rate-of-extension tensile testing machine)*. West Conshohocken, PA: ASTM International.

ASTM D3511. (2015). *Standard test method for pilling resistance and other related surface changes of textile fabrics: Brush pilling tester*. West Conshohocken, PA: American Society for Testing and Materials.

ASTM D3512. (2014). *Standard test method for pilling resistance and other related surface changes of textile fabrics: Random tumble pilling tester*. West Conshohocken, PA: American Society for Testing and Materials.

ASTM D5034-09. (2013). *Standard test method for breaking strength and elongation of textile fabrics (Grab test)*. West Conshohocken, PA: ASTM International.

ASTM D6413/D6413M-15. (2015). *Standard test method for flame resistance of textiles (vertical test)*. West Conshohocken, PA: ASTM International.

ASTM E165/E165M-12. (2012). *Standard practice for liquid penetrant examination for general industry*. West Conshohocken, PA: ASTM International.

ASTM E1131-08. (2014). *Standard test method for compositional analysis by thermogravimetry*. West Conshohocken, PA: ASTM International.

ASTM E1354-16a. (2016). *Standard test method for heat and visible smoke release rates for materials and products using an oxygen consumption calorimeter*. West Conshohocken, PA: ASTM International.

ASTM F1449-08. (2015). *Standard guide for industrial laundering of flame, thermal, and arc resistant clothing*. West Conshohocken, PA: ASTM International.

ASTM F1930-15. (2015). *Standard test method for evaluation of flame resistant clothing for protection against fire simulations using an instrumented manikin*. West Conshohocken, PA: ASTM International.

ASTM F1939-15. (2015). *Standard test method for radiant heat resistance of flame resistant clothing materials with continuous heating*. West Conshohocken, PA: ASTM International.

ASTM F2700-08. (2013). *Standard test method for unsteady-state heat transfer evaluation of flame resistant materials for clothing with continuous heating*. West Conshohocken, PA: ASTM International.

ASTM F2757-09. (2016). *Standard guide for home laundering care and maintenance of flame, thermal and arc resistant clothing*. West Conshohocken, PA: ASTM International.

Atalay, O., Bahadir, S., & Kalaoglu, F. (2015). An analysis on the moisture and thermal protective performance of firefighter clothing based on different layer combinations and effect of washing on heat protection and vapour transfer performance. *Advances in Materials Science and Engineering*, *2015*, 540394.

Barnett, R., & Slater, K. (1991). The progressive deterioration of textile materials, part V: The effects of weathering on fabric durability. *Journal of the Textile Institute*, *82*(4), 417–425.

Bray, A., & Stull, J. (1996). A non-destructive inspection method to determine fatigue in chemical protective suit and shelter materials. *Performance of protective clothing*: *Vol. 5*. West Conshohocken, PA: American Society for Testing and Materials. ASTM STP 1237.

Bresee, R., Annis, P., & Warnock, M. (1994). Comparing actual fabric wear with laboratory abrasion and laundering. *Textile Chemist and Colorist*, *26*(1), 17–23.

Cai, G., & Yu, W. (2011). Study on the thermal degradation of high performance fibers by TG/FTIR and Py-GC/MS. *Journal of Thermal Analysis and Calorimetry*, *104*(2), 757–763.

CAN/CGSB-155.1. (2001). *Firefighters' protective clothing for protection against heat and flame*. Ottawa, ON: Canadian General Standards Board.

Chalmers, J., & Griffiths, P. (2001). *Handbook of vibrational spectroscopy*. New York, NY: John Wiley and Sons.

Chen, L., & Cloud, R. (2000). Effects of abrasion on liquid barrier properties of selected nonwoven fabrics. *Performance of protective clothing: Issues and priorities for the 21st century*: *Vol. 7*. West Conshohocken, PA: American Society for Testing and Materials. ASTM STP 1386.

Cinnamon, M. (2013). *Post use analysis of firefighter turnout gear-phase III* [M.Sc. thesis]. Lexington, KY: University of Kentucky.

Cloud, R., & Lowe, P. (1995). Effects of field-wear abrasion on barrier properties on nonwoven fabrics. *Clothing and Textile Research Journal*, *13*(3), 159–164.

Collier, B., Bide, M., & Tortora, P. (2009). The care of textile products. In V. Anthony (Ed.), *Understanding textiles* (pp. 475–499). Upper Saddle River, NJ: Pearson Prentice Hall.

Cui, Z., Ma, C., & Lv, N. (2015). Effects of heat treatment on the mechanical and thermal performance of fabric used in firefighter protective clothing. *Fibers and Textiles in Eastern Europe*, *23*(2), 74–78.

Davis, R., Chin, J., Lin, C., & Petit, S. (2010). Accelerated weathering of polyaramid and polybenzimidazole firefighter protective clothing fabrics. *Polymer Degradation and Stability*, *95*(9), 1642–1654.

Day, M., Cooney, J., & Suprunchuk, T. (1988). Durability of firefighter's protective clothing to heat and light. *Textile Research Journal*, *58*(3), 141–147.

Dolez, P., & Vu-Khanh, T. (2009). Recent developments and needs in materials used for personal protective equipment and their testing. *International Journal of Occupational Safety and Ergonomics*, *15*(4), 347–362.

Donnelly, M., Davis, W., Lawson, J., & Selepak, M. (2006). *Thermal environment for electronic equipment used by first responders*. Gaithersburg, MD: National Institute of Standards and Technology.

EN 367. (1992). *Protective clothing—Protection against heat and fire—Method of determining heat transmission on exposure to flame*. Brussels, Belgium: European Committee for Standardization.

EN 469. (2005). *Protective clothing for firefighters—Performance requirements for protective clothing for firefighting*. Brussels, Belgium: European Committee for Standardization.

Fortier, C., Montalvo, J., Von Hoven, T., Easson, M., Rodgers, J., & Condon, B. (2014). Preliminary evidence of oxidation in standard oven drying of cotton: Attenuated total reflectance/Fourier transform infrared spectroscopy, colorimetry, and particulate matter formation. *Textiles Research Journal*, *84*, 157–173.

Galiotis, C. (1992). Raman optomechanical studies on fibers, composites and fiber-matrix interfaces. In S. Paipetis & G. Papanicolaou (Eds.), *Phase interaction in composite materials* (pp. 173–184). Wallingford: Omega Scientific.

Garside, P., Wyeth, P., & Zhang, X. (2011). Use of near IR spectroscopy and chemometrics to assess the tensile strength of historic silk. *e-Preservation Science*, *8*, 68–73.

Ghosh, S., Cannon, M., & Roy, R. (1990). Quantitative analysis of durable press resin on cotton fabrics using near-infrared reflectance spectroscopy. *Textile Research Journal*, *60*(3), 167–172.

Goddu, R., & Delker, D. (1960). Spectra-structure correlations for near-infrared. *Analytical Chemistry*, *32*, 140–141.

Gralewicz, G., & Wiecek, B. (2009). Active thermography in qualitative evaluation of protective materials. *International Journal of Occupational Safety and Ergonomics*, *15*(4), 363–371.

Gu, X., Dickens, B., Stanley, D., Byrd, W. E., Nguyen, T., Vaca-Trigo, I., et al. (2008). Linking accelerating laboratory test with outdoor performance results for a model epoxy coating

system. In J. Martin, R. Ryntz, J. Chin, & R. Dickie (Eds.), *Service life prediction of polymeric materials: Global perspectives* (pp. 3–28). Berlin: Springer.

Hadjianfar, M., Semnani, D., & Sheikhzadeh, M. (2010). A new method for measuring luster index based on image processing. *Textile Research Journal*, *80*, 726–733.

Hedrick, S., Bennett, R., Rials, T., & Kelley, S. (2007). Correlation of near-infrared spectroscopy measurements with the properties of treated wood. *Journal of Materials in Civil Engineering*, *19*(4), 279–285.

House, J., & Squire, J. (2004). The effect of wear and washing on the protection afforded by the new Royal Navy fire fighters' protective hood. *International Journal of Clothing Science Technology*, *16*, 368–373.

Houshyar, S., Padhye, R., Nayak, R., & Shanks, R. (2015). Deterioration of polyaramid and polybenzimidazole woven fabrics after ultraviolet irradiation. *Journal of Applied Polymer Science*, *133*(9), 43073.

Hsu, L., & Cheek, L. (1989). Dimensional stability of ramie, cotton, and rayon knit fabrics. *Clothing and Textiles Research Journal*, *7*(2), 32–36.

ISO 6942. (2002). *Protective clothing—Protection against heat and fire—Method of test: Evaluation of materials and material assemblies when exposed to a source of radiant heat*. Geneva: International Standards Organization.

ISO 13506. (2008). *Protective clothing against heat and flame—Test method for complete garments—Prediction of burn injury using an instrumented manikin*. Geneva: International Standards Organization.

Iyer, R., Sudhakar, A., & Vijayan, K. (2006). Decomposition behaviour of Kevlar 49 fibers: Part II. At T values < Td. *High Performance Polymers*, *18*(4), 495–517.

Iyer, R., & Vijayan, K. (1998). Identification of a new parameter controlling the thermally induced effects on Kevlar 49 fibers. *Current Science*, *75*(9), 946–951.

Iyer, R., & Vijayan, K. (1999). Decomposition behaviour of Kevlar 49 fibers: Part I. at T ≈ Td. *Bulletin of Materials Science*, *22*(7), 1013–1023.

Jain, A., & Vijayan, K. (2002). Thermally induced structural changes in Nomex fibers. *Bulletin of Material Science*, *25*(4), 341–346.

Jasinska, I., & Stempien, Z. (2014). An alternative instrumental method for fabric pilling evaluation based on computer image analysis. *Textile Research Journal*, *84*(5), 488–499.

Jiang, Y. Y., Yanai, E., Nishimura, K., Zhang, H., Abe, N., Shinohara, M., et al. (2010). An integrated numerical simulator for thermal performance assessments of firefighters' protective clothing. *Fire Safety Journal*, *45*, 314–326.

Johnson, M. (2005). *The Cambridge handbook of age and aging*. Cambridge: The Cambridge University Press.

Kelley, S. (2003). Method of predicting mechanical properties of decayed wood. Kansas City, MO. Patent No. US 6593572 B2.

Kim, H., Jorgensen, G., King, D., & Czandema, A. (1996). Development of a methodology for service lifetime prediction of renewable energy devices. *Durability testing of nonmetallic materials*. West Conshohocken, PA: American Society for Testing and Materials. ASTM STP 1294.

Kludt, K. (2003). *Use of near infrared spectroscopy technology for predicting bending properties of clear wood specimens* [M.Sc. thesis]. Pullman, WA: Washington State University.

Loftin, D. (1992). The durability of flame resistant fabrics in an industrial laundry environment. *Performance of protective clothing*: *Vol. 4*. West Conshohocken, PA: ASTM International. STP1133.

Makinen, H. (1992). The effect of wear and laundering on flame-retardant fabrics. *Vol. 4. Performance of protective clothing*. West Conshohocken, PA: ASTM International. STP1133.

McClure, F. (2004). Review: 204 years of near infrared technology 1800–2003. *Journal of Near Infrared Spectroscopy*, *11*(6), 487–518.

McQuerry, M., Klausing, S., Cotterill, D., & Easter, E. (2015). A post-use evaluation of turnout gear using NFPA 1971 standard on protective ensembles for structural fire fighting and NFPA 1851 on selection, care, and maintenance. *Fire Technology*, *51*(5), 1149–1166.

McSherry, W., Reeves, W., Markezich, A., & Cooper, A. (1975). Effect of laundry detergents on flame retardant cotton fabrics. *The Journal of Fire and Flammability: Fire Retardant Chemicals*, *2*, 151–160.

Mettananda, C. (2009). *Effects of oily contamination and decontamination on combustion and flame resistance of thermal protective textiles* [Ph.D. thesis]. Edmonton, AB: University of Alberta.

Mettananda, C., & Crown, E. (2010). Quantity and distribution of oily contaminants present in flame-resistant thermal-protective textiles. *Textile Research Journal*, *80*(9), 803–813.

Mora, C. (2009). *Rapid techniques for screening wood properties in forest plantations* [Ph.D. thesis]. Athens, GA: University of Georgia.

Mosquera, M., Jamond, M., Martinez-Alonzo, A., & Tascon, J. (1994). Thermal transformations of Kevlar aramid fibers during pyrolysis: Infrared and thermal analysis studies. *Chemistry of Materials*, *6*(11), 1918–1924.

Nazare, S., Davis, R., Peng, J., & Chin, J. (2012). *Accelerated weathering of firefighter protective clothing: Delineating the impact of thermal, moisture, and ultraviolet light exposures*. Technical note 1746 Gaithersburg, MD: National Institute of Standards and Technology.

NFPA 1851. (2014). *Selection, care, and maintenance of protective ensembles for structural fire fighting and proximity fire fighting*. Quincy, MA: National Fire Protection Association.

NFPA 1971. (2013). *Standard on protective ensembles for structural fire fighting and proximity fire fighting*. Quincy, MA: National Fire Protection Association.

NFPA 2113. (2015). *Standard on selection, care, use, and maintenance of flame-resistant garments for protection of industrial personnel against short-duration thermal exposures*. Quincy, MA: National Fire Protection Association.

Onions, W., & Slater, K. (1967). The automatic comparison of roving and yarn irregularities during drafting. *Textile Institute Journal*, *58*, 210–219.

Ozgen, B., & Pamuk, G. (2014). Effects of thermal aging on Kevlar and Nomex Fabrics. *Industria Textila*, *65*(5), 254–262.

Park, S., Seo, M., Ma, T., & Lee, D. (2002). Effect of chemical treatment of Kevlar fibers on mechanical interfacial properties of composites. *Journal of Colloid and Interface Science*, *252*(1), 249–255.

Penn, L., & Milanovich, F. (1979). Raman spectroscopy of Kevlar 49 fiber. *Polymer*, *20*(1), 31–36.

Pickett, J., & Sargent, J. (2009). Sample temperatures during outdoor and laboratory weathering exposures. *Polymer Degradation and Stability*, *94*(2), 189–195.

Pinto, R., Carr, D., Helliker, M., Girvan, L., & Gridley, N. (2012). Degradation of military body armor due to wear: Laboratory testing. *Textile Research Journal*, *82*(11), 1157–1163.

Poli, T., Toniolo, L., & Sansonetti, A. (2006). Durability of protective polymers: The effect of UV and thermal aging. *Macromolecules in Cultural Hertiage*, *238*(1), 78–83.

Prasad, K., & Grubb, D. (1990). Deformation behavior of Kevlar fibers studied by Raman spectroscopy. *Journal of Applied Polymer Science*, *41*(9), 2189–2198.

Randall, D. (1998). *Instruments for the measurement of color*. Charlotte, NC: Datacolor International.

Rezazadeh, M. (2014). *Evaluation of performance of in-use firefighter's protective clothing using non-destructive tests* [Ph.D. thesis]. Saskatoon, SK: Department of Mechanical Engineering, University of Saskatchewan.

Rezazadeh, M., & Torvi, D. (2011). Assessment of factors affecting the continuing performance of firefighters' protective clothing: A literature review. *Fire Technology*, *47*(3), 565–599.

Richardson, E., Martin, G., Wyeth, P., & Zhang, X. (2008). State of the art: Non-invasive interrogation of textiles in museum collections. *Microchimica Acta*, *162*(2), 303–312.

Rodgers, J., Fortier, C., Montalvo, J., Cui, X., Kang, S. Y., & Martin, V. (2010). Near infrared measurements of cotton fiber micronaire by portable near infrared instrumentation. *Textile Research Journal*, *80*, 1503–1515.

Rossi, R., Bolli, W., & Stampfli, R. (2008). Performance of firefighter's protective clothing after heat exposure. *International Journal of Occupational Safety and Ergonomics*, *14*(1), 55–60.

Shull, P. (2002). Introduction to NDE. In P. Shull (Ed.), *Nondestructive evaluation: Theory, techniques, and applications* (pp. 1–15). New York, NY: Marcel Dekker Inc.

Sipe, J. (2004). *Development of an instrumented dynamic mannequin test to rate the thermal protective performance provided by protective clothing* [M.Sc. thesis]. Worcester: Worcester Polytechnic Institute.

Slater, K. (1986). The progressive deterioration of textile materials, part I: Characteristics of degradation. *Journal of the Textile Institute*, *77*(2), 76–87.

Slater, K. (1987). The progressive deterioration of textile materials, part II: A comparison of abrasion testers. *Journal of Textile Institute*, *78*(1), 13–22.

Slater, K. (1991). Textile degradation. *Textile Progress*, *21*(1), 1–150.

Stull, J., Dodgen, C., Connor, M., & McCarthy, R. (1996). Evaluating the effectiveness of different laundry approaches for decontaminating structural fire fighting protective clothing. *Performance of protective clothing*: *Vol. 5*. West Conshohocken, PA: ASTM International. STP1237.

Szostak-Kotowa, J. (2004). Biodeterioration of textiles. *International Biodeterioration and Biodegradation*, *53*(3), 165–170.

Thorpe, P. (2004). *Assessment of in-use firefighter's protective clothing* [M.Sc. thesis]. Saskatoon: University of Saskatchewan.

Tian, M., Wang, Z., & Li, J. (2016). 3D numerical simulation of heat transfer through simplified protective clothing during fire exposure by CFD. *International Journal of Heat and Mass Transfer*, *93*, 314–321.

Timiras, P., Quay, W., & Vernadakis, A. (1995). *Hormones and aging*. Boca Raton, FL: CRC Press.

Torvi, D., & Hadjisophocleous, G. (2000). Development of methods to evaluate the useful lifetime of firefighters' protective clothing. *Vol. 7. Performance of protective clothing: Issues and priorities for the 21st century*. West Conshohocken, PA: ASTM International. STP1386.

Torvi, D., Rezazadeh, M., & Bespflug, C. (2016). Effects of convective and radiative heat sources on thermal response of single and multiple-layer protective fabrics in bench top tests. In *Tenth symposium on performance of protective clothing and equipment: Risk reduction through research and testing, STP 1593, West Conshohocken, PA: ASTM International* (pp. 132–159).

Torvi, D. A., & Threlfall, T. G. (2006). Heat transfer model of flame resistant fabrics during cooling after exposure to fire. *Fire Technology*, *42*, 27–48.

Udayraj, Talukdar, P., Das, A., & Alagirusamy, R. (2016). Heat and mass transfer through thermal protective clothing – A review. *International Journal of Thermal Sciences*, *106*, 32–56.

Vanderschaaf, C., Batcheller, J., & Torvi, D. (2015). Combined effects of laundering and abrasion on the protective performance of flame resistant fabrics. In *Proceedings of the combustion institute—Canadian section spring technical meeting, Saskatoon, SK* (pp. FS6–FS11).

Vogelpohl, T. (1996). *Post-use evaluation of firefighter's turnout coats* [M.Sc. thesis]. Lexington, KY: University of Kentucky.

Vogelpohl, T., & Easter, E. (1997). Post-use evaluation of fire fighters turnout coats. In *Proceedings of the fifth scandinavian symposium on protective clothing (NOKOBETEF). Elsinore, Denmark, General Workers Union* (pp. 68–73).

Wang, M., & Li, J. (2016). Thermal protection retention of fire protective clothing after repeated flash fire exposure. *Journal of Industrial Textiles*, *46*(3), 737–755.

Wang, Z., Li, J., & Tian, M. (2015). Thermal protective performance evaluation of fire proof garment eliminating air gaps effect based on computational fluid dynamics simulation. *Journal of Fire Sciences*, *33*(6), 445–458.

Wang, N., Liu, Z., Tang, C., Zhao, S., Shi, M., & Yu, J. (2014). Study of the near-infrared transmission of woven fabrics based on statistical analysis. *Fibers and Polymers*, *15*(9), 2016–2018.

Ward, Y., & Young, R. (2001). Deformation studies of thermotropic aromatic copolyesters using NIR Raman spectroscopy. *Polymer*, *42*(18), 7857–7863.

Washer, G., Brooks, T., & Saulsberry, R. (2009). Characterization of Kevlar using Raman spectroscopy. *Journal of Materials in Civil Engineering*, *21*(5), 226–234.

You, X., & Tonon, F. (2012). Event-tree analysis with imprecise probabilities. *Risk Analysis: An International Journal*, *32*(2), 330–345.

Zhang, H., Zhang, J., Chen, J., Hao, X., Wang, S., & Feng, X. (2006). Effects of solar UV irradiation on the tensile properties and structure of PPTA fiber. *Polymer Degradation and Stability*, *91*(11), 2761–2767.

Zhang, C., Zhang, Q., Xue, Y., Li, G., Liu, F., Ji, X., et al. (2014). Effect of draw ratio on the morphologies and properties of BPDA/PMDA/ODA polyimide fibers. *Chemical Research in Chinese Universities*, *30*(1), 163–167.

Zhao, H., Zhang, M., Zhang, S., & Lu, J. (2012). Influence of fiber characteristics and manufacturing process on the structure and properties of aramid paper. *Polymer-Plastics Technology and Engineering*, *51*(2), 134–139.

Zhu, C., Liu, X., Guo, J., Zhao, N., Li, C., Wang, J., et al. (2013). Relationship between performance and microvoids of aramid fibers revealed by two-dimensional small-angle X-ray scattering. *Journal of Applied Crystallography*, *46*(4), 1178–1186.

Further reading

ASTM D3938-13. (2013). *Standard guide for determining or confirming care instructions for apparel and other textile products*. West Conshohocken, PA: ASTM International.

ASTM D4966-12e1. (2012). *Standard test method for abrasion resistance of textile fabrics (Martindale abrasion tester method)*. West Conshohocken, PA: ASTM International.

Stull, J., & Stull, G. (2010). Determining when PPE needs to be retired. *Fire and Rescue News*. May 25 (Accessed 22 July 2016).

Torvi, D., & Hadjisophocleous, G. (1999). Research in protective clothing for firefighters: State of the art and future directions. *Fire Technology*, *35*(2), 111–130.

Zhu, X., Yuan, L., Liang, G., & Gu, A. (2014). Unique UV-resistant and surface active aramid fibers with simultaneously enhanced mechanical and thermal properties by chemically coating Ce0.8 Ca0.2 O1.8 having low photocatalytic activity. *Journal of Materials Chemistry A*, *29*(2014), 11286–11298.

This page intentionally left blank

Advanced chemical testing of textiles

6

Y. Shao, V. Izquierdo, P.I. Dolez
CTT Group, Saint-Hyacinthe, QC, Canada

6.1 Introduction

The chemical composition and nature of textile finishes play an important role in their properties, functions, and applications. Therefore, textile manufacturing plants and testing laboratories often conduct fiber content and composition analysis of textiles as well as chemical assessments of textile finishes.

Textile finishing dates back to 1929, when cotton fabrics were treated with urea-formaldehyde resin for a wrinkle-free appearance (Lane, 1934). Because of the toxicity of formaldehyde, durable pressing (DP) finishing are generally now low formaldehyde or formaldehyde free (Oeko-Tex 1000, 1995).

Besides DP finishing, different finishes have been and are being developed to provide textiles with functionalities for special applications, such as antimicrobial, insect-repellent, stain-free, and UV protection. In particular, UV protection is not only important to limit the degradation of textiles; textile finishes may also protect the wearer from the harmful effect of UV on the skin.

In addition, for some applications, textiles may need to offer some resistance to various chemicals—acids, alkalis, or organic solvents for instance. The resistance of textiles to chemicals may be evaluated by measuring the residual performance after a period of immersion in the chemical of interest.

Textiles may also have to act as a barrier for toxic chemicals. These may be liquids, gases, vapors, or particulates. In the case of clothing, a reasonable permeability to air and/or water vapor may be desired to provide some level of comfort to the wearer.

Finally, for better environmental sustainability, a textile material should ideally be recyclable, reusable, and/or biodegradable after use. Usually, natural fibers and manufactured regenerated cellulose fibers are more biodegradable than synthetic fibers. Some biodegradable synthetic fibers have also been developed. Biological degradation tests allow assessing the capacity of textiles to biodegrade.

This chapter provides a description of chemical tests assessing the nature and function of textiles and finishes. Caution must be exercised when performing these tests because the chemicals used may be dangerous. Standard laboratory atmospheres (air conditions) to be used for testing textile materials may be found in the standards CAN/CGSB 4.2 No. 2–M88 (2013), ISO 139 (2005), or ASTM D1776 (2016).

Advanced Characterization and Testing of Textiles. https://doi.org/10.1016/B978-0-08-100453-1.00007-6

6.2 Measurement of extractable content

Textile extractable content or nonfibrous materials, which may be either natural constituents of the fibers (such as cotton wax, wool grease, etc.) or additives (such as spinning oils, finishes, etc.), can be removed by extraction. For example, soap and cationic finishing may be removed from textiles by aqueous extraction. Starch and gelatin may be eliminated with an enzyme treatment. Waxes, oils, and greases may be removed by petroleum extraction, while some resin finishes may be removed using phosphoric acid and urea treatment.

According to the standard test method CAN/CGSB 4.2 No. 15 (2003), test specimens are first oven-dried at 105–110°C or conditioned until they reach a constant weight; for example, general textiles are generally conditioned at 20 ± 2°C and 65 ± 2% RH (CAN/CGSB 4.2 No. 2–M88, 2013), while nonwovens can be conditioned at 23 ± 2°C and 50 ± 5% RH (ASTM D1776, 2016).

In addition to the standard extraction procedures described below, it is possible to analyze the result of the extraction using analytical techniques such as FT-IR (see Section 6.3). This is a procedure generally used to confirm the nature of the nonfibrous material extracted from the textile materials. It is also performed in some cases for defect analysis.

6.2.1 Extraction of water soluble species

The oven-dried or conditioned specimen is immersed in distilled water at 50°C at a liquor ratio of 100:1 for 30 min (CAN/CGSB 4.2 No. 15, 2003). Then the specimen is thoroughly rinsed and oven-dried or conditioned to a constant weight. The difference in weight of the specimen before and after extraction is attributed to the water soluble materials in the textile.

6.2.2 Extraction of starch and sizing compounds by enzyme treatment

The oven-dried or conditioned specimen is immersed in an aqueous solution of enzymes at the conditions (temperature, liquor ratio, time, etc.) suggested by the enzyme supplier (CAN/CGSB 4.2 No. 15, 2003). Then the specimen is thoroughly rinsed and oven-dried or conditioned to constant weight. The difference in weight of the specimen before and after extraction is attributed to the enzyme extractable materials in the textile.

6.2.3 Extraction of nonfibrous materials by solvent extraction

The oven-dried or conditioned specimen is extracted with a solvent for 2 h (at least 12 siphons) in a Soxhlet extractor (CAN/CGSB 4.2 No. 15, 2003). It is then allowed to air dry in a fume hood before being oven-dried or conditioned to a constant weight. The difference in weight of the specimen before and after extraction is attributed to the solvent extractable materials in the textile.

A list of solvents to be used depending on the species to extract is provided in the standard test method CAN/CGSB 4.2 No. 15 (2003). For example, hexane may be used for oils, waxes, softeners, and silicones. Extraction of small amounts of unfixed polymers—polyester, acrylic, polyurethane, or polyvinyl acetate resins—may be carried out with 1,1,1-trichloroethane.

6.2.4 Extraction of amino-formaldehyde resin finishes by urea and phosphoric acid treatment

The oven-dried or conditioned specimen is immersed in an aqueous solution containing 5% urea and 1.5% phosphoric acid with a liquor ratio around 100:1 at 80°C for 1 h (CAN/CGSB 4.2 No. 15, 2003). It is then rinsed thoroughly with warm water, neutralized with a few drops of ammonia, rinsed again, and oven-dried or conditioned to constant weight. The difference in weight of the specimen before and after extraction is attributed to the amino-formaldehyde resin finish in the textile.

6.3 Analysis of fiber content

Textile industries, commercial markets, and testing laboratories often require qualitative and/or quantitative analysis of fiber content in textiles. Textile fibers can be classified as natural or man-made. Natural fibers comprise cellulose-based fibers such as cotton, hemp, and linen; protein-based fibers such as silk and wool; and mineral fibers such as asbestos. It is to be noted that asbestos fibers are banned in many countries because of their effect on health (CCOHS, 2017). Man-made fibers include cellulose-based fibers, e.g., rayon, acetate, and triacetate fibers; and synthetic fibers, e.g., acrylic, nylon, modacrylic, polyester, para-aramid (e.g., Kevlar®), and meta-aramid (e.g., Nomex®).

Several organizations have published standard test methods for qualitative and/or quantitative analysis of fiber contents in textiles (e.g., AATCC TM 20A, 2014; ASTM D629, 2015; CAN/CGSB 4.2 No. 14, 2005). These methods propose a combination of different tests to identify the fiber nature, including solubility tests, microscopic observation, refractive index measurement, infrared spectroscopic analysis, burning test and melting point test, etc. In particular, a series of analytical methods is suggested for the separation and quantification of binary fiber mixtures based on differences in solubility in various solvents. For instance, polyester—olefins mixes are analyzed by dissolving olefin fibers in boiling xylene while polyester mixed with acetate and/or nylon 6 or 66 is quantified by dissolving the nylon and/or acetate fibers in 90% formic acid (ASTM D629, 2015). However, these analytical techniques are difficult to use if the composition of the textile sample is unknown or if there are more than two components in the textile.

In order to overcome these difficulties, a step-by-step analysis protocol has been developed at CTT Group (Canada) to allow identifying the nature of the fibers in a sample of unknown composition (Shao & Filteau, 2004). It is based on a succession of solubility tests conducted with various solvents (Table 6.1). After the nonfibrous content has been removed (see Section 6.2.3), the textile specimen is dried in an oven at 105°C until it reaches a constant weight. That dry weight (around 1–2 g) is recorded:

Table 6.1 Step-by-step analysis by solubility tests of the fiber content of a sample of unknown composition (Shao & Filteau, 2004)

Specimen 1		Specimen 2		Specimen 3	
Step 1: Treated with formic acid (85%) at room temperature for 10 min	*Yes*[a]: Contains nylon, acetate, or triacetate	*Step 2*: Treated with acetone (99%) at room temperature for 25 min	*Yes*: Contains acetate and/or triacetate *No*[a]: Weight loss in step 1 due to nylon	*Step 3*: Treated with acetone (65%) at room temperature for 25 min	*Yes*: Presence of acetate *No*: Weight loss in step 2 due to triacetate
Step 4: Treated with dimethylformamide at 60–93°C for 5 min	*Yes*: Contains acrylic, modacrylic, PVC, and/or spandex; Proceed to step 5 *No*: Proceed to step 6	*Step 5*: Treated with boiling cyclohexanone (99%) for 5 min	*Yes*: Contains modacrylic PVC, and/or spandex[b] *No*: Weight loss in step 4 due to acrylic		
Step 6: Treated with boiling xylene (97%) for 5 min	*Yes*: Contains polyolefins[b]				
Step 7: Treated with sulfuric acid (75%) at 40–50°C for 25 min	*Yes*: Contains cotton,[b] linen, ramie, rayon and/or silk; Proceed to step 8 *No*: Proceed to step 10	*Step 8*: Treated with a solution of zinc chloride in formic acid (85%) at 40°C for 2 h	*Yes*: Contains rayon and/or silk; proceed to step 9 *No*: Weight loss in step 7 due to cotton, ramie, or rayon; proceed to step 10	*Step 9*: Treated with boiling sodium hydroxide (10%) for 10 min	*Yes*: Contains silk *No*: Weight loss in step 8 due to rayon

Step 10: Treated with sodium hypochlorite (5%) at room temperature for 45 min	*Yes*: Contains wool *No*: Proceed to step 11				
Step 11: Treated with boiling nitrobenzene (99%) for 5 min	*Yes*: Contains polyester *No*: Proceed to step 12				
Step 12: Treated with boiling sodium hypochlorite (5%) for 15 min	*Yes*: Contains para-aramid (Kevlar) *No*: Proceed to step 13				
Step 13: Treated with boiling sulfuric acid (75%) for 10 min	*Yes*: Contains meta-aramid (Nomex) *No*: Possible presence of inorganic fibers				

[a] "Yes" means that some weight loss is measured after the treatment. "No" means that the treatment does not generate any weight loss.
[b] Needs further confirmation by other techniques (see below).

it corresponds to W_0 in the equation used to compute the fiber content (Eq. 6.1 on the next page). Two or three specimens of the textile sample are needed for parallel tests and confirmation. This step-by-step analysis protocol has been included in a standard (CAN/CGSB 4.2 No. 14, 2005), which is regularly revised.

At some instances in the step-by-step analysis protocol in Table 6.1, it is mentioned that the nature of the fiber needs to be confirmed by other techniques. These include infrared spectroscopy (IR), differential scanning calorimetry (DSC), and microscopy. For example, in Step 5, the PVC, spandex, and modacrylic fibers may be identified by IR. Fig. 6.1 gives an example of spandex and PVC IR spectra. If residues are left at the end of Step 13, IR analysis may also be used to identify if these are glass fibers.

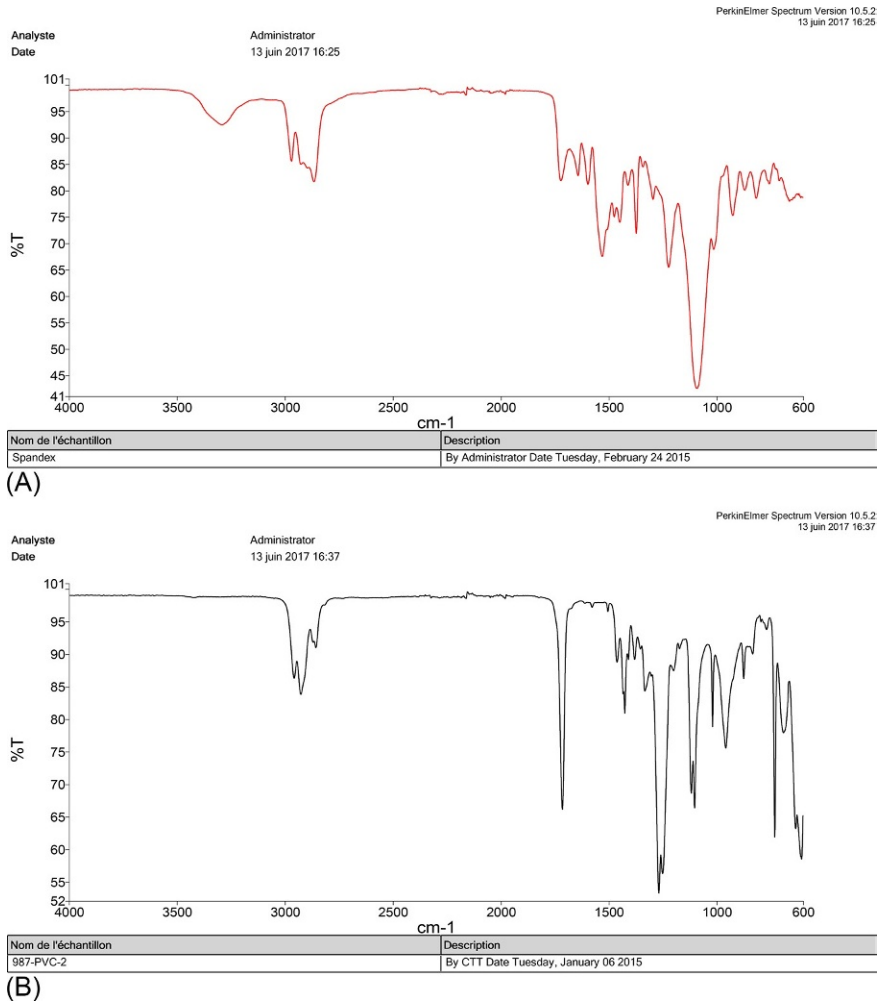

Fig. 6.1 Examples of (A) Spandex and (B) PVC IR spectrum.

On the other hand, the type of nylon and polyolefin in Step 2 and 6 respectively may be identified based on their melting point: for example, polyethylene has a melting point of 135°C, and polypropylene has a melting point of 170°C; Nylon 6 melts between 213°C and 225°C, and nylon 66 melts between 256°C and 265°C. Fig. 6.2 gives an example of a melting curve obtained by differential scanning calorimetry (DSC); the sample is polypropylene with a melting point of 160°C.

In Step 7, cotton and ramie may be identified by microscopic observation. AATCC Technical Manual (AATCC TM 20, 2013) provides the melting point, appearance, and infrared spectrum of some textile materials. Microscopic pictures of the cross-section and longitudinal view of textile fibers are also included in this standard test method.

At the end of each step of the analysis protocol presented in Table 6.1, the specimen is rinsed thoroughly with water if water soluble chemicals are used. If the treatment involves the use of an acid, it is first neutralized with sodium bicarbonate and then rinsed with hot water. In the case of nonwater soluble solvents, the specimen is thoroughly washed with acetone or ethanol and then rinsed with water. After rinsing, the specimen is dried in an oven at 105°C until a constant weight is obtained. The fiber content in dry conditions at the end of step n is provided by the following equation:

$$\text{Fiber content}(\%)\,|_n = \frac{W_n - W_{n-1}}{W_0} \times 100 \tag{6.1}$$

with W_n and W_{n-1} being the weight of the dry specimen at the end of step n and $(n-1)$ respectively; and W_0 is the initial dry weight of the specimen. As an illustration, the polyester fiber content in the specimen provided by the analysis performed in step 11 can be computed as follows:

$$\text{Polyester fiber content}(\%)\,|_{11} = \frac{W_{11} - W_{10}}{W_0} \times 100 \tag{6.2}$$

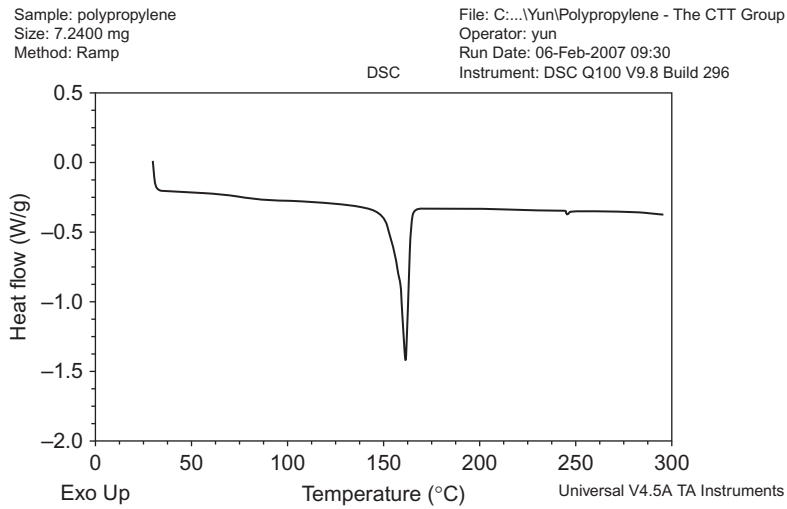

Fig. 6.2 DSC curve of polypropylene.

where W_{11} and W_{10} represent the dry weight of the specimen at the end of the treatment of step 11 and step 10 respectively.

The fiber content may also be expressed on a commercial moisture regain basis using tabulated values of moisture regain contained in ASTM D1909 (2013) or CAN/CGSB-4.2 No. 0 (2001).

6.4 Chemical testing of functional finishes

6.4.1 Antibacterial finishes

Antibacterial treatments are a large part of textile finishes, especially for protective clothing, medical garments, carpets, and daily hygiene products. The antimicrobial function can be brought by the polymer itself or by antibacterial finishes applied on the textiles.

For instance, some polymers such as those containing quaternary ammonium atoms, guanidine, halogens, or phospho- and sulfo-derivatives exhibit inherent antimicrobial activity (Muñoz-Bonilla & Fernández-García, 2012). Other polymers may be imparted with an antibacterial function by chemical modification, addition of low molecular weight antimicrobial compounds, blend with antimicrobial polymers, or addition of metal particles or metal oxides. These antimicrobial polymers may then be used as the raw material to manufacture textile fibers or filaments.

Antibacterial finishes usually involve quaternary ammonium, *N*-halamine, or silver or copper salts (Qian & Sun, 2003). Quaternary ammonium salts are the main group of antimicrobial finishing agents and include, for example, *n*-alkyldimethylbenzylammonium chloride and benzyldimethyldodecylammonium chloride (BDMDAC). Ferreira, Pereira, Pereira, Melo, and Simoes (2011) studied the mechanism of action of BDMDAC against the bacteria *Pseudomonas fluorescens*: BDMDAC binds to the bacteria cell membrane through ionic and hydrophobic interaction and induces changes in the membrane properties and functions such as cellular disruption and loss of membrane integrity. Quaternary ammonium salts may be extracted with isopropanol and their content measured by potentiometric titration according to the standard test method ASTM D5070 (1990).

N-halamine is another group of antimicrobial agents. Its mechanism of action follows the reaction below (Qian & Sun, 2003):

$$=\mathrm{N}-\mathrm{Cl}+\mathrm{H_2O}\rightarrow =\mathrm{N}-\mathrm{H}+\mathrm{Cl}^{+}+\mathrm{OH}^{-} \qquad \text{(Reaction 1)}$$

The chlorine slowly released by the *N*-halamine compound kills bacteria by direct transfer of positive halogens to receptors near or at the cell outer membrane. The two large advantages of this antimicrobial solution are that no development of resistance has been observed and, after the active compounds have been depleted, the antimicrobial efficiency can be restored by treatment with halogen-releasing chemicals such as bleach:

$$=\mathrm{N}-\mathrm{H}+\mathrm{Cl}^{+}+\mathrm{OH}^{-}\rightarrow =\mathrm{N}-\mathrm{Cl}+\mathrm{H_2O} \qquad \text{(Reaction 2)}$$

In order to increase the washing durability of *N*-halamine-treated textiles, the *N*-halamine compound has been grafted to cellulose using 3-methylol-2,2,5,5-tetramethylimidazolidin-4-one (Qian & Sun, 2003). The resulting fabrics contain a more stable yet less reactive amine *N*-halamine structure, thus providing a slow but durable biocidal function. The *N*-halamine treated fabrics are used for surgical gowns, drapes, and medical gloves for instance.

The *N*-halamine content on textiles may be determined by chlorine titration (Li et al., 2015). *N*-halamine grafted cotton fabric swatches are chlorinated by exposure to a 10% sodium hypochlorite (0.5% NaClO) solution at a pH of 7 at room temperature for 1 h. The chlorinated swatches are washed thoroughly with distilled water and dried at 45°C for 1 h to remove free chlorine from the surface of the cotton fabric. The chlorine loading in the swatches is determined by iodometric/thiosulfate titration. The chlorine content of the cotton swatches is calculated using the following equation:

$$\mathrm{Cl}^{+}(\%) = \frac{35.45N \cdot V}{2W} \times 100 \tag{6.3}$$

where Cl^{+} (%) is the weight percent of oxidative chlorine in the samples, *N* and *V* are the normality (eq./L) and volume (L) of the titrant sodium thiosulfate, respectively, and *W* (g) is the initial weight of fabric swatch. The chlorine captured by the testing specimen can be converted to yield the content of *N*-halamine according to the stoichiometric ratios in Reaction 2.

Another antimicrobial solution is based on the use of silver particles. For instance, SilverClear® is a silver salt-containing commercial antimicrobial, bactericidal, and antiodor product patented by Tessier, Radu, and Filteau (2009, 2015). Applied as a liquid, it forms a transparent, durable coating at the surface of the textile yarns/fibers once it has been properly cured to cross-link the polymer matrix.

A procedure has been developed at CTT Group (Canada) to measure the silver content in fabrics treated with SilverClear®. It involves the following steps: (1) Prepare a specimen of around 2 g of the fabric to be tested and weigh it precisely to the nearest 0.1 mg; (2) Soak the specimen in 150 mL of a solution of 1 N nitric acid at 40°C for 20 min under stirring conditions; (3) Transfer the solution without the test specimen in a 250 mL volumetric bottle; (4) Soak the test specimen in 80 mL of fresh 1 N nitric acid at 40°C for 10 min under stirring conditions; (5) Add that new soaking solution without the test specimen to the same 250 mL volumetric bottle, dilute with distilled water to 250 mL, and shake well; (6) Withdraw 10 mL of the extracted solution, transfer to a 100 mL volumetric bottle, dilute with distilled water to 100 mL, and shake well. (7) Prepare at least 5 standard silver solutions from a standard 1000 ppm silver solution—for example, 1, 5, 10, 15, and 20 ppm; (8) Use atomic absorption analysis (AAA) or an inductively coupled plasma (ICP) spectrometer to analyze the standard silver solutions and obtain a calibration curve; (9) Measure the silver concentration (in ppm) in the solution obtained in step 6. The silver content in the tested specimen can be calculated by the following equation:

$$\mathrm{Silver}(\%) = R \cdot W\left(\frac{250}{1000}\right) \cdot \left(\frac{100}{10}\right) \cdot \left(\frac{100}{1000}\right) = 0.25R \cdot W \tag{6.4}$$

in which the factors (250/1000) and (100/10) correspond to the dilution steps and the factor (100/1000) is related to conversion from mg/g to %. The test should be repeated at least twice.

6.4.2 Insect repellent finishes

Insect repellent finishes for textiles are usually based on permethrin or *N*,*N*-diethyl-3-methylbenzamide (DEET). DDT (dichlorodiphenyltrichloroethane) was widely used for that purpose in the 1960s. However, it has since then been banned worldwide because of its toxicity and polluting effect on the environment.

DEET was developed as a pesticide by the US Department of Agriculture in 1944 (AMCA, 2014). It was registered for use by the general public in 1957. It is effective against mosquitoes, biting flies, chiggers, fleas, and ticks. DEET concentration in today's products ranges from 5% (with a 90 min lasting effect) to 100% (yielding 10 h of protection from insect bites). DEET is mainly applied on the skin and has been deemed safe to use with a concentration of up to 30% by anyone over the age of two months by the American Academy of Pediatrics.

On the other hand, permethrin is a synthetic version of pyrethrum, which is a powerful rapidly acting insecticide derived from the dried flowers of the *chrysanthemum* plant (Wolverton, 2013). Permethrin works as a contact insecticide with a knockdown action by inducing nervous system toxicity. It is effective on mosquitos, fleas, ticks, human lice, etc. Permethrin may be sprayed on clothing and other fabrics but should not be used directly on the skin. Permethrin may be assessed by measuring its knockdown efficiency on insects. For the test, a sample of permethrin treated fabric is placed in an enclosed space containing insects for a specified period of time, after which the sample is removed and the insects' reaction is recorded. Wolverton (2013) used this technique to assess the launderability of permethrin-treated blankets. The residual efficiency with mosquitos and ticks was 100% after 25 washes and 90% after 50 washes.

The permethrin content in textiles may also be obtained by extraction and infrared spectroscopic analysis. Indeed, permethrin is not soluble in water but is soluble in alcohols, ethanol for instance. The residue of the extraction after ethanol evaporation can be further analyzed by IR.

6.4.3 Stain-free finishes

Antisoiling properties of textiles come from a change in the interfacial energy leading to a high contact angle (Fig. 6.3). In Fig. 6.3, γ_{LG}, γ_{SL}, and γ_{SG} are the liquid/gas, solid/liquid, and solid/gas interfacial energies respectively. θ_c is the contact angle of the liquid on the solid surface. They meet Young's equation (Young, 1855):

$$\gamma_{LG} \cos\theta_c = \gamma_{SG} - \gamma_{SL} \tag{6.5}$$

From the above equation, it can be seen that the contact angle increases with decreasing the surface energy of the solid γ_{SG}. When the contact angle increases above 150 degrees (Fig. 6.3B), the liquid does not wet the surface of the solid, thus it cannot

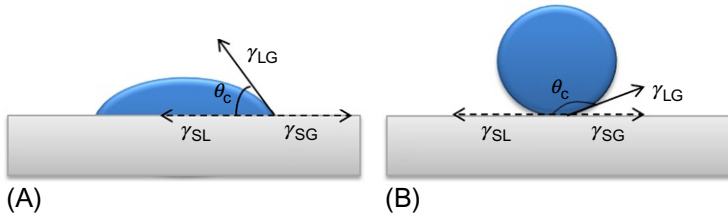

Fig. 6.3 Contact angle of a liquid on a solid surface: (A) low contact angle; (B) high contact angle.

stain the solid. This is the main method used to impart textiles with stain-resistant properties.

Stain-resistant finishes for textiles generally involve the use of fluorocarbon or polysiloxane compounds, which have a low surface tension (Wang & Liu, 2009). In addition, nanoparticles may be used to coat the surface of textiles and lead to water contact angles of more than 150 degrees, i.e., leading to a superhydrophobic behavior. For instance, Arfaoui, Dolez, Dubé, and David (2016a; 2016b) have provided recycled jute fibers and nonwovens with stable superhydrophobic properties using zinc oxide (ZnO) or titanium dioxide (TiO_2) nanoparticles combined with a fatty acid.

Fluorocarbon or polysiloxane content in textiles may be analyzed by IR spectroscopy after extraction with hexane according to the standard test method CAN/CGSB 4.2 No. 15 (2003). Examples of the IR spectrum of fluorocarbons and polysiloxanes are shown in Fig. 6.4.

Nanoparticle coatings on textiles may be observed using a field emission scanning electron microscope (FE-SEM). For instance, Fig. 6.5 provides pictures of ZnO nanorods grown on jute fibers. The metal oxide content in the textile may be obtained by AAA or ICP using the same procedure described in Section 6.4.1 for silver quantification of the SilverClear® antibacterial textile treatment.

The oil repellency of a fabric may be evaluated according to the standard test method AATCC TM 118 (2007). Eight different liquids with different surface tensions are used for the tests, ranging from Kaydol (high surface tension, liquid No. 1) to *n*-heptane (low surface tension, liquid No. 8). Five drops of liquid No. 1 are deposited on the fabric specimen and observed for 30 ± 2 s. If there is no penetration or wetting or wicking of the fabric by the liquid, the test is repeated with the liquid with the next highest number until failure is recorded, i.e., when three of five drops show complete wetting or wicking with loss of contact angle.

Using the same principle of wetting and wicking of droplets on the fabric surface, the standard test method AATCC TM 193 (2012) was developed to measure the aqueous liquid repellency using different water-alcohol solutions having surface tensions from 24 to 59 dynes/cm at 25°C. In this method, the evaluation is performed during a 10-s period.

The soil repellency of a fabric may be assessed by staining the fabric with corn oil (AATCC TM 130, 2000). The stained specimen is covered by a piece of glassine paper and loaded with a 5 pound weight for 1 h. Then, the stained fabric is washed and dried according to a specific laundering procedure. Finally, the residual stain on the test

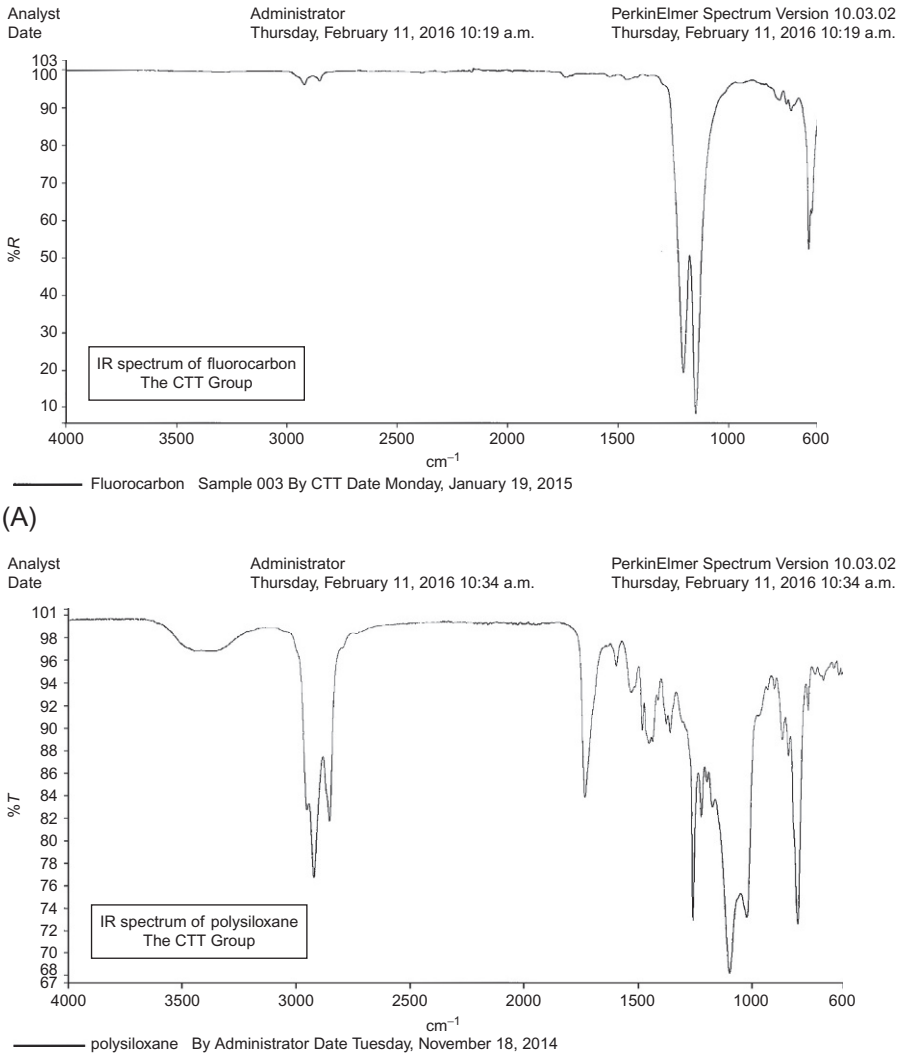

Fig. 6.4 Examples of FTIR spectrum of (A) a fluorocarbon and (B) a polysiloxane.

specimen is graded using a stain release rating scale. Grade 1 represents a low stain removal and Grade 5 represents a perfect stain removal.

6.4.4 UV protection

UV radiation is usually classified into three regions: UVA (320–400 nm), UVB (290–320 nm), and UVC (100–290 nm). Most of the UVC radiation is blocked by the ozone layer around the earth. On the other hand, a large amount of UVA and UVB radiations passes through the atmosphere. The high energy of the UV radiation induces

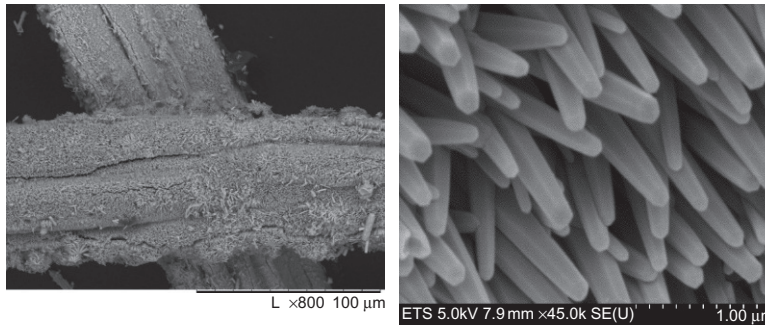

Fig. 6.5 SEM pictures of ZnO nanorods in jute fibers: (A) magnification ×800; (B) magnification ×5000 (Arfaoui et al., 2016a).

beneficial as well as harmful effects on health. For instance, UV is responsible for the synthesis of vitamin D in humans and other land vertebrates. However, it may also cause skin cancer, have damaging effects on the eye, suppress the immune system, and aggravate several skin conditions and diseases (NASA, 2014).

Some textiles and textile structures may provide some level of UV protection to the wearer. For instance, Shao and Nantel (1998a, 1998b) studied the effect of factors such as fiber content, textile structures, dyes, pigments, and anti-UV agents on the UV protection of textiles.

UV radiation may also induce a premature aging of textiles. In order to improve the resistance of textiles to UV, anti-UV agents may be added directly into polymers before spinning or applied as dyes, coating, or finishes on textiles. The three main types of anti-UV agents are UV absorbers, quenchers, and hindered amine light stabilizers (HALS) (Gerard, 2014). UV absorbers convert UV radiation into harmless infrared radiation (or heat). Carbon black is one of the most effective and commonly used UV absorbers. Another UV absorber is titanium dioxide. It is effective in the 300–400 nm range but has limited efficiency in the UVB range below 315 nm. Hydroxybenzophenone and hydroxyphenylbenzotriazole are also often employed as UV stabilizers since they can provide clear UV coatings. Quenchers return chromophores from excited to ground state before the photo-oxidation reaction proceeds any further. They are generally organic complexes of transition metals such as nickel, iron, or chromium. However, their use is limited by their inherent color as well as the toxicity of the heavy metals. HALS trap free radicals formed during the photo-oxidation reaction and stop the progress of the degradation process. They all have a 2,2,6,6-tetramethylpiperidine ring structure. HALS are effective for polypropylene, polyethylene, and polyurethane but not for PVC.

In addition to the traditional UV absorbers mentioned above, metal oxides such as TiO_2 and ZnO display increased UV-blocking properties when at the nanoscale thanks to their very large surface area (Zhang, 2009). Moreover, they have the advantage of being transparent, nontoxic, and chemically stable under exposure to both high temperatures and UV.

The resistance of textiles to UV degradation can be assessed using aging tests—for instance, CAN/CGSB-4.2 No. 69–M91 (2013), AATCC TM 169 (2009), AATCC TM 16.3 (2014), and ASTM G155 (2013). The specimen is installed in a xenon-arc apparatus for a defined period of time at specific UV radiation and temperature conditions. It may also be exposed simultaneously to water spray. After the aging period, the specimen is observed, and its residual performance such as tensile strength is measured and compared with the initial condition.

The nature of the UV absorbers in the textile may be identified by IR. Their content may be assessed by AAA or ICP or even HPLC-MS analysis after extraction by a proper solvent.

On the other hand, the protection offered by textiles to UV radiation is rated in terms of the ultraviolet protection factor (UPF) (AATCC TM 183, 2014; AS/NZS 4399, 1996). It is defined as the following (AS/NZS 4399, 1996):

$$\mathrm{UPF} = \frac{\sum_{290}^{400} E_\lambda \cdot S_\lambda \cdot \Delta\lambda}{\sum_{290}^{400} E_\lambda \cdot S_\lambda \cdot \tau_\lambda \cdot \Delta\lambda} \tag{6.6}$$

in which λ is the wavelength, E_λ is the relative erythemal spectral effectiveness on human skin, S_λ is the solar spectral irradiance, and τ_λ is the spectral transmittance of the specimen. The UPF may be obtained directly from a measuring device such as the UV-2000 F (Labsphere). Otherwise, the transmission of the UV radiation through the specimen may be measured with a UV spectrometer.

The durability of the UPF performance is addressed by subjecting specimens to aging treatments prior to the UPF measurement. Suggestions of these pretreatments may be found in the standard practice ASTM D6544 (2012). It consists, for instance, of UV exposure as per AATCC TM 16.3 (2014), multiple washings as per AATCC TM 135 (2015), or exposure to chlorinated pool water (AATCC TM 162, 2011) or nonchlorine bleach laundering (AATCC TM 172, 2016).

6.5 Measurement of the resistance to chemicals

The test method described in Section 6.3 to analyze the fiber content of textiles takes advantage of the varied response different fibers display when exposed to chemicals. For example, acetate fibers are sensitive to acetone; nylon fibers dissolve in formic acid; cotton fibers are hydrolyzed in sulfuric acid; while wool fibers have a low resistance to alkalis.

Table 6.2 gives a rating of the resistance of different textile materials to different concentrations of chemicals at 20°C and 60°C. In some instances, an increase in temperature or in the chemical concentration leads to a decrease in the textile resistance to that chemical.

The resistance of textiles to chemicals can be assessed by immersion in the chemical. For instance, the test method ISO 8096-2 (1989) describes a procedure in which a fabric, a coated fabric, or a plastic specimen is immersed in a solution of 40 g/L of

Table 6.2 Resistance to chemicals of some textile materials (A: negligible effect; B: limited effect; C: considerable effect; D: dissolves or decomposes)

	Nylon		Polyester		Polypropylene		Polyethylene		Kevlar®	
Chemicals	**20°C**	**60°C**	**20°C**	**60°C**	**20°C**	**60°C**	**20°C**	**60°C**	**20°C**	**60°C**
Carbon tetrachloride	A	A	A	A	C	C	B	C	A	A
Chlorine gas	D	D			D	D	C	C		
Hydrochloric acid										
10%	C	C	B	B	A	A	A	A	C	D
38%	D	D	C	C	A	B	A	A	D	D
Hydrogen peroxide										
10%	D	D	B	C	A	B	A	B		
30%	D	D	B	D	B	C	A	B		
Methyl ethyl ketone	A		A		A	C	A	A	A	A
Motor oil	A	A	A	A	B	D	A	A	A	A
Nitric acid										
10%	D	D	A	B	A	B	A	A	B	C
70%	D	D	C	D	C	D	A	B	D	D
Phenol	D	D	C	D	C	D	B	C		
Silicon oil	A	A	A	A	A	A	B	C		
Sulfuric acid										
10%	C	D	B	C	A	A	A	A	C	D
98%	D	D	D	D	C	C	B	C	D	D
Sodium hydroxide										
10%	A	A	A	B	A	A	A	A	B	C
50%	B	C	D	D	A	A				
Toluene	A	A	A	A	B	C	B	C	A	A
Xylene	A	A	A	A	C	C	B	D		

Adapted from Miller. (2017). Harness textiles—Resistance to chemicals and other information. Miller by Sperian.

boiling sodium hydroxide (NaOH) for 10 min. The treated specimen is then washed under cold running water for 4 h. The effect of immersion in NaOH is evaluated by observation of the textile aspect (e.g., sign of delamination) and determination of the residual performance—for example, tensile strength, water penetration resistance, or any other property of concern.

For geosynthetics, the standard test method ASTM D5322 (2017) may be used instead. According to the laboratory immersion procedure described, test specimens are immersed in a tank containing the challenge liquid. The tank is sealed and kept at 23°C or 50°C. Specimens are collected after exposure periods of 1, 2, 3, and 4 months. The condition of the textile specimens before and after exposure to the challenge liquid is evaluated by physical testing.

6.6 Measurement of the permeability to air, water vapor, solvents, particles, and toxic chemicals

6.6.1 Permeability to liquids, water vapor, and air

Permeability to solvents and toxic chemicals is critical for protective clothing and filters. It is also relevant for clothing used daily. In the case of clothing, it may be desirable that liquids are blocked while a certain level of air and water vapor permeability out of the clothing is allowed to improve the comfort of the wearer.

Indeed, as indicated by Budd (1981), the metabolic heat produced by an individual at rest is about 70 W. That heat rises to around 1000 W under strenuous exercise conditions. The metabolic heat causes the temperature inside the clothing to rise by 3°C in 10 min. In addition, about 10 L of sweat are produced every 8 h during heavy exercise (Smith et al., 1995). In the United States, fire fighters' deaths caused by heat stress or overexertion reached 56% in 2012 and 35% in 2013 (USFA, 2014). These grime data illustrate how important water vapor permeability is to allow dissipating the metabolic heat of the clothing wearer and limit heat stress.

For instance, Gore-Tex® (Gore, 1976) is a waterproof yet breathable membrane. Invented in 1969, the stretched microporous polytetrafluoroethylene (PTFE) membrane is able to repel liquid water while allowing water vapor to pass through. It is often used as a barrier in protective clothing to block toxic liquid chemicals inward but let water vapor go out to prevent metabolic heat buildup. An alternative strategy developed by Stedfast with its Stedair® membrane is based on a combination of laminated layers with various hydrophilic and oleophobic properties (Stedfast, 2017).

The resistance of a fabric to liquid penetration may be tested according to ASTM F903 (2017). A conditioned specimen is installed in a penetration test apparatus and exposed to the challenge liquid on one side for a specified time and pressure. For example, procedure C involves 5 min of exposure at 0 psig followed by 1 min at 2 psig and then 54 min at 0 psig. Visual signs of the presence of the challenge liquid on the other side of the specimen are recorded and lead to test failure. A fluorescent dye, food coloring, or an acid-base indicator may be added to the challenge liquid to enhance droplet visibility.

The water vapor permeability may be tested on conditioned specimens using ISO 15496 (2004), ASTM E96 (2005), or CAN/CGSB-4.2 No. 49–99 (2013). ASTM E96 (2005) includes a desiccant method and a water method. In the desiccant method, the test specimen is sealed over the open mouth of a test dish containing a desiccant. The assembly is placed in a controlled atmosphere. Periodic weightings determine the rate of water vapor movement through the specimen into the desiccant. In the water method, the dish contains distilled water and the weightings determine the rate of water vapor movement through the specimen to the controlled atmosphere. The inverted cup option is a variation of the water method allowing the water to be in contact with the test specimen. This allows the evaluation of water vapor permeability of materials when the liquid water is in direct contact with the fabric.

ASTM D737 (2004) and CAN/CGSB 4.2 No. 36–M89 (2013) provide a standard test method for measuring the air permeability of textiles. The conditioned specimen is secured onto the test head of the air permeability testing apparatus. The rate of air flow passing perpendicularly through the specimen is adjusted to obtain the desired air pressure differential between the two faces of the textile. The rate of air flow at the specified pressure differential between the two fabric surfaces is used as a measurement of the fabric air permeability. Ten specimens of the tested fabric should be measured.

6.6.2 Permeability to particles

The passage of particles through textiles is controlled by filtration mechanisms (Lawrence, 2014). The particle liquid or air carrier goes through the textile while some of the particles, usually the coarser ones, are stopped. The performance of a filter largely depends on the pore size and filter cross-plane permeability.

In the case of liquid filtration, the filtration efficiency depends on the pore size and size distribution of the filter; on the viscosity and density of the liquid; as well as on the density, size, shape, hardness, and abrasiveness of the particles (Lynch, 2007). Nonwovens are often used for liquid filtration, for example, in engine oil filters, as well as for air filtration in respirators, medical masks, etc. (Hutten, 2007). They are also found in filter bags and multipleated filters used for air filtration for industrial plants such as in the aluminum refining industry.

Filter porosity may be characterized using the apparent opening size (AOS). In a test method for geotextiles, spherical solid glass beads are dry sieved through the textile specimen for a specified time at a specified frequency of vibration (ASTM D4751, 2012). The amount of beads retained by the geotextile specimen is then measured. The test is carried out for a range of sizes of glass beads. The AOS corresponds to the bead size for which 95% of the glass beads are retained above and within the textile. It is important to note that the opening size of sieves decreases as the pore size increases; e.g., a US Standard Sieve Size of 70 corresponds to a 0.212 mm particle size, whereas a US Standard Sieve size of 100 corresponds to a 0.149 m particle size and a US Standard Sieve Size of 30 corresponds to a 0.595 mm particle.

The filtration efficiency of filters may be determined using a number of test methods that are specific to the intended application. For instance, the efficiency of a vacuum cleaner system may be measured using ASTM F1977 (2004). Six discrete particle

sizes (0.3, 0.5, 0.7, 1.0, 2.0, and >3 μm) of neutralized potassium chloride (KCl) are used as the challenge medium. The total emission of the vacuum cleaner system, whatever the sources, is measured at the nozzle at each of the six particle size levels with a normal airflow rate produced by restricting the inlet to the nozzle adapter with a 1¼-inch orifice while the vacuum cleaner system is being operated in a stationary test condition. The filtration efficiency is computed by comparing the amount of upstream and downstream challenge particles.

6.7 Biodegradability testing

Environmental protection is best when a textile material is recyclable, reusable, or biodegradable after use (Oeko-Tex 1000, 1995). Usually, natural fibers and regenerated fibers are more biodegradable than synthetic fibers. Some biodegradable synthetic fibers have also been developed, such as poly(lactic acid) (PLA), polycaprolactone, and polyglycolide.

PLA is a thermoplastic aliphatic polyester derived from renewable plant sources, such as corn starch and sugar. It may be obtained by direct condensation of lactic acid (2-hydroxy propionic acid) monomers. It is biodegradable and compostable. It is more hydrophilic than typical polyester fibers (Ren, Dong, & Yang, 2006).

Polycaprolactone is also biodegradable but has a low melting point (60°C). The most common use of polycaprolactone is as a coating for applications requiring a high resistance to oils, solvents, and chlorine (Labet & Thielemans, 2009).

Finally, polyglycolide provides high strength, high modulus biodegradable fibers with a melting point around 225–230°C. Polyglycolide is widely used as a biomaterial, e.g., for bone tissue engineering (Gentile, Chiono, Carmagnola, & Hatton, 2014).

The biodegradability of a material can be computed according to the following equation (EC 648, 2004):

$$\text{Biodegradability}(\%) = \frac{\text{BOD} - B}{\text{TOD}} \times 100 \tag{6.7}$$

in which BOD is the biochemical oxygen demand of the material, B is the medium oxygen demand, and TOD is the theoretical oxygen demand when the material is completely oxidized.

BOD is a procedure aimed at determining the dissolved oxygen consumed by microbial life while oxidizing the sample (EPA 405.1, 1974). In general, the test is conducted over 5 days and is called BOD5. The specimen is introduced in a bottle containing microorganisms, a carbon nutrient source of glucose-glutamic acid, and dissolved oxygen (DO). It is then incubated for 5 days at 20°C in the dark. The BOD of the sample is provided by the difference between the initial (prior to incubation) and final (after 5 days of incubation) DO readings. The DO may be determined using the Winkler titration method, which consists in fixing dissolved oxygen in water using a series of reagents (manganese sulfate, alkaline iodide azide, and concentrated sulfuric acid). The acid compound that is formed is then titrated with sodium thiosulfate using a starch solution to identify the titration endpoint.

In Eq. (6.7), *B* is obtained by conducting the same procedure as for the determination of BOD, but without including a material specimen in the incubating bottle.

Finally, TOD may be measured by recording the oxygen level in a carrier gas when a material specimen is thermally oxidized in an oven. It may also be calculated based on the stoichiometric ratios of the chemical reaction of the material with oxygen. For example, the oxidation of cotton fibers can be expressed as the following:

$$-\left(C_6H_{10}O_5\right)_n - +6nO_2 \rightarrow 6nCO_2 + 5nH_2O \qquad \text{(Reaction 3)}$$

The degradation of 1.62 mg of cotton fibers (which is equal to one unit of glucose) thus requires 1.82 mg of oxygen.

6.8 Future trends

Traditional textile laboratories used to have, in their chemical section, ovens, hotplates, chemicals for reactions, and titration devices; colorfastness to various types of agents was a common assessment. Over the years, chemical testing of textile materials has become more and more complex. This evolution is driven by new needs of the industry, new regulations mostly targeting materials safety, and an increased education and interest of consumers.

For instance, new techniques and instruments are needed to detect the presence of substances of concern and quantify them. This usually requires a long process in the laboratory involving digestion, dilution, and the use of analytical techniques with high performance equipment. For example, formaldehyde content is measured using a standard reaction with NASH reagent followed by a UV absorption test using a spectrometer (CAN/CGSB 4.2 No. 63.4, 2016; CAN/CGSB 4.2 No. 63.5, 2016; AATCC TM 112, 2014). Heavy metals are detected and analyzed using flame atomic absorption (FAA) or inductive coupled plasma (ICP) after acid digestion. Volatile organic compounds (VOC) are qualitatively and quantitatively analyzed using a series of specific sampling bags (obtained directly from the manufacturing location according to test method California 01350 (2010)), extraction chambers, collector tubes, and thermal desorbers followed by gas chromatography (GC-MS) and high performance liquid chromatography (HPLC-MS) analysis. Perfluorinated and polyfluorinated chemicals (PFCs) are also tracked to identify the presence of long chain chemicals such as perfluorooctane sulfonate (PFOS) and perfluorooctanoic acid (PFOA) used as surface treatment on textiles. These chemicals are banned in some countries and there is a need to develop internationally recognized test methods to detect them properly.

On the other hand, fast detection techniques are developed to give the possibility to laboratories to obtain a rapid estimate of the content of substances of concern. For instance, X-ray fluorescence (XRF) lead testing guns are now available and provide an almost instantaneous result in terms of lead content of materials including coatings and polymers. In addition, in-house methods are developed by laboratories to perform "spot tests" used as decision-making tools to perform or not full scale test evaluations.

Finally, there is still a need to develop test protocols to identify certain materials used in the textile industry. This includes for example regenerated cellulose produced with bamboo or other sources. In addition, dyes made of almond shells, saw palmetto, rosemary leaves, and other natural Archroma earth color products cannot currently be differentiated from dyes of petroleum origin because their final chemical structures are similar. The traceability of materials, from the production site to the store, is a solution proposed to guarantee their origin.

6.9 Conclusions

The composition and finishes of a textile material play an important role in its properties, functions, and applications. Textile manufacturing plants and testing laboratories often conduct analyses of the composition (fiber content) of the textile and its eventual finishes. These tests include the extractable or nonfibrous content, both from natural origin (e.g., cotton wax, wool grease, etc.) and resulting from the manufacturing process (e.g., spinning oils, finishes, etc.), as well as the textile fiber content. To that extent, a step-by-step protocol has been developed at CTT Group (Canada) to allow the identification of the nature of the fiber components in a textile sample of unknown origin.

Test methods also exist to assess the nature of the compound used and its efficiency as antibacterial, insect-repellent, stain-free, and UV protective additive and/or finish. In the latter case, UV protection involves both the wearer of the clothing as well as the textile itself. Resistance to chemicals may also be assessed in terms of the effect of the chemical on the textile material as well as the permeability of the textile to chemicals in solid, liquid, vapor, and gas form. In particular, maintaining the certain level of air and water vapor permeability thought clothing is critical to prevent heat build-up and the associated effects on health.

Finally, because sustainable manufacturing has become a concern for all, test methods have been developed to quantify the ability of a textile to biodegrade. It is expected that the demand for these types of tests will increase as an increasing number of "greener" yet well performing textile materials will make the transition from the laboratory to the market.

References

AATCC Test Method 16.3. (2014). *Colorfastness to light: Xenon-Arc*. Durham, NC: American Association of Textile Chemists and Colorists.

AATCC Test Method 20A. (2014). *Fiber analysis: Quantitative*. Durham, NC: American Association of Textile Chemists and Colorists.

AATCC Test Method 20. (2013). *Fiber analysis: Qualitative*. Durham, NC: American Association of Textile Chemists and Colorists.

AATCC Test Method 112. (2014). *Formaldehyde release from fabric, determination of sealed jar method*. Durham, NC: American Association of Textile Chemists and Colorists.

AATCC Test Method 118. (2007). *Oil repellency: Hydrocarbon resistance test*. Durham, NC: American Association of Textile Chemists and Colorists.

AATCC Test Method 130. (2000). *Soil release: Oily stain release method*. Durham, NC: American Association of Textile Chemists and Colorists.
AATCC Test Method 135. (2015). *Dimensional changes of fabrics after home laundering*. Durham, NC: American Association of Textile Chemists and Colorists.
AATCC Test Method 162. (2011). *Colorfastness to water: Chlorinated pool*. Durham, NC: American Association of Textile Chemists and Colorists.
AATCC Test Method 169. (2009). *Weather resistance of textiles: Xenon lamp exposure*. Durham, NC: American Association of Textile Chemists and Colorists.
AATCC Test Method 172. (2016). *Colorfastness to powdered non-chlorine bleach in home laundering*. Durham, NC: American Association of Textile Chemists and Colorists.
AATCC Test Method 183. (2014). *Transmittance or blocking of erythemally weighted ultraviolet radiation through fabrics*. Durham, NC: American Association of Textile Chemists and Colorists.
AMCA. (2014). The American Mosquito Control Association, Mount Laurel, NJ. http://www.mosquito.org/repellents.
Arfaoui, M. A., Dolez, P. I., Dubé, M., & David, É. (2016a). *Hydrophobic treatment for jute fibres based on zinc oxide nanoparticles*. In: *Proceedings of nanotech 2016 conference & expo, Washington, DC, May 22–25*.
Arfaoui, M. A., Dolez, P. I., Dubé, M., & David, É. (2016b). *Preparation of hydrophobic nonwoven using recycled jute fibre and a titanium dioxide /fatty acid coating*. In: *2nd world congress and expo on recycling, Berlin, Germany, July 25–27*.
AS/NZS 4399. (1996). *Sun protective clothing—Evaluation and classification*. Homebush, Australia: Australian/New Zealand Standard.
ASTM D629. (2015). *Standard test methods for quantitative analysis of textile*. West Conshohocken, PA: ASTM International.
ASTM D737. (2004). *Standard test method for air permeability of textile fabrics*. West Conshohocken, PA: ASTM International.
ASTM D1776. (2016). *Standard practice for conditioning and testing textiles*. ASTM International.
ASTM D1909. (2013). *Standard tables of commercial moisture regains and commercial allowances for textile fibers*. West Conshohocken, PA: ASTM International.
ASTM D4751. (2012). *Test method for determine apparent opening size of a geotextile*. West Conshohocken, PA: ASTM International.
ASTM D5070. (1990). *Standard test method for synthetic quanternary ammonium salts in fabrics by potentiometric titration*. West Conshohocken, PA: ASTM International.
ASTM D5322. (2017). *Laboratory immersion procedure for evaluating the chemical resistance of geosynthetics to liquids*. West Conshohocken, PA: ASTM International.
ASTM D6544. (2012). *Standard practice for preparation of textiles prior to ultraviolet (UV) transmission testing*. West Conshohocken, PA: ASTM International.
ASTM E96. (2005). *Standard test method for water vapor transmission of materials*. West Conshohocken, PA: ASTM International.
ASTM F903. (2017). *Standard test method for resistance of materials used in protective clothing to penetration by liquids*. West Conshohocken, PA: ASTM International.
ASTM F1977. (2004). *Standard test method for determine initial, fractional, filtration efficiency of a vacuum cleaner system*. West Conshohocken, PA: ASTM International.
ASTM G155. (2013). *Standard practice for operating xenon arc light apparatus for exposure of non-metallic materials*. West Conshohocken, PA: ASTM International.
Budd, G. M. (1981). Clothing physiology. *Fire Safety Journal*, *4*, 77–81.
California 01350. (2010). *Standard method for the testing and evaluation of volatile organic chemical emissions from indoor sources using environmental chambers*. Sacramento, CA: California Department of Public Health.

CAN/CGSB-4.2 No. 0. (2001). *Textile test methods moisture regain values, SI units used in CAN/CGSB-4.2 and fibre, yarn, fabric, garment and carpet properties*. Ottawa, ON, Canada: Canadian General Standards Board.

CAN/CGSB 4.2 No. 2–M88. (2013). *Textile test methods conditioning textile materials for testing*. Ottawa, ON, Canada: Canadian General Standards Board.

CAN/CGSB 4.2 No. 14. (2005). *Textile test methods—Quantitative analysis of fibre mixture*. Ottawa, ON, Canada: Canadian General Standards Board.

CAN/CGSB 4.2 No. 15. (2003). *Textile test methods—Non-fibrous materials on textiles*. Ottawa, ON, Canada: Canadian General Standards Board.

CAN/CGSB 4.2 No. 36–M89. (2013). *Textile test methods—Air permeability*. Ottawa, ON, Canada: Canadian General Standards Board.

CAN/CGSB-4.2 No. 49–99. (2013). *Textile test methods resistance of materials to water vapour diffusion*. Ottawa, ON, Canada: Canadian General Standards Board.

CAN/CGSB 4.2 No. 63.4. (2016). *Textile test methods: Textiles—Determination of formaldehyde—Part 1: Free and hydrolyzed formaldehyde (water extraction method)*. Ottawa, ON, Canada: Canadian General Standards Board.

CAN/CGSB 4.2 No. 63.5. (2016). *Textile test methods: Textiles—Determination of formaldehyde—Part 2: Released formaldehyde (vapour absorption method)*. Ottawa, ON, Canada: Canadian General Standards Board.

CAN/CGSB-4.2 No. 69–M91. (2013). *Textile test methods weather resistance—Xenon arc radiation*. Ottawa, ON, Canada: Canadian General Standards Board.

CCOHS. (2017). *Asbestos—Health effects*. Hamilton, ON, Canada: Canadian Center for Occupational Health and Safety. https://www.ccohs.ca/oshanswers/chemicals/asbestos.

EC 648. (2004). *Health & consumer protection directorate regulation 648/2004 of parliament and of council on detergents*. Brussels, Belgium: The European Commission.

EPA 405.1. (1974). *Biochemical oxygen demand (5 Days, 20°C)*. Washington, DC: United States Environmental Protection Agency.

Ferreira, C., Pereira, A. M., Pereira, M. C., Melo, L. F., & Simoes, M. (2011). Physiological changes induced by the quaternary ammonium compound benzyldimethyldodecylammonium chloride on *Pseudomonas fluorescens*. *Journal of Antimicrobial Chemotherapy*, *66*(5), 1036–1043.

Gentile, P., Chiono, V., Carmagnola, I., & Hatton, P. V. (2014). An overview of poly(lactic-*co*-glycolic) acid (PLGA)-based biomaterials for bone tissue engineering. *International Journal of Molecular Sciences*, *15*(3), 3640–3659.

Gerard, K. (2014). *The top 3 plastic additives for UV stabilization*. Hudson, NY: Craftech Industries. http://info.craftechind.com/blog/bid/383570/The-Top-3-Plastic-Additives-for-UV-Stabilization.

Gore, W. L. (1976). Process for producing porous products. U.S. Patent 3,953,566. Alexandria, VA: US Patent Office.

Hutten, I. M. (2007). *Handbook of non-woven filter media*. Oxford, UK: Elsevier.

ISO 139. (2005). *Textiles—Standard atmosphere for conditioning and testing*. Geneva, Switzerland: International Organization for Standardization.

ISO 8096–2. (1989). *Rubber- or plastics-coated fabrics for water-resistant clothing—Specification—Part 2: Polyurethane- and silicone elastomer-coated fabrics*. Geneva, Switzerland: International Organization for Standardization.

ISO 15496. (2004). *Textiles—Measurement of water vapour permeability of textiles for the purpose of quality control*. Geneva, Switzerland: International Organization for Standardization.

Labet, M., & Thielemans, W. (2009). Synthesis of polycaprolactone: A review. *Chemical Society Review*, *38*(12), 3484–3504.

Lane, R. P. (1934). *Cotton and cotton seeds*. Washington, DC: U.S. Department of Agriculture. p. 84.

Lawrence, C. A. (2014). *High performance textiles and their applications*. Cambridge, UK: Woodhead Publishing.
Li, X. L., Liu, Y., Du, J., Li, R., Ren, X., & Huang, T. S. (2015). Biocidal activity of N-halamine methylenebisacrylamide grafted cotton. *Journal of Engineering Fabrics and Fabrics*, *10*(2), 147–154.
Lynch, J. (2007). *Liquid filtration testing basics*. Nashville, TN: American Filtration and Separations Society (AFSS).
Muñoz-Bonilla, A., & Fernández-García, M. (2012). Polymeric materials with antimicrobial activity. *Progress in Polymer Science*, *37*, 281–339.
NASA. (2014). *The Electromagnetic Spectrum - Ultraviolet Waves*. https://science.nasa.gov/ems/10_ultravioletwaves.
Oeko-Tex 1000 Standard. (1995). Zürich, Switzerland: Oeko-Tex International.
Qian, L., & Sun, G. (2003). Durable and regenerable antimicrobial textiles: Synthesis and applications of 3-methylol-2,2,5,5-tetramethyl-imidazolidin-4-one (MTMIO). *Journal of Applied Polymer Science*, *89*(9), 2418–2425.
Ren, Z., Dong, L., & Yang, Y. (2006). Dynamic mechanical and thermal properties of plasticized poly(lactic acid). *Journal of Applied Polymer Science*, *101*, 1583–1590.
Shao, Y., & Filteau, M. (2004). A systematic analysis of fiber contents in textiles. *AATCC Review*, *4*(6), 18–21.
Shao, Y., & Nantel, R. (1998a). Première partie: Étude du facteur de protection ultraviolette (FPU) des textiles. *Canadian Textile Journal*, *115*(3), 40–44.
Shao, Y., & Nantel, R. (1998b). Deuxième partie: Étude du facteur de protection ultraviolette (FPU) des textiles. *Canadian Textile Journal*, *115*(4), 46–48.
Smith, D. L., Cairns, B. A., Ramadan, F., Dalston, J. S., Fakhry, S. M., & Rutledge, R. (1995). Effect of acclimatization on the sweat rate and rectal temperature relationship. *Journal of Applied Physiology and Occupational Physiology*, *71*, 223–229.
Stedfast. (2017). *STEDAIR® 4000*. Stedfast Advanced Barrier Technologies. http://www.stedfast.com/stedair-4000.html.
Tessier, D., Radu, I., & Filteau, M. (2009). *Antimicrobial solution comprising a metallic salt and a surfactant. Canadian patent, 2,604,020*. Gatineau, QC, Canada: Canadian Intellectual Property Office.
Tessier, D., Radu, I., & Filteau, M. (2015). *New antimicrobial compositions and uses thereof. US patent application publication, US20150201622*. Alexandria, VA: US Patent Office.
USFA. (2014). *Firefighter fatalities in the United States in 2013*. Emmitsburg, MD: US Fire Administration. November.
Wang, J., & Liu, J. (2009). Surface modification of textiles by aqueous solutions. In Q. Wei (Ed.), *Surface modification of textiles* (pp. 269–295). Cambridge, UK: Elsevier.
Wolverton, S. E. (2013). *Comprehensive dermatologic drug therapy* (3rd ed.). Edinburgh, London, New York, Oxford, Philadephia, St Louis, Sydney, Toronto: Elsevier - Saunders.
Young, T. (1855). *Miscellaneous works*. London: Murry.
Zhang, J. Z. (2009). *Optical properties and spectroscopy of nanomaterials*. Singapore: World Scientific Publishing Co.

Further reading

Miller. (2017). *Harness textiles—Resistance to chemicals and other information*. Franklin, PA: Miller by Sperian.

This page intentionally left blank

Toxicity testing of textiles

7

P.I. Dolez, H. Benaddi
CTT Group, Saint-Hyacinthe, QC, Canada

7.1 Introduction

Textiles come into intimate contact with our skin, 24 h a day, 7 days a week; they are everywhere around us at any moment of our lives: the clothing we wear; our bed and linens; our cleansing and hygiene products; the floor of our home and office; and in our means of transportation; they cover our furniture and decorate our house; they protect wounds; and they are hidden within composite material parts of our car and inside the walls of buildings; these are just a few examples. It is therefore critical that textiles pose no harm to human health and the environment both in cases of short and long term exposure.

Yet, many chemicals are used at all steps of the textile manufacturing process (Luongo, 2015). For instance, scouring, which allows removing hydrophobic substances from the fibers, employs compounds such as anionic or nonionic surfactants, dispersing and reducing agents, and/or chelating agents. Bleaching is applied on fibers to improve the whiteness of the textile and requires hypochlorite and hydrogen peroxide combined with auxiliary compounds such as stabilizers, costabilizers, wetting agents, activators, and anticorrosion agents. The mercerizing treatment, which uses chemicals such as alcohol sulfates, anionic surfactants, and cyclohexanol, enhances the fiber dyeability and increases its strength, dimension stability, and luster. Dying may be applied on the fiber, the yarn, or the fabric using azo dyes, anthraquinone dyes, and metal complex dyes. Printing also uses dyes or pigments, and organic solvents. Finally, various types of finishing treatments may be applied on the fiber, the yarn, the fabric, or the final product. This includes flame retardancy with bisphenol A and brominated compounds, crease resistance with formaldehyde, stain-repellence and waterproofing with perfluorinated chemicals, fungus resistance with dimethylfumarate, and antibacterial and antiodor functions with organotin and silver. Chemicals may also be found in polymer coatings applied on textiles—for example, phthalates used as a plasticizer in polyvinyl chloride.

Most of these chemicals are found in textile products (Table 7.1). Yet, some of them have been shown to be toxic to human health and the environment. For instance, heavy metals such as lead, antimony, and cadmium used as dyes and pigments are prone to bioaccumulation leading to neurotoxic, mutagenic, and carcinogenic effects (Chowdhury & Chandra, 1987). Azo dyes, which make 60%–70% of all commercial colorants, may cause allergic contact dermatitis as well as release carcinogenic and mutagenic aromatic amines (KEMI, 2014). Reproductive toxicity has been reported as a result of exposure to textile articles containing brominated flame retardants, highly fluorinated water and stain repellants, phthalates, and antibacterial agents.

Advanced Characterization and Testing of Textiles. https://doi.org/10.1016/B978-0-08-100453-1.00008-8

Table 7.1 List of potentially toxic chemicals detected in finished product textiles and foams

	UV-clothes	Baby carriers	Prams	Teddy bears	Toys	Kid snowsuits	Kid rain suits	Kid restrains	Push-chairs	Kid pajamas	Underwear	Bodysuits	Mats	Changing pads	Stuffed animals
Phthalates	X		X		X		X			X	X	X	X		
NPE[a]	X	X		X	X						X				
PAH[a]					X	X		X	X		X				X
CFR[a]		X	X		X			X	X					X	
Toxic dyes					X										
Heavy metals					X					X	X		X	X	
Organotin					X			X							
Formaldehyde					X			X		X		X	X		
Fluorinated compounds			X			X									

[a] NPE: nonylphenol ethoxylates; PAH: polycyclic aromatic hydrocarbons; CFR: chlorinated flame retardants.
Adapted from ANEC/BEUC (2016)

Nonylphenol ethoxylates (NPE) used as a cleaning, dyeing, and rinsing agent for textiles and a stabilizer for polymers, have been shown to cause endocrine disruption in fish and eventually in humans (Guenther et al., 2002). Finally, some volatile organic compounds (VOCs)—which include trichloroethane used for scouring, chlorobenzenes used as dyeing carriers, formaldehyde used as a finishing agent in crease-resistant/no-ironing products, and tetrachloroethylene used in dry-cleaning—have direct toxic effects on humans ranging from carcinogenesis to neurotoxicity; they also form ground-level ozone, a major component of smog (Islas-Espinoza, 2014).

Efforts have been made in the recent years to better control the amount of chemicals used in textile processes and limit those that are the most toxic. For instance, NPE, which had been banned from use within its borders by the European Union for 20 years, has also recently been voted by all EU member states to be excluded from textile imports (Flynn, 2015). In response to the larger interest of consumers for green products and sustainable development, a majority of textile companies are now including environmental management systems (EMS) such as ISO 14001 and/or the adhesion to voluntary ecolabels (Section 7.9) as part of their business model (TexEASTile, 2014).

This chapter describes test methods for various types of toxic chemicals that may be found in textiles, including heavy metals, VOC, pesticide and fungicide residues, azo dyes, and phthalates. It presents also some existing ecotextile certifications. It ends with a look at future trends towards toxic chemical-free textiles.

7.2 Testing for heavy metals

Many heavy metal elements and salts are used in textile processing (Podsiki, 2008; Bulan-Brady, 1990; Zeiner, Reziæ, & Steffan, 2007; KEMI, 2014):

- Aluminum as a textile dying mordant;
- Antimony as a catalyst for the production of polyester, flame retardant, and dyeing mordant;
- Arsenic as a textile mordant, silk weighting agent, pigment, and printing agent;
- Barium as a dyeing mordant and pigment;
- Boron (boric acid) as a flame retardant and insecticide;
- Calcium (calcium acetate) as a mordant in textile dyeing and printing;
- Cadmium as a pigment and dye;
- Chromium IV as a dyeing and printing mordant, silk weighting agent, and pigment;
- Cobalt as a dye and dyeing mordant;
- Copper as a dye as well as a mordant and an oxidizing agent for textile dyeing;
- Iron as a dyeing mordant;
- Lead as a textile mordant and silk weighting agent;
- Manganese as a dye;
- Mercury as a pigment and dyeing catalyst;
- Nickel as a dye;
- Silver as a biocide and antiodor agent;
- Tin as a textile mordant;
- Titanium as a pigment; and
- Uranium, vanadium, zinc, and zirconium as textile mordants.

For instance, the use of chromium as a mordant in dyes is key to obtaining wash fastness for black wool and nylon fabrics (Zeiner et al., 2007). Mordants work by forming a coordination complex with the dye.

The typical mass fraction of heavy metals used in dyes is the following (in $\mu g\,g^{-1}$): 1.0–1.4 for arsenic, up to 1.0 for cadmium, 3–83 for chromium, 1.0–3.2 for cobalt, 33–110 for copper, 6–52 for lead, 0.5–1.0 for mercury, and 3–32 for zinc (Zeiner et al., 2007). Values of 0.2–200 $\mu g\,g^{-1}$ of antimony, 0.054 $\mu g\,g^{-1}$ of arsenic, 12.5 $\mu g\,g^{-1}$ of barium, 1.5–660 $\mu g\,g^{-1}$ of bromine, 0.016–0.25 $\mu g\,g^{-1}$ of cadmium, 0.093–4.5 $\mu g\,g^{-1}$ of chromium, 0.02–0.082 $\mu g\,g^{-1}$ of cobalt, 0.05–341 $\mu g\,g^{-1}$ of copper, 230–140,000 $\mu g\,g^{-1}$ of fluorine, 3.55–34.3 $\mu g\,g^{-1}$ of iron, 0.02–7.5 $\mu g\,g^{-1}$ of lead, 1.02–2.50 $\mu g\,g^{-1}$ of manganese, 1.20–4.69 $\mu g\,g^{-1}$ of nickel, 0.4–38.8 $\mu g\,g^{-1}$ of silver, 0.05–0.21 $\mu g\,g^{-1}$ of vanadium, and 0.5–120 $\mu g\,g^{-1}$ of zinc were reported for various textile products (Tuzen, Onal, & Soylak, 2008; KEMI, 2013).

A number of these metals and their compounds have well documented effects on health and the environment (Table 7.2). For instance, lead has been shown to induce blood poisoning, impair neurobehavioral development, reduce hearing acuity and speech ability, generate growth retardation and attention deficit, and lead to lower intelligence quotient in children (Tchounwou, Yedjou, Patlolla, & Sutton, 2012). The effects on adults include reproductive problems both in men and women, brain and kidney damage, and gastrointestinal diseases in the case of acute exposure, and harmful impacts on the blood, central nervous system, kidney, and vitamin D metabolism.

Cadmium is reported as a severe pulmonary and gastrointestinal irritant as well as a cytotoxic agent and a human carcinogen (Tchounwou et al., 2012). Chromium IV is easily absorbed by cells where it is reduced to reactive intermediates leading to cytotoxic, genotoxic, and carcinogenic effects. Mercury is a largely prevalent environmental toxicant and pollutant that induces severe adverse health effects on humans and animals. Finally, although arsenic-containing compounds are used to treat some tropical diseases and have recently been approved by the US Food and Drug Administration for the treatment of a certain form of leukemia, arsenic has demonstrated cytotoxic, mutagenic, and carcinogenic effects during in-vitro and epidemiology studies.

Regulations have been put forward by some countries to limit the exposure of workers and end-users to heavy metals. For instance, the European regulation REACH prohibits the use of cadmium to stabilize vinyl chloride polymers or copolymers in articles of apparel and clothing accessories as well as impregnated, coated, covered, or laminated textile fabrics (EC, 2009). In addition, with the exception of safety applications, the concentration of cadmium pigments is restricted to <0.01 wt.% for coloring polyvinylchloride (PVC), polyurethane, low-density polyethylene (LDPE) (except for the production of master batches), cellulose acetate (CA), cellulose acetate butyrate (CAB), epoxy resins, melamine-formaldehyde (MF) resins, urea-formaldehyde (UF) resins, unsaturated polyesters (UP), polyethylene terephthalate (PET), polybutylene terephthalate (PBTP), transparent/general-purpose polystyrene (PS), acrylonitrile methylmethacrylate, cross-linked polyethylene, high-impact polystyrene, and polypropylene (PP). Finally, the use of cadmium and its compounds is also prohibited for plating metallic products or components in equipment and machinery for the

Table 7.2 Specific toxicity of heavy metals relevant to textiles (Zeiner et al., 2007; Förstner & Wittmann, 2012)

	Nervous	Cardiovascular	Gastrointestinal	Endocrine	Immune	Renal	Hepatic	Respiratory	Hematic	Dermic	Environmental pollutant
Aluminum	X							X			
Arsenic	X		X	X			X	X	X	X	X
Cadmium	X	X	X			X		X			X
Chromium			X		X	X		X		X	X
Cobalt	X	X	X	X	X			X		X	X
Copper	X		X						X		X
Iron	X		X				X	X			
Lead	X	X	X	X	X	X			X	X	X
Manganese	X			X	X			X			
Mercury	X		X			X		X			X
Nickel					X			X		X	X
Zinc			X						X		X

production of textiles and clothing. Mercury compounds are proscribed as well for the impregnation of heavy-duty industrial textiles and yarns. Nickel is banned in articles that come into direct and prolonged contact with the skin such as rivets, zippers, and metal marks used in garments.

In the United States, the use of lead for textile surface coating and printing is limited to an extractable content of 90 ppm (AAFA, 2013). The Consumer Product Safety Improvement Act (CPSIA) also limits the total lead content in accessible parts of children's products to 100 ppm (CPSIA, 2008). However, undyed and dyed natural and manufactured fibers may not have to be tested unless the textile has been treated in a way that could result in the addition of lead into the material, knowing that dyes are not considered to be a material that may result in the addition of lead to textiles. Occupational exposure levels for heavy metals relevant to textiles, including aluminum, arsenic, cadmium, cobalt, chromium, copper, iron, mercury, manganese, nickel, lead, and zinc, have also be set by the US Occupational Safety and Health Administration (Podsiki, 2008).

Various methods have been developed for the detection, identification, and quantification of heavy metals in and on textile materials. They rely on different analysis techniques including thin layer chromatography (TLC), UV-VIS spectrometry, graphite furnace atomic absorption spectrometry (GFAAS), flame atomic absorption spectrometry (FAAS), inductively coupled plasma-optical emission spectrometry (ICP-OES), and inductively coupled plasma-mass spectrometry (ICP-MS) (Zeiner et al., 2007). Protocols have also been developed for sampling, sample preservation, and sample preparation because these steps are critical for the quality of the information obtained. For instance, care should be taken to prevent any change in the sample composition after collection that may result from physical, chemical, and biological processes. Sample preparation may involve extraction or digestion processes to allow the analytes to be released from the matrix.

Heavy metal extraction may be conducted with an artificial acidic sweat solution. The solution is prepared using 0.5 g of L-histidine monohydrochloride monohydrate, 5 g of sodium chloride, and 2.2 g of sodium dihydrogen orthophosphate dehydrate per liter (ISO 105-E04, 2013). The solution is brought to a pH of 5.5 with 0.1 mol L^{-1} of sodium hydroxide. The textile specimen is first immersed in the freshly prepared artificial acidic sweat solution at room temperature during 30 min. Then, it is inserted between two glass or acrylic-resin plates and subjected to a pressure of 12.5 kPa at 37°C during 4 h. The determination of the extractable heavy metal content may be carried out by atomic absorption spectrometry (AAS), ICP spectrometry, or spectrophotometry (OEKO-TEX 200, 2010). This technique applies to antimony, arsenic, lead, cadmium, chromium, copper, cobalt, nickel, and mercury.

In the case of organic tin compounds, the extraction with the artificial acidic sweat solution described above is followed by derivatization with sodium tetraethylborate (OEKO-TEX 200, 2010). The sample is analyzed by gas chromatography with mass selective detection (GC-MSD).

In the case of nickel-coated articles that are in direct and prolonged contact with the skin such as rivets, zippers, and metal marks used in garments, the specimen is first subjected to a corrosion treatment at 50°C for 2 h followed by a wear treatment

at 30 rpm for 5 h using abrasive pastes (EN 12472, 2009). This procedure is designed to simulate 2 years of normal use. The specimen is then kept for 168 h (7 days) in an artificial sweat solution at 30°C (EN 1811, 2011). That artificial sweat solution is prepared with sodium chloride, lactic acid, urea, and ammonia. The nickel content in the extraction solution is analyzed via ICP spectrometry.

A method has also been developed to simulate the heavy metal extraction that may result from an object, for instance a toy, having accidently been swallowed and that would stay for 4 h in the alimentary tract (ASTM F963, 2011; EN 71-3, 2014). The coating is scraped off the surface and grinded through a 0.5-mm nominal opening metal sieve. If the coating cannot be grinded because of its elastic, rubber, or plastic nature, it may be tested as removed from the surface. For other materials like laminates, textile-reinforced composites, and textiles, <6-mm dimension specimens shall be obtained with the thinnest cross-section possible. The test sample is then placed in a 0.07 mol L^{-1} hydrochloric acid solution at 37°C and the pH is adjusted to be between 1.0 and 1.5. The solution shall be protected from light. The mixture is shaken continuously for 1 h, and then left standing at 37°C for another hour. Next, solids are immediately separated from the mixture by membrane filtration, with the addition of up to 10 min of centrifuge treatment. If the sample cannot be analyzed within one working day, the solution shall be stabilized by the addition of hydrochloric acid so that the resulting HCl concentration is 1 g L^{-1}. This method may be used to detect and quantify antimony, arsenic, barium, cadmium, chromium, lead, mercury, and strontium.

For the determination of the total lead content in surface coatings, the scraped coating sample is subjected to a digestion treatment before being filtered and analyzed by an ICP or AA spectrometer (CPSC-CH-E1003-09, 2009). Hot plate digestion is conducted using a solution of concentrated nitric acid in hydrogen peroxide (ASTM E1645, 2016) or in water (HC PartB-C-02.2, 2011) at 100°C. For the microwave digestion, concentrated nitric acid or a solution of concentrated nitric acid, concentrated hydrochloric acid, and water is used (ASTM E1645, 2016). The microwave digestion program includes a heating ramp of 20 min to a temperature of 210°C followed by a hold at that temperature for 10 min (HC PartB-C-02.2, 2011), or a heating ramp of 10 min to a temperature of 180°C followed by a hold at that temperature for 15 min (ASTM E1645, 2016).

The total lead content in nonmetal, nonsiliceous products for children, including polymers and textiles, is also measured after microwave acid digestion (CPSC-CH-E1002-08.1, 2010). The test specimen is cut into small pieces or cryo-milled to obtain a fine powder. Concentrated nitric acid is added in the microwave vessel. The microwave program involves a 20-min ramp to at least 200°C, followed by a 10-min hold at that temperature. The diluted sample is then analyzed by an ICP or AA spectrometer. An alternative technique based on energy dispersive X-ray fluorescence spectrometry (EDXRF) may also be used for homogeneous polymers (ASTM F2617, 2015). It is recommended that tests conducted on undigested samples using EDXRF analysis are completed by an ICP analysis on digested specimens if the lead content measured is greater than 70% of the Consumer Product Safety Improvement Act requirements (CPSC-CH-E1002-08.1, 2010).

Variants of the acid digestion methods described in the above two paragraphs using alternative digestant solutions may be employed to obtain the total content in antimony,

arsenic, barium, cadmium, chromium, lead, mercury, and strontium in toys and toy components and materials (ASTM F963, 2011). For instance, concentrated nitric acid is replaced by aqua regia, which consists of three parts concentrated hydrochloric acid to one part concentrated nitric acid. A mixture of three parts concentrated nitric acid to one part 30% hydrogen peroxide may be used to achieve complete digestion of some polymers like polyvinyl chloride. The digested material is filtered and diluted before being analyzed.

The selection of the analytical technique may be made based on the element to quantify, the level of precision required, and the equipment available. TLC can separate and simultaneously identify a number of metal components, and requires small amounts of samples and chemical reagents (Zeiner et al., 2007). However, it is generally limited to qualitative and semiquantitative analysis since its limit of detection is relatively high for certain metals and it has a poor quantitative reproducibility. UV-VIS spectrometry may be used after converting the metals to colored complexes. This method has a high sensitivity and selectivity, and it allows relatively straightforward measurements. However, the sample preparation is time intensive, and there might be interference issues with other colored substances in the sample.

AAS allows determining metals in very low mass concentrations ($\mu g\,L^{-1}$-range) (Zeiner et al., 2007). Two types of AAS may be used for heavy metal determination in textiles: flame AAS (FAAS) and graphite furnace (GFAAS). GFAAS allows much lower limits of detection to be reached than FAAS. Testing protocols for the determination of lead by FAAS and GFAAS are available in ASTM E1613 (2012).

Inductively coupled plasma-optical emission spectrometry (ICP-OES), which is also called ICP-AES for atomic emission spectroscopy, may be used to analyze up to 70 elements in one step (Zeiner et al., 2007). One of its disadvantages is its high argon consumption. In addition, it requires a larger sample size than GFAAS and the achievable limits of detection are higher. A test protocol with calibration standards, ICP parameters, and limits of detection and quantification is provided in EN 71-3 (2014) for the quantification of aluminum, antimony, arsenic, barium, boron, cadmium, chromium, cobalt, copper, lead, manganese, mercury, nickel, selenium, strontium, tin, and zinc after extraction. Specific details for the determination of lead concentration in sample digestate and extract may be found in ASTM E1613 (2012).

Inductively coupled plasma-mass spectrometry (ICP-MS) adds a further step and separates atoms and ions based on their mass-to-charge ratios (Zeiner et al., 2007). While still a multielement analysis, this allows higher sensitivity and lower detection limits to be reached than ICP-OES. This technique can also provide information about the isotope composition. However, its operational costs are high because of the high amount of argon it uses and it suffers from a high susceptibility to salt concentrations present in digest solutions or in sweat and gastric extraction solutions. Test protocols with calibration standards, testing procedure, ICP parameters, and limits of detection and quantification are available in EN 71-3 (2014) and EPA 6020A (2007) for the quantification of a series of heavy metals.

The speciation of chromium III and VI may be achieved by adding ethylenediamine tetraacetic acid (EDTA) to the previously neutralized extract solution (EN 71-3, 2014). EDTA reacts with chromium III to form a complex. Chromium III and chromium VI

may then be separated by liquid chromatography and further quantified using an LC-ICP-MS technique. A test protocol with calibration standards, ICP parameters, and limits of detection and quantification can be found in EN 71-3 (2014).

In the case of organotin compounds, because most of them are too polar to be directly analyzed by gas chromatography, they are first derivatized using tetraethylborate to produce ethyl organic tin derivatives (EN 71-3, 2014). They are then extracted with hexane and analyzed by GC/MS either in full scan mode or single ion mode for quantification purposes. Because they are already per-alkylated, tetra-alkylated organic tin compounds such as tetrabutyltin can be determined directly without derivatization.

7.3 Testing for VOCs

VOCs refer to organic carbon-containing compounds with low vapor pressures. However, the exact definition may differ depending on the country/state. For instance, in Europe, the vapor pressure limit is set at 0.01 kPa at a temperature of 293.15 K (EC, 1999). In the United States, the California standard on VOCs defines the vapor pressure range between that of *n*-pentane and that of *n*-heptadecane, i.e., from 10^{-4} to 58 kPa (California Specification 01350, 2010). For its part, Canada excludes a series of compounds including acetone, methane, ethane, methyl chloroform, methylene chloride, chlorofluorocarbons (CFCs), fluorocarbons (FCs), and hydrochlorofluorocarbons (HCFCs) due to their negligible photochemical reactivity (CCME, 2002). However, halogenated hydrocarbons are included in Quebec's list of 175 VOCs (MDDELCC, 2016).

VOCs may be classified according to their chemical nature: alkanes, alkenes, alcohols, alkynes, aldehydes, ketones, halogenated derivatives, nitro-derivatives, esters, ethers, aromatic hydrocarbons, and halogenated hydrocarbons. They may also be categorized based on their boiling points (Bp) (WHO, 1989):

- Very volatile (VVOCs): Bp < 50–100°C
- Volatile (VOCs): 50–100°C < Bp < 240–260°C
- Semivolatile (SVOCs): 240–260°C < Bp < 380–400°C

VOCs and VOC-emitting chemicals enter at several points in the textile manufacturing process (EPA, 1997): For instance, polyvinyl acetate used in sizing operations and methanol-etherated formaldehyde resins employed during finishing are both methanol emitters. The last one is also a source of formaldehyde. Methyl ethyl ketone and toluene are used as solvents in coating processes, and xylenes are employed in printing operations. Table 7.3 lists some VOCs encountered in textile products.

As a result, potential exposure to VOCs may take place in occupational settings during slashing/sizing, desizing, scouring, heat-setting, dying, printing, and finishing operations (EPA, 1997). For example, increased free radical and antioxidant enzyme activity was detected in textile paint workers and attributed to long-term exposure to organic solvents (Bayil, Cicek, Cimenci, & Hazar, 2008). In addition, formaldehyde allergy was observed to be more common among people exposed to that chemical at work (KEMI, 2014).

Table 7.3 VOCs potentially encountered in textile products (Greenguard, 2016)

Acetaldehyde	Hexane (*n*-)
Benzene	Isophorone
Carbon disulfide	Isopropanol
Carbon tetrachloride	Methyl chloroform
Chlorobenzene	Methylene chloride
Chloroform	Methyl t-butyl ether
Dichlorobenzene (1,4-)	Naphthalene
Dichloroethylene (1,1)	Phenol
Dimethylformamide (*N*,*N*-)	4-Phenylcyclohexene
Dioxane (1,4-)	Propylene glycol monomethyl ether
Epichlorohydrin	Styrene
Ethylbenzene	Tetrachloroethylene
Ethylene glycol	Toluene
Ethylene glycol monoethyl ether	Trichloroethylene
Ethylene glycol monoethyl ether acetate	Vinyl acetate
Ethylene glycol monomethyl ether	Xylenes (*m*-, *o*-, and *p*-)
Ethylene glycol monomethyl ether acetate	1-Methyl-2-pyrrolidinoneG
Formaldehyde	

Consumers may also be exposed to VOCs during the use and care of their textile goods, which has prompted some groups to promote alternatives to toxic chemicals (Yernaux, 2015). For instance, a number of VOCs, including acetic acid, caprolactam, ethyene and propylene glycol, alkylbenzenes, and other unidentified substances, were still emitted by carpets at concentrations between 40 and 3300 $\mu g\, m^{-3}$ after 28 days in the sampling chamber (Wilke, Jann, & Brçdner, 2004). An increase in the release of 4-phenylcyclohexene by textile floor coverings was measured when the temperature was raised from 23°C to 50°C, which may be a concern in the case of sub-floor heating (Igielska, Wiglusz, Sitko, & Nikel, 2003). In the case of textile articles intended to be in direct contact with the skin, a study conducted in 2007 showed that 11% of them contained more than 30 mg formaldehyde per kg of textile (KEMI, 2014).

The concern is that some of these VOCs are toxic for health and the environment. Methanol, a common solvent, is directly absorbed from the gastrointestinal and respiratory tracts and is converted to formaldehyde and formic acid (EPA, 1997). At high doses, toxic effects observed in humans included damage to the central nervous system and blindness, while long-term exposure via inhalation caused liver and blood damage in animals. Methanol also reacts with air in the atmosphere to produce formaldehyde. Toluene, another solvent, may cause headaches, weakness, confusion, and memory loss upon inhalation or ingestion. It may also affect the kidney and liver function. On the environmental perspective, it contributes to the formation of ground-level ozone. Another solvent, methyl ethyl ketone, can generate neurotoxic effects including headaches, dizziness, nausea, toe and finger numbness, and even unconsciousness when inhaled at moderate doses for short periods of time; it can also cause skin, eye, nose, and throat irritation. In the long term, it may lead to liver and kidney defects

upon repeated exposure. For their part, xylenes are readily absorbed in the body upon exposure through inhalation, ingestion, and skin contact. Short-term exposure to high concentrations of xylenes may cause skin and mucosal irritation, respiratory difficulty, and effects on the nervous system, the kidney, and the liver. It can be noted that none of these solvents have demonstrated carcinogenic effects.

Other VOCs used in or released by textiles have known carcinogenic and developmental effects. For instance, tetrachloroethylene, which is used for dry-cleaning, has been shown to induce liver, kidney, and blood cancer in rodents (Watts, 2006). It was also associated with a larger prevalence of esophageal, cervical, and kidney cancers, non-Hodgkin's lymphoma as well as reproductive effects such as menstrual disorders, miscarriages, and reduced fertility in workers exposed to tetrachloroethylene. Chronic exposure to benzene, which is used as a solvent for rubberizing/waterproofing coatings, an industrial degreaser, and a precursor of polyester and other polymers, causes acute myeloid leukemia and may also be associated with risks of acute and chronic lymphocytic leukemia, non-Hodgkin's lymphoma, and multiple myeloma (WHO, 2010).

Formaldehyde is another example of a toxic VOC used in the textile industry. It is typically employed to enhance wrinkle resistance in textiles and may cause nausea, asthma aggravation, and cellular changes leading eventually to the development of tumors upon inhalation (GAO, 2010). It has also been shown that chronic inhalation exposure may trigger cancer. Even at low levels (around 50 ppb), it has been shown to create a subclinical inflammatory response in the airways of healthy children (Franklin, Dingle, & Stick, 2000). However, the largest concern with formaldehyde in textiles may be related to dermal exposure, which is the cause of allergic and irritant contact dermatitis, two forms of eczema that create rashes, blisters, and an itchy or burning flaky, dry skin (GAO, 2010). Between 2.3% and 8.2% of patients showing textile dermatitis are sensitized to formaldehyde (KEMI, 2014).

Because of concerns for health and the environment, the use of VOCs and VOC-emitting chemicals has been restricted by a number of countries. For instance, Europe and Japan have a limit of 0.1 wt.% for a series of solvents including pentachloroethane, trichloroethane, tetrachloroethane, dichloroethylene, tri and tetrachloroethylene (Japan only), carbon tetrachloride, and chloroform in apparel and footwear products (AAFA, 2013). The maximum quantity of chlorinated solvents in PVC artificial leather is fixed to $20\,g\,m^{-2}$ by China. Europe also bans the presence of a list of hydro- and perfluorocarbons in apparel and footwear products. In the case of dioxins and furans, which enter in the synthesis of a number of polymers including PVC, Germany has set maximum total values as low as $0.1\,\mu g\,kg^{-1}$ of the finished product for Group 1 and Group 4 chemicals. Formaldehyde is also regulated by a large number of countries. Europe requires that a label warning about risks of sensitive or allergic skin reactions is affixed to a textile intended to be in contact with the skin if it contains more than $1500\,mg\,kg^{-1}$ of free formaldehyde (TUV, 2013). For kids under the age of 3, the free and hydrolyzed formaldehyde content in accessible textiles is limited to $30\,mg\,kg^{-1}$ (EN 71-9, 2007). In Japan, that level is set to an undetectable level (i.e., below $20\,mg\,kg^{-1}$) (AAFA, 2013). Above 3 years of age, the value is raised to $75\,mg\,kg^{-1}$ in case of direct skin contact and $300\,mg\,kg^{-1}$ with no direct skin contact.

The measurement of VOCs emitted by textile products involves three steps (Srivastava & Majumdar, 2011): sampling the VOCs emitted by the product, extracting the VOCs from the sample, and detecting/quantifying the VOCs. VOC sampling may be carried out directly at the location where the textile product is being used, for example in a car or in a house, by active sampling using a pump to draw ambient air through an adsorbent cartridge, by grab sampling using an evacuated canister, by passive sampling using an adsorbent contained in a tube, or directly with an online analyzer measuring the total VOC concentration without chemical speciation/identification. For instance, standard test methods EPA TO-1 (1984) and EPA TO-2 (1984) both refer to active sampling to capture the chemicals of interest on Tenax® (poly(2,6-diphenyl phenylene oxide) resin and carbon molecular sieve adsorbent, respectively. The determination of the sampling conditions takes into account the characteristic retention volume of each compound of interest, which shall not be exceeded. The air flow rate is generally in the range of 10–100 mL min^{-1} and the sampling time is in the order of minutes to hours (Srivastava & Majumdar, 2011).

VOC sampling may also be conducted using environmental chambers of different sizes (EPA, 2015). This includes the following:

- Full-scale chambers with dimensions in the order of 30 m^3 (ASTM D6670, 2013; ISO 16000-9, 2006; GGTM.P066, 2008)
- Small-scale chambers with dimensions between a few liters and a few m^3 (ASTM D5116, 2010; ISO 16000-9, 2006; California Specification 01350, 2010; GGTM.P066, 2008)
- Micro-scale chambers with dimensions ranging from a few milliliters to about 150 mL (ASTM D7706, 2011; ISO 12219-3, 2012)
- Emission cells with a volume of 0.035 L, which are tightly secured against the surface of the product test specimen (ISO 16000-10, 2006; ASTM D7143, 2011).

Reducing the size of the chamber allows the time to reach equilibrium, amount of sample necessary for the test, and cost to decrease (Salthammer, 2009). However, it increases the influence of the sample inhomogeneity and the recovery of SVOC. In addition, the level of information shifts from emission to content.

The air change rate is set to one chamber volume per hour in the case of full- and small-scale chambers and more than 100 volumes per hour for micro-scale chambers and emission cells (EPA, 2015). With micro-scale chambers, the gas flow rate is in the 150–500 mL min^{-1} range for formaldehyde and other carbonyls, and it is in the 30–100 mL min^{-1} range for other VOCs (ASTM D7706, 2011). Tests are generally conducted at 23°C and 50% relative humidity, but environmental conditions may be varied depending on the specific situations to be simulated (EPA, 2015).

A critical aspect to insure the quality of the VOC emission quantification testing deals with product sampling, storage of samples, and preparation of test specimens. For instance, product samples shall be collected as soon as possible after they have been manufactured (ISO 16000-11, 2006). They shall be immediately properly packaged, and transported and stored in appropriate conditions in order to avoid any chemical contamination or the action of physical or chemical aging agents (e.g., heat, light, moisture). The time between sample unpacking and test specimen preparation shall be as short as possible and recorded. The moment when the test specimen preparation is completed is considered to be the starting time of the VOC emission test. Examples

of test specimen preparation procedures may be found in standards ISO 16000-11 (2006), GGTM.P066 (2008), ASTM D6177 (2014), and California Specification 01350 (2010) for various types of products.

After the specimen has been prepared, it may be inserted directly into the chamber or conditioned for a set period of time. Some standards specify a conditioning time designed to simulate realistic use conditions of the product. For instance, a conditioning period of 10 days followed by a 4-day test is proposed to simulate a 14-day delay before first occupancy after a building construction or major renovation (California Specification 01350, 2010).

VOCs may be collected from the environmental chambers using sorbent materials contained in air-tight cartridges (ASTM D5116, 2010). The selection of the sorbent or combination of sorbent materials is based on the nature of the chemicals to be captured. VOCs that may be trapped using Tenax® resin sorbent include some hydrocarbons, chlorinated hydrocarbons, esters, glycol ethers, aldehydes, ketones, and alcohols (ISO 16000-6, 2011). The list of VOCs that can be collected with activated carbon cartridges includes methyl ethyl ketone and tetrachloroethylene (ASTM D3686, 2013). The XAD-27 resin may be considered for semivolatile compounds, i.e., with a boiling point above 180°C (ASTM D5116, 2010). Cartridges containing silica gel coated with 2,4-dinitrophenylhydrazine (DNPH) reagent are designed for formaldehyde but may also be used for a series of other carbonyl compounds, i.e., aldehydes and ketones (ISO 16000-3, 2011). Other sorbent materials include glass beads, Ambersorb, and graphitized carbon (ASTM D5116, 2010). In the case of large chambers, the emitted VOC sample may also be collected with a syringe, in a sampling bag or vessel, or through a closed-loop sampling system.

After collection on sorbent materials, VOCs need to be desorbed to perform identification and/or quantification analysis. Available methods include chemical desorption using an organic solvent, thermal desorption at a high temperature (generally in the range of 200–380°C), solvent extraction, solid phase microextraction, and membrane extraction (Srivastava & Majumdar, 2011). Thermal desorption is generally performed with Tenax® sorbent cartridges and may be combined with a secondary cold trap (ISO 16000-6, 2011). In the case of silica gel coated with DNPH used for formaldehyde and low molecular weight aldehydes, desorption is conducted using acetonitrile (ISO 16000-3, 2011).

The last step of the VOC emission measurement involves the analysis of the liquid or gas sample. In the case of gas samples generated for instance by thermal desorption, gas chromatography is generally used as the separation technique (Srivastava & Majumdar, 2011): the liquid stationary phase adsorbed onto the surface of the inert solid packing material in the column provides different elution times depending on the chemical physical properties such as it polarity, molecular weight, structure, etc. Identification and quantification may be carried out with a wide range of detection techniques including mass spectroscopy (MS), flame ionization (FID), thermal conductivity (TCD), electron capture (ECD), flame photometry (FPD), photo-ionization (PID), and Hall electrolytic conductivity. MS is the most accurate and versatile detector: its typical sensitivity of 10^{-9} g in scan mode can be increased to 10^{-12} g with an ion trap or when analyzing known compounds in the selected ion mode (ASTM D5116, 2010).

MS is listed as one of the recommended detection techniques in a number of VOC emission standard test methods (ISO 16000-6, 2011; California Specification 01350, 2010; ASTM D5116, 2010; GGTM.P066, 2008; EPA TO-1, 1984; EPA TO-2, 1984). FID detectors are also widely used (ASTM D5116, 2010): They have a sensitivity of 10^{-11} g and respond to a wide variety of VOCs.

For liquid samples obtained when analyzing formaldehyde and low molecular weight aldehydes, analysis is conducted with high performance liquid chromatography (HPLC) equipped with a UV detector or a diode array detector (ISO 16000-3, 2011; California Specification 01350, 2010; GGTM.P066, 2008).

The results of the measurement of VOC emissions by textile materials and products may be expressed in terms of individual compound identification (California Specification 01350, 2010; ISO 16000-6, 2011; GGTM.P066, 2008). This is performed by comparing the retention time and mass spectrum obtained for the sample with that of pure compounds (or hydrazone derivatives of the pure compounds in the case of aldehydes) analyzed with the same instrument. Libraries of chemicals (e.g., NIST electronic database) may also be used for a preidentification run. That identification should be performed at least for the chemicals corresponding to the 10 highest peaks, those present at concentrations above $2\,\mu g\,m^{-3}$, as well as all VOCs of concern listed in the test methods.

The concentrations of the individual compounds in the sampled air are determined by calibrating the analytical system with standard solutions with various concentrations of the corresponding chemicals (ISO 16000-6, 2011; ISO 16000-3, 2011). Indeed, the peak area corresponding to a compound in the chromatogram is proportional to the mass of the compound injected. The mass of VOC (or DNPH derivative in the case of aldehydes) extracted from the cartridge is provided by subtracting the mass of analyte in a blank cartridge. Finally, the mass concentration of VOCs in the original air sample is obtained by dividing the result by the sampling volume. In the case of aldehydes, the calculation has also to take into account the ratio of molar mass between the carbonyl compound and the DNPH derivative. The carbonyl compound concentration may be converted to volume fraction (ppm or parts per million) by multiplying the mass concentration by the ratio of the ideal gas volume and the molar mass of the carbonyl compound (ISO 16000-3, 2011; GGTM.P066, 2008).

The total VOC (TVOC) concentration is obtained by considering the entire area of the chromatogram between *n*-hexane and *n*-hexadecane (ISO 16000-3, 2011; GGTM.P066, 2008) or *n*-pentane and *n*-heptadecane (California Specification 01350, 2010). Toluene response is used as a reference to convert the area into mass units of toluene (ISO 16000-3, 2011; GGTM.P066, 2008; California Specification 01350, 2010). The analysis of TVOC is a semiquantitative measure since individual compounds in the mixture may respond differently than toluene. In addition, formaldehyde and acetaldehyde are not included in the TVOC calculation.

The emission factor (EF, also called area specific emission rate), which is the mass of VOC emitted from a specific unit area of product surface per unit time, is given by the following equation (ASTM D5116, 2010; GGTM.P066, 2008):

$$EF = \frac{C_s \cdot N}{L},$$

with C_s, the mass concentration of the considered VOC in the chamber, N, the air exchange rate in the chamber, and L, the loading factor defined as the ratio of the area of the test specimen exposed surface to the chamber volume. This equation can be used if the emission rate is constant and the chamber has reached steady-state (ASTM D5116, 2010). If this is not the case, a time-dependent emission factor profile may be obtained from the time-concentration profile:

$$EF\left(t_i\right) = \frac{1}{L}\left(\frac{\Delta C_i}{\Delta t_i} + N \cdot C_i\right),$$

with C_i being the concentration at time t_i and $(\Delta C_i/\Delta t_i)$ being the slope of the time-concentration curve at time t_i.

Long-term emission modeling may also be performed. If the product emission source decreases in time, the emission factor variation may be modeled with a first-order decay or a power law decay (GGTM.P066, 2008).

In the case of formaldehyde, additional specific methods exist for determining the free and partially releasable formaldehyde from fabrics. In a first series of test methods targeting formaldehyde release in air under hot and humid conditions, the fabric specimen is suspended over a measured volume of distilled water in a sealed container (AATCC TM112, 2014; ISO 14184-2, 2011; CAN/CGSB-4.2 N°63.5, 2007). Depending on the method, the container is left for 20 h at 49°C or for 4 h at 65°C. The formaldehyde released in the water is further reacted with a Nash reagent (a solution of ammonium acetate, glacial acetic acid, and acethylacetone in water) at 40°C for 30 min or 58°C for 6 min. The absorbance of the reacted sample aliquot is measured at 412 nm with a spectrophotometer and compared to that of standards prepared by adding the Nash reagent to solutions of known concentrations in formaldehyde, yielding the amount of aldehyde released by a unit mass of fabric. These test methods cover the range of releasable formaldehyde between 20 and 3500 mg kg^{-1} of fabric.

A second series of test methods based on water extraction gives access to the amount of free formaldehyde and formaldehyde extracted partly through hydrolysis in fabrics (ISO 14184-1, 2011; CAN/CGSB-4.2 N°63.4, 2007). The fabric specimen is immersed in deionized water in a sealed container at 40°C during 60 min. These test methods also use a Nash reagent to react with formaldehyde extracted from the fabric and absorbance measurements at 412 nm against calibration solutions to quantify the concentration of formaldehyde in the water. The amount of formaldehyde extracted from the fabric is obtained by dividing the concentration of formaldehyde in the sample water aliquot by the weight of the specimen. These test methods are also intended for free and hydrolyzed formaldehyde between 20 and 3500 mg kg^{-1} of the fabric.

7.4 Testing for toxic dyes

Dyeing is an important step of textile finishing (or wet processing) and may be performed at any stage of the manufacturing process, i.e., on fibers, yarns, fabrics, and final products, to add color and intricacy to the textile product (EPA, 1997). If the use

of natural dyes extracted from vegetables, fruits, flowers, insects, and fish can be dated back to 3500 BC, the foundation of the synthetic dye manufacturing industry can be attributed to Sir William Henry Perkin after his accidental discovery in 1856 of a purple, stable dye extracted from aniline and called mauveine (Kant, 2012). Currently, more than 3600 different textile dyes are manufactured by the industry. In fact, more than half of the annual world production of dyes and organic pigments, about 550,000 tons per year, is used by the textile industry (Freedonia, 2015).

The coloring function of dyes is generally based on the combined action of a chromophore providing the color and an auxochrome group that increases the intensity of light absorption of the chromophore and/or shift its main absorption band to a longer wavelength (Gurr, 2012). The use of a mordant, such as heavy metals discussed in Section 7.2, is sometimes necessary to improve the bonding efficiency on the fiber and increase colorfastness. Table 7.4 shows the different categories of dyes used in textile manufacturing as well as the type of fibers they are suitable for. For instance, 30–60 g of dyestuff is used to dye 1 kg of cotton with reactive dyes, along with 600–800 g of NaCl and 70–150 L of water (Babu, Parande, Raghu, & Kumar, 2007).

Azo dyes constitute the most important class of synthetic dyes with 70% of commercial organic colorants (POST, 2015). Their advantages include a low dyeing temperature (60°C), compared to 100°C for azo-free dyes, an extensive range of colors, a better color fastness, and at least four times the intensity of azo-free dyes. With their –N=N– group chromophore, azo dyes are commonly found in acid dyes, metal complex dyes, direct dyes, basic dyes, and disperse dyes (Erkurt, 2010). They also make up 95% of reactive dyes (CIEC, 2013).

The problem with azo dyes is their propensity to release aromatic amines upon cleavage of azo groups under certain conditions (POST, 2015). These conditions are met for instance in the intestinal tract, the liver, and other mammalian organs (Chequer et al., 2013). Some of the aryl amines thus created can show carcinogenic effects. For instance, a case was documented where 100% of workers exposed to 2-naphthylamine in a dye manufacturing plant developed bladder cancer (POST, 2015). Aromatic amines have also been linked to other types of cancers such as splenic sarcomas and hepatocarcinomas. In addition, mutagenic and genotoxic effects in cultured cells have been evidenced with azo dyes and industrial effluents contaminated with azo dyes (KEMI, 2014). Other textile dyes such as anilines and anthraquinones are also classified as carcinogenic and/or mutagenic. Yet, concentrations of up to 576 $\mu g\,g^{-1}$ of dinitroanilines

Table 7.4 Dyes used in textile dyeing operations (EPA, 1997)

Dye category	Types of fibers
Acid	Wool, nylon
Basic	Acrylic fibers, some polyesters
Direct	Cotton, rayon and other cellulosic fibers
Disperse	Polyester, polyamide, acetate, other synthetic fibers
Reactive	Cotton and other cellulosic fibers, wool
Sulfur	Cotton and other cellulosic fibers
Vat	Cotton and other cellulosic fibers

were detected in pieces of clothing (Luongo, 2015). Similarly, wastewaters containing toxic dyes, most of which escape conventional wastewater treatment processes, adversely affect the environment, including soil fertility, aquatic organisms, and animals (Puvaneswari, Muthukrishnan, & Gunasekaran, 2006).

Another issue with textile dyes is related to irritant and allergic contact dermatitis (KEMI, 2014). Contact allergy mostly concerns dispersive dyes. It is a clinically relevant problem because 3.6% of patients suffering from contact allergy are sensitive to disperse dyes. The disperse dye molecules include an azobenzene or an anthraquinone group. However, a study showed that, among the patients diagnosed as having contact allergy to disperse dyes, 25% did not react to the dye molecule itself but to other substances in the dye. A few cases were also reported of textile dermatitis caused by acid, basic, and reactive dyes.

Several countries have enacted strong regulations to limit the use of toxic dyes in textiles. For instance, limit concentrations for a number of aromatic amine-releasing azo dyes have been set to 20 ppm by China and 30 ppm by Europe, i.e., below detection limit (AAFA, 2013). This includes 4-aminodiphenyl/xenylamine/biphenyl-4-ylamine, benzidine, 4-chloro-*o*-toluidine, and 2-naphthylamine, which are considered Category 1 carcinogens in REACH (POST, 2015). The 30 ppm limit is used by Japan too (JTF, 2015). Azo dyes are also banned by other Asian countries—Indonesia, South Korea, Taiwan, and Vietnam—as well as by Egypt and Switzerland (AAFA, 2013). A list of disperse, acid, basic, and direct dyes is also subject to prohibition in textiles in Germany, Egypt, and South Korea.

The determination of aromatic amines derived from azo colorants is conducted by subjecting a colored test specimen to color extraction in the case of disperse dyes and/or direct reduction for other dyes (EN 14362-1, 2012). Disperse dye color extraction is performed by suspending the textile specimen in an extractor above boiling chlorobenzene. After the chlorobenzene extract has been further concentrated at 45–60°C, the residue is dispersed in methanol. The reductive cleavage of the azo groups is carried out with sodium dithionite in a citrate-buffered aqueous solution at 70°C in a closed vessel. In the case of nondisperse dyes, the textile test specimen is directly subjected to reduction with sodium dithionite in a citrate-buffered aqueous solution at 70°C in a closed vessel. For textiles dyed with a combination of disperse and nondisperse dyes, the extracted test specimen is added to the methanolic solution of the disperse dye for a combined reduction reaction after having being washed with an appropriate solvent and let dry. Derived amines are then transferred to a t-butyl methyl ether phase by liquid-liquid extraction with a diatomaceous earth column. After concentration of the t-butyl methyl ether extract, the amine detection and quantification may be conducted by a series of chromatography techniques: TLC, HPLC, GC/MS, and capillary electrophoresis. If any amine is detected by a chromatography technique, the result shall be validated by another chromatography technique. If the result is confirmed, the determination of a calibration curve using calibration solutions of at least three different concentrations of the detected amine is made to allow quantifying the amine content in the sample. The weight concentration of the amine in the textile specimen is computed and compared with maximum limits set by regulations. German test methods are also available for carcinogenic azo dyes (OEKO-TEX 200, 2010). It is to be noted

that white is not considered a color. Therefore, white products/product sections are not required to be tested for aromatic amines (EN 14362-1, 2012).

In the case of 4-aminoazobenzene-releasing azo colorants, which cannot be reliably ascertained using the EN 14362-1 (2012) test method, a specific procedure shall be used (EN 14362-3, 2012). The difference between the two test methods relates to the reduction treatment. It shall still be carried out with sodium dithionite in a closed vessel for 30 min. However, in the case of 4-aminoazobenzene-releasing azo colorants, the solution is alkaline and the treatment temperature is 40°C.

The detection of disperse dyes and other colorants may be conducted by extracting the crushed textile test specimen with methanol in an ultrasonic bath (DIN 54231, 2005). The extract is filtered and then separated with HPLC or TLC. The quantification may be carried out by optical or mass spectrometric detection, or by densitometry.

7.5 Testing for pesticide residues

The cultivation of natural fibers like cotton for textile manufacturing requires the use of large quantities of pesticides including insecticides, fungicides, herbicides, and rodenticides (Aktar, Sengupta, & Chowdhury, 2009). In addition, seeds are generally treated with fungicides and insecticides while biocides and fungicides are applied for the safe transportation and storage of fibers and textiles (Deguine, Ferron, & Russell, 2008). Chemicals used as pesticides include organochlorines, organophosphates, carbamates, phenoxys, and pyrethroids (Aktar et al., 2009). Table 7.5 lists the top 50 pesticides applied on cotton in California in 2012 (Kegley, Hill, Orme, & Choi, 2016). It also includes the use, chemical class, total amount used, and application rate. An increasing number of textile products are also provided with antimold, antiodor, and antibacterial functions using silver, triclosan, and triclocarban for instance (KEMI, 2014).

Yet, these chemicals may be toxic for other species than the ones they are intended to fight. Many pesticides currently used in agriculture have been classified as possibly or probably carcinogenic for humans (PAN, 2012). For instance, studies have revealed possible correlations between pesticide use and various types of cancers such as non-Hodgkin's lymphoma, leukemia, sarcoma, multiple myeloma, brain tumors as well as cancers of the prostate, pancreas, lungs, ovaries, breasts, testicles, liver, kidneys, and intestine. Acute pesticide poisoning may also cause neurotoxic effects including fatigue, headaches, dizziness, nausea, impaired vision, tremors, and in severe cases, coma and death. Some pesticides like dimethyl fumarate may also trigger strong allergic reactions (Giménez-Arnau et al., 2009). In addition, the excessive use of biocides may contribute to accelerating the problem of bacterial resistance to antibiotics (KEMI, 2014).

If the use of these pesticides is a major issue for the health of agricultural workers, people living nearby, and the environment, risks may not be totally ruled out for workers transforming the raw material as well as end-users of the finished product. For instance, residues of nine different organochlorine pesticides and herbicides, including 2,4-dichlorophenoxy, 2-methyl-4-chlorophenoxy acetic acid, 2,4,5-trichlorophenoxy, 2-methyl-4-chlorophenoxy butyric acid, betaendosulfan, 2,2-bis (*p*-chlorophenyl)-1,

Table 7.5 List of top 50 pesticides applied to cotton in California in 2012 (Kegley et al., 2016)

Name	Use	Chemical class	Amount used (lb)	Application rate (lb/acre)
Glyphosate, potassium salt	Herbicide	Phosphonoglycine	649,674	1.4
Urea dihydrogen sulfate	Plant growth regulator, herbicide	Inorganic	536,824	2.39
Ethephon	Plant growth regulator	Organophosphorus	363,304	1.01
Sodium chlorate	Defoliant, herbicide, microbiocide	Inorganic	308,764	5
Paraquat dichloride	Herbicide	Bipyridylium	167,896	0.65
Vegetable oil	Insecticide	Oil-vegetable	151,187	1.1
Glyphosate, isopropylamine salt	Herbicide	Phosphonoglycine	141,130	1.25
Pendimethalin	Herbicide	2,6-Dinitroaniline	102,398	1.22
Chlorpyrifos	Insecticide, nematicide	Organophosphorus	97,769	0.91
Unrefined mineral oil	Insecticide, adjuvant, herbicide, fungicide	Petroleum derivative-aromatic	78,805	0.53
Nonyl phenoxy poly (ethylene oxy) ethanol	Adjuvant, plant growth regulator, soap/surfactant	Polyalkyloxy compound	54,856	0.07
Naled	Insecticide	Organophosphorus	52,299	1.12
Phorate	Insecticide, nematicide	Organophosphorus	49,277	1.27
Cottonseed oil	Insecticide	Oil-vegetable	38,610	1.07
Acephate	Insecticide	Organophosphorus	33,226	0.99
Methyl soyate	Adjuvant	Fatty acid ester	31,086	0.26
Oxamyl	Insecticide, nematicide	*N*-Methyl Carbamate	29,168	0.97
Trifluralin	Herbicide	2,6-Dinitroaniline	26,501	0.76
Ammonium sulfate	Herbicide, pH adjustment	Inorganic	24,137	0.09
Metolachlor	Herbicide	Chloroacetanilide	23,720	1.27
Metam-sodium	Fumigant, herbicide, fungicide, microbiocide, algaecide	Dithiocarbamate-MITC	23,592	33.8
Flonicamid	Insecticide	Unclassified	23,200	0.09

Continued

Table 7.5 Continued

Name	Use	Chemical class	Amount used (lb)	Application rate (lb/acre)
Lecithin	Fungicide	Botanical	22,491	0.09
S,*S*,*S*-Tributyl phosphorotrithioate	Defoliant, plant growth regulator	Organophosphorus	21,820	1
Oxyfluorfen	Herbicide	Diphenyl ether	20,727	0.36
Thidiazuron	Defoliant, plant growth regulator	Urea	19,461	0.05
Isopropyl alcohol	Microbiocide, solvent	Alcohol/ether	18,810	0.09
Propionic acid	Fungicide, microbiocide, preservative	Animal derived	16,967	0.07
Azoxystrobin	Fungicide	Strobin	15,501	0.16
Iprodione	Fungicide	Dicarboximide	15,110	0.24
Mepiquat chloride	Plant growth regulator	Quaternary ammonium compound	14,891	0.04
Refined mineral oil	Herbicide, plant growth regulator, insecticide, adjuvant, solvent	Petroleum derivative-saturated	14,477	0.66
p-Nonylphenyl polyoxyethylene dihydrogen phosphate ester	Adjuvant, soap/surfactant	Polyalkyloxy compound	12,887	0.07
Acetamiprid	Insecticide	Neonicotinoid	11,731	0.07
Alkylaryl poly(oxyethylene) glycol	Adjuvant	Polyalkyloxy compound	11,498	0.15
Metolachlor	Herbicide	Chloroacetanilide	10,799	1.32
Dimethoate	Insecticide	Organophosphorus	10,618	0.44
Citric acid	pH adjustment, fungicide, microbiocide	Botanical	10,380	0.04
Buprofezin	Insect growth regulator	Unclassified	10,225	0.34
Undecyl polyoxyethylene (ethylene oxide)	Adjuvant	Polyalkyloxy compound	10,191	0.09

Metam potassium	Fumigant, fungicide, microbiocide, algaecide, nematicide	Dithiocarbamate-MITC	10,019	59.4
Dicofol	Insecticide	Organochlorine	9961	1.31
Ammonium propionate	Preservative, microbiocide	Unclassified	9954	0.07
Diuron	Herbicide	Urea	9732	0.03
Oleic acid, methyl ester	Adjuvant	Fatty acid ester	9126	0.56
Fatty acids, C16-C18 and C18-unsaturated, methyl esters	Adjuvant	Fatty acid ester	8661	0.25
Fatty acids, mixed	Adjuvant	Fatty acid	8552	0.02
Phosphoric acid	Fungicide, pH adjustment, herbicide, microbiocide	Inorganic	8234	0.04
Prometryn	Herbicide	Triazine	7312	1.65

1-dichloroethene, were found in cotton textiles, with peak concentrations ranging from 0.5 to 2 mg kg^{-1} (Zhang, Liao, & Zhang, 2007). The presence of another organochlorine pesticide, pentachlorophenol, which is used as fungicide during transportation, has also been reported in textiles (Gebefügi, 1989). Dimethyl fumarate, which is used as a biocide to prevent mold problems during transport, has also been detected in furniture textiles and shoe materials (ECHA, 2011) and well as in clothing (Foti et al., 2009).

Several countries have enacted regulations to limit the use of toxic pesticides in textiles. For instance, Canada, Finland, Swizerland, South Korea, and Japan have banned or limited to below detection level the use of a series of pesticides in textile goods (AAFA, 2013). Depending on the country, this may include dichloro-diphenyldichloroethane (DDD), dichloro-diphenyldichloroethylene (DDE), dichloro-diphenyltrichloro ethane (DDT), polycholorinated biphenyl (PCB), and polychlorinated terphenyl (PCT). In the United States, the Environmental Protection Agency (EPA) regulates the distribution, sale, and use of pesticides intended to provide antimicrobial or other pesticidal characteristics to clothing or textiles (NIST, 2013). In Europe, the use of dimethyl fumarate has been prohibited in consumer products since 2009 (TUV, 2013). It is now limited to 0.1 mg kg^{-1} under the European Union REACH regulation since 2012, with the detection limit of the test method being at 0.05 mg kg^{-1}.

Test methods available for pesticides are generally based on the analysis of cleaned-up extracts by gas chromatography with selective detection (OEKO-TEX 200, 2010). Aqueous samples of organochlorine and organophosphorus pesticides may be extracted at neutral pH with methylene chloride using separatory funnel, continuous liquid-liquid extractor, or solid-phase extraction techniques (EPA 8081B, 2007). In the case of solid samples, extraction may be conducted with hexane-acetone (1:1) or methylene chloride-acetone (1:1) using Soxhlet, pressurized fluid, microwave, ultrasonic, or supercritical fluid extraction. Other solvents and other extraction techniques may also be employed. Extracts shall then be cleaned up to avoid interferences with the matrix and other analytes. Except for PCBs, techniques include alumina, Florisil, silica gel, gel permeation chromatography, and sulfur clean-up. In the case of PCBs, a sequential sulfuric acid/potassium permanganate clean-up allows removing many single component organochlorine or organophosphorus pesticides to provide better quality PCB data (EPA 8082A, 2007). Organochlorine pesticide and PCB extracts are then analyzed by injecting a measured aliquot into a gas chromatograph equipped with a narrow-bore or wide-bore fused-silica capillary column, and an electron capture or an electrolytic conductivity detector (EPA 8081B, 2007; EPA 8082A, 2007). In the case of organophosphorus pesticides, extract analysis is conducted using gas chromatography equipped with a flame photometric or nitrogen-phosphorus detector (EPA 8141B, 2007). Protocols using high performance liquid chromatography for organochlorine pesticides (Zhang et al., 2007) and solid-phase microextraction followed by gas chromatography with mass spectrometry for organophosphorus pesticides (Zhu et al., 2009) have also been developed by researchers. Besides, a specific test method exists for analyzing the concentration of pentachlorophenol (PCP) in textiles (XP-G08 015, 2000) and in leather (ISO 17070, 2015).

The test method for chlorinated herbicides is based on capillary gas chromatography combined with methylation or pentafluorobenzylation derivatization (EPA 8151A, 1996). Water samples are extracted with diethyl ether and further esterified with diazomethane or pentafluorobenzyl bromide. In the case of solid samples, extraction and esterification are performed with diazomethane or pentafluorobenzyl bromide. The derivatives obtained are analyzed by gas chromatography with an electron capture detector.

Finally, in the case of insecticides found in wool and wool-containing textiles, testing first involves extracting the chemical of interest with a specific solvent mixture (Woolmark TM27, 2003). Then, depending on the herbicide tested, the extract is analyzed using high performance liquid chromatography, gas liquid chromatography, or gas chromatography equipped with a flame ionization detector.

7.6 Testing for flame retardants

Flame retardants are currently widely used in textile products in order to provide them with the fire retardancy performance required by fire safety regulations. This started right before the Second World War with army canvas tents that were treated with halogenated hydrocarbons and waxes (Morgan & Wilkie, 2009). It now covers a large range of applications, from clothing to upholstery to transportation.

Textile flame retardant strategies include inherently flame-resistant fiber materials, fiber blends, additives/copolymers, nanocomposite, and surface treatment (Kandola, 2009). Flame-resistant fiber materials have a decomposition temperature above 375°C and a limiting oxygen index (LOI) of 30% or more. This comprises meta-aramids like Nomex®, para-aramids like Kevlar®, phenolic-based novoloid fiber Kynol®, oxidized acrylic such as Panox®, polybenzylimidazole (PBI), polyphenylene benzobisoxazole (PBO), and polytetrafluoroethylene (PTFE). For its part, fiber blending may involve cotton and polyester, or cotton and nylon for instance; if the right ratio of material content is used, the flammability of the blend may be lower than the flammability of the individual components. Additives and copolymers may also be included prior to polymerization or extrusion. For example, flame retardant additives/copolymers used in polyester comprise phosphinic acid comonomer, bisphenol-S-oligomer derivatives, cyclic phosphonates, and phosphinate salts. Another type of additives is nanoparticles. In particular, the incorporation of nanoclay particles is thought to promote char formation. However, it is still at the research stage as obtaining an exfoliation of the nanoclay while preserving the mechanical performance of the fiber is a challenge.

The last strategy for fire-proofing textiles is based on the application of surface treatments on the fiber, the yarn, or the textile (Kandola, 2009). The most common flame-retardant finishes and coatings are phosphorous-, boron- or halogen-based treatments. They may be applied as finishes that are impregnated in the fabric or coatings that are applied as a layer on the surface of the fabric using traditional textile technologies such as knife-coating or more recent ones like plasma.

However, several of the chemical compounds used for these flame-resistant surface treatments on textiles have been shown to have toxic effects on health and the environment. For instance, polybrominated diphenyl ether (PBDE), which is a largely used flame retardant in textiles, has been detected in water, soil, air, animals, and human tissues (Costa, Giordano, Tagliaferri, Caglieri, & Mutti, 2008). Possible adverse health effects of PBDEs include endocrine disruption and developmental neurotoxicity. Exposure to brominated flame retardants has also been observed to induce reproductive toxicity in animal studies (KEMI, 2014). In general, halogenated flame retardants have shown adverse effects in animals and humans that include endocrine and thyroid disruption, immunotoxicity, reproductive toxicity, cancer, and fetal and child development and neurologic toxicity (Shaw et al., 2010). Boron-based compounds may eventually also have negative impacts on health due to the influence of boron on a variety of enzymes, involving both stimulation and inhibition effects (Woods, 1994). In the case of phosphorous-based flame retardant surface treatments, halogen-containing compounds are carcinogenic (van der Veen & de Boer, 2012). Tricresylphosphate (TCP) is harmful in contact with the skin as well as toxic to aquatic organisms. Triphenyl phosphate (TPhP) and diphenylcresylphosphate (DCP) are also toxic to aquatic organisms. Finally, diethylphosphinic acid and tris(2-chloroethyl)phosphate (TCEP) are considered to be very persistent.

This has prompted a number of countries to issue regulations to ban these toxic chemicals. For instance, the presence of polybrominated biphenyls (PBBs) in textiles is prohibited in the European Union as well as in Canada, the United States, Turkey, Switzerland, South Korea, and Egypt (AAFA, 2013), while penta-bromodiphenyl ether (penta-BDE) and octa-bromodiphenyl ether (octa-BDE) are banned in Europe, the United States, Switzerland, and South Korea (it applies only to bed and night clothes in the case of South Korea). Chlorinated paraffins, tris (2,3-dibromopropyl) phosphate (TRIS), bis (2,3-dibromopropyl) phosphate, and tris (1-aziridinyl)-phosphine oxide (TEPA) are also banned in some countries. Canada is also planning to add hexabromocyclododecane (HBCD) and polybrominated diphenyl ethers (PBDEs) to its list of substances prohibited from manufacture, use, sale, and import (Environment Canada, 2015). This also applies to the products that contain them.

In terms of test methods, the analysis proceeds by solvent extraction and quantification using GC-MS or LC-MS (AAFA, 2013). Methanol is recommended as the solvent for PBB and TRIS extraction. In the case of TEPA, a digestion process is conducted using potassium hydroxide or sodium hydroxide. It is followed by GC-MS headspace analysis for ethyleneimine. Health Canada has also published a series of test methods relative to flame retardants (Health Canada, 2016):

- Sample preparation technique for the determination of flame retardants in textile, foam and other similar consumer products (C47)
- Determination of flame retardants in textile, foam and other similar consumer products by GC-MS (C46)
- Determination of elements in fire retardants in textiles by microwave digestion and ICP-MS analysis (C02.6)
- Determination of tris (2,3-dibromopropyl) phosphate (TRIS) in textiles and similar consumer products (C19)

- Determination of tris (2-chloroethyl) phosphate (TCEP) in polyurethane children's product and similar consumer products by Soxhlet extraction (C38)
- Determination of tris (2-chloroethyl) phosphate (TCEP) in polyurethane children's product and similar consumer products by accelerated solvent extraction (ASE) (C38.1)

7.7 Testing for phthalates

Phthalates were developed in the 1930s and are mainly used as a plasticizer for PVC (Krauskopf & Godwin, 2005). In the textile industry, phthalates are a major component of plastisol printing pastes used for direct printing and transfer printing (Lacasse & Baumann, 2012): the process is solvent-free and the PVC homopolymer is dispersed in a liquid phthatate plasticizer. For instance, phthalate contents of up to 37.6 wt.% were reported for clothing products (Brigden, Labunska, House, Santillo, & Johnston, 2012). However, since there is no covalent bond between phthalates and the polymer and because of their low molecular weight, they may be released in the air upon exposure to high temperature, leach out in the saliva of infants chewing toys, or be absorbed by dermal contact with the skin (Wormuth, Scheringer, Vollenweider, & Hungerbühler, 2006).

Yet, several phthalates have been identified as toxic for human health and the environment. For instance, the effects of phthalates observed in animal studies include reproductive and developmental toxicities as well as liver and kidney abnormalities (Hauser & Calafat, 2005). This can be attributed to the fact that they act as endocrine disruptors. In addition, the formation of liver tumors has been reported in rodents exposed to diethylhexyl phthalate (DEHP) and diisononyl phthalate (DINP) (CHRP, 2009). Recent studies have also evidenced some possible additive effects (KEMI, 2014). Even if it is thought that these hepatocarcinogenic effects are unlikely to occur in humans (CHRP, 2009), some organizations/states/countries have classified DEPH and/or DINP as possible human carcinogens (Canadian Cancer Society, 2016).

The DEHP and DINP content in baby and child textile products has thus been limited by several countries such as the European Union, the United States and South Korea (AAFA, 2013). Other specific types of phthalates are also regulated: di-*n*-octyl phthalate (DNOP), benzyl butyl phthalate (BBP), di-*n*-butyl phthalate (DBP), di-isodecyl phthalate (DIDP), dimethyl phthalate (DMP), diisobutyl phthalate (DIBP), 1,2-benzenedicarboxylic acid, di-C7-11-branched and linear alkyl esters (DHNUP), 1,2-benzenedicarboxylic acid, di-C6-8-branched alkyl esters, C7-rich (DIHP), bis(2-methoxyethyl) phthalate (DMEP), diisopentylphthalate (DIPP), *N*-pentylisopentyl phthalate (NPIPP), and 1,2-benzenedicarboxylic acid, dipentylester, branched and linear (DPP). In some cases, the limitation concerns a phthalate considered individually, while, in other cases, the restriction applies to a group of phthalates considered together.

Test methods for phthalate content generally involve extraction of the phthalates with an organic solvent followed by analysis of the clean-up extract by GC-MS (OEKO-TEX 200, 2010). For instance, phthalates may be extracted with tetrahydrofuran (CPSC-CH-C1001-09.3, 2009). The PVC polymer is then precipitated with

hexane. The solution is diluted with cyclohexane before being analyzed by GC-MS. Alternative extraction methods may include soxhlet extraction, pressurized fluid extraction, microwave extraction, and ultrasonic extraction. Ultrasonic extraction with THF is also prescribed in the ISO 14389 standard (2014). It is possible as well to add a step of cryogenic milling to reduce the sample in a fine powder prior to extraction (CPSC-CH-E1001-09.1, 2010). Finally, ethyl acetate:cyclohexane (1:1) has also been successfully used to extract DMP, DEP, DBP, DIBP, BBP, DEHP, DNOP, DINP, and DIDP (Brigden et al., 2012).

7.8 Testing for other toxic chemicals

This section deals with additional chemicals of interest in the textile industry, namely nonylphenol and nonylphenol ethoxylates (NPE), as well as dioxins and furans.

NPEs are used as a surfactant at several stages of textile processing: scouring, fiber lubrication, and dye leveling (Lacasse & Baumann, 2012). They are particularly useful as a detergent and a conditioning agent for wool because they do not adsorb in wool as anionic surfactants. Nonylphenol is produced when NPEs break down. Yet, both NPEs and nonylphenol have been reported as environmental estrogens (Nimrod & Benson, 1996). They may cause health effects in humans and wildlife through disruption of the endocrine system. They are particularly toxic for aquatic life, with long-lasting effects (Swedish Chemicals Agency, 2013). When NPEs are used in textile manufacturing processes, they may leave residues in the final product. For instance, NPE contents of up to 45,000 $mg\,kg^{-1}$ have been measured in branded clothing articles (Brigden et al., 2012). These NPE residues will be washed away during laundering and released in the environment (KEMI, 2014): this process has been identified as an important source of exposure to NPE for the aquatic environment. Some countries have placed regulations on NPEs and nonylphenol. For example, their concentration in substances and in mixtures used in textile and leather processing has been limited to 0.1 wt.% in the European Union (EC, 2006). This restriction will be toughened in 2021 because the limitation will be extended to textiles sold within the EU, i.e., it will also apply to imported textiles (EC, 2016). In addition, the residual NPE content in textile articles that can be washed in water will be restricted to 0.01 wt.%. If no standard test method for NPE quantification in solid products has been identified, some techniques developed by researchers have been found in the literature. For instance, some have performed NPE extraction using a 70:30 acetonitrile-water mixture (Brigden et al., 2012). The extract was then analyzed with reversed-phase. HPLC. Others used boiling methanol under reflux and GC-MS analysis (Votavová, Dobiáš, Voldřich, & Čížková, 2009).

Dioxins and furans may also be found in textiles. For instance, dioxins may be present as an intermediate product in dyes and pigments used in textiles (Križanec & Le Marechal, 2006). They also exist as impurities in organochlorine pentachlorophenol (PCP), a chemical used as a preservative for cotton to prevent the formation of mildew during storage and sea shipping (PANUPS, 1994). Furan derivatives also enter in the manufacture of synthetic fibers (Zeitsch, 2000). For instance, tetra hydro-2,5-dimethyl *cis* furan was detected in polyester fiber extracts (Le Marechal, Križanec, Vajnhandl, &

Volmajer Valh, 2012), while 2,5-dimethylfuran and 2-methylfuran were emitted by drapes and drapery lining (Andrady, 2003). Polychlorinated dibenzo-*p*-dioxins (PCDD) and dibenzofurans (PCDF) were also measured in washing machine effluent and shower runoff water (Horstmann & McLachlan, 1995). In the latter case, it was attributed to a possible chemical transfer from contaminated textiles to the skin surface (Klasmeier, Mühlebach, & McLachlan, 1999). Yet, dioxins and furans are toxic persistent environmental pollutants. For instance, dioxins have been shown to be carcinogenic in animals and humans as well as induce endocrine, reproductive, and developmental effects (Kogevinas, 2001). In particular, dibenzo-*p*-dioxins and polychlorinated dibenzofurans with chlorine atoms at positions 2, 3, 7, 8 are especially toxic (Le Marechal et al., 2012). However, only Germany appears to have regulated the content of dioxins and furans in goods such as textiles (AAFA, 2013): 5 groups of chemicals are defined based on their toxicity and maximum combined weight concentrations for each group or series of groups are defined. For instance, the maximum combined concentration for Group 1, which includes 2,3,7,8-tetrachlorodibenzo-*p*-dioxin, 1,2,3,7,8-pentachlorodibenzo-*p*-dioxin, 2,3,7,8-tetrachlorodibenzofuran, and 2,3,4,7,8-pentachlorodibenzofuran is $1\,\mu g\,kg^{-1}$. The method used to measure the concentration of dioxins and furans in textiles proceeds through extraction according to a procedure selected on the basis of the sample consistency (EPA 8290A, 2007). Afterwards, the extracts are purified with an acid-based washing treatment and a column chromatography clean-up on alumina, silica gel, and activated carbon. Finally, the detection and quantitative measurement of PCDDs and PCDFs is conducted with high-resolution gas chromatography and high-resolution mass spectrometry. This test method is appropriate for concentrations of part-per-trillion (ppt) to part-per-quadrillion (ppq).

7.9 Eco-textile certifications

In addition to regulations set by countries and states to limit the concentration of toxic chemicals in consumer products and in the environment, such as REACH for the European Union (ECHA, 2016) and the Section 01350 Standard Practice of the California Special Environmental Specifications (California Specification 01350, 2010), a series of voluntary ecolabels have also been implemented.

One of the earliest eco-certification programs relevant to textiles is EcoLogo. It was launched in 1988 by the Canadian government as an environmental certification program (UL, 2016). The objective was to foster demand for products and services that are less damaging for the environment. The EcoLogo certification takes into account the entire life cycle of the product/service, from manufacture to disposal. Products undergo testing and auditing by a third-party laboratory. Criteria cover materials, energy use, health and environment, product performance and use, and product stewardship and innovation. The EcoLogo label is now recognized by manufacturers and buyers of eco-sensitive products all over North America and overseas. It is currently carried by more than 7000 products and is one of the only North American label programs compliant with ISO 14024 and approved by the Global Ecolabelling Network (GEN).

In Europe, the OEKO-TEX 100 certification was introduced in 1992 by the Hohenstein Institute in Germany (OEKO-TEX, 2016). It is an independent testing and certification system for textile products at all stages of the manufacturing process: fibers, yarns, fabrics, nontextile accessories, and finished products. It defines four product classes based on the intimacy and intensity of contact between the product and the skin as well as the sensitivity of the skin (OEKO-TEX 100, 2010):

- Product class I: Articles for babies and toddlers up to 3 years old
- Product class II: Articles with direct, prolonged and/or large-area skin contact
- Product class III: Clothing that is worn away from the skin
- Product class IV: Upholstery/decoration materials

The certification combines general requirements related to an operational effective quality assurance system as well as the legally binding signing of undertakings and conformity declarations by the applicant, with product specific requirements corresponding to limit values for physical properties (pH, color fastness, and odor) and weight concentration or emission of a series of banned, regulated, or known to be harmful to health substances (OEKO-TEX, 2016). The list currently includes formaldehyde, heavy metals, chlorinated phenols, chlorinated benzenes and toluenes, polycyclic aromatic hydrocarbons, volatiles, organic tin compounds, colorants, chemical residues, biological active products, flame retardant products, and asbestos. More than 150,000 OEKO-TEX 100 certificates have been issued for over 10,000 participating companies along the textile chain. A companion certification system, the OEKO-TEX Standard 1000, was introduced in 1995 for environmentally friendly production sites in the textile and clothing industry.

The GREENGUARD certification was introduced in 2000 by the Underwriters Laboratories (Greenguard, 2016). It is aimed at building products and interior finishes to ensure that they meet criteria for low emissions of VOCs into indoor air. Two certification programs are proposed: GREENGUARD Certification for furniture and commercial building products and GREENGUARD Gold for schools and healthcare facilities. Certification criteria are set for total VOC (TVOC), formaldehyde, total aldehyde, 4-phenylcyclohexene, particle matter $<10\,\mu m$, as well as individual VOCs. More than 30,000 products currently hold the GREENGUARD certification/GREENGUARD Gold labels.

Bluesign technologies was also founded in 2000 (Bluesign, 2016). The objective of the Bluesign system is to link chemicals suppliers, textile manufacturers, and brands together to foster a healthy, responsible, and profitable textile industry while reducing its impact on people and the environment. Its four principles are the following:

- Uniting the textile supply chain
- Eliminating substances posing risks to people and the environment from the beginning
- Responsibly using resources
- Providing safety for people and the environment

Each chemical is rated in one of 3 categories: “Blue” for components that meet all of the Bluesign criteria and requirements, “Gray” for components that shall only be used under certain appropriate conditions; and “Black” for components that do not meet the Bluesign criteria. In addition, production sites and companies are evaluated according to the requirements for each step of the process chain in compliance with the five principles of sustainability as well as criteria regarding social responsibility.

Finally, the Cradle-to-Cradle concept was developed in the 1990s at the Environmental Protection Encouragement Agency (EPEA) in Hambourg (C2C, 2016). It is a biomimetic approach to product and system design based on three principles:

- Waste equals nutrients: every waste is food for someone;
- Use solar energy: this is a free, renewable resource which is safe for the environment;
- Celebrate diversity: Nature favors variety and complexity.

Materials are classified into two categories: technical nutrients that can be reused again and again without being downcycled and biological nutrients that, once used, decomposed in the soil into food for small life forms. Each category has its own life cycle. Climatex, a compostable upholstery fabric developed in 1993, was the first product certified Cradle to Cradle.

7.10 Conclusion and future trends

Among the 1900–2400 chemicals used in the textile industry, 165 have currently been identified as carcinogenic, mutagenic, toxic to reproduction, allergenic, and/or with environmentally hazardous, long-term effects (KEMI, 2013). As a result, some regulations and voluntary ecolabels have been implemented by countries, states, and private organizations for textile processes and products to better protect health and the environment from these harmful chemicals. Corresponding test methods aimed at detecting and quantifying these compounds have also been developed: some have been adopted at standards.

However, much remains to be done. In particular, textile manufacturing may still be considered as one of the most polluting industries (Roy Choudhury, 2014): use of harmful chemicals, consumption of large quantities of water and energy, generation of large amounts of waste, transportation over long distances of input and output materials at all stages of the manufacturing process, and the use of nonbiodegradable materials. With the increasing awareness of governments and the general public about potential risks for health and the environment posed by noneco-responsible practices, tougher chemical regulations and a larger demand for eco-certified products can be expected in a very near future. In addition, as new processes and alternative chemical solutions are proposed for more eco-friendly textile products, test methods will have to be adapted and/or developed to ensure that these improvements do not hold loopholes. Finally, as knowledge progresses, new chemicals will be added on the watch or exclusion list while some others may find their way out.

7.11 Sources of further information and advice

ASTM Committee D22 on Air Quality (www.astm.org/COMMIT/SUBCOMMIT/D2205.htm). It was formed in 1951, has a membership of about 400, and meets twice a year. The Committee has jurisdiction of over 145 standards distributed among seven technical subcommittees including Quality Control, Ambient Atmospheres and Source Emissions, Workplace Air Quality, Indoor Air, Sampling and Analysis of Asbestos, and Sampling and Analysis of Mold.

CENTEXBEL (www.centexbel.be) is a Belgian textile research center. Its activities include testing, certification of products and processes, research and development, and services to the industry. In terms of chemical analysis, its capacities comprise assessment of textile-chemical parameters, measurement of protective clothing performance, instrumental analysis of functional additives and health parameters, and characterization of product emission.

CTT Group (www.groupecttgroup.com) is a Quebec/Canada-based testing and R&D laboratory for technical textiles, geosynthetics, and advanced textile-based materials. Founded in 1983 as a college technology transfer center, it serves the industry in the sectors of protection, transportation, aerospace, health, buildings, sports, military, and civil engineering among others. It has a strong expertise in the chemical testing of textiles and its team members have been involved in the development of a number of test methods and standards.

European Chemicals Agency (ECHA, echa.europa.eu) is leading the implementation of the EU's chemicals legislation, REACH (Registration, Evaluation, Authorization and Restriction of Chemicals). It helps companies to comply with the legislation, promotes the safe use of and provides information on chemicals, and addresses chemicals of concern.

ISO Technical Committee ISO/TC 38 on Textiles (www.iso.org/iso/home/standards_development/list_of_iso_technical_committees/iso_technical_committee.htm?commid=48148). It was formed in 1947 and has 133 standards under its responsability. It has five subcommittees:

- SC 1: Tests for colored textiles and colorants
- SC 2: Cleansing, finishing, and water resistance tests
- SC 20: Fabric descriptions
- SC 23: Fibers and yarns
- SC 24: Conditioning atmospheres and physical tests for textile fabrics

And it has eight work groups:

- WG 9: Nonwovens
- WG21: Ropes, cordage, slings, and netting
- WG22: Composition and chemical testing
- WG23: Testing methods for antimicrobial activity and odor
- JWG26: Antistatic
- WG27: Fabric properties relating to moisture
- WG29: Tests for anti house dust mite
- WG30: Tests for biodegradability

References

AAFA. (2013). *Restricted substances list (RSL)*. Washington, DC: American Apparel & Footwear Association (64 p.).

AATCC Standard TM112. (2014). *Formaldehyde release from fabric, determination of: Sealed jar method*. Durham, NC: American Association of Textile Chemists and Colorists (3 p.).

Aktar, M. W., Sengupta, D., & Chowdhury, A. (2009). Impact of pesticides use in agriculture: Their benefits and hazards. *Interdisciplinary Toxicology*, *2*(1), 1–12.

ANEC/BEUC. (2016). *Protecting consumers from hazardous chemicals in textiles*. Brussels, Belgium: The European Association for the Co-ordination of Consumer Representation in Standardisation (ANEC)/The European Consumer Organisation (BEUC).

Andrady, A. L. (2003). *Plastics and the environment*. Hoboken, NJ: John Wiley & Sons (762 p.).

ASTM Standard D3686. (2013). *Standard practice for sampling atmospheres to collect organic compound vapors (activated charcoal tube adsorption method)*. West Conshohocken, PA: ASTM International (7 p.).

ASTM Standard D5116. (2010). *Standard guide for small-scale environmental chamber determinations of organic emissions from indoor materials/products*. West Conshohocken, PA: ASTM International (16 p.).

ASTM Standard D6177. (2014). *Standard practice for determining emission profiles of volatile organic chemicals emitted from bedding sets*. West Conshohocken, PA: ASTM International (4 p.).

ASTM Standard D6670. (2013). *Standard practice for full-scale chamber determination of volatile organic emissions from indoor materials/products*. West Conshohocken, PA: ASTM International (21 p.).

ASTM Standard D7143. (2011). *Standard practice for emission cells for the determination of volatile organic emissions from indoor materials/products*. West Conshohocken, PA: ASTM International (20 p.).

ASTM Standard D7706. (2011). *Standard practice for rapid screening of VOC emissions from products using micro-scale chambers*. West Conshohocken, PA: ASTM International (9 p.).

ASTM Standard E1613. (2012). *Standard test method for determination of lead by inductively coupled plasma atomic emission spectrometry (ICP-AES), flame atomic absorption spectrometry (FAAS), or graphite furnace atomic absorption spectrometry (GFAAS) techniques*. West Conshohocken, PA: ASTM International (9 p.).

ASTM Standard E1645. (2016). *Standard practice for preparation of dried paint samples by hotplate or microwave digestion for subsequent lead analysis*. West Conshohocken, PA: ASTM International (5 p.).

ASTM Standard F963. (2011). *Standard consumer safety specification for toy safety*. West Conshohocken, PA: ASTM International (68 p.).

ASTM Standard F2617. (2015). *Standard test method for identification and quantification of chromium, bromine, cadmium, mercury, and lead in polymeric material using energy dispersive X-ray spectrometry*. West Conshohocken, PA: ASTM International (12 p.).

Babu, B. R., Parande, A. K., Raghu, S., & Kumar, T. P. (2007). Cotton textile processing: Waste generation and effluent treatment. *Journal of Cotton Science*, *11*, 141–153.

Bayil, S., Cicek, H., Cimenci, I. G., & Hazar, M. (2008). How volatile organic compounds affect free radical and antioxidant enzyme activity in textile workers. *Arhiv za Higijenu Rada i Toksikologiju*, *59*(4), 283–287.

Bluesign. (2016). *Bluesign® technologies.* www.bluesign.com.

Brigden, K., Labunska, I., House, E., Santillo, D., Johnston, P. (2012). *Hazardous chemicals in branded textile products on sale in 27 countries during 2012*. Greenpeace Research Laboratories Technical Report 06-2012, Greenpeace Research Laboratories, Exeter, UK (45 p.).

Bulan-Brady, J. (1990). Use of heavy metals in textile wet processing. *Textile Chemist & Colorist*, *22*(1), 23–27.

C2C. (2016). *What is cradle to cradle?* Environmental Protection Encouragement Agency. http://www.epeaparis.fr/cradle-to-cradle/principes.

California Specification 01350. (2010). *Standard method for the testing and evaluation of volatile organic chemical emissions from indoor sources using environmental chambers*. Sacramento, CA: California Department of Public Health (52 p.).

CAN/CGSB Standard 4.2 No. 63.4. (2007). *Textiles—Determination of formaldehyde—Part 1: Free and hydrolyzed formaldehyde (water extraction method)*. Ottawa, ON, Canada: Standards Council of Canada (16 p.).

CAN/CGSB Standard 4.2 No. 63.5. (2007). *Textiles—Determination of formaldehyde—Part 2: Released formaldehyde (vapour absorption method)*. Ottawa, ON, Canada: Standards Council of Canada (20 p.).

Canadian Cancer Society. (2016). *Phthalates.* http://www.cancer.ca/ [Accessed 18 October 2006].

CCME. (2002). *Recommended CCME standards and guidelines for the reduction of VOC emissions from Canadian industrial maintenance coatings*. Winnipeg, MB, Canada: Canadian Council of Ministers of the Environment (32 p.).

Chequer, F. M. D., de Oliveira, G. A. R., Ferraz, E. R. A., Cardoso, J. C., Zanoni, M. V. B., de Oliveira, D. P., et al. (2013). Textile dyes: Dyeing process and environmental impact. In M. Gunay (Ed.), *Eco-friendly textile dyeing and finishing*. InTech. https://doi.org/10.5772/53659 Available from http://www.intechopen.com/books/eco-friendly-textile-dyeing-and-finishing/textile-dyes-dyeing-process-and-environmental-impact.

Chowdhury, B. A., & Chandra, R. K. (1987). Biological and health implications of toxic heavy metal and essential trace element interactions. *Progress in Food & Nutrition Science*, *11*(1), 55–113.

CHRP (Committee on the Health Risks of Phthalates). (2009). *Phthalates and cumulative risk assessment: The tasks ahead*. Washington, DC: National Academies Press (208 p.).

CIEC. (2013). *Colorants*. The Essential Chemical Industry online www.essentialchemicalindustry.org/materials-and-applications/colorants.html.

Costa, L. G., Giordano, G., Tagliaferri, S., Caglieri, A., & Mutti, A. (2008). Polybrominated diphenyl ether (PBDE) flame retardants: Environmental contamination, human body burden and potential adverse health effects. *Acta Biomed*, *79*, 172–183.

CPSC-CH-E1002-08.1 Standard. (2010). *Standard operating procedure for determining total lead (Pb) in non-metal children's products, revised*. Gaithersburg, MD: U.S. Consumer Product Safety Commission (6 p.).

Standard. (2010). *Standard operating procedure for determination of phthalates*. Gaithersburg, MD: U.S. Consumer Product Safety Commission (8 p.).

CPSC-CH-C1001-09.3 Standard. (2009). *Standard operating procedure for determination of phthalates*. Gaithersburg, MD: U.S. Consumer Product Safety Commission (8 p.).

CPSC-CH-E1003-09 Standard. (2009). *Standard operating procedure for determining lead (Pb) in paint and other similar surface coatings*. Gaithersburg, MD: U.S. Consumer Product Safety Commission (7 p.).

CPSIA. (2008). Consumer Product Safety Improvement Act of 2008. Public Law 110–314, 122 STAT. 3016–3077. Consumer Product Safety Commission, Bethesda, MD.

Deguine, J., Ferron, P., & Russell, D. (2008). Sustainable pest management for cotton production. A review. *Agronomy for Sustainable Development*, *28*, 113–137.

DIN Standard 54231. (2005). *Textiles—Detection of disperse dyestuffs*. Berlin, Germany: Deutsches Institut für Normung (11 p.).

EC. (1999). Council Directive 1999/13/EC of 11 March 1999 on the limitation of emissions of volatile organic compounds due to the use of organic solvents in certain activities and installations. *Official Journal of the European Union*, *L 85*, 1–22.

EC. (2006). Commission regulation (EC) No 1907/2006 of the European Parliament and of the Council of 18 December 2006 concerning the Registration, Evaluation, Authorisation and Restriction of Chemicals (REACH), establishing a European Chemicals Agency, amending Directive 1999/45/EC and repealing Council Regulation (EEC) No 793/93 and Commission Regulation (EC) No 1488/94 as well as Council Directive 76/769/EEC and Commission Directives 91/155/EEC, 93/67/EEC, 93/105/EC and 2000/21/EC. *Official Journal of the European Union*, *L 396*.

EC. (2009). Commission regulation (EC) No 552/2009 of 22 June 2009 amending Regulation (EC) No 1907/2006 of the European Parliament and of the Council on the Registration, Evaluation, Authorization and Restriction of Chemicals (REACH) as regards Annex XVII. *Official Journal of the European Union*, *L 164*, 7–31.

EC. (2016). Commission Regulation (EU) 2016/26 of 13 January 2016 amending Annex XVII to Regulation (EC) No 1907/2006 of the European Parliament and of the Council concerning the Registration, Evaluation, Authorisation and Restriction of Chemicals (REACH) as regards nonylphenol ethoxylates. *Official Journal of the European Union*, *L 9*, 1–3.

ECHA. (2011). *Opinion on an Annex XV dossier proposing restrictions on Dimethylfumarate (DMFu)*. ECHA/RAC/RES-O-0000001305-83-04/F Helsinki, Finland: European Chemicals Agency (8 p.).

ECHA. (2016). *REACH*. European Chemicals Agency. https://echa.europa.eu/regulations/reach.

EN Standard 71-3. (2014). *Safety of toys—Part 3: Migration of certain elements*. Brussels, Belgium: European Committee for Standardization (52 p.).

EN Standard 71-9. (2007). *Safety of toys—Part 9: Organic chemical compounds—Requirements*. Brussels, Belgium: European Committee for Standardization (22 p.).

EN Standard 1811. (2011). *Reference test method for release of nickel from all post assemblies which are inserted into pierced parts of the human body and articles intended to come into direct and prolonged contact with the skin*. Brussels, Belgium: European Committee for Standardization (34 p.).

EN Standard 12472. (2009). *Method for the simulation of wear and corrosion for the detection of nickel release from coated items*. Brussels, Belgium: European Committee for Standardization (18 p.).

EN Standard 14362-1. (2012). *Textiles—Methods for determination of certain aromatic amines derived from azo colorants—Part 1: Detection of the use of certain azo colorants accessible with and without extracting the fibres*. Brussels, Belgium: European Committee for Standardization (33 p.).

EN Standard 14362-3. (2012). *Textiles—Methods for determination of certain aromatic amines derived from azo colorants—Part 3: Detection of the use of certain azo colorants, which may release 4-aminoazobenzene*. Brussels, Belgium: European Committee for Standardization.

Environment Canada. (2015). Regulations amending the prohibition of certain toxic substances regulations 2012. *Canada Gazette*, *149*(14).

EPA. (1997). *Profile of the textile industry*. Report EPA 310-R-97-009 Washington, DC: United States Environmental Protection Agency (148 p.).

EPA. (2015). *Indoor exposure product testing protocols*. EPA Document# 740-S1-5001 Washington, DC: United States Environmental Protection Agency (41 p.).

EPA Method 6020A. (2007). *Inductively coupled plasma-mass spectrometry*. Washington, DC: United States Environmental Protection Agency (30 p.).

EPA Method 8081B. (2007). *Organochlorine pesticides by gas chromatography*. Washington, DC: United States Environmental Protection Agency (57 p.).

EPA Method 8082A. (2007). *Polychlorinated biphenyls (PCBs) by gas chromatography*. Washington, DC: United States Environmental Protection Agency (56 p.).

EPA Method 8141B. (2007). *Organophosphorus compounds by gas chromatography*. Washington, DC: United States Environmental Protection Agency (44 p.).

EPA Method 8151A. (1996). *Chlorinated herbicides by GC using methylation or pentafluorobenzylation derivatization*. Washington, DC: United States Environmental Protection Agency.

EPA Method 8290A. (2007). *Polychlorinated dibenzodioxins (PCDDs) and polychlorinated dibenzofurans (PCDFs) by high-resolution gas chromatography/high resolution mass spectrometry (HRGC/HRMS)*. Washington, DC: United States Environmental Protection Agency (72 p.).

EPA TO-1. (1984). *Method for the determination of volatile organic compounds in ambiant air using Tenax® adsorption and gas chromatography/mass spectrometry (GC/MS)*. Washington, DC: United States Environmental Protection Agency.

EPA TO-2. (1984). *Method for the determination of volatile organic compounds in ambiant air by molecular sieve adsorption and gas chromatography/mass spectrometry (GC/MS)*. Washington, DC: United States Environmental Protection Agency.

Erkurt, H.A. (Ed.) (2010). *Biodegradation of azo dyes*. Berlin, Germany: Springer Science & Business Media.

Flynn, V. (2015). EU countries agree textile chemical ban. *The Guardian*, Tuesday 21 July 2015.

Förstner, U., & Wittmann, G. T. W. (2012). *Metal pollution in the aquatic environment*. Berlin, GE: Springer Science & Business Media.

Foti, C., Zambonin, C. G., Cassano, N., Aresta, A., Damascelli, A., Ferrara, F., et al. (2009). Occupational allergic contact dermatitis associated with dimethyl fumarate in clothing. *Contact Dermatitis*, *61*(2), 122–124.

Franklin, P., Dingle, P., & Stick, S. (2000). Raised exhaled nitric oxide in healthy children is associated with domestic formaldehyde levels. *American Journal of Respiratory and Critical Care Medicine*, *161*(5), 1757–1759.

Freedonia. (2015). *World dyes & organic pigments*. Cleveland, OH: The Freedonia Group, Inc.

GAO. (2010). *Formaldehyde in textiles—While levels in clothing generally appear to be low, allergic contact dermatitis is a health issue for some people*. Report GAO-10-875 Washington, DC: US Government Accountability Office (53 p.).

Gebefügi, I. (1989). Chemical exposure in enclosed environments. *Toxicological & Environmental Chemistry*, *20–21*(1), 121–127.

GGTM Standard P066. (2008). *Standard method for measuring and evaluating chemical emissions from building materials, finishes and furnishings using dynamic environmental chambers*. Marietta, GA: GREENGUARD Environmental Institute (62 p.).

Giménez-Arnau, A., Silvestre, J. F., Mercader, P., De la Cuadra, J., Ballester, I., Gallardo, F., et al. (2009). Shoe contact dermatitis from dimethyl fumarate: Clinical manifestations, patch test results, chemical analysis, and source of exposure. *Contact Dermatitis*, *61*, 249–260.

Greenguard. (2016). *GREENGUARD Certification from UL Environment*. GREENGUARD. greenguard.org.

Guenther, K., Heinke, V., Thiele, B., Kleist, E., Prast, H., & Raecker, T. (2002). Endocrine disrupting nonylphenols are ubiquitous in food. *Environmental Science and Technology*, *36*(8), 1676–1680.

Gurr, E. (2012). *Synthetic dyes in biology, medicine and chemistry*. London and New York: Academic Press.

Hauser, R., & Calafat, A. M. (2005). Phthalates and human health. *Occupational and Environmental Medicine*, *62*, 806–818.

Health Canada. (2016). *Chemistry methods*. http://www.hc-sc.gc.ca/cps-spc/prod-test-essai/method-chem-chim-eng.php.

HC PartB-C-02.2. (2011). *Determination of total lead in surface coating materials in consumer products*. Ottawa, Canada: Health Canada.

Horstmann, M., & McLachlan, M. S. (1995). Concentrations of polychlorinated dibenzo-p-dioxins (PCDD) and dibenzofurans (PCDF) in urban runoff and household wastewaters. *Chemosphere*, *31*(3), 2887–2896.

Igielska, B., Wiglusz, R., Sitko, E., & Nikel, G. (2003). Release of volatile organic compounds from textile floor coverings in higher temperatures. *Roczniki Państwowego Zakładu Higieny*, *54*(3), 329–335.

Islas-Espinoza, M. (2014). Airborne toxic pollutants. In A. De Las Heras (Ed.), *Sustainability science and technology: An introduction* (pp. 195–2010). Boca Raton, FL: CRC Press.

ISO Standard 105-E04. (2013). *Textiles—Tests for colour fastness—Part E04: Colour fastness to perspiration*. Geneva, Switzerland: International Organization for Standardization (10 p.).

ISO Standard 12219-3. (2012). *Interior air of road vehicles—Part 3: Screening method for the determination of the emissions of volatile organic compounds from vehicle interior parts and materials—Micro-scale chamber method*. Geneva, Switzerland: International Organization for Standardization (21 p.).

ISO Standard 14184-1. (2011). *Textiles—Determination of formaldehyde—Part 1: Free and hydrolysed formaldehyde (water extraction method)*. Geneva, Switzerland: International Organization for Standardization (14 p.).

ISO Standard 14184-2. (2011). *Textiles—Determination of formaldehyde—Part 2: Released formaldehyde (vapour absorption method)*. Geneva, Switzerland: International Organization for Standardization (18 p.).

ISO Standard 14389. (2014). *Textiles—Determination of the phthalate content—Tetrahydrofuran method: Ultrasonic extraction with tetrahydrofuran (THF)*. Geneva, Switzerland: International Organization for Standardization (22 p.).

ISO Standard 16000-3. (2011). *Indoor air—Part 3: Determination of formaldehyde and other carbonyl compounds in indoor air and test chamber air—Active sampling method*. Geneva, Switzerland: International Organization for Standardization (34 p.).

ISO Standard 16000-6. (2011). *Indoor air—Part 6: Determination of volatile organic compounds in indoor and test chamber air by active sampling on Tenax TA® sorbent, thermal desorption and gas chromatography using MS or MS-FID*. Geneva, Switzerland: International Organization for Standardization (36 p.).

ISO Standard 16000-9. (2006). *Indoor air—Part 9: Determination of the emission of volatile organic compounds from building products and furnishing—Emission test chamber method*. Geneva, Switzerland: International Organization for Standardization (16 p.).

ISO Standard 16000-10. (2006). *Indoor air—Part 10: Determination of the emission of volatile organic compounds from building products and furnishing—Emission test cell method*. Geneva, Switzerland: International Organization for Standardization (24 p.).

ISO Standard 16000-11. (2006). *Indoor air—Part 11: Determination of the emission of volatile organic compounds from building products and furnishing—Sampling, storage of samples and preparation of test specimens*. Geneva, Switzerland: International Organization for Standardization (20 p.).

ISO Standard 17070. (2015). *Leather—Chemical tests—Determination of tetrachlorophenol-, trichlorophenol-, dichlorophenol-, monochlorophenol-isomers and pentachlorophenol content*. Geneva, Switzerland: International Organization for Standardization (9 p.).

JTF. (2015). *Guidelines for nonuse of harmful substances for textiles and clothing*. Tokyo, Japan: Japan Textile Federation.

Kandola, B. (2009). Flame retardancy design for textiles. In C. A. Wilkie & A. B. Morgan (Eds.), *Fire retardancy of polymeric materials*. (2nd ed.). Boca Raton, FL: CRC Press.

Kant, R. (2012). Textile dyeing industry an environmental hazard. *Natural Science*, *4*(1), 22–26.

Kegley, S. E., Hill, B. R., Orme, S., & Choi, A. H. (2016). *PAN pesticide database—California pesticide use*. North America: Pesticide Action Network (PAN). www.pesticideinfo.org.

KEMI. (2013). *Hazardous chemicals in textiles—Report of a government assignment*. Sundbyberg, Sweden: Swedish Chemicals Agency (114 p.).

KEMI. (2014). *Chemicals in textiles—Risks to human health and the environment*. Sundbyberg, Sweden: Swedish Chemicals Agency (142 p.).

Klasmeier, J., Mühlebach, A., & McLachlan, M. S. (1999). PCDD/Fs in textiles—Part II: Transfer from clothing to human skin. *Chemosphere*, *38*(1), 97–108.

Kogevinas, M. (2001). Human health effects of dioxins: Cancer, reproductive and endocrine system effects. *Human Reproduction Update*, *7*(3), 331–339.

Krauskopf, L. G., & Godwin, A. (2005). Plasticizers. In C. E. Wilkes, C. A. Daniels, & J. W. Summers (Eds.), *PVC handbook* (pp. 173–198). Cincinnati, OH: Hanser Gardner Publications.

Križanec, B., & Le Marechal, A. M. (2006). Dioxins and dioxin-like persistent organic pollutants in textiles and chemicals in the textile sector. *Croatica Chemica Acta*, *79*(2), 177–186.

Lacasse, K., & Baumann, W. (2012). *Textile chemicals: Environmental data and facts*. Berlin, Germany: Springer Science & Business Media (1180 p.).

Le Marechal, A. M., Križanec, B., Vajnhandl, S., & Volmajer Valh, J. (2012). Textile finishing industry as an important source of organic pollutants. In T. Puzyn & A. Mostrag-Szlichtyng (Eds.), *Organic pollutants ten years after the Stockholm convention—Environmental and analytical update* (pp. 29–54). Rijeka, Croatia: InTech.

Luongo, G. (2015). *Chemicals in textiles—A potential source for human exposure and environmental pollution*. [Doctoral thesis] Stockholm University [Doctoral thesis].

MDDLECC. (2016). *List of volatile organic compounds (VOC) measured in the atmosphere*-http://www.mddelcc.gouv.qc.ca/air/cov/liste.htm.

Morgan, A. B., & Wilkie, C. A. (2009). An introduction to polymeric flame retardancy, its role in materials science, and the current state of the field. In C. A. Wilkie & A. B. Morgan (Eds.), *Fire retardancy of polymeric materials*. (2nd ed.). Boca Raton, FL: CRC Press.

Nimrod, A. C., & Benson, W. H. (1996). Environmental estrogenic effects of alkylphenol ethoxylates. *Critical Reviews in Toxicology*, *26*(3), 335–364.

NIST. (2013). *A guide to United States apparel and household textiles compliance requirements*. GCR 12-970, Gaithersburg, MD: National Institute of Standards and Technology (36 p.).

OEKO-TEX. (2016). *OEKO-TEX® confidence in textiles*. International Association for Research and Testing in the Field of Textile Ecology. www.oeko-tex.com/en.

OEKO-TEX Standard 100. (2010). *General and special conditions*. Zürich, Switzerland: International Association for Research and Testing in the Field of Textile Ecology (26 p.).

OEKO-TEX Standard 200. (2010). *Testing procedures*. Zürich, Switzerland: International Association for Research and Testing in the Field of Textile Ecology (14 p.).

PAN. (2012). *Pesticides and health hazards—Facts and figures*. Hamburg, Germany: Pestizid Aktions-Netzwerk e.V (16 p.).

PANUPS. (1994). Dioxins from PCP treated cotton. *Pesticide action network North America updates service*. Finland, MN: Organic Consumers Association. https://www.organicconsumers.org/old_articles/clothes/dioxins_cotton_pcp.php.

Podsiki, C. (2008). *Chart of heavy metals, their salts and other compounds*. Washington, DC: American Institute for Conservation of Historic and Artistic Works (24 pp.). www.conservation-us.org/docs/default-source/resource-guides/chart-of-heavy-metals-their-salts-and-other-compounds-nbsp-.pdf (Accessed 17 August 2016).

POST. (2015). *The environmental, health and economic impacts of textile azo dyes*. London, United Kingdom: Parliamentary House of Science and Technology (5 p.).

Puvaneswari, N., Muthukrishnan, J., & Gunasekaran, P. (2006). Toxicity assessment and microbial degradation of azo dyes. *Indian Journal of Experimental Biology*, *44*(8), 618–626.

Roy Choudhury, A. K. (2014). Environmental impacts of the textile industry and its assessment through life cycle assessment. In S. S. Muthu (Ed.), *Roadmap to sustainable textiles and clothing—Environmental and social aspects of textiles and clothing supply chain* (pp. 1–39). Singapore: Springer.

Salthammer, T. (2009). Environmental test chambers and cells. In T. Salthammer & E. Uhde (Eds.), *Organic indoor air pollutants: Occurrence, measurement, evaluation*. Weinheim, Germany: John Wiley & Sons.

Shaw, S. D., Blum, A., Weber, R., Kannan, K., Rich, D., Lucas, D., et al. (2010). Halogenated flame retardants: Do the fire safety benefits justify the risks? *Reviews on Environmental Health*, *25*(4), 261–305.

Srivastava, A., & Majumdar, D. (2011). Monitoring and reporting VOCs in ambient air. In N. A. Mazzeo (Ed.), *Air quality monitoring, assessment and management* (pp. 137–148). Rijeka, Croatia: InTech.

Swedish Chemicals Agency. (2013). Proposal for a restriction—Nonylphenol and nonylphenolates in textiles. *REACH Annex XV restriction report*. Sundbyberg, Sweden: European Union (372 p.).

Tchounwou, P. B., Yedjou, C. G., Patlolla, A. K., & Sutton, D. J. (2012). Heavy metals toxicity and the environment. *EXS*, *101*, 133–164.

TexEASTile. (2014). Green tools handbook for textile industries. *TexEASTile sustainable innovation for textile in South East Europe.* http://www.euroimpresa.it/sites/default/files/GREEN_TOOLS_Handbook.pdf.

TUV. (2013). *Regulations on harmful substances in textiles and leather products*. Köln, Germany: TÜV Rheinland LGA Products GmbH.

Tuzen, M., Onal, A., & Soylak, M. (2008). Determination of trace heavy metals in some textile products produced in Turkey. *Bulletin of the Chemical Society of Ethiopia*, *22*(3), 379–384.

UL. (2016). *ECOLOGO product certification*. Underwriters Laboratories. http://industries.ul.com/environment/certificationvalidation-marks/ecologo-product-certification.

van der Veen, I., & de Boer, J. (2012). Phosphorus flame retardants: Properties, production, environmental occurrence, toxicity and analysis. *Chemosphere*, *88*, 1119–1153.

Votavová, L., Dobiáš, J., Voldřich, M., & Čížková, H. (2009). Migration of nonylphenols from polymer packaging materials into food simulants. *Czech Journal of Food Science*, *27*, 293–299.

Watts, P. (2006). Concise International Chemical Assessment Document 68: Tetrachloroethene. *International Programme on Chemical Safety (IPCS)*. Geneva, Switzerland: World Health Organization (123 p.).

WHO. (1989). Indoor air quality: Organic pollutants. *EURO Reports and Studies 111*. Geneva, Switzerland: World Health Organization Regional Office for Europe.

WHO. (2010). *Exposure to benzene: A major public health concern*. Geneva, Switzerland: World Health Organization (5 p.).

Wilke, O., Jann, O., & Brçdner, D. (2004). VOC- and SVOC-emissions from adhesives, floor coverings and complete floor structures. *Indoor Air*, *14*(Suppl. 8), 98–107.

Woods, W. G. (1994). An introduction to boron: History, sources, uses, and chemistry. *Environmental Health Perspectives*, *102*(Suppl. 7), 5–11.

Woolmark Test Method TM27. (2003). *Insect resist (IR) agent: Chemical assay for content*. The Rocks, Australia: The Woolmark Company (20 p.).

Wormuth, M., Scheringer, M., Vollenweider, M., & Hungerbühler, K. (2006). What are the sources of exposure to eight frequently used phthalic acid esters in Europeans? *Risk Analysis*, *26*(3), 803–824.

XP-G08 015 Standard. (2000). *Textiles—Determination of pentachlorophenol*. Paris, France: AFNOR (Association Française of Normalisation).

Yernaux, B. (2015). *10 toxic chemicals to avoid in your products*. The Ethical Fashion Forum Source. http://source.ethicalfashionforum.com/ (Published July 30, 2015).

Zeiner, M., Reziæ, I., & Steffan, I. (2007). Analytical methods for the determination of heavy metals in the textile industry. *Kemija u Industriji*, *56*(11), 587–595.

Zeitsch, K. J. (2000). (1st ed.). *The chemistry and technology of furfural and its many by-products*. (Vol. 13). Elsevier Science.

Zhang, X., Liao, Q., & Zhang, Y. (2007). Simultaneous determination of nine organochlorine pesticide residues in textile by high performance liquid chromatography. *Se Pu*, *25*(3), 380–383.

Zhu, F., Ruan, W., He, M., Zeng, F., Luan, T., Tong, Y., et al. (2009). Application of solid-phase microextraction for the determination of organophosphorus pesticides in textiles by gas chromatography with mass spectrometry. *Analytica Chimica Acta*, *650*(2), 202–206.

Testing fabrics for flammability and fire safety

8

V. Izquierdo
CTT Group, Saint-Hyacinthe, QC, Canada

8.1 Introduction

Since the origin of human beings, textile materials have been designed to protect people against weather conditions: sun, rain, cold. In addition, because of the sometimes-tense relationships between tribes and countries, textile materials were also aimed at providing protection against mechanical risks: arrows, swords, etc. In modern days, protection against flammability is of concern for various professional applications (e.g., welders, oil and gas industry workers, firefighters), transportation applications (e.g., cars, trains, and aircrafts), and general consumer use (e.g., fireplaces, gas cooktops).

The main purpose for flammability testing of textile materials is to enhance the safety of end users, whether consumers or workers.

This chapter provides a description of the different aspects of textile flammability behavior used in standard test methods. It describes various ignition sources to illustrate the variety of test methods developed to mimic, on a laboratory scale, conditions that may occur in the field. The third part of this chapter presents some test methods mainly used in the North American market for flame-resistant fabrics.

8.2 Flammability properties of fabrics

The flammability properties of fabrics can be evaluated in different ways: by application of a direct flame, application of heat, or a chemical reaction. Different test methods were developed over the years while taking into account the textile's end use and its associated risk assessment. The measurement of potential damages is presented in this section.

The vocabulary and definitions related to the burning behavior of textile materials can be found in standard test methods such as ISO 4880 (1997), CAN/CGSB 4.175 (2011), or ASTM E176 (2015).

8.2.1 Damage measurement

8.2.1.1 Ignitability

This simple concept is used to verify the ease of ignition of a textile material. This type of evaluation is found in some standard test methods such as ISO 6940 (2004). The principle is to apply a flame to a vertically fixed fabric specimen under controlled conditions, in a controlled environment, at incremental durations starting at 1 second.

Advanced Characterization and Testing of Textiles. https://doi.org/10.1016/B978-0-08-100453-1.00009-X

This duration of flame application is incrementally increased until the ignition of the fabric is observed. The maximum flame application time is 20 seconds. Depending on the textile end-use, the flame can be applied either on the surface or the edge. This method is highly demanding in terms of number of specimens tested since a new specimen is needed for each flame application.

8.2.1.2 Damaged length/char length

In the majority of standard test methods, the flame is applied to the specimen for a specific duration. After the flame has been removed, the damaged or char length is recorded based on the visual observation of the damage caused to the specimen. The way of measuring the char length varies depending on the standard test method. In some instances, it corresponds to the original specimen length minus the length of the intact material (NFPA 701, 2015). In other cases, it is the length of a visually damaged portion after a tearing force is applied (ASTM D 6413, 2015; CAN/CGSB 4.2 No 27.10, 2000; CAN/ULC S109, 2014; IMO A.563(14), 1985). That tearing force depends on the fabric mass per unit area as illustrated in Table 8.1.

8.2.1.3 Weight loss (NFPA 701)

In some standard test methods, evaluation of a fabric's behavior when exposed to heat and flame is based on weight loss. For instance, NFPA 701 test method 1 (NFPA 701, 2015), also known as the "small scale" test, describes a procedure in which the specimen is weighed before and after application of the flame. A fabric passes or fails, based upon the average percentage of mass lost by the 10 specimens tested, with an allowance based on the calculated standard deviation.

8.2.1.4 After-flame time and afterglow duration

During a flame test of a fabric, after-flame and afterglow are important. These describe a fabric's capacity to prevent the propagation of a flame to other elements in a fire

Table 8.1 Tearing force applied prior to damaged length measurement

CAN/ULC S109	Material mass (g/m^2)	68–200	200–510	510–780	>780
	Mass applied (g)	110	230	340	450
ASTM D 6413	Material mass (g/m^2)	68–203	203–508	508–780	>780
	Mass applied (g)	100	200	300	475
CAN/CGSB 4.2 No 27.10	Material mass (g/m^2)	Up to 100	100–200	200–330	>330
	Mass applied (g)	57	113	227	340
IMO A.563(14) (1985)	Material mass (g/m^2)	<200	200–600	>600	
	Mass applied (g)	100	200	400	

situation. Generally, the after-flame time is recorded in seconds and corresponds to the length of the flame's persistance after the applied flame is removed.

The afterglow time (also recorded in seconds) is the duration of continuous incandescence once the after-flame ceased on the fabric surface, or once the source of the flame has been removed.

In fabric specifications, there is usually a maximum allowable after-flame time measured on fabrics during a flame test. On the other hand, there is generally no maximum afterglow time set.

8.2.1.5 Flaming debris, melting, and dripping

During the exposure of a material to heat and/or flame, it is possible for some pieces of the material to fall from the specimen and keep on burning. Another possibility is melting of the material, with or without flame generation. Dripping may also be observed. Definitions and restrictions on dripping may be found in specifications and requirements for personal protective equipment. Some specification tests require the measurement (in seconds) of the duration of the melting debris' flaming, as this behavior is part of the acceptance criteria.

8.2.2 Barrier effect: Thermal protective performance, skin burn injury

Protecting workers in various environments is of great importance. This has led to the development of a series of standard test methods to evaluate heat penetration through layers of textile materials. Most of these standard test methods are based on the Stoll and Chianta study (Stoll & Chianta, 1969).

Their work is based on the observation of the relationship between the intensity of heat applied to human subjects' skin and the duration of exposure necessary to create a second-degree burn. The aim of their study was to develop a simple laboratory procedure that provided a rating system for protective fabrics. If the study was based on time-to-pain and heat exposure corresponding to time-to-pain, the resulting standard test methods specifically indicate that the evaluations do not give an estimate of second-degree burn risk.

The result of the work of Stoll and Chianta is largely used in standard test methods, such as ASTM F2700 (2008) or ASTM F 2703 (2008), aimed at evaluating the protection performance of materials against heat and flame. It is also used in standard performance specifications such as NFPA 1971 (2013), NFPA 2112 (2012), etc.

8.2.3 Opacity of smoke

For some applications, the opacity of a burning material's smoke is a critical characteristic. This evaluation consists in causing a material to combust, with or without flame exposure, and evaluating the smoke's opacity by optical measurement in a closed chamber. Usually, a spectrophotometer (ASTM E662, 2017) or a laser beam (ASTM E1354, 2017) are used to measure smoke obscuration in real time during the testing procedure.

8.2.4 Flame propagation

In terms of flame propagation, various test methods have been developed depending upon the main end use of the tested material. For instance, the FMVSS 302 (2011) Standard measures the burn rate according to the distance traveled by the flame on a horizontal specimen exposed to a flame. The result is given in inches per minute.

The standard ASTM E162 (2015) defines the flame spread index as the product of the heat increase by the flame propagation of a burning material. The value reported has no unit.

ASTM E648 (2017) is designed to evaluate the flame properties of flooring materials. It defines the Critical Radiant Flux as the distance after which a flame-out of the specimen is observed, converted in watts per square centimeter using the heat flux profile of the test calibration.

8.2.5 Heat release rate; toxicity of gases

Caloric content is another flammability property which is relevant for some applications. For instance, in the rail industry, the effective heat of combustion, or total heat release rate, is used to evaluate the overall caloric content of mass transportation systems. Mainly used for solid materials such as composite products, it may also apply to flooring textile materials, upholstery assemblies, and mattresses. Usually, an oxygen consumption calorimeter is used to determine the effective heat of consumption, for specific testing conditions (16 CFR 1633, 2006; ASTM E1354, 2017).

8.3 Testing the flammability of fabrics

Various test procedures have been developed over time to measure fabric behavior when exposed to heat and flame. This section presents different sources of ignition typically used to evaluate textile materials' flame resistance, as well as procedures for small-size and garment specimen testing.

8.3.1 Sources of ignition

8.3.1.1 Flame ignition

Flame ignition appears to be the simplest way to evaluate the flaming behavior of textile materials. Different burners may be used, with specific gas mixes and different pressures.

Flame ignition is usually provided using a burner tube such as a Bunsen burner (CAN/ULC S-109, 2014), a Meker burner (NFPA 701 test method 1, 2015), or other tubes. The fuel is usually a gas such as propane (CAN/CGSB 4.2 No 27.10, 2011; ISO 6940, 2004) or butane (ASTM D1230, 2010; CAN/CGSB 4.2 No 27.5, 2008). Great care should be taken in the preparation of the flame using these burners. For instance, the adjustment of a Bunsen burner may vary from one operator to another. Most standard test methods precisely describe how to adjust the burner to obtain the proper flame size, but the procedure description may be less explicit in some test methods.

When the test flame is applied onto the specimen at an angle, the procedure usually involves adjusting the flame length when the burner is vertical, then tilting the burner to the prescribed test angle, for instance 30 degrees or horizontally (CAN/CGSB4.2 No 27.10, 2000; ISO 6940, 2004), before exposing the specimen to the flame.

8.3.1.2 Radiant heat

Radiant heat is a source of heat mainly used in textile flammability testing for evaluating resistance to heat penetration. The radiant heat source is commonly built with a bank of five infrared 500 W quartz tubes (ASTM F1939-08, 2015; ASTM F2702, 2015) or six silicon carbide tubes (ISO 6942, 2002). For these methods, the heat source is oriented vertically, with the specimen to be tested facing the tubes, and the thermal sensor placed on the back of the textile material. The intensity of the radiant heat source is provided in the test methods and can be either 21 or 84 kW/m^2.

For the smoke density test described in ASTM E662 (2017), the radiant source is an electrically powered furnace with a 7.6 cm internal diameter. It delivers 2.5 W/cm^2 of radiant heat to the specimen.

For the measurement of the heat release rates and effective heat of combustion using the cone calorimeter (ASTM E1354, 2017), a radiant heat source is used, coupled with an electric spark igniter to induce the flaming of the material. For this test method, the standard heat flux to be used is 50kW/m^2.

8.3.1.3 Combination of flame and radiant heat

To evaluate the protection offered by textile materials for specific end uses, such as firefighter suit composite materials, standard test methods have been developed to measure the resistance to heat penetration under combined flame and radiant exposure. Originally called thermal protection performance (TPP), and now more properly named Heat Transfer Performance (HTP), this test is described in the standards ASTM F2700 (2008) and ISO 17492 (2003). The combination of radiant heat and flame is produced by a bank of quartz tubes for the pure radiant heat component, and two Meker burners are placed at a specific angle for the conductive heat part. The objective is to get access to both the heat and flame response of textile materials when they are exposed to a 50% convective heat/50% radiant heat, simulating a real fire situation.

8.3.1.4 Contact heat

Another source of heat used for testing purposes is a hotplate directly placed in contact with the textile material (ASTM F1060, 2008). For this test method, the heat source is a hotplate at a controlled temperature prescribed by the end user or the specification. For instance, it is 280°C in NFPA 1971 (2013). The specimen is pressed against the hot plate, with a thermal sensor on the back recording the energy transfer through the material associated with a temperature rise.

8.3.1.5 Cigarette ignition

Cigarette ignition is measured using standard test methods for specific applications, usually upholstery materials or bedding products. For instance, the standard ASTM

E1353 (2016) describes various test procedures to evaluate fabrics' resistance to a smoldering cigarette exposure. For this purpose, a standard cigarette is used with specific properties in terms of length, weight, and smoldering rate. Such cigarettes are identified as Standard Reference Materials (SRM). They are available at the National Institute of Standards and Technology (NIST). The use of SRM is of practical interest, considering the great variety of cigarettes available on the market and the variations in characteristics that may occur over time.

8.3.1.6 Electric arc

Electrical workers are potentially exposed to another source of heat which is generated by an electric arc. To evaluate the protection performance of fabrics used for this type of professional activity, test methods were specifically developed. The principle is to expose the face of a fabric to the energy generated by an electric arc. The standard test method ASTM F1959 (2014) describes the equipment and procedure used to evaluate the protection level of flame-resistant fabrics intended to be used for workers potentially exposed to electric arcs from 84 to 25,120 kW/m^2.

Using a high-current energy source, three specimens are exposed simultaneously to an electric arc of variable duration. Based on the Stoll and Chianta predictive curve for second-degree burn injury, the laboratory statistically evaluates a minimum of 21 fabric specimens.

In this standard, the arc thermal protective value (ATPV) is defined as the incident energy in kW/m^2 required to create a 50% probability of a second-degree burn using the Stoll and Chianta burn injury curve.

Another result of importance in this test method is the breakopen threshold energy that represents the incident energy associated with a 50% probability of generating one or more holes in the fabric.

8.3.1.7 Molten substances

Molten substances are another important source of heat for professional activities. This is a crucial hazard for both welding and the foundry industry. For instance, ASTM F955 (2015) describes a procedure and quantity of molten metal to pour on the surface of a protective fabric to evaluate the heat increase on the back side of the material. For this test, the heat source is 1000 g of molten substance that can be iron at a minimum temperature of 1538°C, aluminum (minimum of 760°C), or brass (minimum of 1149°C).

The test method ISO 9150 (1988) used for the specification ISO 11611 (2015) describes a procedure to evaluate the number of small splashes of molten metal necessary to generate a 40 K heat increase on the back of a protective fabric intended to be used for welding activities.

8.3.2 Small-size specimen testing

Small-size specimen testing is convenient from a laboratory point of view because of the small size of the equipment required. It is also of interest for fabric manufacturers who wish to test prototype materials and samples with low availability.

Specimens are cut from the material using specific procedures: they are usually distributed diagonally to avoid having the same yarn used in each test specimen. The number of specimens varies depending on the test method used. As an example, CAN/ULC S109 (2014) specifies that two specimens are cut along the width and two specimens along the length for large-scale testing in the fold configuration, while ASTM F1959 (2014) may require testing a minimum of 21 specimens to perform the statistical evaluation. The usual number of specimens tested is five along the length and five along the width of the fabric.

For most of the test methods, the specimens are placed either horizontally or vertically. Some standards require other specimen orientations such as a 45-degree angle (16 CFR 1610, 2009; CAN/CGSB 4.2 No 27.5, 2008). These two test methods are designed to evaluate the performance of general clothing textiles. The flame is applied to the surface of a material for 1 second.

When a specification requires washing of specimens prior to testing, they are washed prior to cutting the specimen in order to allow for any potential shrinkage.

8.3.3 Garment flame test

If small-specimen size tests can help evaluate the fabrics' ignitability and the protection they offer against heat and/or flame, it may be necessary to estimate the fire response on a 3D shape form, using an instrumented manikin dressed with a garment made of the fabric. This allows the assessment of fabric behaviors such as shrinkage during exposure, heat accumulation and transfer through a garment's sublayers. Other potential risks due to seam placement, closure systems (zippers, buttons, hooks, loops, etc.), emblems, and identification patches covering garments are difficult to evaluate with a small specimen test and are more easily evaluated at the garment level.

8.3.3.1 Hydrocarbon flash fire

Two test methods have been developed for evaluating fabrics or garments for protection against hydrocarbon flash fire: ISO 13506 (2008), which is referred to as an optional test in the specifications EN 469 (2006) and ISO 11612 (2008), and ASTM F1930 (2017) which is requested by the specification NFPA 2112 (2012). The principle of these tests is to evaluate the fire response of a full garment with a standardized shape and form when placed on a 1.80 m tall male manikin (the size and shape of a female manikin have not been established yet for this test).

For this purpose, a particular garment design is described in the test method ASTM F1930 (2017). The garment is a coverall with no pant cuffs nor pockets, one full-length metal zipper in the front, and specific fit allowances for the thermal manikin on which it is tested.

In the NFPA 2112 (2012) specification, the test is to be performed following ASTM F1930 (2017), with the standard garment exposed to a heat flux of 84 kW/m^2 for 3 seconds. The garment is worn over an underwear made of 100% cotton.

For the specifications EN 469 (2006) and ISO 11612 (2008), the flash fire test is optional and performed following the ISO 13506 (2008) test method. A 4-second exposure at 84 kW/m^2 is suggested, but it may go up to 8 seconds for multilayer assemblies.

8.3.3.2 Electric arc safety

Specific work activities involving a risk of exposure to electric arcs require evaluation of personal protective equipment particularly designed for such use.

The standard test method ASTM F887 (2016) covers requirements for climbing equipment. It includes a test method to evaluate the ability of harnesses and lanyards to keep the worker safe after exposure to a standard electric arc. For that purpose, harnesses and lanyards are exposed to an electric arc as per the standard ASTM F1958 (2012) using a manikin. Three specimens for lanyards or four specimens for harnesses on the front and the same mount of specimens are exposed on the back. The requirements are no electric arc ignition, no after-flame greater than 5 seconds, no melting or dripping. In addition, the harness/lanyard should pass the drop test after the electric arc exposure.

Another document provides guidelines to evaluate finished garments when exposed to an electrical arc: ASTM F2621 (2012). This provides a procedure for evaluating the design performance of protective garments, replicating incident behavior, and verifying the performance of used garments. The test is performed at the electric arc incident energy level obtained from a material initial evaluation test (see ASTM F 1959 (2014) in Section 8.3.1).

8.4 Test methods for fire-resistant fabrics

8.4.1 Personal protective equipment

8.4.1.1 Flammability tests

Fabrics for personal protective equipment are an important part of textile flammability testing.

The standard test method ASTM D6413 (2015) is used in most of the specifications for fire and heat protection in North America. For this test, the specimen is secured in a vertical position. The flame is applied at the bottom of the specimen for a period of 12 seconds. After removal of the flame, the after-flame and afterglow time are recorded. Then the specimen is removed from the specimen holder, a dead weight is applied to one end of the specimen, and the damaged length is measured (see Section 8.2.1.2). A total of 10 specimens are tested: five in the fabric length direction and five in the fabric width direction. Each specimen measures 300 mm by 76 mm. The specimens are tested after being conditioned in the standard atmosphere for textile testing as per ASTM D1776 (2116), that is, in a 21°C and 65% relative humidity environment. The burner is a tube with a 10-mm inner diameter and a pilot flame tube beside the main burner. This equipment is based on a modified Bunsen burner or a Tirril burner. The distance between the burner and the specimen is 19 mm. The gas used is 99% pure methane delivered at a 17.2 kPa pressure at the burner inlet. The flame length has to be 38 mm. The average damaged length and average after-flame time determine whether a fabric passes or fails specifications for this standard test method. Most of the time, the afterglow time is not considered part of the acceptance criteria.

Another standard used in North America is CAN/CGSB 4.2 No 27.10 (2000). This test, which is based on the international standard ISO 6940 (2004), is also a flame test with vertically oriented specimens. Two positions of the burner are proposed: horizontal while facing the specimen, and at a 30 degree angle with the flame underneath the bottom edge of the specimen. This last option is the one generally requested in performance specifications using this test method. The flame is applied at the bottom edge of the vertically oriented specimen. The duration of the flame's application is 12 seconds. After removal of the flame, the after-flame time and afterglow time are recorded. Then the specimen is removed from the specimen holder, a dead weight is applied to one end of the specimen, and the damaged length is measured (see Section 8.2.1.2). Ten specimens are tested: five in the fabric length direction and five in the fabric width direction. Each specimen measures 200 mm by 80 mm. The specimens are tested after being dried in an oven at 105°C for 1 hour then cooled in a desiccator for a minimum of 30 minutes. It is crucial in this procedure that any humidity that may be contained in the textile materials be removed prior to the flame test. The burner is of a design specifically described in the test method and uses commercial grade propane gas. The flame length is adjusted when the burner is vertically oriented and has to be 40 mm long. During the 30 degree angle test, the distance between the burner and the bottom edge of the specimen is 20 mm.

The standard test method ISO 15025 (2016) is used for flame-resistant fabrics included in protective apparel as described in the ISO 11612 (2008) performance specification. Three specimens in the length and three specimens in the width direction of the fabric are tested. Each specimen is 200 mm × 160 mm. They are tested after being conditioned in a standard atmosphere of 20°C and 65% relative humidity. Two options are available for this test: the burner may be placed horizontally for the surface ignition test, or at a 30-degree angle from the vertical for the edge test. For both options, the flame is applied for 10 seconds. The gas used is a commercial grade of propane, butane, or a mixture of the two. In the ISO 11612 (2008) specification, the criteria associated with procedure A (surface ignition) for an A1 classification are the absence of any flame spread to the vertical edges or the upper edge of each specimen, no flaming or molten debris for each specimen, after-flame time and afterglow time below 2 seconds, and no formation of a hole greater than 5 mm. Procedure B (edge ignition) can be added to a material performance evaluation for an A2 classification as described by ISO 11612 (2008). The performance criteria are similar to those described for the A1 classification except for the hole formation that is not applicable for such a test configuration.

Flame impingement (or ignitability) is also a property relevant for products used in situations where the primary protection concern is not flame resistance. For instance, the specification ANSI/ISEA 105 (2016) relative to the performance evaluation of gloves refers to the standard test method ASTM F1358 (2016) to evaluate the ignition resistance of safety gloves. According to this test method, a fabric specimen is folded in half. A flame is applied at the fold location. The burner and flame parameters are the same as for the ASTM D6413 (2015) test method described above. However, this procedure differs in terms of specimen preparation and flame application. In ASTM F1358 (2016), the flame is applied on the folded edge of the specimen for a 3-second

period; it is recorded if flaming occurs. If there is no flaming, the same specimen is subjected to a 12-second exposure. When flaming occurs, the after-flame and afterglow time are recorded. Then the burned length is measured on the specimen pressed flat. A total of 10 specimens are tested, 5 in the length direction and 5 in the width direction of the fabric. Five levels of performance in terms of ignition and burning resistance are defined in ANSI/ISEA 105 (2016). Level 0 corresponds to an after-flame time equal to/lower than 2 seconds, while Level 5 corresponds to no flaming at either the 3- or the 12-second flame exposure.

8.4.1.2 Thermal protective performance tests

One important aspect of personal protective equipment is thermal protective performance. For such an evaluation, there are typically three different test options: radiant heat exposure (ASTM F1939-08, 2015; ISO 6942, 2002), convective heat exposure (using direct flame such as in CAN/CGSB 4.2 No 78.1, 2001), and a combination of both radiant heat and flame exposure (ASTM F2700, 2008; ASTM F2703, 2008; ISO 17492, 2003). The main principle of these tests is to apply a heat source (which is generated using the different energy sources) on one side of a fabric, and measuring the temperature rise over time on the other side of the fabric. The endpoint criteria depend on the test method and historical approach for the protective evaluation of fabrics. It can be either a comparison with the Stoll curve for second-degree burn empirical data, or the total energy required to generate a temperature rise of 12°C or 24°C (according to HTI-Heat Transfer Index in ISO 17492, 2003).

8.4.2 Fabrics for the transportation industry: Automotive, railroad, aviation

8.4.2.1 Automotive

The standard specification FMVSS 302 (2011) is mandatory for automotive interior materials; it includes the test procedure and a performance requirement. This requirement is valid for multiple elements in the vehicle interior, for example, seat cushions, seat back, seat belts, flooring materials, headliner, engine compartment covers, etc.

The FMVSS 302 (2011) standard test method was originally published in the early 1970s and has not been significantly updated since then. It is applicable to materials in passenger cars, multipurpose passenger vehicles, trucks, and buses. The principle is to apply a 1.5-in. long natural gas flame to one end of a specimen, which is placed horizontally in a closed cabinet. The specimen is 4 by 14 in. in dimension and may be a single layer or a composite material depending on its physical end use in the vehicle interior. The flame is applied for 15 seconds. Performance is based on a horizontal burn rate: either the flame self-extinguishes before reaching a timing zone, or the burn rate within this timing zone is less than 4 in. per minute.

Different variations of this standard have been put in place by car manufacturers. They include, for instance, accelerated aging such as exposure to 80°C and 100°C, up to 100 hour, applied prior to flame testing.

8.4.2.2 Railroad

In North America, the NFPA 130 (2017) specification is applicable to railroad materials. This document establishes a test list and performance criteria for fire safety. Textile materials are covered in "Chapter 8—Vehicles" of the NFPA 130 (2017) standard, among other products.

In this specification, floor coverings have to be evaluated for smoke density generated by burning materials per ASTM E662 (2017), and for critical radiant flux at extinguishment per ASTM E648 (2017). Carpeting materials that are used in wall or ceiling coverings have to be evaluated to ASTM E162 (2015) and ASTM E662 (2017), with their own specific requirements (paragraph 8.4.1.11 of NFPA 130, 2017). Other textile materials such as seat upholstery, curtains, draperies, and woven seat cover suspensions are evaluated per 14 CFR 25 (2012) in Appendix F Part I (vertical test), and per ASTM E662 (2017).

The smoke density generated by burning materials is tested per ASTM E662 (2017). The specimen is 3 by 3 in. in dimension, with a maximum thickness of 1 in. The principle of the test is to measure the opacity of the smoke formed when the material is exposed to radiant heat, with and without flaming impingement. The test is performed in a closed chamber in which a spectrophotometer is installed. The light source is on the floor of the chamber, and the photoreceptor is on the ceiling.

The material is placed in front of a furnace generating a radiant heat of 2.5 W/cm^2. Two variations of the test have to be performed for a complete evaluation: nonflaming mode and flaming mode. The flaming mode variation is performed with an extra burner assembly in front of the specimen to generate a potential ignition. The burner is made of a six-tube assembly and is fuelled with propane gas. The flame is applied to the bottom part of the specimen.

During the material's combustion, the photoreceptor records the intensity over time of the light transmitted through the smoke generated by the burning material, for a maximum of 20 minutes. At the end of the test, a correction of the smoke opacity measured is performed by measuring the light transmittance after all the smoke is removed from the test chamber to access the "clear beam" value, taking into account soot deposited in the optical path. The report indicates the optical density measured at any time (usual practice considers 1.5-minute and 4-minute tests [Ds1.5 and Ds4]) and the maximum optical density (Dm) with the corrected maximum optical density (Dm corrected).

The critical radiant flux at extinguishment is measured with ASTM E648 (2017) using a radiant panel placed at a 30-degree angle from the horizontal over a 1 m-long specimen. The test chamber has a radiant flux profile ranging from 1 to 0.1 W/cm^2. The test begins when the specimen is ignited by a burner at the highest heat flux location. The speed of the flame front is measured visually over time, and the distance at self-extinguishment is combined with the heat flux profile to provide the critical heat flux at extinguishment.

The radiant spread index of carpeting materials covering walls and ceilings measured with ASTM E162 (2015) uses a similar radiant panel, but with a vertical orientation. The radiant panel is fuelled with an air-gas mixture to obtain a radiant output

equivalent to 670°C. The specimen, measuring 6 by 18 in., faces the radiant panel at a 30-degree angle from the vertical and is ignited by an acetylene torch placed at the top edge of the specimen closest to the radiant panel. If ignition occurs, the flame front moves down to the bottom edge of the specimen. The speed of this flame front is recorded while the heat generated by the exposed sample is measured with eight thermocouples placed in a stack over the specimen. A total of four specimens are tested. The radiant panel index is the product of the flame spread factor and the heat evolution factor.

The vertical flame test as per 14 CFR 25 (2012, Appendix F Part I) is a standard test method also found in the airworthiness directive. The principle of this test is to evaluate the flame resistance of textile materials when exposed to a Bunsen burner flame for a 12-second period. The specimen, 3×12 in. in dimension, is exposed to the flame, and observations are made concerning the after-flame and drip-burn time. In NFPA 130 (2017), the requirement is based on the burned length and after-flame time only.

It is important to note that when materials are cleanable, there are usually requirements to evaluate the flame resistance after they have been subjected to standard washing and/or dry cleaning processes. The number of cycles for such cleanings depends on the performance criterion expected within the standard. For instance, NFPA 130 (2017) refers to the washing instructions described in ASTM E2061 (2015) Annex A1 that suggests cleaning procedures for hand washing, machine washing, and dry cleaning.

8.4.2.3 Aviation

For aircraft materials that need to be evaluated for flame resistance, the main standards have been developed by the Federal Aviation Association and are published under the Federal Aviation Regulation documents FAR 25.853 (1986). Various tests apply depending on the material's location in the aircraft and its end use. For instance, fabric materials intended to be used in crew and passengers' areas, including floor coverings, draperies and upholstery fabrics, seat cushions, padding, and coated fabrics are tested for vertical flame resistance, with a 12-second flame impingement. A 60-second flame impingement test exists also for materials intended to be used in the cargo and baggage compartments not occupied by crew or passengers. The principle of the test is the same in both situations: a Bunsen or Tirrill burner is located 19 mm underneath the vertically oriented specimen, with a flame that is 38 mm long with a minimum temperature of 843°C in the center. After the 12-second or the 60-second flame application, the burner is removed and the after-flame time is recorded. During the test, the occurrence of dripping has to be noted and the flaming duration of drips after they fall on the cabinet floor is recorded. Depending on the material location in the aircraft, the criterion for burned length varies between 6 and 8 in., the after-flame time is 15 seconds at most, and the dripping flaming ranges between 3 and 5 seconds.

In addition to these tests and requirements, other parts of the aircraft such as the cargo or baggage compartments may have liners or floor panels that must meet the burn criteria with a 45-degree angle flame test. This procedure is also based on a small-size specimen, placed at a 45-degree angle. The burner, which is the same as for the vertical test, is placed underneath in the middle of the specimen, 25 mm away

from its exposed surface. The flame is applied for 30 seconds, and then the burner moved at least 3 in. from the specimen holder. The after-flame time and afterglow time are recorded for each specimen; the burn-through evaluation is performed by visual observation for each specimen during the flame application.

In addition to small-size specimen tests, a specific flammability test exists for evaluating an entire set of seat cushions in an intense fire. The oil burner test for seat cushions is designed to evaluate the flame propagation and weight loss of the seat cushion system. The typical seat cushion includes a central cushioning foam or foam assembly, a fire blocker to prevent the flame from penetrating the foam elements, and an upholstery textile. The principle of this test is to create a mock-up of a seat using a production seat cushion and back cushion with the production seams and closure system. The assembly is precisely weighed and placed in the test position. Then, a specific burner fuelled with kerosene or fuel oil (with a regulator set to deliver 2 gal. per hour, providing a heat flux of 11.9 W/cm^2) is used to expose the specimen to an open flame for 2 minutes. Then a period of self-extinguishment over a maximum of 5 minutes is observed. Immediately after that period has elapsed, the specimen is removed and weighed again. Then, the burned length is measured to evaluate the propagation of the damage due to the flame along the materials. The performance criteria are based on the average burned length (maximum 17 in.) and average weight loss (maximum 10%), with a requirement that two-thirds of the total number of specimens meet each of these criteria.

Other textile materials such as insulation blankets and covers used for the protection of cargo elements, and thermal and acoustic liners used within the pressurized part of the aircraft have their own test criteria in terms of flammability.

8.4.3 Flooring materials

Flooring materials, including textile carpeting, can be evaluated for flame resistance in various ways. For instance, the code of federal regulation in the United States describes two standard performance specifications; 16 CFR 1630 (2006) is designed for all types of carpet and rugs where one dimension is greater than 6 ft and the surface area is greater than 24 ft^2, while 16 CFR 1631 (2006) is used for smaller carpets and rugs.

The principle of these two tests is based on flame propagation observed using a standard methenamine tablet that is ignited on the surface of a 9×9-in. specimen. After the methenamine tablet is ignited, flame propagation may occur along the surface of the material. A circular frame placed over the specimen serves as a guideline to measure how far the flame propagates from the center position of the methenamine tablet. The measurement is taken along the radius. According to 16 CFR 1630 (2006), the distance from the outer edge of the frame to the burned area has to be a minimum of 1 in. A total of eight specimens are tested, and a maximum of one specimen may fail to meet the criterion. Before testing, each specimen is dried in an oven at 105°C and then cooled in a desiccator.

If a carpet or rug has a flame-retardant treatment, or if the fibers used for the manufacture of this carpet and rug received a flame-retardant treatment, the material must

be washed 10 times per AATCC TM 124 (2014) before the flame test may be performed. This test method describes the equipment and procedure to perform washings and dryings of textile materials under standard conditions.

The standard ASTM D2859 (2016) is similar to 16 CFR 1630 and 16 CFR 1631 and is used as a reference in the life safety code NFPA 101 (2015).

Another test for flooring materials used for public buildings is ASTM E648 (2017). It is referred to in NFPA 254 (2015) on the critical radiant flux for floor-covering systems (see Section 8.4.2.2 on Railroad). This test is also used by NFPA 101 (2015) with specific requirements: the minimum critical radiant flux (CRF) should be 0.1 W/cm^2; with Class I materials having a minimum CRF of 0.45 W/cm^2 and Class II materials a CRF between 0.22 and 0.45 W/cm^2.

The standard test method CAN/ULC S102.2 (2010) is used for evaluating flooring materials using a tunnel test. The specimen covers the floor of a tunnel which has a 450-mm width and a 300-mm depth. The test chamber (which corresponds to the length of the inner part of the tunnel itself) is 7600 mm. The flooring material is placed on the floor of the test chamber. One end of the tunnel is equipped with a burner designed to ignite the surface of the specimen. An opening for air supply is found at this end of the tunnel. The flame propagation along the specimen is recorded as well as the temperature increase during the test. The smoke obscuration is measured with a photoreceptor and a light source across the exhaust part of the tunnel, between 4.8 and 12 m from the tunnel end. The measurements obtained from this test are the Smoke Developed Value (SDV) and the Flame Spread Value (FSV).

8.4.4 Drapes/curtains/window shades

In North America, two main test methods are used for window shades: NFPA 701 (2015) and CAN/ULC S109 (2014). They both include a small-size and a large-size specimen test, also known as the small-scale and large-scale tests.

For CAN/ULC S109 (2014), the small-flame test is performed using a Bunsen burner placed underneath the vertically oriented specimen. The Bunsen burner is positioned at a 25-degree angle from the vertical. The flame is generated by methane or natural gas, and must have a length of 40 mm. The flame is applied for 12 seconds on the bottom edge of the specimen with a distance of 20 mm from the top opening of the burner. Five specimens per direction of material are tested for the statistical evaluation (for a total of 10 specimens). The occurrence of flaming debris and the duration of this flaming are recorded for the compliance criterion; a maximum of 2 seconds is allowed. The damaged length is measured with a dead weight to confirm the burned area: a maximum of 165 mm is allowed on average, with no specimen having a damaged length larger than 190 mm.

Test method 1 of NFPA 701 (2015) (formerly the small-scale test) is performed on a vertically oriented specimen with a Meker burner positioned horizontally to have the flame facing the surface of the specimen. The burner is fuelled with methane gas at 17.5 kPa, generating an intense 100 mm long blue flame when the burner is vertically placed. The flame is applied on the specimen for 45 seconds. Ten specimens cut in the length direction of the material are tested for the statistical evaluation. Flaming

debris is observed after falling on the bottom of the test chamber for the duration of the flaming. In addition, the tested specimen is weighed before and after flame exposure; weight loss is determined for acceptance criteria. Falling debris must not continue to burn for an average of 2 seconds, and weight loss must be 40% or less.

A large-flame test is also described in both test methods. For CAN/ULC S109 (2014), the specimen is 750–2100 mm long. It is hung in a test chamber with a Bunsen burner placed at a 25-degree angle from the vertical. The flame is generated by methane or natural gas at a pressure of 1.06 kPa; the burner is set to create a 280 mm long oxidizing flame. The flame is applied for 120 seconds with a distance of 100 mm between the top of the burner and the bottom edge of the specimen. The vertical axis of the flame is perpendicular to the vertical plane of the specimen. Depending on the material's stiffness, two configurations may apply: a folded configuration for soft products (two specimens per direction tested), and a flat configuration for materials that can hardly be folded (five specimens per direction). Eventual flaming debris is observed and the duration of its flaming is recorded for compliance criterion; a maximum of 2 seconds is allowed. The damaged length is measured by visual observation and compared to its original condition, after discarding soot deposit. The criterion for acceptance is a burned length that doesn't exceed 635 mm from the top of the test flame during the flame application for folded materials, or 250 mm for the flat configuration.

The test method 2 of NFPA 701 (2015) (large-scale test) is performed using the same type of test chamber. A Bunsen burner is used with a 25-degree angle from the vertical and placed in a way that the vertical axis of the flame is parallel to the vertical plan of the specimen. The flame is 280 mm long and applied for 120 seconds. During the test, flaming debris is recorded for flame duration of dripping materials. After-flame time is recorded after the burner has been removed from the bottom edge of the specimen. The burned length is measured after the test is completed. Depending on the material's stiffness, two configurations may also apply: a folded configuration for soft products (4 specimens tested), and a flat configuration for materials that can hardly be folded (10 specimens cut from the length direction). The criterion for burned length is a maximum of 1050 mm for the folded configuration and a maximum of 435 mm for the flat configuration. Flaming debris must not continue to burn after 2 seconds, and the after-flame time is also a maximum of 2 seconds. Retests are possible within the NFPA 701 test methods 1 and 2 in the case of some particular specimen behavior.

Depending on the manufacturer's claims regarding the durability of the flame resistance performance, aging treatments may be applied prior to flame testing. For NFPA 701 (2015), the aging procedures include three dry cleanings using conventional commercial dry cleaning, five laundering cycles per AATCC TM 124 (2014), and water leaching during a minimum of 72 hours for products intended to be used outdoors.

When testing is performed as per CAN/ULC S109 (2014), aging procedures include 10 cycles of laundering (per CAN/CGSB 4.2 No 24, 2002), 10 cycles of commercial dry cleaning, water leaching with 300 strokes of scrubbing with a stiff bristle brush on each side of the fabric, and 360 hours of accelerated UV aging with a carbon-arc or a xenon-arc (ASTM G155, 2013, cycle 7) weathering machine including water spray.

8.4.5 Home furnishings

Upholstery fabrics and components of upholstered furniture are evaluated using a mock-up assembly. The standard test method ASTM E1353 (2016) gives some test procedures to evaluate various components of furniture. It originates from the UFAC classification fabric test method 1990 (UFAC, 1990). This test is based on a mini mock-up assembly and a decking material tester. The main objective is to be able to access the individual behavior of the various components of a furniture assembly using the same mock-up set-up and standard materials. For instance, the cover fabric test is designed to measure the ignition characteristics of the tested fabric over standard polyurethane foam. Then, the ignitability of the interior fabric is tested using standard polyurethane foam and a standard cover fabric. The same concept applies to welt cord, filling and padding components, and barrier materials. For each mock-up configuration, the ignition source is a standard cigarette with a specific smoldering rate.

For the California Technical Bulletin 117 (CTB 117, 2013), the ignition source is a standard reference material that is obtained from NIST (SRM 1196). It uses the same testing configuration as the standard specification NFPA 260 (2013). The Technical Bulletin 117 standard test method and requirements are based on ASTM E1353 (2016), with additional requirements.

8.4.6 Mattresses

The flammability of mattresses is a safety concern in both homes and institutional care facilities. In the United States, the Code of Federal Regulation 16 CFR 1632 (2014) describes a test procedure to be performed with prototypes and provides performance criteria for materials used for mattress manufacturing. The method applies to mattresses, mattress pads, and ticking materials. The main objective is to evaluate resistance to smoldering cigarettes placed all over the mattress. The test is divided into two parts. The bare mattress test consists in placing a set of 9 lit cigarettes over the surface of a bare mattress. The two sheets test consists in placing a set of 9 lit cigarettes on a portion of a mattress covered with a standard bed sheet material, and cover these cigarettes with the same bed sheet. The same type of observation is performed in both cases: the maximum char length from the cigarette has to be a maximum of 2 in., and no ignition may occur during the test.

Another method using an entire mattress is described in 16 CFR 1633 (2006). It uses two gas burners placed on the edge and over the mattress as an ignition source. The principle is to have a full mattress on a bed frame burning freely to measure its heat release rate. The mattress is placed under a hood equipped with an oxygen consumption calorimetry system to calculate the heat release rate. The requirements corresponding to this specification are that, at any moment, the peak of heat released should not be more than 200 kW during the 30-minute test and the total heat release shall not be more than 15 MJ during the first 10 minutes of the test.

8.5 Future trends

With the variety of tests being developed over time based on specific activities, there are a large number of standard test methods with small variations among them. Standardization bodies tend to harmonize these standard test methods to facilitate innovation, promote better market access for manufacturers, and potentially reduce cost for end users.

In addition, new technologies would be helpful in terms of laboratory equipment and test procedures to reduce specimen size and facilitate interpretation of the burning behaviors of textile materials. For instance, the microscale combustion calorimetry test such as the one described in ASTM D7309 (2013) may offer better understanding of the specific burning behavior of textiles using small-size specimens.

Finally, fire-retardant chemicals applied to textile materials to enhance their flame resistance performance are suspected to have potential side effects on human health and the environment. The development of inherently flame-resistant fibers or flame-retardant treatments which are more health- and environment-friendly is a potentially promising avenue of research.

8.6 Conclusion

Many test methods and performance criteria are available to evaluate the flame resistance of textile materials based on the nature of the products and their end use. It is important for textile specialists to identify the proper regulations that may apply to their product. The main difficulty is that regulations may be issued by countries, states, municipalities, or professional corporations.

When textile development is involved, the right specification has to be identified at the beginning of the project to guide the evaluation of the performance during the development process.

8.7 Sources of further information and advice

- The Canada Consumer Safety Act dictates the state regulation regarding flammability of textile materials (http://laws-lois.justice.gc.ca/eng/acts/C-1.68/).
- Health Canada website lists the reference documents for flammability testing on various consumer products (http://www.hc-sc.gc.ca/cps-spc/prod-test-essai/method-inflammab-eng.php).
- Canadian test methods for flammability, including specifications are developed by the Canadian General Standard Board, under the Public Services and Procurement of Canada (https://www.tpsgc-pwgsc.gc.ca/ongc-cgsb/programme-program/normes-standards/index-eng.html).
- For regulation information on consumer products, the US Consumer Product Safety Commission is a good reference where information regarding flammability requirements is described (https://www.cpsc.gov).

- The American Society for Testing and Materials has a specific committee ASTM E05 to work on Fire Standards (not only for textile materials), see references below (https://www.astm.org/COMMITTEE/E05.htm).
- The American Society for Testing and Materials has a specific committee ASTM F23 to work on Personal Protective Clothing and Equipment that design specification for performance evaluations, using standard test methods (https://www.astm.org/COMMITTEE/F23.htm).
- The American Society for Testing and Materials has a specific committee ASTM F18 to work on Electrical protective equipment for workers (https://www.astm.org/COMMITTEE/F18.htm).
- The International Maritime Organization—Fire Test Procedure code: IMO FTP Code (http://imo.org).

References

14 CFR 25, 2012 14 CFR 25. (2012). *Airworthiness standards: Transport category airplanes*. Code of federal regulation. United States Consumer Product Safety Commission.

16 CFR 1610. (2009). *Standard for the flammability of clothing textiles*. Code of federal regulation. United States Consumer Product Safety Commission.

16 CFR 1630. (2006). *Standard for the surface flammability of carpets and rugs (FF 1-70)*. Code of federal regulation. United States Consumer Product Safety Commission.

16 CFR 1631. (2006). *Standard for the surface flammability of small carpets and rugs (FF 2-70)*. Code of federal regulation. United States Consumer Product Safety Commission.

16 CFR 1632. (2014). *Standard for the flammability of mattresses and mattress pads*. Code of federal regulation. United States Consumer Product Safety Commission.

16 CFR 1633. (2006). *Standard for the flammability (open flame) of mattress sets*. Code of federal regulation. United States Consumer Product Safety Commission.

AATCC TM124. (2014). *Smoothness appearance of fabrics after repeated home laundering*. Research Triangle Park, NC: American Association of Textile Chemists and Colorists.

ANSI/ISEA 105. (2016). *Hand protection classification*. American National Standards Institute.

ASTM D1230-10. (2016). *(e1) Standard test method for flammability of apparel textiles*. West Conshohocken, PA: ASTM International.

ASTM D1776/D1776M. (2016). *Standard practice for conditioning and testing textiles*. West Conshohocken, PA: ASTM International.

ASTM D2859. (2016). *Standard test method for ignition characteristics of finished textile floor covering materials*. West Conshohocken, PA: ASTM International.

ASTM D6413/D6413M. (2015). *Standard test method for flame resistance of textiles (vertical test)*. West Conshohocken, PA: ASTM International.

ASTM D7309. (2013). *Standard test method for determining flammability characteristics of plastics and other solid materials using microscale combustion calorimetry*. West Conshohocken, PA: ASTM International.

ASTM E162. (2015). *Standard test method for surface flammability of materials using a radiant heat energy source*. West Conshohocken, PA: ASTM International.

ASTM E176. (2015). *(ae1), Standard terminology of fire standards*. West Conshohocken, PA: ASTM International.

ASTM E648. (2017). *Standard test method for critical radiant flux of floor-covering systems using a radiant heat energy source*. West Conshohocken, PA: ASTM International.

ASTM E662. (2017). *Standard test method for specific optical density of smoke generated by solid materials*. West Conshohocken, PA: ASTM International.
ASTM E1353. (2016). *Standard test methods for cigarette ignition resistance of components of upholstered furniture*. West Conshohocken, PA: ASTM International.
ASTM E1354. (2017). *Standard test method for heat and visible smoke release rates for materials and products using an oxygen consumption calorimeter*. West Conshohocken, PA: ASTM International.
ASTM E2061. (2015). *Standard guide for fire hazard assessment of rail transportation vehicles*. West Conshohocken, PA: ASTM International.
ASTM F887. (2016). *Standard specifications for personal climbing equipment*. West Conshohocken, PA: ASTM International.
ASTM F955. (2015). *Standard test method for evaluating heat transfer through materials for protective clothing upon contact with molten substances*. West Conshohocken, PA: ASTM International.
ASTM F1060. (2008). *Standard test method for thermal protective performance of materials for protective clothing for hot surface contact*. West Conshohocken, PA: ASTM International.
ASTM F1358. (2016). *Standard test method for effects of flame impingement on materials used in protective clothing not designated primarily for flame resistance*. West Conshohocken, PA: ASTM International.
ASTM F1930. (2017). *Standard test method for evaluation of flame resistant clothing for protection against fire simulations using an instrumented manikin*. West Conshohocken, PA: ASTM International.
ASTM F1939-08. (2015). *Standard test method for radiant heat resistance of flame resistant clothing materials with continuous heating*. West Conshohocken, PA: ASTM International. http://www.astm.org.
ASTM F1958/F1958M. (2012). *Standard test method for determining the ignitability of non-flame-resistant materials for clothing by electric arc exposure method using mannequins*. West Conshohocken, PA: ASTM International.
ASTM F1959/F1959M. (2014). *(e1), Standard test method for determining the arc rating of materials for clothing*. West Conshohocken, PA: ASTM International.
ASTM F2621. (2012). *Standard practice for determining response characteristics and design integrity of arc rated finished products in an electric arc exposure*. West Conshohocken, PA: ASTM International.
ASTM F2700. 2008. (2013). *Standard test method for unsteady-state heat transfer evaluation of flame resistant materials for clothing with continuous heating*. West Conshohocken, PA: ASTM International.
ASTM F2702. (2015). *Standard test method for radiant heat performance of flame resistant clothing materials with burn injury prediction*. West Conshohocken, PA: ASTM International.
ASTM F2703. 2008. (2013). *Standard test method for unsteady-state heat transfer evaluation of flame resistant materials for clothing with burn injury prediction*. West Conshohocken, PA: ASTM International.
ASTM G155. (2013). *Standard practice for operating xenon arc light apparatus for exposure of non-metallic materials*. West Conshohocken, PA: ASTM International.
CAN/CGSB 4.175-2011 Part 1/ISO 4880. (1997). *Burning behaviour of textiles and textile products—Vocabulary*. Canadian General Standards Board.
CAN/CGSB 4.2 No 24. 2002. (2013). *Textile test methods: Colourfastness and dimensional change in commercial laundering*. Canadian General Standards Board.

CAN/CGSB 4.2 No 27.5. (2008). *Textile test methods flame resistance—45° angle test—One-second flame impingement*. Canadian General Standards Board.

CAN/CGSB 4.2 No 27.10-2000. *Textile test methods flame resistance—Vertically oriented textile fabric or fabric assembly test*. Canadian General Standards Board.

CAN/CGSB-4.2 No. 78.1. 2001. (2013). *Textile test methods—Thermal protective performance of materials for clothing*. Canadian General Standards Board.

CAN/ULC-S102.2-10. *Standard method of test for surface burning characteristics of flooring, floor coverings, and miscellaneous materials and assemblies*. Underwriters Laboratories of Canada.

CAN/ULC S109. (2014). *Standard method for flame tests of flame resistant fabrics and films*. Underwriters Laboratories of Canada.

CTB 117. (2013). *Requirements, test procedure and apparatus for testing the smolder resistance of materials used in upholstered furniture, technical bulletin*. Bureau of Electronic & Appliance Repair Home Furnishings & Thermal Insulation 4244 South Market Court, Suite D, Sacramento, CA 95834-1243. www.bearhfti.ca.gov.

EN 469. (2006). *Protective clothing for firefighters—Performance requirements for protective clothing for firefighting*. European Committee for Standardization.

FAR 25.853. (1986). *Airworthiness standards: Transport category airplanes*. United States Department of Transportation, Federal Aviation Administration.

FMVSS 302. (2011). *Flammability of interior materials*. Federal Motor Vehicle Safety, United States Department of Transportation, National Highway Traffic Safety Administration.

IMO A.563(14). (1985). *Amendments to the recommendation on test method for determining the resistance to flame of vertically supported textiles and films (resolution A.471(XII))*. London, UK: International Maritime Organization.

ISO 4880. (1997). *Burning behaviour of textiles and textile products—Vocabulary*. Geneva, CH: International Standard Organisation.

ISO 6940. (2004). *Textile fabrics—Burning behaviour—Determination of ease of ignition of vertically oriented specimens*. Geneva, CH: International Standard Organisation.

ISO 6942. (2002). *Protective clothing—Protection against heat and fire—Method of test: Evaluation of materials and material assemblies when exposed to a source of radiant heat*. Geneva, CH: International Standard Organisation.

ISO 9150. (1988). *Protective clothing—Determination of behaviour of materials on impact of small splashes of molten metal*. Geneva, CH: International Standard Organisation.

ISO 11611. (2015). *Protective clothing for use in welding and allied processes*. Geneva, CH: International Standard Organisation.

ISO 11612. (2008). *Protective clothing—Clothing to protect against heat and flame*. Geneva, CH: International Standard Organisation.

ISO 13506. (2008). *Protective clothing against heat and flame—Test method for complete garments—Prediction of burn injury using an instrumented manikin*. Geneva, CH: International Standard Organisation.

ISO 15025-2016: *Protective clothing—Protection against flame—Method of test for limited flame spread*. Geneva, CH: International Standard Organisation.

ISO 17492. (2003). *Clothing for protection against heat and flame—Determination of heat transmission on exposure to both flame and radiant heat*. Geneva, CH: International Standard Organisation.

NFPA 101. (2015). *Life safety code®*. Quincy, MA: National Fire Protection Association.

NFPA 130. (2017). *Standard for fixed guideway transit and passenger rail systems*. Quincy, MA: National Fire Protection Association.

NFPA 254. (2015). *Standard method of test for critical radiant flux of floor covering systems using a radiant heat energy source*. Quincy, MA: National Fire Protection Association.
NFPA 260-2013: *Standard methods of tests and classification system for cigarette ignition resistance of components of upholstered furniture*. Quincy, MA: National Fire Protection Association.
NFPA 701. (2015). *Standard methods of fire tests for flame propagation of textiles and films*. Quincy, MA: National Fire Protection Association.
NFPA 1971. (2013). *Standard on protective ensembles for structural fire fighting and proximity fire fighting*. Quincy, MA: National Fire Protection Association.
NFPA 2112-2012: *Standard on flame-resistant garments for protection of industrial personnel against flash fire*. Quincy, MA: National Fire Protection Association.
NIST, National Institute for Science and Technologies, 100 Bureau Drive, Gaithersburg, MD 20899.
Stoll, A. M., & Chianta, M. A. (1969). Method and rating system for evaluation of thermal protection. *Aerospace Medicine*, *40*, 1232–1238.
UFAC. (1990). *Fabric classification test method*. High Point, NC: Upholstered Furniture Action Council.

Further reading

ASTM F1506. (2015). *Standard performance specification for flame resistant and arc rated textile materials for wearing apparel for use by electrical workers exposed to momentary electric arc and related thermal hazards*. West Conshohocken, PA: ASTM International.
Canada. (2011). *Hazardous products (tents) regulation SOR/90-245*. Ottawa: Minister of Justice.
DOT/FAA/AR-00/12. (2000). *Aircraft materials fire test handbook*. Springfield, VA: U.S. Department of Transportation, Federal Aviation Administration.

This page intentionally left blank

Testing of Hot-water and Steam Protective Performance Properties of Fabrics

9

S. Mandal, M. Camenzind, S. Annaheim, R.M. Rossi
Empa, Swiss Federal Laboratories for Materials Science and Technology, St. Gallen, Switzerland

9.1 Introduction

Nowadays, occupational hazards have become more complicated; this has subsequently increased the demand for safety and comfort measures for firefighters and defense personnel. Reports have confirmed that every year, many firefighters and defense personnel (army and navy) sustain burn injuries or lose their lives while fighting fires, rescuing people, and responding to hazardous material incidents (Brushlinsky, Ahrens, Sokolov, & Wagner, 2016; Fahy, LeBlanc, & Molis, 2014). Additionally, numerous oil and gas industry workers and restaurant cooks/chefs are injured at their workplaces due to burns (Sati et al., 2008; Zhang, McQueen, Batcheller, Paskaluk, & Murtaza, 2015b). The solution to mitigate skin burn injuries is the use of high performance protective clothing by these high-risk sector workers, namely firefighters, defense personnel, industrial workers, and cooks/chefs (Kahn, Patel, Lentz, & Bell, 2012; Mandal, Song, Ackerman, Paskaluk, & Gholamreza, 2013; Rossi, 2003). In this context, it is notable that the protective performance of the clothing is dependent on the types of thermal exposures faced by these high-risk sector workers (Mandal & Song, 2016a,2016b).

It has been observed that the workers of the high-risk sectors (e.g., firefighting, defense, oil and gas, restaurant kitchen) are often exposed to many types of thermal exposures including hot water and steam (Barker, 2005; Lawson, 1996; Mandal et al., 2013; Mandal & Song, 2014; Sati, Crown, Ackerman, Gonzalez, & Dale, 2008; Zhang, McQueen, Batcheller, et al., 2015b). In particular, the fire extinguishing water used by firefighters can become hot and could be splashed or sprayed over the firefighters' bodies. Sometimes, this hot water may accumulate on the ground and firefighters need to crawl into this puddle to effectively complete their duty. While crawling, firefighters' clothed body parts (knees, elbows, and lower legs) are immersed in the puddle while at the same time the clothing gets compressed on the floor (Barker, 2005; Lawson, 1996). In another firefighting scenario, the hot water may convert into steam and cause harm to the firefighters' bodies (Mandal, Lu, Wang, & Song, 2014); notably, the exposure to steam is also prevalent for defense personnel (Desruelle & Schmid, 2004). Additionally, oil and gas industry workers may be exposed to hot water splash/spray and steam while extracting bitumen from oil sands or engaging in the production

Advanced Characterization and Testing of Textiles. https://doi.org/10.1016/B978-0-08-100453-1.00017-9

of heavy oil (Sati et al., 2008). Similarly, cooks/chefs are often exposed to hot water splash/spray and steam while preparing food in busy restaurant kitchens (Zhang, McQueen, Batcheller, et al., 2015b). Altogether, the hot water splash/spray, hot water immersion with compression, and/or steam hazards could cause significant burns on firefighters', defense personnel's, industrial workers', and cooks/chefs' bodies.

Considering the above situations, many researchers have studied the hot water and steam protective performance of the clothing usually worn by the firefighters, defense personnel, oil and gas industry workers, and/or cooks/chefs (Barker, 2005; Lawson, 1996; Lu, Song, & Li, 2013b; Lu, Song, Li, & Paskaluk, 2013c; Lu, Song, Ackerman, Paskaluk, & Li, 2013a; Mandal et al., 2013, 2014; Sati et al., 2008; Zhang, McQueen, Batcheller, et al., 2015b). In this context, some researchers have evaluated and characterized the protective performance of fabrics used in the clothing under exposure to hot water splash, hot water immersion with compression, and steam (Mandal et al., 2013; Mandal et al., 2016; Murtaza, 2012), while other researchers have evaluated and characterized the protective performance of whole garments under the exposure of hot water spray and steam (Lu, Song, et al., 2013a; Mandal et al., 2014).

The subsequent sections of this chapter describe standardized or customized bench-scale and full-scale test methods for evaluating the protective performance of fabrics and garments, respectively, under hot water splash, hot water immersion with compression, hot water spray, and/or steam exposures. Previous research on the characterization of fabrics and clothing under these exposures is also briefly reviewed and summarized. Some key issues related to the hot water and steam protective performance of the clothing are discussed towards the end of this chapter. This chapter could help guide textile or materials engineers when developing high performance hot water and steam protective clothing that could provide optimum occupational safety for firefighters, defense personnel, industrial workers, and cooks/chefs.

9.2 Tests for evaluating the hot water and steam protective performance of the clothing used by high-risk sector workers

9.2.1 Sensors

In order to evaluate the hot water and steam protective performance of clothing, one of the prime requirements is sensors (Barker, Hamouda, Shalev, & Johnson, 1999; Mandal & Song, 2015). These sensors should be able to act as the wearers' (workers) skin and measure temperature and heat flux through these sensors under exposure to hot water and steam; these temperature or heat flux values are further used for predicting the extent of the burn injury on the wearers' bodies. Currently, several types of these sensors are available in the market, including copper slug sensors, embedded sensors, skin simulant sensors, PyroCal sensors, and water-cooled sensors (Barker et al., 1999). Among all of these sensors, the copper slug sensors and the skin simulant

sensors have been widely used for evaluating the hot water and steam protective performance of fabrics and clothing (ASTM International, 2008; Mandal et al., 2014; Mandal & Song, 2016a). In the following paragraphs, a summary of these two types of sensors is presented. By employing these sensors, different bench-scale and full-scale tests have been developed to evaluate the hot water and steam protective performance of fabrics and clothing, respectively. In the following subsections, these tests methods are discussed in detail.

9.2.1.1 Burn injury prediction using copper slug sensors

This sensor comprises a copper (electrical grade copper) disk 1.6 mm in thickness and 40 mm in diameter (ASTM International, 2008). The mass of the disk is 18 ± 0.5 g. On the back surface of the disk, a single iron-constantan (ANSI type J) or a single nickel-chromium/nickel-aluminum (ANSI type K) thermocouple wire bead (0.254 mm wire diameter or finer) is bonded mechanically (by mechanically deforming the copper disk material around the thermocouple bead) or by using a high melting (>280°C) point solder. In order to control the emissivity of the overall sensor, the front surface of the disk is painted with a thin coating of flat black high temperature spray that has an absorptivity of 0.9 or greater. The thermocouple wire bead of the sensor can measure the surface temperature of the copper disk during thermal exposure to hot water and steam, for instance. This temperature can further be used to determine the thermal energy (heat flux) through the sensor. In this sensor, the heat flux under a particular thermal exposure is calculated using Eq. (9.1), where q = heat flux (J/cm^2), M = mass of the disk (g), Cp = specific heat of the disk (J/g°C), A = area of the disk (cm^2), ΔT = temperature rise of the disk (°C), and Δt = exposure time (s); here, M can be further represented by Eq. (9.2), where, A = area of the disk (cm^2), b = thickness of the disk (cm), and ρ = density of the disk (g/cm^3) (Song, Mandal, & Rossi, 2016).

$$q = \frac{M.Cp.\Delta T}{A.\Delta t}, \tag{9.1}$$

$$M = A.b.\rho, \tag{9.2}$$

The calculated heat flux values can be used in the Stoll second-degree burn criterion (described below) to predict the time to second-degree burn on wearers' bodies.

A research group at the United States Aerospace Medical Research Department, Naval Air Development Center in Pennsylvania conducted burn injury studies (on pigs, rats, and sailors of the US Navy) in the late 1950s and early 1960s (Stoll, 1962; Stoll & Chianta, 1968; Stoll & Greene, 1959). Based on their studies, Stoll and Chianta (1969) established a range of thermal exposure times and corresponding heat fluxes (i.e., local heat gain in the human tissue) to generate second-degree burns on human bodies. Some data were based on the observed exposure times required to produce second-degree burns on blackened human skin subjected to incident heat fluxes from 4.2 to 16.8 kW/m^2; other data were theoretically determined for heat fluxes from 16.8 to 41.9 kW/m^2 (Stoll & Greene, 1959). For the range of thermal

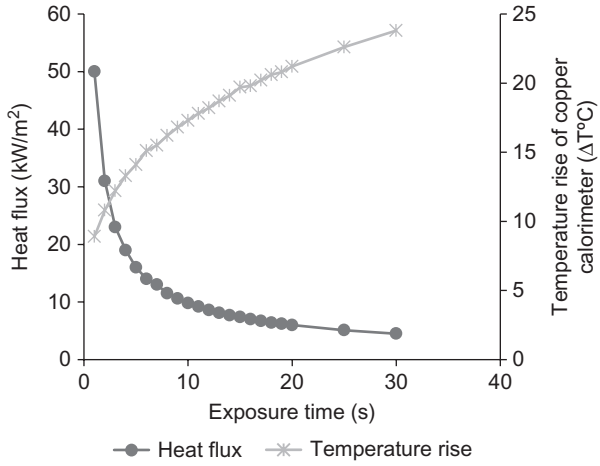

Fig. 9.1 Stoll curve.

exposure times and corresponding heat fluxes, the temperature rise (ΔT°C from the initial temperature of 32°C) of a copper slug calorimeter was recorded and a relationship plot between exposure times, temperature increases, and heat flux was developed as the "Stoll curve" (Fig. 9.1) (Fire Resistant Flight Line Garment, 2010). By employing the Stoll curve, the temperature rise or heat flux of the copper slug sensor under a particular thermal exposure is used to calculate the time required for second-degree burn injuries on human bodies. The main advantage of this Stoll second-degree burn criterion is its simplicity and the fact that it does not require any sophisticated numerical calculation to predict skin burns. However, this criterion is limited to predicting the burn time in a certain range of heat fluxes (up to 41.9 kW/m^2); therefore, the prediction of burn time beyond this range of heat fluxes is objectionable. This model is also inapplicable in the case of "nonrectangular" or "nonsquared" heat flux histories with exposure time (Barker et al., 1999). Additionally, this method is limited to predictions of the time required for a second-degree burn; thus, the prediction of other degree of burns (first- and third-degree) is impossible (Song et al., 2016).

9.2.1.2 Burn injury prediction using skin simulant sensors

This sensor uses a colorceron slab that is 32 mm in thickness and 19 mm in diameter. A type-T thermocouple (copper constantan) is held on the surface of a colorceron slab by an epoxy-phenolic adhesive that can tolerate temperatures of up to 370°C; a hole is drilled along the length of the colorceron slab to allow the thermocouple to be inserted inside the sensor. The thermocouple attached surface is generally painted black to control the emissivity of the sensor. The thermocouple measures the temperature increase in any low- to high-intensity thermal environment; this increase can be used to calculate the thermal energy (heat flux) through the sensor using Duhamel's theorem

(Eq. 9.3, where T_i = initial uniform surface temperature (°C), $T_s(t)$ = surface temperature (°C) at time t (s), and $q''(t)$ = heat flux (W/m^2) at time t) (Dale, Crown, Ackerman, Leung, & Rigakis, 1992; Torvi, 1997).

$$q''(t) = \sqrt{\frac{k\rho Cp}{\pi}}\left[\frac{1}{2}\int_t^0 \frac{T_s(t) - T_i}{t^{1/2}}\right], \tag{9.3}$$

The temperature rise of the sensor can also be used to predict the burn injury on wearers' bodies using the Henriques Burn Integral (HBI) equation (described below) developed in the middle of the 20th century.

In 1947, Henriques and Moritz (1947) found that the destruction (injury) of the tissue layer located at the epidermis/dermis interface in human skin starts when the tissue temperature of the epidermis rises above 44°C (Moritz & Henriques, 1947). Based on this finding, Henriques and Moritz (1947) modeled the destruction rate of human skin as a first-order biochemical reaction using the Arrhenius relationship. To develop this model, they critically considered the time for which the temperature of the epidermis was above 44°C (Eq. 9.4).

$$\frac{d\Omega}{dt} = P\exp\left(\frac{-\Delta E}{RT}\right) \tag{9.4}$$

Eq. (9.4) was further integrated to produce Eq. (9.5), where Ω was assigned as a quantitative measure of burn damage at the epidermis or at any depth in the dermis (dimensionless); P = preexponential factor (s^{-1}), ΔE = the activation energy for human skin (J/mol), R = the universal gas constant (8.315 J/kmol K), T = absolute temperature at the epidermis or at any depth in the dermis (K), and t = total time for which t is above 44°C (s).

$$\Omega = \int_t^0 P\exp^{-(\Delta E/RT)}\,dt \tag{9.5}$$

According to Eq. (9.5), first-, second-, and third-degree burns occur at $\Omega = 0.53$, $\Omega = 1$, and $\Omega = 1$, respectively. In order to calculate the first- and second-degree burn time, the temperature T of the base of the epidermis layer is required (by comparison, the temperature of the base of the dermis is used to predict third-degree burn time). In Eq. (9.5), T is usually calculated by Pennes' bio-heat transfer equation (Eq. (9.6), where ρ = density of skin (kg/m^3), c = specific heat of skin (J kg°C), k = thermal conductivity of skin (W m/°C), x = skin depth (m), G = blood perfusion rate (m^3/s/m^3 of tissue), ρ_b = density of blood (kg/m^3), c_b = specific heat of blood (J kg°C), and T_c = core temperature of human body (37°C)] (Pennes, 1948).

$$\rho c\frac{\partial T}{\partial t} = k\frac{\partial^2 T}{\delta x^2} - G\left(\rho_b c_b\right)\left(T - T_c\right) \tag{9.6}$$

Overall, the main advantage of the HBI equation is that this model is applicable to predict first-, second-, and third-degree burn time at any heat flux; however, this prediction

method is more time-consuming, cumbersome, and requires the use of a computer and specialized software (Song, 2004; Song, Barker, Grimes, & Thompson, 2005; Torvi, 1997).

9.2.2 Bench-scale tests for evaluating the hot water and steam protective performance of the fabrics used in the clothing

In order to evaluate the hot water and steam protective performance of fabrics using bench-scale tests, three different test approaches are available. These approaches are mainly aimed at evaluating the protective performance under hot water splash, hot water immersion with compression, and steam exposures.

9.2.2.1 Hot water splash test

The protective performance of fabrics under the hot liquid (including hot water) splash exposure can be measured according to the ASTM F 2701 standard (ASTM International, 2008). This standard is used to measure thermal energy transmission through hot water protective woven or knit fabrics, battings, and sheet fabrics with permeable or impermeable coating. In this standard, a fabric specimen (355 × 560 mm) is conditioned at 25 ± 3°C and 50% ± 10% relative humidity for at least 8 h and then mounted on a 45 degrees inclined sensor board (406 mm × 254 mm × 13 mm) (Fig. 9.2); this high temperature and thermal shock resistant sensor board is fabricated with a nonconductive, liquid, and heat resistant material with a thermal conductivity value of <0.15 W/m K. On the lengthwise centerline of this sensor board, two copper slug sensors are positioned: the distance from the top of the board to the center of the mounted sensors is maintained at 102 and 204 mm, respectively. At 19 mm above the center of the upper sensor, a funnel cone is fixed to hold water at a determined temperature. In this method, a total of 1 L of water (at 25°C) is added in a heating container and the container is heated on a hot plate until the temperature of the water is raised up to 5°C

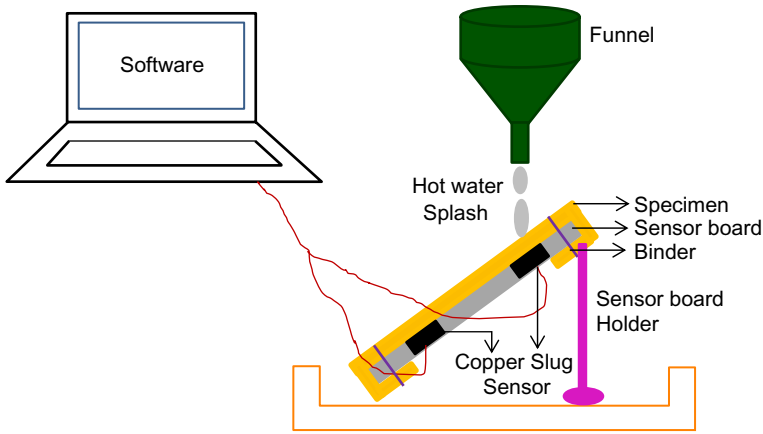

Fig. 9.2 Schematic diagram of the 45°C hot water splash exposure test (ASTM F 2701 test).

above the determined temperature; thereafter, the heating container is removed from the hot plate and the hot water is poured into the funnel within 3–5 s (it is expected that the temperature of the water would reduce by ~5°C within these 3–5 s). Hot water flows from the funnel cone onto the fabric specimen at a determined pouring rate that depends upon the size of the orifice (usually 12 mm) of the funnel. The amount of thermal energy (heat flux) transmitted through the fabric specimen during and after the hot water exposure is measured using the two instrumented copper slug sensors. This measurement is carried out for a total duration of 60 s (10 s before the hot water pouring has been initiated + during the 10 s of the hot water exposure + 40 s after the hot water exposure has been completed). Furthermore, the amount of transmitted thermal energy to cause a second-degree skin burn injury is measured using the Stoll second-degree burn criterion described above. This thermal energy for the second-degree burn is interpreted as the hot water protective performance of the fabric specimen.

Although ASTM F 2701 is a standard test method, the hot water pouring procedure in this method appears awkward, which could affect the hot water pouring rate or repeatability of the test and may cause injuries to the test operator. Considering this, a group of researchers from the Protective Clothing and Equipment Research Facility (PCERF) at the University of Alberta (U of A), Canada, improved the repeatability of the test method by modifying the hot water pouring procedure (Fig. 9.3). According to this new procedure, hot water is poured on the fabric specimen with a low-pressure hot water jet (Jalbani, Ackerman, Crown, Keulen, & Song, 2012). The funnel in the ASTM F 2701 standard is replaced with a small pipe directly fed by a temperature-controlled circulating hot water bath via a small pump and through a hose and valve system. This modified device can allow the consistent application of a given quantity of water at a controlled temperature and flow rate. In this modified device, the water temperature, flow rate, and pressure can be

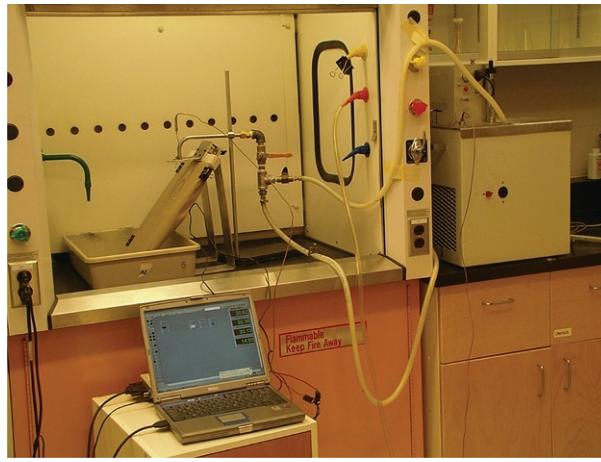

Fig. 9.3 45°C hot water splash exposure test modified from ASTM F 2701 (Jalbani et al., 2012).

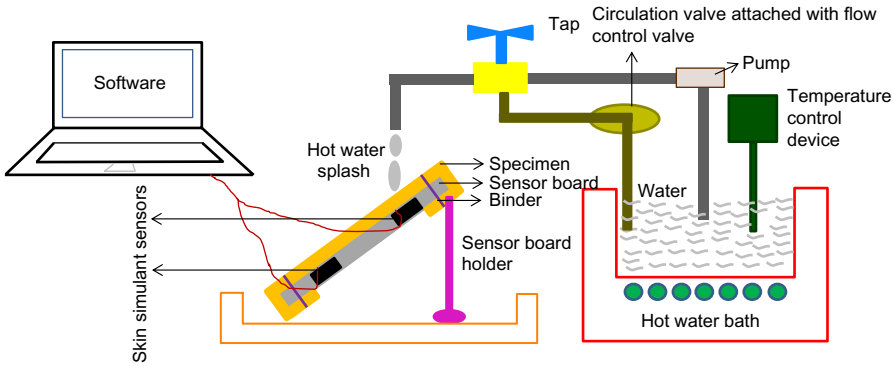

Fig. 9.4 Schematic diagram of the 45°C hot water splash exposure test modified from ASTM F 2701.

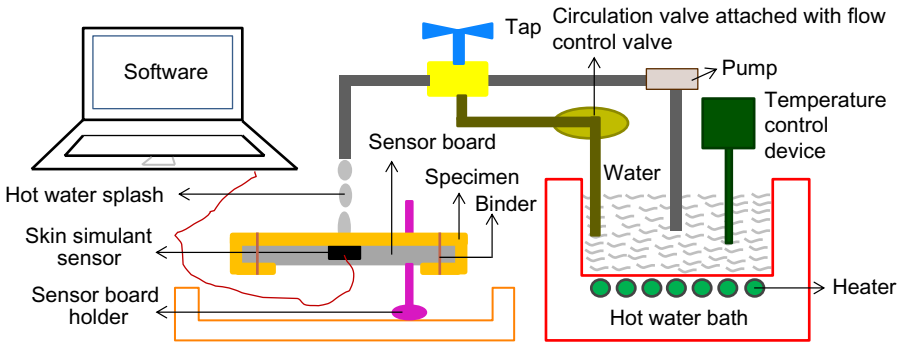

Fig. 9.5 Schematic diagram of the horizontal hot water splash exposure test modified from ASTM F 2701.

controlled as per the requirements of the experimenters. Later, Mandal et al. (2013) modified the sensor board of this device and replaced the two copper slug sensors by two skin simulant sensors in an attempt to more accurately simulate human skin for predicting burn injuries using HBI equation-based software (Fig. 9.4). Finally, in the ASTM F 2701 (ASTM International, 2008) test method, the fabric specimen can only be exposed to the hot water according to one configuration (45 degrees); however, there is a need to conduct tests at different fabric positions (horizontal, vertical, etc.) in order to accurately simulate the exposure of fabrics to hot water. Considering this, Mandal, Song, and Gholamreza (2016) recently modified this device by horizontally positioning the sensor board with the skin simulant sensors (Fig. 9.5).

9.2.2.2 Hot water immersion with compression test

Recently, the PCERF research team has developed a test method for evaluating the protective performance of fabrics under exposure to hot water immersion with compression (Fig. 9.6) (Mandal et al., 2016; Mandal & Song, 2016a). In this test, a metal

Fig. 9.6 Hot water immersion with a compression testing device (Mandal et al., 2014).

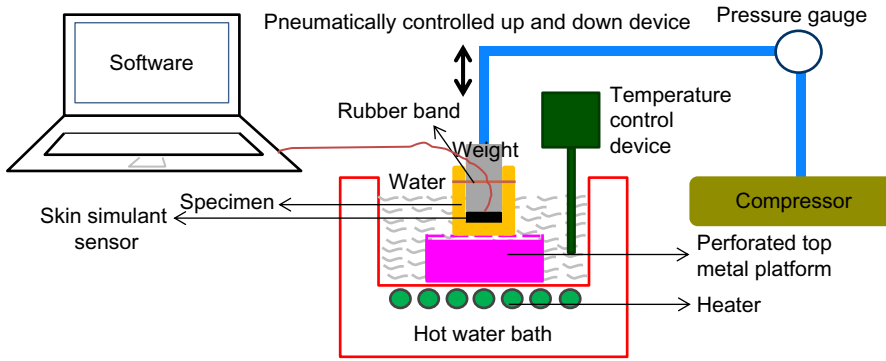

Fig. 9.7 Schematic diagram of the hot water immersion with compression test.

platform with a perforated top surface is positioned at the bottom-center of a hot water bath (Fig. 9.7). Water is poured into the bath up to a level of 6 cm above the perforated top surface. The water temperature is maintained at 85°C using a temperature control device. Next, a 30.5 cm × 30.5 cm fabric specimen is attached with a rubber band to the skin simulant sensor mounted on a cylindrical weight. This specimen-covered sensor is immersed into the hot water bath using a pneumatic device until the whole assembly (specimen + sensor) rests flat on the center of the perforated surface. Pressure is applied to compress the specimen between the sensor and the perforated surface and is pneumatically controlled at 56 kPa. Thermal energy (heat flux) transmitted through the compressed specimen is measured by the sensor for a period of 120 s. Based on the thermal energy measurement, the time required to generate a second-degree skin burn is calculated with a customized HBI software. Using this device and technique, Mandal (2016) studied the hot water protective performance of fabrics at different water temperatures (75°C, 85°C, and 95°C) and compression pressures (14, 28, and 56 kPa). He concluded that this device could successfully evaluate and discriminate the protective performance at different hot water temperatures and pressures, if required.

9.2.2.3 Steam test

Since the end of 20th century, many researchers have investigated the steam protective performance of fabrics by developing their customized steam testing device. Initially, Le, Ly, and Postle (1995) developed a device that can predict the heat (temperature) and mass (water) transfer through multilayered fabrics under the exposure to steam at a temperature of 100.9°C and a pressure of 130 kPa (Fig. 9.8). In this device, a vertical steaming chamber was sealed at the bottom and open to atmospheric pressure at the top. The side wall of the chamber was wrapped by a heating element to preheat it at the steam temperature; this arrangement was made to prevent the condensation of the steam inside the chamber. Then, a perforated plate was horizontally placed in the middle of the chamber and the different layers of the fabric specimen were placed on it. Over the top of the fabric layers, another perforated plate was placed to press and control the overall volume of the fabric layers. Then, steam was imposed on the bottom of the fabric layers through an inlet attached with regulating valve; here, a cone was placed on the steam inlet to disperse the flow of the steam. In order to ensure the dryness of the steam, any excess water from the steam was drained off. In this study, the temperature at the bottom of the fabric layers and between the fabric layers was recorded by copper constantan thermocouples at 1 s intervals with a resolution of ±0.1°C. The weight of the fabric layers before and after the test was measured: the weight difference was used as a measure of the weight of water condensed inside the fabric layers.

Furthermore, Rossi, Indelicato, and Bolli (2004) developed steam testing devices in the Laboratory for Protection and Physiology (LPP) at Empa (Swiss Federal Laboratories for Materials Science and Technology), Switzerland, for evaluating the steam protective performance of fabrics in flat and cylindrical configurations. In this case, steam was generated by heating a water containing chamber through a Bunsen burner. The chamber was closed with a synthetic cork that contained a tube. The fabric specimens were placed flat on the top of the tube so that they were

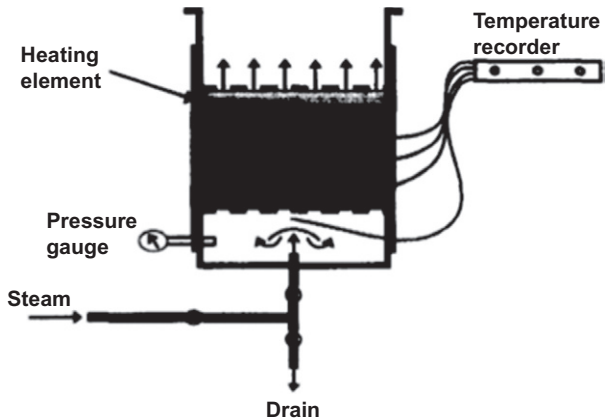

Fig. 9.8 Steam testing device developed by Le et al. (1995).

freely exposed to flowing steam; a copper slug sensor was placed behind the specimen. During the steam exposure, the times to reach a sensor temperature increase of 12°C and 24°C were recorded. These times were defined as the steam transfer index (STI); in this study, STI12 and STI24 were interpreted as the steam protective performance of the exposed fabric specimens. In order to evaluate the steam protective performance of a cylindrically configured fabric, the fabric specimen was wrapped on a metallic cylinder (this configuration was chosen to simulate a fabric wrapped onto a human arm); this metallic cylinder was equipped with sweating nozzles in order to simulate the active sweating on human arm. Then, the clothed cylinder was horizontally placed in front of the steam tube. The steam flow was adjusted in such a way that it hit the cylinder perpendicularly in the middle of the surface. During the steam exposure, the average heating power to keep the cylinder to 35°C (this 35°C temperature was chosen to simulate in realistic manner the human arm under a warm to hot exposure) was recorded. Using another experimental protocol developed by Rossi et al. (2004), the cylinder was heated with a constant heating power during the steam exposure and the mean temperature increase of the whole cylinder was assessed. Overall, the changes in the heating power and surface temperature provided the required information for the assessment of the steam protective performance of the tested fabric specimen.

Considering the requirements for evaluating the steam protective performance of fabrics used in the French Navy clothing, the steam laboratory of the Institut de Médecine Navale du Service de Santé des Armées (IMNSSA) has developed their own testing device (Desruelle & Schmid, 2004). In this device, the fabric specimen was wrapped on a cylinder made of an aluminum sheet and covered by an external black resin layer to minimize the radiant-heat flux; the resin layer of the cylinder was instrumented with heat flux evaluating sensors. The middle part of the clothed cylinder was exposed to the steam (up to a maximum steam temperature and pressure of 142°C and 300 kPa, respectively) generated by a steam generator. During the steam exposure, the sensors measured the heat flux and temperature of the resin layer; the heat flux and temperature values were interpreted as the steam protective performance of the fabrics.

The devices developed by Le et al. (1995), Rossi et al. (2004), and Desruelle and Schmid (2004) for evaluating the steam protective performance of fabrics considered low-pressure steam exposures (lower than 300 kPa). Consequently, these devices are not suitable to simulate the high pressure steam exposures usually faced by oil and gas industry workers. Considering this requirement, the research team of the PCERF has developed a new device that can be used to predict the protective performance of fabrics under high pressure steam exposures (Fig. 9.9) (Sati et al., 2008). A cylinder 230 mm in diameter and 460 mm in height (built with fiberglass and polyester resin and fixed to a steel frame) was instrumented with nine uniformly distributed skin simulant sensors; in this device, the instrumented cylinder actually simulates the human torso. A fabric specimen was tightly wrapped on the cylinder and the clothed cylinder was exposed to high temperature (150°C), high pressure (up to 345 kPa) steam through a nozzle (a thermocouple was placed in front of the nozzle to monitor the steam temperature). During the steam exposure, the temperature rise of the sensors was recorded as a

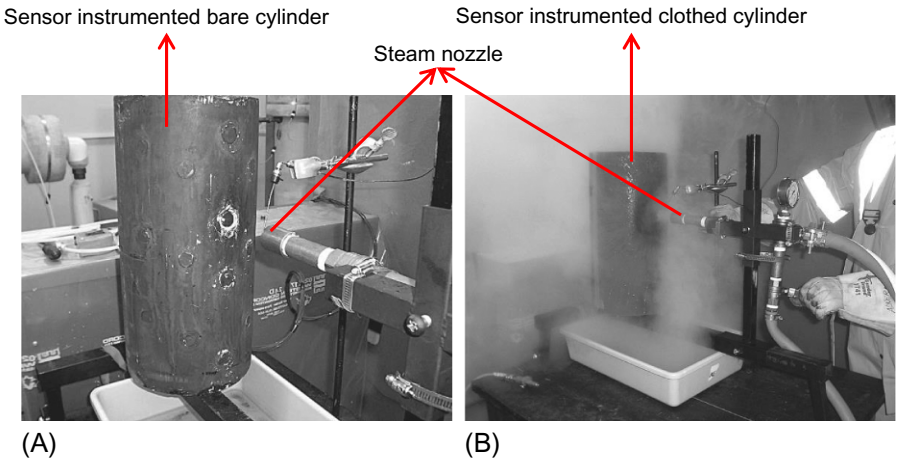

Fig. 9.9 Steam testing device developed by Sati et al. (2008). (A) Before testing and (B) during testing.

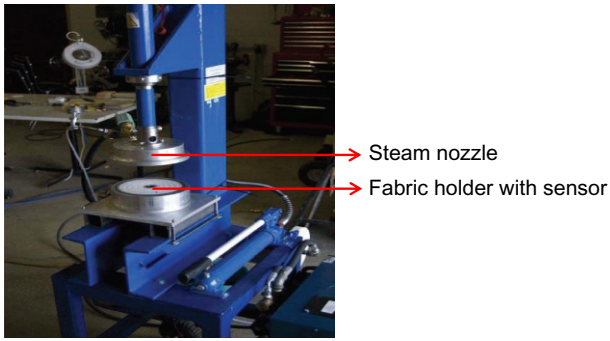

Fig. 9.10 Steam testing device developed by Ackerman et al. (2012).

function of time. From this temperature rise, several parameters (peak temperature, peak heat flux, time to reach peak heat flux, and total absorbed energy by sensors or skin) were calculated for evaluating the steam protective performance of the fabrics.

However, the capacity of the steam pressure of this device developed by the PCERF research team was still very low (345 kPa) compared to the steam pressures (more than 600 kPa) that are sometimes encountered in the oil and gas industry; additionally, this steam testing device was instrumented with several sensors, which makes the device expensive. Considering these shortcomings, the PCERF research team developed another device for evaluating the steam protective performance of fabrics (Fig. 9.10). A schematic diagram of this steam testing device is shown in Fig. 9.11 (Ackerman et al., 2012). In this device, steam is generated by a 3 kW boiler at a temperature of 150°C. The fabric specimen (150 mm diameter) is placed on a Teflon plated specimen holder equipped with a skin simulant sensor. The saturated and superheated steam is impinged at a pressure of 69–620 kPa from 50 to 150 mm above the fabric specimen

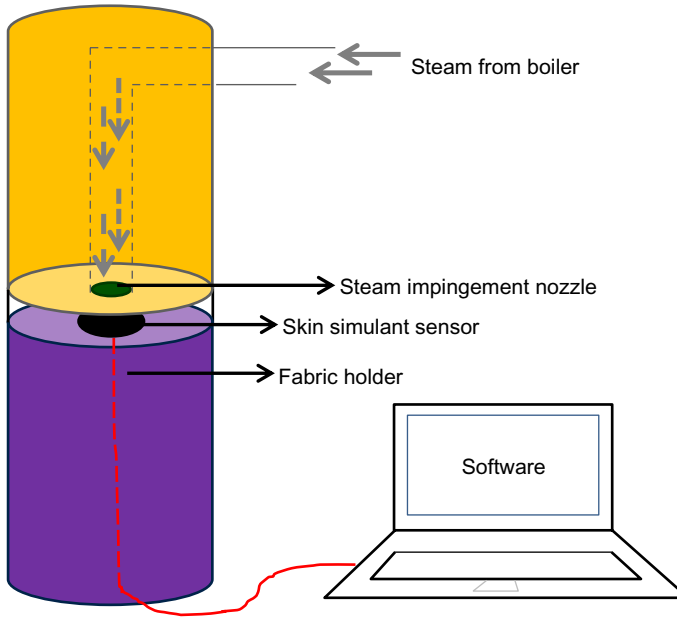

Fig. 9.11 Schematic diagram of the steam testing device developed by Ackerman et al. (2012).

through a nozzle with a diameter of 4.6 mm. The duration of the steam exposure was initially set at 10 s. During and after steam exposure, the heat flux through the fabric specimen is recorded by the skin simulant sensor and the time required to generate a skin burn is calculated by a customized HBI program. Mandal et al. (2013, 2014) recently used this steam testing device and were able to control the exposure time according to the structure of the tested fabric specimen in order to predict a second-degree burn injury from the sensor. Although the normal steam exposure time for this device was set at 10 s by Ackerman et al. (2012), the steam exposure time used for the thickest fabric specimen in the study of Mandal et al. (2013, 2014) was 30 s.

9.2.3 *Full-scale instrumented manikin tests for evaluating the hot water and steam protective performance of whole garments*

In order to evaluate the hot water and steam protective performance of garments using full-scale instrumented manikin tests, two different test approaches are available. These approaches are mainly used to evaluate the protective performance under hot water spray and steam exposures.

9.2.3.1 *Hot water spray test*

Recently, a full-scale instrumented manikin test was developed at PCERF for evaluating the hot water protective performance of a whole garment (Lu, Song, et al., 2013a;

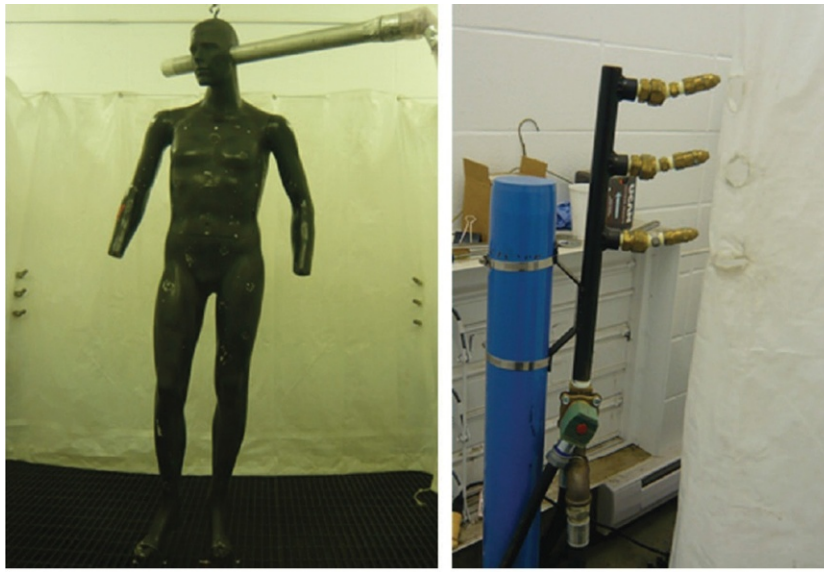

Fig. 9.12 Hot water spray manikin test. (A) Nude manikin, (B) hot water spray systems (Lu, Song, et al., 2013a; Mandal et al., 2014).

Mandal et al., 2014). In this test, the protective performance of the garment is evaluated under hot water spray exposure. For the hot water spray testing, a fiber glass and resin based 40-size manikin is instrumented with 110 skin simulant sensors. These sensors are uniformly distributed over the surface of the manikin (Fig. 9.12A). The garment is placed on the manikin, and the clothed manikin is hung by its head and fastened at the feet by two fetters to keep it in an upright posture. Hot water (85°C) is sprayed at a pressure of 250 kPa on the manikin for 10 s by four groups of automatically controlled 3-nozzle cylinder spray jets (Fig. 9.12B). During and after the spraying, the temperature rise in the sensors is measured and used to calculate the thermal energy (heat flux) transmitted through the garment specimen. This temperature rise is also used to calculate the amount or percentage of skin surface area affected by second-degree scalds/burns. These predicted amounts of second-degree scalds/burns of a particular specimen are used as the hot water protective performance value of the garment.

9.2.3.2 Steam test

In the beginning of the 21st century, Desruelle and Schmid (2004) developed a thermal manikin to evaluate the protective performance of garments under a steam atmosphere. This thermal manikin was divided into nine areas, and the surface of these areas was made of a copper sheet. Furthermore, the manikin included a water cooling system in order to control the temperature for each area separately between 20°C and 40°C. This system contributed to limiting internal heat storage and natural

convection within the manikin. The temperature of the input water was controlled between 20°C and 40°C and the water flow to each zone was regulated between 0.06 and 1 L/min. For the testing, the garment was put on the manikin and the clothed manikin was placed in a steam atmosphere. The steam atmosphere was created in a climatic chamber (a 7-m^3 chamber that allowed the generation of a fully saturated atmosphere at 80°C) by an air conditioner (heating system and humidifier) working in a closed circuit. The humidity of the climatic chamber was increased step by step to obtain a saturated atmosphere. For each step, the mean temperature of the surface of each area of the manikin was regulated at 33°C. Temperature and water flow were measured for each step over 7 min. From the temperature and water flow, the local and total heat fluxes were then calculated for each step, and the heat fluxes at saturation were calculated by extrapolation. These heat flux values were interpreted as the steam protective performance of the garment. However, this test procedure of maintaining a constant manikin surface temperature of 33°C during the steam exposure test may not correspond in a realistic way to real life scenarios (Sati et al., 2008). Indeed, the skin surface temperature would rise during the exposure, resulting in reduced heat transfer rates in response to reduced temperature differences (between human skin and outer surface of the fabric).

9.3 Characterization of the hot water and steam protective performances of clothing used by the high-risk sector workers

The previous section described a series of bench-scale tests developed in the last few decades for evaluating the hot water and steam protective performance of fabrics. Additionally, some full-scale manikin tests have been developed for evaluating the hot water and steam protective performance of whole garments as well. With these bench-scale and full-scale tests, researchers have evaluated and analyzed the hot water and steam protective performance of fabrics and garments. In the following sections, these previous research are critically reviewed.

9.3.1 Hot water and steam protective performances of fabrics used in the clothing

9.3.1.1 Protective performance of fabrics under hot water splash

Lu, Song, et al. (2013b, 2013c) compared the protective performance of single-layered fabrics against different hot liquid (water, drilling mud, and canola oil) splashes at 85°C. They found that the protective performance of the fabrics evaluated depended on the liquid properties. It was evident that the fabric performance was lower when exposed to water or drilling mud than when exposed to canola oil. This was thought to be because the heat capacity of water and drilling mud is higher than the heat capacity of canola oil. Basically, the amount of heat per unit mass of hot water or drilling mud was higher due to their higher heat capacities, and this higher heat content lowered

the protective performance of the fabrics selected in Lu et al.'s study. Recently, Lu, Song, Zeng, Zhang, and Li (2014) found that the flow pattern of liquids on the fabrics varied depending on the surface tension between the liquid molecules and fabrics. Generally, a very hot liquid or a highly rough fabric surface significantly influences the surface tension and thus increases the wettability of the fabric. In the case of a fabric with high wettability, the liquid easily penetrates through the fabric due to wicking and causes burns on wearers' skins. Lu et al. (2014) further mentioned that the liquid applied can be stored in the fabric or transmitted through the fabric depending on the fabric properties (thickness, density, and air permeability). The fabric offers a high initial protective performance if it stores more liquid and prevents its transmission through the fabric. They also found that the addition of a thermal liner along with a single-layered shell fabric can help store more and transmit less liquid, thus enhancing the performance of the shell fabric.

Mandal et al. (2014) stated that the structural configuration (e.g., fiber content, weave structure) and properties (e.g., weight, thickness, and air permeability) of the fabrics could significantly affect the protective performance under hot water splash exposure. They found that a fabric can show a high hot water protective performance if an ultrathin polymer layer is encapsulating the fibers/yarns of a fabric. They also concluded that an air-impermeable and thick fabric could provide a higher hot water protective performance in comparison to an air-permeable and thin fabric (Ackerman & Song, 2011; Mandal et al., 2013; Mandal & Song, 2011). This is because air-permeable and thin fabrics allow a rapid transfer of heat and mass (hot water) towards wearers' bodies through their structure, which generates quick burns on the wearers' skins. On the other hand, the air-impermeable and thick fabrics allow a negligible amount of hot water transfer towards wearers' bodies, which causes less burns on wearers' skins. In that context, Gholamreza and Song (2013) reported that a multilayered fabric with an air-impermeable outer layer provided better protection against hot water splash than a multilayered fabric with an air-permeable outer layer. Zhang, McQueen, Batcheller, Ehnes, and Paskaluk (2015a) and Zhang, McQueen, Batcheller, et al. (2015b) reported also that the hot water protective performance of a multilayered fabric increases by incorporating a larger number of permeable fabric layers; this is attributed to the fact that these permeable fabrics could store the water and enhance the protective performance. Mandal et al. (2013) also indicated that depending upon the pressure of the hot water splash, some amount of conductive heat transfer occurs through the fabrics, and may cause burn injuries to wearers.

Recently, Mandal et al. (2016) mentioned that the spatial orientation of the fabrics also affects their protective performance under hot water splash exposure. According to them, the protective performance of horizontally positioned fabrics is much lower than the protective performance of 45 degrees-oriented fabrics. This is attributed to the fact that a horizontally positioned fabric could hold hot water on its surface for a longer period of time, which could help transmit the heat and mass through the fabric over time. This situation actually lowers the thermal protective performance of the fabric.

9.3.1.2 *Protective performance of fabrics under hot water immersion with compression*

In order to evaluate the hot water protective performance of fabrics, Mandal and Song (2016a) tested a set of multilayered fabrics under hot water immersion with compression. In this study, it was found that the conductive heat and hot water mass transfer mainly occurs through the fabric towards the wearers' bodies, which can lower the protective performance by causing significant burn injuries on wearers' bodies. It was further explained that the fabric thickness is the key for resisting the heat transfer through the fabric, whereas the fabric air permeability is important to obstruct the mass transfer through the fabric systems. By properly utilizing thick and impermeable fabrics, it is possible to prevent burn injuries on wearers' bodies. To ensure optimum protection from exposure to hot water immersion with compression, Mandal and Song (2016a) recommended to use a multilayered fabric that comprises a moisture barrier as its outer layer because it could effectively prevent the mass transfer through the fabric layers and lower the risk of burn injuries on wearers' bodies (Mandal et al., 2016).

Although Mandal et al. (2016) and Mandal and Song (2016a) extensively studied the protective performance of fabrics under hot water immersion with compression, they only evaluated the performance at one water temperature (85°C) and one compression pressure (56 kPa). To further explore the phenomenon, Mandal (2016) recently studied and compared the protective performance of the same set of fabrics at different water temperatures (75°C, 85°C, and 95°C) and compression pressures (14, 28, and 56 kPa). He identified that fabric thickness is less significant in comparison to the fabric evaporative resistance and air permeability when analyzing the protective performance at different water temperatures and compression pressures. Actually, the evaporative resistance and air permeability are the most significant properties to affect the performance because the mass transfer through the fabrics is the most prominent mechanism under hot water immersion and compression exposures. Nevertheless, the evaporative resistance of a fabric is more significant for protective performance than the fabric air permeability, even though both of these properties are mutually dependent. Mandal (2016) concluded that the evaporative resistance has more impact on the protective performance at a low water temperature of 75°C. At this low temperature, a fabric system with a high evaporative resistance may not allow significant mass transfer through the fabric system, and this may increase the time to obtain a second-degree burn or it may enhance the thermal protective performance of the fabric system. However, the water molecules (in the hot water bath) spread slightly further apart from each other and their speed elevates at high temperature of 95°C. In this situation, water molecules can easily or forcefully penetrate through the fabric system. Eventually, evaporative resistance has less impact on second-degree burn time or thermal protective performance of the fabric system at high temperatures. He also concluded that the impact of evaporative resistance on the protective performance is not significantly different at different compression pressures. However, increasing the compression pressure of 14–56 kPa may

reduce the thickness of the fabric or air trapped inside the fabrics, which could lower the protective performance of the fabrics.

9.3.1.3 Protective performance of fabrics under steam

Le et al. (1995) studied the steam protective performance of highly water absorbing multilayered wool fabrics. They found that heat and mass transfer mainly occurs through the fabrics under exposure to steam and that convection is the prime mode of heat and mass transfer through the fabric. It was evident that some amount of steam may condense inside the layers of the fabrics depending upon the moisture regain of the fabrics. If a great amount of steam is condensed in the fabrics, it may generate an increase in the temperature of the fabric layers; that could lower the steam protective performance by generating burns on wearers' bodies due to severe heat release through the fabrics.

Rossi et al. (2004) concluded that water vapor permeability is the most important fabric property to consider for effective protection in a steam exposure. They suggested that a water vapor impermeable membrane inside the fabric layers might significantly prevent steam transfer and could reduce burn injuries. It was also confirmed that a thick fabric with a water vapor impermeable membrane provides a better protection from steam than a thick fabric with a semipermeable membrane (Keiser, Wyss, & Rossi, 2010; Keiser & Rossi, 2008). Keiser et al. (2010) also mentioned that the thermal conductivity and heat capacity of the fabric may change as a result of exposure to steam and ultimately affect the protective performance of a fabric.

Desruelle and Schmid (2004) found that at the beginning of the steam exposure experiment, permeable fabrics showed a peak of heat flux probably due to a complex phenomenon of condensation, diffusion, and absorption of water inside the sample, which resulted in the release of high levels of heat; however, this phenomenon did not occur in the case of impermeable fabrics. They concluded that this is the reason why impermeable fabrics show a higher steam protective performance. Desruelle and Schmid (2004) also mentioned that a denaturation of the impermeable fabric may occur in the course of the steam exposure, which could render the impermeable fabric permeable. In this situation, the steam protective performance of the fabric could be lowered. A similar finding is also reported by Sati et al. (2008). Sati et al. (2008) further mentioned that the pressure of the steam and the distance between the source of the steam and the tested fabric are important for evaluating the steam protective performance of a fabric.

Recently, Mandal et al. (2013, 2014) indicated that fabrics may come in direct contact with the human skin under exposure to high pressure steam. In this situation, an air-impermeable fabric may not allow transferring the mass (steam or condensed hot water) through it; however, it may transfer the conductive heat towards the wearers' skins and that could cause the significant burn injuries on wearers' bodies. Nevertheless, Mandal et al. (2013, 2014) did not recommend any technique for reducing this conductive heat transfer through the fabrics under the high pressure steam exposure.

9.3.2 Hot water and steam protective performance of whole garments

9.3.2.1 Protective performance of whole garments under hot water spray

Lu, Song, et al. (2013a) showed that different sizes of garments have distinct protective performances under hot water spray exposure. This is because different sizes of garments can result in a variation in the dimension of the air gap (microclimate region) between the garment and wearers' body. This air gap controls the heat and mass (hot water) transfer through the garment towards wearers' bodies and could be critical to provide effective protection to wearers.

It was also reported that an impermeable garment demonstrates better protective performance than a semipermeable/permeable garment and that a proper air gap between the garment and a wearer's body is a crucial aspect for improving the hot water protective performance (Mandal et al., 2014). However, high pressure hot water spray and water flow may compress the garment on the wearer's body and significantly reduce the air gap between the garment and the wearer's body. This situation results in a lower hot water protective performance of the clothing. Furthermore, the thermal conductivity and heat capacity of the clothing may change during exposure to hot water spray, which could affect the protective performance.

The thickness and structure of the layered fabrics used, along with the design features of the garment (pocket, closures, and vents), significantly affect the hot water protective performance of an impermeable or a semipermeable garment; however, the effect of fabric weight on the protective performance is minimal. Lu, Song, et al. (2013a) concluded that fabric thickness has less impact on the protective performance in comparison to the garment design. This is because the design of a garment could more holistically affect the protective performance than the properties of the fabrics used in the garment. In this context, a notable point is that the incorporation of some essential/functional design features (e.g., reflective tape for enhancing visibility at night, closures near the collar, and cuff of a garment) on clothing may enhance the garment's performance by trapping some insulative dead air inside the garment, thus providing some extra protection to wearers, namely firefighters or industrial workers (Mandal et al., 2014).

9.3.2.2 Protective performance of whole garments under steam

Similar to hot water spray, Desruelle and Schmid (2004) found that the steam protective performance of a garment is highly dependent on the permeability of the fabrics used in the garment. In their study, it was evident that an air-impermeable garment could provide a better protection than an air-permeable garment. They also confirmed that loose-fitting cut garments include an insulated air gap between the garment and the wearers' bodies: this air gap could enhance the steam protective performance of the garment. However, Desruelle and Schmid (2004) expressed a

concern that enhancing the protective performance of garment using this air gap concept may have some ergonomic consequences on the actual wearing conditions of the workers.

9.3.3 Summary

The discussion above shows that several researchers evaluated the hot water and steam protective performance of fabrics and garments. These researchers mainly tried to identify different factors that could affect the protective performance. From their studies, it can be concluded that the different fabric construction concepts and properties, garment designs, and characteristics of hot water and steam exposure mainly affect protective performance of clothing. Concerning fabric construction, it has been found that the presence of a moisture barrier and/or the type of fibers used in a fabric may significantly affect the protective performance. In general, an air-impermeable and thick fabric system may have high evaporative and thermal resistances and could provide the better protection to wearers under exposure to hot water and steam. However, it must be noted that this type of fabric may cause a lot of heat stress on wearers' bodies by limiting the evacuation of metabolic heat and sweat vapor from wearers' bodies (Song & Mandal, 2016). Furthermore, the design of the garment is equally important for the protective performance along with its fabric properties. For example, the size, fit, and style of a garment could control the insulation features of the microclimate region (which exists between the wearer and the garment) and significantly affect its protective performance under exposure to hot water and steam. Although fabric properties and garment design have a significant impact on the protective performance, it is notable that the performance also considerably depends upon the characteristics of the hot water and steam exposure. Depending upon the temperature and/or pressure of the hot water and steam, the protective performance of a fabric and garment may significantly vary.

9.4 Key issues related to the hot water and steam protective performance of clothing

Although many researchers studied the hot water and steam protective performance of fabrics, there are still some unattended key issues in the field. For example, the thermophysical properties (heat capacity, thermal conductivity) of a fabric may deteriorate over time under exposure to high temperature, high pressure, hot water, and steam. This situation could lower the protective performance of the fabric. To date, no research has been carried out to study the changes of the thermophysical properties of a fabric under exposure to hot water and steam. In addition, because previous researchers studied the protective performance using a limited set of fabric properties (namely thickness, weight, and air permeability), other fabric properties (e.g., surface friction coefficient and bending rigidity) could also be incorporated in future studies to determine the parameters controlling the performance or quality

of a fabric/garment (Mandal, 2009). Additionally, the heat and mass transfer phenomena under these exposures are very complex and involve a combination of convection, conduction, condensation, and/or (hot water, moisture, or steam) diffusion. However, only limited research has been carried out to theoretically model the heat and mass transfer through fabrics or clothing under high temperature, high pressure hot water/steam exposure. This kind of study could advance the field of heat and mass transfer through fabrics.

Although previous researchers developed hot water and steam testing devices for evaluating the protective performance of fabrics, it is notable that the evaluation of performance using these devices is cumbersome, expensive, and difficult to carry out on a routine basis. Therefore, there is a need for some more user-friendly empirical models that can effectively predict the hot water and steam protective performance of fabrics and clothing. Considering this, Mandal (2016) recently developed and validated multiple linear regression and artificial neural network models for predicting the protective performance of fabrics under the exposure to hot water and steam. However, these models were developed using a small data set. In the future, it would be interesting to develop and/or validate these models with large data-sets. Also, it would be valuable to extend these empirical modeling techniques for evaluating the protective performance of the whole garments under exposure to hot water and steam.

Lastly, fabric materials typically used in hot water and steam protective clothing mainly comprise a moisture barrier and a thermal liner. As indicated by Song and Mandal (2016), these types of fabrics may impede the metabolic heat and sweat vapor transfer from wearers' bodies to the environment and cause a large amount of heat stress during moderate to intensive physical activity. New fabric materials are thus needed and may take advantage of the latest technologies (nanotechnologies and smart textiles) for providing a combination of effective protection and comfort to wearers under exposure to hot water and steam. It is expected that these new fabric materials should be lightweight and water or steam impermeable but sweat vapor permeable. These innovative novel fabric materials could provide effective protection and comfort to high-risk sector workers worldwide.

9.5 Summary and conclusion

High-risk sector workers (firefighters, defense personnel, oil and gas industry workers, and cooks/chefs) may be frequently exposed to hot water and steam while on duty; this situation may cause significant burn injuries on their bodies. In order to provide them effective protection, there is a need to effectively evaluate the hot water and steam protective performance of their clothing.

Considering the above requirements, researchers from renowned laboratories (e.g., LPP, Empa-Swiss Federal Laboratories for Materials Science and Technology, Switzerland; PCERF, University of Alberta, Canada; Steam laboratory, IMNSSA, France) have developed test methods and setups for evaluating the hot water and steam protective performance of fabrics and clothing. They can provide some insights into

first-, second-, and/or third-degree burn injuries on wearers' bodies as a result of exposure to hot water and steam.

In addition, in the last few decades, researchers from different laboratories have studied the hot water and steam protective performance of fabrics and clothing. From their studies, it can be concluded that fabric properties (e.g., thickness, air permeability), garment designs (e.g., fit, style), and characteristics of the hot water or steam exposure (e.g., temperature, pressure) could significantly affect the protective performance.

By scientifically analyzing and implementing the above mentioned factors, it should be possible in the future to provide solutions to the different key issues related to the hot water and steam protective performance of fabrics. These solutions could allow an increase in the occupational health and safety for high-risk sector workers worldwide.

9.6 Sources for further information

Any further queries related to the research, development, and testing of hot water and steam protective clothing may be directed to the following laboratories:

- Laboratory for Protection and Physiology, Empa- Swiss Federal Laboratories for Materials Science and Technology, Switzerland (https://www.empa.ch/web/s401)
- Protective Clothing and Equipment Research Facility, University of Alberta, Canada (http://pcerf.ualberta.ca)
- The Textile Protection And Comfort Center, North Carolina State University, United States (https://textiles.ncsu.edu/tpacc)
- Apparel Innovation Center, Calgary, Canada (http://www.apparelinnovation.org/services/#apparel-testing)

References

Ackerman, M. Y., Crown, E. M., Dale, J. D., Murtaza, G., Batcheller, J., & Gonzalez, J. A. (2012). Development of a test apparatus/method and material specifications for protection from steam under pressure. *Performance of protective clothing and equipment: emerging issues and technologies*. *Vol. 9*. West Conshohocken, PA: American Society for Testing and Materials. STP1544, pp. 308–328.

Ackerman, M. Y., & Song, G. (2011). Analyzing thermal protective clothing performance against the impact of small splashes of hot liquid. In *ASTM ninth symposium on performance of protective clothing and equipment: Emerging issues and technologies, California, USA*.

ASTM International. (2008). ASTM F 2701: Standard test method for evaluating heat transfer through materials for protective clothing upon contact with a hot liquid splash. *Vol. 11.03. Annual Book of ASTM Standards*. West Conshohocken, PA: American Society for Testing and Materials. 8 pp.

Barker, R. L. (2005). *A review of gaps and limitations in test methods for first responder protective clothing and equipment*. Pittsburgh, PA: National Personal Protection Technology Laboratory. pp. 1–98.

Barker, R. L., Hamouda, H., Shalev, I., & Johnson, J. (1999). *Review and evaluation of thermal sensors for use in testing firefighters protective clothing*. Gaithersburg, MD: National Institute of Standards and Technology. pp. 1–49.

Brushlinsky, N. N., Ahrens, M., Sokolov, S. V., & Wagner, P. (2016). *World fire statistics*. Russia: Center of Fire Statistics, International Association of Fire and Rescue Services. pp. 1–62.

Dale, J. D., Crown, E. M., Ackerman, M. Y., Leung, E., & Rigakis, K. B. (1992). Instrumented manikin evaluation of thermal protective clothing. In J. P. McBriarty & N. W. Henry (Eds.), *Performance of protective clothing* (pp. 717–733). West Conshohocken, PA: American Society for Testing and Materials. ASTM STP 1133.

Desruelle, A., & Schmid, B. (2004). The steam laboratory of the Institut de Me´decine Navale du Service de Sante´ des Arme´ es: A set of tools in the service of the French Navy. *European Journal of Applied Physiology*, *92*, 630–635.

Fahy, R. F., LeBlanc, P. R., & Molis, J. L. (2014). *Firefighter fatalities in the United States-2012*. Quincy, MA: National Fire Protection Association. pp. 1–30.

Fire Resistant Flight Line Garment. (2010). Retrieved from: http://ecbiz108.inmotionhosting.com/~ltprot5/documents/Final%20report%20-%20Garment.pdf (Accessed 12 December 2013).

Gholamreza, F., & Song, G. (2013). Laboratory evaluation of thermal protective clothing performance upon hot liquid splash. *The Annals of Occupational Hygiene*, *57*(6), 805–822.

Henriques, F. C., & Moritz, A. R. (1947). Studies of thermal injury I. The conduction of heat to and through skin and the temperatures attained therein: A theoretical and an experimental investigation. *The American Journal of Pathology*, *23*(4), 530–549.

Jalbani, S. H., Ackerman, M. Y., Crown, E. M., Keulen, M., & Song, G. (2012). Apparatus for use in evaluating protection from low pressure hot water jets. *Vol. 9. Performance of protective clothing and equipment: Emerging issues and technologies*. West Conshohocken, PA: American Society for Testing and Materials. STP1544, 329-339.

Kahn, S. A., Patel, J. H., Lentz, C. W., & Bell, D. E. (2012). Firefighter burn injuries: Predictable patterns influenced by turnout gear. *Journal of Burn Care & Research*, *33*(1), 152–156.

Keiser, C., & Rossi, R. M. (2008). Temperature analysis for the prediction of steam formation and transfer in multilayer thermal protective clothing at low level thermal radiation. *Textile Research Journal*, *78*(11), 1025–1035.

Keiser, C., Wyss, P., & Rossi, R. M. (2010). Analysis of steam formation and migration in firefighters' protective clothing using X-ray radiography. *International Journal of Occupational Safety and Ergonomics*, *16*(2), 217–229.

Lawson, J. R. 1996. *Fire fighter's protective clothing and thermal environments of structural fire fighting*. Gaithersburg, MD: National Institute of Standards and Technology. pp. 1–22.

Le, C. V., Ly, N. G., & Postle, R. (1995). Heat and mass transfer in the condensing flow of steam through an absorbing fibrous media. *International Journal of Heat and Mass Transfer*, *38*(1), 81–89.

Lu, Y., Song, G., Ackerman, M. Y., Paskaluk, S. A., & Li, J. (2013a). A new protocol to characterize thermal protective performance of fabrics against hot liquid splash. *Experimental Thermal and Fluid Science*, *46*, 37–45.

Lu, Y., Song, G., & Li, J. (2013b). Analysing performance of protective clothing upon hot liquid exposure using instrumented spray manikin. *The Annals of Occupational Hygiene*, *57*(6), 793–804.

Lu, Y., Song, G., Li, J., & Paskaluk, S. (2013c). Effect of an air gap on the heat transfer of protective materials upon hot liquid splashes. *Textile Research Journal*, *83*(11), 1156–1169.

Lu, Y., Song, G., Zeng, H., Zhang, L., & Li, J. (2014). Characterizing factors affecting the hot liquid penetration performance of fabrics for protective clothing. *Textile Research Journal*, *84*(2), 174–186.

Mandal, S. (2009). *Studies on seam quality with sewing thread size, stitch density and fabric properties* [M. Phil thesis]. Kowloon: The Hong Kong Polytechnic University.

Mandal, S. (2016). *Studies of the thermal protective performance of textile fabrics used in firefighters' clothing under various thermal exposures* [Ph.D. thesis]. Edmonton: University of Alberta.

Mandal, S., Lu, Y., Wang, F., & Song, G. (2014). Characterization of thermal protective clothing under hot water and pressurized steam exposure. *AATCC Journal of Research*, *1*(5), 7–16.

Mandal, S., & Song, G. (2011). *Characterization of protective textile materials for various thermal hazards*. In: *Fiber society spring conference, Kowloon, Hong Kong, May 23-25*.

Mandal, S., & Song, G. (2014). An empirical analysis of thermal protective performance of fabrics used in protective clothing. *The Annals of Occupational Hygiene*, *58*(8), 1065–1077.

Mandal, S., & Song, G. (2015). Thermal sensors for performance evaluation of protective clothing against heat and fire: A review. *Textile Research Journal*, *85*(1), 101–112.

Mandal, S., & Song, G. (2016a). Characterizing fabrics in firefighters' protective clothing: Hot water immersion and compression. *AATCC Journal of Research*, *3*(2), 8–15.

Mandal, S., & Song, G. (2016b). Characterizing thermal protective fabrics of firefighters' clothing in hot surface contact. *Journal of Industrial Textiles*, https://doi.org/10.1177/0123456789123456.

Mandal, S., Song, G., Ackerman, M., Paskaluk, S., & Gholamreza, F. (2013). Characterization of textile fabrics under various thermal exposures. *Textile Research Journal*, *83*(10), 1005–1019.

Mandal, S., Song, G., & Gholamreza, F. (2016). A novel protocol to characterize the thermal protective performance of fabrics in hot water exposures. *Journal of Industrial Textiles*, *46*(1), 279–291.

Moritz, A. R., & Henriques, F. C. (1947). Studies of thermal injury II. The relative importance of time and surface temperature in the causation of cutaneous burns. *The American Journal of Pathology*, *23*(5), 695–720.

Murtaza, G. (2012). *Development of fabrics for steam and hot water protection* [MSc Thesis]. Edmonton, Canada: University of Alberta.

Pennes, H. H. (1948). Analysis of tissue and arterial blood temperatures in resting human forearm. *Journal of Applied Physiology*, *1*(1), 93–122.

Rossi, R. (2003). Firefighting and its influence on the body. *Ergonomics*, *46*(10), 1017–1033.

Rossi, R., Indelicato, E., & Bolli, W. (2004). Hot steam transfer through heat protective clothing layers. *International Journal of Occupational Safety and Ergonomics*, *10*(3), 239–245.

Sati, R., Crown, E., Ackerman, M., Gonzalez, J., & Dale, J. D. (2008). Protection from steam at high pressure: Development of a test device and protocol. *International Journal of Occupational Safety and Ergonomics*, *14*(1), 29–41.

Song, G. (2004). *Modeling thermal protection outfit for fire exposures* [Ph.D. thesis]. Raleigh, NC: North Carolina State University.

Song, G., Barker, R., Grimes, D. R., & Thompson, D. (2005). Comparison of methods used to predict the burn injuries in tests of thermal protective fabrics. *Journal of ASTM International*, *2*(2), 88–98.

Song, G., & Mandal, S. (2016). Testing and evaluating thermal comfort of clothing ensembles. In L. Wang (Ed.), *Performance testing of textiles: Methods, technology, and applications* (pp. 39–64). United Kingdom: Woodhead Publishing.

Song, G., Mandal, S., & Rossi, R. (2016). *Thermal protective clothing: A critical review*. United Kingdom: Woodhead Publishing.

Stoll, A. M. (1962). Thermal protective capacity of aviator's textiles. *Aerospace Medicine*, *33*(7), 846–850.

Stoll, A. M., & Chianta, M. A. (1968). Burn production and prevention in convective and radiant heat transfer. *Aerospace Medicine*, *39*(10), 1097–1100.

Stoll, A. M., & Chianta, M. A. (1969). Method and rating system for evaluation of thermal protection. *Aerospace Medicine*, *40*(11), 1232–1238.

Stoll, A. M., & Greene, L. G. (1959). Relationship between pain and tissue damage due to thermal radiation. *Journal of Applied Physiology*, *14*(3), 373–382.

Torvi, D. A. (1997). *Heat transfer in thin fibrous materials under high heat flux conditions* [Ph.D. thesis]. Edmonton: University of Alberta.

Zhang, H., McQueen, H. R., Batcheller, C. J., Ehnes, L. B., & Paskaluk, A. S. (2015a). Characterization of textiles used in chefs' uniforms for protection against thermal hazards encountered in the kitchen environment. *The Annals of Occupational Hygiene*, *59*(8), 1058–1073.

Zhang, H., McQueen, H. R., Batcheller, C. J., Paskaluk, A. S., & Murtaza, G. (2015b). Clothing in the kitchen: Evaluation of fabric performance for protection against hot surface contact, hot liquid and low-pressure steam burns. *Textile Research Journal*, *85*(20), 2136–2146.

This page intentionally left blank

Part Three

Testing by applications

This page intentionally left blank

Specific testing of geotextiles and geosynthetics

10

P.I. Dolez
CTT Group, Saint-Hyacinthe, QC, Canada

10.1 Introduction

Geosynthetics have been developed to offer a quality-controlled, manufactured alternative to materials traditionally used in geotechnics and civil engineering like concrete, rocks, and clay. They include geotextiles, geomembranes, geogrids, geonets, geosynthetic clay liners, geofoams, and geocomposites. They are the result of the creativity, ingenuity, and hard work of pioneers who have inspired following generations of researchers in this field.

Geosynthetics are generally made of polymeric materials (Koerner, 2012). The main functions provided by geosynthetics are separation, reinforcement, filtration, drainage, and containment. Their advantages versus traditional civil engineering materials include their controlled performance, rapidity of deployment, ability to allow otherwise impossible designs and applications, wide availability, and low carbon footprint.

The first documented modern use of textiles in civil engineering can be traced back to 1926, when the South Carolina Highway Department made an attempt to reinforce roads with cotton fabrics (Beckman & Mills, 1957). The material did not hold long due to biodegradation. Polymer geosynthetics were developed in the early 1950s with geomembranes targeting civil engineering and agricultural applications (Kolbasuk, 2005). Polyethylene was first used in Europe and South Africa, while the United States initially elected polyvinyl chloride as geomembrane raw material (Koerner, 2012).

The first polymer geotextiles appeared in the late 1950s as an alternative to granular soil filters (Koerner, 2012): a woven fabric was used in combination with interlocking concrete blocks to protect from erosion the beach at the Florida home of Carthage Mills' president (Barrett, 1966). In the late 1960s Rhone-Poulenc in France started working with needle-punched nonwovens for separation and/or reinforcement in roads, railroad ballast, embankments, and earth dams (Koerner, 2012). In 1970, J.P. Giroud designed the first earth dam for which a geotextile was used (Giroud, Gourc, Bally, & Delmas, 1977): The Valcros dam drainage system in France included a needle-punched nonwoven fabric wrapped around the gravel downstream drain. As of the last assessment, conducted in 2002 after 21 years of service, the system is still performing satisfactorily (Artieres, Oberreiter, & Aschauer, 2009).

Advanced Characterization and Testing of Textiles. https://doi.org/10.1016/B978-0-08-100453-1.00010-6

For their part, geogrids were developed in the United Kingdom by Netlon Ltd., now Tensar (Shukla, 2012): the first sample was produced in their Blackburn laboratories in July 1978. Geonets came a little later, with the first documented environmental application in 1984 in a double-lined hazardous liquid waste pond in Hopewell, VA. Geosynthetic clay liners appeared both in the United States and Germany during the same period (Koerner, 2012). The product developed in the United States contained bentonite mixed with an adhesive and bonded between two geotextiles. It was first used in 1986 for solid waste containment as a secondary liner in complement to a geomembrane. In the German product, the bentonite was needle-punched between two geotextiles. Finally, extruded and expanded polystyrene geofoam has initially been used for the thermal insulation of roads, railways, and airfield pavements in the mid-1960s (Horvath, 1996). It later found an application as light fill in bridge embankments.

With the multiplication of geosynthetic products and applications, and their increasing regulatory requirement, came the need for standard test methods to assess their performance under service conditions, as well as for quality control during deployment. If attempts towards standardization started in the mid-1970s, no real progress was made until committees dedicated to geosynthetics were formed (Suits, 2006). This was the case with the ASTM Committee D35 on Geotextiles and related products that was established in 1986 (and later became Committee D35 on Geosynthetics). It currently oversees over 155 approved standards. In Europe, the CEN Technical Committee 189 on Geosynthetics was formed in 1989. It holds a portfolio of 69 published standards. At the international level, the ISO Technical Committee 221 on Geosynthetics was approved in 2000. It has 36 published standards under its responsibility.

This chapter focuses on geotextiles and other textile-based geosynthetics like geogrids, geocomposite clay liners, and drainage composites. For each category of product, it provides a description of the main test methods grouped according to the type of property/performance: physical, composition, mechanical, hydraulic, thermal, and durability. Textile reinforcement may also be used in geomembranes, with a woven scrim encapsulated between layers of high performance polyethylene. Details about test methods for geomembranes, including measurement of the resistance to delamination of the reinforced geomembranes (also called ply adhesion) can be found in (Scheirs, 2009).

10.2 Geotextiles

According to ISO, geotextiles are defined as “planar, permeable, polymeric (synthetic or natural) textile material, which may be nonwoven, knitted, or woven, used in contact with soil and/or other materials in geotechnical and civil engineering applications” (ISO 10318, 2015). About 95% of polymeric geotextiles are made of polypropylene (Koerner, 2012). Other polymers used to manufacture geotextiles are polyester, polyethylene, and polyamide. They can be found as staple fiber, monofilament, multifilament, staple fiber yarn, and slit-film mono- and multifilament. Natural fibers such as

jute, coir, sisal, kenaf, ramie, palm leaves, wood, and split bamboo are also used to manufacture geotextiles for short-term geotechnical applications (Desai & Kant, 2016).

Woven geotextiles involve the interlacing of warp and weft yarns according to a regular pattern. Most geotextiles are plain weave (i.e., with a 1:1 configuration; Koerner, 2012). Woven geotextiles are generally stronger but less stretchable than other textile structures. Nonwovens are directly produced from the polymer or using staple fibers (i.e., without going through a yarn processing step). The fibers are disposed in a more or less random manner and formed into a three-dimensional structure. The web thus obtained is further consolidated using mechanical, thermal, and/or chemical means. The advantages of the nonwoven process include a high manufacturing rate, low cost, capacity to handle a wide variety of fibers, lower level of requirements in terms of fiber properties, and wide range of functions. This makes them the most frequent textile structure used for geotextiles (Bérubé & Saunier, 2016). Finally, knitted geotextiles are more marginally encountered. They are produced by interlacing symmetrically disposed loops together. This provides knitted geotextiles with a very large extensibility and directional mechanical performances. More details on geotextile manufacturing techniques can be found in (Bérubé & Saunier, 2016).

In terms of function, geotextiles may be used to provide separation, reinforcement, filtration, and drainage (Koerner, 2012). For instance, they can be employed to separate dissimilar materials such as subgrade and stone base in roads, foundation and embankment soil in earth and rock dams, and geomembrane and sand drainage layer in landfills. In addition, geotextile reinforcements may be found over soft soils in airfields, railroads, and landfills, over unstable landfills in closure systems, as well as in earth and rock dams, soil slopes, and embankments for example. Cross-plane flow filtration may also be provided by geotextiles positioned in place of granular soil filters, around crushed stone, perforated pipes or drain-molded cores, beneath leaching landfills, stone riprap, and gabions, as a snow or silt fence, etc. Finally, geotextiles are used for in-plane flow drainage in earth dams, retaining walls, roof gardens, and earth fills, as well as beneath geomembranes and railroad ballast, for instance.

10.2.1 Sampling and specimen preparation and conditioning

Geotextile sampling protocols have been developed to allow providing test results representative of the general product behavior and ensuring the best possible statistical significance of the average finding (ISO 9862, 2005). When geotextiles are supplied in rolls, samples should be taken from the third winding of the roll onward and cut over its full width. The sample length is defined by the tests to be conducted. Specimens should be distributed over the roll width, with the exception of a 100-mm section from each edge on the cross-machine direction. The last two windings of the roll should also be excluded, as well as any section which appears damaged during visual examination.

The cross-machine direction is generally marked with an arrow on the geotextile sample/specimens (ISO 9862, 2005). Other information to be reported on samples includes manufacturer and product name, and unit identification and dimension (ISO 10320, 1999). Samples and specimens shall be kept at room temperature in a dry and dark place, free from dust and other potential physical and chemical agents until tested

(ISO 9862, 2005). When tests require exact dimensions for the specimen, specimens should be cut using a punching die.

Specific onsite sampling procedures are also recommended depending on whether the sampling is conducted for manufacturer's quality control (MQC) testing, manufacturer's quality assurance (MQA) testing, or purchaser's specification conformance testing (ASTM D4354, 2012). They specify different numbers of units to be selected as lot sample as a function of the units in the lot.

Before being tested, it is generally required that geotextiles are conditioned at standard laboratory atmospheric conditions until moisture equilibrium has been reached, as evidenced by a stable mass. Conditions generally prescribed for geotextiles are a temperature of 21°C and a relative humidity of 65%, or a temperature of 23°C and a relative humidity of 50% (ASTM D1776, 2016; ISO 554, 1976). A conditioning period of 24 h is generally sufficient for geotextiles that do not exhibit excessive moisture on reception (ASTM D5199, 2012).

10.2.2 Physical properties

Physical properties most commonly assessed in the case of geotextiles include thickness and mass per unit area. In addition, information about the physical characteristics of the geotextile fiber constituents is sometimes sought. Finally, test methods for some application-specific performance are described: liquid absorbency and light penetration for erosion control products, and asphalt retention for paving fabrics.

Geotextile thickness is generally measured using a presser-foot apparatus equipped with a thickness gauge (ASTM D5199, 2012; ISO 9863-1, 2016). The pressure to be used for geotextiles is 2 kPa, and the presser-foot diameter is 56.4 mm. The dimension of the circular test specimens should be larger than 1.75 times the presser-foot diameter (ISO 9863-1, 2016), or such that the specimen extends 10 mm beyond the edge of the presser foot (ASTM D5199, 2012). The thickness is measured 5 s (ASTM D5199, 2012) or 30 s (ISO 9863-1, 2016) after the pressure has been applied to the specimen with the presser foot. The measurement should be performed on 10 specimens spread across the full width of the geotextile roll. The average thickness of the 10 specimens measured, as well as the coefficient of variation, are reported. Other values of pressure applied and dimension of the presser foot may also be used for specific types of geotextiles (ASTM D1777, 1996). In the case of erosion control products, the pressure is 0.2 kPa and the pressure foot diameter is 150 mm (ASTM D6525, 2016). For multilayer products, it is possible to determine the thickness of each layer by stacking five specimens on top of each other with a separator plate between each specimen and identifying the boundaries between the individual layers using a magnifying system (ISO 9863-2, 1996).

The mass per unit area of geotextiles is generally determined by measuring the weight of specimens of known dimensions (ASTM D5261, 2010). Depending on the test method, a minimum of 5 specimens (ASTM D5261, 2010) or 10 specimens (ISO 9864, 2005) should be tested. All specimens should have the same dimension, be distributed over the width of the sample, and their combined surface area should be at least 100,000 mm^2 (ASTM D5261, 2010; ISO 9864, 2005). For each specimen, the

mass per unit area is computed by dividing its weight by its surface area. The average mass and standard deviation are reported. For turf reinforcement mats (ASTM D6566, 2014) and erosion control blankets (ASTM D6475, 2006), the combined surface area of the specimens should be 230,000 and 500,000 mm^2, respectively. Test methods are also available for full rolls, full width samples, small swatches of fabric, and narrow fabrics (ASTM D3776, 2009). In these cases, the specimen dimensions are adjusted to be relevant to the product or specimen size.

Typical fiber morphological characterization includes length, diameter, and crimp. Staple fiber average length and length distribution are assessed by manually measuring the length of 50 individual fibers (ASTM D5103, 2007). Each fiber is fully extended on a board without stretching using tweezers securing it at the tips, and measured using a precision scale. Most standard techniques used to measure fiber diameter involve cutting small sections of fibers and estimating the diameter from a longitudinal view of the fiber snippets placed on a microscope slide using a projection microscope (ASTM D2130, 2013) or an optical fiber diameter analyzer (ASTM D6500, 2000). An alternative technique disperses the fiber snippets in isopropanol and uses a Sirolan-Laserscan fiber diameter analyzer that computes the fiber diameter based on the reduction in laser beam intensity created when the fiber snippets are passing through the measuring cell (ASTM D6466, 2010). The fiber diameter may also be measured using cross-sectional images of fiber bundles (AATCC TM20, 2013). Finally, the crimp frequency of manufactured staple fibers may be characterized using one of three techniques (ASTM D3937, 2012). Method 1 is performed on 25 individual fibers laid on a plush, color-contrasting board while method 2 involves fiber chips. In both cases, the crimps are visually observed, with the eventual help of a magnifier, and counted. The crimp frequency is computed by dividing the number of crimps by the length of the straightened specimen. In method 3, the fibers are placed on microscope slides and imaged with a 10× magnification projector.

The liquid absorbency of erosion control nonwoven products can be characterized in terms of absorbency time, absorptive capacity, and wicking rate (EDANA 10.3, 1999). The liquid absorbency time is measured by dropping a specimen strip loosely rolled in a wire basket onto the surface of a liquid from a height of 25 cm and recording how long it takes for the basket to sink below the surface of the liquid. The liquid absorptive capacity is determined by measuring the weight of a specimen after specific periods of immersion in a liquid and further free vertical drainage. Finally, the wicking rate is assessed by measuring the rate of the vertical capillary rise in the specimen strip suspended in a liquid.

Light penetration is also an important parameter for erosion control products as it affects the growth of the plants underneath. The turf reinforcement mat specimen is secured vertically in a light penetration box with a light bulb on one side and a light meter on the other side (ASTM D6567, 2014). The percentage of light penetration is computed by dividing the reading of the light meter with the specimen in place by the reading without the specimen.

Finally, the asphalt retention of fabrics used in asphalt paving is characterized by weighing specimens before and after they have been immersed in heated asphalt cement and drained (ASTM D6140, 2000). The asphalt cement temperature is 135°C and

the immersion time is 30 min. The draining procedure involves hanging the specimens in a mechanical convection oven at 135°C for 30 min on each side. The asphalt-coated specimens are cooled down for 30 min before being weighed. The asphalt retention is calculated as the weight difference before and after exposure divided by the initial specimen surface area.

10.2.3 Composition

A first step in the analysis of the geotextile composition is identifying the nature of the fiber(s) used to manufacture the geotextile and quantify their proportion in the case of blends. Two strategies are available for fiber identification (ASTM D276, 2012): one is based on the analysis of the solubility of the fiber in a series of chemicals while the other one relies on the use of a Fourier transform infrared spectrometer (FTIR) or a double-beam spectrometer. In both cases, the identification of the fiber class is made using a decision scheme. These methods apply to a list of 29 types of synthetic and natural fibers. It includes the four polymers mostly used in geotextiles, i.e., polypropylene, polyester, polyethylene, and polyamide, yet without distinguishing between the different polyolefins. The methods also apply to some natural fibers relevant to geotextiles: jute and ramie. An analysis of the fiber longitudinal and cross-section view by microscopy allows distinguishing between species for plant-based and animal hair fibers. The fiber physical properties such as its density, melting point, refractive index, and birefringence are also characterized to confirm the identification. For instance, differential scanning calorimetry can provide the melting and crystallization temperatures (ASTM D3418, 2015; ASTM E794, 2006) and enthalpies (ASTM E793, 2006) of polymers, which may be used to differentiate between polypropylene and polyethylene.

A quantitative analysis of fiber blends is possible once they have been properly identified and the nonfibrous materials have been removed (CAN/CGSB-4.2 No 14, 2005). Techniques to remove the nonfibrous materials can be found in Annex A of ISO 1833-1 (2006). A first strategy of quantitative analysis of fiber blends is based on the manual separation of the fibrous components (CAN/CGSB-4.2 No 14, 2005): the weight of each component fiber in two specimens is measured after manual dissection and sorting, followed by oven drying, and is normalized by the weight of the oven-dried original specimen. A second strategy uses chemicals to dissolve the different components of the blend in turn. The weight of the residue is measured after each step to allow computing the original composition of the blend (CAN/CGSB-4.2 No 14, 2005; ISO 1833-1, 2006). Corrections often have to be made as the solvent used to dissolve one fiber may also affect to a certain level the other components of the blend. For instance, polypropylene may be dissolved using xylene heated at 115°C and separated from certain types of fibers including nylon (CAN/CGSB-4.2 No 14, 2005; ISO 1833-16, 2006). A 75% sulfuric acid solution heated at 50°C or a 20% hydrochloric acid solution at room temperature may be used to dissolve nylon in a blend with polyester (CAN/CGSB-4.2 No 14, 2005). Formic acid can also provide the ratio of nylon fibers in binary blends with polyester or polypropylene (ISO 1833-7, 2006). Other methods relevant to geotextiles include the use of sulfuric acid to obtain the composition of

blends of polyester with natural and regenerated cellulose fibers (ISO 1833-11, 2006) and phenol and tetrachloroethane to quantify the ratio of polyester and polypropylene in binary mixtures (ISO 1833-24, 2010). Protocols are also available for ternary fiber mixtures (ISO 1833-2, 2006).

In terms of chemical analysis, titration is used to determine the carboxyl end group (CEG) content of poly(ethylene terephthalate) (PET) yarns (GRI GG7, 1998). Orthocresol is employed as the solvent to dissolve PET yarns at 80°C. The resulting PET solution is titrated using potassium hydroxide. A low value of CEG content indicates a high resistance of the yarn to hydrolysis (Torosian & Mac Millan, 2016).

10.2.4 Mechanical properties

Tests performed to characterize geotextile mechanical performance were initially based on textile test methods (Zanzinger, 2016). Geotextile-specific test methods were then developed to better describe their behavior in service, particularly the interaction with soil and loading configurations unique to geotechnical applications.

Two categories of short-term mechanical test methods may be identified (Zanzinger, 2016): those involving stress-strain behavior, either in tensile, compression, or shear, and those characterizing the ability of the material/product to preserve its integrity, which are generally based on the assessment of tearing, puncture, and abrasion resistance. It may be noted that, in some instances, for example for soil-reinforcement geotextiles, the ability of the product to survive stresses applied during installation is better characterized using tensile tests than conventional integrity test methods. Furthermore, the evaluation of long-term mechanical performance, for example under cyclic loading, may be critical for some applications: it is covered in Section 10.2.7.

The assessment of geotextile stress-strain behavior may start at the fiber or yarn scale, for example using ASTM D3822 (2014) or ASTM D2256 (2010), respectively. When the final product is considered, three test modes are most often used: tensile, compression, and shear.

Tensile tests performed on geotextiles involve a wide variety of specimen geometries, dimensions, and loading rates. For instance, the strip (or small width) test is carried out on 25 or 50 mm-wide rectangular specimens using grips that are at least as wide as the specimen (Fig. 10.1A) (ASTM D5035, 2011). It includes the raveled strip test for woven fabrics, where the specimen is raveled on each side over 5 to 7.5 mm

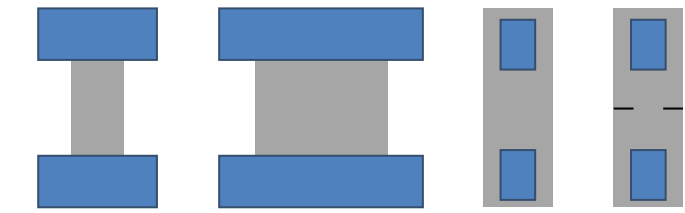

Fig. 10.1 Tensile test configurations, (A) strip, (B) wide width, (C) grab, and (D) modified grab.

depending on the final specimen width, and the cut strip test for nonwovens and coated fabrics. In both cases, the test frame loading rate is 300 mm/min, and the gauge length is 75 mm. This test is not recommended for knitted or other highly deformable fabrics. Five specimens are tested in the machine direction and eight in the cross direction. Any result for which the specimen slips in the jaws or fails on the edge of or in the jaws is discarded; new specimens shall be tested until the required number of valid breaks has been reached. The average breaking force and apparent elongation at specified force or breaking force are computed. The test may be conducted on dry, conditioned specimens as well as on wet specimens. The cut strip test principle is also used for rolled erosion control products (ASTM D6818, 2014). The gauge length and loading rate are the same but the specimen width is larger at 100 mm.

For the wide width tensile test, the width of the specimen is 200 mm, much larger than its gauge length of 100 mm (Fig. 10.1B; ASTM D4595, 2011; ISO 10319, 2015). This configuration allows reducing stress concentrations in the specimen during the test, thus giving better access to real plane strain tensile conditions (Zanzinger, 2016). It is also used to evaluate the tensile strength of stitched or bonded geotextile seams (ASTM D4884, 2014; ISO 10321, 2008). The strain rate is relatively low, either 10% (ASTM D4595, 2011) or 20%/min (ISO 10319, 2015). The number of specimens tested in the machine and cross direction is five (ISO 10319, 2015) or six (ASTM D4595, 2011). That number may also be computed if a reliable estimate of the coefficient of variation of individual data is available. Some test methods require the use of an extensometer (ISO 10319, 2015) while others only recommend it when the material's modulus is to be obtained (ASTM D4595, 2011). Three types of clamps are recommended: capstan or roller wedge clamps, or roller clamps. The results are generally expressed in terms of tensile strength, elongation at maximum force, and secant tensile modulus (ASTM D4595, 2011; ISO 10319, 2015). The initial tensile modulus, offset tensile modulus, and breaking toughness (or work-to-break per unit surface area) may also be reported (ASTM D4595, 2011). In the case of seams, the seam efficiency is computed by dividing the tensile strength of the seam by that of the unseamed material tested in the same direction (ASTM D4884, 2014; ISO 10321, 2008).

For their part, grab tests are performed on 100 mm-wide specimens (ASTM D4632, 2015). Each clamp jaw is equipped with one 25×50 mm face, its longest dimension being parallel to the direction of the applied load (Fig. 10.1C). The initial distance between the clamps is 75 mm. The test is conducted at 300 mm/min until the specimen has failed. The average breaking load as well as the apparent elongation at breaking load are computed. The number of specimens to be tested depends on the test method: for instance, it is ten per direction or as given by the estimate of the coefficient of variation when available for ASTM D4632 (2015) or five in the machine direction and eight in the cross direction for ASTM D5034 (2009). In addition, specimen results are discarded if the specimen breaks at the edge of or in the jaws (ASTM D4632, 2015). A modified grab test method is also available where the specimen is slit on both sides of its width to leave an intact 25 mm-wide central section (Fig. 10.1D) (ASTM D5034, 2009). Grab and modified grab tests may be performed on dry or wet woven and nonwoven geotextiles, but not on knitted fabrics (ASTM D4632, 2015; ASTM D5034, 2009).

The stiffness (or flexural rigidity) of geotextiles may be assessed using the cantilever or heart loop test. In the cantilever test for geotextiles, a 50 × 900 mm specimen is slid at 120 mm/min on a platform overhanging an indicator inclined at an angle of 41.5 degrees below the plane of the platform (ASTM D7748, 2014). The length of the overhang is measured when the specimen tip touches the indicator under its own weight. Alternative specimen dimensions of 25 × 200 mm are also provided in a similar test method aimed at fabrics (ASTM D1388, 2014). The cantilever principle is also applied to determine the stiffness of turf reinforcement mats (ASTM D6575, 2016); specimens are 101.6 × 457.2 mm in that case. The heart loop test is recommended for fabrics that have a tendency to curl or twist (ASTM D1388, 2014). It involves measuring the length of a heart-shaped loop formed with a 25–75 mm-wide and 15, 20, or 25 mm long strip of fabric when it hangs vertically under its own weight. In both cases, the bending length and flexural rigidity may be computed.

In the case of erosion control products, performance may also be characterized in terms of compression and resiliency. The short-term compression behavior of turf reinforcement mats is assessed by the deformation experienced under short-term compressive loading (ASTM D6454, 1999). In practice, five specimens of at least 120 × 120 mm are subjected to compressive loading between two parallel plates at a rate of 10%/min or 1 mm/min. The compressive stress and residual thickness at yield point (or at a point where a significant change in the stress-strain curve is observed if the material does not display a well-defined yield point) are reported. The resiliency is evaluated by measuring the thickness recovery of turf reinforcement mats after they have been subjected to three compression loading cycles at 689 kPa for 1 min per cycle (ASTM D6524, 2016). Specimens are 100 × 100 mm and 10 specimens are generally tested. The resiliency is defined as the ratio between the residual and initial thickness of the specimens.

A last test method characterizing the behavior of geotextiles under load deals with their shear strength against soil or another geosynthetic. The geotextile is installed in a direct shear box of at least 300 × 300 mm and slid against standard sand (ISO 12957-1, 2005) or any other relevant material (ASTM D5321, 2014). The friction behavior of the geotextile/contact material system is characterized under normal stresses representative of field conditions at a constant rate of displacement (ASTM D5321, 2014; ISO 12957-1, 2005). The rate of displacement is generally set at 1 mm/min for geotextile/sand and other soil systems and at 5 mm/min for geotextile/geosynthetic systems. In the case of excess pore pressure at the interface, the displacement rate may be decreased to as low as 0.025 mm/min (ASTM D5321, 2014). The shear force is recorded as a function of the shear displacement as one section of the shear box moves relative to the other section. The variation of the peak shear stress as a function of the applied normal stress defines the Mohr-Coulomb shear strength envelope of the tested system. In practice, a minimum of three test points are usually measured at different normal stresses. Values of 50, 100, and 150 kPa may be used for the characterization of geotextile friction behavior against standard sand (ISO 12957-1, 2005). Other normal stress values more relevant to field conditions may also be used (ASTM D5321, 2014). The Mohr-Coulomb friction angle is provided by the slope of a best fit straight line through the peak shear stress vs. applied normal stress data points. If the geotextile is

tested against soil, it may be necessary to add water to produce the desired water content. Depending on the type of soil, standing times of up to 36 h prior to compaction may be required. Specific conditions such as separate wetting, soaking, or hydration of the geotextile are also possible.

A series of puncture tests are available to assess the ability of the geotextile to maintain its integrity during installation and service. Some use a mechanical test frame and small diameter probes to evaluate the maximum puncture force in static mode for specimens secured between ring clamps: for instance, the FTMS 101C/2065 (1982) test method has a 6.3 mm diameter probe tip and a 25 mm clamp ring internal diameter, with a 500 mm/min puncture probe displacement. The probe diameter of the ASTM D4833 (2007) standard test method is slightly larger at 8 mm and has a chamfered flat end; the clamp ring opening is 45 mm in diameter, and the displacement rate is 300 mm/min. However, these test methods may not be appropriate for some woven geotextiles or other geotextiles with large openings. Other static puncture tests use a 50 mm diameter probe with a flat tip to apply a multidirectional force on the geotextile (ASTM D6241, 2014; ISO 12236, 2006). This test is sometimes called the CBR Test. The hole in the plates securing the specimen has a diameter of 150 mm and the probe displacement rate is 50 mm/min. The mean push-through force provides a measurement of the material puncture strength. The displacement at maximum puncture force may also be reported.

An alternative geometry for the puncture probe is a square pyramid. When this test is used to assess the protective efficiency of nonwoven geotextiles for geomembranes against gravel, the pyramid is 12.5 mm high with a 90 degrees apex angle and a 25-mm diameter (ASTM D5494, 1993). The geomembrane/geotextile system may be allowed to deform during the test, in which case the specimen is fixed between two 50 mm internal diameter ring clamps and the probe displacement rate is 50 mm/min. Water is placed underneath the specimen, and puncture is detected when an electrical contact is established between the puncture probe and the underlying water medium. In another configuration, the geomembrane/geotextile system is placed on a rigid aluminum plate which prevents it from deforming during puncture. The force at which puncture occurs is also detected by electrical means. In that case, the probe displacement rate is 1 mm/min. Geotextiles may also be tested on their own with a square pyramid probe (NF G38- 019, 1988). In that case, the puncture force corresponds to the maximum force recorded during the test. For that test, the pyramid has a 27.5 mm side and a 90 degrees apex angle, the specimen is held in a 50-mm internal diameter ring clamp, and the probe displacement rate is 50 mm/min.

The pyramid geometry may also be used in hydrostatic puncture tests involving a large-scale pressure vessel, typically 500 mm in diameter (ASTM D5514, 2014). The geotextile is placed over a test base consisting of four pyramids positioned 90 degrees apart on a 200-mm diameter circle. Clean Ottawa sand is used to fill the area between the pyramids and control their exposed height. The geotextile is covered with a 0.4 mm thick latex sheet to create an impermeable barrier with the overlaying water layer that should reach 127 mm over the pyramid top. The pressure vessel is pressurized with 0.7 kPa increments every 30 min until rupture occurs or the maximum pressure is reached. If no failure is obtained, the test is started over with increasing the pyramid

height by 13 mm increments. The data are used to compute the critical height, which is the maximum exposed pyramid height that will not cause a failure of the geotextile at a specified hydrostatic pressure. The geotextile thickness deformation at the indentation sites immediately after failure as well as the thickness recovery 90 min after the load has been removed are also recorded. This test may also be performed using three cones disposed 120 degrees apart instead of the four pyramids, or site-specific soil or other materials. A modified version of the ASTM D5514 (2014) test method was proposed to assess the efficiency of geotextiles as protective cushions against puncture for geomembranes (Blond, Bouthot, Vermeersch, & Mlynarek, 2003); it involves a replication of the entire lining system, including the subgrade and drainage layer in the case of double lining systems, in the pressure vessel. An appropriate friction reduction system is installed over the inside wall of the vessel.

Dynamic puncture may be conducted by dropping a conic probe from a certain height on the geotextile secured with clamping rings (ISO 13433, 2006). The 1-kg, 45 degrees tip angle stainless-steel cone is dropped, point first, from a distance of 500 mm onto the center of the 150 mm diameter specimen surface. The resistance of the geotextile to cone penetration is assessed by measuring the size of the hole using a narrow-angle graduated cone.

The ability of the geotextile to maintain its integrity during installation and service may also be characterized using burst tests. Ball burst tests involve exerting a force on a circular specimen using a steel ball replacing one of the clamps in a mechanical test frame (ASTM D3787, 2016; CAN/CGSB 4.2-11.2, 1989). The steel ball is 25.4 mm in diameter, and the specimen clamp rings have an internal diameter of 45.45 mm. The ball displacement rate is 300 mm/min. The ball-bursting strength is provided by the average of the maximum force at burst of 5–10 specimens depending on the test method. Some standards require the use of a constant-rate-of-traverse test frame, with the ball replacing the fixed clamp while the specimen holder is installed on the movable arm (ASTM D3787, 2016). Specimens may be tested in the wet condition (CAN/CGSB 4.2-11.2, 1989). An alternative to ball burst involves the use of a hydraulic or pneumatic diaphragm tester (ASTM D3786, 2013; CAN/CGSB 4.2-11.1, 1994). This test is sometimes called the Mullen test. The specimen is clamped over an expandable diaphragm using 31-mm internal diameter rings. The pressure under the diaphragm is increased at a rate that allows recording a burst in about 20 s. The pressure reading at specimen burst is corrected by subtracting the pressure required to extend the diaphragm membrane without the specimen at the same height at which the specimen burst has been recorded. Measurements are performed on ten specimens, leading to a mean bursting strength. Specimens may be tested in the wet condition (CAN/CGSB 4.2-11.1, 1994).

A last series of tests aimed at assessing the geotextile ability to maintain its integrity during installation and service comprise tearing and abrasion. Tear strength may be tested using the trapezoid method (ASTM D4533, 2015; CAN/CGSB 4.2-12.2, 2012). It measures the force required to propagate a tear in the geotextile. The non-parallel sides of an isosceles trapezoid specimen (75 mm length and 25 mm and 100 mm long bases) are clamped in the jaws of the mechanical test frame. A 15-mm cut is made in the middle of the 25-mm base of the trapezoid specimen. The tearing force is generally

given by the maximum force recorded when the tear is propagated at a rate of 300 mm/min. In the case of woven fabrics, some test methods specify disregarding the initial peak and averaging the maximum force values recorded for the next five successive 5-mm tearing intervals (CAN/CGSB 4.2-12.2, 2012). Depending on the test method, 5–10 specimens are tested in the machine and cross direction (ASTM D4533, 2015; CAN/CGSB 4.2-12.2, 2012). Specimens may be tested in the wet condition (ASTM D4533, 2015). Geotextile resistance to abrasion may be assessed using the sliding block method. The test specimen is mounted on a fixed rectangular platform loaded with a weight (ASTM D4886, 2010; ISO 13427, 2014). An opposing rectangular block covered with a 100-grit emery cloth is rubbed against the specimen using a uniaxial horizontal motion. A fixed number of rubbing cycles at a specific frequency is applied, for instance 250 cycles at 30 cycles per minute for ASTM D4886 (2010) and 750 cycles at 90 cycles per minute for ISO 13427 (2014). The resistance to abrasion is quantified in terms of loss in tensile breaking force as a result of the abrasion treatment compared to the original condition (ASTM D4886, 2010; ISO 13427, 2014). Specimens may be tested in the wet condition (ASTM D4886, 2010).

10.2.5 Hydraulic and barrier properties

Hydraulic properties of geotextiles are controlled by their pore size, pore size distribution, and porosity (Carroll, 1987). Due to the difficulty in assessing precisely these characteristics in fabrics, criteria related to hydraulic performance are measured instead: opening size, permittivity, gradient ratio, and transmissivity.

Several test methods exist to measure the opening size of geotextiles, which characterizes their ability to retain soil particles (Blond, Vermeersch, & Diederich, 2015). The apparent opening size (AOS) of geotextiles is determined using a series of glass beads of calibrated dimensions and dry sieving (ASTM D4751, 2016). It corresponds to the approximate largest particle size of which 5% or less would pass through the geotextile. In practice, ten different ranges of glass bead diameters between 0.075 and 2.0 mm are used. Starting from the smallest range, 50 g of glass beads are placed on the geotextile specimen secured with a hoop inside a 200-mm diameter sieve frame or between two sieve frames. The sieve frame is covered and installed in a mechanical shaker equipped with a tapping arm imparting a lateral and vertical motion to the sieve. After 10 min, both the glass beads still on the surface of the specimen and those that have passed through it are weighted. The operation is repeated with increasingly larger bead ranges until the fraction of glass beads that have passed through the specimen is less than or equal to 5%. The AOS value may be computed by plotting the percentage of passing beads as a function of their size and determining the bead diameter corresponding to a 5% passing ratio by connecting with a straight line the data just above and below the 5% passing ratio. Otherwise the AOS value is attributed to the largest bead diameter of which 5% or less passed through the specimen.

An alternative technique also uses glass beads but relies on hydrodynamic forces rather than shaking action to provide the filtration opening size (FOS) of geotextiles (CAN/CGSB 148.1-10, 1994). Glass beads of dimensions covering a range of relevant diameters are placed on the specimen supported by wire grids on both sides and

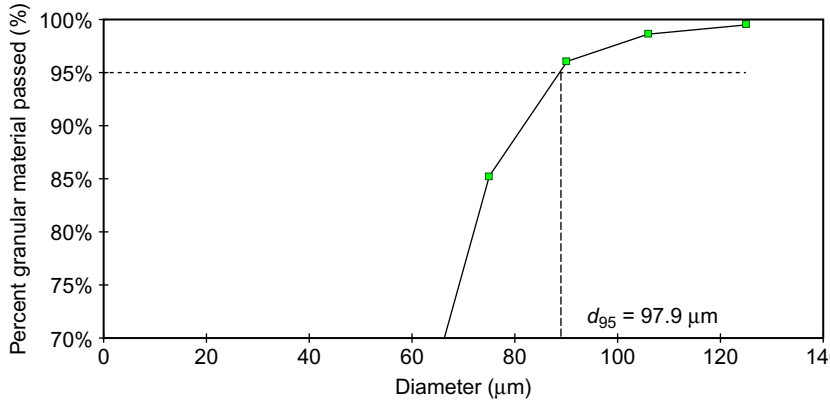

Fig. 10.2 Typical FOS cumulative grading curve measured according to CAN/CGSB 148.1-10.

installed in a cylinder. That cylinder is alternatively immersed in water until water has infiltrated through the specimen up to a height of 100 mm and emerged from the water until no water is left on the specimen. The immersion/emersion cycle is repeated 1000 times. When the test is over, the beads that have fallen in the water reservoir are collected and dried. They are then sieved to determine the fraction corresponding to each diameter range. The filtration opening size d_{95} is computed from the resulting cumulative grading curve as the diameter such that 95 wt.% of the beads having passed through the specimen are smaller (Fig. 10.2).

Wet sieving combines the action of a shaker with wet conditions to provide another measurement of geotextile opening size (ISO 12956, 2010). A cohesion-less granular material of dimensions covering a range of relevant diameters is placed on the geotextile specimen that has been presaturated with water for 12 h before being clamped on a sieve frame with a wire grid support. The specimen and the granular material are maintained in a wet condition during the test using a water sprinkler. The sieving device is shaken at a frequency of 50–60 Hz with an amplitude of 1.5 mm during 600 s. Upon test completion, the passed granular material is collected, dried, and graded. The cumulated percentage of passed granular material as a function of the corresponding sieve size is plotted to yield the d_{90} opening size value, which corresponds to the particle size for which 90% of the mass fraction is smaller than the total mass of measured particles.

A last technique providing a measurement of geotextile opening size is based on the determination of the bubble point (ASTM F316, 2003). It is appropriate for membrane filters with maximum pore size between 0.1 and 15 µm. The geotextile is prewetted with a liquid selected from a list of available reagents to completely wet the geotextile. This list consists of water, denatured alcohol, petroleum distillate, mineral oil, and Freon. Air or nitrogen gas pressure is progressively increased upstream of the specimen until gas bubbles start forming in the liquid layer on the other face of the specimen, which indicates the passage of gas through the maximum pore size of the geotextile. The limiting diameter of the maximum pore size is related to the gas pressure at bubble

point and liquid surface tension. This test method also provides the filter pore size distribution by comparing the gas flow rates of a wet and a dry geotextile at the same pressure.

In complement to the opening size, the Percent Open Area (POA) is determined as the sum of the open areas of the geotextile divided by its total surface area (CW-02215, 1986). The traditional method is based on the use of light projection. The magnified open spaces may be measured with a planimeter. An increase in the measurement sensitivity and a decrease in the measurement time were made possible by the introduction of image analysis (Mlynarek & Lombard, 1997). A binary image is taken with a microscope or a camera; the image is analyzed by counting black and white pixels corresponding to filaments/fibers and openings, respectively. The number of constrictions is also a property of nonwoven geotextiles that complements the opening size in predicting their filtration behavior (ASTM D7178, 2016). A constriction corresponds to a space delimited by three or more fibers. It can be computed based on the geotextile thickness and mass per unit area as well as fiber count and percentage per class of fiber count and type of polymer.

Geotextile permittivity and permeability characterize the way water moves through the fabric in the normal direction. Permittivity gives the volume of water which can pass through a geotextile per unit cross-section area per unit head under laminar flow conditions. The geotextile permeability is obtained by dividing the permittivity by the geotextile thickness. However, as geotextile thickness may be difficult to measure under test conditions and may not lead to a fair comparison of flow capacity between fabrics, the use of permittivity is generally favored for geotextiles (Carroll, 1987). In the uncompressed state, i.e., without load applied, geotextile permittivity may be measured using a water flow apparatus either with a constant or a falling head, or an air flow apparatus (ASTM D4491, 2016). In the constant head, water flow test, the flow rate through the geotextile is recorded for different values of water head to determine the region of laminar flow defined as the initial straight line portion of the flow rate vs. head plot. The value of water head used for the calculation of the geotextile permittivity should be located in the mid- (ASTM D4491, 2016) to upper part (CAN/CGSB 148.1-4, 1994) of the laminar flow region. The permittivity is computed by dividing the measured flow rate by the water head and the specimen test area (ASTM D4491, 2016; CAN/CGSB 148.1-4, 1994). A correction should be made when the water temperature is different from 20°C. When the flow rate of water through the geotextile is slow enough to obtain accurate measurements, the falling head test method may be used to measure the material permittivity (ASTM D4491, 2016). It consists in letting a column of water flow through the geotextile and recording readings of head change vs. time, for instance between 80 and 20 mm. The same principles, i.e., water flow test with constant or falling head, may be used to provide the flow velocity for a 50 mm head loss, V_{H50} (ISO 11058, 2010). With the air flow apparatus, the flow rate and differential pressure are measured while the geotextile is subjected to increasing air flow (ASTM D4491, 2016). The water permittivity for a water head of 50 mm is computed using flow rate data points at 250 and 500 Pa.

Geotextile permittivity may also be measured under load. Indeed, the geotextile internal structure of voids may change with an increase in compressive stress, thus

affecting the material permittivity (ASTM D5493, 2006). The test method uses a constant head permeameter which allows measuring the water flow rate through a geotextile specimen at a constant water head under an applied normal stress of up to 200 kPa. The geotextile specimen is saturated with water for at least 2 h before being installed in the testing apparatus between two wire mesh supports. The flow rate is measured under four hydraulic heads of approximately 15, 25, 50, and 75 mm, and three normal loads of 2, 20, and 200 kPa. The permittivity in the laminar region is provided by the initial constant value obtained when plotting the calculated permittivity data as a function of the water head corrected for the applied load. The thickness of the geotextile under the applied normal stress may be recorded. The same testing principle may also be used to measure the water flow velocity at a 50 mm water head under a 2, 20, and 200 kPa normal stress (ISO 10776, 2012).

The flow rate through the geotextile may be affected by the soil with which the product may be in contact. Depending on the plasticity index of the soil, one of two test methods shall be used: the Gradient Ratio Test (ASTM D5101, 2012) for soil plasticity index lower than 5 (or hydraulic conductivity greater than 5×10^{-2} cm/s) and the Hydraulic Conductivity Ratio (ASTM D5567, 1994) for soil plasticity index higher than 5 (or hydraulic conductivity less than 5×10^{-2} cm/s). The Gradient Ratio Test allows observing the change in the soil-geotextile interface permeability as a function of time under a series of hydraulic gradients between 1 and 10 with a soil-geotextile permeameter (ASTM D5101, 2012). The distribution of hydraulic gradients in the vicinity of the soil-geotextile interface is recorded using pressure transducers. A continuous decrease in the gradient ratio over time and the presence of soil having passed through the permeameter are indications of the tendency of the soil-geotextile system for piping. Gradient ratio values larger than 1 generally point towards system clogging. A variant of the Gradient Ratio Test has been developed by researchers to allow reproducing at the laboratory scale the conditions experienced by a soil-geotextile system in applications involving reversing flow and static or dynamic mechanical stress (Daqoune & Blond, 2010). For its part, the Hydraulic Conductivity Ratio test uses a flexible wall permeameter which is installed in a triaxial pressure chamber filled with water (ASTM D5567, 1994). The pressure in the triaxial chamber and the specimen influent and effluent systems are controlled precisely. After back-pressure saturation and soil consolidation under the desired level of stress, the flow of liquid across the soil-geotextile system under a hydraulic gradient selected to be relevant to what is expected in the field is recorded over time. A somewhat higher hydraulic gradient may also be selected to accelerate testing. The test is terminated when the hydraulic conductivity has reached a constant value or has fallen below a predetermined design limit, or if the effluent remains cloudy after 30 pore volumes have elapsed, which indicates continuous soil piping through the system. The final Hydraulic Conductivity Ratio is obtained by dividing the final by the initial value of hydraulic conductivity.

In addition, a test method has recently been developed by researchers for characterizing the hydraulic behavior of geotextiles with fine-grained tailings, which exhibit a hydraulic conductivity too low for the Gradient Ratio Test (Dolez, Chappel, & Blond, 2014). It consists in a 3-in. internal diameter cylindrical cell (Fig. 10.3). The 12-in. high main chamber holds a volume of tailings and water over a geotextile specimen

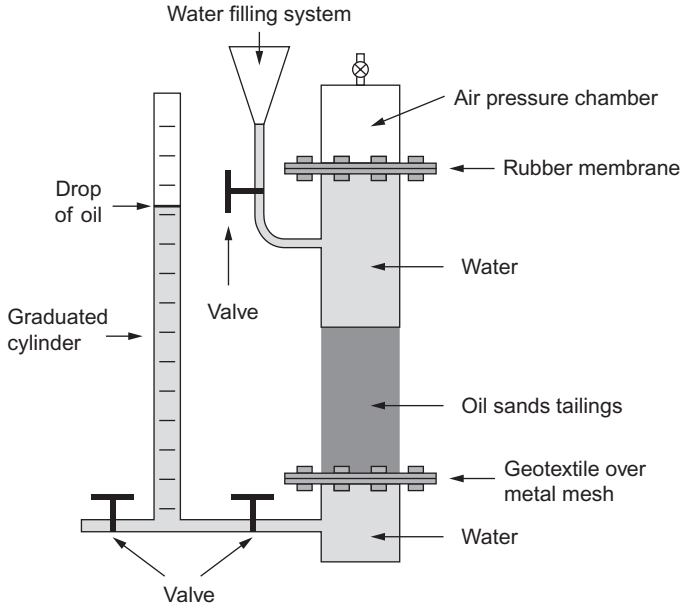

Fig. 10.3 Schematic of the filtration cell for low hydraulic conductivity fine-grained tailings (Dolez et al., 2014).

supported by a wire mesh. The lower chamber is filled with water. Both the water used in the lower and main chamber is recovered from tailings dewatering experiments so that it has the relevant chemistry. The lower chamber is connected to a graduated cylinder to allow recording the volume of water crossing the tailings/geotextile system. Water evaporation from the graduated cylinder is prevented by a supernatant drop of oil. The top chamber is separated from the main chamber by a rubber membrane and is pressurized to 20 kPa to simulate conditions near the surface in a tailings pond, i.e., equivalent to the stress applied by a 1.5-m-thick layer of oil sands tailings for instance. A system allows adding water at regular intervals in the main chamber to maintain the rubber membrane in a low deformation state.

Standard test methods have also been developed to simulate specific applications of geotextiles. For instance, standard test methods ASTM D7701 (2011) and ASTM D7880 (2013) provide a measurement of the flow rate of water and suspended solids from a geosynthetic permeable bag and a geosynthetic permeable closed bag respectively. These bags are used to contain high water content slurries such as dredge material. Hanging bags are assembled using the geotextile material to be tested (ASTM D7701, 2011). They are filled with site-specific dredge material and attached to a frame. Water and sediment expelled from the bag by gravity flow are collected at regular intervals. For each collected sample, the flow rate and solids content are computed. The flow rate and filtering efficiency of sediment retention devices such as silt fence, silt barrier, and inlet protector are measured by placing the geotextile specimen at the bottom end of a flume inclined with an 8% slope (ASTM D5141, 2011). Site-relevant soil dispersed in water is released at the upper end of the flume. The flow rate

is calculated based on the time elapsed until no water remains behind the geotextile. The solids content in the collected filtrate is used to compute the sediment retention geotextile filtering efficiency.

The flow of water within the plane of the geotextile is also of paramount interest for drainage applications. Planar hydraulic transmissivity is measured in a transmissivity test rig under constant water head while the geotextile is subjected to varying normal compressive stress (ASTM D4716, 2014; ISO 12958, 2010). This confining pressure simulates the weight of the backfill material as well as any live load such as traffic. According to ISO 12958 (2010), the test is conducted at hydraulic gradients of 0.1 and 1.0 under normal stress of 20, 100, and 200 kPa. Foam rubber sheets are placed in contact with the geotextile specimen to simulate typical backfill material, unless the product is intended to be used against rigid boundaries. The flow measurement is initiated a few minutes after the normal stress has been applied on the specimen/foam system. A minimum of 0.5 L of water passing through the system is collected within a minimum of 5 s and a maximum of 600 s. The in-plane water flow capacity is computed at each hydraulic gradient and normal stress. Test standard ASTM D4716 (2014) prescribes selecting three gradients between 0.05 and 1.0 and three applied normal stresses between 10 and 500 kPa, based on material specifications or specific site conditions. The hydraulic transmissivity is computed at each value of the normal stress. This ASTM standard recommends the use of site-specific soils as substrate and superstrate for the geotextile specimen when relevant to simulate soil intrusion in the geotextile openings. This has been shown to provide more reliable results than the foam rubber of the ISO test method (Bamforth, 2009). Another characteristic of the ASTM test method is that the confining pressure is applied for 1 h before the flow rate measurement starts (ASTM D4716, 2014). As a result, the data obtained provide some information about the long-term behavior of the geotextile-soil system (Bamforth, 2009).

For geotextiles whose transmissivity is independent of the orientation of the flow and $<2\times10^{-4}\,m^2/s$, a radial flow apparatus may be used (ASTM D6574, 2013). Water is fed at the center of a torus-shaped specimen and flows radially outward. The test may be conducted at different constant heads between 0.1 and 1.0 and different normal compressive stresses between 5 and 50 kPa. The seating time before the flow rate measurement is started is typically 15 min. The hydraulic transmissivity is computed from the flow rate measurements for each head and stress condition.

Geotextile barrier properties against liquids are tested using a Mullen-type hydrostatic tester. One technique involves applying a specified constant pressure to a 31-mm diameter specimen exposed surface area for 5 min (ASTM D751, 2006, Method A). Any appearance of water on the other side of the geotextile during this period indicates a failure. A quantitative assessment of the hydrostatic resistance is made possible if the water pressure is gradually increased until water passage is detected. Depending on the test method, the criterion may be a first appearance of water (ASTM D751, 2006, Method A), the formation of continuous droplets on the surface of the specimen (EN 13562, 2000), or three separate water penetration points (CAN/CGSB 4.2-26.3, 1995; ISO 811, 1981). Differences in terms of exposed specimen surface area and rate of pressure increase also exist between these test methods.

10.2.6 Thermal properties

As polymers are sensitive to the effect of temperature, the performance of polymer-based geotextiles may change with temperature (Torosian & Mac Millan, 2016). The mechanical properties of plant-based fibers are also affected by temperature (Célino et al., 2013).

The effect of temperature on the stability of geotextiles may be characterized by its impact on the specimen tensile strength and elongation at break (ASTM D4594, 1996). Tests are conducted in a mechanical tensile test frame equipped with an environmental chamber. Temperatures used for specimen conditioning and testing are those at which the geotextile will be exposed in the field and/or will have to perform. They may range between −40°C and 100°C. The measurements are carried out according the standard test method ASTM D1682 (which was withdrawn and has been replaced by ASTM D5035 (2011)) at a deformation rate of 305 mm/min using 50.8-mm cut or raveled strip tensile test specimens (depending on the type of geotextile) prepared according to ASTM D5035 (2011). The change in tensile strength and elongation at break at a certain temperature is calculated by comparison with the results obtained in a standard atmosphere for testing geotextiles, i.e., a temperature of 21°C and a relative humidity of 60%.

10.2.7 Durability

The assessment of geotextile durability is critical when one considers the detrimental effect various environmental and service conditions such as UV exposure or contact with chemicals have both on polymers (Verdu, 1984) and plant-based fibers (Azwa, Yousif, Manalo, & Karunasena, 2013) that form geotextiles. For instance, polyethylene exposed to UV becomes brittle and rapidly loses its strength (Struick, 1985); the loss in mechanical performance is about 50% after half a year to one year of exposure to outdoor conditions. Durability assessment of geotextiles is all the more important that service life of 100 years or more may be required in the case of acid generating or radioactive waste for example (Renken, Mchaina, & Yanful, 2005), or for primary leachate collection systems in landfills (Rowe, 2005).

A series of test methods is available to assess the durability of geotextiles (ASTM D5819, 2005; EN 12226, 2000; ISO 13434, 2008). They generally involve subjecting the geotextile to the action of an environmental or service degradation factor in an accelerated manner by increasing its frequency, its severity, and/or the temperature. Degradation mechanisms include thermo-oxidation, photo-oxidation, hydrolysis, chemical attack, swelling by solvents, biological attack, wear or other mechanical damage, and creep. The geotextile residual performance is then measured based on end-of-life criteria dictated by its function: mechanical performance, hydraulic capacity, barrier properties, etc.

The resistance of geotextiles to oxidation may be characterized by exposing specimens to high temperature over a fixed time period by suspending them in an air oven (EN 14575, 2005; ISO 13438, 2004). Upon exposure, the residual tensile strength and elongation at break are measured and compared to that of control specimens. This

test is primarily intended for polypropylene and polyethylene materials. In EN 14575 (2005), the oven temperature is set at 85°C, and the exposure time is 90 days. Control specimens are prepared by subjecting them to the 85°C temperature condition during 16 to 24 h. No test method is specified for measuring the mechanical performance at break of the exposed and control specimens: it is only mentioned that a test method relevant to the type of application of the geotextile should be used. The percentage of retained strength and elongation at break is computed by dividing the result obtained for the exposed specimens by that of the control specimens. Test method ISO 13438 (2004) provides different aging temperatures depending on the polymer: 110°C for polypropylene and 100°C for polyethylene. For each of them, two exposure durations may be used depending if the product is intended for a nonreinforcing or a reinforcing application: 14 or 28 days for polypropylene, and 28 or 56 days for polyethylene, respectively. The control specimens should be exposed for 6 h at the same temperature. The tensile strength and strain at maximum load of the exposed and control specimens are measured according to the test methods indicated in EN 12226 (2000). The results are used to compute the percentage of retained performance of the product. An alternative test method based on the use of a sodium bicarbonate ($NaHCO_3$) aqueous solution enriched with oxygen is described in ISO 13438 (2004). The specimens are immersed in the liquid at 5000 kPa and 80°C for 14 days for nonreinforcing applications and 28 days for reinforcing applications. Control specimens are prepared by subjecting them to the same conditions during 24 h. The mechanical performances at break of the exposed and control specimens are also tested according to the methods indicated in EN 12226 (2000).

In addition, thermal aging may also induce a reduction over time in the content of antioxidants and other stabilizers that are generally added to polyolefins used to manufacture geotextiles to increase their durability (Allen, 2016). Indeed, polyolefins are highly sensitive to oxidative degradation, which involves the formation of free radicals; after an induction time during which no significant loss in performance is recorded, the material's degradation rate increases rapidly, it becomes brittle and eventually loses all its strength. The measurement of the oxidative induction time (OIT) by differential scanning calorimetry has been shown to provide a good estimate of the antioxidant concentration in polyolefin products. In practice, a 5–10 mg specimen is heated at 200°C, i.e., above its melting temperature, in an inert atmosphere (nitrogen gas) at atmospheric pressure (ASTM D3895, 2014). When that temperature is reached, the gas is switched to oxygen with a flow rate of 50 mL/min. The isothermal operation is maintained until the maximum exotherm has been reached (Fig. 10.4). The time between the switch to oxygen and the onset of the oxidative exotherm corresponds to the OIT. For geotextiles containing hindered amine light stabilizer (HALS), which is an important class of antioxidants that is most efficient at ambient temperature but cannot be detected by the standard OIT test (Allen, 2016), the HP-OIT test method has been developed. It uses a high-pressure differential scanning calorimeter that allows applying oxygen at a pressure of 3.4 MPa in the specimen chamber (ASTM D5885, 2015). The flow of oxygen is started during the initial temperature ramp at 20°C/min. Once a temperature of 150°C is reached, the isothermal is started. The HP-OIT value is measured from the start of the isotherm to the onset of the oxidative exotherm.

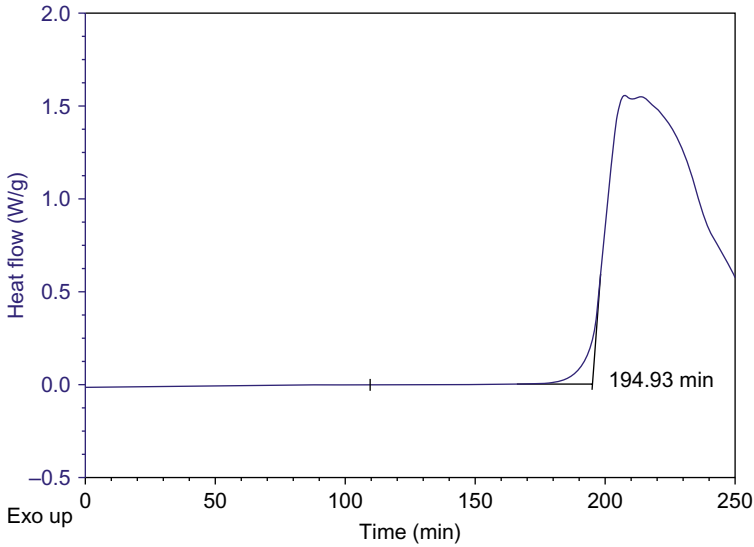

Fig. 10.4 Typical OIT curve measured according to ASTM D3895.

When geotextiles contain other stabilizers in addition to HALS, it is recommended to conduct both OIT and HP-OIT tests as the HALS response during the HP-OIT test may mask that of other stabilizers present.

Degradation due to weathering generally involves exposure to a combination of UV light, moisture, and heat (ISO 13434, 2008). The resistance to weathering may be characterized by outdoor exposure tests conducted at a location selected to be relevant to the product use conditions (ASTM D5970, 2016). Geotextile coupons are exposed with an angle of 45 degrees from the horizontal and facing the equator for time periods of 1, 2, 4, 8, 12, and 18 months. Their breaking strength and elongation at break are measured after exposure according to test method ASTM D5035 (2011) using 50 mm-wide strip specimens, a 75-mm gauge length, and a 305 mm/min displacement rate. The retained mechanical properties at the different exposure times are computed by dividing the results obtained for the exposed specimens by that for unexposed specimens tested in the same conditions (ASTM D5970, 2016).

Accelerated weathering test methods have also been developed with higher levels of radiation coupled with cycles of exposure to high temperature and moisture to reduce test durations (ISO 13434, 2008). The resistance of geotextiles to accelerated weathering is often characterized using fluorescent (ASTM G154, 2016) or Xenon arc (ASTM G155, 2013) UV light apparatus. Four programs of artificial weathering using fluorescent light are proposed in ISO 4892-3 (2016). They include different levels of irradiance, durations of light cycle, temperatures, timings of dry/wet cycle, and use of condensation and/or water spray for exposure to moisture. The irradiance is 0.76 W/(m^2 nm) with UVA-340 lamps in the case of alternating light/dark cycles and 45 W/m^2 with 290–400 nm lamp combination in the case of continuous light exposure. Depending on the program, the temperature is between 50°C and 70°C during dry

periods, at 50°C during eventual condensation periods, and at 25°C during eventual water spray periods. The changes in appearance and properties of the exposed material, including its mechanical performance, are characterized according to test method ISO 4582 (2007). On the other hand, EN 12224 (2000), which specifically targets geotextiles, specifies a radiant exposure of 50 MJ/m^2, with alternating wet/dry cycles. This corresponds to 1 month of exposure in southern Europe during summer. The temperature is 25°C with water spray during the wet cycle and 50°C with 10% relative humidity during the dry cycle. The percentage retained strength and elongation at break are recorded.

Xenon arc lamps may sometimes be preferred since, when properly filtered, they most closely match the sun radiation spectrum (Shah, 2007). Standard test method ISO 4892-2 (2013) provides examples of exposure programs for artificial weathering under continuous light exposure. For all programs, the irradiance is kept at 0.51 W/(m^2 nm) at 340 nm and the 120 min wet/dry cycle includes 18 min of water spray. Differences may be found in the black-panel temperature (65°C or 100°C) and the chamber temperature and relative humidity (not controlled or set at specific values). The standard mentions the possibility of applying more complex cycles with alternating dark periods involving high humidity or the formation of condensation. The changes in appearance and properties of the exposed material are characterized according to test method ISO 4582 (2007). For its part, standard test ASTM D4355 (2014) specifies an exposure program for characterizing geotextile degradation under light, moisture, and heat using a Xenon arc apparatus. The irradiance is 0.35 W/(m^2 nm) at 340 nm. It has a 90 min light-only period at 65°C and 50% relative humidity, followed by a 30 min period with light and water spray. Specimens are exposed for 150, 300, and 500 h. Their residual breaking strength is measured according to test method ASTM D5035 (2011) using 50 mm-wide strip specimens, a 75 mm gauge length, and a 305 mm/min displacement rate. The percent loss in strength from the unexposed material is computed at each exposure time.

Geotextiles may also be exposed to various chemicals while in service. First of all, geotextiles, in particular polyester and polyamide, may be susceptible to hydrolysis in water resulting from soil moisture (EN 12447, 2001). Specimens are immersed in water heated at 95°C to accelerate the degradation kinetic and obtain measurable effects over the test duration of 28 days. The specimens should be free of significant load during immersion. Control specimens are exposed to the same environmental conditions for 1 h. The changes in visual appearance and mechanical performance at break of the exposed material are characterized according to test method EN 12226 (2000). Geotextiles may also be in contact with aqueous acid or alkaline solutions. The test method involves immersing geotextile specimens either in an inorganic acid containing sulfuric acid, ferrisulfate, and ferrosulfate or in an inorganic base prepared with calcium hydroxide without any mechanical stress applied (EN 14030, 2001). In both cases, the liquid is kept at 60°C and the test lasts 3 days. Control specimens should be immersed in water at 60°C for 1 h. Upon exposure, specimens shall be rinsed appropriately and dried before being tested. The changes in properties are characterized according to test method EN 12226 (2000).

A more general laboratory immersion procedure is available in standard ASTM D5322 (1998) for evaluating the resistance of geotextiles to chemicals, liquid waste,

and leachate. Specimens are immersed in the liquid which is generally maintained under constant stirring conditions. Recommended immersion temperatures are 23°C and 50°C. The immersion solutions may have to be replaced periodically if their chemistry changes with time. The material should be tested unexposed as well as after four different immersion times. Standard immersion periods are 1–4 months. Tests to evaluate the chemical resistance of geotextiles to liquids may be found in ASTM D6389 (1999). They include physical, mechanical, and hydraulic properties as well as composition. The specimens may also be subjected to immersion testing directly in the field (ASTM D5496, 2015). For that purpose, they are placed in a container immersed in the fluid-containing tank or sump. The sides and bottom of the container are perforated to allow a complete flooding of the specimens by the fluid. At the end of the exposure period, the container is drained and washed with water with the specimens left inside. Within 30 min of removal from the tank or sump, the container should be tightly wrapped in heavy-duty polyethylene bags, so that the geotextile specimens remain wet during the overnight shipping to the testing laboratory.

Finally, a test method is available for specifically determining the chemical resistance to liquid waste under laboratory immersion (EN 14414, 2004). The procedure includes chemical compounds chosen to generate the types of chemical degradation relevant to municipal, agricultural, and industrial wastes: an acid solution made of sulfuric acid; a basic solution prepared with calcium hydroxide; a solvation/swelling solution containing a mixture of diesel fuel, paraffin, and lubricating oil; and a synthetic leachate prepared with acetic, propionic, isobutyric, butyric, isovaleric, valeric, hexanoic, and heptanoic acid, glucose, sodium chloride, sodium sulfate, calcium chloride, magnesium sulfate, diammonium hydrogen phosphate, and water (the pH is adjusted with ammonia solution and sodium hydroxide). The immersion test may also be conducted with a site-specific leachate. The specimens are immersed for 56 days in the solutions at 50°C under constant stirring. After the exposure time has elapsed, the specimens are rinsed and visually observed for any sign of degradation; their residual elongation at break is measured according to test method EN 12226 (2000).

Geotextiles may also be sensitive to biological degradation resulting from attack by bacteria or fungi. Their microbiological resistance is assessed by subjecting specimens to a soil-burial test (ASTM G160, 2012; EN 12225, 2000). In EN 12225 (2000), the soil is at 60% of its saturation moisture content and incubated at 28°C in an environmental at 97% relative humidity for a month. Its microbial activity is verified with a bleached, untreated woven cotton fabric; the residual tensile strength of 100×25 mm specimens buried for 7 days in the soil should be less or equal to 25% of their original strength. For the test, geotextile specimens are buried in the soil kept in a dark environment at 26°C and 95% relative humidity for 16 weeks along with one specimen of cotton reference. When the exposure time has elapsed, the test specimens are recovered from the soil and observed visually before being disinfected with an ethanol-water mixture, cleaned under running water, and dried. Additional visual observations are made and the residual tensile strength of the exposed specimens is assessed according to test method EN 12226 (2000). For comparison purposes, the mechanical performance of unexposed, control specimens subjected to a similar disinfection, cleaning, and drying process as the exposed specimens is also measured. In ASTM G160 (2012),

the composition of the active soil is specified to comprise 1/3 of fertile top soil, 1/3 of well-rotted and shredded horse manure, and 1/3 of coarse sand. It is aged for 3 months and sifted through a ¼-in. mesh screen when produced as well as twice during the aging period. The soil should be maintained between 20% and 30% moisture and at a pH between 6.5 and 7.5, and kept in an environment at 30°C with a relative humidity between 85% and 95%. The biological activity of the soil after the 3-month aging period is tested with an untreated cotton cloth: it should display a loss in tensile strength of at least 50% after a 5-day burial in the soil. The default exposure period of the geotextile specimens is 60 days. A minimum of four specimens are buried for each exposure period. Upon retrieval and gentile cleaning, the specimens are evaluated for microbial staining as well as changes in the physical and mechanical properties. The soil burial assessment may also be conducted on specimens previously subjected to UV aging.

Biological species may also affect the hydraulic performance of geotextile filters. Their resistance to biological clogging is assessed by measuring the variation over time of their flow capacity when they are in contact with a site-specific soil or exposed to an eventually biologically active fluid, for instance leachate (ASTM D1987, 2007). The test may be conducted under constant or falling head conditions. It generally runs for extensive periods of time, up to 1000 h, to allow the biological activity to initiate. The flow rate or permittivity may remain constant over time, which indicates an absence of biological clogging. It may also experience a more or less steep decrease, indicative of a clogging activity. The flow rate may also remain steady for some time before dropping rapidly, which is a sign of retarded clogging. In addition to biological clogging, filter hydraulic properties may be reduced over time by the progressive ingress of soil particles into the filter structure. Tests methods exist to characterize this mechanism of filter clogging: Gradient Ratio test (ASTM D5101, 2012) for soil plasticity index lower than 5 and Hydraulic Conductivity Ratio test (ASTM D5567, 1994) for soil plasticity index higher than 5; they have already been described in Section 10.2.5.

When geotextiles are kept under load for extended periods of time, they may experience both creep, i.e., a persistent extension under a constant stress, and stress relaxation (Allen, 2016). If not controlled, creep and stress relaxation may have catastrophic consequences for the geotechnical work in which the geotextile is used. This situation may be especially relevant for geotextiles used as reinforcement in steepened slopes and retaining walls. In the traditional testing strategy, a fixed load is applied on unconfined specimens across their full width at a constant temperature (ASTM D5262, 2007; ISO 13431, 1999). Large specimens (200 × 200 mm) are used to limit the effect of edge contraction. In tensile creep tests, the specimen elongation is recorded for 1000 h under four loads selected between 5% for ISO 13431 (1999) or 20% for ASTM D5262 (2007), and 60% of the ultimate tensile strength of the geotextile. The test is performed at room temperature. In addition, test method ASTM D5262 (2007) recommends carrying out creep tests at two other temperatures that are relevant to the geotextile service conditions on site. Measurements of the specimen elongation are conducted at increasing time intervals up to 1000 h (exact numbers depend on the test method). Creep curves show the variation in percent strain as a function of time

on a semilogarithmic scale. If the results are used for design purposes, the test duration may have to be extended to a minimum of 10,000 h to avoid extrapolating creep data beyond one order of magnitude. Tensile creep rupture tests may also be conducted. In that case, the measurement of the specimen elongation lasts until the specimen fails (ASTM D5262, 2007; ISO 13431, 1999). Tests should be conducted at four loads selected in the range of 50%–90% of the ultimate tensile strength of the geotextile. As in the case of creep testing, additional measurements at two temperatures other than room temperature are suggested by test method ASTM D5262 (2007). Results are reported in terms of creep rupture load as a function of time on a semilogarithmic scale.

To circumvent the length of creep tests, accelerated methods have been developed based on the time-temperature superposition principle (Williams, Landel, & Ferry, 1955). According to this principle, the variation as a function of time of properties of viscoelastic materials measured at different temperatures may be shifted on a single master curve on a semilogarithm scale (ASTM D5262, 2007). The shift factors vary with temperature according to the Arrhenius law. Using a stepped isothermal method (SIM), which involves applying load increments at a sequence of increasing temperatures, creep measurements can be made on a single specimen and in a much shorter time, typically 24 h (Thornton, Allen, Thomas, & Sandri, 1998). The SIM creep test is done with a mechanical test frame equipped with an environmental chamber capable of applying very rapid temperature changes (ASTM D6992, 2016). Tests are conducted on 50 mm wide strip specimens. A tensile test conducted at 20°C with a strain rate of 10%/min is used to determine the ultimate tensile strength of the geotextile and select the load increments. The specimen elongation is recorded as a function of time as these load increments are applied simultaneously with small temperature increments (<7°C for polyolefins and <14°C for other polymers) between isotherm dwell times of typically 10,000 s (Fig. 10.5A). The raw data are then plotted on a semilogarithmic scale with the time of each temperature/load segment being adjusted to achieve a matching slope with the end of the preceding segment (Fig. 10.5B). Finally, the individual curve segments are shifted onto the 20°C reference data to yield a master curve that can serve to predict long-term creep behavior (Fig. 10.5C).

The resistance to mechanical stressors applied over long periods of time may also affect the geotextile durability. For instance, geotextiles used in road and railway applications experience dynamic loading or fatigue and standards recommend evaluating the performance of geotextiles intended to operate under severe dynamic loading (ISO 13434, 2008). The dynamic loading in tension may be tested according to ASTM D7556 (2010). A 200×200 mm specimen is clamped over its entire width and subjected to successive series of 1000 loading cycles at axial strains of 0.5%, 1.0%, 1.5%, 2%, 3%, and 4%. The cyclic loading is ±0.1% of the axial strain value applied at a rate of 10%/min of the gauge length. The average modulus is computed for the last 10 cycles of each 6-load step. In addition, geotextile performance under compressive dynamic loading between two layers of granular materials may be assessed using test method ISO 10722 (2007). Specimens are installed over a 75 mm thick layer of compacted synthetic aggregate composed of 5–10 mm diameter sintered aluminum oxide particles. A 75 mm thick loose layer of the same aggregate is placed above the specimen. The assembly is subjected to 200 loading cycles between 5 and 500 kPa using

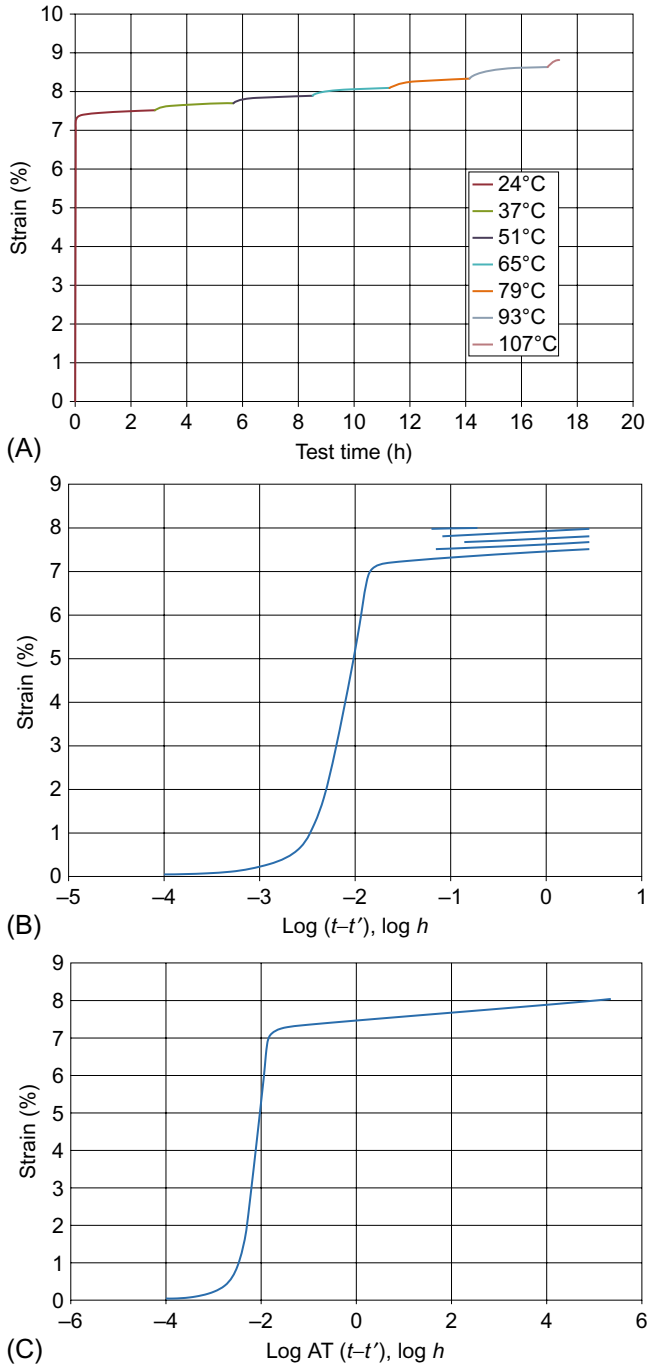

Fig. 10.5 Principle of the SIM creep test method: (A) raw data; (B) strain-time curves before shifting; and (C) master curve with shifted individual curve sections.

a 100×200 mm loading plate. After the test is over, the specimen is examined for signs of damage. Its residual performance is also assessed using a wide-width tensile test (ISO 10319, 2015) or any other relevant test method for mechanical or hydraulic properties. Another important dynamic mechanical stressor for geotextiles deals with abrasion. Test methods are based on the sliding block principle (ASTM D4886, 2010; ISO 13427, 2014). They are described in Section 10.2.4.

Alternatively to the use of methods simulating the effect of aging agents, the long-term behavior of geotextiles can also be assessed by subjecting samples to field aging (ISO 13437, 1998). These tests allow as well establishing the validity of the accelerated aging procedures described above. As much as possible, samples should be exposed to the same physical, mechanical, hydraulic, and chemical environments that the geotextile experiences in the structure. The recommended retrieval schedule includes a first retrieval directly following construction, which allows assessing installation damages, a second retrieval after 10 years, followed by retrieval every 20 years or less until the end of the expected life service, upon which a final retrieval is made. Special care should be paid not to damage samples during retrieval: mechanical digging should be stopped 30 cm before reaching the sample and the final layer of material should be removed manually with a shovel and a trowel. If no durability samples had been installed during construction and it is necessary to sample a piece of geotextile in service, a procedure for repair of the hole left in the geotextile should be defined. Control specimens should be taken from the material before installation, placed in black polyethylene bags, stored at a temperature between 0°C and 20°C and a relative humidity between 50% and 65%, and tested at the same time as retrieved samples. Tests to be done on retrieved samples and control specimens include wide-width tensile test according to ISO 10319 (2015), solution viscosity measurement, and scanning electron microscopy examination for signs of chemical or biological attack, surface degradation, or environmental stress cracking. In addition, retrieved samples may be weighted and their water permeability measured.

10.3 Geogrids

Geogrids are defined as "a geosynthetic formed by a regular network of integrally connected elements with apertures >6.35 mm to allow interlocking with surrounding soil, rock, earth, and other materials to primarily function as reinforcement" (ASTM D4439, 2015). They are composed of interconnected longitudinal and transverse ribs. The development of geogrids was made possible by the arrival of high-modulus polymers prepared by tensile drawing (Koerner, 2012). In addition to the stiffness and strength of the ribs, the strength of the junctions between longitudinal and transverse ribs is critical as the load might have to be transmitted from the transverse to the longitudinal ones.

Three main categories of geogrids may be distinguished (Koerner, 2012). Two of them are manufactured by polymer-type processes while the last one is textile-based. The first geogrid category is grounded on the original technique used to produce geogrids. These unitized or homogeneous geogrids are manufactured by punching holes

in a heavy-gauge polymer sheet, which is then drawn in a uniaxial, biaxial or triaxial manner. Uniaxial geogrids, which are reserved for walls and slopes where the main stress direction is known, are generally made of high density polyethylene (HDPE). Bidirectional and tridirectional geogrids are used for base and foundation reinforcement and are generally made of polypropylene. The second geogrid category employs polyester or polypropylene rods or straps that are laid in a square network and joined by laser or ultrasonic welding. These are the stiffest and generally the strongest geogrids. Finally, textile-type geogrids are produced by weaving high-tenacity polyethylene terephthalate (PET), fiberglass, polyamide or polyvinyl alcohol yarns into an open structure with intertwined or knitted junctions. The entire structure is then coated with polyvinyl chloride (PVC), latex or bitumen for dimensional stability and increased protection. Depending on the design and manufacturing process, the geogrid apertures can be elongated ellipses, squares with more or less rounded corners, or rectangles.

These high-strength, high-modulus, low-creep open polymeric structures have found a very large number of applications, mostly as reinforcement but sometimes also for separation with very coarse granular materials (Koerner, 2012). Geogrids are used for instance beneath or within aggregate on unpaved roads and ballast in railroad construction; as wraparound walls; as reinforcement of embankment fills and earth dams; as gabions for wall and bridge abutments and erosion control structures; as basal reinforcement over soft soils and karst areas; and to construct mattresses for fills over soft soils.

10.3.1 Sampling and specimen preparation and conditioning

Geogrid sampling and specimen preparation are described in ISO 9862 (2005) for instance. It is similar to what is prescribed for geotextiles (see Section 10.2.1). Conditioning requirements are also the same for geogrids than for geotextiles (ISO 554, 1976).

10.3.2 Physical properties

Physical properties of most interest for geogrids are thickness, aperture dimensions, percent open area, mass per unit area, and intrinsic viscosity for polyethylene terephthalate geogrids.

As for geotextiles, the thickness of geogrids is measured using a presser-foot apparatus equipped with a thickness gauge (ASTM D5199, 2012; ISO 9863-1, 2016). The pressure used is generally 2 kPa. However, since geogrids generally exhibit a non-uniform thickness over their surface, with different values at ribs and junctions for instance, clear indications should be provided of the part(s) to be tested (ISO 9863-1, 2016). That information should also be recorded in the test report. If the overall thickness of the geogrid is sought, a presser-foot larger than the 25 cm^2 surface area typically used for geosynthetics other than polymeric and bituminous geosynthetic barriers might be needed to ensure that the presser-foot surface is in contact with the specimen on at least three points evenly distributed over its surface. If the thickness of

individual parts of the geogrid is sought, one may use two presser points with a 1-mm radius at the tip facing each other on the top and bottom plates of the presser-foot and a 0.6 N applied pressure.

The dimensions of the geogrid apertures, which are typically 10–100 mm wide, are a critical component in the design of geotechnical structures reinforced with geogrids as they control the ability of the surrounding soil, aggregate, and other granular material to strike through their plane (Koerner, 2012). The aperture inside dimensions are measured in each principal direction using vernier calipers (ASTM D5947, 2011). No standard test method exists with a procedure for the measurement of the aperture dimensions; however, it is good practice to record values for a number of apertures randomly distributed over the sample so that a result representative of the product may be obtained. The strike-through capacity can also be characterized by the Percent Open Area (POA). Like for geotextiles, it is determined using light projection as the sum of the open areas divided by the total surface area (CW-02215, 1986).

The determination of the mass per unit area of geogrids is conducted with the same test methods as for geotextiles (ASTM D5261, 2010; ISO 9864, 2005). However, because of the large size of the openings, the dimensions of the specimens should be increased to be representative of the product. In particular, some test methods recommend that the specimen includes at least 5 constitutive elements (i.e., ribs) in each direction (ISO 9864, 2005). In addition, the specimen's edges should be located halfway between two junctions and the surface of each specimen should be measured individually.

10.3.3 Composition

In the case of PET geogrids, the determination of the intrinsic viscosity may be of interest as it is related to the composition and molecular weight of the polymer. The intrinsic viscosity is measured with a glass capillary viscometer (ASTM D4603, 2003). Specimens of the geogrid material are dissolved in a 60 wt.% phenol/40 wt.% 1,1,2,2-tetracholorethane mixture at 110°C under stirring conditions for 15 min. The flow time of the polymer solution and pure solvent through the viscometer capillary at 30°C is measured and used to compute the intrinsic viscosity at a polymer concentration of 0.5% g/dL.

The carboxyl end group (CEG) content of PET geogrids may also be obtained by titration (ASTM D7409, 2015; GRI GG7, 1998). After the geogrid coating has been completely removed, for example using methyl ethyl ketone in the case of a PVC coating, 2 mm long pieces of the geogrid longitudinal yarns are dissolved in ortho-cresol at 80°C for 25 min under constant stirring condition. After the solution has cooled down, it is diluted with methylene chloride before being titrated against potassium hydroxide dissolved in methanol using a potentiometric or colorimetric method. A low CEG content has been associated with a high resistance to hydrolysis (Hsuan, Koerner, & Lord, 1993).

10.3.4 Mechanical properties

The tensile strength of single ribs is characterized by subjecting rib specimens to a tensile test at a constant rate of deformation of 10%/min of the gauge length (ASTM D6637, 2015, Method A). The specimen should contain at least one intersecting rib

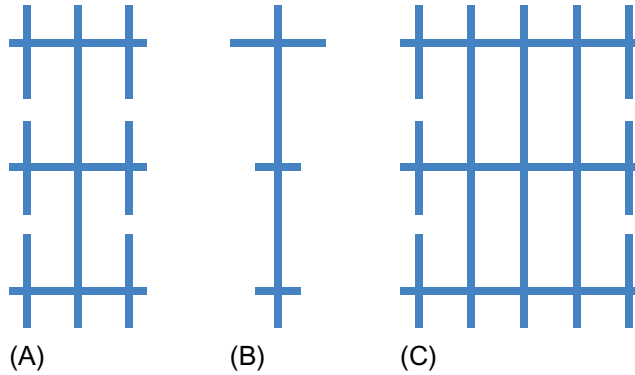

Fig. 10.6 Specimen configuration for (A) single rib, (B) rib junction, (C) multirib tensile test according to ASTM D6637.

crossing the testing direction and at least three junctions in the direction of testing, or be at least 300 mm long (Fig. 10.6A). The initial distance between the clamps should be selected such that at least one transverse rib is within the gauge length. At least one clamp is installed on a free swivel to ensure that the force is applied in the geogrid plan. The tensile force required to bring the specimen to failure is recorded as well as the elongation at break. The test is performed on six specimens.

The tensile strength of rib junctions (or nodes) is also assessed with a tensile test at a constant rate of deformation but with special clamps that grip the transversal rib on each side of the junction to allow applying a tensile or shearing force to the junction while minimizing rotation and peeling (ASTM D7737, 2015; GRI GG2, 2005). Specimens are generally prepared with a "T" shape (Fig. 10.6B). Depending on the geogrid morphology, two designs are proposed for the top clamp that holds the junction: in the case of unitized or homogeneous geogrids, the preferred design is a clamp that secures the horizontal rib on each side of the junction with unconstrained rotation; for textile, rod, and strap geogrids, the best results are obtained with a clamp that constrains the rotation of the junction. The bottom clamp is a standard rib tensile clamp. The test is conducted at 50 mm/min on ten specimens. The maximum force measured at junction failure allows computing the average junction strength per rib as well as the average junction strength per unit width.

Tensile tests may also be conducted on a wider specimen to evaluate the performance of the product as a whole. The test is performed in the machine direction for unidirectional geogrids, and both in machine and cross direction for bidirectional and tridirectional geogrids (Koerner, 2012). Method B in standard ASTM D6637 (2015) refers specifically to multirib tensile test for geogrids. The specimen should be at least 200 mm wide with five ribs and at least 300 mm long with three junctions (Fig. 10.6C). The outermost ribs are generally cut prior to testing to limit specimen slippage in the clamps that should hold the entire specimen width. The strain rate is 10%/min of the gauge length and five specimens per direction are measured. The force per unit width, percent strain, and secant modulus at a specified elongation are reported. The use of an external extensometer is required with roller clamps. Otherwise, it is encouraged since

a modulus is measured. In the case of standard test method ISO 10319 (2015), which contains specific provisions for testing geogrids, the specimen is wider than long, with a minimum of 100-mm length and 200-mm width, to reduce the risk of necking. In addition, the use of an extensometer is required when strain measurement is involved. The strain rate is 20%/min of the gauge length which should be at least 60 mm and contain at least one node. The reference points for the extensometer should be at least 60 mm apart, be separated by at least one node, and be located at the center of ribs. Jaw designs suitable for testing geogrids are provided in the standard.

The out-of-plane bending stiffness or flexural rigidity of geogrids is characterized using the cantilever test procedure (ASTM D1388, 2014; ASTM D7748, 2014; GRI GG10, 2001). The test conditions are the same as those for geotextiles (see Section 10.2.4), i.e., with a bending angle of 41.5 degrees and a sliding rate of 120 mm/min. However, the specimen should include at least two geogrid apertures in width, but no more than four, for a width as close to 100 mm as possible (ASTM D7748, 2014; GRI GG10, 2001). In addition, the ribs should be cut exactly midway between junctions both in the machine and cross directions. This test provides a measurement of the bending length and flexural rigidity.

The in-plane shear modulus of bidirectional geogrids may be measured to characterize the aperture stability for pavement and subgrade reinforcement applications among others (ASTM WK24635, 2011). The geogrid specimen is secured in a 230 mm internal side square frame with a node in the middle (GRI GG9, 2004). Incremental moments are applied to the central node with a torqueing device. The specimen should be supported at the central node location to avoid applying an out-of-plane stress to the geogrid. At each increment, the corresponding torsional rotation produced in the central node is recorded. The geogrid is then unloaded. The loading-unloading cycle is repeated three other times for the same specimen. The measurement is conducted on four different specimens. The geogrid torsional behavior is characterized in terms of the initial tangent modulus of the applied moment vs. angular rotation curve. If the response curve is bilinear, which is characteristic of flexible textile-type geogrids, the offset tangent modulus corresponding to the second linear portion of the applied moment vs. angular rotation curve is also reported.

The mechanical behavior of geogrids in relation to the surrounding media is also of great importance. The interface shear strength with soil is tested using a similar setup and procedure as what is done for textiles (Koerner, 2012) and is described in Section 10.2.4. The maximum shear stress is recorded as the geogrid specimen fixed to a block is forced to slide against standard sand or any other soil in a shear box while under various values of normal stress (ASTM D5321, 2014; ISO 12957-1, 2005). However, the dimensions of the shear box should be adjusted so that at least two longitudinal and three transverse ribs are contained within the contact surface area between the upper and lower parts of the shear box throughout the test (ISO 12957-1, 2005). In addition, if a rigid plate is used to hold the geogrid specimen in the lower box, calibration measurements between the plate and sand should be made at each normal stress value to assess the impact of the support plate/substrate friction on the geogrid/substrate friction angle. It is also possible to use standard sand in both the upper and lower parts of the shear box.

The resistance of geogrids to soil pull-out is assessed using a laboratory pull-out box (ASTM D6706, 2001). The box is equipped with a side door containing a horizontal slot where the load transfer sleeve is positioned. The box length should be at least five times the maximum geogrid aperture size. The specimen width should be at least 305 mm and include five ribs or more. The minimum specimen length to width ratio is 2. Resin may be used to allow a uniform load transfer from the geogrid to the clamping device used to apply the horizontal pulling force to the geogrid. The geogrid attached to the pulling device is embedded horizontally between two layers of soil. The force required to pull the geogrid out of the soil at a rate of 1 mm/min is recorded for different values of normal compressive stress applied to the top soil layer. Values of normal stress of up to 250 kPa are generally used. The pull-out resistance at each normal compressive stress is calculated by dividing the maximum load by the geogrid width. The deformation of the different parts of the geogrid during pull-out may also be recorded with steel wires fixed to nodes and attached to dial indicators on the other end, as well as with strain gauges secured to the longitudinal ribs (Koerner, 2012).

Finally, two test methods are available to assess the behavior of geogrids in relation with segmental concrete block units used in the construction of reinforced soil retaining walls. A first one assesses the geogrid wall connection anchorage strength by pulling horizontally on a 750 mm wide or more geogrid specimen anchored between two rows of dry stacked modular concrete blocks subjected to a normal load (ASTM D6638, 2011). The displacement rate is 10%/min of the initial free length of the geogrid specimen. The tensile load is recorded as a function of the geogrid displacement at the back of the concrete blocks. Tests should be performed at a minimum of five values of the normal load within the range of what is typically seen in wall design. At each normal load, the peak connection strength, which is provided by the maximum tensile load, and the service state connection strength at a prescribed displacement criterion are determined. The second test method characterizes the shear strength of two rows of segmental concrete block units between which a geogrid is sandwiched (ASTM D6916, 2006). The lower concrete block row is restrained while the upper row is pulled horizontally at a displacement rate of 5 mm/min. A normal load is applied to the whole system. The shear load and concrete block displacement are recorded for a minimum of five applied normal loads within the range of what is typically seen in wall design. At each value of the normal load, the peak shear strength and service state shear strength at a prescribed displacement criterion are computed.

10.3.5 Durability

The same types of degradation mechanisms and corresponding test methods are used for geogrids as what has been described for geotextiles (Section 10.2.7). This includes resistance to oxidation (ISO 13438, 2004), resistance to UV (ASTM D4355, 2014; ISO 4892-2, 2013; ISO 4892-3, 2016), resistance to hydrolysis (EN 12447, 2001), chemical resistance for landfill applications (EN 14414, 2004), and field aging (ISO 13437, 2008). In the case of resistance to chemicals (ASTM D5322, 1998), the standard method ASTM D6213 (1997) specifies tests to be used to assess the impact of immersion in chemicals on the physical and mechanical properties of geogrids: visual

aspect, weight change, rib tensile test, wide width tensile test, melt index for polyolefin geogrids, and inherent viscosity for polyester geogrids. In dynamic tensile (ASTM D7556, 2010) and compressive (ISO 10722, 2007) loading tests, the size of the specimen may have to be adjusted to requirements specific to geogrids, for instance with at least 5 ribs in the width direction and the length comprising at least 3 nodes and being at least 300 mm for dynamic tensile loading (ASTM D7556, 2010).

In terms of durability, creep behavior is a critical aspect for the design of structures using geogrids (Koerner, 2012). Similar to geotextiles, tension creep and creep rupture may be measured with conventional test methods (ASTM D5262, 2007; ISO 13431, 1999). A 10% strain limit is generally considered the maximum allowable amount of creep for geogrids (Koerner, 2012). Accelerated creep testing, in particular using the SIM method (ASTM D6992, 2016), has allowed reducing the negative impact of interspecimen variation on the results (Koerner, 2012). Data obtained on geogrids show, for instance, that both creep strain and creep rupture mechanisms need to be taken into account to predict the geogrid behavior.

Stress cracking is another degradation mechanism to which geogrids made of highly crystalline polymers such as HDPE might be sensitive as a result of construction-induced damage (Elias, Carlson, Bachus, & Giroud, 1998). The resistance to stress cracking is assessed using the notched constant tensile load (NCTL) test method for geomembranes (ASTM D5397, 2007). A dumbbell-shaped notched specimen is subjected to a constant tensile load at elevated temperature and in the presence of a surface-active agent. The reactive agent is a 10% nonylphenoxy poly(ethyleneoxy) ethanol (Igepal) solution in water. Its role is to amplify the initiation and propagation of stress cracks as a result of its concentrated absorption at locations under dilational stress, for instance at crack tip (Wright, 1996). The specimens are loaded at various percentages ranging from 20% to 65% of their room temperature yield stress by 5% increments (ASTM D5397, 2007). The bath temperature is 50°C. The time to failure is recorded at the different applied loads. Percent yield stress vs failure time curves may exhibit a bilinear (knee), overshoot (nose), or tri-linear (step) shape. An analysis about the best notch location, specimen geometry, and notch depth for NCTL testing of geogrids may be found in Elias et al. (1998).

10.4 Geosynthetic clay liners

Geosynthetic clay liners (GCL) have been developed as a manufactured hydraulic barrier (ASTM D4439, 2015). They consist in clay being bonding to one or several layers of geosynthetic materials. The thin layer of bentonite eventually mixed with a polymer is held in sandwich between geotextiles and/or geomembranes through needling, stitching, or the use of a chemical adhesive (Koerner, 2012). In North America, all GCL products use sodium bentonite with a mass per unit area of 3.2–6 kg/m^2, and a thickness between 4 and 6 mm. Sodium bentonite is composed primarily of montmorillonite, which has a large specific surface, high cation exchange capacity, and the ability for interlayer swelling, which imparts it with a very low hydraulic conductivity, below 10^{-8} cm/s (Shackelford, Benson, Katsumi, Edil, & Lin, 2000).

The main types of GCLs include (Koerner, 2012):

- A layer of bentonite powder mixed with an adhesive and bonded between two geotextiles;
- A layer of bentonite powder needle-punched between two geotextiles;
- A layer of bentonite powder stitch-bonded between two geotextiles;
- A layer of bentonite powder mixed with an adhesive and bonded to a HDPE or LLDPE geomembrane.

Upon manufacturing, GCL rolls are covered with a plastic film to maintain the optimal 10%–35% humidity-equilibrated moisture state during storage and transportation until the product is installed.

GCLs are used beneath geomembranes in primary and secondary landfill liners, in landfill covers, in composite liners for surface impoundments, heap leach ponds, and coal ash piles; adjacent to geomembranes in vertical cutoff walls; above geomembranes as puncture protection; and on their own as single liners for canals, surface impoundments, agricultural waste treatment, as secondary liners for underground storage tanks, and for the containment of deicing solutions in airport and deicing salts in roads in sensitive areas for instance (Koerner, 2012). Their advantages over compacted clay liner systems (CCL) is that they are faster and easier to install, have better hydraulic performance, are self-healing and self-sealing, and are more resistant to changes in weather conditions.

10.4.1 Sampling and specimen preparation and conditioning

The conditions for sampling GCLs are described in ASTM D6072 (2009). Great care should to be taken in minimizing bentonite loss from the sample. For that purpose, GCL samples collected prior to installation, i.e., on finished and/or packaged GCL rolls, are manually rolled around a core at least 75 mm in diameter with wide strapping tape wound around both roll ends. GCL samples may be exhumed from the field after installation either using a hand cutting or a coring method. In the first case, the sample is slid on a nonporous rigid plate to minimize the risk of bending or distorting the GCL. In the second case, the sampling tube is capped immediately after retrieval.

Both for samples collected before and after installation, great precaution should also be taken to preserve the GCL moisture content throughout the handling, transportation, and storage process until testing (ASTM D6072, 2009). For that purpose, samples are sealed inside at least two layers of plastic sheeting; a thin cellophane film may be used for the inner wrapping to secure the sample while the outer sheeting should be at least 0.15 mm thick. Time between collection and testing should be minimized to limit changes in the sample moisture content. Physical and mechanical sources of disturbance for the GCL samples, such as very high or freezing temperatures, mechanical distortion, vibrations, impacts, etc., should also be avoided.

Unlike the rest of geosynthetics, GCL samples should generally be tested as received, i.e., without conditioning (ASTM D6768, 2004). In addition, to limit changes in the sample moisture content, the interval between the moment when the sample package is open and the sample is tested should be minimized (ASTM D6072, 2009).

10.4.2 Physical properties

GCL thickness is measured using the same test method as for geotextiles (Section 10.2.2), i.e., with a presser-foot apparatus at 2 kPa equipped with a 56.4 mm diameter foot (ASTM D5199, 2012; ISO 9863-1, 2016). Samples are tested in the as-received condition.

A test method for measuring GCL weight, water content, and bentonite content is provided in ASTM D5993 (2014). The weight of GCL specimens is first determined after they have reached moisture equilibrium in the atmosphere of the laboratory they will be tested, which should be at 23°C with a relative humidity below 70%. They are then dried in an oven at 110°C until the mass remains constant, and weighted again when cooled down. The mass per unit area of the GCL specimen is determined by dividing its initial weight by its surface area. The mass per unit area of the dry clay component, which may include adhesives, polymers, and other additives, is computed by subtracting the nominal mass per unit area of the geosynthetic components, measured according to ASTM D5261 (2010) or ISO 9864 (2005) for instance, from the mass per unit area of the dried GCL specimen. Finally, the percent initial moisture content of the GCL clay component is estimated by dividing the difference between the initial mass per unit area of the GCL specimen and the nominal mass per unit area of the geosynthetic components by the mass per unit area of dry clay (ASTM D5993, 2014). Different techniques are suggested to limit clay loss at the specimen edge during the cutting process, which strongly affects the GCL weight determination.

10.4.3 Mechanical properties

The tensile strength of GCLs may be tested in a wide width configuration to simulate its behavior when it is installed on a steep slope and anchored in a trench at the top of the slope (GRI GCL5, 2011). A 100 × 200 mm specimen in the as-received condition is secured across its entire 100 mm width in the grips of a tensile frame and loaded at 300 mm/min until it ruptures (ASTM D6768, 2004). The appropriate pressure should be used for specimen clamping to prevent slippage or crushing. The measurement is conducted on five specimens cut in the machine direction. The tensile strength is calculated using the peak value obtained for each specimen. Alternatively, the GCL wide width tensile tests may be performed using the ASTM D4595 (2011) or ISO 10319 (2015) test methods, with a 200-mm width and a 100-mm length. Tensile tests may also be conducted on GCLs using the ASTM D4632 (2015) grab test method for geotextiles.

When the GCL is constructed with two geotextiles needle-punched on both sides of a layer of clay, it is important to assess the peel strength of the assembly. The measurement may be performed according to ASTM D6496 (2004), where the top and bottom layers of a 100 × 200 mm specimen are gripped individually over their entire width and pulled apart at a rate of 300 mm/min. The specimen is tested as received, i.e., without conditioning, and is prepared by manually separating the top and bottom layers of the GCL for the first 50 mm using a knife or a razor blade. The bonding peel strength is calculated by dividing the average peeling force recorded over the entire peeling process by the specimen width. As the initial portion of the curve corresponds

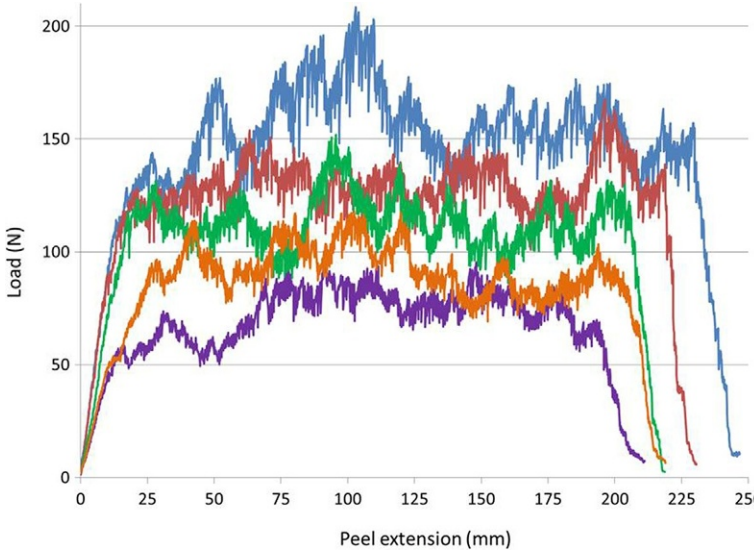

Fig. 10.7 Typical GCL peeling test data measured according to ASTM D6496.

to the initial loading and deformation of the geotextile tabs prior to peeling (Fig. 10.7), it has been proposed to exclude the data corresponding to the first 50 mm displacement from the calculation of the bonding peeling force (CETCO, 2014). An alternative test method is based on a modification of the geotextile grab test method ASTM D4632 (2015). This is in fact the way GCL manufacturers initially measured the peel strength of their product before a test method was specifically developed for GCLs (CETCO, 2014). The modified version of ASTM D4632 (2015) involves the same specimen and clamp dimensions as well as displacement rate as what is used in ASTM D6496 (2004). The only difference is that, in the case of the modified ASTM D4632, the bonding peel strength is reported in terms of maximum peak force. It may be noted that the possibility to express the peeling performance in terms of peak peel strength is also provided in ASTM D6496 (2004).

Even if GCLs have the capability to self-heal, a characterization of the puncture performance may be justified by their relative thinness and brittleness (Koerner, 2012). Measurements may be performed using the same test methods available to geotextiles and described in Section 10.2.4: small scale puncture with an 8-mm diameter probe (ASTM D4883, 2007), medium scale puncture with a 50-mm diameter CBR probe (ASTM D6241, 2014; ISO, 12236, 2006), or large-scale hydrostatic puncture conducted with pyramids, cones, or site-specific soil (ASTM D5514, 2014).

Knowledge of both the internal and interface shear strength is also critical for structure design using GCLs (GRI GCL5, 2011). Both properties may be measured in a direct shear box using test method ASTM D6243 (2016). The GCL internal shear strength is determined by securing one surface of the GCL specimen to the lower section of the 300 × 300 mm shear box and the other specimen surface to the top shear box section. This may be done using gripping surfaces or clamps so that the applied

shear force is transferred through the outside specimen surfaces into the GCL inside. The measurement is conducted at a constant horizontal displacement rate in the area of 0.1 mm/min under at least three different values of the normal stress applied to the GCL specimen. Specimens are tested in the as-received condition in the standard atmosphere for testing geosynthetics and should be allowed consolidating under the applied normal load before the measurement is started. Samples may also be tested in a wet condition by inundating the specimen after it has been installed in the shear box. For the GCL interface shear strength measurement, a section of the shear box is filled with compacted soil while the GCL specimen is fixed to the other section. A normal load is applied to the system which is allowed to consolidate before testing. The shear force and horizontal displacement are measured while one section of the shear box moves relative to the other section at a rate of 1 mm/min or less. The test is conducted with a minimum of three different normal stresses. For both internal and interface shear strength measurements, the peak shear force is determined for each normal stress and a Mohr-Coulomb shear strength envelope is developed by expressing the peak shear stress as a function of the applied normal stress, leading to the Mohr-Coulomb friction angle. In all instances, the locus of failure should also be reported. Alternatively, standard test method ISO 12957-1 (2005), which employs standard sand as contact soil, may be used. Other interface materials of interest include geomembranes (GRI GCL5, 2011).

10.4.4 Hydraulic and barrier properties

The water-clay interaction has large effects on the GCL hydraulic performance. It may be characterized by three properties: the swell index, water absorption, and fluid loss. These properties are generally measured on the as-received bentonite prior to GCL manufacturing. The swell index evaluates the swelling ability of bentonite under zero normal stress (Koerner, 2012). It is measured by adding 2 g of finely ground bentonite that has been oven dried at 105°C to 100 mL of reagent water by 0.1 g increments (ASTM D5890, 2011). After a minimum hydration period of 16 h, the volume of hydrated clay mineral is recorded. Bentonite water absorption may be measured according to ISO 10769 (2011). A 0.25 g specimen which has been ground, sieved below 0.25 mm, and dried at 60°C is deposited on the glass filter plate of a water absorption device that records the variation in the weight of water absorbed over a 24-h period. The water absorption value is computed by dividing the weight of absorbed water by the weight of dry bentonite. Finally, the fluid loss properties of bentonite are determined by measuring the amount of liquid collected when a film prepared with a well-mixed 6% solids bentonite/water slurry is filtered under 689 kPa during 22.5 min using an ambient temperature/low-pressure filter press and a 90 mm filter paper (ASTM D5891, 2002).

Hydraulic measurements may also be conducted on the GCL material. For GCL products having a geotextile backing, the flux through the GCL may be evaluated using water (ASTM D5887, 2016). A flexible wall triaxial permeameter equipped with a constant head, falling head, or constant rate of flow system is used for the measurement. The first step of the test consists in saturating and consolidating the 100 mm

diameter GCL specimen with deionised water under a stress of 550 kPa and a back-pressure of 515 kPa for 48 h. Then the pressure at the base of the specimen is increased to 530 kPa, so an upward flow is produced through the specimen under a pressure gradient of 15 kPa. The inflow and outflow rates should be within 25% of each other. At least three values of flow rate are determined over a minimum 8-h time period; they should not show any upward or downward trend. The flux is computed by dividing the average of the last three recorded flow rate values, which are taken as the average of the inflow and outflow rates, by the specimen surface area. The measurement may also be conducted with another aqueous permeant that is potentially incompatible with the GCL, for example leachate (ASTM D6766, 2012). In that case, a permeant interface device including a flexible bladder membrane is added when the permeant is hazardous, corrosive, or volatile. The 48 h saturation/consolidation step may be performed either with deionized water or with the liquid of interest. Although the hydraulic conductivity (also referred to as coefficient of permeability) could be provided by the same test protocol, difficulties in assessing the specimen thickness have prompted those who drafted standard test method ASTM D5887 (2016) to limit the test output to the value of the flux (Koerner, 2012). On the other hand, details of the calculation of the hydraulic conductivity are provided in ASTM D6766 (2012) for the different configurations of the hydraulic system: constant head, falling head (with constant or increasing tailwater pressure), and constant flow rate. Some indications are also provided regarding the measurement of final dimensions of the specimen.

The gas barrier properties of GCLs are also of great interest. They may be characterized under a normal stress of 20 kPa using a 15 kPa differential pressure of nitrogen gas (ISO 10773, 2011). The GCL specimen is first brought to a water content around 110% and left consolidating at these conditions under 20 kPa for one week. Then it is installed in the test cell over a base layer of 1–2 mm diameter glass beads, sealed on the edges with bentonite paste, and covered with another layer of glass beads over which the loading piston is positioned. A 20 kPa normal load is applied. It is increased to 35 kPa at the same time a 15 kPa differential pressure of nitrogen gas is applied across the GCL specimen, with the downstream pressure being atmospheric pressure. The steady-state nitrogen gas flow is recorded for three specimens at different values of water content around 110% (e.g., 100%, 110%, and 120%). That water content value is determined by weighting the specimen immediately after the test is over and after it has been dried out. The gas flux of nitrogen at a 110% GCL water content is determined by interpolation using a best-fit regression of the three data points.

10.4.5 Durability

The assessment of GCL durability involves tests performed both on the individual components as well as on the finished product (ASTM D5819, 2005; ISO 13434, 2008). A description of test methods relative to the resistance of the geotextile components to environmental and service degradation may be found in Section 10.2.7. This includes UV resistance according to ISO 4892 (2013), chemical resistance to liquids using test methods EN 14030 (2001) and/or EN 14414 (2004), chemical immersion procedures using test methods ASTM D5322 (1998) and/or ASTM D5496 (2015), and resistance

to micro-organisms using test methods EN 12225 (2000) and/or ASTM G160 (2012). In instances where the geotextile is tested while being in contact with an external medium, for instance for characterizing its long-term hydraulic behavior, that medium should be hydrated bentonite (Koerner, 2012).

Depending on the application, it may also be relevant to characterize the resistance of the GCL textile components to leaching in hot water, alkaline solutions, and organic alcohols (EN 14415, 2004). Specimens are prepared by removing the bentonite from the GCL using compressed air, washing, or any appropriate method. They are initially weighted after a 24 h period at 50°C followed by a cooling period in a desiccator until they reach the test temperature of 20°C. Then, they are immersed either in distilled or demineralized water, in a saturated suspension of calcium hydroxide, or in a mixture composed of 30% by volume of methanol, 30% by volume of 2-propanol, and 40% by volume of 1,2-ethane diol. In all three cases, the solution is maintained at 50°C with constant stirring conditions in an opaque and airtight container. After 56 days of immersion, the specimens are removed from the bath, dried at 50°C, and weighted once cooled down. A visual observation is made of any sign of degradation. In addition, the residual elongation at beak is measured and compared to that of control specimens that have also been conditioned at 20°C and 65% relative humidity.

The clay portion of the GCL may also be tested for its chemical compatibility with liquids (ASTM D6141, 2014). For that purpose, the swell index and fluid loss of the bentonite are measured according to the traditional test methods described in Section 10.4.4 (ASTM D5890 (2011) for swell index and ASTM D5891 (2002) for fluid loss) while using the solution of interest as the test liquid. If the liquid has to be generated in the laboratory for a site-specific soil, a slurry is prepared by mixing one volume of the soil with two volumes of distilled water and allowing the mixture to condition for 24 h in a sealed container (ASTM D6141, 2014). The test liquid is obtained by decantation followed by an eventual filtration, and stored in a sealed container.

Other important aspects of GCL durability are related to freeze-thaw cycles, wet-dry cycles, water/solute breakout time, and ion exchange (Koerner, 2012). The effect of freezing-thawing cycles on the permeability of GCL may be characterized according to EN 14418 (2014). A GCL sample is saturated under a pressure of 4 kPa for 48 h at room temperature. It is then kept in a freezer at −5°C for 24 h. After being allowed to thaw at room temperature, it is submerged again for 24 h at room temperature. The cycle is repeated three other times before 100 mm diameter specimens are cut. Their flux is determined with a flexible wall permeameter that is initially subjected to a cell pressure of 550 kPa and a back pressure of 515 kPa for a period of 48 h before the flow of deionized water is initiated by raising the pressure on the inlet side of the test specimen to 530 kPa. The flux of the frozen-thawed specimen is determined under equal inflow and outflow levels and compared to that of control specimens that have been subjected to similar cycles except for the cold temperature. The measurement of the effect of wetting-drying cycles on the permeability of GCL follows the same principle (EN 14417, 2014). However, in that case, the freezing part of the cycle is replaced by a 24 h drying period under a pressure of 4 kPa in an oven at 110°C. In case of water/solute breakout time, if no dedicated standard test method appears to have been

published yet, it has been proposed to assess it by performing a flux measurement test on the as-received dry GCL product instead of the fully saturated specimen used in the traditional flux measurement test (Koerner, 2012). For water breakout time, the test may be conducted according to ASTM D5887 (2016) while ASTM D6766 (2012) is used for solute breakout time. No standard test method exists either to characterize the sensitivity of GCLs to ion exchange and its impact on the material hydraulic conductivity. However, guidance may be found in the work done by Kolstad, Benson, and Edil (2004). They performed their measurements with a flexible wall permeameter under falling head conditions with constant tailwater elevation and used a list of aqueous multispecies solutions of the inorganic salts with various ionic strength and relative amounts of monovalent and divalent cations as the permeant solutions.

Resistance to root penetration is another aspect of GCL durability that is assessed on the full product. A short-term evaluation may be performed according to EN 14416 (2014). GCL specimens are placed horizontally in clay flower pots between two layers of soil. Lupin seeds are sown on the soil and allowed to grow outside during 6 weeks in summer (or eight weeks in winter with the pots placed in a heated greenhouse with additional artificial light). A control experiment is carried out by replacing the GCL specimen by a 20-mm thick layer of bitumen. After the test is over, the pots are emptied and the upper and lower surfaces of the GCL specimens are inspected for signs of roots having penetrated into or through them. The bitumen control specimen is also inspected to verify the vitality of the plants: if roots have not penetrated the bitumen, the test shall be repeated. If needed, the long-term resistance to root penetration may eventually be assessed over a 2-year period in a climate-controlled greenhouse using pyracantha shrubs (EN 13948, 2007).

10.5 Drainage geocomposites

Drainage geocomposites are generally constituted of a polymeric drainage core encapsulated with a geotextile (Koerner, 2012). The objective is to increase the in-plane flow capacity of the geotextile. The drainage core may be a geogrid bonded to a needle punched nonwoven geotextile; the resulting geocomposite combines tensile strength and in-plane drainage. These types of geocomposites are often used for the internal drainage of low permeability backfill soils in reinforced walls and slopes. The drainage core may also be a geonet, in which case the composite provides simultaneously separation, filtration, and drainage. These types of geocomposites are installed horizontally in landfill liner and cover systems to catch and transport leachate and gases, or beneath pond liners to conduct water and vapor.

In a third category of drainage composites, the polymeric drainage core is a 3D quasirigid structure produced by extrusion or thermoforming for example (Koerner, 2012). This includes prefabricated vertical drains (PVD), which are also called wick or strip drains. They are generally composed of a 100 mm wide by a 5 mm thick plastic fluted or nubbed cores enclosed in a geotextile filter. These products have all but taken over from the use of sand drains as a way to rapidly consolidate saturated fine grained soils. Indeed, in addition to offering similar performance in terms of drainage, their

deployment is simpler and less time consuming and costly as they are supplied in rolls and installed using a conventional soil insertion rig. They also provide an additional reinforcement to soft soils with tensile strength usually in the range of 5–15 kN. This third category of drainage geocomposites comprises prefabricated edge drains as well. They are typically 500 mm high and 20–30 mm wide and are installed next to highway and airfield pavements for lateral drainage out of the pavement section. In that case, the water flow goes downward in the drain contrary to strip drains.

Another type of 3D quasirigid structure core drainage composites is sheet drains (Koerner, 2012). The core is composed of perforated panels that bear nubs, columns or dimples or are formed as a 3D mesh of entangled filaments. They generally have one layer of geotextile on one side which acts as a filter or separator while the polymer core provides the drainage function. They typically display higher flow rate than geonet drainage composites. They are installed on the backfilled side of retaining walls and plaza decks, and behind mechanically stabilized earth walls and slopes. A last example of 3D quasirigid structure core drainage composites is planar drain-tube geocomposites. These products were developed in the late 1990s and include two or three layers of nonwoven geotextiles assembled by needle punching between which parallel rows of corrugated perforated pipes are regularly positioned (Saunier & Blond, 2009). They have been shown to sustain extremely high normal loads without significant changes in transmissivity and display no sensitivity to creep. These planar drain-tube geocomposites have been successfully used for the drainage of embankments, backfills, pavements and floor slabs, parks, gardens and sports fields, landfill caps and long-term exposed slopes as well as for deep vertical drainage, protection of pond geomembranes, and collection of leachate at the bottom of landfills.

10.5.1 Sampling and specimen preparation and conditioning

The characterization of drainage composite properties and performance involves measurements conducted on the individual components, i.e., geotextiles, geogrids, geonets, dimpled, columned or nubbed polymer sheets, 3D plastic filament mesh, corrugated perforated drainage pipes, etc., as well as on the assembled product. In most cases, these materials are supplied in rolls. A sampling and specimen preparation protocol may be found in ISO 9862 (2005) and has been described in Section 10.2.1. Conditioning requirements are also generally the same than for geotextiles, with atmospheres at 21°C/65% RH or 23°C/50% RH.

10.5.2 Physical properties/composition

Test methods for the measurement of the physical properties of the geotextile components of drainage geocomposites are described in Section 10.2.2. This includes single and multilayer thickness measurements according to standard test methods ASTM D5199 (2012), ISO 9863-1 (2016), ASTM D1777 (1996), and ISO 9863-2 (1996), as well as mass per unit area (ASTM D3776, 2009; ASTM D5261, 2010; ISO 9864, 2005).

In the case of the polymeric drainage core, it may be of interest to measure the density, melt index, and carbon black content. The density of plastic solids may be

determined by the displacement method (ASTM D792, 2013). After being conditioned for at least 40 h at 23°C/50% RH, a 1–50 g one-piece specimen with smooth surfaces and edges is weighted in air. It is then suspended by a wire and immersed in air-free, distilled or demineralized water at 23°C. The mass of the suspended specimen is recorded. The mass of the partially immersed wire as well as that of a sinker eventually used with plastics with a specific gravity lower than 1 are also determined. This test method provides the specific gravity of the plastic material as well as its density. If the plastic is affected by or lighter than water, other liquids might be used. Their specific gravity at 23°C is measured before the test using a pycnometer. Plastic density may also be determined by the density-gradient technique (ASTM D1505, 2010). Three specimens are gently immersed in a graduated tube containing a system of two liquids at 23°C selected to cover the relevant range of density as well as calibrated glass floats evenly distributed throughout that density range. After equilibrium has been obtained, the height of each specimen and each float is recorded. The density of the specimens is obtained graphically or by numerical interpolation.

The melt flow rate of thermoplastics is determined with an extrusion plastometer (ASTM D1238, 2013). This parameter provides information on the polymer molecular weight. A quantity of resin between 2.5 and 8 g (depending on the expected melt flow rate) is inserted in the cylinder bore of the plastometer at a temperature selected based upon the polymer tested and loaded with a piston and a dead-weight. The plastometer may be equipped with a standard die with an orifice of 2.095 mm diameter and 8 mm length or a half die with an orifice of 1.048 mm internal diameter and 4 mm length (for polyolefins that exhibit a high melt flow rate). After a 7-min preheat period, the timer is started: the amount of resin extruded over a set period of time is collected and weighted. The melt flow rate is expressed in terms of grams of extruded material/10 min at the test temperature and weight. In the case of polyethylene, the flow rate obtained at 190°C with a dead-weight of 2.16 kg is customary referred to as the melt index.

Different techniques are available to quantify the carbon black content in polyolefins based on the particle size range, presence of other mineral fillers, and type of polymer. For polyethylene compounds that contain channel black (10–30 nm diameter particles) or furnace black (10–80 nm diameter particles) with eventually other mineral fillers but no thermal black (150–500 nm diameter particles), a muffle furnace at 600°C is used to prevent the combustion of the residual carbon black once the air in the furnace has been oxygen-depleted (ASTM D4218, 2015). A 1 g specimen is initially weighted; it is reweighted after a 3-min pyrolysis treatment in the muffle furnace. If the presence of other mineral fillers is suspected, a second heating is applied for 10 min or more until only light-colored ashes remain. The true carbon black content is obtained by subtracting the mass of the residual ashes from the carbon black mass. For polyethylene, polypropylene, and polybutylene compounds containing no other nonvolatile pigments or fillers than carbon black, the specimen pyrolysis is conducted in an electric oven at 600°C in nitrogen for at least 15 min (ASTM D1603, 2014). After the specimen has cooled down, it is weighed. For very low carbon black content, the measurement is corrected for the presence of residual inorganic matter in the sample by subjecting it to a second 10 min heating treatment in air at 600°C. Finally, in the

case of planar drain-tube geocomposites, the outside diameter of the drainage pipe may be determined with a flat-anvil micrometer, vernier calipers, a tapered sleeve gage, a sleeve window gage, or a circumferential wrap tape (ASTM D2122, 2016).

10.5.3 Mechanical properties

Some mechanical performances of drainage composites are assessed on the product individual components. In the case of the geotextile layer(s), this includes tensile tests according to the strip method (ASTM D5035, 2011), grab method (ASTM D4632, 2015), and wide width method (ASTM D4595, 2011; ISO 10319, 2015), trapezoidal tear tests (ASTM D4533, 2015), and puncture tests with the 8-mm diameter probe (ASTM D4833, 2007) and the 50 mm diameter CBR probe (ASTM D6241, 2014; ISO 12236, 2006). A description of these tests may be found in Section 10.2.4.

In the case of geonet-geotextile geocomposites, the mechanical performance in tension of the geonet component may be assessed on 102 mm wide by 203 mm long specimens loaded at a rate of 300 mm/min in a constant rate of extension mechanical test frame (ASTM D7179, 2007). The grips should be at least as wide as the specimens and initially distanced by 100 mm. The test is performed on five specimens cut in the machine direction. The result is reported in terms of breaking force. For the polymeric drainage core of strip drains, tensile strength may be measured according to the grab method (ASTM D4632, 2015) or on dumbbell-shaped test specimens (ASTM D638, 2014).

The compressive strength of the strip drain core is determined using compression platens and a loading system (ASTM D1621, 2016). Specimens with a surface area between 25.8 and 232 cm^2 are placed between the two flat plates, one of which is equipped with a spherical seating mechanism to compensate for any source of nonparallelism. Load-deflection data are recorded as one of the plates moves toward the other at a rate of 2.5 mm/min for each 25.4 mm of specimen thickness. The results are generally expressed in terms of compressive strength at a set value of deflection, for example 20%, or at yield point. For planar drain-tube geocomposites, the pipe stiffness may be characterized under parallel-plate loading conditions (ASTM D2412, 2011). A 150 mm long pipe specimen is loaded between two rigid parallel flat plates that are moving towards each other at a rate of 12.5 mm/min. The pipe stiffness at a specific level of deflection, 5% for instance, is calculated from the recorded load-deflection data.

Some mechanical properties are also assessed on the assembled product. For instance, the same test method used to measure the compressive strength of the strip drain core, i.e., ASTM D1621 (2016), may also apply to the core-geotextile geocomposite (Fig. 10.8). Alternate test methods may also be used. For example, standard test method ASTM D6364 (2006) uses specimens that are at least 120 × 120 mm or contain at least five support points along each main axis in the case of dimpled, columned, or nubbed core geocomposites to characterize their short-term compression behavior. The specimens are loaded in compression using parallel plates at a rate of 10% of the nominal specimen thickness per min or 1 mm/min. The plates may be horizontal

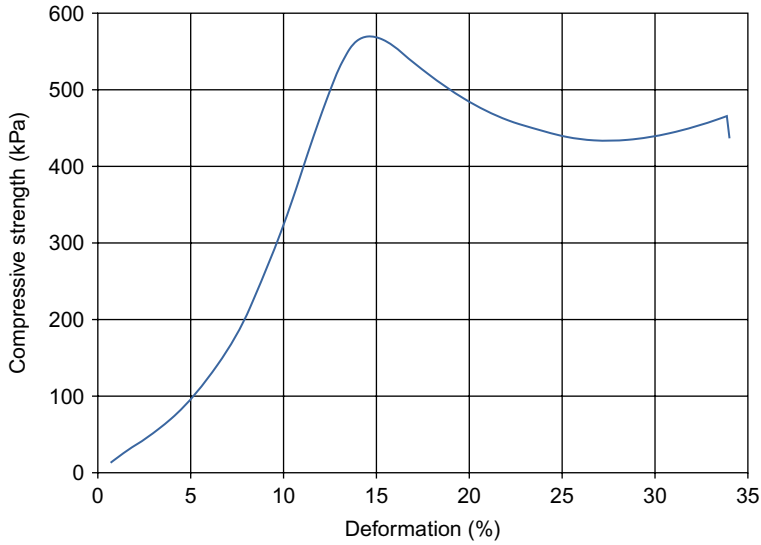

Fig. 10.8 Example of compressive test data on a strip drain measured according to ASTM D1621.

or inclined, in which case their surface is roughened to keep the specimen from sliding. The load and residual thickness at yield point are usually reported as well as the residual thickness at specific loads. The short-term compression behavior of geocomposites may also be measured using ISO 25619-2 (2008). In that case, specimens are at least 100 × 100 mm or contain at least three support points along each main axis in the case of dimpled, columned or nubbed core geocomposites. A 5 kPa preload is applied on the specimen installed between two horizontal parallel plates. The loading is conducted at a rate of 10% of the initial specimen thickness per min. The compressive stress and strain at failure are computed as well as the strain at 1 MPa.

The vertical strain and change in core area of geocomposite edge drains may also be characterized under vertical compression (ASTM D6244, 2006). The specimen length should correspond to the height of the drain in the field and be 298.5 mm wide. It is installed along the back wall of a 304.8 mm long, 106.7 mm wide, and 610 mm high compression chamber. The large front and back walls of the chamber are made of aluminum covered with a Teflon film on the inside to reduce friction. The narrow side walls are made of tempered glass and are protected from scratch with clear plastic spacers on the inside of the chamber. The chamber is backfilled with natural sand oven-dried and sieved to a specific gradation. The initial open area of the core is traced on one side of the chamber by shining a light source through the open core from the other side. The initial core height is also recorded. Then, a vertical load is applied to the system at 445 N/min using a loading plate placed on the top of the compression chamber and a compression machine. The loading is stopped and the load held constant when a value of 1112.5 N has been reached to allow measuring the core height and open area. Then the loading is resumed until a value of 3337.5 N, and then 4450 N have been reached.

Each time, the loading is put on hold and the core height and open area are measured. The test is stopped at 4450 N. The percent decrease in core height and open area as a function of the vertical stress applied or at a nominal load is reported.

The ability of the drainage geocomposite to maintain its integrity may be assessed using peel tests. For instance, standard test method ASTM D7005 (2016), which was developed specifically for geocomposites, uses specimens of 101.6 × at least 200 mm whose individual plies have been initially separated by mechanical means over a distance of at most 50 mm. The separated ends of the specimen are clamped in the grips of a tensile test machine with an initial grip distance of 50 mm. If the specimen contains a rigid ply, for instance a geonet, that end shall be bent by hand to form an angle of approximately 45 degrees relative to the axis of the grips. The grips are then pulled apart at a rate of 300 mm/min. The bond strength or ply adhesion is determined by dividing the average force between 25 and 100 mm of separation by the specimen width. Test method ASTM F904 (2016) is also sometimes used for geocomposites. However, it has been developed for similar laminates made from flexible materials and the specimen width is much smaller (25.4 mm), which may not allow testing a representative sample of the product. This test method offers alternative ply separation techniques to mechanical means with the use of heat or solvents. It also specifies to disregard the initial peak in the calculation of the average force and record if the failure is cohesive, i.e., within one of the two adjacent layers to the bonded area, or adhesive. ASTM D413 (1998) applies to the case when rubber is involved as the adhesive or the substrate and the surfaces are relatively plane or uniformly circular. It allows testing with a 90-degree peeling angle in addition to the usual 180-degree angle. The force may be applied in a dynamic manner with a tensile test machine as well as in a static process using dead-loads hanging freely from the specimen. In the latter case, the separation rate per unit width under a specific force is reported. However, the specimen width is only 25.4 mm and restrictions exist in terms of thickness (6 or 13 mm depending on the test method (90 or 180 degrees peel)). It should be noted that in all the test methods described above, the contribution of the bending force of the individual layers is included in the result of the bond strength measurement.

The mechanical interaction of the drainage geocomposite with its surrounding medium is also of paramount importance. As already described in Section 10.2.4, the geocomposite may be tested in direct shear against standard sand (ISO 12957-1, 2005) or any other relevant material (ASTM D5321, 2014). It is also possible to determine its friction performance against soils under low normal stress using an inclined plane apparatus (ISO 12957-2, 2005). The geocomposite specimen is installed either on a rigid plate or on soil in the lower section of the shear box. The upper section of the shear box is filled with compacted soil or standard sand and positioned above the geocomposite specimen. A normal load is applied to the soil using a system of weights so that the normal stress is 5 kPa. Then the lower section of the shear box is inclined at a constant rate of 3 degrees/min while the position of the upper section is recorded. The angle at which the upper box section starts sliding over the geocomposite is used to compute the friction angle of the geocomposite/soil system.

10.5.4 Hydraulic properties

The assessment of the hydraulic properties of drainage geocomposites generally includes a characterisation of the filter component's AOS according to ASTM D4751 (2016) and water permittivity according to ASTM D4491 (2016). In the case of in-plane water flow capacity or transmissivity, measurements may be conducted on the core component or the assembled geocomposite using test methods ASTM D4716 (2014) and ISO 12958 (2010). A description of these different test methods is available in Section 10.2.4. In the case of geocomposite in-plane water flow capacity measurements, the dimension of the geocomposite specimen is dictated by the component requiring the largest minimum size (ASTM D4716, 2014). It has also been shown with tubular drainage geocomposites that the length of the specimen affects the transmissivity measured (Blond, Saunier, Daqoune, & Fourmont, 2013); the value obtained with the 300-mm specimen length typically used in ASTM D4716 (2014) and ISO 12958 (2010) may be considered to be conservative for drainage lengths of 1 m or more.

In addition, crimps induced in vertical strip drains by soil consolidation around may affect the drain in-plane water flow rate (ASTM D6918, 2009). To assess this effect, the vertical strip drain is sealed in a waterproof membrane; its ability to conduct water along its plane in a crimped condition under constant head is compared to that in the uncrimped condition. Crimp may be generated either using a 90-degree tip wedge or with air pressure at 300 kPa applied over a 300 mm long section of the vertical strip drain to simulate earth pressure. In the latter case, the strip drain specimen is wrapped in a rubber membrane cylinder. The percent change in flow velocity between the uncrimped and crimped condition is computed.

The efficiency of vertical strip drain products at increasing the consolidation rate of specific compressible soils from construction project sites may also be assessed for design purposes using a large-scale consolidation test (ASTM D7498, 2009). A vertical strip drain specimen with a 508-mm length is positioned vertically in the center of a 254-mm diameter by 558.6 mm long PVC cylinder. The cylinder is then filled up to a 381-mm height with compressible soil from the project site which is molded around the specimen. The top of the soil is sealed with wax with the vertical strip drain specimen protruding up through the seal. The bond between the wax and the cylinder inner surface is carefully broken with a spatula. A 25.4-mm thick sand drainage blanket is placed above the soil with the vertical strip drain specimen draining into it. Drainage ports are located in the cylinder wall just above the initial wax level. A double cup rubber seal positioned atop the sand drainage blanket allows applying incremental loads to the system. First, an air pressure of 103.42 kPa is used and the soil consolidation is monitored over 3 days or until plots of deflection readings versus the log and the square root of elapsed time indicate at least three data points beyond the 100% primary consolidation phase. Then, the air pressure is increased to 206.84 kPa and deflection readings are taken until at least three data points are beyond the 100% primary consolidation phase. The same procedure is repeated with a 50-mm sand drain in place of the vertical strip drain. For each load applied to the soil, the coefficients of consolidation of the vertical strip drain and the sand drain are computed for 50% and 90% consolidation.

10.5.5 Durability

The durability of drainage composites is generally assessed using the same test methods as those employed for geotextiles (ASTM D5819, 2005; EN 12226, 2000; ISO 13434, 2008) and described in Section 10.2.7. This includes resistance to oxidation according to ISO 13438 (2004), UV resistance using fluorescent light (ASTM G154, 2016; EN 12224, 2000; ISO 4892-3, 2016) or Xenon arc (ASTM D4355, 2014; ASTM G155, 2013; ISO 4892-2, 2013), chemical compatibility according to ASTM D5322 (1998), and resistance to liquid waste and landfill chemicals according to EN 14414 (2004). In particular, resistance to biological clogging is of critical importance for applications of drainage geocomposites in leachate collection (Blond, Fourmont, Bloquet, & Budka, 2012). Exposure to aging conditions may be conducted on the individual components or the assembled product. The residual physical, mechanical, and hydraulic properties are generally assessed on the individual components according to ASTM D6389 (1999) for geotextiles, ASTM D6213 (1997) for geogrids, and ASTM D6388 (1999) for geonets, for instance, in the case of liquid chemical resistance. A description of onsite installation, retrieval, and testing protocols for the field aging of textile-based products according to ISO 13437 (1998) is also available in Section 10.2.7.

In addition, test methods also exist to assess the resistance of drainage geocomposites to compressive creep. For instance, compressive creep may be measured by subjecting drainage geocomposite specimens to a constant vertical load and recording the change in thickness over time (ISO 25619-1, 2008). Each specimen is at least 100×100 mm and contains at least three contact points in each main direction. A metal top plate is used to distribute the load over the entire specimen surface area: the stress it generates on the specimen shall be lower than 2 kPa. Normal stresses applied to specimens shall include at least four of the five following values: 20, 50, 100, 200, and 500 kPa. The specimen thickness is recorded at specific times: 1, 2, 4, 15, 30, and 60 min; 2, 4, 8, and 24 h; and 2, 4, 7, 14, 28, and 42 days. The test is generally conducted for 1000 h; it may be terminated if the thickness of the specimen becomes $<10\%$ of its initial value. The compressive creep strain and total compressive strain are computed at 1 and 1000 h for each applied normal stress. The test may be conducted with the specimen immersed in water if any component of the geocomposite contains a hydrophilic polymer. For products that display a columnar or cuspated structure and may be sensitive to shear failure, it is also possible to add a shear load to the compressive load. This may be done with inclined upper and lower plates in contact with the specimen or with a system of dead weights applying a horizontal force on the top plate. The shear force shall be 20% of the normal force. The surface of the upper and lower plates is roughened to permit a transfer of the shear force to the specimen. The specimen thickness and its horizontal displacement are recorded over time. In cases where the drainage geocomposite is intended to be installed on a slope, for instance in a landfill, it may be critical to assess the long-term performance of the product under combined normal and shear stresses as premature local failures may occur and compromise the structural stability of the system (Zhao, Blond, & Recalcati, 2012).

The compressive creep test duration may be reduced by using a SIM procedure similar to what has been described in Section 10.2.7 for tensile creep. Specimens are at least 120 × 120 mm and are positioned between two horizontal loading platens in the environmental chamber of a testing machine (ASTM D7361, 2007). The specimen thickness is recorded as a function of time as load increments are applied simultaneously with small temperature increments (<7°C for polyolefins) between isotherm dwell times of at least 10,000 s. The data expressed in terms of compressive creep modulus or compressive strain are analysed in a similar manner as for tensile SIM, i.e., by adjusting the time of each temperature/load segment to achieve a matching slope with the end of the preceding segment and by shifting the individual curve segments onto the initial dwell temperature reference data. In addition, the data are corrected for the system thermal expansion.

10.6 Future trends

Large progress has been accomplished since work on test method development for geotextiles and other textile-based geosynthetics was initiated in the 1970s. There are currently more than 250 standards available to characterize the properties and performance of geotextiles and other geosynthetics. However, efforts are still needed to improve existing test methods and develop new ones.

A first driver is the trend towards sustainable manufacturing with a larger use of recycled and biosourced materials. For instance, postproduction and postconsumer recycled materials may enter in the production of geotextiles (Bérubé & Saunier, 2016). Corrugated pipes containing recycled polyethylene are also already being manufactured for some applications (Thomas & Cuttino, 2011). However, as there may be differences between the properties of the recycled and virgin material, great attention should be paid so that the performances of the final product are not compromised. One aspect of particular concern is the presence of potential contaminants, for instance polypropylene and mineral additives in the case of recycled polyethylene, which may affect both the short and long term behavior of the geotextiles and textile-based geosynthetics. Another aspect to be considered is the larger variability in the recycled resin quality observed as postconsumer recycling becomes more widespread (Hopewell, Dvorak, & Kosior, 2009). This may require an adjustment of the sampling frequencies to capture this variability. In terms of biosourced materials, the larger prevalence of some aging mechanisms, for instance hydrolysis and biodegradation, compared to synthetic materials may call for different testing programs. In addition, the quality of biosourced materials is also inherently largely variable (Kozlowski, 2012).

A second driver for progress in standard test methods for geotextiles and other textile-based geosynthetics is related to the development of new applications for these products. For instance, GCLs are increasingly being used for mining applications. This includes liners and covers for mine tailings, liners for oil field pits, containment for heap leach pads, and secondary containment around fuel, brine, and acid tanks (Rowe, 2014). In some cases, the environment they are exposed to may be highly severe: very

aggressive chemicals, high or low pH solutions, hot or cold temperatures, etc. For example, a GCL has been used as part of a containment system for jet-fuel contaminated soil resulting from a spill in the Arctic (Bathurst, Rowe, Zeeb, & Reimer, 2007). Another example of new application in the mining industry includes the accelerated dewatering of mine tailings using an electrokinetic drainage geocomposite (Dolez, Blond, & Saunier, 2016). New applications may also be found in coastal engineering (Heerten, Jackson, Restall, & Saathoff, 2000), road infrastructure (Doulala-Rigby & Black, 2016), marine construction (Kulju, 2016), and waste management (Kelsey, 2017) for instance. Test methods have to be developed for these new applications both to assess the properties of the product relevant to the application as well as its performance. For instance, a test method was recently designed to characterize the hydraulic behavior of geotextiles with fine-grained tailings, which exhibit a hydraulic conductivity too low for the traditional gradient ratio test (Dolez et al., 2014).

A third driver is the development of new types of geotextiles and other textile-based geosynthetics that would require modifications of existing test methods and/or the development of new ones. For instance, there are currently new developments in the area of geogrids and GCLs (Koerner, 2012). As an example, a new geogrid composite made of a continuous filament, needle-punched nonwoven geotextile bonded to a biaxial geogrid offers three functions in a single layer: soil separation, filtration, and reinforcement (Kelsey, 2014). Research is also going on for the use of nanoclay as a replacement for part of the bentonite in GCLs to improve the hydraulic barrier performance and self-healing capacity (Salemi, Abtahi, Rowshanzamir, & Hejazi, 2016). Nanoclay has also been added to produce nanocomposite polyester fiber nonwoven geotextile in order to enable it to remove toxic and organic compounds from leachate solutions (Jeon, 2016). Nanofiber-based geotextiles are identified as a solution to improve the chemical/biological reactivity of the geotextile-based products, with applications for instance for gas collection in landfill cover systems (Ko, 2004). Smart materials are also looked at for providing new functionalities to geotextiles. For instance, sensor-enabled geosynthetics for the health-monitoring of reinforced soil slopes and embankments may be developed by combining electrically conductive fillers like carbon black or carbon nanotubes with a polymer matrix (Yazdani, Hatami, Hawa, & Grady, 2013). Thanks to the smart-material technology, geotextiles and geosynthetics may eventually be able one day to change their properties based on the external conditions, making them adaptive products.

Finally, another trend that is seen in standard test method development is the concern to better simulate field conditions. Indeed, it has been observed, for instance, that GCLs absorb much less moisture over time when they undergo thermal cycles simulating heating produced by daily sun exposure and thermal gradients resulting from the contact with the ground than when they are kept at constant temperature (Sarabian & Rayhani, 2013). As a result, if index test methods are useful to perform an initial screening of products (as well as for quality control and conformance testing as they are simple to perform) performance test methods which simulate field conditions as closely as possible (but are much more complex to run) are critical to ensure that the product will perform well in service (Narejo, 2016). An intermediate strategy is conducting quasiperformance tests combined with empirical design methods. However, the empirical design methods will ultimately also need to be corroborated by performance tests or field testing.

10.7 Conclusion

Thanks to the creativity, ingenuity, and hard work of pioneers in geosynthetics and of those who have pursued their mission, several test methods have been developed over the years to characterize the properties and performance of geotextiles and textile-based geosynthetics: physical, composition, mechanical, hydraulic, thermal, and durability. This chapter provides a description of many of the test methods relative to geotextiles, geogrids, geosynthetic clay liner, and drainage geocomposites under the jurisdiction of the International Organization for Standardization (ISO), ASTM International, and the European Committee for Standardization (CEN). It also includes some standards published by the American Association of Textile Chemists and Colorists (AATCC), AFNOR, the Canadian General Standards Board (CAN/CGSB), EDANA, the Geosynthetic Research Institute (GRI), the U.S. Army Corps of Engineers, and the U.S. General Services Administration. If large efforts have already been made and have led to great accomplishments in terms of providing tools to oversee the manufacture, installation, and short- and long-term performance of geotextiles and other textile-based geosynthetics, work is still needed to take into account the increasing content in recycled and biosourced materials, cover requirements related to new applications, encompass the new types of products developed, and better simulate field conditions.

10.8 Sources of further information and advice

More information may be obtained through standardization Committees dedicated to geotextiles and other geosynthetics, for instance:

- ISO Technical Committee 221 on Geosynthetics: http://www.iso.org/iso/standards_development/technical_committees/other_bodies/iso_technical_committee.htm?commid=270590
- ASTM Committee D35 on Geosynthetics: http://www.astm.org/COMMITTEE/D35.htm
- CEN Technical Committee 189 on Geosynthetics: https://standards.cen.eu/dyn/www/f?p=204:7:0::::FSP_ORG_ID:6170&cs=1954FF59BA83960998FFB63D729325FED

Acknowledgments

The author wishes to thank Eric Blond and Jacek Mlynarek from CTT Group for fruitful discussions on geosynthetics testing. She also wants to acknowledge the help of Sylvie Dalpé and David Beaumier in preparing some of the figures.

References

AATCC TM20. (2013). *Fiber analysis: Qualitative*. Park, NC: American Association of Textile Chemists and Colorists, Research Triangle. 19 pp.

Allen, S. R. (2016). Geotextile durability. In R. Koerner (Ed.), *Geotextiles: From design to applications* (pp. 177–214). Duxford, UK: Woodhead Publishing.

Artieres, O., Oberreiter, K., & Aschauer, F. (2009). *Geosynthetic systems for earth dams—35 years of experience*. In: Proceedings of the 2nd international conference on long term behaviour of dams. Graz (Austria), October 12–13. (pp. 98–103).

ASTM D276 Standard. (2012). *Standard test methods for identification of fibers in textiles*. West Conshohocken, PA: ASTM International. 12 pp.

ASTM D413 Standard. (1998). *Standard test methods for rubber property—Adhesion to flexible substrate*. West Conshohocken, PA: ASTM International. 5 pp.

ASTM D638 Standard. (2014). *Standard test method for tensile properties of plastics*. West Conshohocken, PA: ASTM International. 17 pp.

ASTM D751 Standard. (2006). *Standard test methods for coated fabrics*. West Conshohocken, PA: ASTM International. 19 pp.

ASTM D792 Standard. (2013). *Standard test methods for density and specific gravity (relative density) of plastics by displacement*. West Conshohocken, PA: ASTM International. 6 pp.

ASTM D1238 Standard. (2013). *Standard test method for melt flow rates of thermoplastics by extrusion plastometer*. West Conshohocken, PA: ASTM International. 16 pp.

ASTM D1388 Standard. (2014). *Standard test method for stiffness of fabrics*. West Conshohocken, PA: ASTM International. 6 pp.

ASTM D1505 Standard. (2010). *Standard test method for density of plastics by the density-gradient technique*. West Conshohocken, PA: ASTM International. 7 pp.

ASTM D1603 Standard. (2014). *Standard test method for carbon black content in olefin plastics*. West Conshohocken, PA: ASTM International. 4 pp.

ASTM D1621 Standard. (2016). *Standard test method for compressive properties of rigid cellular plastics*. West Conshohocken, PA: ASTM International. 5 pp.

ASTM D1776/D1776M Standard. (2016). *Standard practice for conditioning and testing textiles*. West Conshohocken, PA: ASTM International. 5 pp.

ASTM D1777 Standard. (1996). *Standard test method for thickness of textile materials*. West Conshohocken, PA: ASTM International. 5 pp.

ASTM D1987 Standard. (2007). *Standard test method for biological clogging of geotextile or soil/geotextile filters*. West Conshohocken, PA: ASTM International. 6 pp.

ASTM D2122 Standard. (2016). *Standard test method for determining dimensions of thermoplastic pipe and fittings*. West Conshohocken, PA: ASTM International. 5 pp.

ASTM D2130 Standard. (2013). *Standard test method for diameter of wool and other animal fibers by microprojection*. West Conshohocken, PA: ASTM International. 10 pp.

ASTM D2256/D2256M Standard. (2010). *Standard test method for tensile properties of yarns by the single-strand method*. West Conshohocken, PA: ASTM International. 13 pp.

ASTM D2412 Standard. (2011). *Standard test method for determination of external loading characteristics of plastic pipe by parallel-plate loading*. West Conshohocken, PA: ASTM International. 7 pp.

ASTM D3418 Standard. (2015). *Standard test method for transition temperatures and enthalpies of fusion and crystallization of polymers by differential scanning calorimetry*. West Conshohocken, PA: ASTM International. 7 pp.

ASTM D3776/D3776M Standard. (2009). *Standard test methods for mass per unit area (weight) of fabric*. West Conshohocken, PA: ASTM International. 5 pp.

ASTM D3786/D3786M Standard. (2013). *Standard test method for bursting strength of textile fabrics—Diaphragm bursting strength tester method*. West Conshohocken, PA: ASTM International. 4 pp.

ASTM D3787 Standard. (2016). *Standard test method for bursting strength of textiles—Constant-rate-of-traverse (CRT) ball burst test*. West Conshohocken, PA: ASTM International. 4 pp.

ASTM D3822/D3822M Standard. (2014). *Standard test method for tensile properties of single textile fibers*. West Conshohocken, PA: ASTM International. 10 pp.
ASTM D3895 Standard. (2014). *Standard test method for oxidative-induction time of polyolefins by differential scanning calorimetry*. West Conshohocken, PA: ASTM International. 8 pp.
ASTM D3937 Standard. (2012). *Standard test method for crimp frequency of manufactured staple fibers*. West Conshohocken, PA: ASTM International. 4 pp.
ASTM D4218 Standard. (2015). *Standard test method for determination of carbon black content in polyethylene compounds by the muffle-furnace technique*. West Conshohocken, PA: ASTM International. 3 pp.
ASTM D4354 Standard. (2012). *Standard practice for sampling of geosynthetics and rolled erosion control products(RECPs) for testing*. West Conshohocken, PA: ASTM International. 3 pp.
ASTM D4355/D4355M Standard. (2014). *Standard test method for deterioration of geotextiles by exposure to light, moisture and heat in a xenon arc type apparatus*. West Conshohocken, PA: ASTM International. 5 pp.
ASTM D4439 Standard. (2015). *Standard terminology for geosynthetics*. West Conshohocken, PA: ASTM International. 6 pp.
ASTM D4491/D4491M Standard. (2016). *Standard test methods for water permeability of geotextiles by permittivity*. West Conshohocken, PA: ASTM International. 8 pp.
ASTM D4533/D4533M Standard. (2015). *Standard test method for trapezoid tearing strength of geotextiles*. West Conshohocken, PA: ASTM International. 6 pp.
ASTM D4594/D4594M Standard. (1996). *Standard test method for effects of temperature on stability of geotextiles*. West Conshohocken, PA: ASTM International. 3 pp.
ASTM D4595 Standard. (2011). *Standard test method for tensile properties of geotextiles by the wide-width strip method*. West Conshohocken, PA: ASTM International. 13 pp.
ASTM D4603 Standard. (2003). *Standard test method for determining inherent viscosity of poly(ethylene terephthalate) (PET) by glass capillary viscometer*. West Conshohocken, PA: ASTM International. 4 pp.
ASTM D4632/D4632M Standard. (2015). *Standard test method for grab breaking load and elongation of geotextiles*. West Conshohocken, PA: ASTM International. 5 pp.
ASTM D4716/D4716M Standard. (2014). *Standard test method for determining the (In-plane) flow rate per unit width and hydraulic transmissivity of a geosynthetic using a constant head*. West Conshohocken, PA: ASTM International. 10 pp.
ASTM D4751 Standard. (2016). *Standard test methods for determining apparent opening size of a geotextile*. West Conshohocken, PA: ASTM International. 9 pp.
ASTM D4833/D4833M Standard. (2007). *Standard test method for index puncture resistance of geomembranes and related products*. West Conshohocken, PA: ASTM International. 4 pp.
ASTM D4884/D4884M Standard. (2014). *Standard test method for strength of sewn or bonded seams of geotextiles*. West Conshohocken, PA: ASTM International. 6 pp.
ASTM D4886 Standard. (2010). *Standard test method for abrasion resistance of geotextiles (sand paper/sliding block method)*. West Conshohocken, PA: ASTM International. 3 pp.
ASTM D5034 Standard. (2009). *Standard test method for breaking strength and elongation of textile fabrics (grab test)*. West Conshohocken, PA: ASTM International. 8 pp.
ASTM D5035 Standard. (2011). *Standard test method for breaking force and elongation of textile fabrics (strip method)*. West Conshohocken, PA: ASTM International. 8 pp.
ASTM D5101 Standard. (2012). *Standard test method for measuring the filtration compatibility of soil-geotextile systems*. West Conshohocken, PA: ASTM International. 8 pp.
ASTM D5103 Standard. (2007). *Standard test method for length and length distribution of manufactured staple fibers (single-fiber test)*. West Conshohocken, PA: ASTM International. 4 pp.

ASTM D5141 Standard. (2011). *Standard test method for determining filtering efficiency and flow rate of the filtration component of a sediment retention device*. West Conshohocken, PA: ASTM International. 6 pp.
ASTM D5199 Standard. (2012). *Standard test method for measuring the nominal thickness of geosynthetics*. West Conshohocken, PA: ASTM International. 4 pp.
ASTM D5261 Standard. (2010). *Standard test method for measuring mass per unit area of geotextiles*. West Conshohocken, PA: ASTM International. 3 pp.
ASTM D5262 Standard. (2007). *Standard test method for evaluating the unconfined tension creep and creep rupture behavior of geosynthetics*. West Conshohocken, PA: ASTM International. 16 pp.
ASTM D5321/D5321M Standard. (2014). *Standard test method for determining the shear strength of soil-geosynthetic and geosynthetic-geosynthetic interfaces by direct shear*. West Conshohocken, PA: ASTM International. 11 pp.
ASTM D5322 Standard. (1998). *Standard practice for immersion procedures for evaluating the chemical resistance of geosynthetics to liquids*. West Conshohocken, PA: ASTM International. 3 pp.
ASTM D5397 Standard. (2007). *Standard test method for evaluation of stress crack resistance of polyolefin geomembranes using notched constant tensile load test*. West Conshohocken, PA: ASTM International. 5 pp.
ASTM D5493 Standard. (2006). *Standard test method for permittivity of geotextiles under load*. West Conshohocken, PA: ASTM International. 5 pp.
ASTM D5494 Standard. (1993). *Standard test method for the determination of pyramid puncture resistance of unprotected and protected geomembranes*. West Conshohocken, PA: ASTM International. 4 pp.
ASTM D5496 Standard. (2015). *Standard practice for in field immersion testing of geosynthetics*. West Conshohocken, PA: ASTM International. 3 pp.
ASTM D5514/D5514M Standard. (2014). *Standard test method for large scale hydrostatic puncture testing of geosynthetics*. West Conshohocken, PA: ASTM International. 5 pp.
ASTM D5567 Standard. (1994). *Standard test method for hydraulic conductivity ratio (hcr) testing of soil/geotextile systems*. West Conshohocken, PA: ASTM International. 9 pp.
ASTM D5819 Standard. (2005). *Standard guide for selecting test methods for experimental evaluation of geosynthetic durability*. West Conshohocken, PA: ASTM International. 11 pp.
ASTM D5885/D5885M Standard. (2015). *Standard test method for oxidative induction time of polyolefin geosynthetics by high-pressure differential scanning calorimetry*. West Conshohocken, PA: ASTM International. 4 pp.
ASTM D5887/D5887M Standard. (2016). *Standard test method for measurement of index flux through saturated geosynthetic clay liner specimens using a flexible wall permeameter*. West Conshohocken, PA: ASTM International. 8 pp.
ASTM D5890 Standard. (2011). *Standard test method for swell index of clay mineral component of geosynthetic clay liners*. West Conshohocken, PA: ASTM International. 7 pp.
ASTM D5891/D5891M Standard. (2002). *Standard test method for fluid loss of clay component of geosynthetic clay liners*. West Conshohocken, PA: ASTM International. 3 pp.
ASTM D5947 Standard. (2011). *Standard test methods for physical dimensions of solid plastics specimens*. West Conshohocken, PA: ASTM International. 10 pp.
ASTM D5970/D5970M Standard. (2016). *Standard test method for deterioration of geotextiles from outdoor exposure*. West Conshohocken, PA: ASTM International. 3 pp.
ASTM D5993 Standard. (2014). *Standard test method for measuring mass per unit of geosynthetic clay liners*. West Conshohocken, PA: ASTM International. 4 pp.

ASTM D6072/D6072M Standard. (2009). *Standard practice for obtaining samples of geosynthetic clay liners*. West Conshohocken, PA: ASTM International. 4 pp.
ASTM D6140 Standard. (2000). *Standard test method to determine asphalt retention of paving fabrics used in asphalt paving for full-width applications*. West Conshohocken, PA: ASTM International. 3 pp.
ASTM D6141 Standard. (2014). *Standard guide for screening clay portion and index flux of geosynthetic clay liner (GCL) for chemical compatibility to liquids*. West Conshohocken, PA: ASTM International. 3 pp.
ASTM D6213 Standard. (1997). *Standard practice for tests to evaluate the chemical resistance of geogrids to liquids*. West Conshohocken, PA: ASTM International. 5 pp.
ASTM D6241 Standard. (2014). *Standard test method for static puncture strength of geotextiles and geotextile-related products using a 50-mm probe*. West Conshohocken, PA: ASTM International. 6 pp.
ASTM D6243/D6243M Standard. (2016). *Standard test method for determining the internal and interface shear strength of geosynthetic clay liner by the direct shear method*. West Conshohocken, PA: ASTM International. 12 pp.
ASTM D6244 Standard. (2006). *Standard test method for vertical compression of geocomposite pavement panel drains*. West Conshohocken, PA: ASTM International. 5 pp.
ASTM D6364 Standard. (2006). *Standard test method for determining short-term compression behavior of geosynthetics*. West Conshohocken, PA: ASTM International. 6 pp.
ASTM D6388 Standard. (1999). *Standard practice for tests to evaluate the chemical resistance of geonets to liquids*. West Conshohocken, PA: ASTM International. 4 pp.
ASTM D6389 Standard. (1999). *Standard practice for tests to evaluate the chemical resistance of geotextiles to liquids*. West Conshohocken, PA: ASTM International. 4 pp.
ASTM D6454/D6454M Standard. (1999). *Standard test method for determining the short-term compression behavior of turf reinforcement mats (TRMs)*. West Conshohocken, PA: ASTM International. 4 pp.
ASTM D6466 Standard. (2010). *Standard test method for diameter of wool and other animal fibers by sirolan-laserscan fiber diameter analyser*. West Conshohocken, PA: ASTM International. 9 pp.
ASTM D6475 Standard. (2006). *Standard test method for measuring mass per unit area of erosion control blankets*. West Conshohocken, PA: ASTM International. 3 pp.
ASTM D6496/D6496M Standard. (2004). *Standard test method for determining average bonding peel strength between top and bottom layers of needle-punched geosynthetic clay liners*. West Conshohocken, PA: ASTM International. 4 pp.
ASTM D6500 Standard. (2000). *Standard test method for diameter of wool and other animal fibers using an optical fiber diameter analyser*. West Conshohocken, PA: ASTM International. 12 pp.
ASTM D6524/D6524M Standard. (2016). *Standard test method for measuring the resiliency of turf reinforcement mats (TRMs)*. West Conshohocken, PA: ASTM International. 3 pp.
ASTM D6525/D6525M Standard. (2016). *Standard test method for measuring nominal thickness of rolled erosion control products*. West Conshohocken, PA: ASTM International. 4 pp.
ASTM D6566 Standard. (2014). *Standard test method for measuring mass per unit area of turf reinforcement mats*. West Conshohocken, PA: ASTM International. 3 pp.
ASTM D6567 Standard. (2014). *Standard test method for measuring the light penetration of a turf reinforcement mat (TRM)*. West Conshohocken, PA: ASTM International. 5 pp.
ASTM D6574/D6574M Standard. (2013). *Standard test method for determining the (in-plane) hydraulic transmissivity of a geosynthetic by radial flow*. West Conshohocken, PA: ASTM International. 5 pp.

ASTM D6575/D6575M Standard. (2016). *Standard test method for determining stiffness of geosynthetics used as turf reinforcement mats (TRMs)*. West Conshohocken, PA: ASTM International. 4 pp.
ASTM D6637/D6637M Standard. (2015). *Standard test method for determining tensile properties of geogrids by the single or multi-rib tensile method*. West Conshohocken, PA: ASTM International. 6 pp.
ASTM D6638 Standard. (2011). *Standard test method for determining connection strength between geosynthetic reinforcement and segmental concrete units (modular concrete blocks)*. West Conshohocken, PA: ASTM International. 7 pp.
ASTM D6706 Standard. (2001). *Standard test method for measuring geosynthetic pullout resistance in soil*. West Conshohocken, PA: ASTM International. 8 pp.
ASTM D6766 Standard. (2012). *Standard test method for evaluation of hydraulic properties of geosynthetic clay liners permeated with potentially incompatible aqueous solutions*. West Conshohocken, PA: ASTM International. 9 pp.
ASTM D6768/D6768M Standard. (2004). *Standard test method for tensile strength of geosynthetic clay liners*. West Conshohocken, PA: ASTM International. 3 pp.
ASTM D6818 Standard. (2014). *Standard test method for ultimate tensile properties of rolled erosion control products*. West Conshohocken, PA: ASTM International. 8 pp.
ASTM D6916 Standard. (2006). *Standard test method for determining the shear strength between segmental concrete units (modular concrete blocks)*. West Conshohocken, PA: ASTM International. 7 pp.
ASTM D6918 Standard. (2009). *Standard test method for testing vertical strip drains in the crimped condition*. West Conshohocken, PA: ASTM International. 6 pp.
ASTM D6992 Standard. (2016). *Standard test method for accelerated tensile creep and creep-rupture of geosynthetic materials based on time-temperature superposition using the stepped isothermal method*. West Conshohocken, PA: ASTM International. 8 pp.
ASTM D7005/D7005M Standard. (2016). *Standard test method for determining the bond strength (Ply adhesion) of geocomposites*. West Conshohocken, PA: ASTM International. 4 pp.
ASTM D7178 Standard. (2016). *Standard practice for determining the number of constrictions "m" of non-woven geotextiles as a complementary filtration property*. West Conshohocken, PA: ASTM International. 5 pp.
ASTM D7179 Standard. (2007). *Standard test method for determining geonet breaking force*. West Conshohocken, PA: ASTM International. 3 pp.
ASTM D7361 Standard. (2007). *Standard test method for accelerated compressive creep of geosynthetic materials based on time-temperature superposition using the stepped isothermal method*. West Conshohocken, PA: ASTM International. 8 pp.
ASTM D7409 Standard. (2015). *Standard test method for carboxyl end group content of polyethylene terephthalate (PET) yarns*. West Conshohocken, PA: ASTM International. 3 pp.
ASTM D7498/D7498M Standard. (2009). *Standard test method for vertical strip drains using a large scale consolidation test*. West Conshohocken, PA: ASTM International. 6 pp.
ASTM D7556 Standard. (2010). *Standard test methods for determining small-strain tensile properties of geogrids and geotextiles by in-air cyclic tension tests*. West Conshohocken, PA: ASTM International. 6 pp.
ASTM D7701 Standard. (2011). *Standard test method for determining the flow rate of water and suspended solids from a geotextile bag*. West Conshohocken, PA: ASTM International. 7 pp.
ASTM D7737/D7737M Standard. (2015). *Standard test method for individual geogrid junction strength*. West Conshohocken, PA: ASTM International. 8 pp.
ASTM D7748/D7748M Standard. (2014). *Standard test method for flexural rigidity of geogrids, geotextiles and related products*. West Conshohocken, PA: ASTM International. 6 pp.

ASTM D7880/D7880M Standard. (2013). *Standard test method for determining flow rate of water and suspended solids retention from a closed geosynthetic bag*. West Conshohocken, PA: ASTM International. 5 pp.

ASTM E793 Standard. (2006). *Standard test method for enthalpies of fusion and crystallization by differential scanning calorimetry*. West Conshohocken, PA: ASTM International. 4 pp.

ASTM E794 Standard. (2006). *Standard test method for melting and crystallization temperatures by thermal analysis*. West Conshohocken, PA: ASTM International. 4 pp.

ASTM F316 Standard. (2003). *Standard test methods for pore size characteristics of membrane filters by bubble point and mean flow pore test*. West Conshohocken, PA: ASTM International. 7 pp.

ASTM F904 Standard. (2016). *Standard test method for comparison of bond strength or ply adhesion of similar laminates made from flexible materials*. West Conshohocken, PA: ASTM International. 3 pp.

ASTM G154 Standard. (2016). *Standard practice for operating fluorescent ultraviolet (UV) lamp apparatus for exposure of nonmetallic materials*. West Conshohocken, PA: ASTM International. 11 pp.

ASTM G155 Standard. (2013). *Standard practice for operating xenon arc light apparatus for exposure of non-metallic materials*. West Conshohocken, PA: ASTM International. 11 pp.

ASTM G160 Standard. (2012). *Standard practice for evaluating microbial susceptibility of nonmetallic materials by laboratory soil burial*. West Conshohocken, PA: ASTM International. 3 pp.

ASTM WK24635 draft Standard. (2011). *Standard test method for determining the aperture stability modulus of geogrids*. West Conshohocken, PA: ASTM International. 13 pp.

Azwa, Z. N., Yousif, B. F., Manalo, A. C., & Karunasena, W. (2013). A review on the degradability of polymeric composites based on natural fibres. *Materials & Design*, *47*. 424–442.

Bamforth, A. (2009). *Interpretation of in-plane flow capacity of geocomposite drainage by tests to ISO 12958 with soft foam and ASTM D4716 with various natural backfill materials*. In: GIGSA GeoAfrica, Cape Town. 9 pp.

Barrett, R. (1966). Use of plastic filters in coastal structures. *Coastal Engineering Proceedings*, *1*(10). 1048–1067.

Bathurst, R. J., Rowe, R. K., Zeeb, B., & Reimer, K. (2007). A geocomposite barrier for hydrocarbon containment in the Arctic*International Journal of Geoengineering Case Histories*, *1*(1). 18–34.

Beckman, W. K., & Mills, W. H. (1957). Cotton fabric reinforced roads. *Engineering News Records*, *115*(14). 453–455.

Bérubé, D., & Saunier, P. (2016). Manufacturing process of geotextiles. In R. Koerner (Ed.), *Geotextiles: From design to applications*. (pp. 25–60). Duxford, UK: Woodhead Publishing.

Blond, E., Bouthot, M., Vermeersch, O., & Mlynarek, J. (2003). *Selection of protective cushions for geomembranes puncture protection*. In: Proceedings of the 56th annual conference of the Canadian Geotechnical Society, Winnipeg, Canada, October. 7 pp.

Blond, E., Fourmont, S., Bloquet, C., & Budka, A. (2012). *Biological clogging resistance of tubular drainage geocomposites in leachate collection layers*. In: Proceedings of the 5th European Geosynthetics Congress EuroGeo V, Valencia, Spain, September. 10 pp.

Blond, E., Saunier, P., Daqoune, T., & Fourmont, S. (2013). *Assessment of the effect of specimens dimensions on the measured transmissivity of planar tubular drainage geocomposites*. In: Proceedings of the 66th canadian geotechnical conference and the 11th Joint CGS/IAH-CNC groundwater conference—GeoMontreal 2013, Montréal, Canada, Sept. 29–Oct. 3. 9 pp.

Blond, E., Vermeersch, O., & Diederich, R. (2015). *A comprehensive analysis of the measurement techniques used to determine geotextile opening size: AOS, FOS, O90, and 'bubble point'*. In: 2015 Geosynthetics conference, Portland, OR, 15–18 Feb. (pp. 1190–1199).

CAN/CGSB-148.1 No 10. (1994). *Geotextiles—Filtration opening size*. Gatineau, QC: Canadian General Standards Board. 11 pp.
CAN/CGSB-148.1 No 4. (1994). *Geotextiles—Normal water permeability under no compressive load*. Gatineau, QC: Canadian General Standards Board. 7 pp.
CAN/CGSB-4.2 No 11.1. (1994). *Bursting strength—Diaphragm pressure test*. Gatineau, QC: Canadian General Standards Board. 9 pp.
CAN/CGSB-4.2 No 11.2. (1989). *Bursting strength—Ball burst test*. Gatineau, QC: Canadian General Standards Board. 10 pp.
CAN/CGSB-4.2 No 12.2. (2012). *Tearing strength—Trapezoid method*. Gatineau, QC: Canadian General Standards Board. 9 pp.
CAN/CGSB-4.2 No 14. (2005). *Textile test methods—Quantitative analysis of fibre mixtures*. Gatineau, QC: Canadian General Standards Board. 55 pp.
CAN/CGSB-4.2 No 26.3. (1995). *Textile fabrics—Determination of resistance to water penetration—Hydrostatic pressure test*. Gatineau, QC: Canadian General Standards Board. 6 pp.
Carroll, R. C. (1987). Hydraulic properties of geotextiles. In J. E. Fluet (Ed.), *Geotextile testing and the design engineer*. (pp. 7–20). West Conshohocken, PA: ASTM International.
Célino, A., Fréour, S., Jacquemin, F., & Casari, P. (2013). The hygroscopic behavior of plant fibers: a review. *Frontiers in Chemistry*, *1*(43). 12 pp.
CETCO. (2014). *Peel testing of needlepunched GCLs*. Accessed 8 January 2017, www.cetco.com.
CW-02215 Test Method. (1986). *Geotextiles used as filters. Civil works construction guide specification*. U.S. Army Corps of Engineers.
Daqoune, T., & Blond, E. (2010). In: Proceedings of the 9th international conference on geosynthetics: geosynthetics, advanced solutions for a challenging world ICG 2010, Guaruja, Brazil. 4 pp.
Desai, A. N., & Kant, R. (2016). Geotextiles made from natural fibres. In R. Koerner (Ed.), *Geotextiles: From design to applications*. (pp. 61–87). Duxford, UK: Woodhead Publishing.
Dolez, P. I., Blond, E., & Saunier, P. (2016). *Assessing the range of applicability of electrokinetic drainage geocomposite dewatering for mine tailings*. In: Tailings and mine waste 2016, Keystone, Colorado, October 2–5. (pp. 673–683).
Dolez, P. I., Chappel, M. J., & Blond, E. (2014). *Evaluating the use of geotextile filters to dewater MFT*. In: Proceedings of the 10th international conference on geosynthetics, Berlin, Germany, Sept. 21–24.
Doulala-Rigby, C., & Black, M. (2016). *The design and construction of a bridge approach embankment utilizing mechanically stabilized earth walls with geogrid-reinforced pulverized fuel ash fill*. In: GeoAmericas 2016. Apr. 10–13, Miami, FL. (pp. 1650–1661).
EDANA 10.3. (1999). *Recommended test method: Nonwoven absorption*. EDANA. 10 pp.
Elias, V., Carlson, D., Bachus, R., & Giroud, J. P. (1998). *Stress cracking potential of HDPE geogrids*. Report No. FHWA-RD-97-142 US Federal Highway Administration.
EN 12224 Standard. (2000). *Geotextiles and geotextile-related products. Determination of the resistance to weathering*. European Committee for Standardization. 12 pp.
EN 12225 Standard. (2000). *Geotextiles and geotextile-related products. Method for determining the microbiological resistance by a soil burial test*. Brussels: European Committee for Standardization. 12 pp.
EN 12226 Standard. (2000). *Geotextiles and geotextile-related products—General tests for evaluation following durability testing*. Brussels: European Committee for Standardization. 12 pp.
EN 12447 Standard. (2001). *Geotextiles and geotextile-related products. Screening test method for determining the resistance to hydrolysis in water*. Brussels: European Committee for Standardization. 10 pp.

EN 13562 Standard. (2000). *Geotextiles and geotextile-related products—Determination of resistance to penetration by water (hydrostatic pressure test)*. Brussels: European Committee for Standardization. 12 pp.

EN 13948 Standard. (2007). *Flexible sheets for waterproofing. Bitumen, plastic and rubber sheets for roof waterproofing. Determination of resistance to root penetration*. Brussels: European Committee for Standardization. 18 pp.

EN 14030 Standard. (2001). *Geotextiles and geotextile-related products. Screening test method for determining the resistance to acid and alkaline liquids*. Brussels: European Committee for Standardization. 10 pp.

EN 14414 Standard. (2004). *Geosynthetics. Screening test method for determining chemical resistance for landfill applications*. Brussels: European Committee for Standardization. 14 pp.

EN 14415 Standard. (2004). *Geosynthetic barriers. Test method for determining the resistance to leaching*. Brussels: European Committee for Standardization. 14 pp.

EN 14416 Standard. (2014). *Geosynthetic barriers. Test method for determining the resistance to roots*. Brussels: European Committee for Standardization. 12 pp.

EN 14575 Standard. (2005). *Geosynthetic barriers. Screening test method for determining the resistance to oxidation*. Brussels: European Committee for Standardization. 12 pp.

EN/TS 14417 Standard. (2014). *Geosynthetic barriers. Test method for the determination of the influence of wetting-drying cycles on the permeability of clay geosynthetic barriers*. Brussels: European Committee for Standardization. 12 pp.

EN/TS 14418 Standard. (2014). *Geosynthetic Barriers. Test method for the determination of the influence of freezing-thawing cycles on the permeability of clay geosynthetic barriers*. Brussels: European Committee for Standardization. 12 pp.

FTMS 101C Test Method 2065. (1982). *Puncture Resistance and Elongation (1/8 inch radius probe method)*. Washington, DC: U.S. General Services Administration. 5 pp.

Giroud, J. P., Gourc, J. P., Bally, P., & Delmas, P. (1977). *Comportement d'un textile non tissé dans un barrage en terre*. In: Proceedings of the international conference on the use of fabrics in geotechnics, Paris, France, April. (pp. 213–218).

GRI GCL5 Standard. (2011). *Standard guide for design considerations for geosynthetic clay liners (GCLs) in various applications*. Folsom, PA: Geosynthetic Research Institute. 34 pp.

GRI GG10 Standard. (2001). *Standard test method for determination of the flexural rigidity of geogrids*. Folsom, PA: Geosynthetic Research Institute. 8 pp.

GRI GG2 Standard. (2005). *Standard test method for individual geogrid junction strength*. Folsom, CA: Geosynthetic Research Institute. 9 pp.

GRI GG7 Standard. (1998). *Standard test method for carboxyl end group content of polyethylene terephthalate (PET) yarns*. Folsom, PA: Geosynthetic Research Institute. 5 pp.

GRI GG9 Standard. (2004). *Standard test method for torsional behavior of bidirectional geogrids when subjected to in-plane rotation*. Folsom, PA: Geosynthetic Research Institute. 6 pp.

Heerten, G., Jackson, A., Restall, S., & Saathoff, F. (2000). *New geotextile developments with mechanically-bonded nonwoven sand containers as soft coastal structures*. In: Proceeding of the 27th international conference on coastal engineering (ICCE), July 16-21, Sydney, Australia.

Hopewell, J., Dvorak, R., & Kosior, E. (2009). Plastics recycling: Challenges and opportunities. *Philosophical Transactions of the Royal Society B*, *364*(1526), 2115–2126.

Horvath, J. S. (1996). Geofoam geosynthetic: Past, present, and future. *Electronic Journal of Geotechnical Engineering.*., *1*(1). 16 pp.

Hsuan, Y. G., Koerner, R. M., Lord, A. E., Jr. (1993). A review of the degradation of geosynthetic reinforcement materials and various polymer stabilization methods. In S. C. J. Cheng (Ed.), *Geosynthetic soil reinforcement testing procedures*. (pp. 228–244). West Conshohocken, PA: ASTM International ASTM STP 1190.

ISO 554 Standard. (1976). *Standard atmospheres for conditioning and/or testing–specifications*. Geneva, CH: International Organization for Standardization. 1 pp.
ISO 811 Standard. (1981). *Textile fabrics–Determination of resistance to water penetration–Hydrostatic pressure test*. Geneva, CH: International Organization for Standardization. 3 pp.
ISO 1833-1 Standard. (2006). *Textiles—Quantitative chemical analysis—Part 1: General principles of testing*. Geneva, CH: International Organization for Standardization. 26 pp.
ISO 1833-2 Standard. (2006). *Textiles—Quantitative chemical analysis—Part 2: Ternary fibre mixtures*. Geneva, CH: International Organization for Standardization. 14 pp.
ISO 1833-7 Standard. (2006). *Textiles–Quantitative chemical analysis–Part 7: Mixtures of polyamide and certain other fibres (method using formic acid)*. Geneva, CH: International Organization for Standardization. 3 pp.
ISO 1833-11 Standard. (2006). *Textiles–Quantitative chemical analysis—Part 11: Mixtures of cellulose and polyester fibres (method using sulfuric acid)*. Geneva, CH: International Organization for Standardization. 2 pp.
ISO 1833-16 Standard. (2006). *Textiles—Quantitative chemical analysis—Part 16: Mixtures of polypropylene fibres and certain other fibres (method using xylene)*. Geneva, CH: International Organization for Standardization. 2 pp.
ISO 1833-24 Standard. (2010). *Textiles—Quantitative chemical analysis—Part 24: Mixtures of polyester and certain other fibres (method using phenol and tetrachloroethane), 2010*. Geneva, CH: International Organization for Standardization. 3 pp.
ISO 4582 Standard. (2007). *Plastics—Determination of changes in colour and variations in properties after exposure to daylight under glass, natural weathering or laboratory light sources*. Geneva, CH: International Organization for Standardization. 16 pp.
ISO 4892-2 Standard. (2013). *Plastics–Methods of exposure to laboratory light sources–Part 2: Xenon-arc lamps*. Geneva, CH: International Organization for Standardization. 13 pp.
ISO 4892-3 Standard. (2016). *Plastics–Methods of exposure to laboratory light sources–Part 3: Fluorescent UV lamps*. Geneva, CH: International Organization for Standardization. 16 pp.
ISO 9862 Standard. (2005). *Geosynthetics—Sampling and preparation of test specimens*. Geneva, CH: International Organization for Standardization. 12 pp.
ISO 9863-1 Standard. (2016). *Geosynthetics—Determination of thickness at specified pressures–Part 1: Single layers*. Geneva, CH: International Organization for Standardization. 5 pp.
ISO 9863-2 Standard. (1996). *Geotextiles and geotextile-related products–Determination of thickness at specified pressures—Part 2: Procedure for determination of thickness of single layers of multilayer products*. Geneva, CH: International Organization for Standardization. 7 pp.
ISO 9864 Standard. (2005). *Geosynthetics—Test method for the determination of mass per unit area of geotextiles and geotextile-related products*. Geneva, CH: International Organization for Standardization. 2 pp.
ISO 10318-1 Standard. (2015). *Geosynthetics–Part 1: Terms and definitions*. Geneva, CH: International Organization for Standardization. 8 pp.
ISO 10319 Standard. (2015). *Geosynthetics–Wide-width tensile test*. Geneva, CH: International Organization for Standardization. 14 pp.
ISO 10320 Standard. (1999). *Geotextiles and geotextile-related products—Identification on site*. Geneva, CH: International Organization for Standardization. 8 pp.
ISO 10321 Standard. (2008). *Geosynthetics—Tensile test for joints/seams by wide-width strip method*. Geneva, CH: International Organization for Standardization. 10 pp.
ISO 10722 Standard. (2007). *Geosynthetics—Index test procedure for the evaluation of mechanical damage under repeated loading—Damage caused by granular material*. Geneva, CH: International Organization for Standardization. 6 pp.

ISO 10769 Standard. (2011). *Clay geosynthetic barriers—Determination of water absorption of bentonite*. Geneva, CH: International Organization for Standardization. 7 pp.
ISO 10773 Standard. (2011). *Clay geosynthetic barriers—Determination of permeability to gases*. Geneva, CH: International Organization for Standardization. 9 pp.
ISO 10776 Standard. (2012). *Geotextiles and geotextile-related products—Determination of water permeability characteristics normal to the plane, under load*. Geneva, CH: International Organization for Standardization. 9 pp.
ISO 11058 Standard. (2010). *Geotextiles and geotextile-related products–Determination of water permeability characteristics normal to the plane, without load*. Geneva, CH: International Organization for Standardization. 17 pp.
ISO 12236 Standard. (2006). *Geosynthetics—Static puncture test (CBR test)*. Geneva, CH: International Organization for Standardization. 6 pp.
ISO 12956 Standard. (2010). *Geotextiles and geotextile-related products—Determination of the characteristic opening size*. Geneva, CH: International Organization for Standardization. 10 pp.
ISO 12957-1 Standard. (2005). *Geosynthetics—Determination of friction characteristics—Part 1: Direct shear test*. Geneva, CH: International Organization for Standardization. 8 pp.
ISO 12957-2 Standard. (2005). *Geosynthetics—Determination of friction characteristics—Part 2: Inclined plane test*. Geneva, CH: International Organization for Standardization. 10 pp.
ISO 12958 Standard. (2010). *Geotextiles and geotextile-related products—Determination of water flow capacity in their plane*. Geneva, CH: International Organization for Standardization. 13 pp.
ISO 13427 Standard. (2014). *Geosynthetics—Abrasion damage simulation (sliding block test)*. Geneva, CH: International Organization for Standardization. 4 pp.
ISO 13431 Standard. (1999). *Geotextiles and geotextile-related products—Determination of tensile creep and creep rupture behaviour*. Geneva, CH: International Organization for Standardization. 16 pp.
ISO 13433 Standard. (2006). *Geosynthetics—Dynamic perforation test (cone drop test)*. Geneva, CH: International Organization for Standardization. 6 pp.
ISO 13437 Standard. (1998). *Geotextiles and geotextile-related products—Method for installing and extracting samples in soil, and testing specimens in laboratory*. Geneva, CH: International Organization for Standardization. 9 pp.
ISO 13438 Standard. (2004). *Geotextiles and geotextile-related products—Screening test method for determining the resistance to oxidation*. Geneva, CH: International Organization for Standardization. 9 pp.
ISO 25619-1 Standard. (2008). *Geosynthetics—Determination of compression behaviour—Part 1: Compressive creep properties*. Geneva, CH: International Organization for Standardization. 20 pp.
ISO 25619-2 Standard. (2008). *Geosynthetics—Determination of compression behaviour—Part 2: Determination of short-term compression behaviour*. Geneva, CH: International Organization for Standardization. 12 pp.
ISO/TS 13434 Standard. (2008). *Geosynthetics—Guidelines for the assessment of durability*. Geneva, CH: International Organization for Standardization. 42 pp.
Jeon, H.-Y. (2016). Geotextile composites having multiple functions. In R. Koerner (Ed.), *Geotextiles: From design to applications*. (pp. 413–425). Duxford, UK: Woodhead Publishing.
Kelsey, C. (2014a). *Riding the Rails: Track extension on composite, biaxial geogrids*. http://www.Geosynthetica.net 29 October 2014.
Kelsey, C. (2014b). *CCR closure and geocomposite drainage*. http://www.Geosynthetica.net 26 January 2017.

Ko, F. K. (2004). *From textile to geotextiles. Seminar in honor of professor Robert Koerner*. September 13 Philadelphia, PA: Department of Materials Science and Engineering, Drexel University, Philadelphia University. 20 pp.

Koerner, R. M. (2012). *Designing with geosynthetics*. (Vol. 1). Bloomington, IN: Xlibris Publishing Co..

Kolbasuk, G. (2005). *Opportunities and solutions, development and growth of the geomembrane industry*. In: Robert M. Koerner symposium on geosynthetics and geosynthetic-engineered structures, Baton Rouge, Louisiana, June 1–3.

Kolstad, D. C., Benson, C. H., & Edil, T. B. (2004). Hydraulic conductivity and swell of nonprehydrated geosynthetic clay liners permeated with multispecies inorganic solutions. *Journal of Geotechnical and Geoenvironmental Engineering*, *130*(12), 1236–1249.

Kozlowski, R. M. (2012). *Handbook of natural fibres, volume 2—Processing and applications*. Oxford, Cambridge, Philadelphia, New Delhi: Woodhead Publishing.

Kulju, J. (2016). *Behind the [turbidity] curtain. Geosynthetics*. Roseville, MN: IFAI Publication October 1st.

Mlynarek, J., & Lombard, G. (1997). *Significance of percent open area in the design of woven geotextile filters*. In: Proceedings of geosynthetics'97, IFAI, Long Beach, CA, March. (pp. 1093–1107).

Narejo, D. (2016). Geotextiles use for cushioning. In R. Koerner (Ed.), *Geotextiles: From design to applications*. (pp. 395–412). Duxford, UK: Woodhead Publishing.

NF G38–019 Standard. (1988). *Textiles. Articles for industrial use. Tests for geotextiles: Determination of resistance to stamping*. Paris, France: AFNOR. 5 pp.

Renken, K., Mchaina, D. M., & Yanful, E. K. (2005). *Geosynthetics research and applications in the mining and mineral processing environment*. In: Proceeding of the North American geosynthetic society (NAGS)-geosynthetic institute (GSI) conference, Las Vegas, Nevada. 20 pp.

Rowe, R. K. (2005). Long-term performance of contaminant barrier systems. *Geotechnique*, *55*(9), 631–678.

Rowe, R. K. (2014). Performance of GCLS in liners for landfill and mining applications. *Environmental Geotechnics*, *1*(EG1), 3–21.

Salemi, N., Abtahi, S. M., Rowshanzamir, M., & Hejazi, S. M. (2016). A study on the hydraulic performance of sandwich geosynthetic clay liners reinforced with nano-clay particles. *Journal of Sandwich Structures and Materials*, *18*(6), 693–711.

Sarabian, T., & Rayhani, M. T. (2013). Hydration of geosynthetic clay liners from clay subsoil under simulated field conditions. *Waste Management*. *33*, 67–73.

Saunier, P., & Blond, E. (2009). *Behavior of 'Draintube' drainage geocomposites under high compression load*. In: Proceedings of geosynthetics 2009, Salt Lake City, UT, Feb 25–27. (pp. 95–101).

Scheirs, J. (2009). *A guide to polymeric geomembranes*. Chichester: John Wiley & Sons.

Shackelford, C. D., Benson, C. H., Katsumi, T., Edil, T. B., & Lin, L. (2000). Evaluating the hydraulic conductivity of GCLs permeated with non-standard liquids. *Geotextiles and Geomembranes*, *18*, 133–161.

Shah, V. (2007). *Handbook of plastics testing and failure analysis*. Hoboken, NJ: John Wiley & Sons.

Shukla, S. K. (2012). *An introduction to geosynthetic engineering*. London, UK: CRC Press.

Struick, L. C. E. (1985). Degradation. *Encyclopedia of polymer science and engineering*. (Vol. 4). New York, NY: John Wiley & Sons. 630–696.

Suits, L. D. (2006). National and international standards governing geosynthetics. In R. W. Sarsby (Ed.), *Geosynthetics in civil engineering*. (pp. 66–96). Cambridge, UK: Woodhead Publishing.

Thomas, R. W., & Cuttino, D. (2011). *Performance of corrugated pipe manufactured with recycled polyethylene content*. NCHRP report 696 Transportation Research Board of the National Academies. 54 pp.

Thornton, J. S., Allen, S. R., Thomas, R. W., & Sandri, D. (1998). *The stepped isothermal method for TTS and its application to creep data on polyester yarn*. In *Proceedings of the sixth international conference on geosynthetics, Atlanta*. (pp. 699–706).

Torosian, G. T., & Mac Millan, A. (2016). Physical properties, behaviour, and testing of geotextiles. In R. Koerner (Ed.), *Geotextiles: From design to applications*. (pp. 105–113). Duxford, UK: Woodhead Publishing.

Verdu, J. (1984). *Vieillissement des plastiques*. Paris: Association française de normalisation.

Williams, M. L., Landel, R. F., & Ferry, J. D. (1955). The temperature dependance of relaxation mechanisms in amophous polymers and other glass-forminig liquids. *Journal of the American Chemical Society*, *77*(14). 3701–3707.

Wright, D. C. (1996). *Environmental stress cracking of plastics*. Shropshire, UK: iSmithers Rapra Publishing.

Yazdani, H., Hatami, K., Hawa, T., & Grady, B. P. (2013). *Atomic-scale simulation of sensor-enabled geosynthetics for health-monitoring of reinforced soil slopes and embankments*. In: Proceedings of Geo-Congress 2013: Stability and performance of slopes and embankments III, San Diego, California, March 3-7. (pp. 1529–1535).

Zanzinger, H. (2016). Mechanical properties, behaviour, and testing of geotextiles. In R. Koerner (Ed.), *Geotextiles: From design to applications*. (pp. 115–150). Duxford, UK: Woodhead Publishing.

Zhao, A., Blond, E., & Recalcati, P. (2012). *Drainage geonet composites and performance assessment*. In: Proceedings of the 5th European geosynthetics congress EuroGeo V, Valencia, Spain, September. (pp. 325–329).

This page intentionally left blank

Specific testing of protective clothing

11

P.I. Dolez, V. Izquierdo
CTT Group, Saint-Hyacinthe, QC, Canada

11.1 Introduction

According to the US Department of Defense, protective clothing is defined as being "designed, fabricated, or treated to protect personnel against hazards caused by extreme changes in physical environment, dangerous working conditions, or enemy action" (US DoD, 2005). It is part of the personal protective equipment (PPE) suite, which also includes respirators, goggles, helmets, and ear muffs, for example. Interestingly, the ASTM Committee F23 on Personal Protective Clothing and Equipment adds the notion of a barrier preventing the user from being a source of contamination besides the traditional protection of the user from hazards (ASTM International, 1996). A simplified definition of protective clothing could be that it protects the wearer's body.

Threats to human health and safety may come from various sources (Mayer & Grabowsky, 2007):

- Mechanical: cut, puncture, needle puncture, abrasion, impact, blast, etc.
- Chemical: exposure to toxic solids, dusts, aerosols, liquids, and gases through inhalation, skin contact, or ingestion
- Biological: viruses, bacteria, bloodborne pathogens, etc.
- Radiological and nuclear: ionizing radiations, neutrons, microwaves, etc.
- Thermal: heat, cold, flame, bad weather, etc.
- Electrical: static discharge, electric shock, etc.
- Visibility: insufficient or excessive

Protective clothing may also help prevent drowning and falls (Berry, McNeely, Beauregard, & Haritos, 2008). With recent advances in smart textiles, active functions are now being embedded in protective clothing, allowing continuous monitoring of vital signs, external conditions, and position, for instance (Cao, 2013).

It must be noted that in the traditional occupational health and safety approach, protective clothing, as other types of PPE, shall only be considered as a last resort after all other risk management strategies have been implemented, i.e., elimination, substitution, engineering techniques, and administrative controls (Kuhl & Brück, 2014). Indeed, their efficiency is limited by the willingness of the worker to wear them and his/her ability to use and maintain them properly.

Various types of protective clothing can be found depending on the body part it is designed to protect. It includes bunker suits, lab coats, coveralls, gowns, lifejackets, bulletproof vests, safety harnesses, aprons, hoods, gloves, arm guards, gaiters, booties, and boots. They may be made of woven, knitted, or nonwoven textiles alone or

Advanced Characterization and Testing of Textiles. https://doi.org/10.1016/B978-0-08-100453-1.00011-8

laminated/coated/impregnated with a polymer (Mayer & Grabowsky, 2007). Leather and polymer membranes may also be used for protective clothing. It must be noted that, in most instances, protective clothing items are not made of a sole material but generally involve several layers of different materials that provide in combination the level of protection required against the hazards involved.

A large variety of fibers have uses in protective clothing. They include the following (Hearle, 2005):

- Highly extensible elastomeric fibers such as elastane (Lycra/Spandex) used for tight fits, for example in gloves.
- Brittle mineral fibers like rock wool employed for thermal insulation.
- Natural fibers, e.g., wool and cotton. At the basis of the first protective clothing 10,000 years ago along with leather, pelts, and down, they are still used for protection against bad weather, particularly with the help of surface treatments imparting them with water repellent properties, for example.
- Commodity synthetic fibers such as polyolefins, polyester, and polyamide, which display moderate strength (around 1 GPa) but constitute most of the low-requirement protective clothing thanks to their low cost and excellent durability.
- High strength inorganic materials like steel wire and carbon and glass fibers. They are usually combined with other softer materials to form high-performance yarns such as those that are cut-proof.
- High-performance polymer fibers made of polyaramide (e.g., Kevlar®, Nomex®, and Kermel®), ultrahigh molecular weight polyethylene (Spectra®/Dyneema®), polybenzimidazole (PBI), polyphenylene benzobisoxazole (PBO), poly (melamine-formaldehyde) (Basofil®), and oxidized polyacrylonitrile (PANOX®). Developed over the last 50 years, these fibers display high mechanical performance, with an elastic modulus of 70–150 GPa and a tensile strength around 3–5 GPa. In addition, some of these fibers are chemically, thermally, and fire resistant.

Assembled as a yarn, these fibers may be used to produce a woven fabric, which is the most common textile for protective clothing applications, or a knitted fabric (Potluri & Needham, 2005). This last structure allows obtaining complex, three-dimensional geometric forms directly, i.e., without a seam. The intertwined loop configuration also produces a high shear flexibility combined with good strength. Alternatively, fibers may be directly used to produce nonwovens. The advantages of nonwovens include their low production cost, high flexibility, and the air-entrapping characteristic that endows them with thermal insulation.

Specific finishes may be applied on textiles to improve their performance for protective clothing applications. This includes water repellent or fire retardant surface treatments, for example, or lamination/coating/impregnation with a polymer. Polymers may also be used as a standalone material in a mono- or multilayer structure, for example in gloves or boots. The most widespread polymers encountered in protective clothing comprise the following (Mellstrom & Boman, 2005; Potluri & Needham, 2005):

- Elastomers like natural rubber, neoprene rubber, nitrile rubber, and butyl rubber, for their great elasticity combined with interesting barrier properties.
- Thermoplastic or thermosetting polymers such as polyurethane (PU), polyvinylchloride (PVC), polyethylene vinyl alcohol (EVOH), and polyethylene, which display a resistance to some chemicals as well as to abrasion.
- Polytetrafluoroethylene (PTFE), which allows, in its expanded form, the production of a waterproof and chemical resistant yet breathable microporous membrane.

The selection of protective clothing design and materials may proceed through a step-by-step process (Shaw, 2005). The first step consists in identifying the type and severity of the physical and health hazards related to the activity and the environment in which it is placed. This initial hazard assessment phase allows defining the potential risks the individual is exposed to. The second step involves establishing the protective clothing requirements based on standards, specifications, and guidelines relevant to the industry or type of activity, or, if none exists, on the risks identified in step 1. Then, designs and materials are screened based on protection performance. The final selection is conducted by considering other relevant factors like ergonomics, comfort, durability, and cost. In practice, finding the ideal protective clothing is rarely possible because hazards are often from multiple sources (Eiser, 1988); a trade-off between perfect protection and the ability to conduct the activity must generally be considered.

Standard test methods and performance specifications have been mostly developed since the early 1990s by various national and international standardization bodies as a way to assess the performance of protective clothing design and materials (Mäkinen, 2006). This includes ISO (International Organization for Standardization) Technical Committee TC 94 on Protective Clothing and Equipment, CEN (European Committee for Standardization) TC 161 and TC 162 on Footwear and Protective Clothing, ASTM Committee F23 on Personal Protective Clothing and Equipment, and the US National Fire Protection Association (NFPA). The role of these standard test methods and performance specifications is to ensure that the performance data on protective clothing are comparable, meaningful, and usable on the field (Eiser, 1988). They also serve, in combination with performance criteria, for protective clothing marking, which may be mandatory depending on the country, end use, and type of protective clothing.

This chapter proceeds through the presentation of test methods of protective clothing's main properties for a series of activities: industrial/domestic, first responder, law enforcement, military, medical, electrical, construction, marine, and sports. It should be noted that the performance specifications these protective clothing items have to meet generally include other requirements related to size, labeling, laundering, etc. in addition to the properties considered below. Moreover, as with any test performed on textiles, conditioning prior to testing is generally critical and shall be performed at the conditions specified in the test methods. This chapter concludes with a discussion on future trends.

11.2 Testing of industrial/domestic protective clothing

Industrial workers can be found in a wide variety of domains, from natural resource mining and food processing to chemicals and goods manufacturing. The hazards they are exposed to are also of varied and multiple nature: they include dangerous machinery, chemicals, as well as extreme temperatures and fire (Tatiya, 2010). To a certain extent even though generally at a smaller scale, the same types of hazards may be encountered in everyday life, while carrying out domestic chores or performing house repairs. These three categories of hazards—mechanical, chemical, and thermal/fire—therefore constitute priority performance targets for industrial/domestic protective

clothing and have been associated with dedicated test methods. However, it is also crucial to assess the functionality and comfort of those protective clothing items to ensure that their benefits are not surpassed by the negative impact they may have on the ability to conduct the task (Slater, 1996).

11.2.1 Mechanical

The main mechanical risks industrial/domestic protective clothing is intended to protect from are cuts, punctures, and abrasion (ANSI/ISEA 105, 2011). In the case of footwear, the most common risks are crushing and sole puncture (Hrynyk & Irzmańska, 2013). Tearing per se is not associated with a specific hazard but is often used as an indication of the capacity of the PPE item to preserve its mechanical integrity if snagged (Dolez, Soulati, Gauvin, Lara, & Vu-Khanh, 2012a). Most of the tests evaluating the resistance of protective clothing to these hazards are performed on material swatches and do not take into account the clothing design and construction.

Standard test methods developed for assessing the resistance of protective clothing materials to cutting generally consider slicing, i.e., the blade displacement being parallel to its cutting edge (Fig. 11.1A). In the ISO 13997 (1999), ASTM F1790 (2005), and ASTM F2992/F2992M (2015) standards, the specimen is secured on a semicylindrical metal sample holder; a rectangular blade positioned perpendicularly to the sample holder axis is displaced horizontally at a constant speed. The device measures the distance traveled by the blade until it has cut through the specimen; the measurement is repeated for different values of the force applied vertically by the blade on the specimen using weights. Cut resistance corresponds to the force necessary to cut the material with a 20-mm horizontal displacement of the blade. An alternative technique is described in the EN 388 Standard (2004); it is based on a counter-rotating circular blade that applies a constant 5-N force on the specimen. The number of cycles until the blade has cut through the specimen is compared to that measured with a cotton reference material. This method is currently questioned by several experts in the field because of the rapid degradation of the blade cutting edge observed especially with

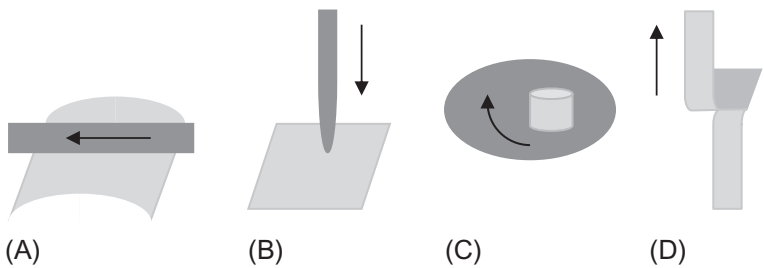

Fig. 11.1 Test configurations corresponding to (A) cutting, (B) puncture, (C) abrasion, and (D) tearing.
Reproduced from Dolez P. I., & Vu-Khanh T. (2009a). Gloves for protection from cold weather. In J. T. Williams (Ed.), *Textiles for cold weather apparel* (pp. 374–398). Woodhead/Cambridge.

glass and other high-performance fiber-containing textiles, which leads to incorrect results (Rebouillat & Steffenino, 2005). A change in the EN 388 standard is presently in discussion to solve this issue.

The resistance to puncture corresponds to the maximum force recorded when a probe passes through a specimen secured between two clamping rings (Fig. 11.1B). Differences between the different corresponding standard test methods mostly concern the probe size and shape. If both the ISO 13996 (1999) and the EN 388 (2004) test methods for protective clothing use a 4.5-mm diameter probe with a 0.5-mm radius tapered head, the ASTM F1342 Standard (2005) offers a choice of three probe geometries which may be more relevant to typical mechanical aggressors: Probe A has a 2-mm diameter and a 0.25-mm radius tapered head, Probe B has a 1-mm diameter and a 0.5-mm radius rounded tip, and Probe C is similar to Probe A but with a 0.5-mm radius tapered head. Indeed, it has been shown that the probe tip size and shape affect the puncture force as well as the mechanisms involved in probe penetration (Nguyen, Vu-Khanh, & Lara, 2005). In the case of footwear, the puncture resistance of the protective sole is assessed with a 4.5-mm diameter probe with a 30 degree angle, 0.5-mm radius conical truncated tip (ISO 20344, 2011; CAN/CSA Z195, 2014). The same issue of relevance of the probe geometry has also been raised in that case (Aschan, 2005).

A test method for abrasion specific to protective gloves is proposed in the EN 388 Standard (2004). A circular specimen is subjected to abrasion under a pressure of 9 kPa with a Martindale apparatus. The cyclic planar motion between the specimen and the abradant follows a Lissajous curve (Fig. 11.1C). The test ends when a hole appears in the specimen. The resistance to abrasion is defined as the number of cycles completed until the end of the test. Other test methods not specific to protective clothing may also be used depending on the type of material: for example, rotary platform abrader (ASTM D3389, 2005), Taber abrader (ISO 5470-1, 1999), and Martindale abrader (ISO 5470-2, 2003) for coated fabrics; and rotary platform, double-head (RPDH) abrader (ASTM D3384, 2009), Martindale abrader (ISO 12947-1, 1998; ASTM D4966, 2012), and oscillatory cylinder (Wyzenbeek) tester (ASTM D4157, 2013) for fabrics. Because these methods work according to different principles, there is no correlation between the results they provide. It must also be noted that the measurement of the resistance of textiles to abrasion is complex because it is strongly affected by the condition of the abradant, the specimen strain condition, the pressure between the specimen and the abradant, and any dimensional change in the specimen among others (ACT, 2010). In addition, the evaluation of the end point criterion may not be very precise because it is not related to an easily measurable parameter such as the loss in mass after a defined number of cycles.

The European standard on protective gloves (EN 388, 2004) describes a test method for the measurement of tearing resistance using a single tongue, or trouser, configuration (Fig. 11.1D). A rectangular specimen is partially split lengthwise; tearing takes place by pulling the legs apart. Tearing resistance is defined as the maximum force recorded over the distance torn in the specimen. This test is similar to CAN/CGSB-4.2 No. 12.1 (2016), ASTM D2261 (2013), and ISO 13937-2 (2000) for textiles. Alternative methods for textiles and coated fabrics include the

double tongue tear test (ISO 13937-4, 2000), the wing-shaped test (ISO 13937-3, 2000), the trapezoidal tear test (ASTM D5587, 2015; CAN/CGSB-4.2 No. 12.2, 2012), and the Elmendorf ballistic pendulum method (CAN/CGSB-4.2 No. 12.3, 2005; ISO 13937-1, 2000). For footwear, in addition to the single tongue, trapezoidal, and pendulum methods used for coated fabrics (ASTM D751, 2011), slit tear resistance may be measured for leather (ASTM D2212, 2000). It involves tearing apart the cross-sectional thickness of a specimen at a slit cut through the leather by a die or a sharp knife. Care should be taken when comparing the results of these different test methods because some define the tearing strength as the maximum force during the tear propagation (EN 388, 2004), while others define it as the average of the five highest peaks during a test or the average of the highest peaks on a predefined tear length.

The resistance to crushing of footwear may be assessed with a 200 J impact test and a 15 kN compression test performed on the entire shoe (ISO 20345, 2011). In both cases, the tested area is the toe cap. No crack shall be generated in the specimen as a result of the impact test; a minimal toe cap free height, whose value depends on the shoe size, shall be maintained after the impact or compression test has been carried out. Alternatively, the impact resistance of the toe cap may be measured on the front section of the footwear comprising a minimum of 25 mm of material behind the rear corners of the protective toe cap (CAN/CSA Z195, 2014). A 25-mm diameter plasticine cylinder is inserted under the toe cap so that it contacts the sole of the footwear and the dome of the toe cap. The impact test is performed with a 22.7 kg, 25 mm diameter striker. Depending on the footwear grade, a 125 J impact energy with a 3.32 m/s impact velocity or a 90 J impact energy with a 2.82 m/s impact velocity is used. The residual plasticine cylinder height is measured after the impact to provide the minimum internal toe clearance after impact. A 22.7 kg, 25-mm diameter striker is also used to assess the impact resistance of the metatarsal protector. In that case, the impact energy is 101.7 J, the impact velocity is 2.99 m/s, and a PU-injected foot form with a 33-mm wide cavity filled with plasticine is used. Compression and impact tests for protective footwear can also be found in the ASTM F2412 Standard (2011).

Risks of stabs and slashes also exist in the food transformation industry as well as when working with various types of materials such as plastics, leather, textile, and paper. The resistance of protective aprons, trousers, and vests to hand knives may be assessed with an impact penetration testing apparatus (ISO 13998, 2003). A 30 degree tip, 1.5-mm thick oiled stainless steel blade is held in a 1-kg block that is dropped from a height of 250 or 500 mm on a material specimen secured over a tray filled with a flesh simulant plastic. The test is performed with the specimen positioned horizontally as well as inclined at 30 degrees to the horizontal. Penetration of the blade through the protective material is determined by measuring the length of the tip of the blade exposed below the tested specimen. The same setup is used for chain mail gloves and arm guards, with rigid arm guards being filled with rice instead of being laid over the flesh simulant-containing tray (ISO 13999-1, 1999). For gloves and arm guards made of leather, fabric, or other materials than chain mail, a drop test apparatus is also used with the same blade geometry (ISO 13999-3, 2002). However, in that case,

the specimen is secured over a circular anvil with a 200-mm radius top surface and a vertical hole in which the blade enters during the test. In addition, the blade holder is only 110 g and the drop height is 600 mm.

11.2.2 Chemical

Two aspects shall be considered in the case of chemical hazards, whether in solid, liquid, aerosol, or gas form (Dolez, Soulati, et al., 2012a). First, the protective clothing shall act as a barrier for the chemicals of interest and prevent both penetration through closures, pores, seams, and all sorts of macroscopic imperfections as well as permeation, which takes place at a molecular level (Stull, 2005). In addition, the protective clothing material shall resist the degradation of its properties by the chemicals, including its protective performance (Dolez, Soulati, et al., 2012a).

The resistance of protective clothing materials to liquid penetration may be assessed using runoff tests and hydrostatic techniques (Stull, 2005). In runoff tests, the specimen is inclined to allow the chemical to run off on its surface (ISO 6530, 2005). The quantity of chemical that penetrates through the specimen under the force of gravity is measured using a blotting material positioned underneath the specimen. Hydrostatic techniques involve pressurizing a liquid above or underneath the specimen and visually detecting when the liquid appears on the other side of the specimen (ASTM F903, 2010). The test may be conducted at a set pressure, leading to a pass/fail result, or with an increasing liquid head. These tests may be used to assess the integrity of seams and closures. In the case of solid particles, aerosols, and gases, the resistance to penetration is only measured on whole clothing items (ISO 16602, 2007). Depending on the protection level and the form of the chemical, tests may include leak tightness, inward leakage, liquid penetration under jet and spray conditions, and penetration by sodium chloride airborne solid particles. These measurements on whole clothing items are generally conducted with human subjects.

The resistance of protective clothing materials to chemical permeation is generally characterized by the breakthrough time and the permeation rate (Stull, 2005). Breakthrough time corresponds to the time it takes for the chemical to be detected on the other side of the specimen; it is therefore highly dependent on the detection method sensitivity. Permeation rate is the steady-state mass flow of chemical through a unit area of material per unit time. These parameters may be assessed using two techniques. In the first one, the specimen makes a tight barrier between a challenge chamber where the chemical of interest is introduced and a collection chamber where the chemical concentration is sampled using a chemical detection method (Fig. 11.2A). Exposure to the chemical may be continuous as in the ISO 6529 Standard (2013) and ASTM F739 Standard (2012) or intermittent as in the ISO 6529 Standard (2013) and ASTM F1383 Standard (2012). These test methods apply to liquids and gases. It may be noted that conditions of intermittent contact do not always lead to longer breakthrough times (Man, Bastecki, Vandal, & Bentz, 1987). For liquids with a sufficiently high volatility, a gravimetric technique may also be employed to measure breakthrough time and permeation rate in situation of continuous contact (ASTM F1407, 2012). In that case, the specimen is secured over the mouth of a cup containing

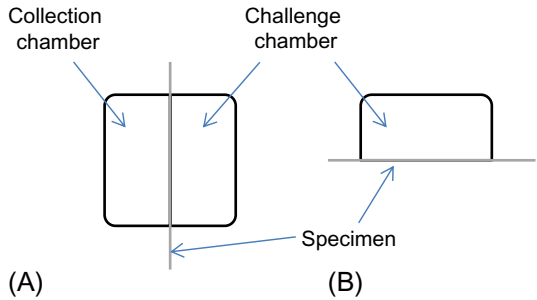

Fig. 11.2 Schematic representation of the (A) chemical detection permeation technique and the (B) gravimetric permeation technique.

the challenge chemical (Fig. 11.2B); the cup is inverted and weighted at regular intervals. A relationship between permeation data and permissible exposure limits might be obtained by using cumulative permeation mass (Stull, 2006).

Degradation tests assess if a change in the material physical properties takes place as a result of exposure to a chemical (Stull, 2005). The effect may be instantaneous, for example, with the lubrication of the material surface by an oily compound, or gradual, with the swelling of an elastomer in a solvent (Dolez, Soulati, et al., 2012a). If no test method specific for protective clothing appears to have been developed yet, various standards relative to rubbers and plastics have been used in the barrier material industry (Stull, 2005). For instance, degradation tests involving immersion in liquids are described in the ASTM D471 Standard (2012) for vulcanized rubber, fabrics coated with vulcanized rubber, and look-alike finished products, and in the ASTM D543 Standard (2014) for plastics of various forms. In both cases, the changes in physical properties such as weight, dimension, strength, and appearance of specimens are recorded after immersion in the liquid for a set period of time. Each of the test methods provides a list of chemicals of interest and specifies the duration and temperature of the immersion. In addition, Section 13 of the ASTM D471 Standard (2012) describes a test method for measuring the change in sample weight when only one side of the specimen is exposed to the liquid. It uses a cylindrical test chamber that is closed by the specimen at the bottom and filled with the liquid from the top. A new method also based on a one-sided exposure to liquids has been developed for glove materials by the International Safety Equipment Association (Stull, 2005). 10-mL crimp top vials closed by a disk of glove material and placed in an inverted position are used to expose specimens to liquids for one hour (ANSI/ISEA 105, 2011). Once the exposure time is over, the vial is positioned upright in a test frame outfitted with the EN 388 (2004) 4.5-mm diameter puncture probe. The puncture force measured with the exposed specimens is compared to that recorded with specimens secured on vials not containing any chemical. An alternative technique developed by researchers studying the impact of oils and greases on the resistance of protective gloves to mechanical risks consisted in measuring the residual cutting, puncture, and tearing force of exposed specimens using the corresponding standard test methods (Section 11.2.1) (Dolez, Gauvin, Lara, & Vu-Khanh, 2010).

11.2.3 Thermal and fire

Several methods are available to assess the level of protection offered by protective clothing to extreme temperatures. For example, in the case of exposure to a source of heat, three modes of heat transfer are considered: conduction, radiation, and convection. For the measurement of contact heat transmission, the mono- or multilayer specimen is positioned horizontally between a heated hot plate and a calorimeter under a defined load (ASTM F1060, 2008; ISO 12127-1, 2015). The amount of heat transmitted by the sample is compared with human tissue tolerance to heat, i.e., pain sensation and second-degree burn. In the case of radiant heat, a vertical specimen is exposed to quartz lamps or heated silicon carbide rods providing an incident heat flux between 5 and 84 kW/m^2 depending on the test method (ASTM F1939, 2008; ISO 6942, 2002). The heat transmitted to a calorimeter through the specimen is recorded and used to compute the radiant heat resistance of the sample. For convective heat, a specimen is positioned horizontally and exposed to an 80 kW/m^2 (ISO 9151, 1995) or 83 kW/m^2 (CAN/CGSB-4.2 No. 78.1, 2001) heat flux produced by a gas burner. The heat transmission index is computed as the time to record a 24°C increase in temperature in a calorimeter positioned on the other side of the specimen or the exposure energy expected to cause a second-degree burn. More details regarding thermal and fire testing of textile materials may be found in Chapter 4 and Chapter 8 of this book.

Alternatively, some testing configurations use the model of a hand (EN 511, 2006), a foot (GCTTG 4006-13) or an entire manikin (ASTM F1291, 2010) to include the effect of the clothing design in the evaluation of the level of thermal insulation they provide. In that case, the thermal resistance is computed from the energy consumed to maintain the hand, foot, or manikin at a certain temperature (30–35°C for the hand, 27°C for the foot, and 35°C for the manikin) while they are exposed to hot or cold temperature in an environmental chamber.

In some instances, industrial workers may also have to be protected against a potential risk of fire. To test the flame resistance of protective clothing materials, small coupons positioned vertically are exposed to the flame of a burner for a set period of time, generally around 12 s (Sadier & Izquierdo, 2015). The flame may be applied to the specimen surface (CAN/CGSB-4.2 No 27.10, 2000), perpendicular to its lower edge (ASTM D6413/D6413M, 2015) or at a 30 degree angle (CAN/CGSB-4.2 No 27.10, 2000) for example (Fig. 11.3). After the flame is removed, the fire resistance of the material is generally characterized by the after flame and afterglow times, char length, and residual tearing force. In addition, no evidence of melting or dripping shall be observed.

Industrial workers may also be exposed to a risk of flash fire, i.e., a fire that spreads rapidly by means of a flame front through a diffuse fuel, like dust, gas, or the vapors of an ignitable liquid, without the production of damaging pressure (NFPA 921, 2011). In that instance, protective garments shall be tested using an instrumented manikin with an exposure heat flux of 84 kW/m^2 and an exposure time of 3 s (NFPA 2112, 2012). The manikin is dressed with 100% cotton underwear under the protective garment. The predicted body burn is assessed using temperature increases recorded by sensors positioned on the manikin surface, excluding hands and feet,

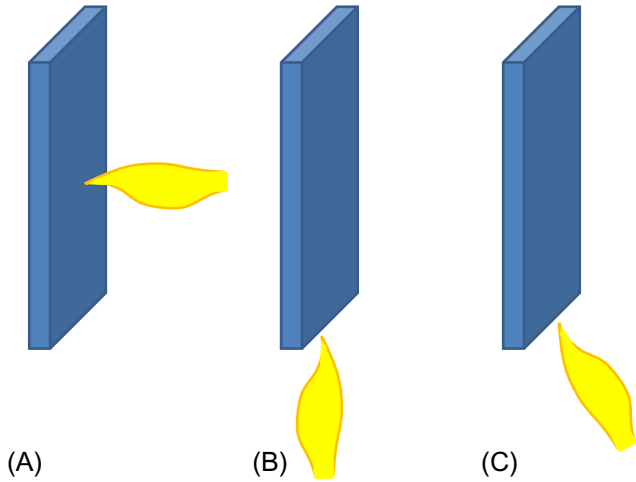

Fig. 11.3 Examples of flame vs specimen surface configurations in flame resistance tests: (A) application on the specimen surface, (B) application on the specimen lower edge, and (C) application at a 30 degree angle.

when the manikin is exposed to a simulated fire environment in a laboratory. More details about this test are available in Section 11.4.3 of this chapter.

Other sources of heat include hot liquid splashes, molten material, and steam. The resistance to hot liquid splashes is characterized by pouring heated oil over an inclined specimen and recording the heat transmitted to a calorimeter positioned beneath (ASTM F2701, 2008). A similar configuration is used in the ASTM F955 Standard (2007) and ISO 9185 Standard (2007) with molten metals (iron, mild steel, aluminum, copper, and brass) and cryolite with the particularity for the ISO 9185 Standard (2007) to employ embossed PVC film as a heat transfer sensor instead of a calorimeter. On the other hand, in the ISO 9150 Standard (1988), which targets protective clothing for welding activities, liquid metal drops are produced from the fusion of a metal rod by a welding torch and are projected on the surface of a vertically mounted specimen using a 45 degree drop guide. Finally, in the case of steam under pressure, a test apparatus and an associated test method have been developed by researchers at the University of Alberta, Canada (Ackerman et al., 2012). The specimen is exposed to an oversaturated water steam jet produced by a combination of a boiler and a super heater for a duration of up to 10 s. Heat transfer through the specimen is measured with a skin simulant sensor. More details about hot water and steam tests may be found in Chapter 9.

Exposure of protective clothing materials to heat and flame may also produce changes in their properties. For example, the resistance of protective clothing materials to convective heat is characterized in a hot air circulating oven (ASTM F2894, 2012; ISO 17493, 2000). Dimensional changes as well as signs of degradation (ignition, melting, separation, etc.) are recorded after a 5-min exposure of the specimens to 185°C or 260°C. Exposure to radiant heat is simulated using heated silicon carbide rods (ISO 6942, 2002). Changes in the specimen appearance are noted after a 3-min exposure to heat flux between 5 and 80 kW/m^2.

11.2.4 Ergonomics and comfort

Assessing the functionality and comfort of protective clothing is a complex task as several of the aspects involved are highly subjective and associated with specific activities. As a result, test methods generally involve human subjects.

For example, the comfort and function of chemical protective ensembles can be qualitatively assessed using an exercise or a work task scenario (ASTM F1154, 2011). The first one involves a series of kneeling, duck squat, body bending, arm extension in various directions, walking, and crawling on hands and knees. In the second one, the subject has to lift boxes, move a 55-gal drum on and off a handtruck, coil, uncoil, connect, and disconnect a hose, open and close an overhead valve, remove and install a bolt with a wrench and a screw with a screwdriver, and climb a ladder. After the test, the subject is asked to rate the level of difficulty of each activity as well as the ensemble function, fit, and comfort.

In the case of protective gloves, the residual dexterity can be assessed by timing a subject picking up 25 9.5-mm diameter, 38-mm long metal pegs and placing them in a pegboard (ASTM F2010/F2010M, 2010) or by identifying the smallest diameter pin a subject can pick up three times within 30 s among a set of 5, 6.5, 8, 9.5, and 11 mm diameter pins (EN 420, 2003). However, a study conducted with nine models of protective gloves covering the three categories of fine, medium, and coarse dexterity revealed a limited capacity of these two dexterity tests, as well as ten others, at discriminating the different gloves (Gauvin, Tellier, Daigle, & Petitjean-Roger, 2006). In particular, no significant effect of the gloves was obtained with the EN 420 (2003) dexterity test, which displayed a degree of sensitivity of 3%. Another test described in the NFPA 1971 (2013) performance specification consists of screwing nuts, washers, and bolts on a vertical board while wearing gloves. The performance is based on the time ratio it takes to perform the test with and without the gloves.

This lack of quantitative or precise data provided by test methods involving human subjects as well as their time-consuming nature have prompted the development of physical test methods enabling the quantitative assessment of ergonomics/comfort of protective clothing (Dolez & Vu-Khanh, 2009b). For example, because the dexterity of gloves has been linked to their suppleness, adherence, and snugness of fit (Bradley, 1969), mechanical tests methods for the measurement of glove flexibility (Harrabi et al., 2008) and grip (Gauvin et al., 2008) have been developed and successfully validated by biomechanical and psychophysical evaluation tests. Another grip test method is described in the NFPA 1971 (2013) performance specification: it uses a 32-mm diameter vertical fiberglass pole attached to an overhead force measuring device. Both the gloves and the pole are wet conditioned. The peak and minimum pull force values are recorded. In the case of protective apparel, fabric comfort has been associated with flexibility and texture (Cowan, Tilley, & Wiczynski, 1988). These properties as well as fabric shear, tension, compression, and friction may be characterized using the Kawabata Evaluation System (KES) developed in 1972 (Kawabata, 1980). Professor Kawabata also proposed an equation expressing the total hand value as a function of the 16 parameters obtained in both fabric directions.

For its part, the sweating hot plate or skin model test simulates the heat and mass transfer processes which occur through a textile-based material next to human skin and contribute to the thermophysiological comfort of the wearer (ASTM F1868, 2014; ISO 11092, 2014). The measurements are performed under steady-state conditions. Thermal resistance is provided by the dry heat flux across the sample in response to a temperature gradient while the evaporative resistance corresponds to the resistance to the flow of moisture vapor from a saturated surface to an environment with a lower vapor pressure. Generally, the test is carried out with the hot plate set at a temperature of 35°C, but other conditions may be selected. Clo is a unit of thermal resistance and is equal to 0.155 K m^2/W (ASTM F1868, 2014).

11.3 Testing of law enforcement protective clothing

Law enforcement personnel, which includes police, court, and correctional officers, are both at risk of unintentional injury and deliberate attack. Personal weapons (e.g., hands, fists, or feet) are most often involved in assaults against law enforcement personnel with 80% of the cases reported for US officers in 2014, while firearms and knives or other cutting instruments accounted for 4% and 2% of the assaults respectively (FBI, 2015). In addition, improvised explosive devices as well as old ammunition, commercial explosives, and fireworks that are found on non-Department of Defense property, are handled by special units comprising public safety bomb technicians (Hughes, 2006). Specific protective clothing has been designed to help reduce the risks associated with these different weapons. On the other hand, slips and falls represent an important cause of injuries for police officers; they accounted for more than 16% of injuries in the Quebec, Canada, police departments between 2005 and 2010, and they represented 20% of the payouts by the Quebec's Occupational Health and Safety Commission (Gauvin et al., 2015). Finally, because of their role as well as the nature and speed of their actions, easy identification and high visibility are of critical importance for law enforcement personnel.

11.3.1 Mechanical

In addition to the mechanical risks already discussed in Section 11.2.1, law enforcement officers may also be exposed to some specific types of hazards. This includes knives and other stabbing objects as well as hypodermic needles, which may be used as weapons or inadvertently encountered during the search of a suspect, an inmate, or their belongings.

The resistance of personal body armor to stabbing may be assessed with a drop weight test using engineered test blades as a probe and a guided rail drop tube to control the dropping location, angle, and velocity (NIJ 0115.00, 2000). Three geometries of test blades are provided in the standard: an engineered knife blade representing a typical single cutting edge, small knife; an engineered knife blade simulating commando-style blades or larger kitchen knives with two cutting edges;

and a spike resembling an ice pick characteristic of a class of pointed weapons encountered in correctional environments. A composite backing material composed of stacked layers of neoprene sponge, polyethylene foam, and rubber is positioned below the body armor panel tested. A sheet of witness paper is inserted between the backing material and the body armor panel. The depth of penetration of the test blade in the body armor panel is determined for two levels of the impact energy. Even if this test method does not directly address slash threats, protection against slash may still be provided as it has been shown that body armors capable of defeating stab threats should perform satisfactorily against slash threats, which are easier to overcome.

A standard test method has also been developed to assess the resistance of protective clothing material to puncture by hypodermic needles (ASTM F2878, 2010). The specimen is clamped between two metal plates with 10–25.4-mm diameter holes serving as puncture guides. The specimen holder is mounted in a mechanical test frame used to measure the maximum force required by a 21-, 25-, or 28-gauge hypodermic needle used as a probe to puncture the specimen. The researchers at the origin of this test method also looked at the effect of needle characteristics (Dolez, Nguyen, Guero, Gauvin, & Lara, 2008), test conditions (Nguyen, Dolez, Vu-Khanh, Gauvin, & Lara, 2010), and mechanical deformations and presence of a support material below the specimen simulating real glove use conditions (Nguyen, Dolez, Vu-Khanh, Gauvin, & Lara, 2013) on the resistance of protective materials to needle puncture.

11.3.2 Ballistics

The ballistic resistance of personal body armor intended to protect against gunfire may be assessed using the test method proposed by the US National Institute of Justice. It applies to flexible vests and jackets, hard armors, and plate inserts (NIJ 0101.06, 2008). Projectiles used for the test include 0.40 S&W full metal jacketed (FMJ); 9 mm full metal jacketed round nose (FMJ RN); 0.357 magnum jacketed soft point (JSP); 0.357 SIG FMJ flat nose (FN); 0.44 magnum semi jacketed hollow point (SJHP); 7.62 mm FMJ, steel jacketed (U.S. Military designation M80); and 0.30 caliber armor piercing (AP) (U.S. Military designation M2 AP) bullets. The armor panel should be strapped on a backing material fixture containing a homogenous block of nonhardening, oil-based modeling clay. The fixture is located 5 m from the test barrel for handgun rounds and at a distance of 15 m for rifle rounds. Sensors situated in the line of fire are used to insure that the bullet velocity meets the test parameter requirements. Back face deformation depth or perforation is recorded for each fair hit and compared with the requirements for each type of personal body armor.

11.3.3 Blast

The NIJ 0117.00 Standard (2012) provides test methods to evaluate the performance of bomb suits. In addition to flame resistance assessment already described in Section 11.2.3, tests are conducted to assess the clothing impact attenuation, fragmentation, and integrity as a result of blast overpressure.

Impact attenuation is measured on facsimile samples of the bomb suit spine protector (NIJ 0117.00, 2012). Specimens are tested using a gravity drop method and an impactor representing a sphere threat. The impact energy is 45 J. Specimens are conditioned at ambient, low, and high temperature prior to testing.

Fragmentation performance is tested on facsimile samples of protection areas containing fabric ballistic resistant materials using fragment-simulating projectiles (FSP) of 0.22, 0.30, and 0.50 caliber fired from a distance of 5 m from the target (NIJ 0117.00, 2012). The V50 ballistic limit, i.e., the velocity required for a particular projectile to penetrate the material at least 50% of the time, is calculated for each projectile tested. Perforations and stops are determined using an aluminum alloy witness plate located behind the specimen tested. Perforation is detected with a light bulb positioned behind the witness plate; light passing through a crack or hole created by the impacting projectile is recorded.

Finally, the result of blast overpressure is measured on the entire bomb suit worn by a male crash test dummy positioned in a kneeling posture (NIJ 0117.00, 2012). A C4 plastic explosive charge located at a distance of 0.6 m from the exterior of the bomb suit is detonated. The bomb suit integrity is assessed by verifying if the protective elements covering the neck, thorax/abdomen, and pelvis protection areas have remained attached to the bomb suit at the anchor points in the donned position, have maintained their shape integrity, and show no evidence of collapse.

11.3.4 Slip

Slip resistance of footwear is usually characterized by the coefficient of friction of the outsole with a test surface representing flooring material. Static friction corresponds to the force that must be overcome to initiate the sliding motion between the outsole and the flooring material. Dynamic/kinetic friction is the force to resist motion while sliding is in progress. If various test methods have been developed to characterize footwear slip resistance, the reliability of the results is often limited as friction is affected by a very large number of parameters, including temperature, surface roughness, presence of solid or liquid contaminants on both surfaces, and even the test method (Bartenev & Lavrentev, 1981).

A first series of test methods involve the use of the whole footwear for the determination of the coefficient of friction. For example, the ASTM F2913 (2011) test method determines the dynamic coefficient of friction of footwear sliding at a rate of 0.3 m/s under a 400 or a 500 N load, depending on the size of the shoes, over a clay quarry tile, a stainless steel plate, or another flat sheet material relevant to flooring. Various lubricants may also be applied on the surface, including distilled or deionized water, a sodium lauryl sulfate detergent solution, and corn oil. The standard test method uses a whole shoe slip tester such as the test machine developed by SATRA whose test method the standard is derived from. This machine allows conducting the test in the following modes: forward heel slip at a 7 degree angled contact, backward forepart slip, and forward flat slip (Fig. 11.4). In addition to whole footwear, the test may also be carried on 76-mm diameter samples. The ISO 13287 (2012) test method is based on the same principle. However, tests are only conducted on whole footwear held with

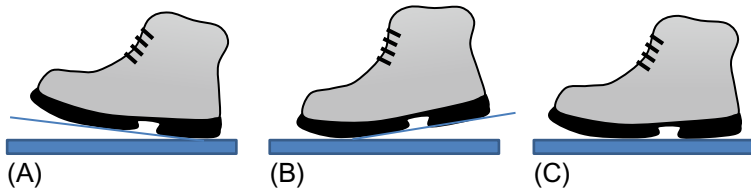

Fig. 11.4 Main slip resistance test modes for whole footwear: (A) forward heel slip at angled contact; (B) backward forepart slip; and (C) forward flat slip.

a shoemaking last or an artificial foot. In addition, test surfaces are limited to stainless steel and pressed ceramic tile of well-defined characteristics, and the use of a sodium lauryl sulfate detergent solution or glycerol aqueous solution lubricant is mandatory.

Other test methods measure the static coefficient of friction. For instance, the ASTM F609 (2013) test method uses a 2700 g horizontal pull slipmeter holding three 12.7 mm diameter cylindrical specimens. The measurement is conducted on dry walkway surfaces in the laboratory and in the field. A modified version of this method can be performed on a standard tensile test frame (Intertek, 2009). A weight is placed in or on a finished footwear or outsole unit, which is pulled horizontally at a fixed speed over the test surface. This test is similar to the ASTM D1894 (2014) method for static and kinetic coefficients of friction of plastic film and sheeting. Two other standard test methods measuring the static coefficient of friction of sole and heel samples have been withdrawn but are still largely encountered in the industry. The ASTM F489 Standard (1996) uses the James machine to apply 36.3 kg to a 76 × 76 mm specimen via a strut with an articulated joint. The test surface is a standard vinyl flooring surface, which can be dry or wet for the test. A portable tribometer based on the same principle and known as Mark II tester is employed in the ASTM F1677 (2005) test method. The 76 × 76 mm sample is loaded with a 4.5 kg weight. The flooring may be dry, wet, or contaminated.

11.3.5 Identification and high visibility

The uniform color provides a first line of identification for law enforcement personnel. Color fastness of law enforcement protective clothing is tested against a series of potentially damaging conditions, including light (ISO 105-B02, 2013), laundering (ISO 105-C06, 2010), dry cleaning (ISO 105-D01, 2010), hot pressing (ISO 105-X11, 1994), and sweat (ISO 105-E04, 2013). Color fastness is assessed by comparing the color change resulting from the exposure of the clothing fabric specimen to the damaging condition with that produced by the same exposure on a reference fabric. Color change may be determined by visual evaluation using gray scales or with a spectrophotometer.

In addition, the ASTM E809 (2008) test method may be employed to measure the photometric characteristics of retroreflector materials used for identification and high visibility purposes on law enforcement protective clothing during night operations. A source of light is directed at the specimen through an aperture of defined dimension. A photoreceptor also equipped with an angular aperture is positioned at a set distance

from the specimen and used to measure the proportion of light reflected in a direction close to the incident axis. The measurement is conducted in a dark photometric range. Various quantities such as the coefficient of luminous intensity, the coefficient of retroreflected luminance, the coefficient of retroreflection, the coefficient of line retroreflection, the reflectance factor, and the coefficient of luminous flux per unit solid angle can be computed from the measured data. In addition, the resistance of the retroreflector material to various service and environmental conditions may be assessed by measuring the residual photometric characteristics of specimens exposed to laundering, abrasion, UV light, or flexing at cold temperature. It may also be measured under water spray conditions simulating rain (CAN/CSA Z96, 2015; ISO 20471, 2013).

11.4 Testing of first responder protective clothing

In addition to the case of police officers already discussed in the previous section, first responders also include fire fighters, emergency medical technicians, and paramedics. Depending on the type of work performed, the requirements for first responder protective clothing may be found, for example, in a series of specification documents published by different standard bodies: the National Fire Protection Association (Haase, 2012), the Canadian General Standard Board (CAN/CGSB 155 series), and the International Standard Organization (under the responsibility of the ISO TC 94/SC 14 Committee on Firefighters' personal equipment), for instance. The main categories of requirements for first responders' protective clothing involve chemical and biological protection, thermal (hot and cold) protection, protection against fire, protection against mechanical hazards, high visibility, and ergonomics.

11.4.1 Chemical and biological

The resistance to chemical and biological hazards, or CB protection, has become an increasing concern with the rise of urban terrorism events. The list of potential CB treats that first responders may be exposed to includes nerve agents, blister agents, toxic industrial chemicals/materials, bacterial agents, viral agents, and biological toxins (Fatah et al., 2007). Performance tests are conducted on material coupons as well as on whole ensembles to evaluate the efficiency of seams, closures, and connections between PPE parts, including with gloves and footwear.

For instance, the man-in-simulant test (MIST) is performed on whole ensembles comprising the respirator, visor, gloves, and footwear (NFPA 1994, 2012). Human subjects wear the ensemble while carrying out a specific physical exercise routine in a chamber at 25°C and 55% relative humidity with a nominal wind speed of 0.9–2.2 m/s. The 30-min exercise routine includes dragging a 70 kg human dummy; performing squats, pivots, body bends, and arm extensions; climbing a ladder; and crawling. The penetration into the protective ensemble of methyl salicylate (MeS) vapor introduced at a concentration of 100 mg/m^3 in the chamber is measured using passive adsorbent dosimeters (PAD) distributed at different locations on the body and affixed directly to

the skin of the test subjects. The concentration of MeS in the PAD is obtained by extraction with a solvent followed by chemical analysis, for example, with UV-vis spectroscopy. The detection limit for the analytical technique is 50 ng of MeS per PAD. The protection factor at each PAD is given as the ratio between the MeS concentration in the chamber and the MeS vapor dosage for the specific PAD.

Liquid tightness is assessed on whole ensembles also. A manikin is dressed with the ensemble worn over a liquid-absorptive inner garment (ASTM F1359, 2007). Water is sprayed on the manikin using five nozzles positioned at the four corners and at the top of the shower at set distance and orientation from the manikin. Pressurized water is delivered through the nozzles at a rate of 3 L/min. A surfactant may be added to the water supply to achieve a surface tension of 0.032 N/m. The manikin is exposed successively to the water spray using four configurations corresponding to different orientations relative to the water nozzle positions. The water exposure duration for each configuration varies depending on the ensemble class (NFPA 1994, 2012): 4 times 5 min for a total of 20 min for class 2 ensembles and 4 times 1 min for a total of 4 min for class 3 ensembles. A qualitative assessment of the liquid tightness of the ensemble is conducted by looking for any sign of wetness of the inner garment. This test is a pass or fail evaluation. A specific test method is available as well for testing gloves and footwear (NFPA 1994, 2012).

The particle inward leakage is also conducted on whole ensemble, including the respirator (NFPA 1994, 2012). A human subject is dressed with the ensemble worn over black undergarments. He performs a specific physical exercise routine during 30 min in a chamber where a challenge aerosol with an aerodynamic mass median diameter of 2.5 µm composed of 50 wt% amorphous silica, 42 wt% tetraethylene glycol, 6 wt% uranine, and 2 wt% Tinopal has been introduced at a concentration of 20 mg/m^3. Particulate inward leakage is assessed by examining the test subject under black light within 10 min of doffing. This test is again a pass or fail evaluation.

Coupons of the CB barrier layers are tested for chemical permeation resistance using a two-chamber permeation cell of the principle of Fig. 11.2A (NFPA 1994, 2012). Liquid and gas/vapor challenge chemicals are used: sulfur mustard, soman, dimethyl sulfate, ammonia, chlorine, acrolein, and acrylonitrile. The challenge chemical in the air stream sweeping across the collection chamber is analyzed for 60 min.

Biopenetration resistance testing is performed on material coupons as well as on seams using the Phi-X174 bacteriophage as a test system (ASTM F1671, 2013). A test specimen is subjected to a nutrient broth containing the virus for 60 min using a specified pressure sequence. The visual assessment of the penetration of the liquid is supplemented by a quantitative evaluation of the passage of viable virus through the material. This test shall be conducted on specimens preconditioned by flexing and/or abrading (NFPA 1994, 2012).

11.4.2 Thermal

In addition to the methods assessing the level of protection offered by protective clothing to extreme temperatures already described in Section 11.2.3, a technique

combining convective and radiant heat is often used in the case of firefighter protective equipment (NFPA 1971, 2013). Also called thermal protective performance (TPP) testing, this test method involves exposing a flame resistant material simultaneously to radiant heat from nine quartz infrared tubes and convective heat generated by two burners whose flames converge at a point situated just beneath the specimen (ISO 17492, 2003). The specimen positioned horizontally is exposed until sufficient heat energy passes through it to cause the equivalent of a second-degree burn injury in human tissue, evidenced by a temperature rise of 24°C in a sensor situated beneath the specimen.

Another specific aspect regarding thermal protection of first responders is the assessment of the thermal energy stored in the clothing as a result of prolonged exposure to heat (Barker, Guerth, Behnke, & Bender, 2000). Indeed, a second-degree burn injury may be observed even at a low level of exposure if the garment is compressed against the body. Standard test methods have been developed to quantify this phenomenon. More specifically, the combination of transmitted and stored energy that occurs in firefighter protective clothing material systems as the result of exposure to prolonged, relatively low levels of radiant heat is measured by exposing a vertically positioned specimen to a low level of radiant heat for a set amount of time, followed by a 60 s compression of the specimen against a sensor under a pressure of 13.8 kPa (ASTM F2731, 2011). The result is provided in terms of radiant heat exposure time to obtain a second-degree burn injury prediction for the protective clothing material system tested or occurrence of a predicted second-degree burn injury for the radiant heat exposure time used.

11.4.3 Fire

Several methods assessing the level of protection offered by protective clothing to fire have already been described in Section 11.2.3. In addition, some specific test methods can be found for gloves and footwear used by first responders, in particular firefighters (NFPA 1971, 2013). In the case of gloves, a rectangular specimen folded in an *L*-shaped configuration using a steel rod is exposed during 12 s to the flame of a burner at the location of the fold. The flame resistance is defined in terms of afterflame time, char length, and percentage of consumed material. For footwear, complete items are tested by exposing them during 12 s to the flame created by the free burn of *n*-heptane in a $305 \times 457 \times 63.5$ mm fuel pan. The footwear flame resistance is assessed in terms of average afterflame time and occurrence of melting, dripping, or burn-through.

Flashfire is also a large issue for firefighters. Already discussed in Section 11.2.3, tests simulating this type of situations involve the use of a fully instrumented male form (a female form is under development) whose surface is covered with over 100 heat flux sensors (ASTM F1930, 2015; ISO 13506, 2008). It is dressed in a complete garment and exposed during a few seconds to an average incident heat flux of 84 kW/m^2 produced by a minimum of eight propane burners, which constitutes a laboratory simulation of a flash fire. Data are recorded during 60 s for single layer garments and 120 s for multilayer garments and ensembles. The measurements can be used to assess

the performance of the garment or protective clothing ensemble under the test conditions, i.e., time to experience pain and first-degree burn injury. They also provide an estimate of the extent and nature of skin damage that a person would suffer if wearing the test garment under similar exposure conditions, in particular the second- and third-degree and total burn injury areas.

11.4.4 Mechanical

First responders' protection clothing is subjected to requirements in terms of resistance to cutting, puncture, tearing, and abrasion. The corresponding test methods are described in Section 11.2.1. In addition, garments may also have to be tested for puncture propagation tear resistance and burst strength (NFPA 1994, 2012). The puncture propagation tear resistance test consists in subjecting a specimen to dynamic puncture and propagation of that puncture (ASTM D2582, 2009). The tear that results from that dynamic puncture simulates a snagging-type hazard. A rectangular specimen is secured over a curved holder with a tear slot. A 3.18 mm diameter truncated conical probe loaded with different carriage weights is dropped from a height of 508 mm. The tear length is used to compute the tear resistance based on the value of the carriage weight. In the case of burst strength, the specimen is positioned in a 44.4 mm diameter ring clamp (ASTM D751, 2011). A 25.4 mm diameter steel ball is pressed against the center of the specimen at a rate of 5 mm/s using a tensile test frame. The force at which rupture occurs is used to compute the burst strength of the material.

11.4.5 High visibility

In daytime, the fluorescence of materials is critical, while the retroreflection performance of photoreflectors is necessary for night time visibility. The method for testing the photometric characteristics of retroreflector materials described in Section 11.3.5 is used with some minor modifications for first responders (NFPA 1971, 2013). The fluorescence of high visibility trims may also be assessed using a one-monochromator method (ASTM E991, 2011). It consists in obtaining the spectrometric data for simulated daylight approximating CIE Standard Illuminant D65 and viewing conditions corresponding to the CIE 1931 Standard Colorimetric Observer or the CIE 1964 Supplementary Standard Colorimetric Observer. These data are then used to compute tristimulus values yielding an evaluation of the color of the fluorescent object. General high visibility requirements may also be found in the ISO 20471 (2013), CAN/CSA Z96 (2015), ANSI/ISEA 107 (2015), and AS/NZS 1906.4 (2010) (see Section 11.8.2 for more details).

In addition, because of the specific conditions encountered by first responders, the effect of rain and heat on the visibility performance of clothing shall also be assessed. In the case of rain, the specimen photometric characteristics are measured while it is subjected to a spray of water at a rate of 110 mm/h (CAN/CSA Z96, 2015; ISO 20471, 2013). The coefficient of retroreflectivity is measured 2 min after the rainfall exposure has started. To assess the effect of heat on the photometric

characteristics of the materials, specimens are subjected to a 10-min exposure at 140°C in an oven (NFPA 1971, 2013). The aging treatment is followed by the usual conditioning procedure before the measurement of the coefficient of retroreflectivity is carried out.

11.4.6 Ergonomics, function, and comfort

A last aspect that is of major importance for first responders' protective clothing is related to ergonomics and comfort. Indeed, concerns with excessive weight of PPE, heat stress, overprotection in the case of nonfire calls, garment fit, restricted mobility, and problems donning the PPE rank high on the list of complaints (Barker et al., 2012).

For instance, a new standard protocol is under development by the ASTM Committee F23 on personal protective clothing and equipment to allow assessing the change in range of motion (ROM) for subjects wearing a protective clothing ensemble (ASTM WK27291, 2016). An ergonomic test protocol will be followed by human subjects to compare the ergonomic performance between ensembles of the same class as well as of different classes (e.g., firefighter ensemble versus HAZMAT suit).

An ISO standard is also under development to assess the physiological heat load associated with protective clothing worn by firefighters (ISO/DIS 18640-2, 2016). Using the data provided by measurements conducted with the sweating torso (ISO/DIS 18640-1, 2016), a statistical model calculates the maximum allowable work time during a defined firefighting scenario under defined environmental conditions before a too high body core temperature is reached and the risk for heat stress and heat stroke occurs.

Some specific assessment methods of the ergonomics and function of first responders' protective gloves are also available. In addition to the modified pegboard dexterity test (ASTM F2010/F2010M, 2010) described in Section 11.2.4, gloves are also evaluated for their impact on the wet gripping capacity of the wearer (NFPA 1971, 2013). For that purpose, gloves are wet conditioned by immersing them in a water container at 21°C for 2 min while being worn by the subject; then they are drained off by hanging then for 2 min with the opening facing down. Afterwards, the wearer puts them on again and pulls on a 3.2-cm diameter vertical fiberglass pole attached to a force measuring device. Prior to testing, the pole is wet conditioned by wiping it with a damp rag. A last test for gloves involves donning/doffing one glove of the pair while the other glove is worn on the opposite hand (NFPA 1971, 2013). The trial is repeated three times. Another series of three donning trials is conducted by immersing the gloved hand in water at 21°C for 10 s before doffing and repeating donning. The donning time for each trial and the eventual detachment of the inner liner or the moisture barrier are recorded.

11.5 Testing of military protective clothing

Military personnel deeply rely on their protective clothing to keep them alive and in good health. Indeed, they need to resist enemy attack in a wide range of environments all over the planet independently of the climatic conditions. In addition, their missions

may last several consecutive days without access to the usual amenities of the industrial world. Five main categories of requirements have been identified for military protective clothing: chemical and biological, thermal, ballistic, camouflage, and comfort.

11.5.1 Chemical and biological

Chemical warfare agents include chlorine, phosgene, mustard gas, and sarin. They have been largely used during World War I and are still been encountered on various battlefields (Truong & Wilusz, 2008). Biological warfare agents comprise anthrax, ricin, botulinum toxin, and other natural and engineered compounds. Their first documented use dates back to the 6th century BC.

Chemical barrier properties of protective clothing swatch may be tested with the US Army TOP-8-2-501 test method (Truong & Wilusz, 2008). The material specimen mounted in a permeation cell is either saturated with liquid chemical agents over its entire surface or laid with droplets of live agent simulants. An exposure density of $10\,g/m^2$ is generally used for a 24 h test. Tests are performed with blister and nerve agent simulants such as distilled mustard, lewisite, sarin, soman, and VX. The agent cumulative vapor permeation through the barrier specimen is recorded using continuous air monitor systems. The reactivity of the barrier materials to the chemical agents may also be assessed. Chemical vapor system testing may also be conducted on entire suits using the MIST test procedure (see Section 11.4.1) and methyl salicylate, a nontoxic simulant for chemical agent vapors (Belmonte, 1998).

The biological barrier properties of military protective clothing may be assessed on a fabric swatch by measuring the penetration of aerosolized MS2 viral and *Bacillus globigii* bacterial spores (Truong & Wilusz, 2008). In addition, the biocidal activity of fabrics against biological warfare agents such as anthrax is characterized either by putting the test fabric in contact with spores of nonvirulent *Bacillus anthracis* grown on a nutrient plate or by growing the spores in the nutrient broth media in the presence of test specimen. Finally, a system test similar to MIST may be performed with corn oil aerosol, which is a physical simulant for biological aerosols (Belmonte, 1998).

11.5.2 Thermal

Military personnel are exposed to a wide range of climatic conditions, from bitter cold to very hot. In some instances like in the desert, large variations may be encountered between day and night. As accommodation conditions may be spartan and heated/air conditioned shelters inexistent, military personnel will largely have to rely on their protective clothing to keep them as much comfortable as possible. In addition, exposure to heat and flame may occur in the battlefield due to thermal and flame weapons, as well as voluntary or accidental ignition of fuel.

The assessment of military protective clothing for cold environments may be conducted in a five-stage process according to an evaluation system developed by NATO (Thwaites, 2008). At the first stage, the thermal and evaporative resistance of each layer of the clothing is measured using the sweating hot plate or skin model test (see Section 11.2.4). The total resistance of a multilayer system is the sum of the

resistance of single layers. At the next stage, the thermal and evaporative resistance of the clothing system is measured with a heated thermal manikin (see Section 11.2.3). The clothing ventilation rate and fabric waterproofness may also be tested at this stage. At stage 3 of the evaluation, the clothing is worn by human subjects in a climatic chamber for physiological assessment under realistic conditions of temperature and relative humidity. Stage 4 involves the physiological evaluation of the clothing in the field, and in stage 5 the clothing is used by a large number of soldiers.

The assessment of the performance of military protective clothing against flame generally proceeds in two stages (Winterhalter, 2008). First, an initial evaluation of the fabrics and materials is conducted for screening purposes using bench-scale testing such as the vertical flame test. Then, the entire clothing system is subjected to the flash fire instrumented manikin test method (see Section 11.4.3), which allows characterizing the fabric performance as well as the effect of the clothing configuration, design, fit, closure systems, interface with other PPE components, and behavior as a system in a flash fire exposure. Based on military medical doctrine, i.e., the accepted criteria for transferring injured soldiers in a burn center, the pass/fail criterion for the instrumented manikin test is to have no more than 20% second-degree and no more than 5% third-degree body burn.

11.5.3 Ballistics

Military personal armor should provide protection against handgun treats, fragmenting munitions, and rifle shots (Dunn, 2008). Materials providing ballistic protection shall prevent entry of the ballistic treat and its fragments into the protected area as well as resist fragmentation and deformation to limit blunt trauma injury. The assessment of the performance of ballistic resistant materials relies on two test methodologies: ballistic limit (V50) testing, and ballistic resistance testing.

V50 testing determines the velocity at which a specific treat has 50% chance of penetrating the armor material (Dunn, 2008). It is based on the average of equal numbers of velocities associated with complete and partial penetration. In particular, the lowest velocity corresponding to a complete penetration as well as the highest velocity corresponding to a partial penetration shall be included in the V50 calculation. The V50 testing can be combined with the casualty reduction testing, which provides the loss in velocity of the projectile when it penetrates the armor material and is used to define the potential lethality of the projectile after penetration. Bullets from fielded guns are used for testing. In case of fragmenting munitions, due to the infinite number of situations encountered, four categories of fragment simulator projectiles have been defined: caliber 0.22 (17 grain), caliber 0.30 (44 grain), caliber 0.50 (207 grain), and 20 mm (830 grain).

Ballistic resistance testing allows verifying if the material is compliant with the minimum performance requirements (Dunn, 2008). It uses the same projectiles as the V50 testing. However, in that case, a fixed number of projectiles are fired and velocities shall be maintained within a fair range. The specimens may have been subjected to various types of environmental exposure prior to testing. Blunt trauma testing

is usually conducted in combination with ballistic resistance testing. The back face deformation produced by the projectile impacting the armor material is characterized using a deformable substance such as nonhardening modeling clay.

11.5.4 Camouflage

Promoting concealment is critical for military clothing. Management of the visual signature takes advantage of two characteristics of the fabric: color and pattern (Gomes, 2008). The soldier blends in the environment by limiting the amount of contrast with his background. Modern camouflage strategy in the US and Canada is based on the use of a digital pattern with pixel-shape color patches. The US Army Combat Uniform (ACU) is a universal pattern designed to blend into several environments. For their part, the Canadian military may choose between the Canadian Disruptive Pattern for Temperate Woodland (CADPAT (TW)) (DSSPM 2-2-80-500, 2012), the Canadian Disruptive Pattern for Arid Regions (CADPAT (AR)) (DSSPM 2-2-80-501, 2012), and the Canadian Disruptive Pattern for Winter Operations (CADPAT (WO)) (DSSPM 2-2-80-502, 2010). The camouflage performance of military fabrics is assessed by chromaticity and infrared reflection measurements.

The fabric colors are computed using the ASTM E308 (2015) test method that is based on the International Committee on Illumination (CIE) system. The color measurement is conducted with a spectrometer over a 380–780 nm wavelength range. It shall use CIE illuminant C, which simulates daylight with a correlated color temperature of 6774 K, a 2 degree observer, and a 1-nm measurement interval (DSSPM 2-2-80-500, 2012; DSSPM 2-2-80-501, 2012). The results are expressed using the CIELAB color coordinates to provide a more uniform color space.

The fabric infrared reflection is assessed in terms of diffuse reflectance factors for the different pattern colors using a spectrophotometer (DSSPM 2-2-80-500, 2012; DSSPM 2-2-80-501, 2012). The measurement is conducted over the same 350–2000 nm wavelength range with a 10 nm measurement interval.

Both color and infrared reflectance measurement shall be carried out on the as-manufactured fabric as well as after 15 laundering cycles performed in accordance with the method specified for the fabric (DSSPM 2-2-80-500, 2012; DSSPM 2-2-80-501, 2012).

11.5.5 Comfort

While the original focus of military clothing was solely directed towards protection, functionality, and identification, there has been an increased awareness that the design of military clothing requires more consideration of comfort (Cardello, 2008). Indeed, heat stress and other discomforts brought by heavy, bulky, and moisture-tight protective clothing may impede the visual, cognitive, and physical performance of the wearer.

Comfort can be defined as a combination of three aspects: tactile, thermal, and physiological (Kilinc-Balci & Elmogahzy, 2008). Fabric handle may be characterized

using indirect evaluation methods such as the Kawabata (KES) system and the fabric assurance by simple testing (FAST) system. They are based on the measurement of a series of fabric properties like stiffness and roughness, which have been identified as representing the fundamental determinants of fabric hand. In addition, direct evaluation methods have been developed to simulate the mechanisms involved in fabric hand. They are generally based in the measurement of the force vs. time profile as the fabric is pulled or pushed through a hole of specific geometry. Finally, a subjective assessment of fabric hand feel can be conducted using the handfeel spectrum descriptive sensory (HSDS) method (Cardello, 2008). It employs 17 handfeel attributes rated on a 15-point intensity scale: grainy, gritty, fuzziness, thickness, tensile stretch, hand friction, fabric-fabric friction, depression depth, springiness, force to gather, stiffness, force to compress, fullness/volume, compression resilience intensity and rate, and noise intensity and pitch.

Thermophysiological comfort characterizes heat and moisture management in the clothing (Kilinc-Balci & Elmogahzy, 2008). Factors that affect thermophysiological comfort include air and radiant temperature, air velocity and water vapor pressure, and activity level. In addition, fabric physical properties such as thermal resistance, water absorption, and moisture transfer, as well as clothing design and the presence of air gaps, play a large role. In particular, a dynamic microclimate system establishes as a result of the energy and fluid exchange between the wearer's body, his clothing, and the environment (Pan, 2008). The clothing thermal and evaporative resistance may be characterized using a thermal/sweating manikin or human subjects (ISO 15831, 2004; ISO 9920, 2007). The measurement is made in a climatic chamber with controlled temperature, relative humidity, and air velocity conditions. The manikin may be standing or in motion.

Finally, a new method has recently been developed at the US Army Natick Soldier Research, Development and Engineering Center for the evaluation of the physiological comfort of military clothing (Cardello, 2008). The CALM scale, which stands for comfort affective labeled magnitude scale, is based on an evaluation of the semantic meaning of 43 phrases related to comfort or discomfort, going from greatest imaginable discomfort to greatest imaginable comfort. Coefficients of variation for these different phrases range from 5% to 42%.

11.6 Testing of medical protective clothing

Medical protective clothing is an essential part of the health care system. Indeed, they shall protect the wearer against external agents as well as prevent him from spreading them from one patient to another (Siegel, Rhinehart, Jackson, & Chiarello, 2007). A special attention should also be put on the PPE removal protocol to avoid contaminating the wearer's skin and clothes (Casanova, Alfano-Sobsey, Rutala, Weber, & Sobsey, 2008). In addition to the corresponding requirements in terms of antibacterial and CB performance, this section also covers the question of protection against radiological hazards which are related to the use of X-ray medical devices for imaging and therapy.

11.6.1 Antibacterial

First, a qualitative assessment of the antibacterial activity of textile materials may be carried out using the parallel streak method (AATCC TM147, 2011). Textile specimens are placed in intimate contact with an agar surface that has been previously inoculated with bacteria. After incubation, the agar surface is examined for a clear area of interrupted growth underneath and along the side of the specimen, which would be the sign of the bacteriostatic activity of the textile. Test organisms include *Staphylococcus aureus* and *Klebsiella pneumoniae*.

For a quantitative characterization of the degree of antibacterial activity of textile finishes, three methods may be used (ISO 20743, 2013): absorption, transfer, and printing. According to the absorption method, the bacterial suspension is inoculated directly onto the specimens. This is also the inoculation technique used in the AATCC TM100 Standard (2012). In the transfer method, the test bacteria are placed on an agar plate and transferred onto the specimens (ISO 20743, 2013). Finally, the printing method consists in placing the bacteria on a filter that is printed onto the specimens. Bacteria count may be determined by the colony plate count method or the adenosine tri-phosphate luminescence method. The antibacterial activity value of the tested textile is provided by the difference in bacteria growth between a control fabric and the antibacterial-treated fabric.

11.6.2 Chemical and biological barrier

Contact with bloodborne pathogens is a critical issue for health care professionals. The testing strategy involves two steps. First, the barrier performance of the protective clothing is assessed against blood (ASTM F1670/1670M, 2008). A solution of synthetic blood comprising a red dye/surfactant, a thickening agent, and distilled water having a surface tension and viscosity representative of blood is used to conduct an hydrostatic penetration test (ASTM F903, 2010) at 13.8 kPa. No droplet of blood appearing on the opposite side of the specimen or no other sign of sample wetness over the 60-min evaluation period corresponds to a pass result for the test. Then, a more rigorous testing may be conducted using a bloodborne pathogen surrogate, Phi-X174 bacteriophage (ASTM F1671, 2013). A description of this test method is provided in Section 11.4.1. It is specifically designed for modeling the viral penetration of hepatitis B and C and human immunodeficiency virus (HIV) carried in blood and other body fluids. The quantitative assessment of the transfer of the Phi-X174 bacteriophage through the protective clothing coupon is performed using the *Escherichia coli* bacteria, type C. It leads to a pass/fail result.

Medical personnel may also be exposed to a large variety of other liquids: body fluids, drugs, solvents, detergents, etc. Performance of their protective clothing against these liquids may be assessed in terms of resistance to penetration under pressure (ASTM F903, 2010), permeation under continuous contact (ASTM F739, 2012; ISO 6529, 2013), and permeation under conditions of intermittent contact (ASTM F1383, 2012; ISO 6529, 2013). A description of these tests is available in Section 11.2.2.

11.6.3 Radiological

The performance of leaded and nonleaded radiation protective clothing materials may be assessed in terms of attenuation of the primary X-ray beam of 60–130 kV X-ray equipment (ASTM F2547, 2006). An X-ray source is used to produce a primary beam with a standardized energy spectrum and constant intensity. The intensity of the X-ray beam is measured with an ionization chamber with and without a protective clothing material specimen positioned between the source and the detection. The attenuation provided by the protective clothing material is defined as the percent reduction in the X-ray beam intensity resulting from its presence.

For the case of medical X-ray fluoroscopy, radiation may be scattered from the body of the patient. A test method involves exposing the protective clothing material specimen to X-rays generated between 60 and 130 kV and scattered through an angle of 90 degrees by a water equivalent material (ASTM F3094, 2014). The test method is designed to include contributions from secondary radiations generated within the protective material and allows a more realistic evaluation of the radiation protection provided by the PPE.

Two other standards are under development by the Subcommittee F23.70 on Radiological Hazards of the ASTM Committee F23 on Personal Protective Clothing and Equipment. The first one is a guide for testing and optimal selection of radiological protection garments (ASTM WK31804, 2016). The second one is a method for the quantitative measurement of defects and damage in radiation protective shielding garments (ASTM WK54740, 2016).

11.7 Testing of electrical protective clothing

Electrical hazards can be encountered everywhere: at work, at home, and even in the wilderness. If prevention is as always the first line of defense, PPE may be required for electrical workers as well as for nonelectrical workers working in specified areas that may expose them to higher than normal electrical risks. This includes welders, heavy equipment operators, excavators, warehouse workers, and painters. The main aspects for electrical protective clothing involve electrical insulation, electrical arc, fire, and mechanical performance.

11.7.1 Electrical insulation

The electrical shock protection of workers exposed to energized electrical conductors or circuit parts is based on the determination of approach boundaries computed from the range and type (alternating (AC) or direct current (DC)) of voltage (NFPA 70E, 2012): the limited approach boundary, from which unqualified persons shall not be permitted to approach; the restricted approach boundary where only qualified workers wearing insulating gloves and sleeves are authorized; and the prohibited approach boundary where additional measures shall be taken to protect uninsulated parts of the body.

Rubber insulating gloves with leather protectors and rubber insulating sleeves required for electrical shock protection shall be initially given a proof-test with a 50-Hz or 60-Hz AC proof-test voltage or a DC proof-test voltage (ASTM D120, 2014) and be retested while in service at least every 6 months for gloves and 12 months for sleeves (ASTM F496, 2014). The test involves filling the glove with water up to a certain level and immersing it vertically in a water tank so that the water levels inside and outside the glove are the same (ASTM D120, 2014): the water inside the glove will form one electrode and the tank water will form the other electrode. In the case of sleeves, the small end of the sleeve may be pulled through to the large end to form an annular trough (ASTM F496, 2014); other techniques for sleeves include sling mounting, hammock mounting, straight mounting with a liquid dielectric or mechanical cuff seal, and the use of a wet sponge or a dry electrically conductive conforming electrode. An increasing AC or DC voltage is applied up to the specified value where it shall remain for 3 min or until failure is obtained. The voltage value and the level of water vary with the class of glove or sleeve.

Insulated footwear may be needed as protection against a step and touch risk on energized electrical conductors or circuit parts. The dielectric overshoes required shall be tested for dielectric strength. The footwear is filled with water or other conducting media up to a certain level and immersed in water or other conducting media up to the same level so that both volumes of water or conducting medium form the electrodes (ASTM F1116, 2014). The AC or DC voltage applied between the electrodes is increased until the prescribed testing voltage is reached or failure occurs. The test period starts when the prescribed testing voltage is reached and lasts between 1 and 3 min.

For low-voltage and low-risk tasks, electrical hazard shoes may be worn to provide a secondary source of protection against electrical hazards by stepping on live electrical circuits and electrically energized conductors. The footwear is tested by placing it on a metal mesh platform electrode (ASTM F2412, 2011). A second electrode is embedded in a layer of small metal spheres packed inside of the footwear. A 60 Hz–18 kV AC voltage is applied between the electrodes and maintained for 1 min. The leakage current is measured. It should be lower than 1.0 mA.

11.7.2 Electrical arc

An arc flash boundary is also defined based on the electrical arc flash hazard (NFPA 70E, 2012): for systems of 50 V and greater, it is defined as the distance at which the incident energy equals 5 J/cm^2. If work has to be conducted within the arc flash boundary, arc-rated clothing and other PPE shall be used to protect all parts of the body inside the arc flash boundary. The arc-rating test shall be performed on materials that have passed the flammability requirements (see Section 11.7.3). It allows determining the heat transport through a material, a fabric, or a fabric system when it is exposed to the heat from an electric arc (ASTM F1959, 2014). Stainless steel electrodes located at a distance of 30.5 mm are powered with an 8 kA arc current. Three specimens, which have been subjected to three laundering cycles prior to the test, are mounted at a distance of 30.5 mm from the arc centerline. The thermal energy transferred through the material is measured using thermal sensors positioned behind the

specimens. The arc-rating may be expressed in terms of the arc thermal performance value (ATPV), which is the incident energy on a material or a multilayer system that results in a 50% probability to obtain a second-degree skin burn injury, or, if the material exhibits a break-open response below the ATPV value, the break-open threshold energy (E_{BT}), which is the incident energy on a material that results in a 50% probability of breaking open. For single layer systems, the afterflame time shall also be determined.

A test method specific for gloves is also available. It allows testing whole gloves mounted on 7.6-cm wide by 1.3-cm thick vertical standoffs (ASTM F2675, 2013). Circular copper slug calorimeters are used as heat sensors. The distance between the glove standoffs and the centerline of the arc electrodes can be varied between 20.0 and 60.0 cm to allow for greater energy levels to be tested. The ATPV or E_{BT} are also reported.

11.7.3 Fire

As already mentioned, arc-rated clothing shall also be flame resistant. The flame is applied perpendicular to the lower edge of the specimen according to the ASTM D6413/D6413M (2015) test method. The flame resistance of the material is assessed in terms of char length and afterflame time. The flame resistance test shall be conducted on fabrics as received as well as after 25 washing using laundering or dry cleaning depending on the garment label indications (ASTM F1506, 2015).

11.7.4 Mechanical

A critical factor for protective clothing, including gloves and footwear, to maintain their efficiency against electrical hazards is preserving their physical integrity. Mechanical requirements are thus established for electrical protective clothing.

In the case of textile materials for wearing apparel, woven fabrics are tested for their breaking load using 100-mm wide by at least 150-mm long specimens loaded at 300 mm/min (grab test), tear resistance according to the falling-pendulum (Elmendorf-Type) test method using 100 × 75 mm notched specimens, and seam slippage (ASTM F1506, 2015). The woven fabric is tested in the machine and cross direction. For knitted fabrics, the requirement is set in terms of bursting strength. It is measured using a hydraulic or a pneumatic diaphragm bursting tester (ASTM D3786/D3786M, 2013). A specimen is clamped over a 31-mm diameter expandable diaphragm that is expanded up to specimen rupture using fluid pressure. The bursting strength is defined as the difference between the total pressure required to rupture the specimen and the pressure required to inflate the diaphragm alone.

The mechanical performance of electrical protective gloves is assessed by measuring their tensile strength, tensile stress at 200% of elongation, ultimate elongation, and tension set using 6-mm wide dumbbell specimens (ASTM D120, 2014). Tear resistance is measured on unnicked test specimens with tab ends and a 90 degree angle on one side, which allows characterizing the material tear initiation strength. A puncture test is performed using the same principle as described in Section 11.2.1 but

with a 5-mm diameter steel needle with a 12 degree tapered end rounded to a radius of 0.8 mm. Finally, the rubber material hardness is measured using a Type A durometer.

In the case of footwear, the preservation of the physical integrity is characterized by a puncture test using a pointed steel pin with a 4.5-mm diameter, a conical truncated tip with a 1-mm diameter, and a 30 degree angle at the tip (ASTM F2412, 2011). In addition, toe impact and compression resistance as well as metatarsal impact resistance are assessed by measuring the deformation made in a clay or wax form inserted inside the footwear as a result of the impact or compression applied to the footwear.

11.8 Testing of construction protective clothing

In the construction industry, falls account for the highest number of fatalities (OSHA, 2005): many accidents may be avoided by using appropriate and well maintained PPE against falls. The question of high visibility is also critical, especially for roadside worksites and night shifts. Finally, construction workers are also exposed to a series of mechanical hazards, including vibrating machinery, cuts, punctures, crushes, etc. It is to be noted that activities involving electrical hazards are already covered in Section 11.7.

11.8.1 Fall from heights

According to regulations, workers shall be protected in the case of a risk of falling from a height of 1.8 m or more (OSHA, 1998). If personal protection is needed, fall arrest systems composed of a full body harness and a secured lanyard may be used to stop workers during the fall and prevent them from hitting the ground.

Harnesses are subjected to head first and feet first drop tests using a torso-shaped, 160 kg wooden weight (CAN/CSA-Z259.10, 2012). The weight is raised by 1 m and dropped. The requirements are set in terms of maximum elongation of the harness and angular position of the weight at rest. The weight should also remain hanging for at least 10 min.

Harnesses may also be subjected to additional requirements depending on the specific tasks to be carried out and the risks associated with them. For instance, if a risk of electric arc exists, as this is the case for welders and power linemen, the electric arc performance of the harness has to be assessed using a manikin exposed to a 40 cal/cm^2 arc (ASTM F887, 2013). Three harness specimens are tested with the arc centered on the chest while three others are tested with the arc centered on the fall arrest attachment located on the back of the harness. The resistance of the harness to electric arc is assessed in terms of afterflame time, electric arc ignition, and dripping. In addition, the specimens exposed to the electrical arc shall be subjected to the required drop test as soon as possible afterwards.

11.8.2 High visibility

As it has been similarly described for law enforcement personnel and first responders, construction protective clothing may be required to exhibit high visibility functionalities. This is the case when performing work at roadside sites or on night shifts, for instance.

The requirements for high visibility safety apparel such as those used by construction workers include an assessment of the color and retroreflection when new and after exposure to a number of conditions (ANSI/ISEA 107, 2015; AS/NZS, 1906.4, 2010; CAN/CSA Z96, 2015; ISO 20471, 2013). Fabric color is characterized by the chromaticity coordinates and luminance factor using a CIE D_{65} illuminant, a 2 degree standard observer, and a 45/0 illuminating and viewing spectrometer geometry. The measurement is conducted over a 400–700 nm wavelength range. Color fastness is assessed after exposure to xenon light, rubbing in a dry and/or wet condition, perspiration using a simulated acid perspiration solution, as well as laundering, dry cleaning, hypochlorite bleaching, and hot pressing.

Retroreflective materials shall also be evaluated for their photometric performance (ANSI/ISEA 107, 2015; AS/NZS, 1906.4, 2010; CAN/CSA Z96, 2015; ISO 20471, 2013). The coefficient of retroreflection R_A (also called the specific intensity per unit area R') is measured at four values of the entrance angle: 5, 20, 30, and 40°; at four values of the observation angle: 12′, 20′, 1°, and 1°30′; and for the 0° and 90° positions of the rotation angle ε using a light projector source, a photodetector, and two goniometers positioned in a photometric range. The photometric performance of retroreflective materials is also assessed after exposure to 5000 abrasion cycles under a 9 kPa weight, 7500 flexing cycles, folding at −20°C, temperature variations between −30°C and 50°C, and five washing and/or dry cleaning cycles performed according to the garment manufacturer's instructions. The measurement of the coefficient of retroreflection may also be conducted while the retroreflective material is subjected to a continuous spray of water droplets to simulate the influence of rainfall.

11.8.3 Mechanical

Construction workers are also exposed to a series of mechanical risks from which appropriate protective clothing can help protect them. For instance, protective gloves may be needed with proper resistance to cutting, puncture, abrasion, and tearing (see Section 11.2.1). In addition, hand-held powered work equipment is of large use in the construction industry. Antivibration gloves may be used to limit the hand-arm vibration syndrome. The transmission of vibrations of a 40-mm diameter handle to the hand palm through the glove is measured using accelerometers positioned at the surface of the handle and at the interface between the glove and the hand of the human subject holding the handle (ISO 10819, 2013). The vibration applied covers the 16–1500 Hz range.

Large risks of foot injury also exist in the construction industry. Workers should wear puncture- and crushing-resistant shoes or boots (see Section 11.2.1 for test methods) with slip-resistant soles (see Section 11.3.4 for test methods).

11.9 Testing of marine protective clothing

Floatation clothing is mandatory for recreational and occupational activities where a risk of drowning exists. There are two types of floatation clothing (Vidito, 2014)—lifejackets with keyholes and personal flotation devices such as vests, suits, and coats.

They may be inherently buoyant, inflatable or combine inherently buoyant and inflatable components. Some may also offer thermal protection.

11.9.1 Flotation

The floatation assessment of clothing involves tests performed on the raw materials as well as on the finished product.

Woven fabrics fulfilling a structural function in the floatation clothing, for instance used as a cover for floatation compartments, shall be tested for tensile strength and elongation at break using the strip method, resistance to tearing using single tear trouser-shaped specimens, resistance to yarn slippage, and weave opening (ISO 12402-7, 2006). In the case of knitted fabrics, the bursting strength is measured using a hydraulic or pneumatic pressure device. Both tensile strength for woven fabrics and bursting strength for knitted fabrics shall be measured on new materials as well as after UV aging and immersion in diesel fuel, IRM oil, and 0.5% detergent. Tearing strength may also be measured with wet specimens using the single-rip method (CAN/CGSB-65.19, 2004). In some instances, the adhesion resistance of the coating is also tested (ISO 12402-7, 2006). In the case of structural webbing and tape, tensile strength is assessed when the fabric is new as well as after UV exposure. The rigidity in torsion of tapes is measured on new materials only.

The density of foam-type floatation materials shall be measured after a 24 h immersion in water as well as after 10 thermal cycles between 65°C and −30°C (ISO 12402-7, 2006). The buoyancy of the material shall also be characterized after a 24 h immersion in water as well as after subjecting the foam to 5 cycles of compression at 50 kPa in water at a rate of 200 mm/min; the buoyancy is computed from the measurement of the weight of a foam material specimen enclosed in a basket immersed in water. The tensile strength of the foam is also measured using dumbbell-shaped specimens. Finally, the resistance to immersion in oil and flexion at −18°C as well as the deformability under compression load are characterized.

Materials used for manufacturing inflatable products shall be subjected to tensile, trapezoidal tearing, and permeability to carbon dioxide (CO_2) tests when new as well as after accelerated thermal aging at 70°C for 168 h (ISO 12402-7, 2006). Residual performance in tension and CO_2 permeability shall also be assessed after a 12-week exposure to laboratory soil burial aimed at evaluating the susceptibility of the materials to microbial attack. The effect of UV aging on tensile strength and of exposure to 95% relative humidity at 65°C on CO_2 permeability is characterized as well. Inflatable chamber materials are also tested for resistance to abrasion. Finally, the adherence of the coating on the textile support is assessed by subjecting pouches made of the material to burst test under pressure when new and after 5000 pressure cycles between 100 and 300 mbar.

Polymer foam coatings are tested without the textile support. They are assessed in terms of tensile strength, maximum elongation, and resistance to tearing when new and after UV aging and exposure to 70°C for 7 days (ISO 12402-7, 2006). Other tests to be conducted include flexibility at −30°C, blocking resistance, effect of abrasion on tensile strength, water absorption, and loss of volatiles. In addition, the adhesion of

the polymer foam coating on the textile support shall be characterized by measuring the peeling force using a mechanical test frame.

The performance of the various assembly materials and closure systems shall also be assessed (ISO 12402-7, 2006): the tensile strength and elongation at break of sewing threads in their original condition and after UV aging as well as the breaking strength of a thread loop; the tensile strength of structural lacings in their original condition and after UV aging; and the operating force and lateral strength of zippers in their original condition and after UV aging, salt spray aging, and immersion in diesel fuel, IRM oil, and 0.5% detergent, as well as the pullout resistance of the zipper, the torsion resistance of the pull tab and slider, and the holding force of the slider locking system.

The buoyancy of the whole immersion suit systems is also assessed by weighting a mesh basket containing the product after it is immersed in water (CAN/CGSB-65.16, 2005). The test is conducted on the product in its original condition as well as after 24 h immersion in fresh water. Some tests are also conducted with human subjects with water temperature at a minimum of 18°C. For instance, the donning time, mobility outside of the water, and ability to swim may have to be assessed. In addition, two tests shall be performed to ensure the floatation stability: freeboard and self-righting. For the freeboard test, the subject steps from a platform situated at least 4.5 m above the water level while wearing the floatation clothing properly secured and adjusted. The time to have the system positioning the subject's mouth above the water surface as well as the freeboard distance reached within 15 s of the water entry are recorded. For the self-righting test, the subject is immersed face down in the water while wearing the floating equipment. His ability to turn over face up unaided, i.e., by the sole action of the floating clothing or under his own power, within 5 s is assessed. The floatation stability as well as the buoyancy shall be retained after the floating clothing has been exposed to the flame of burning gasoline at a distance of 240 mm for 2 s. Test methods for floatation performance assessment may also be found in the CAN/CGSB-65.7 (2007) for life jackets.

11.9.2 Thermal

If the marine protective clothing is intended to provide some level of thermal protection, its thermal performance parameters are assessed using a thermal manikin and human subjects (CAN/CGSB-65.16, 2005). If dry suits are tested, the tests shall be performed with an amount of water introduced inside the clothing prior to testing that corresponds to ingress water that had been measured to penetrate the clothing upon jumping into water and during swimming.

The thermal manikin dressed with the marine protective clothing, including eventually gloves and socks, is placed in a natural floating position in turbulent water at no less than 18°C (CAN/CGSB-65.16, 2005). Once stable conditions have been reached, the thermal protection value, or immersed Clo, is computed from the temperature gradient between the heated manikin and the surrounding water, the heat loss corresponding to the power input, and the manikin surface area.

The test involving human subjects is conducted in calm circulating water between 0°C and 2°C (CAN/CGSB-65.16, 2005). The average body (rectal) temperature and

that of finger, toe, or buttock of subjects wearing the marine protection clothing are recorded every 10 min during the 6 h of the test.

11.9.3 Localization

The color of marine protective clothing is designed to facilitate localization in the case of a fall into the water. The chromaticity coordinates and luminance factor are measured for nonfluorescent and fluorescent colors in dry and wet conditions using a CIE D_{65} illuminant, a 2 degree standard observer, and a 45/0 spectrometer geometry (ISO 12402-7, 2006). The test is conducted on UV aged specimens as well as after exposure to abrasion cycles and immersion in salt water. The color of the exterior of helicopter passenger transportation suit systems designed to increase the chance of survivability in case of an evacuation during transportation over water is also assessed using a CIE D_{65} illuminant, a 2 degree standard observer, and a 45/0 spectrometer geometry (CAN/CGSB 65.17, 2012).

In addition, the area of retroreflective tape above the water level is measured while the floatation clothing is worn by human subjects in a relaxed, floating position in the water (CAN/CGSB-65.16, 2005). For helicopter passenger transportation suit systems, tests also include a measurement of the area of retroreflective tape above the water level, with a specific focus on the hood (CAN/CGSB 65.17, 2012). The amount of retroreflective material within each quadrant of the forearm is characterized as well.

11.10 Testing of sports protective clothing

Protective clothing is also a critical element to enjoy practicing sports in complete safety. Indeed, depending on the sport, risks may include impacts, cuts, abrasion, falls, cold temperature, heat, and flame. For this section, a series of sports have been selected: car racing, motorcycling, hockey playing, and ice skating.

11.10.1 Car racing

Car racing is a dangerous sport, even for spectators. For instance, an in-race injury rate of 1.2 per 1000 competitors has been reported for a circuit in Japan between 1996 and 2000, with the most frequent injuries being bruises and neck sprains (Minoyama & Tsuchida, 2004). In addition, drivers in automobile competitions are also at high risk of exposure to heat and flame. For example, the driver's feet being burned by heat coming from the engine is one of the most common injuries in NASCAR races (Bonsor & Nice, 2001). Finally, excessive heat build-up in the cockpit of the cars and in the protective clothing puts racecar drivers at risk of hyperthermia, eventually causing heat syncope, heat cramps, heat exhaustion, and heat stroke (Potkanowicz & Mendel, 2013).

The standard for protective clothing for automobile drivers of the Federation internationale de l'automobile (FIA) specifies the requirements in terms of protection offered against heat and flame for clothing to be worn by drivers in automobile

competitions (FIA N° 8856-2000, 2012). Tests shall be performed on each material used in the outer garment, undergarment/cooling undergarment, balaclava hood, rainproof overgarment, socks, gloves, and shoes. The flame resistance of all materials shall be tested in the original condition and after 15 washing cycles using surface ignition and limited flame spread. The flame resistance of the sewing thread and the glove seams is also assessed in the original condition. The heat transmission of outer garments and gloves upon flame exposure is tested in the original condition and after 15 washing cycles. The mechanical resistance of the outer garment after exposure to flame is assessed by folding the specimen 5 times in both directions. In addition, the dimensional change of outer garments and gloves after 5 washing or dry cleaning processes and the tensile strength of outer garment seams are measured as well. Finally, the resistance of the cooling undergarment materials to convective heat is characterized at a temperature of 250°C.

11.10.2 Motorcycling

Motorcycling is also a dangerous sport, both on race tracks and on the road. Wearing protective clothing has been shown to reduce the rate and severity of crash-related injuries suffered by motorcyclists (de Rome et al., 2011). Motorcycle clothing comprises jackets, pants, gloves, and boots. Some of them may also include fitted body armor to provide extra protection at the elbows, knees, hips, and back.

The surface area of jackets, trousers, and suits is distributed into four zones depending on the potential of exposure in case of a fall or a crash (EN 13595-1, 2003). Minimum levels of abrasion, burst, and impact cut resistance are defined for each of these four zones. Abrasion resistance is assessed by dropping the fabric specimen secured on a sensor from a defined height on an abrasive strip that moves at a constant speed on a rigid horizontal surface (EN 13595-2, 2003). The time for complete abrasion of the specimen is detected by the sensor. For the burst test, the specimen is positioned over a water-tight inflatable pouch, which is progressively filled with water (EN 13595-3, 2002). The water pressure corresponding to the specimen failure provides the bursting strength. Impact cut resistance is measured by dropping a blade on the specimen from a defined height and recording the penetration depth (EN 13595-4, 2002). In addition, the armor positioned at the shoulder, elbow, hip, and knee of the protective clothing is subjected to an impact test using a dropped weight with a 50 J impact (EN 1621-1, 2013). The test is conducted at room temperature but an option exists in the standard to perform it at 40°C and −10°C as well. Finally, the performance of back protectors is also assessed with a 50 J impact test but with a different anvil geometry and different transmitted energy requirements (EN 1621-2, 2014).

Protective gloves and footwear shall also be tested. They are subjected to abrasion and impact cut tests according to the same methods as jackets, trousers, and suits (EN 13594, 2015; EN 13634, 2016). In addition, the resistance of gloves to tearing as well as the impact resistance of the armor pieces at the knuckles are assessed (EN 13594, 2015). In the case of protective footwear, the transverse stiffness is measured on the entire footwear, the resistance to tearing on the lining, and the pH and chromium VI

content (in the case of leather material) on all of the different footwear components (EN 13634, 2016).

11.10.3 Ice sports

The sharp skates used in ice hockey, ice skating, and other ice sports are the source of a high risk of body lacerations. Protective clothing may be used to protect from these cuts.

For instance, in the case of hockey, the occurrence of several severe injuries, and even deaths, resulting from the skate severing a major artery in the neck prompted the Bureau de normalization du Quebec (BNQ) to develop a standard for neck protectors, which are now mandatory for every ice hockey player in Quebec and every minor league players of ice hockey and ringette throughout Canada (CAN/BNQ 9415-370/2007, 2013). The resistance of the neck protector to contact with a hockey skate blade is assessed using a test bench comprising an artificial neck, a skate blade held by a pendulum mechanism, a pneumatic cylinder capable of moving the artificial neck at a speed of 25 km/h, and a system of weights simulating a 90 kg player. Evidence for cuts through the bottom layer of the neck protector or in the layer of foam at the surface of the artificial neck is looked for. The resistance of the neck protector to laundering is assessed by verifying the protected zone with an anatomical form after three washing/drying cycles.

In the case of ice skating, the International Skating Union requires protective clothing to be tested for cut resistance using the counter-rotating circular blade method (EN 388, 2004).

11.11 Future trends

Large progress has been made over the years for the development of test methods for protective clothing that allow characterizing their performance in a meaningful and reproducible way. However, several challenges remain.

One issue is related to the relevance of the test conditions in comparison with the situations encountered while in service. For instance, even if it has been shown that the probe tip size and shape affect puncture force as well as the mechanisms involved in probe penetration (Nguyen et al., 2005), both ISO and EN puncture test methods (EN 388, 2004; ISO 13996, 1999) still use a 4.5-mm diameter probe with a 0.5-mm radius tapered head, which is not relevant to most of the hand, foot, and body puncture hazards encountered in the field. Another example is related to pointed blades. Currently, most test methods assessing the cutting resistance of protective clothing consider slicing, i.e., the blade displacement being parallel to its cutting edge. However, the prevalence of lacerations produced by pointed blades is very high in several sectors such as food processing and metal machining, while the mechanism of penetration of pointed blades through materials is largely different from that produced during a slicing cut or a puncture test performed according to current standard methods (Dolez, Azaiez, & Vu-Khanh, 2012b).

Another aspect where progress is still needed relates to the assessment of protective material long-term performance. If the assessment of the residual performance after UV aging is generally included in the test program of protective clothing, for instance with moisture barriers in firefighter protective clothing as in the NFPA 1971 Standard (2013), its relevance to real conditions experienced in the field may sometimes be questionable. In addition, other aging agents, for instance heat in that case, may appear equally relevant yet operate according to different mechanisms (Dolez et al., 2011a). Moreover, for this particular case of firefighter protective suits, no evaluation of the long-term performance is conducted on the outer layer, even if research has shown that depending on the material used, a significant loss in the yarn mechanical strength may be produced as a result of exposure to UV, heat, or humidity (Dolez, Arrieta, et al., 2011a). A solution for ensuring that protection is maintained throughout the whole service life of the clothing may be to demand a regular assessment of the residual performance while in use. However, this requires that nondestructive testing methods are available. Efforts have been initiated to that extent for flame protective fabrics (Rezazadeh & Torvi, 2012).

Another sector where efforts need to be pursued relates to new and emerging hazards. For instance, nanoparticles are increasingly encountered at the work place. Preliminary tests have evidenced a risk of penetration through certain types of protective clothing and gloves when the nanoparticles are in colloidal solutions or when the gloves are subjected to repeated deformations simulating those experienced when flexing the hand or the fingers (Vinches et al., 2013) using a test method developed to measure the permeability of protective materials to nanoparticles in conditions simulating occupational use (Dolez, Vinches, Wilkinson, Plamondon, & Vu-Khanh, 2011b). Other test methods have been proposed for aerosols and hydrosols (Dolez, 2015). In a totally different area of activity, extreme sports such as downhill biking, off-track skiing, and acrobatic motorcycling were previously reserved to athletes (Young, 2002). They are gaining in popularity among the general public, which brings new requirements in terms of type and magnitude of hazards from which one should be protected.

New technologies are also introduced into protective clothing, which may require an adjustment of existing performance specifications and testing methods or the development of new ones. For instance, smart textiles are gradually finding their way into protective clothing, allowing integrated position location, physiological monitoring, active cooling and heating, communication, and energy harvesting for example (Dolez & Mlynarek, 2016). New test methods are required to characterize their specific properties, e.g., trigger threshold value, consumed power, magnitude and quality of response, and durability (Decaens, 2014). They shall also probe the effect of the time factor and the different states that the smart material will take during the use of the clothing. Finally, it is critical to assess the eventual occurrence of unexpected side effects caused by the particular nature of the smart textile or some unintended interactions with the conditions the PPE will experience over its use—for example, an increased risk of being struck by lightning because of the presence of conductive elements or a reduced protection efficiency resulting from the presence of a protruding device such as a camera.

11.12 Conclusions

Even though they should only be considered as a last resort after all other risk management strategies have been implemented, protective clothing play a large role in our lives: at work, at home, and during leisure times. They protect us from mechanical hazards, chemicals, biological agents, extreme temperatures, fire, impacts, electric shocks, drowning, or falls for instance. They may also help identify, see or locate us, or, on the contrary, conceal us.

Because their potential impact on the health, safety, and life of those wearing them is so large, it is of major importance to properly assess the performance of protective clothing in a way that is relevant to the situations experienced in service. To that effect, specific test methods have been developed and shall be used to verify the conformity of the protective clothing with requirements established depending on the type of activities/tasks: industrial/domestic use, first responders, law enforcement personnel, military personnel, medical employees, electrical workers, construction workers, marine activities, and sports. Even if great progress has been accomplished over the years, some challenges remain; examples include using test conditions more relevant to situations encountered in service, assessing in a meaningful way the long-term performance of the protective material, and the existance of new and emerging hazards as well as new technologies introduced into protective clothing.

11.13 Sources for further information and advice

Below is provided a nonexhaustive list of sources of further information and advice on the testing of textiles used in protective clothing.

ASTM Committee F23 on Personal Protective Clothing and Equipment (https://www.astm.org/COMMIT/SUBCOMMIT/F23.htm). This Committee was formed in 1977, has a membership of about 260, and meets twice a year. The Committee has jurisdiction of over 44 standards distributed among six technical subcommittees: physical, chemical, biological, human factors, flame and thermal, and radiological.

CEN TC 161 on Foot and leg protectors (https://standards.cen.eu/dyn/www/f?p=204:7:0::::FSP_ORG_ID:6142&cs=19558685DF5F40E1F26956AB43EBB330E). The TC 161 committee was formed in 1988 and is organized in three working groups: WG 1 for test methods; WG 2 for requirements, and WG 3 for test methods for slip resistance.

CEN TC 162 on Protective clothing including hand and arm protection and lifejackets (https://standards.cen.eu/dyn/www/f?p=204:7:0::::FSP_ORG_ID:6143&cs=1172B5BBB1F1411294D97D98575DE977D). This Committee has 13 working groups:

- WG 1: General requirements for protective clothing
- WG 2: Protective clothing against heat and fire
- WG 3: Protective clothing against chemical hazards
- WG 4: Protective clothing against foul weather
- WG 5: Protective clothing against mechanical impact
- WG 6: Lifejackets

- WG 7: High visibility warning clothing
- WG 8: Protective gloves
- WG 9: Motorcycle rider's protective clothing
- WG 10: Buoyancy aids for swimming instruction
- WG 11: Body protection for sports
- WG 12: Diving suits
- WG 13: Permeation of chemicals through materials for protective footwear, gloves, and clothing

CTT Group (Quebec, Canada) is a testing and R & D Laboratory for technical textiles, geosynthetics, and advanced textile-based materials (www.groupecttgroup.com). Founded in 1983 as a college technology transfer center, it serves the industry in the sectors of protection, transportation, aerospace, health, buildings, sports, military, and civil engineering among others. It has strong expertise in protective clothing, and its team members have been involved in the development of a number of test methods and standards.

ISO Technical Committee TC 94 on Protective clothing and equipment (http://www.iso.org/iso/iso_technical_committee%3Fcommid%3D50580). It has eight subcommittees:

- SC 1: Head protection
- SC 3: Foot protection
- SC 4: Personal equipment for protection against falls
- SC 6: Eye and face protection
- SC 12: Hearing protection
- SC 13: Protective clothing
- SC 14: Firefighters' personal equipment
- SC 15: Respiratory protective devices

It also has one task group (TG 1) on compatibility of PPE items. It has published 136 standards.

National Fire Protection Association (http://www.nfpa.org/codes-and-standards). NFPA has more than 250 technical committees and develops and publishes more than 300 consensus codes and standards intended to eliminate death, injury, property, and economic loss due to fire, electrical, and related hazards.

Acknowledgments

The authors wish to thank Mrs. Edith Dion-Marcil for her assistance in preparing the manuscript.

References

AATCC TM100 Standard. (2012). *Antibacterial finishes on textile materials: Assessment of*. Research Triangle Park, NC: American Association of Textile Chemists and Colorists. 3 pp.

AATCC TM147 Standard. (2011). *Antibacterial activity assessment of textile materials: Parallel streak method*. Research Triangle Park, NC: American Association of Textile Chemists and Colorists.

Ackerman, M. Y., Crown, E. M., Dale, J. D., Murtaza, G., Batcheller, J., & Gonzalez, J. A. (2012). Development of a test apparatus/method and material specifications for protection from steam under pressure. In A. M. Shepherd (Ed.), *Emerging issues and technologies*: *Vol. 9. Performance of protective clothing and equipment* (pp. 308–328). West Conshohocken, PA: ASTM International.

ACT. (2010). Abrasion resistance: The full story. ACT white paper series, Association for Contract Textiles.

ANSI/ISEA 105 Standard. (2011). American national standard for hand protection selection criteria. American National Standards Institute.

ANSI/ISEA 107 Standard. (2015). American National Standard for high-visibility safety apparel and headwear. American National Standards Institute. 43 pp.

AS/NZS 1906.4 Standard, (2010). Retroreflective materials and devices for road traffic control purposes—Part 4: High-visibility materials for safety garments. Australian/New Zealand Standards. 30 pp.

Aschan, C. (2005). Discrepancy between real risks and standardized test methods and specifications—The typical case of safety footwear. *Work environment research report series*: *Vol. 16*. Finland: Finnish Institute of Occupation Health. pp. 50–53.

ASTM D120 Standard. (2014). Standard specification for rubber insulating gloves. ASTM International. 9 pp.

ASTM D471 Standard. (2012). Standard test method for rubber property—Effect of liquids. ASTM International. 14 pp.

ASTM D543 Standard. (2014). Standard practices for evaluating the resistance of plastics to chemical reagents. ASTM International. 7 pp.

ASTM D751 Standard. (2011). Standard test methods for coated fabrics. ASTM International. 19 pp.

ASTM D1894 Standard. (2014). Standard test method for static and kinetic coefficients of friction of plastic film and sheeting. ASTM International. 7 pp.

ASTM D2212 Standard. (2000). Standard test method for slit tear resistance of leather. ASTM International. 3 pp.

ASTM D2261 Standard. (2013). Standard test method for tearing strength of fabrics by the tongue (single rip) procedure (constant-rate-of-extension tensile testing machine). ASTM International. 6 pp.

ASTM D2582 Standard. (2009). Standard test method for puncture-propagation tear resistance of plastic film and thin sheeting. ASTM International. 5 pp.

ASTM D3384 Standard. (2009). Standard guide for abrasion resistance of textile fabrics (rotary platform, double-head method). ASTM International.

ASTM D3389 Standard. (2005). Standard test method for coated fabrics abrasion resistance (rotary platform abrader). ASTM International.

ASTM D3786/D3786M Standard. (2013). Standard test method for bursting strength of textile fabrics—Diaphragm bursting strength tester method. ASTM International. 4 pp.

ASTM D4157 Standard. (2013). Standard test method for abrasion resistance of textile fabrics (oscillatory cylinder method). ASTM International.

ASTM D4966 Standard. (2012). Standard test method for abrasion resistance of textile fabrics (Martindale abrasion tester method). ASTM International.

ASTM D5587 Standard. (2015). Standard test method for tearing strength of fabrics by trapezoid procedure. ASTM International.

ASTM D6413/D6413M Standard. (2015). Standard test method for flame resistance of textiles (vertical test). ASTM International. 12 pp.

ASTM E308 Standard. (2015). Standard practice for computing the colors of objects by using the CIE system. ASTM International. 45 pp.
ASTM E809 Standard. (2008). Standard practice for measuring photometric characteristics of retroreflectors. ASTM International. 11 pp.
ASTM E991 Standard. (2011). Standard practice for color measurement of fluorescent specimens using the one-monochromator method. ASTM International. 8 pp.
ASTM F489 Standard. (1996). Standard test method for using a James machine (withdrawn 2005). ASTM International. 3 pp.
ASTM F496 Standard. (2014). Standard specification for in-service care of insulating gloves and sleeves. ASTM International. 8 pp.
ASTM F609 Standard. (2013). Standard test method for using a horizontal pull slipmeter (HPS). ASTM International. 3 pp.
ASTM F739 Standard. (2012). Standard test method for permeation of liquids and gases through protective clothing materials under conditions of continuous contact. ASTM International.
ASTM F887 Standard. (2013). Standard specifications for personal climbing equipment. ASTM International. 30 pp.
ASTM F903 Standard. (2010). Standard test method for resistance of materials used in protective clothing to penetration by liquids. ASTM International. 10 pp.
ASTM F955 Standard. (2007). Standard test method for evaluating heat transfer through materials for protective clothing upon contact with molten substances. ASTM International. 6 pp.
ASTM F1060 Standard. (2008). Standard test method for thermal protective performance of materials for protective clothing for hot surface contact. ASTM International. 7 pp.
ASTM F1116 Standard. (2014). Standard test method for determining dielectric strength of dielectric footwear. ASTM International. 3 pp.
ASTM F1154 Standard. (2011). Standard practices for qualitatively evaluating the comfort, fit, function, and durability of protective ensembles and ensemble components. ASTM International. 7 pp.
ASTM F1291 Standard. (2010). Standard test method for measuring the thermal insulation of clothing using a heated manikin. ASTM International. 5 pp.
ASTM F1342 Standard. (2005). Standard test method for protective clothing material resistance to puncture. ASTM International.
ASTM F1359 Standard. (2007). Standard test method for liquid penetration resistance of protective clothing or protective ensembles under a shower spray while on a Mannequin. ASTM International. 5 pp.
ASTM F1383 Standard. (2012). Standard test method for permeation of liquids and gases through protective clothing materials under conditions of intermittent contact. ASTM International.
ASTM F1407 Standard. (2012). Standard test method for resistance of chemical protective clothing materials to liquid permeation—Permeation cup method. ASTM International.
ASTM F1506 Standard. (2015). Standard performance specification for flame resistant and arc rated textile materials for wearing apparel for use by electrical workers exposed to momentary electric arc and related thermal hazards. ASTM International. 7 pp.
ASTM F1670/1670 M Standard. (2008). Standard test method for resistance of materials used in protective clothing to penetration by synthetic blood. ASTM International. 7 pp.
ASTM F1671 Standard. (2013). Standard test method for resistance of materials used in protective clothing to penetration by blood- borne pathogens using Phi-X174 bacteriophage as a test system. ASTM International. 11 pp.
ASTM F1677 Standard. (2005). Standard test method for using a portable inclineable articulated strut slip tester (PIAST) (withdrawn 2006). ASTM International. 4 pp.

ASTM F1790 Standard. (2005). Standard test method for measuring cut resistance of materials used in protective clothing. ASTM International.
ASTM F1868 Standard. (2014). Standard test method for thermal and evaporative resistance of clothing materials using a sweating hot plate. ASTM International. 19 pp.
ASTM F1930 Standard. (2015). Standard test method for evaluation of flame resistant clothing for protection against fire simulations using an instrumented Manikin. ASTM International. 9 pp.
ASTM F1939 Standard. (2008). Standard test method for radiant heat resistance of flame resistant clothing materials with continuous heating. ASTM International. 12 pp.
ASTM F1959 Standard. (2014). Standard test method for determining the arc rating of materials for clothing. ASTM International. 14 pp.
ASTM F2010/F2010M Standard. (2010). Standard test method for evaluation of glove effects on wearer hand dexterity using a modified pegboard test. ASTM International. 3 pp.
ASTM F2412 Standard. (2011). Standard test methods for foot protection. ASTM International. 17 pp.
ASTM F2547 Standard. (2006). Standard test method for determining the attenuation properties in a primary X-ray beam of materials used to protect against radiation generated during the use of X-ray equipment. ASTM International. 3 pp.
ASTM F2675 Standard. (2013). Standard test method for determining arc ratings of hand protective products developed and used for electrical arc flash protection. ASTM International. 13 pp.
ASTM F2701 Standard. (2008). Standard test method for evaluating heat transfer through materials for protective clothing upon contact with a hot liquid splash. ASTM International. 8 pp.
ASTM F2731 Standard. (2011). Standard test method for measuring the transmitted and stored energy of firefighter protective clothing systems. ASTM International. 13 pp.
ASTM F2878 Standard. (2010). Standard test method for protective clothing material resistance to hypodermic needle puncture. ASTM International. 5 pp.
ASTM F2894 Standard. (2012). Standard test method for evaluation of materials, protective clothing and equipment for heat resistance using a hot air circulating oven. ASTM International. 6 pp.
ASTM F2913 Standard. (2011). Standard test method for measuring the coefficient of friction for evaluation of slip performance of footwear and test surfaces/flooring using a whole shoe tester. ASTM International. 10 pp.
ASTM F2992/F2992M Standard. (2015). Standard test method for measuring cut resistance of materials used in protective clothing with tomodynamometer (TDM-100) test equipment. ASTM International. 10 pp.
ASTM F3094 Standard. (2014). Standard test method for determining protection provided by X-ray shielding garments used in medical X-ray fluoroscopy from sources of scattered X-Rays. ASTM International. 5 pp.
ASTM International. (1996). Committee F23 on Personal Protective Clothing and Equipment. Retrieved December 31, 2015 from www.astm.org/COMMIT/SCOPES/F23.htm.
ASTM WK27291 Standard. (2016). *New practice for ergonomic performance evaluation of first responders protective ensembles*. ASTM International. Retrieved from www.astm.org/DATABASE.CART/WORKITEMS/WK27291.htm [Accessed 12 June 2016].
ASTM WK31804 Standard. (2016). *New guide for testing and optimal selection of radiological protection garments*. ASTM International. Retrieved from www.astm.org/COMMIT/SUBCOMMIT/F2370.htm [Accessed 12 June 2016].
ASTM WK54740 Standard. (2016). *Method for quantitative measurements of defects or damage in radiation protective shielding garments*. ASTM International. Retrieved from www.astm.org/COMMIT/SUBCOMMIT/F2370.htm [Accessed 12 June 2016].

Barker, J., Boorady, L. M., Lin, S.-H., Lee, Y.-A., Esponnette, B., & Ashdown, S. P. (2012). Assessing user needs and perceptions of firefighter PPE. In A. Shepherd (Ed.), *Emerging issues and technologies*: Vol. 9. Performance of protective clothing and equipment (pp. 158–175). West Conshohocken, PA: ASTM International. STP1544.

Barker, R., Guerth, C., Behnke, W., & Bender, M. (2000). Measuring the thermal energy stored in firefighter protective clothing. In C. N. Nelson & N. W. Henry (Eds.), Vol. 7. *Performance of protective clothing: Issues and priorities for the 21st century* (pp. 33–44). West Conshohocken, PA: ASTM International. STP1386.

Bartenev, G. M., & Lavrentev, V. V. (1981). *Friction and wear of polymers*. Amsterdam, Netherlands: Elsevier.

Belmonte, R. B. (1998). *Test results of level A suits—Protection against chemical and biological warfare agents and simulants*. Aberdeen Proving Ground, MD: US Army, Edgewood Research Development and Engineering Center.

Berry, C., McNeely, A., Beauregard, K., & Haritos, S. (2008). *A guide to personal protective equipment*. Raleigh, NC: NC Department of Labor.

Bonsor, K., & Nice, K. (2001). *How NASCAR safety works.* Retrieved from auto.howstuffworks.com [Accessed 1 August 2016].

Bradley, J. V. (1969). Glove characteristics influencing control manipulability. *Human Factors*, *11*(1), 21–35.

CAN/BNQ 9415-370/2007 Standard. (2013). Neck protectors for ice hockey and ringette players. Bureau de normalisation du Québec. 40 pp.

CAN/CGSB-4.2 No. 12.1 Standard. 2016. Textile test methods tearing strength—Single-rip method. Canadian General Standards Board. 11 pp.

CAN/CGSB-4.2 No. 12.2 Standard. (2012). Textile test methods tearing strength—Trapezoid method. Canadian General Standards Board. 9 pp.

CAN/CGSB-4.2 No. 12.3 Standard. (2005). Textile test methods: Textiles—Tear properties of fabrics—Part 1: Determination of tear force using ballistic pendulum method (Elmendorf). Canadian General Standards Board. 24 pp.

CAN/CGSB-4.2 No 27.10 Standard. (2000). Textile test methods flame resistance—Vertically oriented textile fabric or fabric assembly test. Canadian General Standards Board. 13 pp.

CAN/CGSB-4.2 No. 78.1 Standard. 2001. Textile test methods: Thermal protective performance of materials for clothing. Canadian General Standards Board. 15 pp.

CAN/CGSB-65.7 Standard. (2007). Life jackets. Canadian General Standards Board.

CAN/CGSB-65.16 Standard. (2005). Immersion suit systems. Canadian General Standards Board. 33 pp.

CAN/CGSB 65.17 Standard. (2012). Helicopter passenger transportation suit systems. Canadian General Standards Board. 76 pp.

CAN/CGSB-65.19 Standard. 2004. Textile components of life jackets and personal flotation devices. Canadian General Standards Board. 16 pp.

CAN/CSA Z96 Standard. (2015). High-visibility safety apparel. CSA Group. 55 pp.

CAN/CSA Z195 Standard. (2014). Protective footwear. CSA Group. 61 pp.

CAN/CSA-Z259.10 Standard. (2012). Full body harnesses. CSA Group. 48 pp.

Cao, H. (2013). Smart technology for personal protective equipment and clothing. In R. A. Chapman (Ed.), *Smart textiles for protection* (pp. 229–243). Cambridge: Woodhead Publishing.

Cardello, A. V. (2008). The sensory properties and comfort of military fabrics and clothing. In E. Wilusz (Ed.), *Military textiles* (pp. 71–106). Cambridge/Boca Raton, FL: Woodhead/CRC Press LLC.

Casanova, L., Alfano-Sobsey, E., Rutala, W. A., Weber, D. J., & Sobsey, M. (2008). Virus transfer from personal protective equipment to healthcare employees' skin and clothing. *Emerging Infectious Diseases*, *14*(8), 1291–1293.

Cowan, S. L., Tilley, R. C., & Wiczynski, M. E. (1988). *Comfort factors of protective clothing: Mechanical and transport properties, subjective evaluation of comfort*. In S. Z. Mansdorf, R. Sager, & A. P. Nielsen (Eds.), *Performance of protective clothing: Second symposium* (pp. 31–42). Philadelphia, PA: ASTM International.

de Rome, L., Ivers, R., Du, W., Haworth, N., Heritier, S., & Richardson, D. (2011). Motorcycle protective clothing: Protection from injury or just the weather? *Accident Analysis and Prevention*, *43*(6), 1893–1900.

Decaens, J. (2014). *New standards for smart textiles*. In *113th scientific session of institute of textile science, October 7, 2014, Montreal, QC, Canada*.

Dolez, P. (2015). Progress in personal protective equipment for workers exposed to nanomaterials. *Nano engineering: Global approaches to health & safety issues*. Amsterdam, Netherlands: Elsevier. pp. 607–635.

Dolez, P. I., Arrieta, C., El Aidani, R., Tomer, N., Malajati, Y., Vu-Khanh, T., et al. (2011). *Aging of textiles used in fire protective clothing*. In: *Personal protective symposium, partenariat innovation 2011, November 22–23, 2011, Quebec, Canada*.

Dolez, P. I., Azaiez, M., & Vu-Khanh, T. (2012). Characterization of the resistance of protective gloves to pointed blades. In A. M. Shepherd (Ed.), *Emerging issues and technologies*: Vol. 9. Performance of protective clothing and equipment (pp. 354–370). West Conshohocken, PA: ASTM International.

Dolez, P. I., Gauvin, C., Lara, J., & Vu-Khanh, T. (2010). The effect of protective glove exposure to industrial contaminants on their resistance to mechanical risks. *International Journal of Occupational Safety and Ergonomics*, *16*, 169–183.

Dolez, P., & Mlynarek, J. (2016). Smart materials for PPE: Tendencies and recent developments. In V. Koncar (Ed.), *Smart textiles and their applications* (pp. 497–518). Amsterdam: Elsevier.

Dolez, P. I., Nguyen, C. T., Guero, G., Gauvin, C., & Lara, J. (2008). Influence of medical needle characteristics on the resistance to puncture of protective glove materials. *Journal of ASTM International*, *5*(1). 12 pp.

Dolez, P., Soulati, K., Gauvin, C., Lara, J., & Vu-Khanh, T. (2012). *Information document for selecting gloves for protection against mechanical hazards: Studies and Research Projects Series/Report R-783*. Montreal, QC: IRSST. 61 pp.

Dolez, P., Vinches, L., Wilkinson, K., Plamondon, P., & Vu-Khanh, T. (2011). Development of a test method for protective gloves against nanoparticles in conditions simulating occupational use. *Journal of Physics: Conference Series*, *304*, 10, 012066.

Dolez, P. I., & Vu-Khanh, T. (2009b). Recent developments and needs in materials used for personal protective equipment and their testing. *International Journal of Occupational Safety and Ergonomics*, *15*, 347–362.

DSSPM 2-2-80-500 Specification. (2012). Specification for CADPAT™ (TW) [Canadian Disruptive Pattern (Temperate Woodland)]. Department of National Defense Canada. 22 pp.

DSSPM 2-2-80-501 Specification. (2012). Specification for CADPAT™ (AR) [Canadian Disruptive Pattern (Arid)]. Department of National Defense Canada. 12 pp.

DSSPM 2-2-80-502 Specification. 2010. Specification for CADPAT™ (WO) [Canadian Disruptive Pattern (Winter Operations)]. Department of National Defense Canada. 6 pp.

Dunn, D. R. (2008). Ballistics testing of textile materials. In E. Wilusz (Ed.), *Military textiles* (pp. 229–241). Cambridge/Boca Raton, FL: Woodhead/CRC Press LLC.

Eiser, D. N. (1988). *Problems in personal protective equipment selection*. In S. Z. Mansdorf, R. Sager, & A. P. Nielsen (Eds.), *Performance of protective clothing—Second symposium, January 19–21 1987, 1988 Tampa, Fl. 252* (pp. 341–346). Philadelphia, PA: ASTM International.

EN 388 Standard. (2004). Protective gloves against mechanical risks. European Committee for Standardization.

EN 420 Standard. (2003). Protective gloves—General requirements and test methods. European Committee for Standardization. 34 pp.

EN 511 Standard. (2006). Protective gloves against cold. European Committee for Standardization. 32 pp.

EN 1621-1 Standard. (2013). Motorcyclists' protective clothing against mechanical impact. Requirements and test methods for impact protectors. European Committee for Standardization.

EN 1621-2 Standard. (2014). Motorcyclists' protective clothing against mechanical impact. Motorcyclists back protectors. Requirements and test methods. European Committee for Standardization.

EN 13594 Standard. (2015). Protective gloves for motorcycle riders. Requirements and test methods. European Committee for Standardization.

EN 13595-1 Standard. (2003). Protective clothing for professional motorcycle riders. Jackets, trousers and one piece or divided suits. General requirements. European Committee for Standardization.

EN 13595-2 Standard. (2003). Protective clothing for professional motorcycle riders. Jackets, trousers and one piece or divided suits. Test method for determination of impact abrasion resistance. European Committee for Standardization.

EN 13595-3 Standard. (2002). Protective clothing for professional motorcycle riders. Jackets, trousers and one piece or divided suits. Test method for determination of burst strength. European Committee for Standardization.

EN 13595-4 Standard. (2002). Protective clothing for professional motorcycle riders. Jackets, trousers and one piece or divided suits. Test methods for the determination of impact cut resistance. European Committee for Standardization.

EN 13634 Standard. (2016). Protective footwear for motorcycle riders. Requirements and test methods. European Committee for Standardization.

Fatah, A. A., Arcilesi, R. D., Charpentier, L., Lattin, C. H., Mundinger, J., Tassinari, T., et al. (2007). *Guide for the selection of personal protective equipment for emergency first responders: Guide 102-06*. Washington, DC: U.S. Department of Homeland Security.

FBI. (2015). *Law enforcement officers killed and assaulted, 2014*. Retrieved from www.fbi.gov/about-us/cjis/ucr/leoka/2014. U.S. Department of Justice—Federal Bureau of Investigation.

FIA Standard N° 8856-2000. (2012). Protective clothing for automobile drivers. Fédération internationale de l'automobile. 75 pp.

Gauvin, C., Dolez, P. I., Harrabi, L., Boutin, J., Petit, Y., Vu-Khanh, T., et al. (2008). *Mechanical and biomedical approaches for measuring protective glove adherence*. In *52nd annual meeting of the human factors and ergonomics society, September 22–26, 2008, New York* (pp. 2018–2022).

Gauvin, C., Pearsall, D., Damavandi, M., Michaud-Paquette, Y., Farbos, B., & Imbeau, D. (2015). *Risk factors for slip accidents among police officers and school crossing guards—Exploratory study Studies and Research Projects Series/Report R-893*. Montreal, QC: IRSST. 101 pp.

Gauvin, C., Tellier, C., Daigle, R., & Petitjean-Roger, T. (2006). *Evaluation of dexterity tests for gloves*. In *Proceedings of the 3rd European conference on protective clothing and Nokobetef 8, 10–12 May 2006 Gdynia, Poland*. 6 pp.

GCTTG 4006-13 test method. Cote de confort thermique au niveau de pied à sec et humide (Thermal comfort index for the dry and wet foot). CTT Group.

Gomes, C. A. (2008). Designing military uniforms with high-tech materials. In E. Wilusz (Ed.), *Military textiles* (pp. 183–203). Cambridge/Boca Raton, FL: Woodhead/CRC Press LLC.

Haase, Z. S. (2012). *NFPA standards and occupational safety of first responders. An interactive qualifying project report*. Worcester, MA: Worcester Polytechnic Institute. 85 pp.

Harrabi, L., Dolez, P. I., Vu-Khanh, T., Lara, J., Tremblay, G., Nadeau, S., et al. (2008). Characterization of protective gloves stiffness: Development of a multidirectional deformation test method. *Safety Science*, *46*, 1025–1036.

Hearle, J. W. S. (2005). Fibres and fabrics for protective textiles. In R. A. Scott (Ed.), *Textiles for protection* (pp. 117–150). Boca Raton, FL: CRC Press.

Hrynyk, R., & Irzmańska, E. (2013). *Protective footwear—Requirements selection and ergonomy*. OSH Wiki Networking knowledge, European Agency for Safety and Health at Work. Retrieved from oshwiki.eu/wiki/Protective_footwear_%E2%80%93_requirements_selection_and_ergonomy. Accessed 2 January 2016.

Hughes, S. (2006). How to become a Bomb Tech—Working as part of an effective hazardous devices team requires more than donning a bomb suit. *POLICE Magazine*, 2.

Intertek. (2009). *Test methods for determining slip resistance of footwear*. Washington, DC: American Apparel & Footwear Association. 3 pp.

ISO 105-B02 Standard. (2013). Textiles—Tests for colour fastness—Part B02: Colour fastness to artificial light: Xenon arc fading lamp test. International Organization for Standardization. 40 pp.

ISO 105-C06 Standard. 2010. Textiles—Tests for colour fastness—Part C06: Colour fastness to domestic and commercial laundering. International Organization for Standardization. 14 pp.

ISO 105-D01 Standard. 2010. Textiles—Tests for colour fastness—Part D01: Colour fastness to drycleaning using perchloroethylene solvent. International Organization for Standardization. 5 pp.

ISO 105-E04 Standard. (2013). Textiles—Tests for colour fastness—Part E04: Colour fastness to perspiration. International Organization for Standardization. 10 pp.

ISO 105-X11 Standard. 1994. Textiles—Tests for colour fastness—Part X11: Colour fastness to hot pressing. International Organization for Standardization. 3 pp.

ISO 5470-1 Standard. (1999). Rubber- or plastics-coated fabrics—Determination of abrasion resistance—Part 1: Taber abrader. International Organization for Standardization.

ISO 5470-2 Standard. (2003). Rubber- or plastics-coated fabrics—Determination of abrasion resistance—Part 2: Martindale abrader. International Organization for Standardization.

ISO 6529 Standard. (2013). Protective clothing—Protection against chemicals—Determination of resistance of protective clothing materials to permeation by liquids and gases. International Organization for Standardization.

ISO 6530 Standard. (2005). Protective clothing—Protection against liquid chemicals—Test method for resistance of materials to penetration by liquids. International Organization for Standardization. 7 pp.

ISO 6942 Standard. (2002). Protective clothing—Protection against heat and fire—Method of test: Evaluation of materials and material assemblies when exposed to a source of radiant heat. International Organization for Standardization. 11 pp.

ISO 9150 Standard. (1988). Protective clothing—Determination of behaviour of materials on impact of small splashes of molten metal. International Organization for Standardization. 12 pp.
ISO 9151 Standard. (1995). Protective clothing against heat and flame—Determination of heat transmission on exposure to flame. International Organization for Standardization. 9 pp.
ISO 9185 Standard. (2007). Protective clothing—Assessment of resistance of materials to molten metal splash. International Organization for Standardization. 20 pp.
ISO 9920 Standard. (2007). Ergonomics of the thermal environment—Estimation of thermal insulation and water vapour resistance of a clothing ensemble. International Organization for Standardization. 120 pp.
ISO 10819 Standard. (2013). Mechanical vibration and shock—Hand-arm vibration—Measurement and evaluation of the vibration transmissibility of gloves at the palm of the hand. International Organization for Standardization. 36 pp.
ISO 11092 Standard. (2014). Textiles — Physiological effects — Measurement of thermal and water vapour resistance under steady-state conditions (sweating guarded hotplate test). International Organization for Standardization. 22 pp.
ISO 12127-1 Standard. (2015). Clothing for protection against heat and flame—Determination of contact heat transmission through protective clothing or constituent materials—Part 1: Contact heat produced by heating cylinder. International Organization for Standardization. 9 pp.
ISO 12402-7 Standard. (2006). Personal flotation devices—Part 7: Materials and components—Safety requirements and test methods. International Organization for Standardization. 96 pp.
ISO 12947-1 Standard. (1998). Textiles—Determination of the abrasion resistance of fabrics by the Martindale method—Part 1: Martindale abrasion testing apparatus. International Organization for Standardization.
ISO 13287 Standard. (2012). Personal protective equipment—Footwear—Test method for slip resistance. International Organization for Standardization. 20 pp.
ISO 13506 Standard. (2008). Protective clothing against heat and flame—Test method for complete garments—Prediction of burn injury using an instrumented manikin. International Organization for Standardization. 26 pp.
ISO 13937-1 Standard. (2000). Textiles—Tear properties of fabrics—Part 1: Determination of tear force using ballistic pendulum method (Elmendorf). International Organization for Standardization.
ISO 13937-2 Standard. (2000). Textiles—Tear properties of fabrics—Part 2: Determination of tear force of trouser-shaped test specimens (Single tear method). International Organization for Standardization.
ISO 13937-3 Standard. (2000). Textiles—Tear properties of fabrics—Part 3: Determination of tear force of wing-shaped test specimens (Single tear method). International Organization for Standardization.
ISO 13937-4 Standard. (2000). Textiles—Tear properties of fabrics—Part 4: Determination of tear force of tongue-shaped test specimens (Double tear test). International Organization for Standardization.
ISO 13996 Standard. (1999). Protective clothing—Mechanical properties—Determination of resistance to puncture. International Organization for Standardization.
ISO 13997 Standard. (1999). Protective clothing—Mechanical properties—Determination of resistance to cutting by sharp objects. International Organization for Standardization.
ISO 13998 Standard. (2003). Protective clothing—Aprons, trousers and vests protecting against cuts and stabs by hand knives. International Organization for Standardization. 31 pp.

ISO 13999-1 Standard. (1999). Protective clothing—Gloves and arm guards protecting against cuts and stabs by hand knives—Part 1: Chain-mail gloves and arm guards. International Organization for Standardization. 39 pp.

ISO 13999-3 Standard. (2002). Protective clothing—Gloves and arm guards protecting against cuts and stabs by hand knives—Part 3: Impact cut test for fabric, leather and other materials. International Organization for Standardization. 14 pp.

ISO 15831 Standard. (2004). Clothing—Physiological effects—Measurement of thermal insulation by means of a thermal manikin. International Organization for Standardization. 11 pp.

ISO 16602 Standard. (2007). Protective clothing for protection against chemicals—Classification, labelling and performance requirements. International Organization for Standardization. 48 pp.

ISO 17492 Standard. (2003). Clothing for protection against heat and flame — Determination of heat transmission on exposure to both flame and radiant heat. International Organization for Standardization. 26 pp.

ISO 17493 Standard. (2000). Clothing and equipment for protection against heat—Test method for convective heat resistance using a hot air circulating oven. International Organization for Standardization. 13 pp.

ISO 20344 Standard. (2011). Personal protective equipment—Test methods for footwear. International Organization for Standardization.

ISO 20345 Standard. (2011). Personal protective equipment—Safety footwear. International Organization for Standardization.

ISO 20471 Standard. (2013). High visibility clothing — Test methods and requirements. International Organization for Standardization. 34 pp.

ISO 20743 Standard. (2013). Textiles—Determination of antibacterial activity of textile products. International Organization for Standardization. 32 pp.

ISO/DIS 18640-1 Standard. (2016). Protective clothing for fire-fighters- physiological impact—Part 1: Measurement of coupled heat and mass transfer with the sweating TORSO. International Organization for Standardization. 32 pp.

ISO/DIS 18640-2 Standard. (2016). Protective clothing for fire-fighters- physiological impact—Part 2: Determination of physiological heat load caused by protective clothing worn by firefighters. International Organization for Standardization. 24 pp.

Kawabata, S. (1980). *The standardization and analysis of hand evaluation* (2nd ed.). Osaka, Japan: The Textile Machinery Society of Japan. pp. 7–28.

Kilinc-Balci, F. S., & Elmogahzy, Y. (2008). Testing and analyzing comfort properties of textile materials for the military. In E. Wilusz (Ed.), *Military textiles* (pp. 107–136). Cambridge/Boca Raton, FL: Woodhead/CRC Press LLC.

Kuhl, K., & Brück, C. (2014). *Hierarchy of prevention and control measures*. OSH Wiki Networking knowledge, European Agency for Safety and Health at Work. Retrieved from oshwiki.eu/wiki/Hierarchy_of_prevention_and_control_measures#cite_note-Boyle-2 [Accessed 1 January 2016].

Mäkinen, H. (2006). *Protective clothing—Nowadays and vision*. In *Proceedings of the 3rd European conference on protective clothing and Nokobetef 8, 10-12 May 2006 Gdynia, Poland*. 3 pp.

Man, V. L., Bastecki, V., Vandal, G., & Bentz, A. P. (1987). Permeation of protective clothing materials: Comparison of liquid contact, liquid splashes and vapors on breakthrough times. *American Industrial Hygiene Association Journal*, *48*, 551–555.

Mayer, A., & Grabowsky, C. (2007). *Les vêtements de protection: Choix et utilisation*. Paris, France: Institut National de Recherche et de Sécurité. 36 pp.

Mellstrom, G. A., & Boman, A. S. (2005). Gloves: Types, materials and manufacturing. In A. S. Boman, T. Estlander, J. E. Wahlberg, & H. I. Maibach (Eds.), *Protective gloves for occupational use* (2nd ed., pp. 15–28). Boca Raton, London, New York, Washington DC: CRC Press.

Minoyama, O., & Tsuchida, H. (2004). Injuries in professional motor car racing drivers at a racing circuit between 1996 and 2000. *British Journal of Sports Medicine*, *38*, 613–616.

NFPA 70E Standard. (2012). Standard for electrical safety in the workplace. National Fire Protection Association. 225 pp.

NFPA 921 Standard. (2011). Guide for fire and explosion investigations. National Fire Protection Association.

NFPA 1971 Standard. (2013). *Standard on protective ensembles for structural fire fighting and proximity fire fighting*. National Fire Protection Association. 151 pp.

NFPA 1994 Standard. (2012). *Standard on protective ensembles for first responders to CBRN terrorism incidents*. National Fire Protection Association. 63 pp.

NFPA 2112 Standard. (2012). *Standard on flame-resistant garments for protection of industrial personnel against flash fire*. National Fire Protection Association. 29 pp.

Nguyen, C. T., Dolez, P. I., Vu-Khanh, T., Gauvin, C., & Lara, J. (2010). Resistance of protective gloves materials to puncture by medical needles. *Journal of ASTM International*, *7*(5). 16 pp.

Nguyen, C. T., Dolez, P. I., Vu-Khanh, T., Gauvin, C., & Lara, J. (2013). Effect of protective glove use conditions on their resistance to needle puncture. *Plastics, Rubber and Composites: Macromolecular Engineering*, *42*(5), 187–193.

Nguyen, C. T., Vu-Khanh, T., & Lara, J. (2005). A study on the puncture resistance of rubber materials used in protective clothing. *Journal of ASTM International*, *2*, 245–258.

NIJ 0101.06 Standard. (2008). *Ballistic resistance of body armor*. U.S. Department of Justice, Office of Justice Programs, National Institute of Justice. 89 pp.

NIJ 0115.00 Standard. (2000). *Stab resistance of personal body armor*. U.S. Department of Justice, Office of Justice Programs, National Institute of Justice. 46 pp.

NIJ 0117.00 Standard. (2012). *Public safety bomb suit standard*. U.S. Department of Justice, Office of Justice Programs, National Institute of Justice. 87 pp.

OSHA. (1998). *Fall protection for the construction industry*. Part 1926 Subpart M CFR 1926.500 Washington, DC: Occupational Safety & Health Administration, U.S. Department of Labor.

OSHA. (2005). *Worker safety series—Construction*. Washington, DC: Occupational Safety & Health Administration, US Department of Labor. 12p.

Pan, N. (2008). Sweat management for military applications. In E. Wilusz (Ed.), *Military textiles* (pp. 137–157). Cambridge/Boca Raton, FL: Woodhead/CRC Press LLC.

Potkanowicz, E. S., & Mendel, R. W. (2013). The case for driver science in motorsport: A review and recommendations. *Sports Medicine*, *43*(7), 565–574.

Potluri, P., & Needham, P. (2005). Technical textiles for protection. In R. A. Scott (Ed.), *Textiles for protection* (pp. 151–175). Boca Raton, FL: CRC Press.

Rebouillat, S., & Steffenino, B. (2005). Cut performance fundamentals and norms harmonization. *Journal of ASTM International*, *2*, 139–159.

Rezazadeh, M., & Torvi, D. A. (2012). Non-destructive test methods to assess the level of damage to firefighters' protective clothing. In A. M. Shepherd (Ed.), Vol. 9. *Performance of protective clothing and equipment: Emerging issues and technologies* (pp. 202–226). West Conshohocken, PA: ASTM International.

Sadier, I., & Izquierdo, V. (2015). Textile flammability tests. *The Textile Journal*, *132*(2), 30–37.

Shaw, A. (2005). Steps in the selection of protective clothing materials. In R. A. Scott (Ed.), *Textiles for protection* (pp. 90–116). Boca Raton, FL: CRC Press.

Siegel, J. D., Rhinehart, E., Jackson, M., & Chiarello, L. (2007). 2007 guideline for isolation precautions: Preventing transmission of infectious agents in health care settings. *American Journal of Infection Control*, *35*(10—Suppl. 2), S65–S164.

Slater, K. (1996). Comfort or protection: The clothing dilemma. In J. S. Johnson & S. Z. Mansdorf (Eds.), *Performance of protective clothing*: Vol. 5. (pp. 486–497). West Conshohocken, PA: American Society for Testing and Materials.

Stull, J. O. (2005). Civilian protection and protection of industrial workers from chemicals. In R. A. Scott (Ed.), *Textiles for protection* (pp. 295–354). Boca Raton, FL: CRC Press.

Stull, J. O. (2006). *A perspective on realistic material chemical performance requirements: The need to redefine how industry chooses chemical protective suit materials*. In *Proceedings of the 3rd European conference on protective clothing and Nokobetef 8 [CD-ROM]; 2006 May 10–12, Gdynia, Poland*. 6 pp.

Tatiya, R. R. (2010). *Elements of industrial hazards: Health, safety, environment and loss prevention*. Boca Raton, FL: CRC Press.

Thwaites, C. (2008). Cold weather clothing. In E. Wilusz (Ed.), *Military textiles* (pp. 158–182). Cambridge/Boca Raton, FL: Woodhead/CRC Press LLC.

Truong, Q., & Wilusz, E. (2008). Chemical and biological protection. In E. Wilusz (Ed.), *Military textiles* (pp. 242–280). Cambridge/Boca Raton, FL: Woodhead/CRC Press LLC.

US DoD. (2005). *Dictionary of military and associated terms*. US Department of Defense. Retrieved from www.thefreedictionary.com [Accessed 31 December 2015].

Vidito, A. (2014). *Clothing flotation standards in Canada*. In *113th scientific session of the institute of textile science, Montreal, Quebec, Canada, October 7th, 2014*.

Vinches, L., Testori, N., Dolez, P., Perron, G., Wilkinson, K. J., & Hallé, S. (2013). Experimental evaluation of the penetration of TiO2 nanoparticles through protective clothing and gloves under conditions simulating occupational use. *Nanoscience Methods*, *2*(1), 1–15.

Winterhalter, C. (2008). Military fabrics from flame protection. In E. Wilusz (Ed.), *Military textiles* (pp. 326–345). Cambridge/Boca Raton, FL: Woodhead/CRC Press LLC.

Young, C. C. (2002). Extreme sports: Injuries and medical coverage. *Current Sports Medicine Reports*, *1*, 306–311.

This page intentionally left blank

Specific testing for smart textiles

12

J. Decaens, O. Vermeersch
CTT Group, Saint-Hyacinthe, QC, Canada

12.1 Introduction

12.1.1 Markets and applications

Since their emergence, the smart textile technologies have received increasing attention from researchers all around the world as well as support and enthusiasm from users waiting to see and try the latest innovation. Even if, over the last decade, textiles have suffered from delocalization of the production and other economic restrictions, smart textiles have been able to show the customers high value products that have changed the perception people have of the textile industry.

Nowadays, the main sector of smart textiles that has resulted into commercial products has been directly related to wearable electronics and monitoring sensors for healthcare and sports performance (Dalsgaard & Sterrett, 2014). Despite an aging population, people want to stay active and mobile without being stereotyped as elderly due to the use of medical devices required for monitoring their health. These bulky devices have now been replaced by similar products, made entirely of textiles and which are directly integrated into clothing for an aesthetic and discreet look.

Similarly, in sports and leisure activities, sensors can provide feedback on the heartbeat and breathing rate or even muscle activities, which is vital information to optimize training (McGrath & Ní Scanaill, 2013).

Smart textiles are also widely used in the protection market, where the need for performance is often as important as the need for comfort (Tang & Po, 2007). By integrating heating or thermoregulating materials within the worker's uniform, it is already possible to reduce their bulkiness while improving the overall comfort (Scott, 2005).

More generally, smart textiles find applications in a large variety of sectors such as transport, home textiles, construction, and fashion. With expansive research directed towards new topics such as energy harvesting textiles, it is expected for the smart textiles market to continue thriving over the coming years.

12.1.2 Recent evolution of smart textiles

Several generations of smart textiles have succeeded one another over the years (Van Langenhove & Hertleer, 2004). Each new generation offers a higher level of integration. At first, the functional element was simply added at the last step of the assembly, i.e., after finishing. Even though it was easier to manufacture, the level of integration was poor and the wearer's comfort was low. The second generation of smart textiles has shown improvement by working directly at the level of the textile structure:

Advanced Characterization and Testing of Textiles. https://doi.org/10.1016/B978-0-08-100453-1.00013-1

knitted, woven, etc. Finally the upcoming generation might be able to provide functionality through innovative fibers and yarns.

In 2011, the European Committee CEN TC 248 WG 38 gave the following definition of a smart textile material: "Functional textile material, which interacts actively with its environment, i.e., it responds or adapts to changes in the environment (CENTEXBEL, 2017)." However, it appeared that the social or common definition of a smart textile was much broader and required the creation of subcategories: passive smart textiles, active smart textiles and ultrasmart textiles (Singh, 2004).

Passive smart textiles can only sense their environment but are not able to interact in any way with it (Singh, 2004). An example of passive smart textiles is conductive fabrics or optical fiber embedded fabric. Their properties are constant in time and do not vary according to their surroundings. Active smart textiles, on the other hand, have the faculty to act both as a sensor and an actuator. Some examples are phase change materials (PCMs), shape memory polymers, electrically heated clothing, etc. Stimuli from their environment can be used to create a change in their properties.

The last category is directly in line with the definition given by the European Committee because ultra-smart textiles can sense, react, and adapt to their environment. They rely on the integration of electronic devices within the textile so they are able to detect stimuli, analyze them, and modify their structure to adapt to the stimuli. Musical jackets, intended for deaf people, which are able to vibrate and light up according to the music being played in real time, are an example of such ultrasmart systems.

In parallel, a particular attention has been brought onto the durability of the products in order to commercialize them. Not only must the performance be obtained, but it must also be maintained through use and cleaning to ensure the product has a decent lifetime.

12.1.3 Challenges and needs for new standards

These new concerns have raised the question of testing smart materials and developing evaluation methods. Due to the reactivity of smart textiles towards their environment and the perception of external stimuli, existing standard test methods may not be applicable. Any change in mechanical stress, light, humidity, or temperature can trigger the functionality within the textile and change radically the results of the measured parameter. Therefore, the need to develop new methods becomes inevitable. Several aspects of smart textiles must be addressed (Hertleer & Van Langenhove, 2015):

- Characterizing the properties
- Evaluating the performance
- Assessing the durability

In order to do so, it is necessary to first identify and categorize the different types of smart textiles since they will not all have the same working principle neither the same requirements in terms of measured parameters.

12.1.4 Initiatives around the world

The current lack of objective test methods impedes the commercialization process for new smart textiles. Due to the importance of the matter, several research groups

and normalization organizations have launched projects in order to develop new standards. Among them, SUSTASMART (Supporting Standardization for Smart Textiles), a European research consortium including several international partners, has been working on this problem for over 2 years (CEN, 2011). The project ended in March 2014. In North America, the ASTM (American Society for Testing and Materials) holds special workshops to try and gather ideas and information from textile specialists (AATCC, 2016).

Even though an important step has already been accomplished, there is still a lot of work ahead. Every research center that has been working with smart textiles and has developed its own internal test methods must now come together in order to have some test methods officially recognized and approved by standards organizations.

12.2 Testing conductive textile materials

12.2.1 Introduction

Conductive materials are commonly used for smart textile applications since they have the capacity to act both as power transmission media and sensors. The electrical resistance is one the most important characteristics when it comes to conductive materials and the level of requirement varies according to the intended application.

Though the measurement of accurate electrical resistance on solid metals does not present any difficulties, the case of conductive fibers, yarns, or fabrics is more complex. The questions of repeatability of the measurements, number of specimens, values of the mechanical tension applied on the specimens, etc. have been studied by research groups worldwide (Šafářová & Grégr, 2010).

Indeed, most conductive fibers or yarns are produced by applying conductive materials such as silver, copper, polyaniline, or other conductive polymers on polymer fibers and yarns by surface coating or electroplating techniques. Because of the irregularity of the fiber and yarn surface, the process may not lead to fully homogeneous coating, and therefore, the resistivity of the yarns will depend on the location of the measurement contacts (Bashir et al., 2012). The same principle applies also to filaments and yarns containing conductive particles such as carbon. The random dispersion of these particles in the polymeric matrix and the possible formation of clusters can also create variations in the electrical resistance of the yarns (Smith, 2010).

Despite these obstacles, significant advances have been made during the last few years. Some existing standards such as ASTM D4496 (2013) or AATCC TM76 (2011) have been demonstrated to be applicable to measure the surface resistivity of fabrics. In parallel, the European research group Sustasmart has drafted a new standard proposal for measuring the electrical resistivity of yarns, which has been submitted to CEN (European Committee for standardization) and is pending approval (BS-EN-16812, 2016).

12.2.2 Electrical characteristics

Several parameters can be used to characterize the conductivity of materials:

- The electrical resistivity (ρ) only depends on the nature of the material and is constant regardless of its dimensions. It is often expressed in Ohms/m since the diameter of the yarn or cable is so small compared to its length that it becomes not significant. For fabrics, surface resistivity in Ohms/m^2 can be used.
- The electrical resistance (R) depends on the dimensions of the product (length (L), diameter (A)) and is expressed in Ohms. It is possible to compute the electrical resistance of a piece of material by using the following equation:

$$R = \rho * \left(L / A\right) \tag{12.1}$$

  The equation demonstrates the existing relationship between the length of the cable and its electrical resistance. The longer the cable will be, the more the electrical resistance will increase. Contrarily, the larger the diameter of the cable will be, the more the electrical resistance will decrease, since the current will be able to pass more easily.
- Conductance (G) and conductivity (γ) are respectively the inverse of the resistance and the resistivity and are expressed in Siemens and Siemens/m.

Moreover, these parameters can be affected by external factors such as the temperature, compression, stretching, humidity, etc. In some cases, the effect of the environmental parameters on the electrical resistance is documented and can be computed. For example, the resistance will increase as the ambient temperature T decreases according to the following formula (Larrimore, 2005):

$$\rho_T = \rho_0 \left(1 + \alpha \left(T - T_0\right)\right) \tag{12.2}$$

where ρ_T is the resistance at the chosen temperature and ρ_0 is the resistance at 25°C (at T_0).

The general trend for the effect of mechanical compression and stretching on conductive materials is also known: compression increases the contact between the conductive fibers and therefore decreases the resistance, whereas stretching increases it (Ding, Wang, & Wang, 2007). However, there is no mathematical relationship that describes the effect of mechanical compression and stretching on conductive material electrical characteristics since the hardness, elasticity, and other physical characteristics of the material will influence the result.

12.2.3 Measurement of the linear resistivity

The CEN committee TC 248/WG 31 on smart textiles standardization has been working on developing a testing method for measuring the linear resistivity of fibers, yarns, ribbons, and other materials for which the width of the conductive tracks is not significant compared to its length, i.e., $<10^{-1}$ (BS-EN-16812, 2016).

It is important to note that the width of the conductive track does not always correspond to the diameter of the conductive yarns. In the case of a knitted fabric for example, the width will be the loop height, whereas its length will correspond to its course, as illustrated in Fig. 12.1.

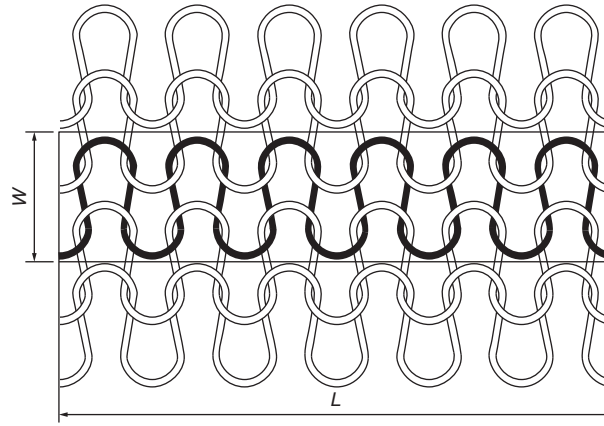

Fig. 12.1 Schematic representation of the width and length of the conductive track of a knitted fabric.
Reproduced with permission from CEN EN 16812.

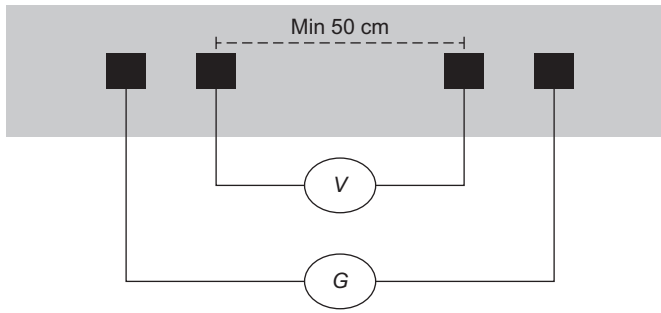

Fig. 12.2 Schematic representation of the test method set-up for measuring linear electrical resistance of conductive tracks.
Adapted from BS-EN-16812. (2016), Determination of the linear electrical resistance of conductive tracks. Brussels: CEN—European Committee for Standardization.

The test method uses four electrodes, connected to the conductive track and aligned over its width. The two inner electrodes are connected to a voltmeter, while the two outer electrodes are connected to a power source. The set-up is represented on Fig. 12.2, where *G* stands for power source and *V* stands for voltmeter.

The resistance (*R*) of the conductive material can then be calculated using the value of current (*I*) supplied by the power source and the voltage (*V*):

$$R = V / I$$

The electrodes must have a flat surface and provide a good contact with the conductive media. To improve this contact and depending on the nature of the conductive tracks, it may be possible to glue them with some conductive epoxy or solder them. In the case of conductive yarns, crimp connectors can also be used as electrodes.

Table 12.1 Values of stress to be applied on the yarn or fabric for the measurement of linear resistivity

Nature	Weight (g/m^2)	Stress applied
Yarns	–	0.5 cN/tex
Not stretchable fabrics	<200	2 N
	200–500	5 N
	>500	10 N
Stretchable fabrics	–	0.5 N

The distance between the voltage electrodes should be at least 10 times the width of the conductive track or a minimum of 50 cm (Fig. 12.2).

A controlled value of stress is applied to the textile before the test. That value depends on the type and weight of the textile (Table 12.1).

The test method requires measuring at least five specimens. For each specimen, two series of five voltage measurements are done. Between the two series, the specimen should be relaxed and then retensioned.

12.2.4 Measurement of the surface resistance

Standardized test methods already exist for the measurement of the DC surface resistance of conductive materials. For instance, ASTM D4496 (2013) describes a testing protocol similar to the four points method used for the measurement of the linear resistivity (Section 12.2.3). The main difference consists in the weight and stress applied to the fabric as well as the position of the electrodes. For the measurement of the surface resistance, instead of having the four electrodes positioned on the same face of the conductive track, they are located on both sides of the fabric, as shown in Fig. 12.3.

Insulating materials can be added between the electrodes to support the fabric specimen and avoid the formation of a concave shape. A first weight is added above the current electrodes. It shall be 300 N/m times the width of the specimen in meter. The second weight over the potential electrodes is 60 N/m times the specimen width. The distance between the potential electrodes shall be superior to 10 mm, and they should be distant from the current electrodes by at least 20 mm.

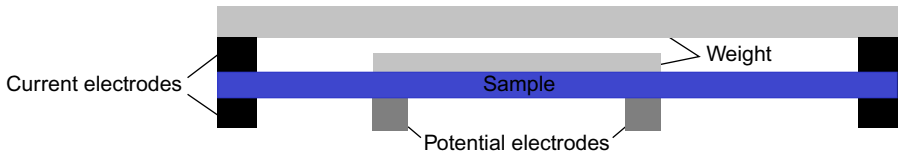

Fig. 12.3 Schematic representation of the electrode position for the measurement of the surface resistance of fabrics.
Adapted from ASTM D4496. (2013). Standard test method for D-C resistance or conductance of moderately conductive materials (5 pp.). West Conshohocken, PA: ASTM InternationalUSA.

The standard AATCC TM76 (2011) proposes a simplified method where the specimens are placed in contact with only two parallel plate or concentric ring electrodes that are distant by 25 mm. The electrodes are connected to an ohmmeter and a power source that is set to deliver 80 V for 1 min or as long as needed to reach a stable value. Two sets of three specimens are to be tested according this method. It is expected that each set will have a different orientation in terms of width and length. All specimens must be conditioned prior to testing; however, the values of temperature and humidity selected may depend on the intended application of the product.

12.2.5 Dynamic measurements

Most of the standards previously described impose controlled testing conditions so that a reference value of the electrical resistance can be accessed. However, electrical resistance depends on a number of environmental factors such as temperature, humidity, and mechanical stress. For instance, the electrical resistance may vary when the fabric is stretched, compressed, or abraded. In addition, that variation may not be the same if the fabric is a knitted or a woven structure.

Therefore, CTT Group has developed specific test methods to evaluate the change in electrical resistance when a mechanical action is applied on the conductive textile. For example, a setup allows evaluating the impact of abrasion on the electrical resistance of narrow woven fabrics comprising conductive yarns (CTT Group, 2011) (Fig. 12.4). It includes an electronic system to record the value of the electrical resistance every 20 abrasion cycles.

Data gathered from this test help determine the behavior and durability of the smart textile over time and under accelerated use conditions. Moreover, the conductive yarns can also be used as aging indicators to monitor the structural integrity of the fabric.

A system has also been developed to investigate the variation in electrical performance of smart fabrics subjected to tensile stress (CTT Group, 2010). As illustrated in Fig. 12.5, the conductive knitted fabric is held between the two clamps of a dynamometer while the resistance measurement is performed.

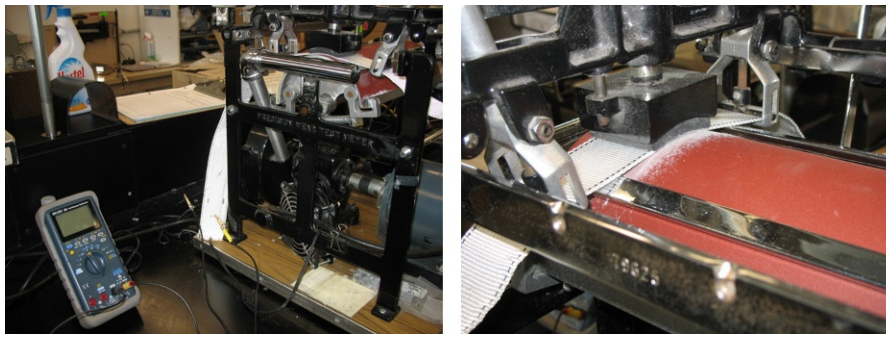

Fig. 12.4 Pictures of the recording device (left) and mechanical abrasion system (right) developed to evaluate the impact of abrasion on the electrical resistance of narrow woven fabrics comprising conductive yarns.

Fig. 12.5 Measurement of the electrical resistance of a conductive fabric under tensile stress.

12.3 Testing smart thermoregulating textiles

12.3.1 Introduction

The human body is designed in a way that allows it to regulate its internal temperature within a certain range, typically from 36°C to 38°C. In order to do so, several possible heat exchange mechanisms may take place (Arens & Zhang, 2006):

- Heat conduction happens through contact between the skin and another surface. If the surface is cooler than the skin, the body will evacuate heat, whereas if it is hotter, the heat will warm up the body.
- Thermal convection depends on the air flow around the body
- Heat radiation comes from infrared rays that reverberate on walls. The warm feeling of the sun behind a glass is an example of heat radiation.
- Sweat evaporation and breathing are other forms of heat transfer that are based on moisture transfer unlike the three others, which are dry exchanges.

However, in extreme climatic conditions such as arctic regions or deserts, the human body faces limitations and cannot provide enough heat or active cooling to keep his core temperature within an acceptable range. Therefore, clothing must act as a protective barrier between the body and his environment.

Thanks to emerging innovative textiles, it is now possible to integrate active functions within the fabric to compensate for the impact of the weather conditions. Several heating garments such as heated gloves, jackets, boots, etc. are already on the market (Wang et al., 2010). Cooling garments are more complex to produce and are still at an early stage of development despite some commercial examples. Developing thermoregulating materials that can provide independently both heat and cooling effects is a challenge that PCMs have not fully overcome yet (Mondal, 2008).

12.3.2 Conductive heating garments

Conductive heating garments come in various forms: nonwovens, knits, wovens, embroideries, etc. They all use the same principle to dissipate heat when they are powered: the Joule effect.

In order to measure how much heat is generated by the heating garment, thermocouples have been used to give a general idea of the textile temperature. However, results are generally not very precise/reproducible. Indeed, if the conductive element is dispersed randomly or inserted according a predetermined pattern, the choice of the position of the thermocouple on the heated surface will greatly impact the result obtained.

To measure a surface temperature rather than a point temperature, thermal infrared cameras are very useful and provide reliable data, generally within ±1.5°C, depending on the accuracy of the emissivity value used. A visual color gradation may be used to reveal the presence of hot points or colder areas as shown in Fig. 12.6.

In order to fully appreciate the color gradation along with the increase in dissipated heat, the range end points must be determined first. The distance between the heating textile and the camera may also have an impact on the results and should always be the same for comparative studies (Michalak, Felczak, & Więcek, 2009; Banaszczyka, Anca, & De Mey, 2009).

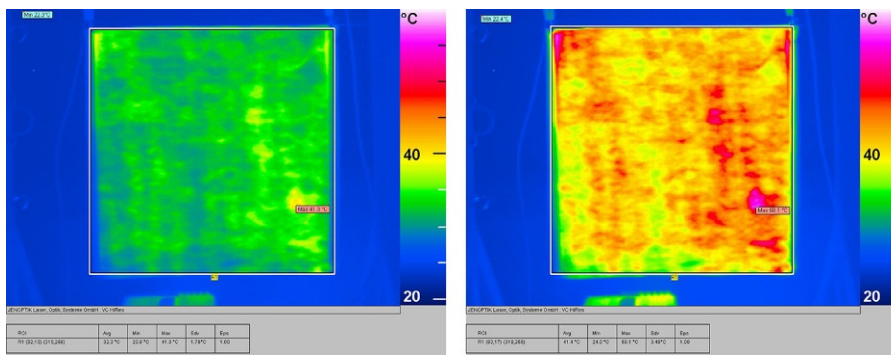

Fig. 12.6 Thermal infrared imaging of heating nonwovens at 35°C (left) and 45°C (right).

Knowing the average surface temperature of a heating element is essential but it is not sufficient to predict the behavior of the heating product while in use in a cold environment. Indeed, the time during which the heating garment will be able to provide heat is another critical element. In particular, low temperatures have a direct impact on the electrical resistance of conductive textiles, which will decrease and therefore require more power to maintain the same level of heating. It is possible to predict the electrical resistance of a heating textile at different temperatures if some characteristics of the conductive element are known (Larrimore, 2005):

$$\rho_T = \rho_0 \left(1 + \alpha \left(T - T_0\right)\right) \tag{12.3}$$

Here, ρ_T and ρ_0 are respectively the resistance at temperature T and T_0. ρ_0 is measured at ambient temperature (T_0). α is a constant that depends on the nature and composition of the materials and refers to the temperature coefficient of the metallic element.

Using an empirical method is another alternative that proved to be sometimes more accurate than the theoretical model since it is closer to the real situation. For instance, heating garments are placed into a climatic chamber while powered, and their resistance is measured over a large range of temperatures.

Once the values of resistance and voltage (fixed) are known, the current can be computed. By dividing the energy contained in the battery (J) used to power the garment by the current (A), the time during which the heating garment will be operating can be calculated.

12.3.3 Cooling garments

Cooling garments are more complex and usually present a level of integration lower than the conductive heating textile. This is mainly due to the fact that current cooling garments are based on water or air circulating within small tubes inserted between two textile layers (Kim et al., 2011).

Currently there are only two existing standardized test methods that allow evaluating the performance of personal cooling system (PCS): ASTM F2371 (2011) and ASTM F2300 (2016). They both offer very different approaches: ASTM F2371 relies on the objective measurements performed on a thermal manikin, whereas ASTM F2300 monitors the physiological parameters of a panel of human subjects.

The standard test method ASTM F2371 (2011) evaluates two main aspects: heat removal rate and the duration of the cooling effect. The heated manikin used for this test shall be equipped with the sweating skin system since the cooling resulting from sweat evaporation represents a large fraction of the heat dissipation and must therefore be taken into account. The conditions specified for the test include an ambient temperature of 35°C with a relative humidity of 40% and an air velocity of 0.4 m/s.

A baseline test shall be conducted to isolate the effect of cooling only. If the PCS is active, the baseline test is conducted while the system is turned off. If the PCS is passive and cannot be turned off such as in the case of ice or gel vests, the garment is

placed into the climatic chamber for 12 h prior to the test in order to attain equilibrium between the PCS and the climatic conditions.

The manikin is dressed with clothes that are intended to be used with the PCS so the output is relevant to the real operating conditions.

The power input needed for the manikin to maintain a skin temperature of 35°C is recorded. An average of measurements carried out once steady-state conditions are reached is calculated and serves as reference for the PCS performance test.

The procedure is similar for the test. However, the PCS is turned on for that step. The manikin's skin temperature, the air temperature, and the power input to the manikin are recorded continuously for 2 h or until the difference between the power input during the test and that corresponding to the baseline test has reached 50 W. It is expected that the power input to the manikin with the PCS turned on is greater than for the baseline test since the PCS should attempt to decrease the skin temperature: Additional heat is thus required to maintain the manikin temperature at 35°C.

Even though only one sample of the PCS is used to conduct the test, the measurement shall be replicated three times to take into account variations in dressing and instrumentations.

The heat removal rate is calculated by dividing the average power input (PCS test minus baseline test) by the cooling duration which is the time it took to reach a difference of 50 W.

The standard ASTM F2300 (2016) may be an interesting alternative if no thermal manikin is available. However, it requires more logistics and time and is more costly as it involves human subjects. In addition, less flexibility is allowed for the under and outer garments worn by the subjects during the test than in the method ASTM F2371. At least five human subjects are required to evaluate the performance of one PCS. Physiological parameters include esophageal, rectal, and skin temperature as well as heart rate and body sweat rate. A treadmill is used to help participants generate a sufficient metabolic energy expenditure that will translate in a temperature rise. The duration of the cooling can be deduced from the time needed for the core temperature to reach 39°C or for the skin temperature to reach 38°C. If none of these two happens within 2 h, the test is stopped.

The test method described by ASTM F2300 provides more details than in ASTM F2371, but is also more complex to interpret and relate directly to the PCS performance. Moreover, it involves much more subjectivity than with the use of an instrumented manikin.

12.3.4 The specific case of PCMs

PCMs have the unique feature of being able to either provide heat or cool down (Mondal, 2008). They are, however, restricted in terms of the duration of this effect. Indeed, they are active only while they are at the transition between the liquid and solid phases (from liquid to solid for a heating effect or the opposite for a cooling effect). In order to evaluate the performance of PCM-based textiles, several methods can be used. The most common is the differential scanning calorimeter (DSC), which is used to measure the phase transition range as well as the enthalpy of both the melting

and the crystallizing process. However, this method is limited by the fact that it does not take into account the thermal barrier effect of the PCM (Sharma et al., 2009).

In 2002, Hittle & Andre developed a test method that was standardized in 2004 as ASTM D7024 (withdrawn, 2013). It is based on the use of an index called the temperature regulating factor (TRF), which is computed using the following equation (ASTM D7024, 2013):

$$\mathrm{TRF} = \frac{\left(T_{\max} - T_{\min}\right)}{\left(Q_{\max} - Q_{\min}\right)} \times \frac{1}{R}$$

where the amplitude of the temperature variation ($T_{\max} - T_{\min}$) is divided by the heat flux variation ($Q_{\max} - Q_{\min}$) and the thermal resistance of the fabric tested. The TRF is a dimensionless number lower or equal to 1.

A specimen of the tested fabric is placed between a hot plate and two cold plates, one on each side of the hot plate/fabric system (Fig. 12.7). The cold plates are maintained at 20°C, whereas the hot plate is subjected to a sinusoidal flux. The midpoint of the sinusoidal flux is 150 W/m^2 and its amplitude is 100 W/m^2 above and below the midpoint. The thermal resistance value is measured under steady-state conditions when the hot plate is submitted to a constant heat flux of 250 W/m^2.

Hittle and Andre have pursued their work in order to take into account other parameters than the latent heat: diameter of the PCMs, amount of PCMs in the fabric, method of incorporation of the PCMs, etc. Another test apparatus has been developed for this purpose and is called the fabric intelligent hand tester (FIHT) (Ying et al., 2004). It is composed of a bottom measuring plate and an upper measuring head which integrates temperature, pressure friction, displacement, and heat flux sensors.

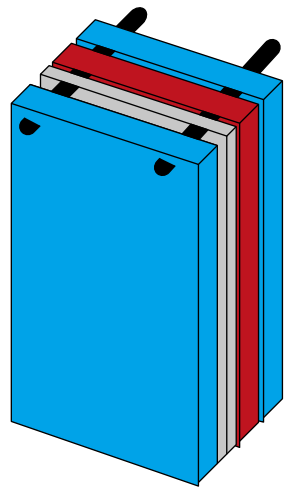

Fig. 12.7 Schematic illustration of the TRF test apparatus with the cold plates in *blue*, the hot plate in *red*, and the test specimen in *gray*.

Several indexes may be calculated using the data collected in order to analyze the performance of the PCMs in a broader way: static thermal insulation (I_s), phase change duration time (Δt_d), PCM heat flux during the phase change period (I_d), and thermal psychosensory intensity (TPI).

More recently, studies have turned towards the guarded hot plate system (ISO 11092, 1993), which is commonly used to determine the static thermal resistance of fabrics, to evaluate the PCM impact on the heat flux variation (Wan & Fan, 2009; Bendkowska & Wrzosek, 2009). In particular, the use of already existing standardized methods is beneficial since they allow comparing passive and active materials.

12.4 Testing ECG, EMG, EEG, and other embedded textile sensors

12.4.1 Introduction

Over the past few years, the healthcare market has invested more than 3 billion dollars in textile materials and research (Dalsgaard & Sterrett, 2014). The medical sector is constantly looking for new technologies that will facilitate the continuous monitoring of patients at risk while not impeding their lifestyle. Smart clothing offer the advantage of direct and permanent contact with the body, allowing access to bioparameters such as ECG (electrocardiogram), EMG (electromyogram), EEG (electroencephalogram), breathing rate and others.

Driven by the need for such products, several companies have developed shirts, chest-belts, and bras that integrate electrodes capable of detected biosignals and transferring them to a data acquisition module. Companies such as Ambiotex, OM Signal, Under Armour, etc., have already made commercial products available on the market. Among them, Zoll Life Vest went even further by embedding not only electrodes but also a defibrillator in a garment (Francis & Reek, 2014). It is programmed to trigger an electric discharge in case of a heart failure.

This last example demonstrates the need to ensure high reliability, accuracy, and robustness of biomonitoring clothing. Due to the high demand context of the application, the tolerance for false signal, lack of thereof, or even drifting is very low. Therefore, biomonitoring garments shall be carefully tested before their market entry as well as on a regular basis during service.

12.4.2 Evaluation of electrode adhesion

ECG measurements are based on the detection of the depolarization of the ventricle when it contracts. The electrical pulse that accompanies the depolarization is channeled through the electrodes to create the signal (Becker, 2006).

In order to reduce the skin-electrode impedance and avoid motion-induced artefacts, the electrodes must perfectly adhere to the skin. Traditional electrodes use adhesive conductive gel to improve the contact at the interface. However, if they are worn during extended periods of time, these electrodes may create skin irritation

(Merritt, 2008). The adhesion strength of this type of electrodes is measured with a standard peel test.

Textile electrodes do not comprise any form of adhesive layer since, thanks to its compressive properties, the base fabric induce the contact with the skin. In this context, peel tests are not relevant.

The measurement of the coefficient of friction of the electrode can, however, help determining its surface properties and identifying if the electrode would tend to slide. The traditional friction test is generally based on the use of a sled over which is positioned the tested material, and which slides over a substrate. The coefficient of friction μ is given by the following equation (Blau, 2001):

$$\mu = f / N \tag{12.4}$$

where f represents the friction force and N is the normal force exerted by the sled. Therefore, the tightness of the shirt around the chest can be taken into account and described through the value of N. Ideally, a material having surface properties similar to skin should be chosen as the substrate on which the sled bearing the electrodes will be slid to determine the coefficient of friction.

Two parameters must be considered: the static coefficient of friction and the dynamic coefficient of friction. The static friction coefficient corresponds to the force necessary to initiate a motion of the upper material (i.e., the electrodes) against the substrate (i.e., the skin analog). The dynamic coefficient of friction is given by the force required to maintain the motion (De Luca et al., 2004).

The standard test method ASTM D1894 (2014) for plastic films and sheeting is commonly used in the textile industry and recommends a displacement speed of 150 ± 30 mm/min. The weight applied on the sled should correspond to the level of compression of the garment over the body.

12.4.3 Measurement of the electrical impedance

The electrical impedance between the skin and the electrode is one of the most determining factors of the signal quality. Indeed, a high value of impedance will induce a small signal/noise ratio and require that the signal is strongly amplified and filtered before being usable.

An equivalent electrical circuit can be established for the skin-electrode impedance. For instance, Swanson and Webster have proposed a model that consists of a resistor (R_e) in parallel with a capacitor (C_e), associated with a second resistor (R_s) in series, as shown in Fig. 12.8 (Assambo et al., 2007; Taji et al., 2014). The skin-electrode impedance can be deduced from measurements of the electrical characteristics of the electrodes and the skin.

Despite the fact that this method is easy to implement, it does not provide very accurate values of the skin-electrode impedance. Indeed, the effect of the body fluid motion and skin surface humidity has to be taken into consideration. To do so, Priniotakis et al. (2007) have used electrochemical impedance spectroscopy to develop an electrochemical cell (Fig. 12.9) with the objective of replicating the contact of the electrodes against the body with the influence of its fluids.

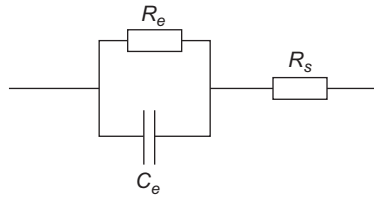

Fig. 12.8 Swanson and Webster single-time constant model for the skin-electrode impedance.

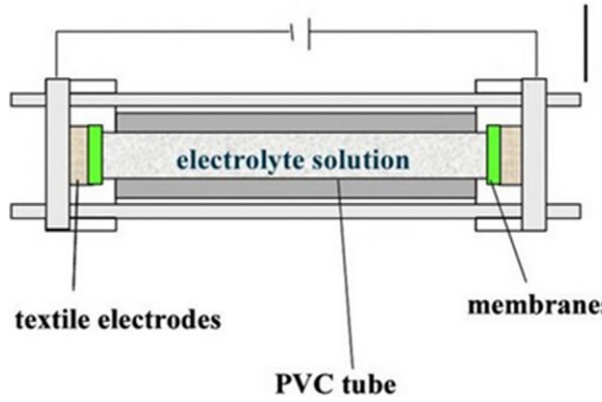

Fig. 12.9 Electrochemical cell developed to characterize the skin-textile electrode impedance. Reproduced from Priniotakis, G., et al. (2007). Electrochemical impedance spectroscopy as an objective method for characterization of textile electrodes. *Transactions of the Institute of Measurement and Control, 29*(3–4), 271–281, with authorization.

The cell is composed of a PVC tube filled with an electrolyte solution replicating the body fluids, two semipermeable membranes on both extremities of the tube, and the two electrodes on the external face of the membranes. The semipermeable membranes simulate the skin. Since skin pore size and density vary from one person to another, different membranes should be used for the test to take into account the variability in human skin properties. In the Priniotakis et al. (2007) study, two membranes were tested with 5 and 0.45 µm pore size.

It is recommended that several textile electrodes are tested to calibrate the electrochemical cell. Indeed, the surface profile of a knitted structure versus a nonwoven one is very different. Because textile structures form a complex network of point contacts with the porous membrane, the impedance cannot be obtained from the global contact surface but is provided by the sum of each individual contact.

12.4.4 Assessment of the sweating impact

The presence of humidity between the skin and the electrode will generate a decrease in the bio-impedance. As the textile electrode gets soaked by the liquid, the charges are able to move more freely through the system, resulting in a lower electrical resistance.

In addition, due to the presence of salts in human sweat, it is expected that the electrical resistance drops even faster than with tap water (Brahme, 2014).

Westbroek et al. have conducted a study on the short- and long-term evolution of the electrical resistance of textile electrodes after exposure to sweat (Westbroek et al., 2006). The electrical resistance of nonwoven electrodes was reduced by 20% just a few minutes after being exposed to synthetic sweat. Lower variations were observed for knitted and woven electrodes. This was attributed to their lower liquid absorption capacity than nonwovens.

Regarding long term exposure, the electrical resistance of all the electrodes had increased by 25% after 4 days and by more than 40% after 20 days (Westbroek et al., 2006). This was attributed to the effect of corrosion. In this experiment, the synthetic sweat solution was produced using 20 g/L of NaCl, 1 g/L of urea, 500 mg/L of salts, and the addition of NaoH or HCl to reach a pH of 5.8.

Standardized recipes for synthetic sweat preparation are available in ISO 11641 (2012), ASTM D4265 (2014), and AATCC TM15 (2002). Artificial perspiration may be acidic or alkaline. For instance, ISO 11641 (2012) recommends reaching a pH of 5.5 ± 0.2 for an acidic solution and 8.0 ± 0.1 for an alkaline solution. In all cases, NaCl remains the most important component of the solution regardless of the pH.

Since the corrosion reaction is mostly due to the presence of chloride, an increase of its concentration in the solution can induce an acceleration of the degradation of the conductive fibers. Therefore, this method can be used to simulate the ageing of the textile electrodes and conclude on their durability.

12.4.5 Assessment of the comfort properties for long-term use

Textile electrodes are preferred to conventional electrodes for long-term monitoring because they can be integrated into clothing and are usually more comfortable to wear for extended period of time.

An important requirement for textile electrodes is that the electrode surface is non-reactive with skin. This property is typically obtained with the use of silver plated yarns that often combine high electrical conductivity and biocompatibility properties.

In order to assess the comfortable feeling associated with wearing the electrodes, two modes of evaluation can be considered:

- The comfort wear test is a subjective evaluation that involves several participants grading the garment based on scales from 1 to 5 while performing specific activities (box lifting, ladder climbing, etc.) (Hollies et al., 1979). The ASTM F1154 (2011) method provides an exercise scenario for the assessment of chemical protective garments, but it may be applied to other clothing items. Although the testing procedure is close to the intended use of the garment, this method of evaluation remains costly and time consuming.
- The Kawabata evaluation method uses a series of 4 instruments to characterize, in an objective way, the fabric properties, including the tensile strength and shear stiffness (KES-FB1), bending rigidity (KES-FB2), compression (KES-FB3), and surface friction and roughness (KES-FB4).

In the context of textile electrodes, the measurement of the coefficient of friction and surface roughness is the most relevant parameter to consider since the electrodes will be integrated within a piece of clothing. Therefore, properties such as bending

rigidity, compression, etc. should be directly tested on the supporting fabric because the contribution of the electrodes generally remains negligible.

The KES-FB4 uses 10 sensors to simulate the fingertip feeling and records the output required to move the fabric at a constant rate of 0.1 cm/s over a distance of 2 cm (Barker, 2002). Simultaneously, a probe is placed on the fabric during its displacement to measure the mounts and valleys, i.e., the roughness of the surface.

The friction coefficient provided by the KES-FB4 ranges between 0 and 1, with 1 representing a very sticky surface. The surface roughness expressed by a number between 0 and 20, where 20 represents a very coarsely-textured fabric.

12.5 Testing cosmetotextiles and smart dermotextiles

12.5.1 Introduction

Due to their close contact with the body, textiles represent ideal substrates to carry and deliver cosmetic products to the skin. The active principles are encapsulated within microspheres which are, then, dispersed either inside the fibers or in a coating paste. Because of friction, chemical reaction with sweat, or change in pH, the microcapsules degrade as time goes on. Upon degradation, they release their active ingredient at a constant and regular rate (Persico & Carfagna, 2013). That rate is controlled by the thickness of the polymeric capsules.

The same principle is also used in medical applications for the controlled release of drugs. In the case of cosmetotextiles or dermotextiles, properties such as moisturizing, slimming, energizing, etc. are targeted and are integrated into pantyhose, underwear, or socks.

Several commercials products have already been launched on the market despite the absence of standards to evaluate their actual performance. Because of the variety of compounds encapsulated as well as their intimate contact with the skin, cosmetotextiles should not be evaluated only for their effectiveness but also in regards with their eventual toxicity and their durability after washing cycles. Finally, specific labeling must be put in place in order to subcategorize products and inform consumers.

12.5.2 Evaluation of the chemical properties of the active ingredient

Before evaluating the efficiency of the cosmetotextiles, the chemical components shall be characterized and quantified. Each ingredient (copper oxide, chitosan, aloe vera, etc.) shall be tested and identified according to specific test methods. For example, the presence of vitamin E can be detected by dripping $FeCl_3$- onto the finished textile (Singh, Varun, & Behera, 2011). The ions Fe^{2+} created by the reaction are evidenced by immersing the textile in a solution of Dipyridyl where the ions Fe^{2+} react to create a red complex which is visible to the naked eye.

The component analysis of perfumed textiles is more complex and requires headspace gas chromatography and mass spectrometry because of the volatile nature of

these compounds (Barel, Paye, & Maibach, 2014). The specimen is placed in a vessel under vacuum and is submitted to temperature variations. The vapors are collected and analyzed for odor issues, identification of polymer additives, or residual solvent. Testing protocols may be found in ASTM D3362 (2005), ASTM D3452 (2012), or ASTM D4128 (2012) for instance.

12.5.3 Evaluation of the efficiency of the claimed effect

Commercially available cosmetotextile products usually claim a wide variety of actions ranging from slimming and moisturizing to energizing and perfuming effects. Since 2009, the European directive 76/768/CEE requires manufacturers of such products to provide evidences of the effects advertised to the competent authorities (Bartels, 2011). In order to do so, four main methods are commonly used (Colipa—European Cosmetics Association, 2008):

- In vivo sensorial testing refers to a visual, tactile, or olfactory evaluation of the product effect by consumers or human subjects. This method is often used for perfuming or deodorizing textiles.
- In vivo instrumental testing also requires the involvement of human subjects. However, in this case, objective criteria or skin properties are measured by bioengineering techniques.
- Ex in vivo instrumental testing is very similar to in vivo instrumental testing. The only difference lies on the fact that the testing does not take place on human subjects but on specific human elements such as hair braids, skin tape strips, etc.
- In vitro testing uses artificial media recreated in laboratory in order to perform the tests.

For example, conductimetry or corneometry measurements may be conducted on human subjects before and after wearing moisturizing cosmetotextiles to determine the efficiency of the product. This technique relies on the electrical conductivity of the outer skin layers, which will directly be modified by any change in hydration.

Another example would be the evaluation of slimming textiles that can be achieved by the quantification of cellulite by echography of the dermal density. Similarly, the firmness and elasticity of the skin can be measured either by cutometry or ballistometry. A negative pressure is induced so that skin is locally sucked up by the instrument while the amplitude and duration of the deformation is noted.

12.5.4 Toxicity and innocuousness

Because of their close contact with the skin, cosmetotextiles may lead to risks of irritation and even toxicity. Indeed, most of cosmetotextiles use a microencapsulation process to contain the active substance. Therefore, chemical agents involved in the production of these microcapsules stay on the skin long after the microcapsules are empty and may lead to skin sensitization or epidermal cell toxicity.

In order to identify these potential negative outcomes, cosmetotextiles should be submitted to testing by either one of those three standards (Barel et al., 2014):

- EN ISO 10993 (ISO 10993, 2009) for medical devices includes two parts of interest for cosmetotextiles and smart dermotextiles:
  - Part 5: Tests for in vitro cytotoxicity

  - Part 10: Tests for irritation and skin sensitization. The method involves both in vitro and in vivo testing. The in vitro procedure uses rat skin and human skin cells, whereas rabbits are used for the in vivo tests. A scale of 0–4 allows the grading of any intracutaneous reactions.
- OECD guidelines for testing of chemicals, section 406 (1992), describes a test method for skin sensitization that is inspired from the guinea pig maximization test (GPMT) by Magnusson and Kligman (Kligman & Basketter, 1995).
- OEKO-TEX is an association of several Institutes of textile research and testing in Europe and Japan that offers a certification for textiles tested for various harmful substances such as heavy metals, formaldehyde, etc. (Niinimäki, 2006). Among the list of agents tested, solvent and other chemical residues would be of interest for cosmetotextiles.

12.5.5 Durability

When it comes to the durability of cosmetotextiles, two aspects should be considered independently: the durability of the active ingredient and the durability of the microcapsules. The release mechanism of the active substance is timed to last a determined number of hours, days, or weeks depending on the intended use. Unless the microcapsules are faulty, the product should be able to deliver the cosmetic effect over the planned period of time.

However, other parameters such as rubbing, temperature change, the presence of sweat, etc. can affect the performance of the binder used to create the adhesion between the microcapsules and the textile, leading to their detachment and loss. In order to verify the presence of the microcapsules on the fabric, the scanning electron microscope (SEM) and transmission electron microscope (TEM) have proven to be useful (Rodrigues et al., 2008; Monllor et al., 2010). Although it is difficult to quantify accurately the microcapsules with microscope imaging, the images provide

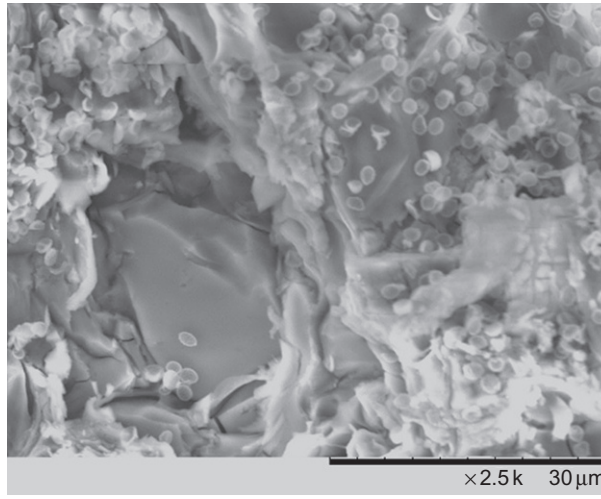

Fig. 12.10 Example of SEM image of microcapsules on a fabric.

a general estimate of the microcapsule concentration as illustrated in Fig. 12.10. Moreover, TEM can be used to identify if the microcapsules present on the fibers still contain the active ingredient or not.

Other techniques may be used to evaluate the residual amount of active ingredient inside the microcapsules. These techniques generally follow two main steps: extraction and quantification (Bartels, 2011). Solvent extraction is most commonly used but, in specific cases, the Soxhlet extractor may also be an option. The obtained solution is then analyzed by GC (Gas chromatography) or HPLC (high performance liquid chromatography) to separate and identify the components.

Azizi et al. reported using UV-visible absorption spectroscopy combined with solvent extraction to quantify the remains of neroline, a perfume component, after several washing cycles (Azizi, Chevalier, & Majdoub, 2014). Diethyl ether was used for the extraction and its UV spectrum had been checked against the UV spectrum of the extracted solution to identify the absorption maxima that would be characteristic of the neroline. The variation in the absorbance ratio was expressed as a function of the number of washing cycles.

12.5.6 Labeling

The European standard CEN/TR 15917 (CEN, 2009) differentiates product labels and the commercialization labels. Except for small articles such as socks or hoses, the product label shall be attached to the textile item, whereas commercialization labels are generally affixed on the package.

The product label shall display at least the following information:

- Fiber composition, based on the European directive 96/74/CE related to textile denomination;
- Care conditions in accordance with EN ISO 3758 (ISO 3758, 2012) "Textiles—Care labeling code using symbols";
- Tracking number (for example, batch or serial number);
- Identification of the cosmetic product.

In Canada, cosmetic product labels shall list all ingredients in descending order of predominance down to the minimum weight of 1% (Canada Health, 2009)

Commercialization labels shall clearly state the following elements:

- The word "cosmetotextile" must be explicitly written.
- All cosmetic ingredients shall be listed in accordance with Article 6 of the European Directive 76/768/CE related to cosmetic products. Products may also be referred to by their INCI (International Nomenclature for Cosmetic Ingredients) code.
- It shall be recommended to keep this information with the product for its entire lifetime.
- The name and address of the manufacturer head office shall be indicated, although abbreviations are allowed.
- An expiry date shall be mentioned if the optimal period of usage is <30 months.
- Any particular precautions for use shall be stated if necessary.
- The main function of the product has to be written on the label unless its representation is clear enough.

12.6 Conclusion

Although there has been a lot of activity in the field of smart textiles standardization, no actual standard has still been approved and is officially being used by the textile industry. Looking back over the last decade, Europe has, so far, been the most proactive region for standard development for smart textiles. In 2006, they created a first task group that led to the well-known project "Sustasmart." Even though the project officially ended in March 2014, work continues: a first draft of the standard proposal titled, "Determination of the linear electrical resistance of conductive track" was submitted in 2015. It is expected to become the first official standard applicable for smart textiles.

In North America, interest for the development of new standards related to the emerging sector of smart textiles increased in 2012 when ASTM organized the first smart textiles workshop for standardization. More recently, a subcommittee of ASTM D13 on textiles dedicated to smart textiles, ASTM D13-50, was created.

In addition, the AATCC organization joined forces with ASTM and organized a joint workshop in March 2016.

It is worth mentioning the importance that people from the electronics sector are represented at these workshops and remain involved in the standardization process. Indeed, smart textiles usually require at least one electronic component or device, for instance a power source. The impact of the electronic part on the product performance can be crucial and should be included in the aspects evaluated by the standards.

In parallel, a number of research centers are developing internal test methods in order to be able to characterize and evaluate the performance of the products they develop and prototype. A large amount of knowledge has thus already been acquired on the topic. However, it lacks homogeneity, objectivity, and comparable basis. For instance, different methods can be used to test the same function, such as a heating textile for example, based on the equipment available: thermal infrared camera, thermocouple, etc.

The involvement of standardization organizations can help turn these various internal methods into a unique objective method that would become the reference for both the industry and the consumers.

References

AATCC. (2016). *AATCC encourages education and discussion on wearable technology and electronic textiles*. AATCC (American Association of Textile Chemists and Colorists) news release. http://www.aatcc.org/wp-content/uploads/2016/02/AATCC_Encourages_Education_and_Discussion_on_Wearable_Technology_and_Electronic_Textiles.pdf (Accessed 29 February 2016).

AATCC TM15. (2002). *Colorfastness to perspiration*. Research Triangle Park, NC: American Association of Textile Chemists and Colorists.

AATCC TM76. (2011). *Electrical surface resistivity of fabrics*. Research Triangle Park, NC: American Association of Textile Chemists and Colorists (2 p.).

Arens, E. A., & Zhang, H. (2006). *The skin's role in human thermoregulation and comfort*. Berkeley: Center for the Built Environment, University of California.

Assambo, C., et al. (2007). Determination of the parameters of the skin-electrode impedance model for ECG measurement. In *Proceedings of the 6th WSEAS international conference on electronics, hardware, wireless and optical communications, Corfu Island, Greece*.

ASTM D1894. (2014). *Standard test method for static and kinetic coefficients of friction of plastic film and sheeting*. West Conshohocken, PA: ASTM International (7 p.).

ASTM D3362. (2005). *Standard test method for purity of acrylate esters by gas chromatography*. West Conshohocken, PA: ASTM International (4 p.).

ASTM D3452. (2012). *Standard practice for rubber—Identification by pyrolysis-gas chromatography*. West Conshohocken, PA: ASTM International (4 p.).

ASTM D4128. (2012). *Standard guide for identification and quantitation of organic compounds in water by combined gas chromatography and electron impact mass spectrometry*. West Conshohocken, PA: ASTM International (8 p.).

ASTM D4265. (2014). *Standard guide for evaluating stain removal performance in home laundering*. West Conshohocken, PA: ASTM International (8 p.).

ASTM D4496. (2013). *Standard test method for d-c resistance or conductance of moderately conductive materials*. West Conshohocken, PA: ASTM International (5 p.).

ASTM D7024. (2013). *Standard test method for steady state and dynamic thermal performance of textile materials*. West Conshohocken, PA: ASTM International (4 p.).

ASTM F1154. (2011). *Standard practices for qualitatively evaluating the comfort, fit, function, and durability of protective ensembles and ensemble components*. West Conshohocken, PA: ASTM International (7 p.).

ASTM F2300. (2016). *Standard test method for measuring the performance of personal cooling systems using physiological testing*. West Conshohocken, PA: ASTM International (8 p.).

ASTM F2371. (2011). *Standard test method for measuring the heat removal rate of personal cooling systems using a sweating heated manikin*. West Conshohocken, PA: ASTM International (5 p.).

Azizi, N., Chevalier, Y., & Majdoub, M. (2014). Isosorbide-based microcapsules for cosmetotextiles. *Industrial Crops and Products*, *52*, 150–157.

Banaszczyka, J., Anca, A., & De Mey, G. (2009). Infrared thermography of electroconductive woven textiles. *Quantitative InfraRed Thermography Journal*, *6*(2), 163–173.

Barel, A. O., Paye, M., & Maibach, H. I. (Eds.), (2014). *Handbook of cosmetic science and technology* (p. 532). Boca Raton, FL: CRC Press.

Barker, R. L. (2002). From fabric hand to thermal comfort: the evolving role of objective measurements in explaining human comfort response to textiles. *International Journal of Clothing Science and Technology*, *14*(3/4), 181–200.

Bartels, V. (Ed.), (2011). *Handbook of medical textiles*. Cambridge, UK: Elsevier.

Bashir, T., et al. (2012). Electrical resistance measurement methods and electrical characterization of poly (3, 4-ethylenedioxythiophene)-coated conductive fibers. *Journal of Applied Polymer Science*, *124*(4), 2954–2961.

Becker, D. E. (2006). Fundamentals of electrocardiography interpretation. *Anesthesia Progress*, *53*(2), 53–64.

Bendkowska, W., & Wrzosek, H. (2009). Experimental study of the thermoregulating properties of nonwovens treated with microencapsulated PCM. *Fibres & Textiles in Eastern Europe*, *17*(5), 76.

Blau, P. J. (2001). The significance and use of the friction coefficient. *Tribology International*, *34*(9), 585–591.
Brahme, A. (2014). Comprehensive biomedical physics. *Newnes*, 157.
BS-EN-16812. (2016). *Determination of the linear electrical resistance of conductive tracks*. Brussels: CEN–European Committee for Standardization.
Canada Health. (2009). *Guide to cosmetic ingredient labelling*. Minister of Health, ISBN: 978-1-100-10897-1.
CEN. (2009). *Textiles—Cosmeto-textiles CEN/TR 15917*. Brussels: European Committee for Standardization (24 p.).
CEN. (2011). *Textiles and textile products—Smart textiles—Definitions, categorisation, applications and standardization need—CEN/TR 16298*. Brussels: European Committee for Standardization (32 p.).
CENTEXBEL. (2017). *Smart Textiles Standardisation*. http://www.centexbel.be/nl/node/858. (Accessed 18 August 2017).
Colipa—European Cosmetics Association. (2008). *Guidelines for the evaluation of cosmetic products*. Brussels: Colipa (18 p.).
CTT Group. (2010). *Méthode de mesure de la variation des caractéristiques électriques d'un textile électro-conducteur ou comportant des zones conductrices en fonction de l'allongement*.
CTT Group. (2011). *Méthode de mesure de la variation des caractéristiques électriques d'un textile électro-conducteur ou comportant des zones conductrices en fonction de l'abrasion*.
Dalsgaard, C., & Sterrett, R. (2014). *White paper on smart textile garments and devices: A market overview of smart textile wearable technologies*. Market Opportunities for Smart Textiles.
De Luca, G. N., et al. (2004). *Sweat test for electro-mechanical stability of the EMG electrode-skin interface*. In: *Proceeding of the international society for electrophysiology and kinesiology*.
Ding, T., Wang, L., & Wang, P. (2007). Changes in electrical resistance of carbon-black-filled silicone rubber composite during compression. *Journal of Polymer Science Part B: Polymer Physics*, *45*(19), 2700–2706.
Francis, J., & Reek, S. (2014). Wearable cardioverter defibrillator: A life vest till the life boat (ICD) arrives. *Indian Heart Journal*, *66*(1), 68–72.
Hertleer, C., & Van Langenhove, L. (2015). Standards for smart textiles. *Handbook of smart textiles*. pp. 843–856.
Hittle, D. C., & Andre, T. L. (2002). A new test instrument and procedure for evaluation of fabrics containing phase-change material. *ASHRAE Transactions*, *108*, 175.
Hollies, N. R. S., et al. (1979). A human perception analysis approach to clothing comfort. *Textile Research Journal*, *49*(10), 557–564.
ISO 3758. (2012). *Care labelling code using symbols*. Geneva (Suisse): International Standard Organisation (22 p.).
ISO 10993. (2009). *Biological evaluation of medical devices*. Geneva (Suisse): International Standard Organisation (21 p.).
ISO 11092. (1993). *Measurement of thermal and water-vapour resistance under steady state conditions (sweating guarded hotplate test)*. Geneva (Suisse): International Standard Organisation (10 p.).
ISO 11641. (2012). *Colour fastness to perspiration*. Geneva (Suisse): International Standard Organisation (7 p.).
Kim, J.-H., et al. (2011). Effects of liquid cooling garments on recovery and performance time in individuals performing strenuous work wearing a firefighter ensemble. *Journal of Occupational and Environmental Hygiene*, *8*(7), 409–416.

Kligman, A. M., & Basketter, D. A. (1995). A critical commentary and updating of the guinea pig maximization test. *Contact Dermatitis*, *32*(3), 129–134.
Larrimore, L. M. (2005). *Low temperature resistivity*. Swarthmore, PA: Swarthmore College Computer Society (11 p.).
McGrath, M. J., & Ní Scanaill, C. (2013). *Wellness, fitness, and lifestyle sensing applications*. Berkeley, CA: Sensor Technologies Press. pp. 217–248.
Merritt, C. R. (2008). *Electronic textile-based sensors and systems for long-term health monitoring*. ProQuest.
Michalak, M., Felczak, M., & Więcek, B. (2009). Evaluation of the thermal parameters of textile materials using the thermographic method. *Fibres and Textiles in Eastern Europe*, *17*(3), 84–89.
Mondal, S. (2008). Phase change materials for smart textiles–An overview. *Applied Thermal Engineering*, *28*(11), 1536–1550.
Monllor, P., et al. (2010). Improvement of microcapsule adhesion to fabrics. *Textile Research Journal*, *80*(7), 631–635.
Niinimäki, K. (2006). Ecodesign and textiles. *Research Journal of Textile and Apparel*, *10*(3), 67–75.
Persico, P., & Carfagna, C. (2013). Cosmeto-textiles: State of the art and future perspectives. *Advances in science and technology* (Vol. 80). Zurich: Trans Tech Publications.
Priniotakis, G., et al. (2007). Electrochemical impedance spectroscopy as an objective method for characterization of textile electrodes. *Transactions of the Institute of Measurement and Control*, *29*(3–4), 271–281.
Rodrigues, S. N., et al. (2008). Microencapsulation of limonene for textile application. *Industrial & Engineering Chemistry Research*, *47*(12), 4142–4147.
Šafářová, V., & Grégr, J. (2010). *Electrical conductivity measurement of fibers and yarns*. In *7th international conference, TEXSCI, Liberec, Czech Republic*.
Scott, R. A. (Ed.), (2005). *Thermal protection*: Textiles for protection. Elsevier. (chapter 7), p. 190.
Sharma, A., et al. (2009). Review on thermal energy storage with phase change materials and applications. *Renewable and Sustainable Energy Reviews*, *13*(2), 318–345.
Singh, M. K. (2004). *The state-of-art smart textiles*. http://www.ptj.com.pk/Web%202004/08-2004/Smart%20Textiles.html (Accessed 12 December 2016).
Singh, M. K., Varun, V. K., & Behera, B. K. (2011). Cosmetotextiles: State of art. *Fibres and Textiles in Eastern Europe*, *19*(4), 27–33.
Smith, W. C. (Ed.), (2010). *Testing of conductive coatings*: Smart textile coatings and laminates. Elsevier. (chapter 6), p. 167.
Taji, B., et al. (2014). Impact of skin–electrode interface on electrocardiogram measurements using conductive textile electrodes. *IEEE Transactions on Instrumentation and Measurement*, *63*(6), 1412–1422.
Tang, S., & Po, L. (2007). Recent developments in flexible wearable electronics for monitoring applications. *Transactions of the Institute of Measurement and Control*, *29*(3–4), 283–300.
Van Langenhove, L., & Hertleer, C. (2004). Smart clothing: A new life. *International Journal of Clothing Science and Technology*, *16*(1/2), 63–72.
Wan, X., & Fan, J. (2009). A new method for measuring the thermal regulatory properties of phase change material (PCM) fabrics. *Measurement Science and Technology*, *20*(2), 025110.
Wang, F., et al. (2010). A review of technology of personal heating garments. *International Journal of Occupational Safety and Ergonomics*, *16*(3), 387–404.
Westbroek, P., et al. (2006). Quality control of textile electrodes by electrochemical impedance spectroscopy. *Textile Research Journal*, *76*(2), 152–159.
Ying, B., et al. (2004). Assessing the performance of textiles incorporating phase change materials. *Polymer Testing*, *23*(5), 541–549.

Specific testing for filtration

13

N. Petillon
IFTS, Foulayronnes, France

Filters are used in a larger number of applications both for ecological and economic reasons. For example:

- Filters prevent industries from polluting the environment when rejecting their effluents directly into rivers or the sea,
- Cities can supply drinking water to their own population by processing available water sources with large scale filter membranes.
- Automotive fuel and oil filters can lead to clean engines and increase component life duration and car power.

This makes filters essential in our lives. The heart of filters is the filter medium. Without an adequate filter medium, even the most sophisticated and ingenious filter is of no use.

The filter medium is a permeable structure which lets the fluid circulate but retains all the undesirable solid contaminants. The variety of filter materials is very large: they can range from metals with mm-diameter holes to microporous membranes whose pore size is about 2 nm. They can be made of synthetic polymers, cellulosic paper, metallic cloth, ceramic, etc. They may have to resist high temperature, creep and stretch, abrasion, and be flexible enough to be pleated or assembled.

Below are described some test methods for properties relevant to filter media. They ensure that filter media offer the required performance towards their ecological and economic purposes.

13.1 Structural properties

A filter medium structure is described by its morphology, the size (diameter, length, etc.) and netting of its fiber, but more importantly by its pore size distribution.

13.1.1 Pore size distribution

Pores have many different shapes but, from a mathematical point of view, they are generally considered to be cylinders, the diameter of which is measured by air-liquid porometry:

Advanced Characterization and Testing of Textiles. https://doi.org/10.1016/B978-0-08-100453-1.00014-3

The air-liquid porometry consists of a fluid with a surface tension γ being pulled outside pores under the application of an increasing pressure P (Wet curve in Fig. 13.1). The pore diameter d is calculated using Jurin's law (Fig. 13.2):

$$P = \frac{4\gamma \times \cos\theta}{d}$$

P = air pressure (kPa)
θ = contact angle between the fluid and the pore material (may be considered as $0 \rightarrow \cos\theta = 1$)
γ = surface tension (mN/m)
d = "pore" diameter (µm)

By comparing the wet flow corresponding to the air flow through the wet filter medium (in a 1st step) vs the dry flow corresponding to the air flow through the dried filter media (in a 2nd step) (Fig. 13.1), we can determine the percentage of cumulative air flow versus the air pressure and by computing this curve in a differential way, we

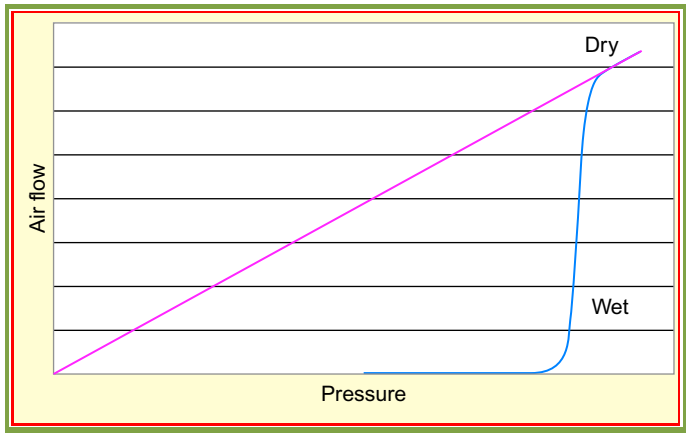

Fig. 13.1 Typical air flow curve.

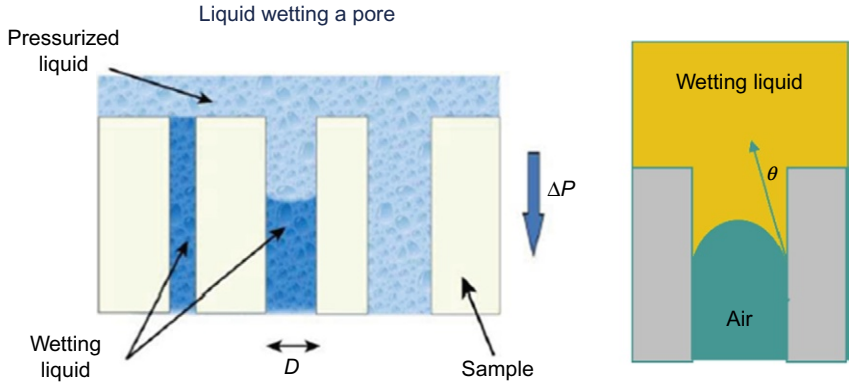

Fig. 13.2 The principle of Jurin's law.

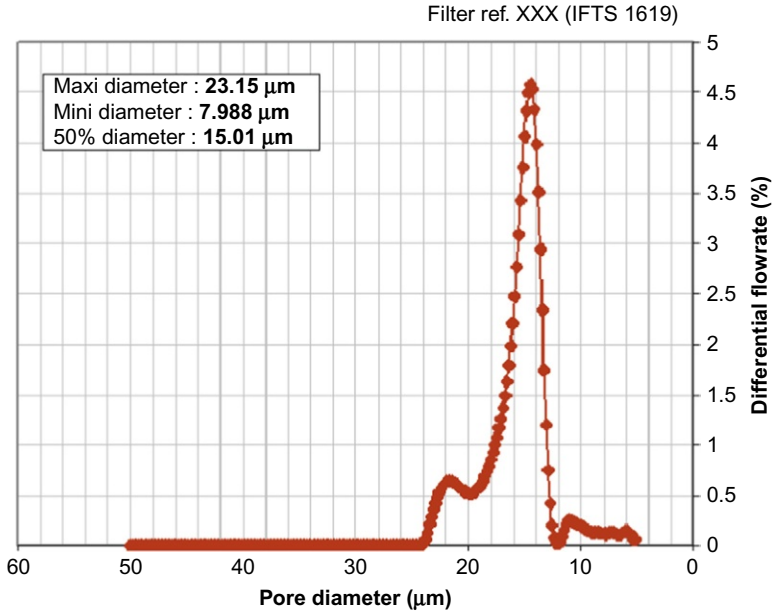

Fig. 13.3 Typical pore size distribution curve of a filter medium.

can draw the differential air flow percentage and consequently the pore size distribution, per Jurin's law (Fig. 13.3).

The pore size distribution is either thin or broad depending on whether there is a surface filter medium (such as metallic sieve, woven medium, or track etched membrane) or a depth filter medium (such as cellulosic medium, nonwoven medium) (Fig. 13.4). This provides an initial insight into the filtration mechanism of the medium and is a useful tool to nondestructively assess the variability of the medium from one manufacturing batch to another.

The air-liquid porometry is mainly for pore sizes larger than 10 µm (possible down to 0.2 µm but at such a level, there are risks of biased results due to dissolved gas relaxation). Air-liquid porometry is standardized as per ASTM F 316-03 (2011) (pore sizes between 0.1 and 15 µm). A test method specific to geotextiles, ASTM D 6767 (2016), also uses the capillary flow principle. It applies to pore sizes ranging from 1 to 200 µm.

The liquid-liquid porometry does not suffer from the dissolved gas issue and can measure pore sizes of 2 nm, under the condition that the filter medium doesn't deform (Fig. 13.5).

13.1.2 Bubble point determination (or bulloscopy)

Bulloscopy characterizes the first bubble point which corresponds to the lowest air bubbling pressure (Fig. 13.6, air bubble occurring outside a filter medium). It is taken as a reference for the largest pore size. This is a value indicative of the integrity of the

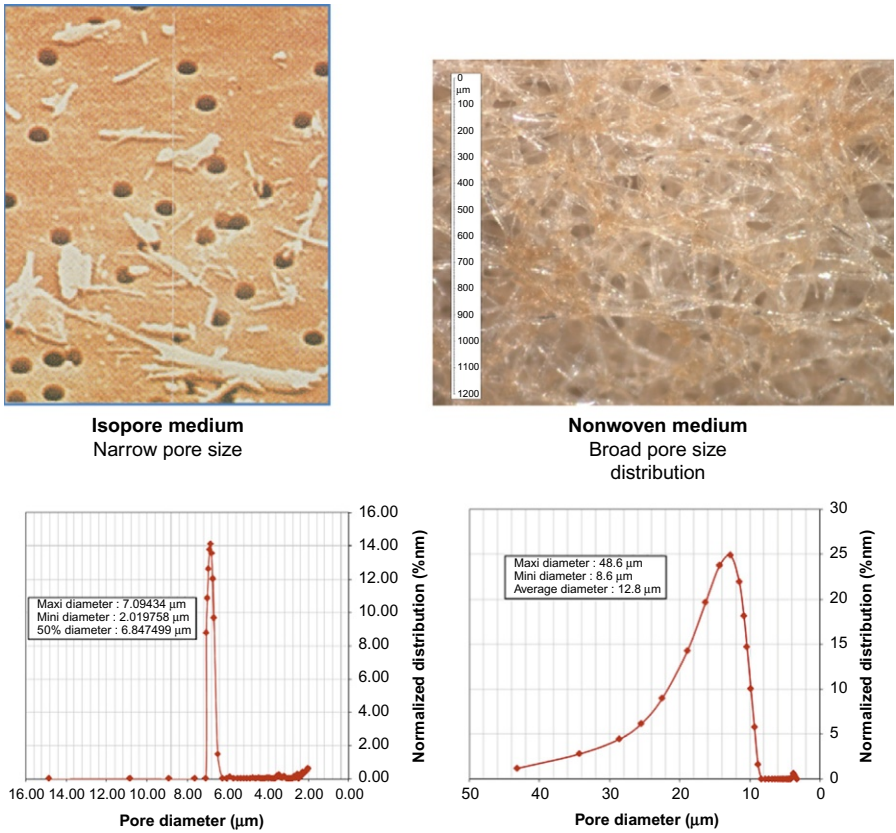

Fig. 13.4 Example of narrow and broad pore size distributions (on the left side: narrow distribution due to the homogeneity of the pore size of the isopore filter medium; on the right side: broad distribution due to the heterogeneity of the pore size of a thick nonwoven filter medium).

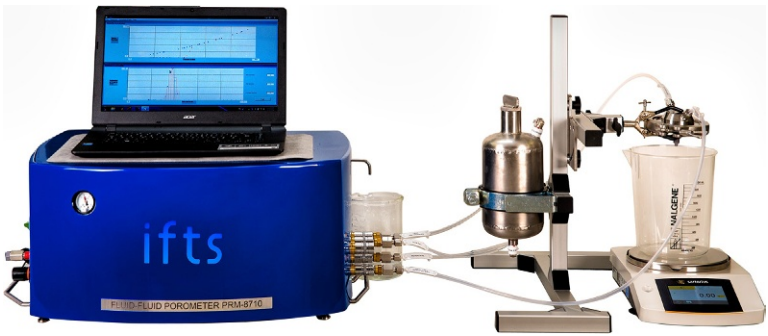

Fig. 13.5 Example of porometer apparatus combining both air-liquid and liquid-liquid porometry.
Courtesy from IFTS.

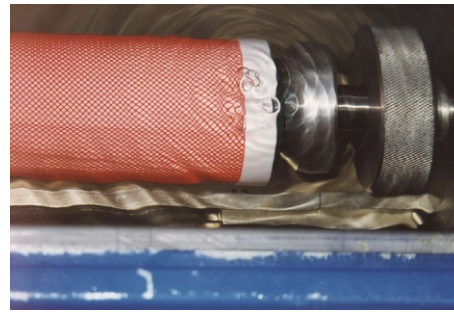

Fig. 13.6 Air bubble occurring outside the filter medium.

filter medium. Other fizzing pressures corresponding to 3 or 10 bubbles in a set time can also be used.

Several standards are available to determine the bubble point pressure, for instance ISO 2942 (2004) and ISO 4022 (1987).

13.2 Hydraulic properties

The permeability characterized by the pressure drop gives some information relative to the percolation of a clean fluid through a filter medium; it is not correlated with the filtration size.

13.2.1 Air and liquid permeability

The permeability value β is calculated with the Darcy law for a fluid circulating in a laminar flow at a given flowrate (Q) through a porous media for a given surface area Ω and a given depth z under a differential pressure ΔP:

$$\beta = \frac{\mu z Q}{\Omega \Delta P}$$

By positioning a flat sheet of the filter medium in an adequate flat sheet holder, the flowrate varies from 20% to 110% of its nominal value (see typical test rig in Fig. 13.7). By knowing the fluid viscosity, it is possible to determine the slope of the curve ΔP vs flow rate and compute the intrinsic permeability β of the flat sheet medium. By considering β as a constant value, it is also possible to extrapolate the ΔP of the flat sheet medium both at high and low viscosity of the fluid (Fig. 13.8).

It is to be noted that the ΔP of the flat sheet medium is calculated on the basis of the following assumption:

$$\Delta P_{\text{flatsheet medium}} = \Delta P_{\text{complete assy}} - \Delta P_{\text{empty holder}}$$

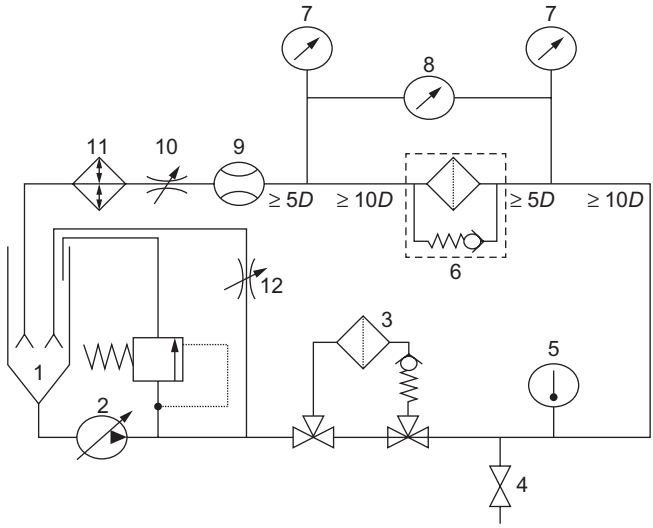

D pipe inside diameter

1. Reservoir
2. Variable speed pump
3. Clean-up filter
4. Sampling valve
5. Thermometer
6. Filter under test
7. Absolute pressure transducer
8. Differential pressure transducer
9. Flowmeter
10. Counter pressure regulating valve
11. Heat exchanger
12. Bypass flow regulating valve

Fig. 13.7 Differential pressure measurement rig.

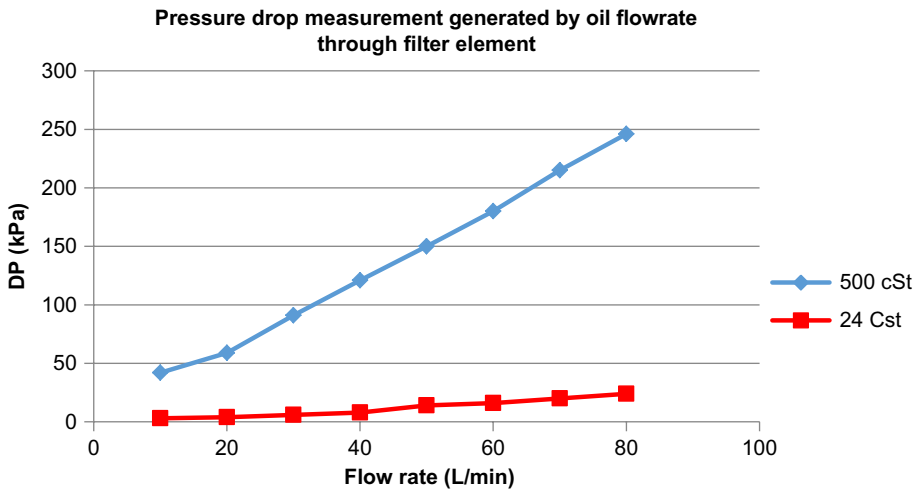

Fig. 13.8 Typical pressure drop curves at two different oil viscosities.

The complete assay is assumed to include both the empty holder and the flat sheet medium.

For filter cloth or any other structured porous medium, the permeability β can be expressed in L/h/m^2 under a specific water flow rate at a pressure of 196 Pa or 20 mmHg or in Nm^3/h m^2 under a specific air flow rate at an air pressure of 196 Pa.

The pressure drop measurement is standardized as per ISO 3968 (2001), ISO 4548-1 (1997), or NF EN 13443-2/IN1 (2007) if it is dealing with filter cartridges or filter samples.

13.2.2 Cleanability of the filter medium

The permeability value of a filter medium or the associated pressure drop is one of the criteria to evaluate the efficiency of a filter cleaning process. Both these values could be evaluated before and after cleaning the clogged filter medium. The clogging process should have occurred in controlled conditions. The cleaning process may use back flow, ultra-sonic dispersion, or chemical attack. Cleanability is important for filter media such as metallic sieves, and membranes which are permanent filter media, and not disposable ones.

13.3 Separative properties

These are the most informative properties because they refer to the filtration performances of the filter medium in terms of:

- Retaining all the particles larger than a given size (absolute glass bead tests, bacterial challenge)
- Retaining a given percentage of particles of a given size at the very early life of the filter medium (initial particulate filtration efficiency, filtration rating, and cut-off of the membrane)
- Retaining a given quantity of specified test dust (retention capacity) up to a given clogging differential pressure (DP)

13.3.1 Absolute glass bead test

This corresponds to the diameter of the largest glass beads being able to go through a flat sheet filter medium under given conditions of pressure. The glass bead size distribution and quantity should be in adequacy with the filtration area and should prevent the formation of a filter cake on the filtration surface (Fig. 13.9). This often correlates with the largest pore value determined by the first bubble point pressure. This test may be performed using MIL F8815 (1995) and NF X45-304 (2000) procedures.

13.3.2 Particulate filtration efficiency

This data is the only characteristic relative to the capability of a filter medium to retain solid particles in suspension.

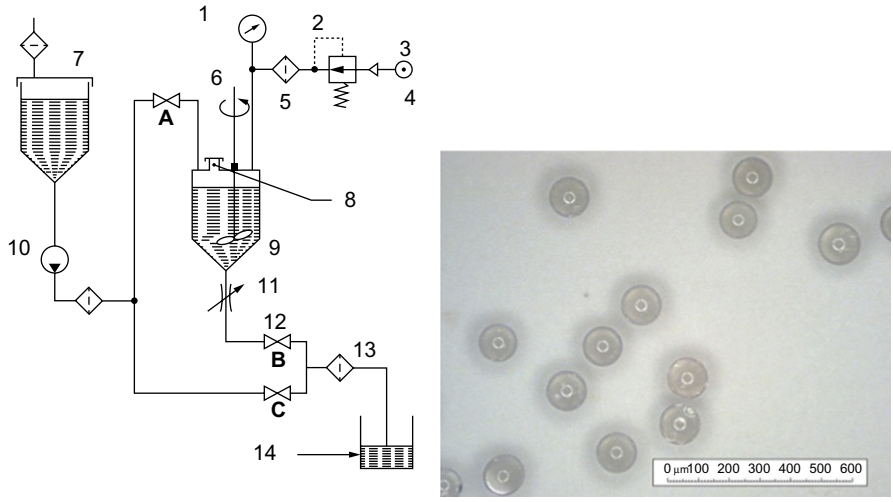

Fig. 13.9 Absolute glass beads test rig and picture of glass beads under microscope.

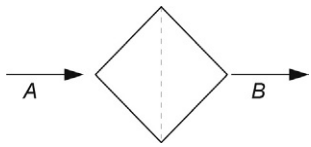

Fig. 13.10 Schematic representation of the incoming (*A*) and the outgoing (*B*) particles passing through a filter medium.

The particulate filtration efficiency E (%) corresponds to the ratio expressed in % between the incoming (A) and the outgoing (B, i.e., not retained) particle quantity (Fig. 13.10). It is related to the β ratio.

$$E(\%) = \frac{A-B}{A} \times 100; \quad \beta = \frac{A}{B}$$

A and B may be measured in terms of turbidity, suspended matters, particle counts (in a cumulative or differential way), bacteria level, etc.

The filtration efficiency of a filter medium depends on many operating parameters such as the physical properties of the fluid, the size distribution of the solid particles to be retained, the flow velocity, the temperature, the current flow or pressure pulsation, the clogging state of the filter medium, etc.

Unfortunately, it is not possible to duplicate real life conditions; that is the reason why some standards have been adopted to evaluate filter media under controlled and standardized operating conditions so that their performance can be compared.

The filtration efficiency measurement applies to any kind of filter medium, whatever its structure. However, it needs some appropriate test rig equipped with the suitable circulation pump, the proper way to maintain the particles in suspension and the right particle counting system (Fig. 13.11).

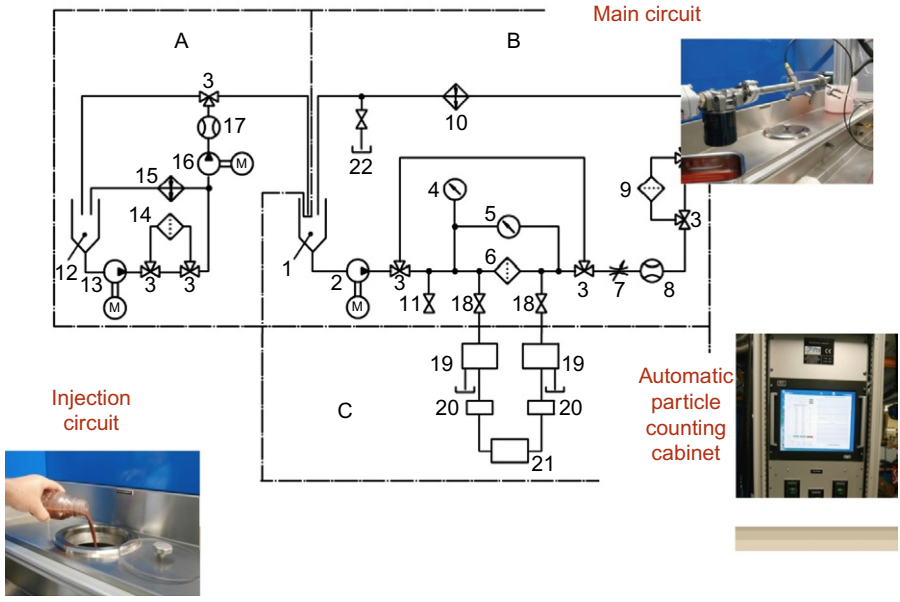

Fig. 13.11 Principle of a multipass test bench used to characterize the particulate filtration efficiency and retention capacity of a filter medium.
Courtesy from IFTS.

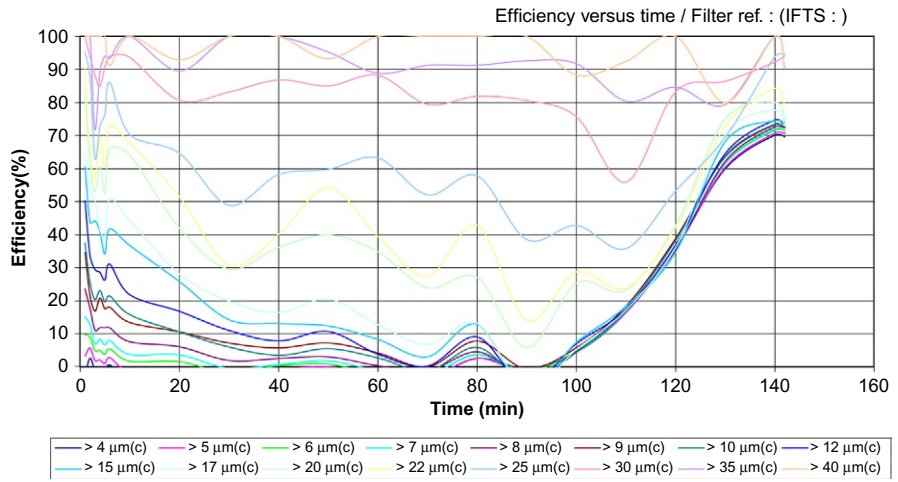

Fig. 13.12 Instantaneous filtration efficiency vs clogging time.

The results can be expressed in terms of instantaneous filtration efficiency vs. duration time (Fig. 13.12), the filtration efficiency being calculated from on-line particle counts N at different sizes ($>x\,\mu m$) upstream and downstream of the filter.

$$\mathrm{Eff}_{x\mu m}(\%) = \frac{N_{\mathrm{up}>x\mu m} - N_{\mathrm{dw}>x\mu m}}{N_{\mathrm{up}>x\mu m}}$$

All the instantaneous filtration efficiency values at each particle size are averaged; the average filtration efficiency curve vs. particle size is obtained (Fig. 13.13).

The particle size distribution of the test dust and the technology of the particle counter have to be suitable for the presumed filtration ratings of the filter cartridge under test (Table 13.1).

NF X45-303 (2000) and NF EN 13443-2/IN1 (2007) standard test methods are available for reference filtration ratings. This corresponds to the particle upper size

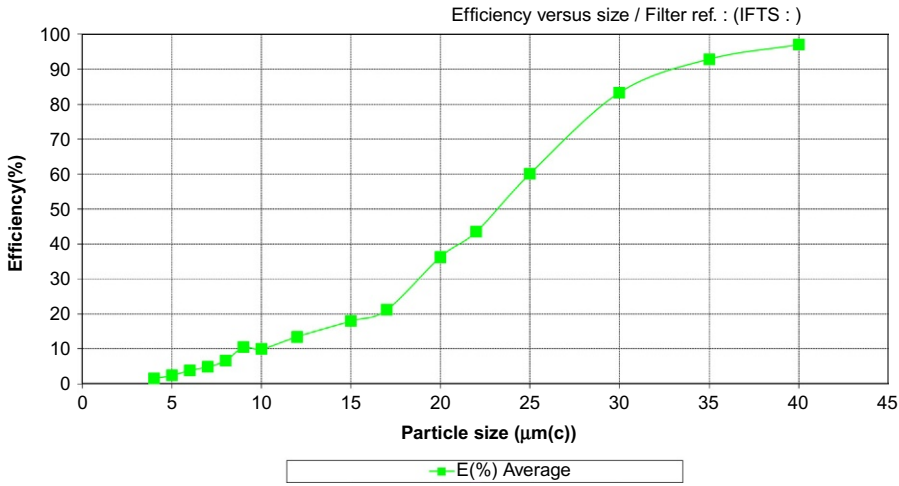

Fig. 13.13 Evolution of the particulate contamination vs time according to different particle sizes.

Table 13.1 Types of test dust and particle counter as a function of the filtration rating of filter medium

Presumed filtration ratings (µm)	Test dust	Particle counting technology
<1	Monodispersed latex beads	On-line light scattering principle
<25	A3 medium silica test dust as per ISO 12103-1 (2016)	On-line light extinction principle
<80	A4 coarse silica test dust as per ISO 12103-1 (2016)	On-line light extinction principle
>80	Glass beads	Off-line optical microscopy after filtration under membrane

in µm which provides a filtration efficiency of 99.8% (or a beta ratio of 500 corresponding to the upstream particles count divided by the downstream particle counts).

13.3.3 Retention capacity

The retention capacity expressed in *g* of test dust per m^2 (in the case of a flat sheet medium) or in g of test dust (in case of a filter cartridge) corresponds to the mass of particles retained by the filter medium up to a specified ΔP, at a given flow rate. Generally, it can be measured simultaneously with the particulate filtration efficiency.

This property can help comparing different filters with each other in terms of life duration and anticipating the evolution of their filtration efficiency until they are fully clogged (Fig. 13.14).

13.3.4 Bacterial challenge

This property is relevant for the qualification of sterilizing membranes. It consists in injecting a suspension of microorganisms (such as *brevundimonas diminuta* or *serraciatiens* bacteria of diameter size between 0.5 and 0.8 µm and length between 1 and 20 µm) upstream of the membrane with a concentration of 10^7 bacteria per cm^2 of filter medium area (Fig. 13.15). The ratio of the logarithm number of upstream bacteria to the logarithm number of downstream bacteria will define the reduction number. As soon as this reduction number is higher than 6, the filter membrane is considered as a sterilizing one.

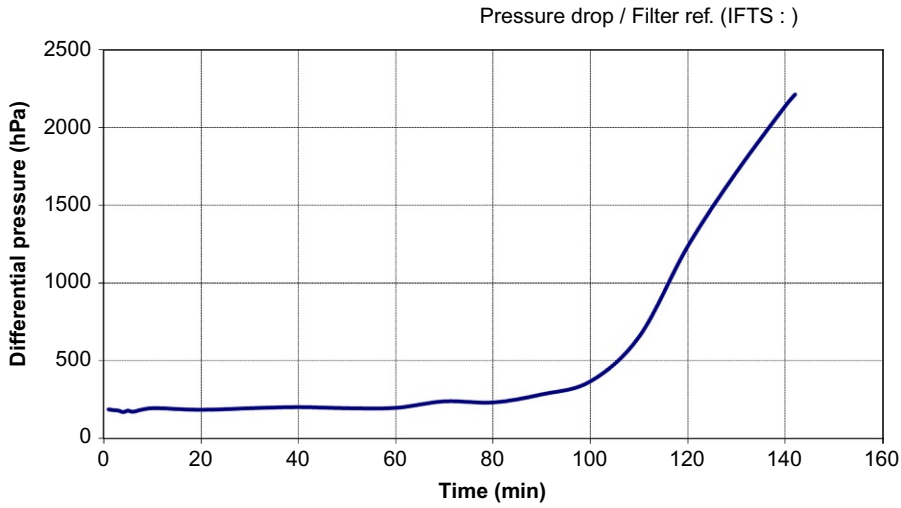

Fig. 13.14 Clogging curve of a filter medium vs test dust injection time.

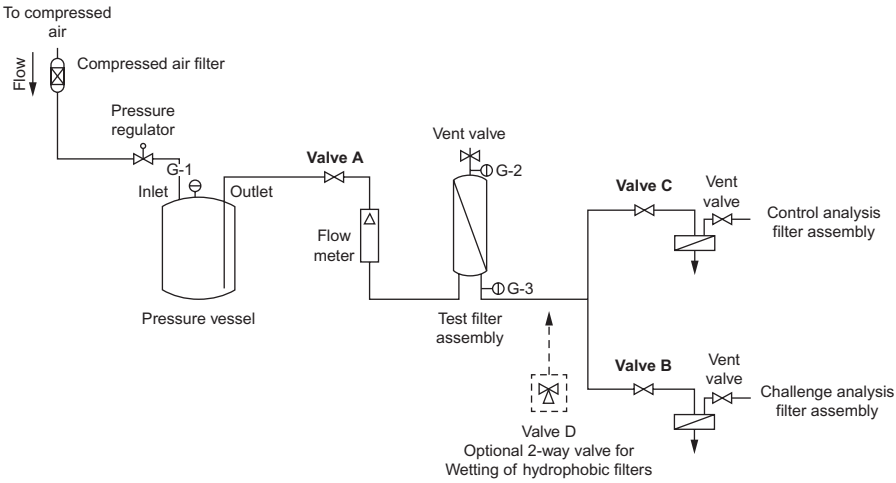

Fig. 13.15 Bacterial challenge test rig as per ASTM F838.

13.4 Physical and physicochemical properties

The physicochemical data corresponding to the interactions between the filter medium and the filtered liquid are of major importance to allow identifying the right filtration system.

13.4.1 Grammage

In case of metal or synthetic flat sheet filter medium, the grammage is calculated as the weight per m^2 of filtration area.

The grammage is related to the size of the fibers or the wires and the density of the material. Its variation during the use of the filter medium may eventually take place if the medium is dry or wet.

13.4.2 Thickness

It is measured under a given pressure with a digital micrometer. It can give access to the compressibility of the filter medium.

13.4.3 Compatibility—chemical and thermal resistance

A filter medium may face chemical, thermal, photo, or mechanical stresses during its use into a filtering cartridge, a filter panel, or a custom-made flat sheet, for instance:

- Pleating, bonding, seaming, calendaring…
- Contact with aggressive fluids such as cleaning fluids, sterilizing fluids, abrasive contaminants, etc.

In addition, in the case of the clarification of industrial liquids, the filter shall not contaminate the downstream fluid; it has to be demonstrated that no toxic or unwanted

substances exist or can migrate as a result of fiber or microparticle release, or dissolution of extractible particles.

The compatibility is demonstrated when:

- the filter material can resist the contact with the final processed fluid;
- the substances constituting the filter are included in the authorized list to be in contact with the final liquid (such as in food or drinking water regulations);
- the main characteristics of the filter (such as the mechanical resistance, ΔP, filtration efficiency) remain unchanged after the filter has being subjected to fluid circulation in given conditions of duration, temperature, concentration, pressure, etc.

13.4.4 Cleanliness of the filter medium

Cleanliness is more and more often requested in common rail diesel fuel or in nuclear applications: the filter medium should not contaminate the downstream fluid. Filter cleanliness quantification is conducted by circulating some clean fluid through the filter medium and collecting the downstream fluid for gravimetrical and specific contaminant analysis. The main standard test methods include ISO 4020 (2001), ISO 16232 (2007), and NF X45-306 (2000).

13.4.5 Mechanical resistance

A filter medium is subjected to mechanical stresses such as ΔP increase, flow variation, pressure variation, and backwash flow conditions. The maximal working pressure is critical and defined by the filter supplier. At higher pressures, the filter performances are not guaranteed any more (Fig. 13.16).

Fig. 13.16 Burst filter cartridge.

Fig. 13.17 Mullen burst test.

The Mullen test provides a way to assess the behavior of a filter medium in relation to pressure. It consists in installing the flat sheet medium over a rubber membrane (Fig. 13.17). The membrane is inflated by increasing the static pressure until the filter medium bursts.

13.4.6 Water removal efficiency of diesel fuel filters

The new common rail technologies require that the fuel circuit to be as clean as possible and free of water, especially just upstream of the fuel nozzles of the injection equipment. That is the reason why diesel fuel filter manufacturers are asked to supply the most efficient fuel water separators to diesel fuel injection equipment manufacturers. Consequently, a new fuel water separation efficiency standard test method, referred to as ISO/TS 16332 (2017), has been developed. It consists in injecting some water droplets of calibrated size at a given condition of concentration and interfacial tension of the diesel fluid upstream of the filter medium. The water removal efficiency is calculated based on the water titration of the diesel fuel upstream and downstream of the filter medium. Some water droplets with calibrated size have been standardized for specific applications: 10 µm diameter for pressure side water separators, and 150 µm diameter for suction side water separators. These water droplet sizes are generated by circulation trough a calibrated orifice (Fig. 13.18).

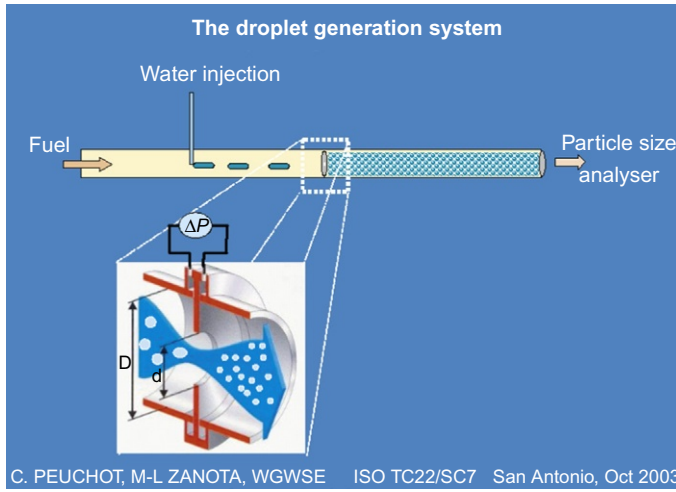

Fig. 13.18 Use of a calibrated orifice to generate certified water droplet size under a given generated differential pressure (ΔP).

Some apparatus allowing a self-adjustment of the orifice are available on the market such as EDGE from IFTS (Fig. 13.19).

Two low and high interfacial tension (IFT) values (respectively 13 ± 2 and 22 ± 2 mN/m) have also been standardized; they correspond to the existing fuel markets in the world.

13.5 Existing standards to qualify filter media

A flat sheet medium is often qualified or certified according to the existing standards whose main principles have been described in the previous sections.

Because of the wide range of clarification needs (from mm to nm) of the numerous filtration applications, there is a large number of filter standards for the different fields of applications which can be used in terms of filter performance comparison. This is an useful first approach from an economical point of view because it eliminated the need to replicate real working conditions. Table 13.2 lists different standards available to characterize filter media and filter cartridges.

Thanks to the experimental feedback between users and manufacturers, standards are improved over time. However, a standard test will never perfectly simulate the end-use conditions of applications in terms of temperature, fluid, contamination, etc. Therefore, its assessment has to be completed with tests in real working conditions in order to confirm the preliminary design of the filters.

Fig. 13.19 Existing equipment generating automatic calibrated orifice as per ISO/TS 16332 (2017). EDGE prototype—courtesy from IFTS.

Table 13.2 Filter medium testing procedures (not an exhaustive list)

Characteristics	Standards
Grammage	ISO 536 (2012)—Paper and board—determination of grammage ISO 3039 (2010)—Corrugated fiberboard—determination of grammage of the component papers after separation
Pore size distribution	ASTM F 316-03 (2011) Standard test methods for pore size charcateristics of membrane filters by bubble point and mean flow pore test ASTM E 128-99 (2011) Standard test method for maximum pore diameter and permeability of rigid porous filters for laboratory use ASTM D 6767 (2016) Standard test method for pore size characteristics of geotextiles by capillary flow test

Table 13.2 Continued

Characteristics	Standards
Bubble point	NF X45-301 (2000): Cartouches filtrantes—méthodes d'essais—contrôle d'intégrité par détermination du point de première bulle ISO 2942 (2004)—Hydraulic fluid power—filter elements—verification of fabrication integrity and determination of the first bubble point ISO 4020 (2001)—Road vehicles—fuel filters for diesel engines—test methods ASTM F 316-03 (2011) Standard test methods for pore size charcateristics of membrane filters by bubble point and mean flow pore test
Liquid permeability (initial pressure drop)	NF X45-101 (1996): Filtration des liquides—membranes poreuses—perméabilité à une eau de référence NF X45-302 (2000): Cartouches filtrantes—Méthodes d'essais—détermination de la pression différentielle en fonction du débit ISO 3968, 2001—Hydraulic fluid power—filters- evaluation of differential pressure versus flow characteristics ISO 4022, 1987—Permeable sintered metal materials—determination of fluid permeability ISO 4548-1, 1997—Methods of test for full-flow lubricating oil filters for internal combustion engines—part 1: differential pressure/flow characteristics
Air permeability	NF X45-311 (2000)—Cartouches filtrantes—méthodes d'essais—détermination de la perméabilité à l'air ASTM F 778-88 (2014) Standard methods for gas flow resistance testing of filtration media
Absolute glass bead test	NF X45-304 (2000)—Cartouches filtrantes—méthodes d'essais—détermination du pouvoir d'arrêt absolu NF E48-679 (1990)—Transmissions hydrauliques- elements filtrants—détermination du pouvoir d'arrêt absolu
Particulate filtration efficiency (glass beads)	ASTM F 795-88 (1993) Standard practice for determining filter medium employing a single liquid test (Withdrawn 2002)
Particulate filtration efficiency (silica test dust)	NF X45-303 (2000): Cartouches filtrantes—méthodes d'essais—détermination de l'efficacité de filtration et de la capacité de rétention ISO 16889 (2008)—Hydraulic fluid power—filters—multipass method for evaluating filtration performance of a filter element ISO 4020 (2001) Road vehicles—fuel filters for diesel engines—test methods ISO 19438 (2003) Diesel fuel and petrol filters for internal combustion engines—filtration efficiency using particle counting and contaminant retention capacity

(Continued)

Table 13.2 Continued

Characteristics	Standards
	JIS D 1611-1 (2003): Automotive parts—lubricating oil filters for internal combustion engines—part 1: general test methods/note ISO 14085-3 (2015) Aerospace series—hydraulic filter elements—test methods—part 3: filtration efficiency and retention capacity ISO 4548-12 (2000) Methods of test for full-flow lubricating oil filters for internal combustion engines—part 12: filtration efficiency using particle counting, and contaminant retention capacity ISO 4548-4 (1997) Methods of test for full-flow lubricating oil filters for internal combustion engines—part 4: initial particle retention efficiency, life and cumulative efficiency (gravimetric method) NF EN 13443-2/IN1 (2007) Appareils de traitement d'eau à l'intérieur des bâtiments—filtres mécaniques—partie 2: particules de taille 1 µm et 80 µm—exigences de performances, de sécurité et essais NF EN 14652 (2007)—Appareils de traitement d'eau à l'intérieur des bâtiments—dispositifs de séparation membranaire—exigences de performance, de sécurité et essais
Membrane filtration efficiency (dextran)	NF X45-103 (1997) Filtration des liquides—membranes poreuses—taux de rétention des membranes d'ultrafiltration et de nanofiltration
Sterilizing filtration efficiency (microorganism)	ASTM D 3862-13 (2013) Standard test method for retention characteristics of 0.2 µm membrane filters used in routine filtration procedures for the evaluation of microbiological water quality ASTM D 3863-87 (2011) Standard test method for retention characteristics of 0.4–0.45 µm membrane filters used in routine filtration procedures for the evaluation of microbiological water quality ASTM F 838-15a (2015) Standard test method for determining bacterial retention of membrane filters utilized for liquid filtration
Water removal efficiency	ISO 16332 (2017) Diesel engines—fuel filters—method for evaluating fuel/water separation efficiency SAE J 1488 (2010): Emulsified water/fuel separation test procedure SAE J 1839 (2010) Coarse droplet water/fuel separation test procedure
Retention capacity	NF X45-303 (2000): Cartouches filtrantes—méthodes d'essais—détermination de l'efficacité de filtration et de la capacité de rétention NF L41-136 (1995) Pollution des circuits de carburant d'aéronefs—filtres et éléments filtrants—mesure de la capacité de rétention avec polluant spécifique des circuits de carburant

Table 13.2 Continued

Characteristics	Standards
	ISO 4548-12 (2000) Methods of test for full-flow lubricating oil filters for internal combustion engines—part 12: filtration efficiency using particle counting, and contaminant retention capacity ISO 4548-4 (1997) Methods of test for full-flow lubricating oil filters for internal combustion engines—part 4: Initial particle retention efficiency, life and cumulative efficiency (gravimetric method) ISO 19438 (2003) Diesel fuel and petrol filters for internal combustion engines—filtration efficiency using particle counting and contaminant retention capacity ISO 16889 (2008) Hydraulic fluid power—filters—multipass method for evaluating filtration performance of a filter element
Fatigue resistance	ISO 23181 (2007) Hydraulic fluid power—filter elements—determination of resistance to flow fatigue using high viscosity fluid
Burst differential pressure	NF X45-310 (2000): Cartouches filtrantes—méthodes d'essais—vérification de la résistance à l'écrasement ou à l'éclatement ISO 2941 (2009) Hydraulic fluid power—filter elements—verification of collapse/burst pressure rating
Axial deformation resistance	ISO 3723 (2015) Hydraulic fluid power—filter elements—method for end load test
Filter media release	NF X45-305 (2000): Cartouches filtrantes—méthodes d'essai—détermination de la masse de substances extractibles par mesurage d'extrait sec
Membrane release	NF EN 12873-4 (2006) Influence sur l'eau des matériaux destinés à entrer en contact avec l'eau destinée à la consommation humaine—influence de la migration—partie 4: méthode d'essai pour les membranes des systèmes de traitement d'eau NF XP P41-270 (2001) Effet des matériaux sur la qualité des eaux destinées à la consommation humaine—Protocole de vérification de l'inertie des matériaux constitutifs des modules de filtration placés au contact des eaux destinées à la consommation humain
Filter media cleanliness	NF X45-306 (2000): Cartouches filtrantes—méthodes d'essai—contrôle de la propreté
Filter cleanliness	ISO 4020 (2001) Road vehicles—fuel filters for diesel engines—test methods ISO 16232 (2007) Road vehicles—cleanliness of components of fluid circuits (part 1–10)

(Continued)

Table 13.2 Continued

Characteristics	Standards
Extractible matters	NF X45-305 (2000) Cartouches filtrantes—méthodes d'essai—détermination de la masse de substances extractibles par mesurage d'extrait sec ASTM D 3861-91 (2011) Standard test method for quantity of water-extractable matter in membrane filters
Chemical compatibility to the process fluid, to the cleaning fluids	NF X45-307 (2000). Cartouches filtrantes—méthodes d'essais—vérification de la résistance des éléments filtrants aux agents chimiques ISO 2943 (1998) Hydraulic fluid power—filter elements—verification of material compatibility with fluids

13.6 Source of further information

More information may be obtained from the standardization committees who developed the different test methods mentioned in this chapter:

- ASTM Subcommittee D19.08 on Membranes and Ion Exchange Materials: https://www.astm.org/COMMIT/SUBCOMMIT/D1908.htm
- ASTM Subcommittee D22.03 on Ambient Atmospheres and Source Emissions: https://www.astm.org/COMMIT/SUBCOMMIT/D2203.htm
- Subcommittee D35.03 on Permeability and Filtration: https://www.astm.org/COMMIT/SUBCOMMIT/D3503.htm
- ASTM Subcommittee E41.01 on Laboratory Ware and Supplies: https://www.astm.org/COMMIT/SUBCOMMIT/E4101.htm
- ASTM Subcommittee E55.03 on General Pharmaceutical Standards: https://www.astm.org/COMMIT/SUBCOMMIT/E5503.htm
- ISO Technical Committee TC 131/SC 6 on Fluid power systems/Contamination control: http://www.iso.org/iso/standards_development/technical_committees/other_bodies/iso_technical_committee.htm?commid=52300
- ISO Technical Committee TC 70/SC 7 on Internal combustion engines/Tests for lubricating oil filters: http://www.iso.org/iso/standards_development/technical_committees/other_bodies/iso_technical_committee.htm?commid=49880
- ISO Technical Committee TC 20/SC 10 on Aircraft and space vehicles/Aerospace fluid systems and components: http://www.iso.org/iso/iso_technical_committee?commid=46570
- ISO Technical Committee TC 22/SC 34 on Road vehicles/Propulsion, powertrain and powertrain fluids: http://www.iso.org/iso/home/standards_development/list_of_iso_technical_committees/iso_technical_committee.htm?commid=5383858
- AFNOR/E48U C Committee—transmissions hydrauliques—Éléments filtrants (hydraulic transmissions—filter elements): http://norminfo.afnor.org/structure/afnore48u/filtration-et-controle-de-la-pollution-des-fluides-hydrauliques/808
- AFNOR/P40R Committee: Appareils de traitement d'eau à l'intérieur des bâtiments (Water Treatment Devices Inside Buildings): http://norminfo.afnor.org/structure/alimentation-en-eau/1351

- AFNOR X45C Committee: Filtration des liquides—membranes poreuses (liquid filtration—porous membranes): http://norminfo.afnor.org/structure/afnorx45c/metrologie-des-membranes-filtrantes/5054
- AFNOR X45D Committee: Cartouches filtrantes (Filter Cartridges): http://norminfo.afnor.org/structure/afnorx45d/cartouches-filtrantes/2300

References

ASTM D 3861-91. (2011). Standard test method for quantity of water-extractable matter in membrane filters. ASTM International. 2 p.

ASTM D 3862-13. (2013). Standard test method for retention characteristics of 0.2 µm membrane filters used in routine filtration procedures for the evaluation of microbiological water quality. ASTM International. 3 p.

ASTM D 3863-87. (2011). Standard test method for retention characteristics of 0.4-0.45 µm membrane filters used in routine filtration procedures for the evaluation of microbiological water quality. ASTM International. 3 p.

ASTM D 6767. (2016). Standard test method for pore size characteristics of geotextiles by capillary flow test. ASTM International. 6 p.

ASTM E 128-99. (2011). Standard test method for maximum pore diameter and permeability of rigid porous filters for laboratory use. ASTM International. 4 p.

ASTM F 316-03. (2011). Standard test methods for pore size charcateristics of membrane filters by bubble point and mean flow pore test. ASTM International. 7 p.

ASTM F 778-88. (2014). Standard methods for gas flow resistance testing of filtration media. ASTM International. 15 p.

ASTM F 795-88. (1993). Standard practice for determining filter medium employing a single liquid test (Withdrawn 2002).

ASTM F 838-15a. (2015). Standard test method for determining bacterial retention of membrane filters utilized for liquid filtration. ASTM International. 6 p.

ISO 536. (2012). Paper and board—Determination of grammage. International Organization for Standardization. 6 p.

ISO 2941. (2009). Hydraulic fluid power—Filter elements—Verification of collapse/burst pressure rating. International Organization for Standardization. 9 p.

ISO 2942. (2004). Hydraulic fluid power—Filter elements—Verification of fabrication integrity and determination of the first bubble point. International Organization for Standardization. 7 p.

ISO 2943. (1998). Hydraulic fluid power—Filter elements—Verification of material compatibility with fluids. International Organization for Standardization.

ISO 3039. (2010). Corrugated fibreboard—Determination of grammage of the component papers after separation. International Organization for Standardization. 8 p.

ISO 3723. (2015). Hydraulic fluid power—Filter elements—method for end load test. International Organization for Standardization. 2 p.

ISO 3968. (2001). Hydraulic fluid power—Filters- evaluation of differential pressure versus flow characteristics. International Organization for Standardization. 11 p.

ISO 4020. (2001). Road vehicles—Fuel filters for diesel engines—Test methods. International Organization for Standardization. 48 p.

ISO 4022. (1987). Permeable sintered metal materials—Determination of fluid permeability. International Organization for Standardization. 9 p.

ISO 4548-1. (1997). Methods of test for full-flow lubricating oil filters for internal combustion engines—Part 1: Differential pressure/flow characteristics. International Organization for Standardization. 9 p.
ISO 4548-4. (1997). Methods of test for full-flow lubricating oil filters for internal combustion engines—Part 4: Initial particle retention efficiency, life and cumulative efficiency (gravimetric method). International Organization for Standardization. 30 p.
ISO 4548-12. (2000). Methods of test for full-flow lubricating oil filters for internal combustion engines—Part 12: Filtration efficiency using particle counting, and contaminant retention capacity. International Organization for Standardization. 26 p.
ISO 12103-1. (2016). Road vehicles—Test dust for filter evaluation—Part 1:Arizona test dust. International Organization for Standardization.
ISO 14085-3. (2015). Aerospace series—Hydraulic filter elements—Test methods—Part 3: Filtration efficiency and retention capacity. International Organization for Standardization. 37 p.
ISO 16232. (2007). Road vehicles—Cleanliness of components of fluid circuits (part 1–10). International Organization for Standardization.
ISO 16889. (2008). Hydraulic fluid power—Filters—Multi-pass method for evaluating filtration performance of a filter element. International Organization for Standardization. 41 p.
ISO 19438. (2003). Diesel fuel and petrol filters for internal combustion engines—Filtration efficiency using particle counting and contaminant retention capacity. International Organization for Standardization. 38 p.
ISO 23181. (2007). Hydraulic fluid power—Filter elements—Determination of resistance to flow fatigue using high viscosity fluid. International Organization for Standardization. 7 p.
ISO/TS 16332. (2017). Diesel engines—Fuel filters—Method for evaluating fuel/water separation efficiency. International Organization for Standardization. 24 p.
JIS D 1611-1. (2003) Automotive parts—Lubricating oil filters for internal combustion engines—Part 1: General test methods/Note: Approved 2013-10-21 JIS, Japanese Industrial Standards.
MIL F 8815. (1995). Military Specification Filter and Filter Elements, Fluid Pressure, Hydraulic Line, 15 Micron Absolute and 5 Micron Absolute, Type II Systems General Specification For.
NF E48-679. (1990). Transmissions hydrauliques-Éléments filtrants—Détermination du pouvoir d'arrêt absolu. Association Française de Normalisation.
NF EN 12873-4 (2006). Influence sur l'eau des matériaux destinés à entrer en contact avec l'eau destinée à la consommation humaine—Influence de la migration—Partie 4: méthode d'essai pour les membranes des systèmes de traitement d'eau. European Standard, Association Française de Normalisation.
NF EN 13443-2/IN1. (2007). Appareils de traitement d'eau à l'intérieur des bâtiments—Filtres mécaniques—Partie 2: particules de taille 1 µm et 80 µm—Exigences de performances, de sécurité et essais. European Standard, Association Française de Normalisation.
NF EN 14652. (2007). Appareils de traitement d'eau à l'intérieur des bâtiments—Dispositifs de séparation membranaire—Exigences de performance, de sécurité et essais. European Standard, Association Française de Normalisation.
NF L41-136. (1995). Pollution des circuits de carburant d'aéronefs—Filtres et éléments filtrants—Mesure de la capacité de rétention avec polluant spécifique des circuits de carburant. Association Française de Normalisation.
NF X45-101. (1996). Filtration des liquides—Membranes poreuses—Perméabilité à une eau de référence. Association Française de Normalisation.
NF X45-103. (1997). Filtration des liquides—Membranes poreuses—Taux de rétention des membranes d'ultrafiltration et de nanofiltration. Association Française de Normalisation.

NF X45-301. (2000). Cartouches filtrantes—Méthodes d'essais—Contrôle d'intégrité par détermination du point de première bulle. Association Française de Normalisation.
NF X45-302. (2000). Cartouches filtrantes—Méthodes d'essais—Détermination de la pression différentielle en fonction du débit. Association Française de Normalisation.
NF X45-303. (2000). Cartouches filtrantes—Méthodes d'essais—Détermination de l'efficacité de filtration et de la capacité de rétention. Association Française de Normalisation.
NF X45-304. (2000). Cartouches filtrantes—Méthodes d'essais—Détermination du pouvoir d'arrêt absolu. Association Française de Normalisation.
NF X45-305. (2000). Cartouches filtrantes—Méthodes d'essai—Détermination de la masse de substances extractibles par mesurage d'extrait sec. Association Française de Normalisation.
NF X45-306. (2000). Cartouches filtrantes—Méthodes d'essai—Contrôle de la propreté. Association Française de Normalisation.
NF X45-307. (2000). Cartouches filtrantes—Méthodes d'essais—Vérification de la résistance des éléments filtrants aux agents chimiques. Association Française de Normalisation.
NF X45-310. (2000). Cartouches filtrantes—Méthodes d'essais—Vérification de la résistance à l'écrasement ou à l'éclatement. Association Française de Normalisation.
NF X45-311. (2000). Cartouches filtrantes—Méthodes d'essais—Détermination de la perméabilité à l'air. Association Française de Normalisation.
NF XP P41-270. (2001). Effet des matériaux sur la qualité des eaux destinées à la consommation humaine—Protocole de vérification de l'inertie des matériaux constitutifs des modules de filtration placés au contact des eaux destinées à la consommation humain. Association Française de Normalisation.
SAE J 1488. (2010). Emulsified Water/Fuel Separation Test Procedure. SAE International.
SAE J 1839. (2010). Coarse Droplet Water/Fuel Separation Test Procedure. SAE International.

This page intentionally left blank

Specific testing of textiles for transportation

14

M. Richaud, O. Vermeersch, P.I. Dolez
CTT Group, Saint-Hyacinthe, QC, Canada

14.1 Introduction

The use of textiles in transportation may be associated with the need to combine comfort and functionality. Sails were used in ships transporting goods; cushions and curtains were used in carriages or trains for the comfort of passengers; and airplane wings were made out of woven canvas for instance. The evolution of each means of transportation along with the increased awareness about the importance of passengers' safety pushed research and development forward towards a larger use of lightweight, fire-resistant, nontoxic, and durable textiles in transportation.

This chapter starts with a presentation of the transportation textile market. Then, different aspects of textile testing relevant to the transportation industry are discussed. The chapter ends with considerations regarding future trends for textiles in transportation.

14.1.1 MobilTech—A growing market

The international trade fair for technical textiles, Techtextil, has set up a classification for technical textiles according to their area of application (Techtextil, 2016). One of these twelve areas—which also include Agrotech, Buildtech, Medtech, and Oekotech—is Mobiltech symbolized by a tire symbol, which covers textiles for ship and aircraft construction as well as all aspects of automobile, railway, and space travel. The Mobiltech sector is in full growth due to the rapid development of all means of transportation and increased safety requirements for passengers (Bertrand, 2005). For instance, the need for fire-retardant materials in the case of a plane or train crash or a car accident is critical to limit the rate of ignition of fabrics and flame propagation; the extra time it will give passengers to exit the wreck will definitely increase their chances of survival.

14.1.1.1 Road vehicles

The automotive sector is the largest consuming sector of technical textiles worldwide (Carrigg & Alarid, 2016). According to the 2015 International Trade Statistics released by the World Trade Organization, the total of world exportations of automotive products was worth $1395 billion, representing 7.5% of the world's merchandise exports (WTO, 2015). In 2014, Europe was exporting around 51.5% of this share, before Asia (23.9%) and North America (20.9%). Technical textiles refer to the manufacture of a wide range of automotive products such as seatbelts, airbags, upholstery, headliners, carpets, tire

Advanced Characterization and Testing of Textiles. https://doi.org/10.1016/B978-0-08-100453-1.00015-5

reinforcements, filters, fiber-reinforced composites, thermal and acoustic insulators, etc. They are used in cars; in recreational vehicles such as motorcycles, snowmobiles, campers, and quads; in public transportation such as buses and streetcars; and in commercial vehicles such as trucks, fire trucks, ambulances, army vehicles, and construction trucks. Textile exports, when considered separately from clothing, accounted for $314 billion in 2014 (WTO, 2015).

Rising concerns for road traffic safety have motivated governments to impose stricter legislations and apply new standards in automotive transportation, such as the compulsory use of 3-point seatbelts and the presence of airbags for drivers as well as front and rear passengers. A study performed by Markets and Markets Analysis predicts that the increase in the demand for premium cars in regions such as Europe, North America, and Asia Pacific should drive the airbag and seatbelt markets upward to $23.6 and $9.0 billion respectively by 2019 (M&M, 2014a).

In the area of composites, the value of the automotive market is expected to reach more than $7 billion by 2019, with a compound annual growth rate of 22% for carbon fiber reinforced polymer composites (M&M, 2014b). Indeed, textile-reinforced composites offer an interesting opportunity to help solve the weight challenge (Wilson, 2015). In 2014, the automotive industry produced 58,000 tons of carbon fiber-reinforced composites, 1.6 million tons of natural fiber-reinforced composites, and 3 million tons of glass fiber-reinforced composites.

14.1.1.2 Aircrafts

The use of technical textiles in aircrafts has long contributed to the reduction in weight and the associated reduction in fuel expenses. But even though the introduction of mandatory seatbelts and the presence of life vests under the seats have contributed to saving many lives, the presence of synthetic fabrics in airplanes has also been the cause of many deaths. According to a study led by the National Transportation Safety Board on 26 plane crashes that occurred between 1983 and 2000, among the 45% passengers who did not survive the accidents, 26% lost their lives because of the violence of the impact while almost 5% died of fire-related causes (NTSB, 2001). In addition, it was observed that, in crashes with a higher survivability rate after impact, the rate of fire-related causalities was higher. As a matter of fact, many polymers used in seats, curtains, cushions, carpets, etc. do not display a high enough flame retardancy and/or they generate toxic fumes while burning (Bertrand, 2005).

Furthermore, in the last 20 years, the proportion of fiber-reinforced composites used in the aerospace industry has increased from 10% to 50%, such as in the Airbus 350 XWB or the Boeing 787 Dreamliner (Airbus, 2016). The objective is to reduce the overall weight of the structure and cut fuel consumption. These materials also require less maintenance thanks to the larger resistance to corrosion. However, the cost of the carbon fiber raw material is still higher than steel or aluminum, for instance, despite the twofold drop over the last decade made possible by the increased production volume and the development of new manufacturing processes. Carbon fiber-reinforced composites are gaining ground and becoming competitive thanks to the reduction in defects and cycle time as well as the development of new resin systems and new fiber

placement and composite manufacturing processes (Rao, Simha, Rao, & Ravi Kumar, 2015); this provides interesting perspectives for aircraft manufacturers willing to push innovation forward in this sector of industry.

14.1.1.3 Marine transportation

Textiles also hold a large place in marine transport (Singha & Singha, 2012): sails, inflatable crafts, life jackets, personal flotation devices, hovercraft skirts, reinforcement for composite parts, securing and lifting webbings, upholstery, etc. In fact, some even wonder if, with a compound annual growth rate expected to exceed 6% by 2020, marine composites would not be one of the key components of the future of the textile industry (Technavio, 2016). Indeed, marine vessels made of textile-reinforced composites are about 50% lighter than those made of steel and more than 30% lighter than those made of aluminum.

In terms of performance, the technical textiles used in the marine industry are subjected to strict requirements to ensure the safety of the passengers and merchandise that are transported. Flame resistance may thus be a critical criterion for some applications. In addition, requirements may include resistance to puncture and tearing as well as to ultraviolet rays, sea salt, and humidity exposure.

These highly demanding requirements have pushed innovation forward within this sector; the use of new materials has been investigated in order to insure the durability of the structures in particular. As a matter of fact, boat hulls are now made of glass fiber reinforced composite with a vinylester matrix, which provides an increased resistance to UV exposure and salt corrosion (Miyano & Nakada, 2009). Other high performance materials used in marine transportation include Spectra®, a high strength/high modulus extended chain polyethylene fiber whose chemical and abrasion resistance is superior to aramids; Treviria, a heat treated polyester fiber fabric; and carbon fibers (Singha & Singha, 2012).

14.1.1.4 Rail transport

The railway industry is another important market for technical textiles. It comprises trains and subways. The growth is fueled by the sustained demand in Asia and Western Europe as well as rising markets in Africa/Middle East and Eastern Europe (Statista, 2016). Textiles are used in flooring (carpets), seats, ceilings, curtains, as well as reinforcement for composite parts. The main driver for textile use in rail transport is, once again, weight.

Requirements for textiles in trains include nontoxicity of smoke, flame resistance, low abrasion, and durability. In particular, the toxicity of smoke in the case of a fire and emissions of volatile organic compounds (VOC) as a result of use are of large concern. Examples of requirements for fabrics and composites used in passenger rail transportation may be found in the standard NFPA 130 (2017) relative to fixed guideway transit and passenger rail systems. It covers seat upholstery, covers, window shades, woven seat cushion suspensions, and other fiber reinforced composite body parts.

14.1.1.5 Other applications

Mass transportation is subject to very high standards in terms of passengers' safety. These translate into high requirements set by national and international regulations on fabric and composite properties and performance. On the other hand, recreational motor vehicles such as snowmobiles, motorcycles, jet skis, and sailing ships are not bound to such strict specifications, for instance, in terms of safety or durability. Requirements on constitutive materials are thus less demanding.

The aerospace industry has also benefited from the significant improvements in terms of mechanical properties of technical textiles. For instance, the thermal protection system of space rockets/shuttles may include fibrous silica batting, graphite rayon fabric-reinforced phenolic resin composite, aramid felts, and/or alumina fiber cloth (Milgrom, 2013). On the other hand, solar sails, made of aluminized carbon fiber fabrics, for instance, may open up new regions of the solar system to exploration by allowing the development of propellant-free interplanetary space crafts (Johnson, 2012).

14.1.2 Regulations, OEM specifications, and standardization organizations

For most applications, the performance of technical textiles used in mass transportation is highly regulated for the sake of the passengers' safety. For that purpose, standards and specifications have been developed and are enforced by national regulations. Tight control of raw materials and components by manufacturers of finished products is also observed.

14.1.2.1 The stakeholders

Over the years, the technical textile market has experienced a steady growth, increasing from less than 15 million tons and about $80 billion in 1995 to more than 23.5 million tons and about $130 billion in 2010 (David Rigby Associates, 2003). The trend is not slowing down: a TechNavio analysis has forecasted that the global technical textile market will reach a compound annual growth rate of 3.71% over the period 2015–19 (Technvio, 2014). Given the broad use of technical textiles on all five continents, this large growth rate has led to a need for manufacturers of technical textiles worldwide to standardize their testing methods for transportation applications.

In particular, the requirements of manufacturers of transportation equipment have increased over time as regulations towards passengers' safety have become more stringent (Pamuk & Çeken, 2009). Part and component suppliers are also experiencing an increase in competition and a request for the improvement in their product quality in order to keep their original partnerships and comply with the market expectations. Being able to rely on the suppliers' constant quality is a concern for manufacturers of transportation equipment. Some original equipment manufacturers (OEM) and their clients have built strong partnerships based on the sharing of common values regarding quality and safety. The key is to offer clients the best products available on the market at the desired price.

Since the creation of the International Organization for Standardization (ISO) in 1947, a series of technical committees have been formed to support the development of standards in the various transportation means, including the following (ISO 2016):

- ISO/TC22 for road vehicles, which was formed in 1947 and has published 839 standards;
- ISO/TC 20 for aircraft and space vehicles, which was also formed in 1947 and has published 649 standards;
- ISO/TC 8 for ships and marine technology, formed in 1947 as well and has published 288 standards;
- ISO/TC 269 for railway applications, which was formed in 2012 and has published 2 standards;

The establishment of these reference testing methods has helped engineers develop products that can easily be exported worldwide.

At the state level, standardization activities in the field of transportation equipment have also been conducted within the American Society for Testing and Materials (ASTM), the Canadian Standards Association (CSA), the Association Française de Normalisation (AFNOR), the Deutsches Institut für Normung (DIN), the British Standards Institution (BSI), the Italian Organization for Standardization (UNI), the Japanese Engineering Standards Committee (JESC), and the Standardization Administration of China (SAC) for instance. In addition, the Society of Automotive Engineers (SAE) is a US-based association whose mission includes the development of standards. Initially limited to the automobile industry, its scope has been broadening in 2016 to include engineers in all types of mobility-related professions.

14.1.2.2 Standards for fire protection and smoke toxicity

Passengers' safety is the major concern for Mobiltech textile manufacturers and has to be ensured by a tight control of the fire performance of the textile components and assemblies. Great efforts have been devoted over the last years to developing fire-resistant and nontoxic smoke generating textiles for airplanes, trains, ships, and road vehicles. In parallel, standards were established to confirm the level of performance of these materials.

For instance, the National Fire Protection Association (NFPA) in the United States has published a series of standards for textiles used in transportation. These documents include good practices in terms of testing methods of the fire behavior on fibers, fabrics, and composites, and the measurement of the level of toxicity of the fumes generated upon burning. The use of these standards is not limited to the United States and has found a large echo among manufacturers of transportation equipment.

A certain hierarchy may be observed regarding fire protection and smoke toxicity requirements. In the case of aircrafts, the US Federal Aviation Administration is the leading authority (Horrocks, 2013). At a second level, aircraft manufacturers (Boeing, Bombardier, Airbus, etc.), as well as part and component suppliers set the performance thresholds along with the certification procedures. For trains, the NFPA is a leader for urban communities (for subways and commuter trains) and states (for other rolling stocks) in North America. In Europe, the standard series EN 45545 relative to fire protection on railway vehicles, which was published in 2010, is gradually being adopted and should prevail over state authorities as well as rolling stock manufacturers.

14.1.2.3 Standards on structural and aesthetic durability

Some textiles used for Mobiltech applications are also subject to various mechanical constraints. Fiber reinforced composites used for structural applications such as in airplane fuselages or wings, car doors, roofs and bodywork parts have to maintain their mechanical properties for the entire lifetime of the structure. It is therefore critical, especially when passengers' safety is at stake, to assess the durability of structural parts and observe the damages induced by mechanical stressors, including impact, fatigue, and abrasion.

In addition, technical textiles used for carpets, curtains, upholstery, and headliners may also have to resist use and abuse, including acts of vandalism. In Europe, fabrics are increasingly used for railway seat manufacturing in order to reach passengers' expectations in terms of comfort but also reduce the overall weight of the train. These fabrics have to be particularly resistant to tearing, cutting, marker and paint, chewing gum stains, etc. Resistance to these aggressors has to be assessed by laboratory tests prior to introducing the product on the market.

Many textiles used inside private or public means of transportation also serve an aesthetic function; thus, this aspect has to be maintained as much as possible over the lifetime of the product. For that purpose, color fastness to ultraviolet or perspiration exposure along with crocking tests are conducted on dyed fabrics, and resistance to pilling is assessed on carpets, curtains, and upholstery.

All of these tests are required by car, airplane, train, and ship manufacturers and must be conducted by Mobiltech textile suppliers. These tests may also be stipulated by competent authorities such as the National Highway Traffic Safety Administration (NHTSA) in the United States, Motor Vehicle Safety (MVS) in Canada, or the European Council for Automotive R&D (EUCAR) in Europe.

14.2 Performance testing related to safety

The testing of automotive equipment safety has been implemented for a long time by the car manufacturers themselves. Some major groups such as Ford Motor Co. and General Motors Corp. in the United States have invested millions of dollars to evaluate safety accessories in high-tech research centers (Johnson, 2005; White, 2015). For instance, Ford invested $65 million in 2005 to improve its safety testing facilities. Efforts include engineering adaptive airbags and seatbelts.

Similarly, the suppliers of safety components and materials are expected to design and manufacture very high quality products with no room for failure, especially when it comes to tires, airbags, seatbelts, emergency handles, oxygen masks in airplanes, and life vests in airplanes and boats. This implies a high safety factor in the design and no manufacturing defects.

14.2.1 Airbags

The first airbag system for cars was developed in 1951 (Hetrick, 1953). It consisted originally of bladders inflated with compressed air. Nowadays, they are made of plain

weave super high tenacity nylon 6,6 or polyester (PET) fabrics (Orme, Walsh, & Westoby, 2014). Some are coated with silicone and equipped with vents in the back as a way to allow a controlled deflation after impact. In addition, a large increase in the airbag inflation rate upon impact has been obtained. They now inflate through a chemical reaction generating nitrogen gas in <50 ms (Tan & Yu, 2012).

During a car crash, the kinetic energy of the car is released into the bodies of the passengers who are propelled toward the windshield. Their acceleration relative to the car depends on the speed of the vehicle prior to the impact and the accumulation of energy during the crash (Sobhani, Young, Logan, & Bahrololoom, 2011). As a complement to seatbelts, the presence of airbags is now considered as a key factor for survival during a crash. Airbags are controlled by a central unit which monitors a series of sensors, including accelerometers that can detect variations in the vehicle speed indicative of a crash. Due to the forces involved and the speed of the airbag deployment and inflation, it has to be constructed out of very high strength fabrics so that it does not explode, distort, or tear during the two most critical phases of its action: inflation and impact of the body. The airbag has thus to be designed so that it does not fail catastrophically, doesn't allow tear propagation, and includes very high safety factors.

A first step in assessing airbag requirements consists of evaluating the different speeds at which bodies will be propelled toward the airbags depending on the weight of the body and the initial car velocity. In the case of a crash involving two moving vehicles, the kinetic energy of the crash may double if the collision is frontal. To help car manufacturers determine the requirements of their airbags, Sobhani et al. (2011) developed a model allowing the estimate of the injury severity in the case of a two-vehicle crash based on the calculation of the collision kinetic energy using the car speed, total mass, angle of collision, etc.

Tests assessing the performance of airbags in the United States may be conducted on the entire system using unbelted 50th-percentile size and weight male instrumented crash dummies seated in the front of a vehicle impacting a fixed rigid barrier perpendicular to its axis of travel at speeds of up to 48 km/h (FMVSS 208). Injury criteria are set in terms of head acceleration, thoracic acceleration, chest deflection, force transmitted axially through the upper leg, and level of neck injury. In addition, all portions of the dummy shall remain inside the passenger compartment. By comparison, the corresponding European test method involves belted crash test dummies (ECE 94, 2003). The airbag module may also be evaluated using a test stand that simulates deployment conditions in a vehicle (ASTM D5428, 2008). The performance is assessed in terms of the variation in the airbag pressure and geometry over time as well as final conditions of the airbag module components.

The requirements may also be set on the airbag fabric, yarn, and sewing thread (Fung & Hardcastle, 2001). Efforts to provide standardized test methods to that extent have been carried out by the ASTM Subcommittee D13.20 on inflatable restraints, the Society of Automotive Engineers (SAE), and car manufacturers, for instance. Table 14.1 provides a list of fabric properties relevant to airbag with examples of associated test methods. In addition, the fabric may be inspected for imperfections using ASTM D5426 (2012).

Table 14.1 Airbag fabric properties and associated test methods

	Property	Test method
Physical (ASTM D5446, 2008)	Thickness	ASTM D1777
	Mass per unit area	ASTM D3776 (option C)
	Coating weight	ASTM D3776 (option C)
	Blocking (coated fabric)	SAE J912-A
	Count of woven fabric	ASTM D3775
	Bow and skew	ASTM D3882
	Nonfibrous content	ASTM D2257 using chloroform as the solvent
	Presence of sizing	ASTM D6613
	pH	AATCC Method 81
	Fogging (volatility)	Ford Test Method BO116-03
	Odor	SAE Practice J 1351
	Flammability	Federal Motor Vehicle Safety Standard 302
	Air permeability	ASTM D737 or DIN 53 887
	Dynamic air permeability	ASTM D6476
	Breaking force and elongation	ASTM D5034
	Stiffness	ASTM D4032 for warp and filling directions or ASTM D1388 (option 2: cantilever) for directional stiffness
	Burst strength	ASTM D3786
	Edgecomb resistance	ASTM D6479
	Tear strength	ASTM D2261 or ASTM D1424 for tongue tear or ASTM D5587 for trapezoid tear
	Abrasion resistance	ASTM D4157
	Coating adhesion	ASTM D4851 or Ford Motor Company FLTM BN-13-1
	Packability	ASTM D6478
Durability (ASTM D5427, 2009)	Cycle aging	ASTM D5427
	Heat aging	ASTM D5427
	Humidity aging	ASTM D5427
	Ozone aging	ASTM D5427

14.2.2 Seat belts

The presence of seat belts in cars dates back to 1930 after two American doctors found that crash related injuries in cars were largely related to the motion of passengers under the effect of their kinetic energy and could be prevented by an appropriate retention system (Imre & Cotetiu, 2014). Lap or 2-point seat belts became compulsory in Europe for front car seats in 1965. A further improvement was the introduction of 3-point seat belts that restrain the motion of the chest toward the steering wheel or the front panel, which proved to be fatal in many cases: They are now mandatory in front and back seats of cars in many countries and are also used in a series of other road

vehicles such as trucks and in the front seats of other commercial vehicles such as buses and ambulances. Lap seat belts are still found in buses and aircrafts for passenger seats. In the case of child safety seats as well as for aircraft and racing car pilots for instance, 4-, 5-, or 6-point seat belts are used with additional buckling belts over the other shoulder and between the legs.

Current 3-point seat belt systems comprise a piece of webbing, a retractor, a pillar-loop, a tongue, a buckle, and a 3rd point anchor. The webbing is generally a multiple layer woven made of high-tenacity continuous filament polyester yarns (Fung & Hardcastle, 2001). It has to have very high strength and good abrasion resistance, be soft and flexible in the longitudinal direction and rigid in the transverse direction, and resist UV degradation.

According to the current process in the car industry, the information about seat belt components is provided to the component manufacturer in a Design Goal Document (DGD) (Imre & Cotetiu, 2014). This includes the positioning of each seat belt component, which depends on the inside layout of the car, as well as the vehicle destination market, which will dictate which standards the seat belt system has to comply with. For instance, Europe refers to ECE R16 (restraints and safety belts) and ECE R44 (child restraints in power driven vehicles), while requirements for seat belts used in the United States are provided in FMVSS 208 (occupant crash protection), FMVSS 209 (seat belt assemblies), FMVSS 210 (anchorages for seat belt assemblies), and FMVSS 213 (child restraint system). If a car manufacturer decides to develop a new component for its seat belts, it will go through several steps of validation before having its component accepted by the competent committees and organisms. Computer aided design (CAD) will help model the component and choose the raw materials. It is also used for running virtual failure analysis through a failure mode and effects analysis (FMEA) and constraint accumulation calculation by finite elements analysis (FEA). Then tests will be run on prototypes, including abrasion, puncture resistance, stiffness, elongation at break, ultimate tensile strength, accelerated fatigue testing, and UV, heat, and humidity aging. Finally, a serial process control (SPC) will determine the stability and predictability of the process.

As in the case of airbags, seat belts may be tested as a system using a 50th percentile adult male dummy in the driver and passenger front seats of a vehicle subjected to frontal barrier crash test, lateral moving barrier crash test, and rollover test (FMVSS 208). The frontal barrier crash test involves the vehicle impacting a fixed rigid barrier perpendicular to its axis of travel at speeds up to 48 km/h. In the lateral moving barrier crash test, the vehicle is impacted laterally on either side by a barrier moving at 32 km/h. The rollover test is conducted at 48 km/h over a concrete surface. Depending on the test performed, injury criteria may be set in terms of head acceleration, thoracic acceleration, chest deflection, force transmitted axially through the upper leg, and/or level of neck injury. In addition, all portions of the dummy shall remain inside the passenger compartment.

Requirements may also apply to the webbing materials. The performance factors to be assessed include the following (TC TSD 209, 2013):

- Width after conditioning for at least 24 h in an atmosphere having a temperature of 23°C and a relative humidity between 48% and 67%;
- Breaking strength measured with a rate of grip separation between 51 and 102 mm/min;

- Elongation when subjected to a force of 11.120 N;
- Resistance to abrasion, measured in terms of residual breaking strength;
- Resistance to light, measured in terms of residual breaking strength and color retention after 100 h exposure to type E carbon-arc at 60°C; and
- Resistance to microorganisms, measured in terms of residual breaking strength.

14.2.3 Tires

If they cannot be considered as a safety accessory per se, tires play a very large role in ensuring the safety of the vehicle. At the interface with the ground, they are a key component that determines the vehicle behavior while it ramps up and brakes. Developed and patented in the mid-19th century by a Scottish engineer, R. W. Thompson, pneumatic tires take advantage of the exceptional performance of vulcanized rubber (Fung & Hardcastle, 2001). A Scottish-born veterinary surgeon, John Boyd Dunlop, rediscovered pneumatic tires at the end of the nineteenth century while trying to improve the rolling comfort of his son's tricycle. His design involved the use of a fabric as reinforcement for the rubber. Another large step was made in 1946 by Michelin, who invented the radial tire method of construction. The more stable structure it produces allows a large increase in the tire longevity, driving safety, and fuel efficiency compared to the original cross-ply construction. They now have taken over most of the passenger road vehicle market, and the use of cross-ply tires is limited to some applications for trucks, trailers, farm equipment, and emerging markets (Lindenmuth, 2006).

Car and light truck radial tires contain about 5% polymer textiles for the carcass and 10%–12% of steel for the belt, which provide strength to the tire (McDonel, 2006). The amount of textile in cross-ply tires is larger with about 21% (Fung & Hardcastle, 2001). Textiles in radial carcasses are primarily composed of polyester, while they are mostly nylon for cross-ply structures (McDonel, 2006). Aramids are also used when high strength-to-weight ratio and temperature resistance are required, for instance, in aircrafts and racing cars (Fung & Hardcastle, 2001). A small amount of aramid and nylon may be found as well in belt overlays (McDonel, 2006). Other tire components include natural and synthetic rubber, reinforcing fillers such as carbon black and silica, and various additives including vulcanization agents, plasticizers, stabilizers, antioxidants, and antiozonants (Lindenmuth, 2006).

Some tests are performed on the whole tire structure as described for instance in the US Federal Motor Vehicle Safety Standard (FMVSS 139) or in its European counterpart (EC 661, 2009). In the case of pneumatic tires, they cover the tire dimensions, high speed performance, endurance, low inflation pressure performance, and strength. In addition, the tire textile components may also be tested at the yarn, cord, and fabric scale (ASTM D885, 2010). Table 14.2 provides a list of the properties tested along with examples of applicable test methods.

14.2.4 Lifting and securing slings

When goods are transported by road, boat, train, and air, they have to be strongly secured to keep them from tilting, sliding, or moving around, which would be a source of danger and/or might damage them (DVSA, 2017). Straps and slings are

Table 14.2 Tire yarn, cord, and fabric properties and associated test methods (Fung & Hardcastle, 2001; ASTM D885, 2010)

Property	Test method
Yarns and cords	
Commercial mass of yarns	ASTM D2494, option II
Commercial mass of cords	As agreed upon between the purchaser and the supplier
Linear density	ASTM D1907 for yarns, ASTM D885 for cords
Thickness of cords	ASTM D885
Twist in yarns and cords	ASTM D885
Identification of fibers	ASTM D276
Extractable matter in yarns and cords	ASTM D2257
Moisture regain	ASTM D885
Breaking strength (force) of conditioned yarns and cords	ASTM D885
Breaking strength (force) of rayon yarns and cords at specified moisture regain level	ASTM D885
Elongation at break of conditioned yarns and cords	ASTM D885
Elongation of rayon yarns and cords at a specified moisture regain level	ASTM D885
Force at specified elongation (FASE) of conditioned yarns and cords	ASTM D885
Breaking tenacity of conditioned yarns and cords	ASTM D885
Modulus of conditioned yarns and cords	ASTM D885
Breaking strength (force) of oven-dried rayon yarns and cords	ASTM D885
Elongation at break of oven-dried rayon yarns and cords	ASTM D885
Force at specified elongation (FASE) of oven-dried rayon yarns and cords	ASTM D885
Breaking tenacity of oven-dried rayon yarns and cords	ASTM D885
Work-to-break of yarns and cords	ASTM D885
Breaking toughness of yarns and cords	ASTM D885
Breaking strength (force) of yarns and cords at elevated temperature	ASTM D885
Shrinkage of conditioned yarns and cords at elevated temperature	ASTM D885, ASTM D4974
Shrinkage force of conditioned yarns and cords at elevated temperature	ASTM D885
Contraction of wet yarns and cords	ASTM D885
Growth of conditioned yarns and cords	ASTM D885
Dip (adhesive) solids pickup on yarns and cords	ASTM D885

Continued

Table 14.2 Continued

Property	Test method
Adhesion of cord to elastomers	ASTM D4393, ASTM D4776, ISO 4647
Longitudinal air permeability of tire of cords and yarns	ASTM D2692
Tire cord fabrics	
Commercial mass of cord fabric	As agreed upon between the purchaser and the supplier
Width	ASTM D3774
Mass of per unit area	ASTM D3776
Count	ASTM D3775 with modification
Stiffness	ASTM D885
Longitudinal air permeability of tire fabrics and cord fabrics	ASTM D2692

generally used to ensure this function. They may also be employed as a way to lift objects to load them on and unload them from the transportation mean. They are generally made with high-tenacity polyamide, polyester, or polypropylene multifilament.

A series of European standards cover the safety aspects of textile slings: flat woven webbing slings made of manmade fibers (EN 1492-1, 2008), roundslings made of manmade fibers (EN 1492-2, 2008), and lifting slings made from natural and manmade fiber ropes (EN 1492-4, 2008). A fourth standard for disposable flat woven slings is in preparation. Properties and performance of slings assessed in these standards comprise the type of polymer and yarn; the webbing construction, width, thickness, and tenacity; the change in webbing width under load; the working load limit and minimum failure force; and the interaction of the sling with fittings. A description of requirements and test methods may also be found in ASME B30.9 (2010) for slings used in conjunction with cranes and ANSI B77.1a (2012) for passenger ropeways (aerial tramways, aerial lifts, surface lifts, tows and conveyors), for instance.

14.3 Testing related to flammability, smoke generation, and toxicity

Tests concerning flammability, smoke generation, and toxicity are very common for a large number of transportation applications because reduced flammability is one of the main safety requirements of almost all textiles used for passenger transportation. However, test methods may vary depending on the conditions the textile will be exposed to while in service. In addition, performance thresholds may also depend on the type of transportation means. For instance, the same textile flammability test may be associated with a more constraining threshold for aerospace applications than in the

automotive industry. Therefore, this section is divided by transportation means. More details about the individual test methods may be found in Chapter 8 on flammability testing.

14.3.1 Road vehicles

For automotive applications, standards concerning flame resistance of materials have been prepared by international and national organizations as well as car manufacturers. For instance, Volvo has broadened the scope of the NHTSA flammability test for motor vehicle interior materials, FMVSS 302, by conducting the test on specimens aged for 14 days at 38°C at 95% RH and at 70°C in addition to conditioned specimens (VCS 5031,19, 2004). Some countries have also adopted modified versions of standards issued by organization such as NFPA, the EU Council, and NHTSA in the United States.

The most common flammability test for road vehicle interior materials measures the horizontal burning rate of specimens exposed to a low-energy flame for 15 s in a combustion chamber (FMVSS 302; ISO 3795, 1989; ASTM D5132, 2011; VCS 5031,19, 2004). The test also determines if and when the flame self-extinguishes. It applies to textiles situated within 13 mm of the occupant compartment air space in passenger cars, multipurpose passenger vehicles, trucks, and buses, as well as for tractors and agriculture and forestry machinery.

Other flammability test methods may involve a test chamber replicating the section of a school bus to assess the burning behavior of upholstered seating used in school buses (ASTM E2574, 2012). The chamber is equipped with two ventilation openings at each end and holds three rows of seats. The ignition source consists of a propane gas burner installed either on top or under one of the seats. The flammability performance is assessed in terms of the time elapsed between ignition and flame extinguishment, mass loss of the seat assembly, occurrence of flame spreading to other seats, and seat material melting or dripping.

14.3.2 Aerospace

In Europe, the European Aviation Safety Agency (EASA) has regulatory authority and executive tasks in the field of civil aviation safety. It works jointly with the National Aviation Authorities (NAAs) of the different European country members of the ESEA in order to ensure that airplane manufacturers and OEMs from these different countries fulfill the various standardization requirements and regulations. EASA also works on technical agreements with its counterparts in the world such as the Federal Aviation Administration (FAA) in the United States or the Canadian Aviation Regulation (CAR). The FAA publishes federal aviation regulations (FAR) and advisory circulars (AC), which provide guidance for compliance with airworthiness standards for airplane manufacturers.

For instance, the FAA standard on airworthiness of airplanes (FAR/CS 25.853) includes several flammability test methods that apply to textile components:

- 12 s vertical flame test, with measurement of the flame time, burn length, and flaming time of drippings;
- 15 s horizontal flame test, with measurement of the average burn rate;

- Seat cushion flame test, with measurement of the burn length and weight loss;
- Radiant heat exposure test, with measurement of the heat released;
- Smoke emission test, with measurement of the specific optical smoke density.

EASA for its part is currently reviewing its legislation on civil aircrafts to take into account the increased air traffic and arrival of new technologies such as drones (Juul, 2016). In particular, it intends to better standardize the way flammability testing is conducted (EASA CM-CS-004, 2013).

Some aerospace companies have also developed their own flammability test standards. For instance, Boeing's BSS fire test standards include vertical, horizontal, and 45 degrees flame tests (BSS 7230), smoke density tests (BSS 7238), gas toxicity tests (BSS 739), and heat release tests (BSS 7322) (AIM-Aerospace, 2015). Airbus has also vertical (AITM 2.0002A and B), horizontal (AITM 2.0003), and 45 degrees (AITM 2.0004) flame tests, heat release test (AITM 2.0006), and smoke density tests (AITM 2.0007). In Canada, Bombardier requires conformance to its SMP 800C test for toxic gas generation.

14.3.3 Rail

The NFPA Standard for Fixed Guideway Transit and Passenger Rail Systems (NFPA 130, 2014) provides guidelines on tests to be performed on materials used in trains. Their behavior in the case of a fire is characterized by their flame resistance and smoke emission. Tests may be carried out on component materials or complete seat or mattress assembly. Table 14.3 lists test methods recommended in the NFPA 130 standard (2014) as well as in other US standards such as ASTM E2061 (2015) and FRA 216 (1999) of the Federal Railroad Administration for the different types of textiles or textile-based items.

The permanence of the surface flammability and smoke emission characteristics of the materials is also verified after dynamic fatigue testing using roller shear or constant force pounding (ASTM D3574, 2016), after washing according to the manufacturer's recommended procedure or ASTM E2061 (2015), and, if relevant, after dry cleaning according to ASTM D2724 (2007).

Table 14.3 Flammability and smoke emission test methods for textiles or textile-based items used in rail vehicles (ASTM E2061, 2015)

Material or item category	Flammability test	Smoke emission test
Cushion and mattress material	ASTM D3675	ASTM E662
Fabrics for upholstery, curtains, covers, wall coverings, drapes, shades, etc.	FAR/CS 25.853, vertical test	ASTM E662
Floor covering	ASTM E648	ASTM E662
Thermal or acoustical insulation	ASTM E162	ASTM E662
Fabric-reinforced composite panels	ASTM E162	ASTM E662
Complete seat assembly	ASTM E1537	ASTM E1537
Complete mattress assembly	ASTM E1590	ASTM E1590

In Europe, a common strategy in terms of fire requirements and test methods for materials used in railway vehicles has been set with the recent publication of the standard EN 45545-2 (2013). Requirements depend on the amount of material, its location, its use, and if it is in contact with another material. Three main categories of performance are measured:

- Ignitability and flame spreading using ISO 5658-2 (2006) for curtains and shades, ISO 12952-2 (2010) for linens and blankets, ISO 9239-1 (2010) for composite flooring, ISO 11925-2 (2010) for air filters
- Heat release rate using a cone calorimeter technique (ISO 5660-1, 2015)
- Smoke generation (ISO 5659-2, 2012)

In addition, flame tests are conducted on complete seats in a large scale chamber according to ISO/TR 9705-2 (2001). The results are obtained in terms of the variation of the heat output and heat release rate with time. The seats are tested in the as-produced condition as well as after damage has been created to simulate an act of vandalism committed with a knife (EN 45545-2, 2013).

14.3.4 Marine

The International Maritime Organization (IMO) has the worldwide authority to set new standards for safety, minimum official requirements, and environmental performance of naval transportation ships. For instance, it has published fire test procedures (FTP) for testing flammability of materials including textiles used onboard. Table 14.4 provides a list of these different tests. The flammability test for vertically suspended textiles and films is also performed on specimens subjected to accelerated aging by dry-cleaning, laundering, water leaching, and weathering (IMO FTP Code, 2010).

Indications about fire test methods for textiles used in marine ships may also be found in the US Code of Federal Regulations 46 CFR Part 72.05-55 subsection relative to structural fire protection for furniture and furnishings for shipping. In addition, ship manufacturers may have to assess the fire characteristics of mattresses and bedding assemblies according to NFPA 267 (1998). The test method uses an open calorimeter environment to determine the heat release, smoke density, weight loss, and generation of carbon monoxide of mattresses and bedding assemblies exposed to a flaming ignition source.

Table 14.4 IMO fire test procedures relevant to textiles onboard ships (IMO FTP Code, 2010)

FTP test	Type of test	Referred test method
Part 1	Noncombustibility test	ISO 1182
Part 2	Smoke and toxicity test	ISO 5659-2
Part 5	Test for surface flammability	ISO 1716
Part 7	Tests for vertically suspended textiles and films	
Part 8	Test for upholstered furniture	
Part 9	Test for bedding components	

14.4 Testing related to hygiene

As closed environments, transportation vehicles may facilitate the transmission of infectious diseases, in particular airborne ones (Santos O'Connor, 2012). For instance, cases of influenza, severe acute respiratory syndrome (SARS), meningococcal disease, tuberculosis, and measles transmission onboard planes are seen relatively frequently. Cruise ships, trains, and school buses have also been documented as potential vehicles for the spreading of various diseases. In an effort to improve air quality, cabin interior air filter systems equipped with nonwoven filters have now become a requirement for many transportation vehicles. Textile filters are also used in other parts of vehicles for air, oil, and fuel filtration. A complementary strategy aimed at limiting the transmission of diseases is based on the use of antimicrobial textiles.

14.4.1 Filtration

Transportation was the leading segment of nonwoven filter media applications in 2014 with 21.2% of the total market revenue (James, 2015). This trend has been maintained since then and may be attributed in part to tougher regulations towards the reduction in carbon emissions from automobiles. Further, with respect to cars, large concerns have also been raised about the air quality inside the passenger compartment (Fung & Hardcastle, 2001). Indeed, research has shown that, because of the tunnel effect, the exhaust gas concentration inside a car may be six times higher than outside. This phenomenon is amplified when a car is driven as a closed distance from the preceding one. The question of inside air filtration is also critical in public transportation, especially for long distance travel segments (Santos O'Connor, 2012).

Cabin air filters may combine three mechanisms (Fung & Hardcastle, 2001): mechanical filtration of the solid particles through the pores of the nonwoven, electrostatic attraction of the solid particles on the charged nonwoven fibers, and adsorption of gases and removal of odors by activated carbon granules distributed across the nonwoven filter.

The performance of air filters may be tested for particulate and gas filtration. For instance, standard ISO/TS 11155-1 (2001) allows assessing the pressure loss, fractional filtration efficiency, and accelerated particulate holding capability of filter elements for road vehicle passenger compartments using standardized laboratory particulate challenges larger than 0.3 μm. The dynamic gas adsorption of the passenger compartment air filters of road vehicles may be characterized according to the test methods described in ISO/TS 11155-2 (2009). The air pressure loss as well as the gas and vapor removal characteristics are measured for a series of relevant contaminants.

14.4.2 Antimicrobial textiles

Textiles used for seats, handles, carpets, etc. may also be treated to provide them with an antimicrobial function. The antimicrobial agent may be applied as a finishing treatment on the yarn or the fabric, or it may be incorporated into the polymer extrusion solution or the spinning bath (Zhao & Chen, 2016). In the latter case, it has to slowly migrate towards the fiber surface to provide its function during use. Finishing

treatments may use conventional exhaust and pad-dry-cure methods as well as newly developed padding, spraying, coating, foam finishing, and microencapsulation techniques. For instance, silver nanoparticles have recently generated interest because they appear as a more health and environmentally friendly antimicrobial alternative to halogenated phenols such as triclosan. In addition, bacteria are less prone to develop resistance to silver nanoparticles than conventional antibiotics (Chernousova & Epple, 2013). Other strategies involve the use of natural compounds such as chitosan to limit the occurrence of side effects on health and the environment (Lim & Hudson, 2004).

The antibacterial activity of textile products may be quantified by directly inoculating fabric swatches with gram-positive *Staphylococcus aureus* and/or gram negative *Klebsiella pneumoniae* organism cultures (AATCC TM100, 2012). The antibacterial activity value of the tested textile is computed using bacteria counts on the samples immediately after inoculation and after the desired contact period. Other standard test methods provide alternative transfer and printing techniques for inoculation (ISO 20743, 2013). More details about antibacterial efficiency test methods are available in Chapter 6.

14.5 Testing of textile-reinforced composites

Fiber reinforced composites have taken an increasing share of transportation applications. Glass reinforced plastics were developed in the 1920s. One of their first use in transportation can be dated back to the late 1940s, with boat hulls made of glass fiber reinforced polyester resin (Bunsell & Renard, 2005). Composites were introduced in military aircrafts in the 1960s. The Renault 5 was the first car in 1972 to have a bumper made of glass fiber reinforced polyester.

Since then, the development of new fibers, for instance carbon and aramid fibers, has allowed an increase in the performance of composites and in the ratio of composite parts in all types of vehicles. For instance, the new Airbus A350 XWB contains 53% of fiber reinforced composites that can be found in the wings, fuselage, empennage, and belly fairing as well as in the skin panels, doublers, joints, and stringers (Airbus, 2016). This has allowed Airbus to save 20% in mass compared to aluminum and 25% in fuel consumption. It has also seen a strong improvement in the resistance of parts to corrosion and fatigue. The Aston Martin One-77 structural core is made of a carbon fiber composite monocoque, making the car weight only 1500 kg (Aston Martin, 2008). In railway applications, Alstom teamed up with France's national railways (SNCF) to develop train noses made of carbon fiber reinforced composite in order to reduce the overall weight and improve the aerodynamics of high speed trains (Mason, 2004). However, all of these composite parts have to go through intense testing in order to fulfill the requirements on which the passengers' lives depend. These may be conducted at the preform and/or composite stage and may involve destructive and nondestructive test methods.

14.5.1 Tests on composite textile reinforcements

Textile reinforcements for composites include yarns, strands, tows or rovings (Strong, 2008). They may be used directly, for instance, in filament winding or fiber placement

processes. They may also be transformed into more complex textile structures such as wovens, knits, and braids with anisotropic properties in all three directions. On the other hand, nonwovens or mats are manufactured directly using fibers or chopped strands that are more or less randomly distributed in the plane of the structure. Recently, noncrimp fabrics (NCF) have been developed to combine the strength and perfect fiber placement of wovens with the flexibility, ease of manufacture, and absence of fiber crimp of nonwovens (Schnabel & Gries, 2011). The 2-D sheet materials may then be assembled by stitching, Z-pinning, or tufting, for instance, to create complex shaped, 3-D structures that will be cut to shape to be fitted in the composite part mold (Mouritz, 2011). Near net-shape preforms may also be prepared directly using 3-D textile manufacturing techniques, which include 3-D interlock and orthogonal noncrimp weaving as well as 3-D braiding. This allows improving the pace of the process and the quality of the composite. The 2-D reinforcements and 3-D preforms may also be delivered as prepregs, i.e., with the textile being coated with the resin only partially cured (Strong, 2008). Prepregs need to be stored in cold conditions to prevent premature complete polymerization.

The properties of the textile reinforcement as well as its compatibility with the matrix play a major role in the performance of the composite material (Strong, 2008). Indeed, the reinforcement gives the composite its strength and stiffness because it bears the stress applied on the composite part, which is transferred by the matrix. Properties measured on the reinforcement include the following:

- Density of the 1-D raw material (fiber/filament/yarn/strand/tow/roving), e.g., using Archimedes' method (ASTM D3800, 2016) or a pycnometer (ASTM D70, 2009; ASTM D5550, 2014);
- Elastic modulus, strength, and elongation at break of the 1-D raw material, e.g., using ASTM D4018 (2017) for continuous filament carbon and graphite fiber tows;
- Dry uniaxial bending of the reinforcement, e.g., based on standard test ASTM D1388 (2014) or using the apparatus developed by Jldain (2015). Buckling of inner yarns may be observed using a translucent bending surface.
- Draping behavior of the reinforcement, e.g., using the double curvature technique developed by Harrabi et al. (2008);
- In-plane shear of the reinforcement using a bias extension or picture frame technique (Long, Boisse, & Robitaille, 2005). In-plane shear is considered to be the main deformation mechanism taking place when the reinforcement is formed to a 3-D geometry. This test also provides a measurement of the maximum deformation, with the yarn locking angle;
- Biaxial in-plane tension of the reinforcement, e.g., using the biaxial tensile device with cruciform specimens described in Long et al. (2005). It allows characterizing the warp and weft yarn interaction in woven fabrics.
- Dry compaction of the reinforcement, e.g., adapted from standard test ISO 5084 (1996). The test involves the application of compression cycles and provides a measurement of the preform thickness under a certain level of normal stress as well as the through-thickness rigidity of the material. It also gives an estimate of the maximum fiber volume fraction that can be achieved (Robitaille & Gauvin, 1998);
- Pore size distribution in the reinforcement, e.g., using microscopy, X-ray microtomography, and capillary flow porometry (Bonnard, Causse, & Trochu, 2017). This last technique allows accessing the dual scale structure of fibrous reinforcements;
- Resin permeability of the reinforcement using unidirectional injection or bidirectional flow measurement from a pointwise injection gate (Demaría, Ruiz, & Trochu, 2007). The test may be conducted with 100 cp silicon oil that behaves as a Newtonian fluid.

In addition, the type of reinforcement also has a large impact on the manufacturing process, which in turn controls the performance of the final composite part.

Defects in the textile reinforcement may also induce reduced performance and/or premature failure in the composite part. These defects include fiber misorientation (Saboktakin, Dolez, & Vu-Khanh, 2011), broken fibers (Mouritz, 2011), wrinkling (Zhu, Yu, Zhang, & Tao, 2011), and local strain concentration due to stitching (Chen, Endruweit, Harper, & Warrior, 2015). Preform inspection may be conducted using x-ray microtomography (Desplentere et al., 2005) or by reconstructing geometries from sections obtained by electronic microscopy (Blanc, Germain, Da Costa, Baylou, & Cataldi, 2006).

14.5.2 Destructive testing of textile-reinforced composites

Depending on its functions, the composite part will have to meet different requirements. These requirements include the following (Mallick, 2007):

- Static mechanical properties: tension, compression, flexion, in-plane shear, interlaminar shear
- Fatigue properties: tension-tension, flexural, interlaminar shear, compressive
- Impact properties: Charpy, Izod, drop-weight
- Long-term behavior: elevated temperature aging, moisture aging, creep
- Other properties: pin bearing, damping, thermal extension, thermal conductivity

Various destructive test methods exist to characterize the properties as well as the short and long-term performance of composite parts. Some tests are conducted on composite specimens (Table 14.5). OEMs have also developed some application-specific test procedures that they may perform on full-scale parts (Kia, 2012; Perret, Mistou, Fazzini, & Brault, 2012).

14.5.3 Nondestructive testing of textile-reinforced composites

As an alternative to destructive testing, nondestructive test (NDT) methods allow looking for defects and damages inside composite parts without cutting them apart or even decreasing their performance. These techniques are critical for in-service inspection but may also be useful for production quality control as well as rapid sample testing. They are categorized as contact and noncontact methods in Table 14.6. For instance, X-ray computed tomography and ultrasound-based techniques were successfully used to detect two significant process-induced defects, namely fiber breakage and ply misorientation, in woven-reinforced composites manufactured by vacuum assisted resin transfer molding (Saboktakin Rizi, 2013).

In addition, new NDT techniques are continuously developed. For instance, a micro-vibrothermography device was designed to detect deep submillimeter flaws in stitched T-joint carbon fiber reinforced polymer (CFRP) composites (Zhang et al., 2016). A burst of ultrasound waves is delivered to the specimen with a 200 Pa ultrasound excitation transducer. The temperature profile is captured with an infrared camera equipped with a microlens. The same team also developed a microlaser line thermography technique, which was successfully used to detect internal microporosities in the same stitched T-joint CFRP composites.

Table 14.5 Short- and long-term properties and performance of composites with examples of test methods used in the transportation industry (ASTM D4762, 2016; ASTM D6856, 2003)

Mechanical properties	
Tension	ASTM D3039, ASTM D638, ASTM D5083, ISO 527-4, ISO 527-5, EN 2561, EN 2597
Through-thickness tension	ATM D7291
Compression	ASTM D695, ASTM D3410, ISO 14126
Combined loading compression (CLC)	ASTM D6641
Short-beam strength (ILSS)	ASTM D2344, EN2563, ISO 14130
Flexion	ASTM D7264, ASTM D790, ASTM D6272, ISO 14125
In-plane shear strength	ASTM D3518, ASTM D3846, ASTM D4255, ISO 14129
V-notched specimen shear	ASTM D5379, ASTM D7078
Lap-shear	ASTM D5868
Filled-hole tension & compression	ASTM D6742
Open-hole tensile strength	ASTM D5766
Open-hole compressive strength	ASTM D6484
Bearing response	ASTM D5961, ASTM D953
Shear bearing/bypass interaction response	ASTM D7248
Fastener pull-through	ASTM D7332
Interlaminar toughness	ASTM D5528, ASTM D6671
Impact	ASTM D256, ASTM D3763, ASTM D7136, ASTM D6264, ASTM D6110, D4812
Composition	
Density	ASTM D792
Fiber, resin, and void content	ASTM D3171, ASTM D2734, ASTM D2584, ASTM C613, ASTM D3529, ASTM D3530
Thermophysical properties	
Glass transition temperature	ASTM E1640, ASTM D7028
Elastic modulus, viscous modulus, and damping coefficient	ASTM D4065, D4440, D5279
Coefficient of thermal expansion	ASTM E831
Long-term performance	
Moisture absorption	ASTM D5229
Creep	ASTM D7337
Fatigue	ASTM D3479, ASTM D6115, ASTM D6873, ASTM D7615, ISO 13003

Table 14.6 Nondestructive test methods for textile-reinforced composites (Gholizadeh, 2016)

Contact methods	Noncontact methods
Pulse echo ultrasonic testing	Through transmission ultrasonic testing
Acoustic emission	Radiography (e.g. X-ray tomography)
Electromagnetic testing (e.g., eddy current)	Thermography (e.g., infrared testing)
Liquid penetrant testing	Holography
Magnetic particle testing	Shearography
	Visual inspection

14.6 Durability testing

If materials and parts used in transportation have to display a certain level of performance when they come out of the production line, they also have to maintain these performance as much as possible over the entire life of the vehicle. For instance, cars today are built to last about 250,000 miles (Gorzelany, 2013). On the other hand, aircraft lifespan is determined by the number of takeoff and landing cycles they experience (Maksel, 2008); aircrafts that only make long flights may last more than 20 years because of the lower number of pressurization cycles. However, textiles used in floorings, upholstery, and draperies in the interior cabin will not last as long and may need to be cleaned, repaired, and/or replaced at regular intervals.

The performances of textile and textile-based materials related to durability for transportation applications include the following (National Research Council, 1995):

- Colorfastness to light
- Resistance to UV
- Resistance to ozone
- Weathering resistance
- Resistance to tearing
- Resistance to crocking
- Resistance to abrasion damage
- Dimensional stability
- Fluid resistance (e.g., solvents and cleaning fluids)
- Resistance to permanent staining
- Resistance to water and moisture absorption
- Resistance to water wicking
- Resistance to corrosion
- Resistance to fungus attack
- Resistance to crazing
- Resistance to impact damage
- Resistance to vibration
- Resistance to fatigue

14.6.1 Environmental aging

A first set of aging agents are environmental. Indeed, temperature, humidity, and UV radiations may induce changes in the materials properties and performance over time. For instance, some polymers like polyolefins are prone to thermo- and photo-oxidation degradation, while polyester and polyamide are especially sensitive to hydrolysis and polyvinylchloride may discolor and become brittle at high temperatures (Verdu, 1984). Polymers and natural fibers may also be degraded by microorganisms.

The resistance of textiles and textile-based materials to heat, moisture, water spray, and UV aging is usually tested using conditions that accelerate the aging process to reduce the duration of the test. Weathering programs simulating climatic conditions to which the material is likely to be subjected in service will combine cycles with variations in temperature, water, and/or radiation conditions. Resistance to microorganisms may also be assessed to evaluate the effect of bacteria, mildew, and rot. The durability is generally characterized in terms of color change as well as effect on mechanical and other physical properties. Table 14.7 provides a list of test methods used in the transportation industry to characterize the resistance of materials to environmental aging. Some of them have been developed by private companies, e.g., Peugeot Citroën (PSA test methods in Table 14.7) and General Motors (GM test methods).

14.6.2 Service aging

Aging may also result from normal wear as well as accidental or intentional damage during service. Damage may be generated by a mechanical action, for instance crocking, pilling, abrasion, snagging, tear, laceration, etc. (Kern, 2014). It may also be of chemical nature, for example, resulting from a water leak, fluid spill, perspiration, soiling by a sick passenger, etc. If the test item is designed to be laundered, colorfastness and resistance to laundering cycles may also have to be assessed. The effect may be visual with a change in color or a stain. A loss in performance and/or physical integrity of the material may also observed. Table 14.8 provides a list of test methods used in the transportation industry to characterize the resistance of materials to aging due to service conditions. Some of them have been developed by private companies like Volkswagen (PV test methods in Table 14.8), Daimler (DBL test methods), and General Motors Europe (GME test methods).

Table 14.7 Test methods assessing the effect of environmental aging (Fung & Hardcastle, 2001; UL, 2016)

Performance	Example of test methods
Resistance to thermal aging	ISO 188; EN ISO 2578; UL 746 B; D45 1139 PSA; D45 1234 PSA
Resistance to UV aging	ISO 4892; ISO 105-B06; ASTM G151; SAE J2412; SAE J2527; SAE J1885; SAE J2212; SAE J2229; SAE J2230; BS 1006; DIN 75202; GM 9125P; PV 1303
Resistance to microorganisms	AATCC Method 30; AATCC Method 100; AATCC Method 174; FTMS 191A Method 5750

Table 14.8 Test methods assessing the effect of service aging on textiles for transportation applications (Fung & Hardcastle, 2001; UL, 2016)

Performance	Example of test methods
Resistance to crocking (wet and dry)	AATCC Method 8; SAE J861; DIN 54021; BS 1006
Resistance to pilling	ISO 12945-3; ASTM D3511; ASTM D3512; ASTM D3514; DIN 53863/3; DIN 53865; DIN 53867; BS 5811; PV 3360
Resistance to abrasion	ISO 105-D02; ISO 12945; ISO 12947; SAE J365; SAE J2509; ASTM D3884-92; ASTM D3885; ASTM D3886; ASTM D 4157; ASTM D4966; AATCC Method 119; AATCC Method 120; DIN EN 105-X12; DIN 53863; DIN 53528; DIN 53754; BS 5690; PV 3353; PV 3356; PV 3366; PV 3949; PV 3968; PV 3961; PV 3975; PV 3906; PV 3908; PV 3987; DBL 5578; DBL 7384_8.9
Resistance to snagging	SAE J948; ASTM D5362; ASTM D3939
Resistance to tearing	ASTM D2261; BS 3242 pt5; ASTM D1117; BS 4443 pt6 Method 15; DIN 1424; DIN 53 356
Scratch resistance	GME 60 280; PV 3952
Resistance to fluids	ISO 175; ISO 1817; ISO 105-E04; DIN 54020; PV 3004
Stain repellency and cleanability	AATCC Method 118; BS 4948
Resistance to maintenance and care processes	ISO 105-X11; DIN 54022; CAN/CGSB-4.2 No 31

14.6.3 Fatigue

Fatigue is a specific aspect of material aging where the part is subjected to loading/unloading cycles. This mechanism is critical for the durability of rigid materials such as textile-reinforced composites. But it is also relevant for textiles and coated textiles which are more flexible.

First of all, fibers themselves exhibit fatigue failure (Miraftab, 2009). Loading may be applied in tension, lateral compression, flexion, and torsion. The damage may come during the manufacture of the woven or braided structure for instance as well as during use. One typical example is the cyclic fatigue experienced by a tire cord. In addition to the mechanical stress mode and conditions of application (frequency, amplitude, offset, etc.), other parameters may affect the fatigue failure of a fiber: its composition and manufacturing process/conditions, its dimensions, the presence of impurities, its environment (temperature, humidity, UV, pH, bacteria), etc. The measurement is conducted by applying cyclic loading conditions in a specified environmental. The result is expressed in terms of stress vs. number of cycles to failure (S-N) curves and survival diagrams.

Fatigue may also be experienced at the textile structure scale. Yet, not much research appears to have been done in that field. In the case of flexural fatigue of woven

fabrics, it was shown that the performance depends on the structure of the fabric, the position and structure of the yarn, and the yarn material (Schiefer & Boyland, 1942). Surface fatigue also contributes to wear behavior upon abrasion (Özdil, Kayseri, & Mengüç, 2012). Fatigue cracks form at the surface of the material due to alternating compression-tension stresses and propagate to subsurface regions where they may rejoin.

Fatigue failure performance is a major component in composite part design and has been the focus of several studies (Carvelli & Lomov, 2015). A series of test methods for textile-reinforced composites has also been developed by various standardization organizations (Table 14.9). In addition, it was shown in a study that the S-N curve should be combined with the time-temperature superposition principle to take into account the effect of the environmental conditions, in that case temperature and water absorption (Miyano & Nakada, 2009).

Table 14.9 Test methods for fatigue resistance in textile-reinforced composites (Carvelli & Lomov, 2015)

Standard number	Standard title
ISO 13003	Fiber-reinforced plastics—Determination of fatigue properties under cyclic loading conditions
ASTM D3479	Standard test method for tension-tension fatigue of polymer matrix composite materials
ASTM D6115	Standard test method for mode I fatigue delamination growth onset of unidirectional fiber-reinforced polymer matrix composites
ASTM D6873	Standard practice for bearing fatigue response of polymer matrix composite laminates
ASTM D7615	Standard practice for open-hole fatigue response of polymer matrix composite laminates
NF T51-120-1	Plastics and composites. Determination of the bending fatigue properties. Part 1: General principles—Plastiques et composites
NF T51-120-2	Plastics and composites. Determination of the bending fatigue properties. Part 2: bending test on test pieces gripped at one end—Plastiques et composites
NF T51-120-3	Plastics and composites. Determination of the bending fatigue properties. Part 3: Three-point bending test on unsecured test pieces—Plastiques et composites
NF T51-120-4	Plastics and composites. Determination of the bending fatigue properties. Part 4: Four-point bending test on unsecured test pieces—Plastiques et composites
NF T51-120-5	Plastics and composites. Determination of the bending fatigue properties. Part 5: Alternating plane-bending test—Plastiques et composites
NF T51-120-6	Plastics and composites. Determination of the bending fatigue properties. Part 6: Buckling bending test—Plastiques et composites
JIS K7082	Testing method for complete reversed plane bending fatigue of carbon fiber-reinforced plastics
JIS K7083	Testing method for constant-load amplitude tension-tension fatigue of carbon fiber-reinforced plastics

14.7 Future trends

Since the beginning of the 21st century, the rising concern about global warming has led the scientific community to integrate sustainable development in its research projects and look for more eco-friendly solutions in the design of new products: improvement in process manufacturing (lower energy consumption and reduction of wastes), product lifetime (lightweight fabrics, low VOC emission, maintenance-free systems), and product afterlife (reuse or recycle). As a result, green fabrics and composites are becoming an interesting alternative to many synthetic products, with the use of natural fibers, biosourced resins, and nontoxic and biodegradable dyes and finishes (Chard, Creech, Jesson, & Smith, 2013). It also pushes research forward into the reduction of greenhouse gases through the development of new lightweight and durable materials in transportation.

14.7.1 Natural fibers

Natural fibers have been used for some time as a replacement for glass and carbon fibers in composites for nonstructural applications. Indeed, in addition to their low cost, they display a low density which can lead to reduced energy consumption as well as competitive specific mechanical properties. They are also biodegradable. In the automotive industry, for instance, jute was used by Mercedes-Benz in 1996 for its E-class vehicle door panels (Koronis, Silva, & Fontul, 2013). A blend of flax and sisal later found its way as reinforcement into Audi's 2000 A2 midrange car door trim panels; kenaf in Toyota's 2003 spare tire cover; bamboo fibers in Mitsubishi Motors' interior components; and wheat straw in Ford 2010 Flex crossover vehicle storage bin and inner lid.

Natural fibers are now considered for more high-performance applications thanks to improvements in their compatibility with polymer matrices (Pickering, Efendy, & Le, 2016). For instance, a green hydrophobic treatment based on zinc oxide nanorods and stearic acid was developed for recycled jute fibers (Arfaoui, Dolez, Dubé, & David, 2017). However some issues remain, including the inherence variability in their physical properties as well as their poor moisture resistance and limited thermal stability (Koronis et al., 2013). This thus requires some adjustments in testing programs to ensure that they perform as required by the application. It may be noted that, to the authors' knowledge, natural fiber-based textiles have not found an application in transportation by themselves, i.e., without being combined with a polymer matrix. This may be eventually attributed to their short life resulting from their biodegradability.

14.7.2 Biosourced resins

Biosourced resins provide an interesting alternative to the recycling dilemma of composites. For instance, Toyota has been using polylactic acid (PLA), a biodegradable thermoplastic polyester derived from renewable resources, in the spare tire cover of its RAUM 2003 (Koronis et al., 2013); it was sugar cane and sweet potato in that case. Other bioderived resins foreseen as a matrix for green composites include poly-L-lactide (PLLA), polyhydroxybutyrate (PHB), poly(3-hydroxybutyrate-co-3-hydroxyvalerate) (PHBV), and thermoplastic starch.

Current issues that limit the use of biosourced resins in the transportation industry include their propensity to biodegrade and their high price (Koronis et al., 2013). A debate also exists on whether or not they represent a real sustainable alternative to conventional plastics. Indeed, they should not reduce the amount of cultivated food available to humans and animals, for instance, by decreasing the amount of fertile lands for edible crops, or increasing land clearing.

14.7.3 Eco-friendly additives and finishes

Many dyes or finishes currently used in the textile industry are highly pollutant and require very important amounts of water and energy for processing. For instance, brominated flame retardants still constitute the most common solution used for seating, curtains, carpets, etc. in transportation vehicles (ICL, 2012). Yet, their effects on health and the environment have been clearly demonstrated (see Section 7.6 in Chapter 7 on toxicity testing of textiles). Other toxic chemicals that may be found in textiles include heavy metals, toxic dyes, pesticides, phthalates, nonylphenol ethoxylates, dioxins, and furans. In addition, some finishes like polybrominated diphenyl ether (PBDE) used in airplane carpets are responsible for the emission of VOCs in confined environments (Allen et al., 2013).

Large efforts are currently deployed to develop eco-friendly additives and finishes for textiles. For instance, phosphorous-based compounds (Salmeia, Gaan, & Malucelli, 2016) as well as nanoclay and carbon nanotube composites (Arao, 2015) are considered as an alternative to halogenated fire retardants. Natural dyes may also ultimately replace the toxic synthetic dyes currently used in the textile industry (Bechtold, Turcanu, Ganglberger, & Geissler, 2003); in addition, their application does not require the use of solvents or other chemicals, and they lead to a reduction in the chemical load released with waste waters.

Tougher regulations are being set to better control the amount of chemicals used in textile processes and limit those that are the most toxic. For instance, Nonylphenol ethoxylates (NPE), which had been banned from use within its borders by the European Union for 20 years, have also recently been voted by all EU member states to be excluded from textile imports (Flynn, 2015). In response to the largest interest of consumers for green products and sustainable development, a majority of textile companies are now including environmental management systems (EMS) such as ISO 14001 and/or the adhesion to voluntary eco-labels as part of their business model (see Chapter 7 on toxicity testing of textiles).

14.7.4 Multifunctional and smart materials

Conferring multifunctionality to fabrics is one of the main contemporary goals of technical textile manufacturers. A fabric that can be made fire-resistant with integrated nanotechnologies such as carbon nanotubes (CNT) or nanoclays while being hydrophobic, self-cleaning, and antibacterial at the same time is gold for public transportation manufacturers (Alongi, Carocio, & Malucelli, 2013).

CNT may also be added to composites to provide them with electrical conduction capabilities, thus reducing the use of cables for carrying information or electricity. In addition,

they can be used for the in-situ detection of defects, cracks or delamination (Nofar, Hoa, & Pugh, 2009). They even displayed an increased sensitivity compared to strain gauges.

Finally, smart textiles are opening new paths in the transportation industry. For instance, smart seat belts for airplanes have been developed by CTT Group in partnership with Belt-Tech (Decaens & Vermeersch, 2016). This smart belt sends a signal if it is not buckled. This technology and the others imply the need to develop new testing methods or adapt existing ones in order to take into account the new material or functionality. In that case, the durability of the connective wire inside the seat belt should be assessed against environmental and service aging among others.

14.8 Conclusion

The remarkable evolution of technical textiles for transportation through the last century has been driven by a constant concern for passenger's safety. Insuring a comfortable and secure journey is also a key marketing strategy for aerospace, railway, marine, and automotive manufacturers, as well as a path towards bigger market shares. These companies are thus pushing research forward into developing state-of-the-art textile products respecting specifications but also featuring unique performances in order to be a step ahead of their competitors.

This has led to the development of test methods assessing the different aspects of textiles in transportation. This includes performance related to safety for airbags, seat belts, tires, and slings; flammability, smoke generation, and toxicity, with test methods and specific requirements for each type of application; hygiene for filters and antimicrobial textiles; destructive and nondestructive tests conducted on textile-reinforced composites at the textile and composite level; and durability. Technical textiles are promised to a bright future in transportation, with new developments involving natural fibers, biosourced resins, eco-friendly additives and finishes, and multifunctional and smart materials among others.

14.9 Sources of further information and advice

More information about test methods may be obtained from dedicated committees in various organizations, including the following:

- ISO/TC22 for road vehicles
- ISO/TC 20 for aircraft and space vehicles
- ISO/TC 8 for ships and marine technology
- ISO/TC 269 for railway applications
- American Society for Testing and Materials (ASTM)
- Canadian Standards Association (CSA)
- Association Française de Normalisation (AFNOR)
- Deutsches Institut für Normung (DIN)
- British Standards Institution (BSI)
- Society of Automotive Engineers (SAE)

Acknowledgments

The authors wish to thank Mr. Valério Izquierdo, Amir Fanaei, and Jonathan Levesque for their assistance in preparing the manuscript.

References

AATCC TM100. (2012). *Antibacterial finishes on textile materials: Assessment of American Association of Textile Chemists and Colorists*. Research Triangle Park, NC: American Association of Textile Chemists and Colorists (3 p.).

AIM-Aerospace. (2015). Flammability lab. http://aim-aerospace.com (Accessed 26 March 2017).

Airbus. (2016). A350 XWB—Cost-effectivness. Retrieved from http://www.a350xwb.com/cost-effectiveness/ (Accessed 8 December 2016).

Allen, J. G., Stapleton, H. M., Vallarino, J., McNeely, E., McClean, M. D., Harrad, S. J., et al. (2013). Exposure to flame retardant chemicals on commercial airplanes. *Environmental Health*, *12*, 17–29.

Alongi, J., Carocio, F., & Malucelli, G. (2013). Smart (Nano) coatings. *Update on flame retardant textiles: State of the art, environmental issues and innovative solutions*. Shawbury, Shrewsbury, Shropshire, UK: A Smithers Group Company (pp. 257–311).

ANSI B77.1a. (2012). *Passenger ropeways—Aerial tramways, aerial lifts, surface lifts, tows and conveyors—Safety requirements*. American National Standards Institute, Anderson, SC: Tile Council of North America, Inc.

Arao, Y. (2015). Flame retardancy of polymer nanocomposite. In P. M. Visakh & Y. Arao (Eds.), *Flame retardants: Polymer Blends, Composites and Nanocomposites* (pp. 15–44). Cham, Heidelberg, New York, Dordrecht, London: Springer International.

Arfaoui, M. A., Dolez, P. I., Dubé, M., & David, É. (2017). Development and characterization of a hydrophobic treatment for jute fibres based on zinc oxide nanoparticles and a fatty acid. *Applied Surface Science*, *397*, 19–29.

ASME B30.9. (2010). *Safety standard for cableways, cranes, derricks, hoists, hooks, jacks, and slings—Slings*. New York, NY: American Society of Mechanical Engineers (80 p.).

ASTM D70. (2009). *Standard test method for density of semi-solid bituminous materials (pycnometer method)*. West Conshohocken, PA: ASTM International (5 p.).

ASTM D885/D885M. (2010). *Standard test methods for tire cords, tire cord fabrics, and industrial filament yarns made from manufactured organic-base fibers*. West Conshohocken, PA: ASTM International (31 p.).

ASTM D1388. (2014). *Standard test method for stiffness of fabrics*. West Conshohocken, PA: ASTM International (6 p.).

ASTM D2724. (2007). *Standard test methods for bonded, fused, and laminated apparel fabrics*. ASTM International (7 p.).

ASTM D3574. (2016). *Standard test methods for flexible cellular materials—Slab, bonded, and molded urethane foams*. West Conshohocken, PA: ASTM International (30 p.).

ASTM D3800. (2016). *Standard test method for density of high-modulus fibers*. West Conshohocken, PA: ASTM International (6 p.).

ASTM D4018. (2017). *Standard test methods for properties of continuous filament carbon and graphite fiber tows*. West Conshohocken, PA: ASTM International (7 p.).

ASTM D4762. (2016). *Standard guide for testing polymer matrix composite materials*. West Conshohocken, PA: ASTM International (22 p.).

ASTM D5132. (2011). *Test method for horizontal burning rate of polymeric materials used in occupant compartments of motor vehicles*. West Conshohocken, PA: ASTM International (8 p.).
ASTM D5426. (2012). *Standard practices for visual inspection and grading of fabrics used for inflatable restraints*. West Conshohocken, PA: ASTM International (6 p.).
ASTM D5427. (2009). *Standard practice for accelerated aging of inflatable restraint fabrics*. West Conshohocken, PA: ASTM International (3 p.).
ASTM D5428. (2008). *Standard practice for evaluating the performance of inflatable restraint modules*. West Conshohocken, PA: ASTM International (4 p.).
ASTM D5446. (2008). *Standard practice for determining physical properties of fabrics, yarns, and sewing thread used in inflatable restraints*. West Conshohocken, PA: ASTM International (5 p.).
ASTM D5550. (2014). *Standard test method for specific gravity of soil solids by gas pycnometer*. West Conshohocken, PA: ASTM International (5 p.).
ASTM D6856. (2003). *Standard guide for testing fabric-reinforced "Textile" composite materials*. West Conshohocken, PA: ASTM International (8 p.).
ASTM E2061. (2015). *Standard guide for fire hazard assessment of rail transportation vehicles*. West Conshohocken, PA: ASTM International (27 p.).
ASTM E2574. (2012). *Standard test method for fire testing of school bus seat assemblies*. West Conshohocken, PA: ASTM International (10 p.).
Aston Martin. (2008). Aston Martin—One-77. Retrieved from http://www.astonmartin.com/en/heritage/past-models/one-77 (Accessed 8 December 2016).
Bechtold, T., Turcanu, A., Ganglberger, E., & Geissler, S. (2003). Natural dyes in modern textile dyehouses—How to combine experiences of two centuries to meet the demands of the future? *Journal of Cleaner Production*, *11*(5), 499–509.
Bertrand, D. (2005). Moving fabric. *The Textile Journal*, *122*(4), 10–15.
Blanc, R., Germain, Ch., Da Costa, J. P., Baylou, P., & Cataldi, M. (2006). Fiber orientation measurements in composite materials. *Composites Part A: Applied Science and Manufacturing*, *37*(2), 197–206.
Bonnard, B., Causse, P., & Trochu, F. (2017). Experimental characterization of the pore size distribution in fibrous reinforcements of composite materials. *Journal of Composite Materials*. https://doi.org/10.1177/0021998317694424.
Bunsell, A. R., & Renard, J. (2005). *Fundamentals of fibre reinforced composite materials*. Bristol & Philadephia: Institute of Physics Publishing.
Carrigg, R., & Alarid, R. (2016). *2016 top markets report—Technical textiles—A market assessment tool for U.S. Exporters*. Washington, DC: US International Trade Administration (59 p.).
Carvelli, V. & Lomov, S. (Eds.), (2015). *Fatigue of textile composites*. (1st ed.) Cambridge, UK: Woodhead Publishing.
Chard, J. M., Creech, G., Jesson, D. A., & Smith, P. A. (2013). Green composites: Sustainability and mechanical performance. *Plastics, Rubber and Composites Macromolecular Engineering*, *42*(10) (6 p.).
Chen, S., Endruweit, A., Harper, L., & Warrior, N. (2015). Inter-ply stitching optimisation of highly drapeable multi-ply preforms. *Composites: Part A*, *71*, 144–156.
Chernousova, S., & Epple, M. (2013). Silver as antibacterial agent: Ion, nanoparticle, and metal. *Angewandte Chemie International Edition in English*, *52*(6), 1636–1653.
David Rigby Associates. (2003). *Technical textiles and nonwovens: World market forecasts to 2010*, (17 p.) http://www.davidrigbyassociates.co.uk.
Decaens, J., & Vermeersch, O. (2016). Wearable technologies for PPE: Embedded textile monitoring sensors, power and data transmission, end-life indicators. In K. Vladan (Ed.), *Smart textiles and their applications* (pp. 519–537). Duxford, UK: Woodhead Publishing.

Demaría, C., Ruiz, E., & Trochu, F. (2007). In-plane anisotropic permeability characterization of deformed woven fabrics by unidirectional injection. Part I: Experimental results. *Polymer Composites*, *28*(6), 797–811.

Desplentere, F., Lomov, S. V., Woerdeman, D. L., Verpoest, I., Wevers, M., & Bogdanovich, A. (2005). Micro-CT characterization of variability in 3D textile architecture. *Composites Science and Technology*, *65*(13), 1920–1930.

DVSA. (2017). *Load securing: Vehicle operator guidance*. United Kingdom: Driver and Vehicle Standards Agency.

EASA CM-CS-004. (2013). *Notification of a proposal to issue a certificate memorandum on Flammability Testing of Interior Materials*. Cologne, Germany: European Aviation Safety Agency (6 p.).

EC 661. (2009). *Type-approval requirements for the general safety of motor vehicles, their trailers and systems, components and separate technical units intended therefor*. Brussels, Belgium: European Commission.

ECE 94. (2003). *Protection of the occupants in the event of a frontal collision*. Geneva, Switzerland: United Nations Economic Commission for Europe.

EN 1492-1. (2008). *Textile slings—Safety—Part 1: Flat woven webbing slings made of man-made fibres for general purpose use*. Brussels, Belgium: European Committee for Standardization (36 p.).

EN 1492-2. (2008). *Textile slings—Safety—Part 2: Roundslings made of man-made fibres for general purpose use*. Brussels, Belgium: European Committee for Standardization (28 p.).

EN 1492-4. (2008). *Textile slings—Safety—Part 4: Lifting slings for general service made from natural and man-made fibre ropes*. Brussels, Belgium: European Committee for Standardization (28 p.).

EN 45545-2. (2013). *Railway applications. Fire protection on railway vehicles. Requirements for fire behaviour of materials and components*. Brussels, Belgium: European Committee for Standardization (78 p.).

FAR/CS 25.853. (n.d.). Airworthiness standards: Transport category airplanes. 14 CFR Part 25 Appendix F. Washington, DC: United States Department of Transportation, Federal Aviation Administration.

Flynn, V. (2015). EU countries agree textile chemical ban. *The Guardian*. Tuesday 21 July 2015.

FMVSS 139. (n.d.). New pneumatic radial tires for light vehicles. 49 CFR 571.139—Federal Motor Vehicle Safety Standard No. 139. Washington, DC: United States Department of Transportation, National Highway Traffic Safety Administration.

FMVSS 208. (n.d.). Occupant crash protection. 49 CFR 571.208—Federal Motor Vehicle Safety Standard No. 208. Washington, DC: United States Department of Transportation, National Highway Traffic Safety Administration.

FMVSS 302. (n.d.). Flammability of interior materials. 49 CFR Part 571.302—Federal Motor Vehicle Safety Standard No. 302, Washington, DC, United States Department of Transportation, National Highway Traffic Safety Administration.

FRA 216. (1999). Passenger equipment safety standards. *49 CFR Part 216*. Washington, DC: United States Department of Transportation, Federal Railroad Administration.

Fung, W., & Hardcastle, M. (2001). *Textiles in automotive engineering*. Cambridge, UK: Woodhead Publishing.

Gholizadeh, S. (2016). A review of non-destructive testing methods of composite materials. *Procedia Structural Integrity*, *1*, 50–57.

Gorzelany, J. (2013). Cars that can last for 250,000 miles (or more). Forbes. Retrieved from https://www.forbes.com (Accessed 30 March 2017).

Harrabi, L., Dolez, P. I., Vu-Khanh, T., Lara, J., Tremblay, G., Nadeau, S., et al. (2008). Characterization of protective gloves stiffness: Development of a multidirectional deformation test method. *Safety Science*, *46*(7), 1025–1036.

Hetrick, J. W. (1953). Safety cushion assembly for automotive vehicles. United States Patent and Trademark Office, 2,649,311.

Horrocks, A. R. (2013). Flame retardant textiles for transport applications. In F. Selcen Kilinc (Ed.), *Handbook of fire resistant textiles* (pp. 603–622). Cambridge, UK: Elsevier.

ICL. (2012). Fire protection for automotive and transportation. ICL Industrial Products. Retrieved from http://icl-ip.com/wp-content/uploads/2015/07/FR-Transportation-2012.pdf (Accessed 2 April 2017).

IMO FTP Code. (2010). *International code for application of fire test procedures*. London, UK: International Maritime Organization (211 p.).

Imre, P. A., & Cotetiu, R. (2014). Contribution to validation and testing of seatbelt components. *Scientific Bulletin Series C: Fascicle Mechanics, Tribology, Machine Manufacturing Technology*, *28*, 54–57.

ISO. (2016). About ISO—What are standards? http://www.iso.org/iso/home/about.htm (Accessed 6 January 2016).

ISO 3795. (1989). *Road vehicles, and tractors and machinery for agriculture and forestry—Determination of burning behaviour of interior materials*. Geneva, Switzerland: International Organization for Standardization (6 p.).

ISO 5084. (1996). *Textiles—Determination of thickness of textiles and textile products*. Geneva, Switzerland: International Organization for Standardization (5 p.).

ISO 5658-2. (2006). *Reaction to fire tests—Spread of flame—Part 2: Lateral spread on building and transport products in vertical configuration*. Geneva, Switzerland: International Organization for Standardization (33 p.).

ISO 5659-2. (2012). *Plastics—Smoke generation—Part 2: Determination of optical density by a single-chamber test*. Geneva, Switzerland: International Organization for Standardization (44 p.).

ISO 5660-1. (2015). *Reaction-to-fire tests—Heat release, smoke production and mass loss rate—Part 1: Heat release rate (cone calorimeter method) and smoke production rate (dynamic measurement)*. Geneva, Switzerland: International Organization for Standardization (55 p.).

ISO 9239-1. (2010). *Reaction to fire tests for floorings—Part 1: Determination of the burning behaviour using a radiant heat source*. Geneva, Switzerland: International Organization for Standardization (25 p.).

ISO 11925-2. (2010). *Reaction to fire tests—Ignitability of products subjected to direct impingement of flame—Part 2: Single-flame source test*. Geneva, Switzerland: International Organization for Standardization (26 p.).

ISO 12952-2. (2010). *Textiles—Assessment of the ignitability of bedding items—Part 2: Ignition source: Match-flame equivalent*. Geneva, Switzerland: International Organization for Standardization (11 p.).

ISO 20743. (2013). *Textiles—Determination of antibacterial activity of textile products*. Geneva, Switzerland: International Organization for Standardization (32 p.).

ISO/TR 9705-2. (2001). *Reaction-to-fire tests—Full-scale room tests for surface products—Part 2: Technical background and guidance*. Geneva, Switzerland: International Organization for Standardization (39 p.).

ISO/TS 11155-1. (2001). *Road vehicles—Air filters for passenger compartments—Part 1: Test for particulate filtration*. Geneva, Switzerland: International Organization for Standardization (38 p.).

ISO/TS 11155-2. (2009). *Road vehicles—Air filters for passenger compartments—Part 2: Test for gaseous filtration*. Geneva, Switzerland: International Organization for Standardization (17 p.).

James, S. (2015). *Nonwoven filter media market to reach $7.18 billion by 2022*. San Francisco, CA: Grand View Research.

Jldain, H. B. (2015). *Behaviour and inspection of novel non-crimp dry thick reinforcement fabrics*. [Ph.D. dissertation] Ottawa, ON: University of Ottawa.

Johnson, M. (2005). Ford beefs up its safety testing facilities. *Automotive Body Repair News*, *44*(11), 32.

Johnson, L. (2012). *Solar sail propulsion*. Huntsville, AL: NASA Marshall Space Flight Center (55 p.).

Juul, M. (2016). *New civil aviation safety rules*. Brussels, Belgium: European Parliamentary Research Service.

Kern, T. (2014). Interior care and maintenance. AviationPros. Retrieved from www.aviationpros.com (Accessed 30 March 2017).

Kia, H. (2012). Focal project 4: Structural automotive components from composite materials. automotive composites consortium. Retrieved from https://energy.gov/sites/prod/files/2014/03/f10/lm049_berger_2012_o_0.pdf (Accessed 31 March 2017).

Koronis, G., Silva, A., & Fontul, M. (2013). Green composites: A review of adequate materials for automotive applications. *Composites: Part B*, *44*, 120–127.

Lim, S.-H., & Hudson, S. M. (2004). Application of a fiber-reactive chitosan derivative to cotton fabric as an antimicrobial textile Finish. *Carbohydrate Polymers*, *56*(2), 227–234.

Lindenmuth, B. E. (2006). An overview of tire technology. *The pneumatic tire*. Washington, DC: National Highway Traffic Safety Administration (NHTSA), U.S. Department of Transportation, 2–27.

Long, A. C., Boisse, P., & Robitaille, F. (2005). Mechanical analysis of textiles. In A. C. Long (Ed.), *Design and manufacture of textile composites* (pp. 62–109). Cambridge, UK: Woodhead Publishing.

M&M. (2014a). *Automotive airbag and seat belt market for passenger cars—A global analysis: By Geography—Trends and forecasts 2014–2019*. Maharashtra, India: MarketsandMarkets Analysis.

M&M. (2014b). *Automotive composites market by type (glass fiber composites, carbon fiber composites, natural fiber composites, metal matrix composites, and ceramic matrix composites) and by application (interior components, exterior components, chassis & powertrain components and others)—Global trends & forecast to 2019*. Maharashtra, India: MarketsandMarkets Analysis.

Maksel, R. (2008). What determines an airplane's lifespan? AIRSPACEMAG.COM. Retrieved from http://www.airspacemag.com (Accessed 30 March 2017).

Mallick, P. K. (2007). *Fiber-reinforced composites: Materials, manufacturing, and design* (3rd ed.). Boca Raton, FL: CRC Press.

Mason, K. F. (2004). Composites aboard high-speed trains. *Composites Technology*, *10*(6), 34–36.

McDonel, E. T. (2006). Tire cord and cord-to-rubber bonding. *The pneumatic tire*. Washington, DC: National Highway Traffic Safety Administration (NHTSA), U.S. Department of Transportation, 80–104.

Milgrom, G. (2013). *Space shuttle thermal protection system*. iBook (18 p.).

Miraftab, M. (2009). Basic principles of fatigue. In M. Miraftab (Ed.), *Fatigue failure of textile fibres* (pp. 3–9). Cambridge, UK: Woodhead Publishing.

Miyano, Y., & Nakada, M. (2009). Accelerated testing for long-term durability of various FRP laminates for marine use. In I. M. Daniel, E. E. Gdoutos, & Y. D. S. Rajapakse (Eds.),

Major accomplishments in composite materials and sandwich structures (pp. 3–25). Dordrecht, Heidelberg, London, New York: Springer.

Mouritz, A. P. (2011). Three-dimensional (3D) fiber reinforcements for composites. In P. Boisse (Ed.), *Composite reinforcements for optimum performance* (pp. 157–199). Oxford, Cambridge, Philadelphia: Woodhead Publishing.

National Research Council. (1995). *Fire- and smoke-resistant interior materials for commercial transport aircraft*. Washington, DC: The National Academies Press.

NFPA 130. (2014). *Standard for fixed guideway transit and passenger rail systems*. Washington, DC: National Fire Protection Association (74 p.).

NFPA 267. (1998). *Standard method of test for fire characteristics of mattresses and bedding assemblies exposed to flaming ignition source*. Washington, DC: Withdrawn, National Fire Protection Association.

Nofar, M., Hoa, S. V., & Pugh, M. (2009). *Self sensing glass/epoxy composites using carbon nanotubes*. In: *Proceedings of the ICCM-17 17th international conference on composite materials*.

NTSB. (2001). *Survivability of accidents involving Part 121 U.S. Air Carrier Operations, 1983 Through 2000*. Washington, DC: National Transportation Safety Board (29 p.).

Orme, B., Walsh, R. V., & Westoby, S. (2014). *Equivalency or compromise? A comparative study of the use of nylon 6,6 and polyester fiber in automotive airbag cushions*. SAE Technical Paper (7 p.).

Özdil, N., Kayseri, G.Ö., & Mengüç, G. S. (2012). Analysis of abrasion characteristics in textiles. In A. Marcin (Ed.), *Abrasion resistance of materials*. Rijeka, Croatia: InTech (29 p.).

Pamuk, G., & Çeken, F. (2009). Research on the breaking and tearing strengths and elongation of automobile seat cover fabrics. *Textile Research Journal*, *79*(1), 47–58.

Perret, A., Mistou, S., Fazzini, M., & Brault, R. (2012). Global behaviour of a composite stiffened panel in buckling. Part 2: Experimental investigation. *Composite Structures*, *94*(2), 376–385.

Pickering, K. L., Efendy, M. G., & Le, T. M. (2016). A review of recent developments in natural fibre composites and their mechanical performance. *Composites Part A: Applied Science and Manufacturing*, *83*, 98–112.

Rao, S. N., Simha, T. G. A., Rao, K. P., & Ravi Kumar, G. V. V. (2015). *Carbon composites are becoming competitive and cost effective*. Whitepaper Pune, India: InfoSys Ltd.

Robitaille, F., & Gauvin, R. (1998). Compaction of textile reinforcements for composites manufacturing. I: Review of experimental results. *Polymer Composites*, *19*, 198–216.

Saboktakin Rizi, A. (2013). *Integrity assessment of preforms and thick textile reinforced composites for aerospace applications*. [Ph.D. dissertation] Quebec, Canada: Ecole de technologie superieure.

Saboktakin, A., Dolez, P., & Vu-Khanh, T. (2011). Damage identification of thin textile-reinforced composite plates using vibration-based testing methods. In *Proceedings of the 26th ASC annual technical conference (the Second Joint US-Canada Conference on Composites) CANCOM2011, September 26–28, 2011, Montréal*.

Salmeia, K. A., Gaan, S., & Malucelli, G. (2016). Recent advances for flame retardancy of textiles based on phosphorus chemistry. *Polymers*, *8*, 319–355.

Santos O'Connor, F. G. (2012). Emerging and re-emerging infectious diseases. In J. N. Zuckerman (Ed.), *Principles and practice of travel medicine* (pp. 146–165). Wiley-Blackwell.

Schiefer, H. F., & Boyland, P. M. (1942). Note on flexural fatigue of textiles. *Journal of Research of the National Bureau of Standards*, *29*, 69–71.

Schnabel, A., & Gries, T. (2011). Production of non-crimp fabrics for composites. In L. Stepan (Ed.), *Non-crimp fabric composites—Manufacturing, properties and applications* (pp. 3–41). Cambridge, UK: Woodhead Publishing.

Singha, M., & Singha, K. (2012). Applications of textiles in marine products. *Marine Science*, *2*(6), 110–119.

Sobhani, A., Young, W., Logan, D., & Bahrololoom, S. (2011). A kinetic energy model of two-vehicle crash injury severity. *Accident Analysis and Prevention*, *43*, 741–754.

Statista. (2016). *Rail industry—Statistics & facts*. New York, NY: Statista.

Strong, A. B. (2008). Fundamentals of composites manufacturing. *Materials, methods and applications*. (2nd ed.). Dearborn, MI: Society of Manufacturing Engineers.

Tan, Y., & Yu, C. (2012). *New device design and performance test on gas generator in automobile airbag*. In: *International conference on control engineering and communication technology*.

TC TSD 209. (2013). *Technical standards document No. 209, revision 2R—Seat belt assemblies*. Ottawa, Canada: Canada Transport.

Technavio. (2016). *Global marine composites market 2016–2020*. London, UK: Infiniti Research Limited.

Technvio. (2014). *Global technical textiles market 2015–2019*. London, UK: Infiniti Research Limited.

Techtextil. (2016). Application areas. Retrieved from http://techtextil.messefrankfurt.com/frankfurt/en/aussteller/messeprofil/anwendungsbereiche.html (Accessed 9 June 2016).

UL. (2016). *Automotive testing and engineering services*. Toronto, Canada: UL Performance Materials.

VCS 5031,19. (2004). *Flammability of interior materials*. Gothenburg, Sweden: Volvo Car Corporation (12 p.).

Verdu, J. (1984). *Le vieillissement des plastiques*. Paris, France: Eyrolles.

White, R. (2015). GM paving way to smarter and safer driving at all-new active safety test area. http://media.gm.com/media/us/en/gm/home.detail.html/content/Pages/news/us/en/2015/jul/0724-asta.html (Accessed 8 May 2016).

Wilson, A. (2015). Vehicle weight is the key driver for automotive composites. *Reinforced Plastics*. Available online 2 November 2015.

WTO. (2015). *International trade statistics 2015*. Geneva, Switzerland: World Trade Organization (170 p.).

Zhang, H., Fernandes, H., Hassler, U., Ibarra-Castanedo, C., Genest, M., Robitaille, F., et al. (2016). Comparative study of microlaser excitation thermography and microultrasonic excitation thermography on submillimeter porosity in carbon fiber reinforced polymer composites. *Optical Engineering*, *56*(4). 041304.

Zhao, Chen. (2016). Halogeneted phenols and polybiguianides as antimicrobial textile finishes. In S. Gang (Ed.), *Antimicrobial textiles* (pp. 141–153). Duxford, UK: Woodhead Publishing.

Zhu, B., Yu, T., Zhang, H., & Tao, X. (2011). Experimental investigation of formability of commingled woven composite preform in stamping operation. *Composites: Part B*, *42*, 289–295.

Specific testing for performance sportswear

15

R.M.Rossi
Empa, St.Gallen, Switzerland

15.1 Introduction

Recent developments in sports technologies have led to different sports apparel aimed at improving athletes' performance. Sportswear should be user-friendly and include different properties like robustness (strength and durability), flexibility, as well as optimized thermal and moisture management at possible moderate costs.

Manufacturers of sports apparel stay under a constant pressure to bring innovation to the market. This market is mainly marketing-driven and therefore, the demonstration of the performance of new sportswear often relies either on simple materials tests or on statements of famous athletes who praise the quality of the new products. The materials tests show the improvement of single material parameters, which are claimed to improve the performance of the athletes. In the last 2 or 3 decades many new materials like PCM (phase change materials), aerogels, shape-memory alloys, or electronical components have been introduced into textiles and their functionality could only be verified with the development of new standards.

During many sports activities, body heat production is much higher than the heat loss, and sportswear has to help the body to evacuate this excess heat to avoid overheating. On the other hand, at extremely cold temperatures, clothing has to help maintain thermal comfort. Textile structures have been developed that aim to support cardiovascular functions and avoid vibrations that may cause damage to muscle tissues and ligaments. Prosthetic devices have also been developed for athletes with a specific disability. In order to maintain or improve the performance of athletes, the clothing thus has to fulfill mainly two criteria: it shall support human thermoregulation and biomechanics.

This chapter gives an overview of specific test methods used to demonstrate thermal and biomechanical characteristics of sportswear for optimal performance.

15.2 Heat and moisture transfer through sportswear

The test methods used to determine the heat and moisture transport through sports textiles and sports garments like guarded hotplates or thermal manikins are not specific for this type of clothing, and therefore, they are described in detail in other chapters of this book. However, in sportswear, some properties of the materials like the wicking effect and the moisture evaporation efficiency are of particular importance to avoid

Advanced Characterization and Testing of Textiles. https://doi.org/10.1016/B978-0-08-100453-1.00016-7

heat stress situations for the athletes. Therefore, the influence of the design of the garment on heat and moisture transfer has to be thoroughly analyzed. The following presents some specific methods to assess the wicking effects of fabrics and discusses the advantages and limitations of thermal manikins for three specific types of sportswear, namely, body-mapping sportswear and active cooling and heating clothing.

15.2.1 Moisture management in sports fabrics

Most of the studies on the thermal comfort and the moisture management performance of sportswear are developed based on human subjects. It has been shown that the human body can distinguish between different amounts of water in fabrics (Ackerley, Olausson, Wessberg, & Mcglone, 2012; Niedermann & Rossi, 2012). However, it has also been shown in different studies that human subject trials may not be the best test method to discriminate between different materials and fabric properties (Macrae, Laing, Wilson, & Niven, 2014). The test scenarios (activity and climate) have to be adequately chosen to be able to differentiate the qualities of different products. Furthermore, these wear trials in laboratory conditions can hardly simulate all the different conditions of wear in real use conditions. For these reasons, the properties of sportswear are mostly tested with laboratory equipment.

One of the most important properties of sportswear is its moisture management, which describes the ability of the fabric to wick liquid moisture (sweat) and cool the body with a high evaporative efficiency. One of the most common test methods for wicking is the moisture management tester described in AATCC 195 (2012). This method measures the changes in electrical conductivity at the top and the bottom of the test specimen when exposed to a sweat simulating solution. However, more and more noninvasive imaging techniques are being used to exactly track the migration of moisture in a fabric, especially in multilayer combinations, in order to optimize the evaporative cooling efficiency. X-ray radiography and tomography methods have already been used several times to determine the spreading of water in single or multilayer assemblies in real-time. These techniques consist of a tube generating X-rays that are projected as a beam onto the object to be tested. After interacting with the sample (i.e., with the atom's electron shells), parts of the beam are being absorbed or scattered and the resulting beam intensity is assessed by a scintillator that usually converts the signal into a gray-shaded image. Radiography is a 2-D technique making a single projection of the sample. Therefore, quick changes in the moisture content of samples, like the evaporation rate of simulated sweat under heat exposure (Keiser & Rossi, 2010) or fast in-plane or transplanar wicking effects between different fabric layers (Birrfelder, Dorrestijn, Roth, & Rossi, 2013; Rossi, Stampfli, Psikuta, Rechsteiner, & Bruhwiler, 2011), can be assessed. On the other hand, with tomography, different projections of the same sample are taken and reconstructed as a 3-D image (Stampfli, Bruhwiler, Rechsteiner, Meyer, & Rossi, 2013; Weder, Laib, & Brühwiler, 2006). This technique requires several minutes of measuring time and is therefore more adapted to slower wicking mechanisms. The validation of these measurements is usually made by comparing the moisture content to the mass of water determined gravimetrically.

Neutron radiography is a method similar to X-ray, but in that case, the neutron beam used interacts mainly with the atomic nucleus instead of the electron shell and gives very good contrast with hydrogen. This allows a visualization and quantification of water inside materials (Weder et al., 2004; Reifler, Lehmann, Frei, & May, 2003). The measurement time usually ranges from a fraction of a second to few seconds depending on the neutron flux (Manke et al., 2008).

Nuclear magnetic resonance (NMR and MRI) has also been used to determine the presence of water in fabrics (Leisen & Beckham, 2001). This method uses a magnetic field and measures the energy absorbed and emitted by the atom nuclei submitted to an electromagnetic wave.

Infrared thermography can precisely measure temperature differences between a wet or dry fabric. Therefore, this method may be used for the measurement of the in-plane water spreading and the drying time of a fabric (Niedermann & Rossi, 2012). Normal optical cameras can also be used for this purpose (Tang, Kan, & Fan, 2015). However, this method is limited to the observation of either the inner or the outer surface of the textile and no information about the transplanar wicking effect can be extracted. Furthermore, for optical cameras, the contrast between wet and dry spots has to be sufficient. Therefore, this method is usually only used for light-colored fabrics, or a dye has to be added to the water for higher resolution.

Recent reviews of different methods to characterize the wicking properties of fabrics and the real-time tracking of the three-dimensional water flow in textile structures can be found in Tang, Kan, and Fan (2014) and Parada, Derome, Rossi, and Carmeliet (2016).

15.2.2 Body-mapping sportswear

Sportswear with different textile structures fulfilling specific requirements for different body parts (elasticity, wicking effects) has become more and more popular in recent years. This “body-mapping clothing” (BMC) is supposed to exactly match the sweat patterns and thermal sensation of the body. In a recent series of studies, the group of George Havenith showed that the thermal sensation of the skin as well as the quantity of sweat production is dependent on the body's location (Smith & Havenith, 2011, 2012). Therefore, in order to be able to realistically assess the effect of a garment on thermal comfort and thermal sensation, the test method has to have a similar differentiation in different body zones as the human body. Indeed, Havenith showed that there are large and statistically significant intra- and inter-segmental variations in sweating rates in the different regions of the human body. Apart from the forehead, the back region, especially above the spine, showed the highest sweating rates. The lowest sweat rates were observed on the hands, feet, cheeks, and chin. The sweating patterns remained the same for two different work intensities. Because the sweat rate, but also the evaporative cooling rate, varies locally, there are regional differences in skin temperatures (Priego Quesada et al., 2015). It has been shown that thermal sensations varied within body segments, particularly in the torso region, where lateral regions were more sensitive than medial areas (Ouzzahra, Havenith, & Redortier, 2012; Fournet, Ross, Voelcker, Redortier, & Havenith, 2013). The lower back and the lateral

abdomen were also the regions where the skin was the most sensitive to cold sensations in relation with wet skin (Filingeri, Fournet, Hodder, & Havenith, 2014). All these studies show the need for test methods to be able to discriminate sweat patterns and thermal sensitivity between the different regions of the body and display a precise segmentation especially in the torso region.

Wang (Wang, Del Ferraro, Molinaro, Morrissey, & Rossi, 2014) measured the heat and moisture transfer performance of such body-mapping shirts using a sweating thermal manikin. However, they found no better performance for the BMC compared to classical sports shirts. They argued that the BMC may only be effective in certain environmental conditions and that they were probably not suitable for the scenarios chosen in their study. Furthermore, the design of the BMC was not specifically adapted to the manikin body shape. The presence of air gaps may have reduced the positive effects of the body-mapping design, and therefore, the authors suggest that analyses of air gap distributions are needed to correctly assess the overall performance of BMC. The same authors (Wang et al., 2016) recently published a study of BMC assessed with human subjects and showed improved thermal performance (skin and body temperatures as well as local subjective sensations) compared to cotton clothing. However, in order to really assess the benefits of the different textile structures of the BMC, these shirts should be compared with classical shirts containing the same type of fibers and yarns as used for the BMC.

15.2.3 Sportswear with cooling or heating elements

The assessment of the thermal performance of clothing with cooling or heating elements faces the same challenges as BMC: the cooling or the heating is usually only applied to specific body segments, and therefore, the measurements with sweating thermal manikins can only lead to realistic results if the clothing is adapted to the manikin shape and segmentation. Furthermore, the heating or cooling elements may lead to local and/or global thermoregulatory responses of the human body (sweating, shivering, vasomotor response) that cannot be simulated with a manikin. It was shown that the cooling power of personal cooling systems used for the precooling of athletes before competitions was overestimated by a factor of 1.5–2 when measured with a manikin in comparison to human subject trials, due to the absence of vasoconstrictive response of the manikin (Bogerd, Psikuta, Daanen, & Rossi, 2010). Despite the drawbacks mentioned, thermal manikins are commonly used to assess the cooling performance of materials like phase change materials (Lu et al., 2015; Zhao et al., 2013b), ice vests or specific ventilation features (Lu et al., 2015; Zhao et al., 2013a; Morrissey & Rossi, 2013), or the heating performance of electrically or chemically heated garments (Song, Lai, & Wang, 2015).

15.2.4 Human simulators

A promising new approach to evaluate the local comfort of body-mapping or cooling/heating garments is the development of human simulators, i.e., the combination of manikin measurements with thermoregulatory prediction models (Fig. 15.1).

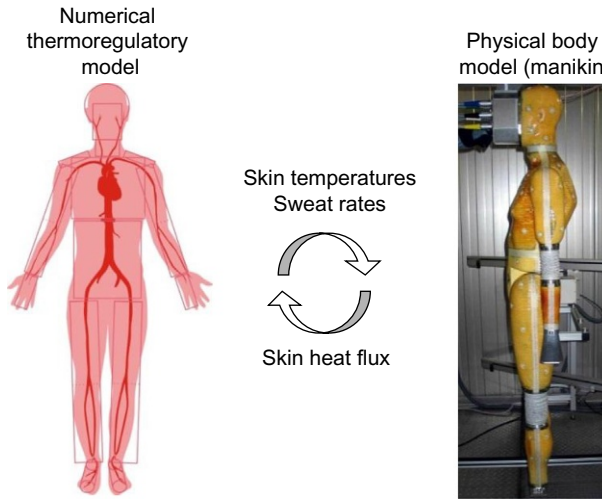

Fig. 15.1 Working principle of a human simulator.

Nowadays, thermal manikins are usually operated with uniform and steady-state surface temperatures, as well as constant sweat rates to determine the overall thermal insulation and the evaporative resistance of the complete clothing. On the other hand, there exist a number of mathematical models of human thermoregulation that usually include the heat and moisture transport mechanisms through the clothing to the environment (Fiala, Lomas, & Stohrer, 1999, 2001; Tanabe, Kobayashi, Nakano, Ozeki, & Konishi, 2002). These models use simplified clothing models that cannot differentiate local thermal effects. A number of efforts have been made in the last decade to couple the physical models (manikins) with numerical codes (Farrington, Rugh, Bharathan, & Burke, 2004; Psikuta, Wang, & Rossi, 2013; Hepokoski et al., 2015; Jie, Wenguo, & Ming, 2014). It has been shown that the manikins have to fulfill several conditions regarding precision under transient conditions (temporal and spatial variations of surface temperatures, heat loss, and sweating) for successful coupling with a numerical model (Psikuta et al., 2015). The thermophysiological model is used to calculate and predict the thermal status of the human body for different activities and environmental conditions and thus to define the manikin parameters like sweat rate and surface temperatures. For an exact control of the manikin, the segmentations of both the manikin and the model have to be compatible. The heat fluxes measured by the manikin determine the amount of heat exchanged with the environment and are used as a feedback system (input parameters) for the numerical model (Psikuta, Richards, & Fiala, 2008). Thus, the global impact of the clothing/environment on the human body can be predicted. However, in order to test the thermal performance of the clothing, additional information about design features is needed. Therefore, more advanced clothing models are needed to account for the coupled heat and mass transport mechanisms in the clothing layers (evaporation, condensation, etc.) (Li & Holcombe, 1998; Fan & Cheng, 2005a, 2005b). These models usually describe the mechanisms on a (one-dimensional) fabric level, but they do not consider factors like

moisture migration processes in multilayer clothing (Weder, Rossi, Chaigneau, & Tillmann, 2008), the evaporative cooling efficiency in relation to the distance to the skin (Havenith et al., 2013), or the presence (and the size) of air gaps (Frackiewicz-Kaczmarek, Psikuta, Bueno, & Rossi, 2015; Hu, Zhao, Li, & Stylios, 2016). In the future, it is expected that thermophysiological models, one- or two-dimensional heat and mass transfer models, as well as air gap/contact area models including the effects of movements and posture will be combined to determine the global and local impact of clothing on thermal comfort.

15.3 Pressure and friction

The mechanical contact of the textile with the human skin defines the sensorial comfort. This feeling is described by fabric properties like stiffness, smoothness, or itchiness and is very difficult to predict objectively. Therefore, a number of studies were performed to relate sensorial comfort with fabric properties like the number of protruding fibers, fiber, and yarn diameters, etc. (Naylor & Phillips, 1997; Wang, Zhang, Postle, & Phillips, 2003; Mcgregor et al., 2013; Stanton et al., 2014). There are only a few objective methods to assess the sensorial properties of a textile, and the most widely recognized is probably the KES-F system developed by Kawabata (Kawabata, 1980).

In sportswear, the mechanical contact with a garment is also related to the prevention of skin injuries due to pressure and friction (blisters, abrasions, or bleeding nipples) (Basler, Hunzeker, Garcia, & Dexter, 2004).

15.3.1 Frictionless sportswear

The textile-skin interactions relative to the formation of blisters were especially studied for the foot, mostly with human subjects (Van Tiggelen, Wickes, Coorevits, Dumalin, & Witvrouw, 2009; Bogerd, Niedermann, Brühwiler, & Rossi, 2012; Laing, Wilson, Dunn, & Niven, 2015; Tasron, Thurston, & Carré, 2015). It has been suggested that the formation of blisters is dependent on different factors like the frictional properties of the socks (and those of the skin), the pressure applied between both frictional partners, and the presence of moisture (Zhong, Xing, Pan, & Maibach, 2006). Therefore, different methods have been developed to determine the static and dynamic friction coefficient in realistic settings, but to the best of our knowledge, no standard test method exists so far. Dong et al. used a commercial tribometer (CSM instrument) with polydimethysiloxane (PDMS) silicone as skin simulant to characterize the friction behavior of newly developed fibers (Dong et al., 2015). Lorica, an artificial leather made of a polyamide fabric coated with polyurethane, shows similar surface properties to the skin (roughness, water contact angle) and was used to simulate the human skin friction against textiles in dry conditions (Derler, Schrade, & Gerhardt, 2007; Cottenden & Cottenden, 2013). This material was integrated into a "textile friction analyzer" (Fig. 15.2) and the friction coefficient measured correlated well to the preferences of participants in a human wear trial (Bertaux et al., 2010).

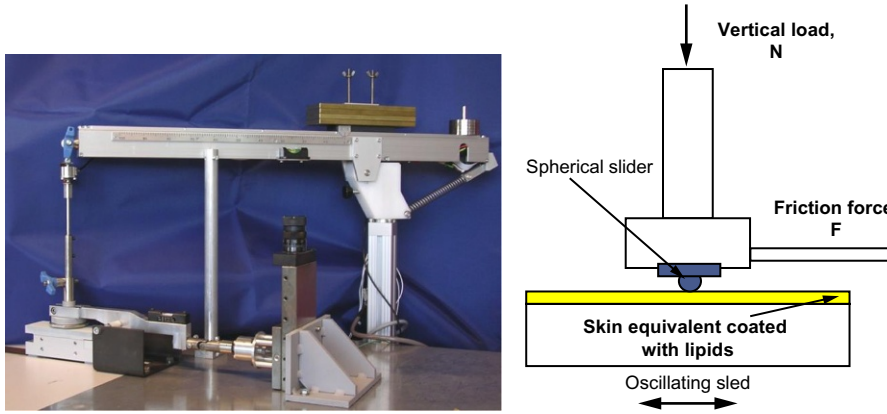

Fig. 15.2 Textile friction analyzer with schematic of the measurement set-up.

This device generates a cyclic sliding movement between the textile and the skin simulant with different normal loads to measure the dynamic friction contact and thus simulate different wear conditions. This method was used to characterize the friction of different sock structures and the effects of different finishes in order to determine their ability to prevent the formation of blisters (Baussan, Bueno, Rossi, & Derler, 2013; Bertaux, Le Marec, Crespy, Rossi, & Hegemann, 2009). A similar principle was used by Van Amber by horizontally pulling a weighted piece of Lorica attached to a sled across the test fabric mounted on a platform attached to a tensile tester (Van Amber et al., 2015). The use of Lorica is limited to the simulation of dry skin; therefore, new materials have been recently proposed to simulate the skin for a wider frictional test range including moist conditions (Nachman & Franklin, 2016; Dąbrowska et al., 2016; Hurtado, Peppelman, Zeng, Van Erp, & Van Der Heide, 2016).

15.3.2 Compression garments

Apart from the friction properties, the pressure existing at the interface between textiles and skin is also relevant for wear comfort. It is obviously directly related to the frictional properties of the textile, but it will also affect the compression of underlying tissues and the blood flow. It is known that the skin blood flow decreases to zero when a pressure of 16 kPa or higher is applied (Holloway, Daly, Kennedy, & Chimoskey, 1976). When carrying loads, is was shown that around 90% of the subjects reported moderate discomfort with an average surface pressure of 20 kPa (Stevenson et al., 1997; cited in Wettenschwiler et al., 2015a). The measurement of the applied pressure is also the main parameter to classify the performance of compression garments that have become very popular among competitive and recreational athletes. The pressure is directly influenced by several garment parameters like the dimension of the garment or the elastic properties of the fabric and the yarns used, as well as the body morphology. Sports compression garments are often made of elastane (also known under the name Lycra or spandex). In order to obtain the required pressure, the compression garment is smaller than the corresponding

body sites. The garment thus has to be highly elastic to allow easy donning. Such compression textiles have been in use for many years in the medical sector to prevent illnesses like blood circulation problems in the legs. Consequently, the effectiveness of compression garments for sports applications can be measured with the same standard. In Germany, the DIN 58133 (2008)/RAL-GZ 387/1 (2008) define the sizes (length and girth), as well as four different compression classes (2.4–2.8 kPa for soft compression and ≥6.5 kPa for very strong compression). In the United Kingdom, three standards (BS 6612, 1985; BS 7563, 1999; BS 7672, 1993) describe the validation procedure of compression hosiery. These test methods consist of a simultaneous stretching of the garment in length and width direction and the measurement of the created tension at different heights of the garment. The study by Hegarty-Craver, Kwon, Oxenham, Grant, and Reid (2015) provides a good overview of currently existing methods. The authors also point out that the different techniques vary in terms of test protocol, and therefore, there are also differences in the measured pressures. However, most of the studies about the compression garments for sports applications use human subjects because the compression has to be directly related to the performance of the athlete. The applied pressures are typically measured at the interface between the garment and the skin. However, the location of the sensors (bones and muscles) as well as the distortion (bending) of the sensors and the presence of moisture may greatly affect the results (Wettenschwiler et al., 2015b; Moffatt, 2008). Furthermore, the mechanisms of compression (i.e., the response of internal tissues to external pressures) are still not fully understood (Dubuis, Avril, Debayle, & Badel, 2012). Consequently, the benefits of sports compression garments are not proven yet (Beliard et al., 2015).

15.4 Aero- and hydrodynamics

Understanding of aero- and hydrodynamics of sportswear helps achieve greater performance in a wide range of high-speed sports like cycling, downhill and cross-country skiing, speed-skating, ski jumping, and swimming. The advantage of optimizing hydrodynamics in sportswear was seemingly demonstrated by swimming suits simulating shark skin, which led to several world records before being banned by the International Swimming Federation in 2010. Mollendorf et al. combined a human trial study with a theoretical model of laminar/turbulent flow at different body sites to demonstrate the positive effect of the shark-skin-like structures on friction and pressure drag (Mollendorf, Termin, Oppenheim, & Pendergast, 2004). In other studies with human subjects, it was shown that these suits decreased the energy costs of swimming and increased the overall performance of the swimmer (Chatard & Wilson, 2008; Falcone, Nagni, & Demarie, 2010). The locomotor performance of shark skin and a shark-skin-like textile was analyzed dynamically under controlled conditions using a robotic device that allowed the determination of the self-propelled swimming speed (Oeffner & Lauder, 2012). The authors found no increased swimming speed with the textile, while the shark skin had an ~12% increase in swimming speed compared to the same skin after removing the microscopic shark scales called

denticles. They suggested that the skin denticles not only reduced the drag but also enhanced thrust, and the skin-like fabric did not contain these microscopic structures. Other authors also questioned the effectiveness of these textile structures for the improvement of swimming speed (Stefani, 2012; Sanders, Rushall, Toussaint, Stager, & Takagi, 2001).

The aerodynamic behavior of sports fabrics has mainly been studied with cylindrical test methods in wind tunnels (Kyle, Brownlie, Harber, MacDonald, & Norstrom, 2004; Moria, Chowdhury, Aldawi, & Alam, 2013; Oggiano, Troynikov, Konopov, Subic, & Alam, 2009; Bardal & Reid, 2014). The cylinders are either placed vertically or with a range of angles of attack to simulate the athlete's body positions. The aerodynamic forces and moments (in the three dimensions) are then measured for different wind speeds in dependence on the cylinder diameter. The calibration of the system is made by measuring the cylinder without fabric. The fabric to be tested is then wrapped around the cylinder with the seam at the rear of the cylinder to minimize its effect (Moria et al., 2013). A review on the influence of athletes' postures, speed, and motion, as well as characteristics of fabrics (yarn types, construction, and coatings) and garments (stretch, wale orientation, seam positioning) can be found in Oggiano et al. (2013). Air permeability was chosen by the International Ski Federation (FIS) as the parameter to be tested in order to regulate the aerodynamic drag with a minimum of 30 L/m^2s (under 10 mm H_2O differential pressure) for racing suits and 40 L/m^2s for ski jumping suits (FIS, 2014). Apart from the aerodynamics, this parameter was introduced to ensure the athletes' health (sufficient air and moisture transport) and safety (increase in the friction between the suit and the snow and thus deceleration of the skier after a fall).

15.5 Conclusions and future trends

The properties of sportswear have to be directly related to their influence on athletes' performance. However, the added value of new features in sportswear is sometimes difficult to demonstrate with human trials. On the other hand, small-scale test methods do not have a large acceptance among end-users. Therefore, the characteristics of garments (especially protective clothing and sportswear aiming at optimizing the performance of the wearer) will be increasingly tested with complex, human-shaped apparatus equipped with intelligent, body-mimicking numerical control (human simulators). The validation of such new test methods remains a challenge. However, non-invasive imaging techniques (e.g., MRI) as well as minimally-invasive electronical devices (e.g., telemetry pill) allow the collection of core body data (temperature, blood flow, and biomechanical stresses) with human trials. This new data will facilitate the establishment of correlations between the human body and body-mimicking manikins and thus increase the acceptance of these new methods.

With the introduction of new textile types, like smart textiles, incorporating sensors and active elements, there is an obvious need for new test methods to be able to adequately classify their performance. In Europe, a new standardization working group was created a few years ago (CEN/TC 248 WG 31 “Smart Textiles”). Their

first publication was a technical report on the definitions of terms used in the field of smart textiles (CEN/TR 16298, 2011). Two main work items were defined and the respective standards were recently published: the first concerns the heat storage and release capacity of textiles containing phase change materials (CEN 16806-1, 2016). A second part of this standard is currently only a preliminary work item and is intended to measure the dynamic heat transfer (PWI/CEN 16806-2, 2016). The second standard defines the linear electrical resistance of conductive textiles (CEN 16812, 2016).

In the field of performance-enhancing textiles and systems, different soft textile-based exoskeletons have been proposed to reduce the metabolic costs of movements and the risks of muscles and joints overloading during high-intensity training (Low, Yeow, Yap, & Lim, 2015; Nycz, Delph, & Fischer, 2015). For these types of systems, new test methods are needed to characterize their biomechanical performance. Either physical models (manikins), like the load carriage systems analyzer proposed by Stevenson (Stevenson et al., 2004), or numerical models can be envisaged for precise performance evaluation.

15.6 Sources of further information

In the following links, further information about test methods for performance sportswear can be found. The links were all accessed in November 2016.

The main standardization organizations working on methods in the field of smart textiles are the following:

CEN/TC 248/WG31 (smart textiles) (https://standards.cen.eu/dyn/www/f?p=204:7:0::::FSP_ORG_ID:636781&cs=1C10B6755CB46A95DB06D279B8C1C5109)
ASTM Subcommittee D13.50 (smart textiles) (https://www.astm.org/COMMIT/SUBCOMMIT/D1350.htm)
AATCC RA 111 (electronically integrated textiles) (http://www.aatcc.org/test/etextiles/)
IEC SG 10 (smart wearable devices) (http://www.iec.ch/dyn/www/f?p=103:85:0::::FSP_ORG_ID,FSP_LANG_ID:12601,25).

Different associations released specific regulations for the use of sportswear in sports competitions. Such regulations exist, for example, for the following activities:

Swimming (https://www.fina.org/content/fina-approved-swimwear)
Alpine skiing (http://www.fis-ski.com/inside-fis/document-library/alpine-skiing/index.html#deeplink=rules)
Cross-country skiing (http://www.fis-ski.com/inside-fis/document-library/cross-country/index.html#deeplink=rules)
Ski jumping (http://www.fis-ski.com/inside-fis/document-library/ski-jumping/index.html#deeplink=rules)
Snowboarding (http://www.fis-ski.com/inside-fis/document-library/snowboard/index.html#deeplink=rules)

References

AATCC 195. (2012). *Liquid Moisture Management Properties of Textile Fabrics*. Research Triangle Park, NC: American Association of Textile Chemists and Colorists.

Ackerley, R., Olausson, H., Wessberg, J., & Mcglone, F. (2012). Wetness perception across body sites. *Neuroscience Letters*, *522*, 73–77.

Bardal, L. M., & Reid, R. (2014). The effect of textile air permeability on the drag of high-speed winter sports apparel. *Sports Engineering*, *17*, 83–88.

Basler, R. S., Hunzeker, C. M., Garcia, M. A., & Dexter, W. (2004). Athletic skin injuries: Combating pressure and friction. *The Physician and Sportsmedicine*, *32*, 33–40.

Baussan, E., Bueno, M. A., Rossi, R. M., & Derler, S. (2013). Analysis of current running sock structures with regard to blister prevention. *Textile Research Journal*, *83*, 836–848.

Beliard, S., Chauveau, M., Moscatiello, T., Cros, F., Ecarnot, F., & Becker, F. (2015). Compression garments and exercise: No influence of pressure applied. *Journal of Sports Science & Medicine*, *14*, 75.

Bertaux, E., Derler, S., Rossi, R. M., Zeng, X., Koehl, L., & Ventenat, V. (2010). Textile, physiological, and sensorial parameters in sock comfort. *Textile Research Journal*, *80*, 1803–1810.

Bertaux, E., Le Marec, E., Crespy, D., Rossi, R., & Hegemann, D. (2009). Effects of siloxane plasma coating on the frictional properties of polyester and polyamide fabrics. *Surface and Coatings Technology*, *204*, 165–171.

Birrfelder, P., Dorrestijn, M., Roth, C., & Rossi, R. M. (2013). Effect of fiber count and knit structure on intra- and inter-yarn transport of liquid water. *Textile Research Journal*, *83*, 1477–1488.

Bogerd, C. P., Niedermann, R., Brühwiler, P. A., & Rossi, R. M. (2012). The effect of two sock fabrics on perception and physiological parameters associated with blister incidence: A field study. *Annals of Occupational Hygiene*, *56*, 481–488.

Bogerd, N., Psikuta, A., Daanen, H. A. M., & Rossi, R. M. (2010). How to measure thermal effects of personal cooling systems: Human, thermal manikin and human simulator study. *Physiological Measurement*, *31*, 1161–1168.

BS 6612. (1985). *Specification for graduated compression hosiery*. London, UK: British Standards Institution.

BS 7563. (1999). *Specification for non-prescriptive graduated support hosiery*. London, UK: British Standards Institution.

BS 7672. (1993). *Specification for compression, stiffness and labelling of anti-embolism hosiery*. London, UK: British Standards Institution.

CEN 16806–1. (2016). *Textiles and textile products—Textiles containing phase change materials (PCM)—Part 1: Determination of the heat storage and release capacity*. Brussels: CEN European Committee for Standardisation.

CEN 16812. (2016). *Textiles and textile products—Electrically conductive textiles—Determination of the linear electrical resistance of conductive tracks*. Brussels: CEN European Committee for Standardisation.

CEN/TR 16298. (2011). *Textiles and textile products—Smart textiles—Definitions, categorizations, applications and standardization needs*. Brussels: CEN European Committee for Standardisation.

Chatard, J., & Wilson, B. (2008). Effect of fastskin suits on performance, drag, and energy cost of swimming. *Medicine and Science in Sports and Exercise*, *40*, 1149.

Cottenden, D. J., & Cottenden, A. M. (2013). A study of friction mechanisms between a surrogate skin (Lorica soft) and nonwoven fabrics. *Journal of the Mechanical Behavior of Biomedical Materials*, *28*, 410–426.

Dąbrowska, A., Rotaru, G. M., Derler, S., Spano, F., Camenzind, M., Annaheim, S., et al. (2016). Materials used to simulate physical properties of human skin. *Skin Research and Technology*, *22*, 3–14.

Derler, S., Schrade, U., & Gerhardt, L.-C. (2007). Tribology of human skin and mechanical skin equivalents in contact with textiles. *Wear*, *263*, 1112–1116.

DIN 58133. (2008). *Medical compression hosiery*. Berlin, Germany: Deutsches Institut für Normung e. V.

Dong, Y., Kong, J., Mu, C., Zhao, C., Thomas, N. L., & Lu, X. (2015). Materials design towards sport textiles with low-friction and moisture-wicking dual functions. *Materials & Design*, *88*, 82–87.

Dubuis, L., Avril, S., Debayle, J., & Badel, P. (2012). Identification of the material parameters of soft tissues in the compressed leg. *Computer Methods in Biomechanics and Biomedical Engineering*, *15*, 3–11.

Falcone, I., Nagni, G., & Demarie, S. (2010). Analysis of high level swim performance in relationship with the introduction of new race swimsuits. *Sport Science Review*, *19*, 177–186.

Fan, J., & Cheng, X.-Y. (2005a). Heat and moisture transfer with sorption and phase change through clothing assemblies Part I: Experimental investigation. *Textile Research Journal*, *75*, 99–105.

Fan, J., & Cheng, X.-Y. (2005b). Heat and moisture transfer with sorption and phase change through clothing assemblies part II: Theoretical modeling, simulation, and comparison with experimental results. *Textile Research Journal*, *75*, 187–196.

Farrington, R. B., Rugh, J. P., Bharathan, D., & Burke, R. (2004). *Use of a thermal manikin to evaluate human thermoregulatory responses in transient, non-uniform, thermal environments*. SAE Technical Paper.

Fiala, D., Lomas, K. J., & Stohrer, M. (1999). A computer model of human thermoregulation for a wide range of environmental conditions: The passive system. *Journal of Applied Physiology*, *87*, 1957–1972.

Fiala, D., Lomas, K. J., & Stohrer, M. (2001). Computer prediction of human thermoregulatory and temperature responses to a wide range of environmental conditions. *International Journal of Biometeorology*, *45*, 143–159.

Filingeri, D., Fournet, D., Hodder, S., & Havenith, G. (2014). Body mapping of cutaneous wetness perception across the human torso during thermo-neutral and warm environmental exposures. *Journal of Applied Physiology*, *117*, 887–897.

FIS. (2014). *Specifications for competition equipment and commercial markings*. International Ski Federation.Retrieved from http://www.fis-ski.com/mm/Document/documentlibrary/AlpineSkiing/04/31/04/Competitionequipment_1415_clean_Neutral.pdf (Accessed 6 November 2016).

Fournet, D., Ross, L., Voelcker, T., Redortier, B., & Havenith, G. (2013). Body mapping of thermoregulatory and perceptual responses of males and females running in the cold. *Journal of Thermal Biology*, *38*, 339–344.

Frackiewicz-Kaczmarek, J., Psikuta, A., Bueno, M.-A., & Rossi, R. M. (2015). Effect of garment properties on air gap thickness and the contact area distribution. *Textile Research Journal*, *85*, 1907–1918.

Havenith, G., Bröde, P., Den Hartog, E., Kuklane, K., Holmer, I., Rossi, R. M., et al. (2013). Evaporative cooling: Effective latent heat of evaporation in relation to evaporation distance from the skin. *Journal of Applied Physiology*, *114*, 778–785.

Hegarty-Craver, M., Kwon, C., Oxenham, W., Grant, E., Reid, L., Jr. (2015). Towards characterizing the pressure profiles of medical compression hosiery: An investigation of current measurement devices and techniques. *The Journal of the Textile Institute*, *106*, 757–767.

Hepokoski, M., Curran, A., Burke, R., Rugh, J., Chaney, L., & Maranville, C. (2015). *Simulating physiological response with a passive sensor manikin and an adaptive thermal manikin to predict thermal sensation and Comfort*. SAE Technical Papers, 2015-April.

Holloway, G. A., Daly, C. H., Kennedy, D., & Chimoskey, J. (1976). Effects of external pressure loading on human skin blood flow measured by 133Xe clearance. *Journal of Applied Physiology*, *40*, 597–600.

Hu, S., Zhao, M., Li, J., & Stylios, G. (2016). Effects of wind direction on sportswear thermal insulation with various ease allowance. *International Journal of Clothing Science and Technology*, *28*(4), 492–502.

Hurtado, M. M., Peppelman, M., Zeng, X., Van Erp, P., & Van Der Heide, E. (2016). Tribological behaviour of skin equivalents and ex-vivo human skin against the material components of artificial turf in sliding contact. *Tribology International*, *102*, 103–113.

Jie, Y., Wenguo, W., & Ming, F. (2014). Coupling of a thermal sweating manikin and a thermal model for simulating human thermal response. *Procedia Engineering*, *84*, 893–897.

Kawabata, S. (1980). *The standardization and analysis of hand evaluation*. Osaka: The Textile Machinery Society of Japan.

Keiser, C., & Rossi, R. M. (2010). Analysis of steam formation and migration in firefighters' protective clothing using X-ray radiography. *Journal of Occupational Safety and Ergonomics*, *16*, 131–143.

Kyle, C., Brownlie, L., Harber, E., MacDonald, R., & Norstrom, M. (2004). The Nike Swift Spin cycling project: Reducing the aerodynamic drag of bicycle racing clothing by using zoned fabrics. *The Engineering of Sport*, *5*, 1.

Laing, R. M., Wilson, C. A., Dunn, L. A., & Niven, B. E. (2015). Detection of fiber effects on skin health of the human foot. *Textile Research Journal*, *85*, 1849–1863.

Leisen, J., & Beckham, H. W. (2001). Quantitative magnetic resonance imaging of fluid distribution and movement in textiles. *Textile Research Journal*, *71*, 1033–1045.

Li, Y., & Holcombe, B. (1998). Mathematical simulation of heat and moisture transfer in a human-clothing-environment system. *Textile Research Journal*, *68*, 389–397.

Low, F.-Z., Yeow, R. C., Yap, H. K., & Lim, J. H. (2015). Study on the use of soft ankle-foot exoskeleton for alternative mechanical prophylaxis of deep vein thrombosis. In *2015 IEEE International Conference on Rehabilitation Robotics (ICORR). IEEE* (pp. 589–593).

Lu, Y., Wei, F., Lai, D., Shi, W., Wang, F., Gao, C., et al. (2015). A novel personal cooling system (PCS) incorporated with phase change materials (PCMs) and ventilation fans: An investigation on its cooling efficiency. *Journal of Thermal Biology*, *52*, 137–146.

Macrae, B. A., Laing, R. M., Wilson, C. A., & Niven, B. E. (2014). Layering garments during rest and exercise in the cold (8°C): Wearer responses and comparability with selected fabric properties. *Ergonomics*, *57*(2), 271–281.

Manke, I., Hartnig, C., Kardjilov, N., Messerschmidt, M., Hilger, A., Strobl, M., et al. (2008). Characterization of water exchange and two-phase flow in porous gas diffusion materials by hydrogen-deuterium contrast neutron radiography. *Applied Physics Letters*, *92*(24), 244101.

Mcgregor, B. A., Naebe, M., Stanton, J., Speijers, J., Beilby, J., Pieruzzini, S., et al. (2013). Relationship between wearer prickle response with fibre and garment properties and Wool ComfortMeter assessment. *Journal of the Textile Institute*, *104*, 618–627.

Moffatt, C. (2008). Variability of pressure provided by sustained compression. *International Wound Journal*, *5*, 259–265.

Mollendorf, J. C., Termin, A. C., II, Oppenheim, E., & Pendergast, D. R. (2004). Effect of swim suit design on passive drag. *Medicine and Science in Sports and Exercise*, *36*, 1029–1035.

Moria, H., Chowdhury, H., Aldawi, F., & Alam, F. (2013). A cylindrical methodology for the study of fabric aerodynamics. *Procedia Engineering*, *56*, 297–302.

Morrissey, M. P., & Rossi, R. M. (2013). The influence of fabric air permeability on the efficacy of ventilation features. *International Journal of Clothing Science and Technology*, *25*, 440–450.

Nachman, M., & Franklin, S. (2016). Artificial Skin Model simulating dry and moist in vivo human skin friction and deformation behaviour. *Tribology International*, *97*, 431–439.

Naylor, G. R. S., & Phillips, D. G. (1997). Fabric-evoked prickle in worsted spun single jersey fabrics.3. Wear trial studies of absolute fabric acceptability. *Textile Research Journal*, *67*, 413–416.

Niedermann, R., & Rossi, R. M. (2012). Objective and subjective evaluation of the human thermal sensation of wet fabrics. *Textile Research Journal*, *82*, 374–384.

Nycz, C. J., Delph, M. A., & Fischer, G. S. (2015). Modeling and design of a tendon actuated soft robotic exoskeleton for hemiparetic upper limb rehabilitation. In *Proceedings of the annual international conference of the IEEE Engineering in Medicine and Biology Society, EMBS* (pp. 3889–3892).

Oeffner, J., & Lauder, G. V. (2012). The hydrodynamic function of shark skin and two biomimetic applications. *Journal of Experimental Biology*, *215*, 785–795.

Oggiano, L., Brownlie, L., Troynikov, O., Bardal, L. M., Sæter, C., & Sætran, L. (2013). A review on skin suits and sport garment aerodynamics: Guidelines and state of the art. *Procedia Engineering*, *60*, 91–98.

Oggiano, L., Troynikov, O., Konopov, I., Subic, A., & Alam, F. (2009). Aerodynamic behaviour of single sport jersey fabrics with different roughness and cover factors. *Sports Engineering*, *12*, 1–12.

Ouzzahra, Y., Havenith, G., & Redortier, B. (2012). Regional distribution of thermal sensitivity to cold at rest and during mild exercise in males. *Journal of Thermal Biology*, *37*, 517–523.

Parada, M., Derome, D., Rossi, R., & Carmeliet, J. (2016). A review on advanced imaging technologies for the quantification of wicking in textiles. *Textile Research Journal*, 0040517515622151.

Priego Quesada, J. I., Martínez Guillamón, N., De Anda, R.M.C.O., Psikuta, A., Annaheim, S., Rossi, R. M., et al. (2015). Effect of perspiration on skin temperature measurements by infrared thermography and contact thermometry during aerobic cycling. *Infrared Physics and Technology*, *72*, 68–76.

Psikuta, A., Kuklane, K., Bogdan, A., Havenith, G., Annaheim, S., & Rossi, R. M. (2015). Opportunities and constraints of presently used thermal manikins for thermo-physiological simulation of the human body. *International Journal of Biometeorology*, *60*(3), 435–446.

Psikuta, A., Richards, M., & Fiala, D. (2008). Single-sector thermophysiological human simulator. *Physiological Measurement*, *29*, 181.

Psikuta, A., Wang, L. C., & Rossi, R. M. (2013). Prediction of the physiological response of humans wearing protective clothing using a thermophysiological human simulator. *Journal of Occupational and Environmental Hygiene*, *10*, 222–232.

PWI/CEN 16806-2. (2016). *Textiles and textile products—Textiles containing phase change materials (PCM)—Part 2: Determination of the heat transfer using a dynamic method*. Brussels: CEN European Committee for Standardisation.

RAL-GZ 387/1. (2008). *Medical compression hosiery*. Sankt Augustin, Germany: RAL Deutsches Institut für Gütesicherung und Kennzeichnung e.V.

Reifler, F. A., Lehmann, E., Frei, G., & May, H. (2003). Water distribution and movement in wet aramid-based ballistic body armor panels detected with neutron radiography. In *2nd European conference on protective clothing and NOKOBETEF 7, Montreux, Switzerland*.

Rossi, R. M., Stampfli, R., Psikuta, A., Rechsteiner, I., & Bruhwiler, P. A. (2011). Transplanar and in-plane wicking effects in sock materials under pressure. *Textile Research Journal*, *81*, 1549–1558.

Sanders, R., Rushall, B., Toussaint, H., Stager, J., & Takagi, H. (2001). Bodysuit yourself: But first think about it. *American Swimming Magazine*, *5*, 23–32.

Smith, C. J., & Havenith, G. (2011). Body mapping of sweating patterns in male athletes in mild exercise-induced hyperthermia. *European Journal of Applied Physiology*, *111*, 1391–1404.

Smith, C. J., & Havenith, G. (2012). Body mapping of sweating patterns in athletes: A sex comparison. *Medicine and Science in Sports and Exercise*, *44*, 2350–2361.

Song, W., Lai, D., & Wang, F. (2015). Evaluating the cold protective performance (CPP) of an electrically heated garment (EHG) and a chemically heated garment (CHG) in cold environments. *Fibers and Polymers*, *16*, 2689–2697.

Stampfli, R., Bruhwiler, P. A., Rechsteiner, I., Meyer, V. R., & Rossi, R. M. (2013). X-ray tomographic investigation of water distribution in textiles under compression - Possibilities for data presentation. *Measurement*, *46*, 1212–1219.

Stanton, J. H., Speijers, J., Naylor, G. R., Pieruzzini, S., Beilby, J., Barsden, E., et al. (2014). Skin comfort of base layer knitted garments. Part 1: Description and evaluation of wearer test protocol. *Textile Research Journal*, *84*, 1385–1399.

Stefani, R. (2012). Olympic swimming gold: The suit or the swimmer in the suit? *Significance*, *9*, 13–17.

Stevenson, J., Bossi, L., Bryant, J., Reid, S., Pelot, R., & Morin, E. (2004). A suite of objective biomechanical measurement tools for personal load carriage system assessment. *Ergonomics*, *47*, 1160–1179.

Stevenson, J., Bryant, J., Pelot, R., Morin, E., Reid, S., & Doan, J. (1997). *Research and development of an advanced personal load carriage system phases II and III. Section D: Development of acceptance criteria for physical tests of load carriage systems*.

Tanabe, S. I., Kobayashi, K., Nakano, J., Ozeki, Y., & Konishi, M. (2002). Evaluation of thermal comfort using combined multi-node thermoregulation (65MN) and radiation models and computational fluid dynamics (CFD). *Energy and Buildings*, *34*, 637–646.

Tang, K. P. M., Kan, C. W., & Fan, J. T. (2014). Evaluation of water absorption and transport property of fabrics. *Textile Progress*, *46*, 1–132.

Tang, K. P. M., Kan, C. W., & Fan, J. T. (2015). Assessing and predicting the subjective wetness sensation of textiles: Subjective and objective evaluation. *Textile Research Journal*, *85*, 838–849.

Tasron, D. N., Thurston, T. J., & Carré, M. J. (2015). Frictional behaviour of running sock textiles against plantar skin. *Procedia Engineering*, *112*, 110–115.

Van Amber, R. R., Lowe, B. J., Niven, B. E., Laing, R. M., Wilson, C. A., & Collie, S. (2015). The effect of fiber type, yarn structure and fabric structure on the frictional characteristics of sock fabrics. *Textile Research Journal*, *85*, 115–127.

Van Tiggelen, D., Wickes, S., Coorevits, P., Dumalin, M., & Witvrouw, E. (2009). Sock systems to prevent foot blisters and the impact on overuse injuries of the knee joint. *Military Medicine*, *174*, 183–189.

Wang, F., Cai, X., Zhang, C., Shi, W., Lu, Y., & Song, G. (2016). Assessing the performance of a conceptual tight-fitting body mapping sportswear (BMS) kit in a warm dry environment. *Fibers and Polymers*, *17*, 151–159.

Wang, F., Del Ferraro, S., Molinaro, V., Morrissey, M., & Rossi, R. (2014). Assessment of body mapping sportswear using a manikin operated in constant temperature mode and thermoregulatory model control mode. *International Journal of Biometeorology*, *58*, 1673–1682.

Wang, G., Zhang, W., Postle, R., & Phillips, D. (2003). Evaluating wool shirt comfort with wear trials and the forearm test. *Textile Research Journal*, *73*, 113–119.

Weder, M., Brühwiler, P. A., Herzig, U., Huber, R., Frei, G., & Lehmann, E. (2004). Neutron radiography measurements of moisture distribution in multilayer clothing systems. *Textile Research Journal*, *74*, 695–700.

Weder, M. S., Laib, A., & Brühwiler, P. A. (2006). Computerized tomography measurements of the moisture distribution in multilayered clothing systems. *Textile Research Journal*, *76*(1), 18–26.

Weder, M., Rossi, R. M., Chaigneau, C., & Tillmann, B. (2008). Evaporative cooling and heat transfer in functional underwear. *International Journal of Clothing Science and Technology*, *20*, 68–78.

Wettenschwiler, P. D., Lorenzetti, S., Stämpfli, R., Rossi, R. M., Ferguson, S. J., & Annaheim, S. (2015). Mechanical predictors of discomfort during load carriage. *PLoS ONE*, *10*, e0142004.

Wettenschwiler, P. D., Stämpfli, R., Lorenzetti, S., Ferguson, S. J., Rossi, R. M., & Annaheim, S. (2015). How reliable are pressure measurements with Tekscan sensors on the body surface of human subjects wearing load carriage systems? *International Journal of Industrial Ergonomics*, *49*, 60–67.

Zhao, M., Gao, C., Wang, F., Kuklane, K., Holmér, I., & Li, J. (2013a). A study on local cooling of garments with ventilation fans and openings placed at different torso sites. *International Journal of Industrial Ergonomics*, *43*, 232–237.

Zhao, M., Gao, C., Wang, F., Kuklane, K., Holmér, I., & Li, J. (2013b). The torso cooling of vests incorporated with phase change materials: A sweat evaporation perspective. *Textile Research Journal*, *83*, 418–425.

Zhong, W., Xing, M. M., Pan, N., & Maibach, H. I. (2006). Textiles and human skin, microclimate, cutaneous reactions: An overview. *Cutaneous and Ocular Toxicology*, *25*, 23–39.

Index

Note: Page numbers followed by *f* indicate figures and *t* indicate tables.

A

Abrasion resistance, 53–55, 305
Absolute glass bead test, 381, 382*f*
Active thermography, 108
Aerodynamics, sportswear, 440–441
Aerospace, 411–412
Aging process, textiles, 93–95
  environmental, and UV aging, 103
  evaluating performance, 105
  exposure, 103–104
  field studies, 104–105
  maintenance/cleaning procedures, 103
  mechanical action, 102–103
  nondestructive tests, 106–114
  research examples, 105–106
  research organizations, 117–118
  research summary, 96*t*
  simulation, 95–105
  standards organizations, 117
  tests for, 95–106
  for transportation
    environment, 420, 420*t*
    fatigue resistance, 421–422, 422*t*
    service, 420, 421*t*
  useful life, predicting, 114–115
  weathering, 103
Airbags, 404–405, 406*t*
Aircrafts, MobilTech, 400–401
Air filters, 414
Air-liquid porometry, 375–377, 378*f*
Air permeability, 142–143, 379–381
Alambeta testing instrument, 82–83
American Association of Textile Chemists and Colorists (AATCC) Technical Manual, 133
American Society for Testing and Materials (ASTM), 117, 352–353
  ASTM Committee D13 on Textiles, 11
  ASTM Committee D22 on Air Quality, 179
  ASTM Committee D35 on Geotextiles, 240, 287
  ASTM Committee F23 on Personal Protective Clothing and Equipment, 301, 303, 320, 326, 337
4-Aminoazobenzene-releasing azo colorants, 168
Amino-formaldehyde resin finish, 129
Antibacterial activity, 325
Antibacterial finishes, 134–136
Antimicrobial textiles, 414–415
Apparent opening size (AOS), 143, 250
Appliances, textile applications in, 6
Arc thermal protective value (ATPV), 194, 327–328
Atomic absorption spectrometry (AAS), 158
Attenuated total reflectance FTIR (ATR-FTIR), 112
Automotive industry, fabrics for, 198
Aviation industry, fabrics for, 200–201
Azo dyes, 151–153, 166

B

Ballistics
  pendulum method, 44–45
  protective clothing, 313, 322–323
Barrier effect, 191
Baseline test, 360–361
Bead test, filter medium, 381, 382*f*
Bench-scale tests, 216–223
Bending length measurement, 39–40
Bending rigidity measurement, 40
Benzene, 160–161
Benzyldimethyldodecylammonium chloride (BDMDAC), 134
Biochemical oxygen demand (BOD), 144
Biodegradability testing, 144–145
Bioengineering techniques, 368
Biosourced resins, 423–424
Bleaching, 151

Blocked structure, stress-strain curve for, 28*f*
Bluesign technologies, 178
Body-mapping clothing (BMC), sportswear, 435–436
Braids, 3–4
Bulloscopy, 377–379
Burn injury prediction
  using copper slug sensors, 213–214
  using skin simulant sensors, 214–216
Burst filter cartridge, 387*f*
Burst strength, 36–37
  hydraulic method, 36–37
  pneumatic method, 37

C

Cadmium, 154
California Technical Bulletin 117, 204
Camouflage, military protective clothing, 323
Carbon nanotubes (CNT), 424–425
Car racing, protective clothing, 333–334
CBR test, 43, 44*f*
CENTEXBEL, 180
Certification, and third-party testing, 9
Chemical testing
  antibacterial finishes, 134–136
  biodegradability testing, 144–145
  insect repellent finishes, 136
  permeability measurement, 142–144
  resistance of textiles, 140–142, 141*t*
  stain-free finishes, 136–138
  UV protection, 138–140
Chlorinated herbicides, 173
Chromium III and VI, 158–159
Chromium IV, 154
Cigarette ignition, 193–194
Civil engineering, textile applications in, 7
Cleanability, filter medium, 381, 387
Clean Ottawa sand, 248–249
Clo test (ASTM D-1518), 76
CNT. *See* Carbon nanotubes (CNT)
Cold protection technologies, 72
Color measurements, 108–110
Comfort testing, 59–60
  ergonomic comfort testing, 66–67
  fabrics, 60
  psychological comfort testing, 67
  skin sensorial wear comfort testing, 62–66
  thermophysiological, 61–62
Comfort wear test, 366
Composition analysis, 127, 129–132, 130*t*
Compression testing
  hot water immersion with, 218–219
  Kawabata compression measurement device, 35
  sodemat thickness measurement apparatus, 34*f*
  sportswear, 439–440
  thickness measurement, 34
Computer aided design (CAD), 407
Cone drop test, 40–41
Constant-rate-of-extension (CRE) tensile tests, 105
Construction protective clothing, 7, 329
  fall from heights, 329
  high visibility, 329–330
  mechanical risks, 330
Consumer Product Safety Improvement Act (CPSIA), 156–157
Contact heat, 77–78, 193
Controlled-condition wearer trials, 61
Cooling garments
  smart textiles, 359–361
  sportswear, 436
Copper slug sensors, 213–214
Cosmetics, textile applications in, 7
Cosmetotextiles, 367
  chemical properties, 367–368
  claimed effect, 368
  corneometry/conductimetry, 368
  durability, 369–370
  labeling, 370
  properties, 367
  toxicity and innocuousness, 368–369
Cradle-to-Cradle concept, 179
Critical Radiant Flux, 192
Cross-plane flow filtration, geotextiles, 241
Curtains, fire-resistant fabrics, 202–203
Cut resistance
  impact cut by hand knives, 50–52
  slicing-type cut by sharp objects, 49–50

D

Degradation, 93–95
Density-gradient technique, 278–279
Dermotextiles, 367–370
Diesel fuel filters, 388–389, 389*f*
N,N-Diethyl-3-methylbenzamide (DEET), 136

Diethylhexyl phthalate (DEHP), 175
Differential scanning calorimetry (DSC), 361–362
  geotextiles, 244, 257–258
  polypropylene, 133, 133*f*
  standard test methods, 79
Diisononyl phthalate (DINP), 175
Dimethyl fumarate, 168–172
Double tear test, 48
Drainage geocomposites, 277
  category, 277–278
  composition, 278–280
  compressive creep test, 284–285
  durability, 284–285
  hydraulic properties, 283
  mechanical properties, 280–282, 281*f*
  physical properties, 278–280
  sampling and specimen preparation, 278
  tensile tests, 280, 282
  3D quasirigid structure core, 278
Drapes, fire-resistant fabrics, 202–203
DSC. *See* Differential scanning calorimetry (DSC)
Duhamel's theorem, 214–215
Durability
  cosmetotextiles, 369–370
  drainage geocomposites, 284–285
  geogrids, 269–270
  geosynthetic clay liners, 275–277
  geotextiles, 256–264
  transportation, 419–422
Dyes, toxic, 165–168
Dying, 151

E

EASA. *See* European Aviation Safety Agency (EASA)
Eco-friendly additives and finishes, 424
EcoLogo label, 177
Eco-textile certifications, 177–179
Elastomers, protective clothing, 302
Electrical impedance, measurement, 364–365, 365*f*
Electrical protective clothing, 326
  electrical arc, 327–328
  electrical insulation, 326–327
  fire resistance, 328
  mechanical performance, 328–329
Electrical resistance, 354, 357
  conductive fabrics, 358*f*
  heating textile, 360
  narrow woven fabrics, 357*f*
  nonwoven electrodes, 366
Electric arc, 194, 196
Electrocardiogram (ECG), 363–367
Electrochemical cell, 364–365, 365*f*
Electrochemical impedance spectroscopy, 364, 365*f*
Electrode adhesion, 363–364
Electroencephalogram (EEG), 363–367
Electromyogram (EMG), 363–367
Electroplating techniques, 353
Emission factor (EF), 164
Energy dispersive X-ray fluorescence spectrometry (EDXRF), 157
Energy, textile applications in, 7
Environmental aging, 103, 420, 420*t*
Environmental management systems (EMS), 424
Environmental Protection Encouragement Agency (EPEA), 179
Enzyme treatment, 128
Equestrian, protective clothing for, 52–53
Ergonomic comfort testing, 66–67
Ethylenediamine tetraacetic acid (EDTA), 158–159
European Aviation Safety Agency (EASA), 411–412
European Chemicals Agency (ECHA), 180
Extractable content, 128–129

F

FAA. *See* Federal Aviation Administration (FAA)
Fabric intelligent hand tester (FIHT), 362
Fabrics
  bench-scale tests, 216–223
  comfort properties, 60
  fire-resistant
    drapes/curtains/window shades, 202–203
    flooring materials, 201–202
    home furnishings, 204
    mattresses, 204
    personal protective equipment, 196–198
    transportation industry, 198–201

Fabrics *(Continued)*
flammability testing
barrier effect, 191
cigarette ignition, 193–194
contact heat, 193
damage measurement, 189–191
electric arc, 194
flame ignition, 192–193
flame propagation, 192
garment flame test, 195–196
heat release rate, 192
molten substances, 194
opacity of smoke, 191
radiant heat, 193
small-size specimen testing, 194–195
hot water immersion with compression, 227–228
hot water splash, 225–226
standard tensile test methods for, 31–32
steam, 228
Federal Aviation Administration (FAA), 411
Federation internationale de l'automobile (FIA), 333–334
Fiber blends, quantitative analysis, 244–245
Fiber-reinforced composites, 400–401, 415–417
Fibers
analysis of, 129–134
solubility tests of, 130*t*
specialty, 83
standard tensile test methods for, 29
stress-strain curve for, 26*f*
tensile tester, 30*f*
Filtration, 375
air bubble occurring outside medium, 379*f*
air flow curve, 376*f*
burst filter cartridge, 387*f*
clogging curve of medium *vs.* test dust injection time, 385*f*
differential pressure measurement rig, 380*f*
existing standards to qualify medium, 389, 390*f*
hydraulic properties
air and liquid permeability, 379–381
cleanability of filter medium, 381
incoming/outgoing particles passing through medium, 382*f*
Mullen burst test, 388, 388*f*
multipass test bench, 383*f*
physical/physicochemical properties, 386
cleanliness of filter medium, 387
compatibility, 386–387
grammage, 386
mechanical resistance, 387–388
thickness, 386
water removal efficiency of diesel fuel filters, 388–389, 389*f*
pressure drop measurement by oil flowrate, 380*f*
separative properties, 381
absolute glass bead test, 381, 382*f*
bacterial challenge, 385, 386*f*
particulate filtration efficiency, 381–385, 383*f*
retention capacity, 385
source of further information, 394–395
structural properties
bubble point determination, 377–379
pore size distribution, 375–377, 377–378*f*
test dust and particle counter, 384*t*
testing procedures, 390*t*
transportation and, 414
Filtration opening size (FOS), geotextiles, 250–251, 251*f*
Finite elements analysis (FEA), 407
Firefighters' protective clothing, 94–95
Fire-resistant fabrics
drapes/curtains/window shades, 202–203
electrical, 328
first responder, 318–319
home furnishings, 204
industrial/domestics, 309–310, 310*f*
mattresses, 204
personal protective equipment
flammability tests, 196–198
thermal protective performance tests, 198
transportation industry, 403
automotive, 198
aviation, 200–201
flooring materials, 201–202
railroad, 199–200
First responder protective clothing, 316
chemical and biological hazards, 316–317
ergonomics, function, and comfort, 320
fire resistance, 318–319
high visibility, 319–320

man-in-simulant test, 316–317
mechanical performance, 319
passive adsorbent dosimeters, 316–317
thermal protection, 317–318
Flame AAS (FAAS), 158
Flame ignition, 192–193
Flame propagation, 192
Flame resistance, 318, 328
protective clothing materials, 309
specimen surface configurations, 310*f*
Flame retardants, testing for, 173–175
Flammability testing, of fabrics, 105
barrier effect, 191
damage measurement
after-flame time, 190–191
afterglow duration, 190–191
damaged length/char length, 190
dripping, 191
flaming debris, 191
ignitability, 189–190
melting, 191
weight loss, 190
flame propagation, 192
garment flame test
electric arc safety, 196
hydrocarbon flash fire, 195
heat release rate, 192
opacity of smoke, 191
personal protective equipment, 196–198
small-size specimen testing, 194–195
sources of ignition
cigarette ignition, 193–194
contact heat, 193
electric arc, 194
flame ignition, 192–193
molten substances, 194
radiant heat, 193
transportation, 410–413, 412*t*
Flexion properties
bending length measurement, 39–40
bending rigidity measurement, 40
Floatation assessment, marine protective clothing, 331–332
Flooring materials, fabrics for, 201–202
Footwear
flame resistance, 318
insulated, 327
physical integrity, preservation of, 329
puncture resistance, 305
resistance to crushing, 306
risks, 304
slip resistance, 314–315, 315*f*
transverse stiffness, 334–335
Formaldehyde, 161, 165
Fragment-simulating projectiles (FSP), 314
Frictionless sportswear, 438–439
Full-scale instrumented manikin tests, 223–225

G

Garment flame test
electric arc safety, 196
hydrocarbon flash fire, 195
Gas chromatography with mass selective detection (GC-MSD), 156
GCL. *See* Geosynthetic clay liners (GCL)
Geogrids, 240, 264
categories, 264–265
composition, 266
durability, 269–270
mechanical properties, 266–269
Percent Open Area, 266
physical properties, 265–266
sampling and specimen preparation, 265
tensile test, 266–270, 267*f*
Geonets, 240, 277, 280, 282, 284
Geosynthetic clay liners (GCL), 12, 240, 270
barrier properties, 274–275
durability, 275–277
hydraulic properties, 274–275
mechanical properties, 272–274
peeling test data measurement, 272–273, 273*f*
physical properties, 272
sampling and specimen preparation, 271
tensile tests, 272
types, 271
Geosynthetics, 142, 239
polymer, 239
Geotextiles, 240–241
apparent opening size, 250
barrier properties, 250–255
CBR Test, 248
composition, 244–245
durability, 256–264
filtration opening size, 250–251, 251*f*
grab test method, 246, 272–273
Gradient Ratio Test, 253–254

Geotextiles *(Continued)*
Hydraulic Conductivity Ratio, 253
hydraulic properties, 250–255, 254*f*
knitted, 241
mechanical properties, 245–250
Mullen test, 249
nanofiber-based, 286
oxidative induction time, 257–258, 258*f*
Percent Open Area, 252
permittivity and permeability, 252–253
physical properties, 242–244
polymer, 239–241
sampling protocols, 241–242
SIM creep test, 262, 263*f*
staple fiber, 241, 243
tensile test configurations, 245–246, 245*f*, 262, 264
thermal properties, 256
woven *vs.* nonwoven, 241
Global Ecolabelling Network (GEN), 177
Gradient Ratio Test, 253
Grammage, filtration, 386
Graphite furnace AAS (GFAAS), 158
GREENGUARD certification, 178

H

N-Halamine, 135
Heating garments
smart textiles, 359–360, 359*f*
sportswear, 436
Heat release rate, 192
Heat stress protection, 72–74
Heavy metals
extraction, 156
testing for, 153–159
Henriques Burn Integral (HBI) equation, 215
High-performance polymer fibers, 302
Home furnishing, 6, 204
Hot water protective performance
bench-scale tests, 216–223
compression test, 218–219, 227–228
high-risk sector workers, 212–225
issues in, 230–231
splash test, 216–218, 225–226
spray test, 223–224
whole garments, 229
Household items, textile applications in, 6
Human simulators, sportswear, 436–438, 437*f*
Hydraulic Conductivity Ratio, 253
Hydraulic method, 36–37
Hydrocarbon flash fire, 195
Hydrodynamics, sportswear, 440–441
Hygiene, textile applications in, 7

I

Ice sports, protective clothing, 335
IMO. *See* International Maritime Organization (IMO)
Impact cut by hand knives, 50–52
Impact resistance, 52–53
Inductively coupled plasma-mass spectrometry (ICP-MS), 158
Inductively coupled plasma-optical emission spectrometry (ICP-OES), 158
Industrial/domestic protective clothing, 7, 303–304
chemical hazards, 307–308
ergonomics and comfort, 311–312
fire resistance, 309–310, 310*f*
flame resistance tests, 309, 310*f*
hydrostatic techniques, 307
Kawabata Evaluation System, 311
Lissajous curve, 305
mechanical risks, 304–307
permeation technique, 308*f*
probe penetration, 305
thermal performance, 309–310
Infrared thermography, sportswear, 435
Inoculation technique, 325
Insect repellent finishes, 136
International Maritime Organization (IMO), 413, 413*t*
International Organization for Standardization (ISO)
ISO Technical Committee ISO/TC 38 on Textiles, 180
ISO Technical Committee 221 on Geosynthetics, 240, 287
ISO Technical Committee TC 94 on Protective clothing and equipment, 338
International Ski Federation (FIS), 441

J

Jurin's law, 376–377, 376*f*

K

Kawabata Evaluation System (KES), 311, 366
  KES-FB1-tension tester, 33*f*
  KES-FB3 compression tester, 35, 35*f*
  tensile curve, 33*f*
Knitted geotextiles, 241
Knitted textiles, 3–4

L

Laboratory accreditation, 14–15
Laboratory information management system (LIMS), 13–14
Law enforcement, protective clothing, 312
  ballistic resistance, 313
  blast overpressure, 313–314
  identification and high visibility, 315–316
  mechanical risks, 312–313
  slip resistance, 314–315, 315*f*
Linear resistivity, measurement, 354–356, 355*f*, 356*t*
Linen, textile applications in, 6
Liquid-liquid porometry, 377, 378*f*
Liquid penetrants, 107–108
Liquid permeability, 142–143, 379–381
Long-term emission modeling, 165
Loose structure, stress-strain curve for, 28*f*
Low stress tensile characterization, 32

M

Manikin testing, 61–62
Man-in-simulant test (MIST), 316–317
Man-made fibers, 4, 129
Manufacturing quality control, 7–8
Marine protective clothing, 330–331
  floatation assessment, 331–332
  localization, 333
  thermal performance, 332–333
Marine transportation
  IMO fire test procedures, 413, 413*t*
  MobilTech, 401
Mark II tester, 315
Mattresses, flammability of, 204
Mechanical resistance, filtration, 387–388
Medical protective clothing, 7, 324
  antibacterial activity, 325
  chemical and biological barrier, 325
  radiation protective, 326
Melt index, 279
Mercerizing treatment, 151
Mercury, 154
Methanol, 160–161
Military protective clothing, 7, 320–321
  ballistics, 322–323
  camouflage, 323
  chemical/biological warfare, 321
  comfort, 323–324
  thermal performance, 321–322
MobilTech, 399
  aircrafts, 400–401
  applications, 402
  International Trade Statistics, 399–400
  marine transportation, 401
  rail transport, 401
  road vehicles, 399–400
Modified transient plane source (MTPS) technique, 81–82
Mohr-Coulomb shear strength, 247–248, 273–274
Moisture management sportswear, 434–435
Molten substances, 194
Motorcycling, protective clothing, 334–335
Motorcyclists' back protectors, 53
Mullen burst test, 388, 388*f*
Mullen-type hydrostatic tester, 255
Multiaxial tensile strength, 28–32
Multilayer fabrics, 83–84
Multipass test bench, filter medium, 383*f*

N

Nanoclay, 286
Nanofiber-based geotextiles, 286
Nanotechnology, 16–17
National Aviation Authorities (NAAs), 411
National Fire Protection Association (NFPA), 117, 403
National Transportation Safety Board, 400
Natural fibers, 4, 129, 240–241, 302, 423
NDT technique. *See* Nondestructive test (NDT) technique
Near infrared spectroscopy, 111–114
Neutron radiography, sportswear, 435
NFPA. *See* National Fire Protection Association (NFPA)
Nickel, 154–156
Noncrimp fabrics (NCF), 415–416

Nondestructive test (NDT) technique
active thermography, 108
color measurements, 108–110
liquid penetrants, 107–108
near infrared spectroscopy, 111–114
purpose of, 106–114
Raman spectroscopy, 110–111
visual inspections, 107
X-ray diffraction, 111
Nonfibrous materials, 128–129
Nonwoven process, 3–4
Nonylphenol, 176–177
Nonylphenol ethoxylates (NPE), 17, 151–153, 176–177
Nuclear magnetic resonance (NMR), 435

O

Occupational hazards, 211
OEKO-TEX 100 certification, 178
OEKO-TEX association, 9
OIT. *See* Oxidative induction time (OIT)
Organochlorine, 172
Organophosphorus pesticides, 172
Oxidative induction time (OIT), 257–258, 258*f*

P

Particles, permeability to, 143–144
Particulate filtration efficiency, 381–385, 383*f*
PCERF research team, 222–223
PCS. *See* Personal cooling system (PCS)
Pendulum testing machine, 45, 45*f*
Pentachlorophenol (PCP), 176–177
Performance-based test methods, 10
Permethrin, 136
Personal cooling system (PCS), 360–361
Personal protective equipment (PPE), 301, 320, 326
Pesticide residues, testing for, 168–173, 169*t*
Phase change materials (PCMs), 85–86, 361–363
Phosphoric acid treatment, 129
Phthalates, testing for, 175–176
Plant-based fibers, 4
Pneumatic method, 37
Poly(lactic acid) (PLA), 144
Polybrominated biphenyls (PBBs), 174
Polybrominated diphenyl ether (PBDE), 174, 424
Polycaprolactone, 144
Polychlorinated dibenzofurans (PCDF), 176–177
Polychlorinated dibenzo-p-dioxins (PCDD), 176–177
Polyethylene, 239, 279
geotextile durability, 256–257
Polyglycolide, 144
Polylactic acid (PLA), 423
Polymer geosynthetics, 239
Polymer geotextiles, 239–241
Polymers, in protective clothing, 302
Polytetrafluoroethylene (PTFE), 142, 302
Polyvinylchloride (PVC) polymer, 175–176
Pore size distribution, filter medium, 375–377, 377–378*f*
Prefabricated vertical drains (PVD), 277–278
Printing, 151
Property-based test methods, 9–10
Protective clothing, 7, 301
bench-scale tests, 216–223
construction, 329
fall from heights, 329
high visibility, 329–330
mechanical risks, 330
cutting resistance, 335
design and material, 303
electrical, 326
electrical arc, 327–328
electrical insulation, 326–327
fire resistance, 328
mechanical performance, 328–329
first responders, 316
chemical and biological hazards, 316–317
ergonomics, function, and comfort, 320
fire resistance, 318–319
high visibility, 319–320
mechanical performance, 319
thermal protection, 317–318
full-scale instrumented manikin tests, 223–225
high-risk sector workers, 212–225
industrial/domestic, 303–304
chemical hazards, 307–308
ergonomics and comfort, 311–312
fire resistance, 309–310, 310*f*

flame resistance tests, 309, 310*f*
hydrostatic techniques, 307
Kawabata Evaluation System, 311
mechanical risks, 304–307
permeation technique, 308*f*
probe penetration, 305
test configurations, 304–305, 304*f*
thermal performance, 309–310
lacerations prevalence, 335
law enforcement personnel, 312
ballistic resistance, 313
blast overpressure, 313–314
identification and high visibility, 315–316
mechanical risks, 312–313
slip resistance, 314–315, 315*f*
marine, 330–331
floatation assessment, 331–332
localization, 333
thermal performance, 332–333
medical, 324
antibacterial activity, 325
chemical and biological barrier, 325
radiation protective, 326
military, 320–321
ballistics, 322–323
camouflage, 323
chemical/biological warfare, 321
comfort, 323–324
thermal performance, 321–322
polymers in, 302
retroreflective materials, 330, 333
sports, 333
car racing, 333–334
ice sports, 335
motorcycling, 334–335
textile applications in, 6
types, 301–302
Psychological comfort testing, 67
Puncture resistance, 305
CBR test, 43
cone drop test, 40–41
pyramid, 43
Pyramid puncture resistance, 43

Q

Quality control, manufacturing, 7–8
Quebec's Occupational Health and Safety Commission, 312

R

Radiant heat, 193
Radiant heat resistance (RHR), 78–79
Radiative protective performance (RPP), 104
Radiography, sportswear, 434
Rail transportation
fabrics for, 199–200
flammability test, 412–413, 412*t*
MobilTech, 401
smoke emission test, 412–413, 412*t*
Raman spectroscopy, 110–111
Recreational vehicles, 399–400, 402
Reproductive toxicity, 151–153
Retention capacity, filter medium, 385
Road vehicles
flammability test, 411
MobilTech, 399–400

S

Scouring, 151
Seat belts, 406–408
Sensors, 212–216
copper slug sensors, 213–214
skin simulant sensors, 214–216
Service aging, on textiles for transportation, 420, 421*t*
Shear properties, 38
Single tear method
with trouser-shaped test specimens, 45–47
with wing-shaped test specimens, 47–48
Single-time constant model, 365*f*
Skin burn injury, 191
Skin-electrode impedance, 363–364, 365*f*
Skin model, 76
Skin sensorial wear comfort testing, 62–66
contact point index measuring device, 64*f*
sorption index measuring equipment, 65, 65*f*
stiffness measurement device, 66*f*
surface index measuring equipment, 64*f*
wet cling index measuring equipment, 64, 65*f*
Skin simulant sensors, 214–216
Slicing-type cut by sharp objects, 49–50
Slip resistance, footwear, 314–315, 315*f*
Smart textiles, 336, 424–425
aspects of, 352
comfort properties for long-term use, 366–367

Smart textiles *(Continued)*
conductive materials testing, 353
dynamic measurements, 357
electrical characteristics, 354
linear resistivity measurement, 354–356, 355*f*, 356*t*
surface resistance, measurement, 356–357, 356*f*
cosmetotextiles, 367–370
dermotextiles, 367–370
electrical impedance, 364–365, 365*f*
electrocardiogram, 363–367
electrode adhesion, evaluation of, 363–364
electroencephalogram, 363–367
electromyogram, 363–367
European Committee, 352
evolution, 351–352
initiatives around world, 352–353
markets and applications, 351
passive *vs.* active, 352
sweating impact assessment, 365–366
thermoregulating materials, 358–359
conductive heating garments, 359–360
cooling garments, 360–361
PCMs, 361–363
Smoke
generation, 410–413, 412*t*
opacity of, 191
toxicity, 403
Solvent extraction, 128–129
Sports protective clothing, 7, 333
car racing, 333–334
ice sports, 335
motorcycling, 334–335
Sportswear, 433
aero- and hydrodynamics, 440–441
body-mapping, 435–436
commercial tribometer, 438
compression garments, 439–440
with cooling/heating elements, 436
frictionless, 438–439
human simulators, 436–438, 437*f*
moisture management, 434–435
non-invasive imaging techniques, 441
properties, 441
textile friction analyzer, 438, 439*f*
thermophysiological model, 436–438
Stain-free finishes, 136–138
Stakeholders, transportation, 402–403
Standardization, 10–11
Standard Reference Materials (SRM), 193–194
Standard tensile test methods
for fabrics, 31–32
for fibres, 29
for yarns, 31
Steam protective performance
bench-scale tests, 220–223
fabrics, 228
full-scale instrumented manikin tests, 224–225
high-risk sector workers, 212–225
issues in, 230–231
whole garments, 229–230
Steam transfer index (STI), 220–221
Stelometer, 30*f*
Stoll curve, 213–214
Stress-strain curve
blocked structure, 28*f*
fibers, 26*f*
loose structure, 28*f*
woven fabric, 27*f*
yarns, 27*f*
Supporting Standardization for Smart Textiles (SUSTASMART), 352–353
Surface resistance, measurement, 356–357, 356*f*
Sweating guarded hotplate (ISO 11092), 76
Sweating thermal manikins, 80–81
Synthetic fibers, protective clothing, 302

T

Tear resistance measurement, 305–306, 319, 328–329
ballistic pendulum method, 44–45
double tear test, 48
pendulum testing specimen, 46*f*
single tear method
with trouser-shaped test specimens, 45–47
with wing-shaped test specimens, 47–48
trouser-shaped test specimen, 46*f*
Temperature regulating factor (TRF), 362, 362*f*
Tenax®, 162–163
Tensile strength, 28–32
Tensile test
drainage geocomposites, 280, 282
geogrids, 266–270, 267*f*

geosynthetic clay liners, 272
geotextiles, 245–246, 245*f*, 262, 264
Tetrachloroethylene, 161
Textile(s)
aging (*see* Aging process, textiles)
applications, 6–7
elasticity, 26–28
extractable content, 128–129
fabrics, 83
finishing, 127
antibacterial finishes, 134–136
insect repellent finishes, 136
stain-free finishes, 136–138
UV protection, 138–140
manufacturing, 3–4
materials, thermal properties of, 71
mechanical behavior of, 25–26
Textile-reinforced composites, transportation and, 415
aging process
environment, 420, 420*t*
fatigue resistance, 421–422, 422*t*
service, 420, 421*t*
destructive testing, 417
nondestructive testing, 417, 419*t*
short-/long-term properties and performance, 418*t*
tests on, 415–417
Textile testing
certification and third-party testing, 9
conditioning and standard atmospheric conditions, 12
defective products
detection, 15
product improvements, strategies for, 16
end-users' perspective, 6
environmentally friendly production processes, 17
importance of, 4–6
laboratory accreditation, 14–15
laboratory equipment, 13
LIMS, 13–14
manufacturers' perspective, 5
manufacturing quality control, 7–8
market development issues, 6
next generation materials, 16–17
performance-based test methods, 10
procurement, trends in, 18
property-based test methods, 9–10
specifiers' perspective, 5
standardization, 10–11
Thermal heat loss (THL), 77
Thermal manikins, 61–62, 80–81
Thermal properties
Alambeta testing instrument, 82–83
applications
multilayer fabrics, 83–84
PCM, 85–86
specialty fibers/yarns, 83
textile fabrics, 83
cold protection, 72
comfort, 71–72
conductivity, 74–75
effusivity, 74–75
heat stress protection, 72–74
resistance, 74
Thermal protection performance (TPP), 104
Barrier effect, 191
fire-resistant fabrics, 198
of materials for hot surface contact, 77–78
standard test method, 77
Thermogravimetric analysis (TGA), 79–80, 105
Thermophysiological comfort testing, 61–62
Thermoplastics, protective clothing, 302
Thermosetting polymers, 302
Third-party testing, 9
Tires, 408, 409*t*
T-joint carbon fiber reinforced polymer (CFRP) composites, 417
Tog test (BS 4745), 76
Toluene, 160–161
Tomography, sportswear, 434
Total VOC (TVOC), 164
Toxic dyes, testing for, 165–168
Toxicity testing
of burned gases, 192
eco-textile certifications, 177–179
for flame retardants, 173–175
for heavy metals, 153–159, 155*t*
for pesticide residues, 168–173
for phthalates, 175–176
for toxic dyes, 165–168
transportation, 410–413, 412*t*
for VOCs, 159–165
Transportation, 399
automotive equipment safety, 404
airbags, 404–405, 406*t*
lifting and securing slings, 408–410

Transportation *(Continued)*
seat belts, 406–408
tires, 408, 409*t*
durability testing, 419–422
flammability, smoke generation, and toxicity, 410–413, 412*t*
MobilTech, 399–402
OEM standards and specifications, 402
fire protection and smoke toxicity, 403
stakeholders, 402–403
structural and aesthetic durability, 404
textile applications in, 7
textile-reinforced composites, 415–417
transmission of infectious diseases, 414–415
TRF. *See* Temperature regulating factor (TRF)
Tricresylphosphate (TCP), 174
Tris (1-aziridinyl)-phosphine oxide (TEPA), 174

U

Ultraviolet (UV)
aging, 103
protection, 138–140
Urea acid treatment, 129

V

Visual inspections, 107
Volatile organic compounds (VOCs), 151–153, 159–165, 160*t*

W

Water soluble species, 128
Water vapor, permeability to, 142–143
Weathering, 103
Weaving, 3
Window shades, fire-resistant fabrics, 202–203
Woven fabric, stress-strain curve for, 27*f*
Woven textiles, 3–4

X

X-ray diffraction (XRD), 111

Y

Yarns
specialty, 83
standard tensile test methods for, 31
stress-strain curve of, 27*f*

THE TEXTILE INSTITUTE BOOK SERIES

Advanced Characterization and Testing of Textiles

Edited by Patricia Dolez, Olivier Vermeersch, and Valerio Izquierdo

A detailed exploration of developments in physical and chemical testing that highlights specific tests for high-performance textiles .

Advanced Characterization and Testing of Textiles explores developments in physical and chemical testing, and specific tests for high-performance textiles. Textiles are tested in order to gauge product quality, assess performance, and ensure regulatory compliance. The increasing variety of end uses and performance requirements associated with textiles has resulted in the evolution of advanced testing processes.

This book introduces the principles of advanced characterization and testing in use in the textile industry. A first series of chapters are organized by textile properties, and provide in-depth coverage of testing each characteristic. Then, tests for specific applications are addressed, with the main focus on high-performance and technical textiles.

About the Editors

Dr. Patricia Dolez has recently joined the Department of Human Ecology at the University of Alberta, Canada, to work as an Assistant Professor in Textile Science. Before that, she had been a researcher at CTT Group in St-Hyacinthe, Quebec, Canada since 2012. Her expertise includes textiles, polymers, and composites. She is especially interested in the application of nanotechnologies, smart textiles, natural fibres, and recycled materials in personal protective equipment and other textile-based products as well as in the aging behavior of protective materials. Dr. Dolez has authored more than 100 articles in books, scientific and technical journals, and conference proceedings.

Olivier Vermeersch is a graduate of ENSISA (Engineering School in Mulhouse, France) and the University of Haute Alsace in France in Textile Materials & Processes Engineering. Dr. Vermeersch has been involved in the technical textile industry since 1990 within the CTT Group, the largest R&D laboratory in Canada in the areas of technical textiles, geosynthetics, and flexible materials. He is Vice-President R&D as well as Chair holder of the NEXTEX Industrial Chair of St-Hyacinthe College.

Valerio Izquierdo graduated in textile engineering from the Institut Textile et Chimique de Lyon (ITECH – France) in 1998. After 3 years at the Institut Textile de France, he joined the CTT Group, St-Hyacinthe, Canada, as a project leader to pilot innovative research and development projects and laboratory testing. He is now Vice-President of the Textile Laboratories and Expertise branch of the CTT Group, involved in the characterization of textile and polymeric materials for the benefit of manufacturers, distributors, and end-users. Valerio also sits as a leading expert on various boards emitting regulatory and specification guidelines for the industry and governing agencies.

Related titles

Understanding and Improving the Durability of Textiles, Annis, 2012, 9780857090874
Simulation in Textile Technology, Veit, 2012, 9780857090294
Modelling and Predicting Textile Behaviour, Chen, 2009, 9781845694166

TEXTILES
ISBN 978-0-08-100453-1
9 780081 004531

ELSEVIER
WP
WOODHEAD PUBLISHING
An imprint of Elsevier
elsevier.com/books-and-journals